Methods in Molecular Biology 1458

Springer Protocols

Josie Ursini-Siegel
Nicole Beauchemin *Editors*

The Tumor Micro-environment

Methods and Protocols

EXTRAS ONLINE

Humana Press

METHODS IN MOLECULAR BIOLOGY

Series Editor
John M. Walker
School of Life and Medical Sciences
University of Hertfordshire
Hatfield, Hertfordshire, AL10 9AB, UK

For further volumes:
http://www.springer.com/series/7651

The Tumor Microenvironment

Methods and Protocols

Edited by

Josie Ursini-Siegel

Lady Davis Institute for Medical Research, Department of Oncology
McGill University, Montreal, QC, Canada

Nicole Beauchemin

Goodman Cancer Research Centre, McGill University, Montreal, QC, Canada

Humana Press

Editors
Josie Ursini-Siegel
Lady Davis Institute for Medical Research
Department of Oncology
McGill University
Montreal, QC, Canada

Nicole Beauchemin
Goodman Cancer Research Centre
McGill University
Montreal, QC, Canada

ISSN 1064-3745 ISSN 1940-6029 (electronic)
Methods in Molecular Biology
ISBN 978-1-4939-3799-8 ISBN 978-1-4939-3801-8 (eBook)
DOI 10.1007/978-1-4939-3801-8

Library of Congress Control Number: 2016945043

Printed on acid-free paper

This Humana Press imprint is published by Springer Nature
The registered company is Springer Science+Business Media LLC New York

Preface

The tumor microenvironment includes the cellular and noncellular constituents that surround and support tumor cells. This includes fibroblasts, blood vessels, innate and adaptive immune cells along with secreted signaling molecules, extracellular vesicles, and components of the extracellular matrix. Indeed, extensive research has firmly established an instrumental role for the tumor microenvironment in supporting cancer initiation, dormancy, progression, and metastatic spread.

This book covers core and emerging in vitro and in vivo protocols that are used to study how various components of the tumor microenvironment are established and subsequently interact with tumor cells to facilitate carcinogenesis. In addition, the book displays research topics including cellular and molecular biology approaches, in vivo genetic approaches, various "omics"-based strategies, therapeutic strategies to target the microenvironment, and, finally, advanced techniques in the fields of tissue engineering and nanotechnology. Written and validated in the laboratories of a number of trusted collaborating authors, these protocols should facilitate further studies in this exciting field.

Thus, this protocol book constitutes a compendium of techniques now available to a broad audience including basic and clinician scientists, systems biologists, and biological engineers.

Montreal, QC, Canada

Josie Ursini-Siegel
Nicole Beauchemin

Contents

Contributors

Arya Afsahi • *Department of Pathology and Molecular Medicine, McMaster Immunology Research Centre, McMaster University, Hamilton, ON, Canada*

Ryuhjin Ahn • *Lady Davis Institute for Medical Research, McGill University, Montréal, QC, Canada*

Bertrand Allard • *Centre de Recherche du Centre Hospitalier de l'Université de Montréal (CRCHUM), Institut du Cancer de Montréal, Montréal, QC, Canada; Faculté de Pharmacie, Université de Montréal, Montréal, QC, Canada*

David Allard • *Centre de Recherche du Centre Hospitalier de l'Université de Montréal (CRCHUM), Institut du Cancer de Montréal, Montréal, QC, Canada; Faculté de Pharmacie, Université de Montréal, Montréal, QC, Canada*

Khalid Al-Nedawi • *Division of Nephrology, Department of Medicine, McMaster University, Hamilton, ON, Canada; Hamilton Centre for Kidney Research (HCKR), St. Joseph's Hospital, Hamilton, ON, Canada*

Lisa M. Arendt • *Department of Comparative Biosciences, School of Veterinary Medicine, University of Wisconsin-Madison, Madison, WI, USA*

Daina Avizonis • *Metabolomics Core Facility, Goodman Cancer Research Centre, McGill University, Montréal, QC, Canada*

Liane Babes • *Department of Physiology and Pharmacology, University of Calgary, Calgary, AB, Canada*

James W. Baish • *Edwin L. Steele Laboratories, Department of Radiation Oncology, Massachusetts General Hospital, Harvard Medical School, Boston, MA, USA; Department of Mechanical and Biomedical Engineering, Bucknell University, Lewisburg, PA, USA*

David J. Beebe • *Division of Cellular and Gene Therapies, Office of Cellular, Tissue, and Gene Therapies, Center for Biologics Evaluation and Research, The US Food and Drug Administration, Silver Spring, MD, USA*

Alice Beigbeder • *Division of Oncology, Centre de Recherche du CHU de Québec, Québec, QC, Canada; Cancer Research Centre, Université Laval, Québec, QC, Canada*

Nicholas R. Bertos • *Rosalind and Morris Goodman Cancer Research Centre, McGill University, Montréal, QC, Canada*

Nicolas Bisson • *Division of Oncology, Centre de Recherche du CHU de Québec, Québec, QC, Canada; Cancer Research Centre, Université Laval, Québec, QC, Canada; Quebec Network for Research on Protein Function, Engineering, and Applications (PROTEO), Université Laval, Québec, QC, Canada; Department of Molecular Biology, Medical Biochemistry and Pathology, Université Laval, Québec, QC, Canada*

Alicia M. Bolt • *Lady Davis Institute for Medical Research, McGill University, Montréal, QC, Canada*

David Bond • *Department of Oncology, University of Alberta, Edmonton, AB, Canada*

Mathieu Bourgey • *McGill University and Genome Quebec Innovation Centre, Montréal, QC, Canada*

Guillaume Bourque • *Department of Human Genetics, McGill University, Montréal, QC, Canada; McGill University and Genome Quebec Innovation Centre, Montréal, QC, Canada*
Jonathan L. Bramson • *Department of Pathology and Molecular Medicine, McMaster Immunology Research Centre, McMaster University, Hamilton, ON, Canada*
Robert D. Cardiff • *Center of Comparative Medicine, University of California, Davis, CA, USA*
Chirayu Chokshi • *McMaster Stem Cell and Cancer Research Institute, McMaster University, Hamilton, ON, Canada*
Esterina D'Asti • *Montréal Children's Hospital, The Research Institute of the McGill University Health Centre, Montréal, QC, Canada*
Manvir Dhillon • *McMaster Stem Cell and Cancer Research Institute, McMaster University, Hamilton, ON, Canada*
Dai Fukumura • *Edwin L. Steele Laboratories, Department of Radiation Oncology, Massachusetts General Hospital, Harvard Medical School, Boston, MA, USA*
Zvi Granot • *Department of Developmental Biology and Cancer Research, Institute for Medical Research Israel Canada, Hebrew University Medical School, Jerusalem, Israel*
Simon-Pierre Gravel • *Department of Biochemistry, McGill University, Montréal, QC, Canada; Goodman Cancer Research Centre, McGill University, Montréal, QC, Canada*
Joanne A. Hammill • *Department of Pathology and Molecular Medicine, McMaster Immunology Research Centre, McMaster University, Hamilton, ON, Canada*
Pardeep Heir • *Department of Laboratory Medicine and Pathobiology, University of Toronto, Toronto, ON, Canada*
Christopher W. Helsen • *Department of Pathology and Molecular Medicine, McMaster Immunology Research Centre, McMaster University, Hamilton, ON, Canada*
Caitlyn Hui • *Department of Microbiology and Immunology, Goodman Cancer Research Center, McGill University, Montréal, QC, Canada; Department of Physiology, Goodman Cancer Research Center, McGill University, Montréal, QC, Canada*
D. Andrew James • *Department of Chemistry, York University, Toronto, ON, Canada*
Craig Jenne • *Snyder Institute for Chronic Diseases, Calgary, AB, Canada; Department of Microbiology, Immunology and Infectious Diseases, Faculty of Medicine, University of Calgary, Calgary, AB, Canada*
José A. Jiménez-Torres • *Division of Cellular and Gene Therapies, Office of Cellular, Tissue, and Gene Therapies, Center for Biologics Evaluation and Research, The US Food and Drug Administration, Silver Spring, MD, USA*
Léon C. van Kempen • *Lady Davis Institute for Medical Research, McGill University, Montréal, QC, Canada; Department of Pathology, Jewish General Hospital, McGill University, Montréal, QC, Canada*
Connie M. Krawczyk • *Department of Microbiology and Immunology, Goodman Cancer Research Center, McGill University, Montréal, QC, Canada; Department of Physiology, Goodman Cancer Research Center, McGill University, Montréal, QC, Canada*
Paul Kubes • *Department of Physiology and Pharmacology, University of Calgary, Calgary, AB, Canada*
John D. Lewis • *Department of Oncology, University of Alberta, Edmonton, AB, Canada*
Marie-Noël M'Boutchou • *Lady Davis Institute for Medical Research, McGill University, Montréal, QC, Canada*

Douglas J. Mahoney • *Alberta Children's Hospital Research Institute, Calgary, AB, Canada; Arnie Charbonneau Cancer Institute, Calgary, AB, Canada; Department of Microbiology, Immunology and Infectious Diseases, Faculty of Medicine, University of Calgary, Calgary, AB, Canada*

Koren K. Mann • *Lady Davis Institute for Medical Research, McGill University, Montréal, QC, Canada*

Nicole McFarlane • *McMaster Stem Cell and Cancer Research Institute, McMaster University, Hamilton, ON, Canada*

Brian Meehan • *Montréal Children's Hospital, The Research Institute of the McGill University Health Centre, Montréal, QC, Canada*

Eelco F.J. Meijer • *Edwin L. Steele Laboratories, Department of Radiation Oncology, Massachusetts General Hospital, Harvard Medical School, Boston, MA, USA*

Alexandre Montpetit • *McGill University and Genome Quebec Innovation Centre, Montréal, QC, Canada*

Hidetoshi Mori • *Center of Comparative Medicine, University of California, Davis, CA, USA*

Victor Naumenko • *Alberta Children's Hospital Research Institute, Calgary, AB, Canada; Arnie Charbonneau Cancer Institute, Calgary, AB, Canada; Snyder Institute for Chronic Diseases, Calgary, AB, Canada; Department of Microbiology, Immunology and Infectious Diseases, Faculty of Medicine, University of Calgary, Calgary, AB, Canada*

Michael Ohh • *Department of Laboratory Medicine and Pathobiology, University of Toronto, Toronto, ON, Canada; Department of Biochemistry, University of Toronto, Toronto, ON, Canada*

Timothy P. Padera • *Edwin L. Steele Laboratories, Department of Radiation Oncology, Massachusetts General Hospital, Harvard Medical School, Boston, MA, USA*

Pudchalaluck Panichnantakul • *Department of Human Genetics, McGill University, Montréal, QC, Canada; McGill University and Genome Quebec Innovation Centre, Montréal, QC, Canada*

Morag Park • *Rosalind and Morris Goodman Cancer Research Centre, McGill University, Montréal, QC, Canada; Department of Experimental Medicine, McGill University, Montréal, QC, Canada; Department of Biochemistry, McGill University, Montréal, QC, Canada; Department of Oncology, McGill University, Montréal, QC, Canada; Department of Pathology, McGill University, Montréal, QC, Canada*

Kelly A. Pike • *Goodman Cancer Research Centre, McGill University, Montréal, QC, Canada*

Janusz Rak • *Montréal Children's Hospital, The Research Institute of the McGill University Health Centre, Montréal, QC, Canada*

Jolene Read • *Division of Nephrology, Department of Medicine, McMaster University, Hamilton, ON, Canada; Hamilton Centre for Kidney Research (HCKR), St. Joseph's Hospital, Hamilton, ON, Canada*

Yasser Riazalhosseini • *Department of Human Genetics, McGill University, Montréal, QC, Canada; McGill University and Genome Quebec Innovation Centre, Montréal, QC, Canada*

Jitka Y. Sagiv • *Department of Developmental Biology and Cancer Research, Institute for Medical Research Israel Canada, Hebrew University Medical School, Jerusalem, Israel*

Camilla Salvagno • *Division of Immunology, Netherlands Cancer Institute, Amsterdam, The Netherlands*

Sheila K. Singh • *McMaster Stem Cell and Cancer Research Institute, McMaster University, Hamilton, ON, Canada; Department of Biochemistry and Biomedical Sciences, Faculty of Health Sciences, McMaster University, Hamilton, ON, Canada; Department of Surgery, Faculty of Health Sciences, McMaster University, Hamilton, ON, Canada*

John Stagg • *Centre de Recherche du Centre Hospitalier de l'Université de Montréal (CRCHUM), Institut du Cancer de Montréal, Montréal, QC, Canada; Faculté de Pharmacie, Université de Montréal, Montréal, QC, Canada*

Konstantin Stoletov • *Department of Oncology, University of Alberta, Edmonton, AB, Canada*

Julie St-Pierre • *Department of Biochemistry, McGill University, Montréal, QC, Canada; Goodman Cancer Research Centre, McGill University, Montréal, QC, Canada*

Kyung E. Sung • *Division of Cellular and Gene Therapies, Office of Cellular, Tissue, and Gene Therapies, Center for Biologics Evaluation and Research, The US Food and Drug Administration, Silver Spring, MD, USA*

Lauriane Vélot • *Division of Oncology, Centre de Recherche du CHU de Québec, Québec, QC, Canada; Cancer Research Centre, Université Laval, Québec, QC, Canada*

Chitra Venugopal • *McMaster Stem Cell and Cancer Research Institute, McMaster University, Hamilton, ON, Canada*

Karin E. de Visser • *Division of Immunology, Netherlands Cancer Institute, Amsterdam, The Netherlands*

Sandra Voels • *Department of Developmental Biology and Cancer Research, Institute for Medical Research Israel Canada, Hebrew University Medical School, Jerusalem, Israel*

Lian Willetts • *Department of Oncology, University of Alberta, Edmonton, AB, Canada*

Yojiro Yamanaka • *GCRC Transgenic Facility, Department of Human Genetics, Goodman Cancer Research Centre, McGill University, Montréal, QC, Canada*

Yoon Kow Young • *Lady Davis Institute for Medical Research, McGill University, Montréal, QC, Canada*

Chapter 1

Methods of Immunohistochemistry and Immunofluorescence: Converting Invisible to Visible

Hidetoshi Mori and Robert D. Cardiff

Abstract

Observing changes in pathophysiological tissue samples often relies on immunohistochemical or immunofluorescence analysis. These techniques show target microanatomy by visualizing marker molecules on cells and their microenvironment. Here, we describe the "pros and cons" in each method, along with alternative procedures and the suggested imaging equipment.

Key words Autofluorescence, Immunofluorescence, Immunohistochemistry, Formalin-fixed paraffin-embedded tissues, Zinc fixation

1 Introduction

Imaging analyses have been extensively performed to identify cellular and microenvironmental changes in tissue sections from biopsies obtained from human patients, or in animal tissues from the laboratory by processing tissues using immunohistochemistry (IHC) or immunofluorescence (IF) methods. Selection of the appropriate method requires consideration of type of specimen under study, the degree of sensitivity, and the cost. Whereas the reaction of a primary antibody to a specific molecular target and using a secondary antibody to visualize the distribution of the target molecule is identical in IF and IHC, the methods for detecting target output signals are different and require different equipment. Target molecule(s) on IHC can be visualized with visible light through chromogenic dyes with enzymatic reactions (e.g., DAB and HRP, X-Gal and β-gal, and Fast Red and AP) which is observed through a bright-field microscope [1]. On the other hand, IF staining uses fluorescence probes conjugated either on the primary or on the secondary antibody against the target. The signal is observed through a conventional epifluorescence microscope or further enhanced with advanced confocal microscopy. IHC is suitable for analyzing the distribution of

Josie Ursini-Siegel and Nicole Beauchemin (eds.), *The Tumor Microenvironment: Methods and Protocols*, Methods in Molecular Biology, vol. 1458, DOI 10.1007/978-1-4939-3801-8_1,

marker-positive cells in a larger area in tissue samples, while analysis with IF is more suitable for subcellular localization of target molecules. The concurrent detection limits of target molecule(s) also differ between IHC and IF. IHC is typically able to detect only two molecules with counterstaining. In contrast, IF can currently visualize 3–5 or more target molecules. However, recent studies have shown that IF can be multiplied by re-probing and re-staining cycle [2–4], which allows visualization of many more target molecules in tissue section. The advantage of IHC is a permanent signal that can be observed with conventional optics and, consequently, a standard uncomplicated microscope can be used. However, the difference in enzymatic reaction time for chromogenic deposition often produces false-positive or -negative results, which requires strict controls for the enzymatic reaction procedures. Although IF can theoretically visualize more targets at once, it has some technical limitations: First, the selection of the multiple combinations of primary and secondary antibodies requires careful selection to avoid overlapping signals. Second, multi-colored-IF may require a sophisticated confocal microscope to detect each specific emission signal. Third, the fluorescence signals can be "bleached" either by excess exposure to the high-energy light source or by long-term storage. Fourth, tissues often express autofluorescence which interferes with positive signals from IF probes. Although both IHC and IF techniques have "pros and cons," they have their respective strengths. The investigator can utilize the respective attributes that are most suitable for the analytical needs of the project.

2 Materials

2.1 Reagents for IHC and IF

1. Formalin solution: Neutral buffered, adjusted to 10% (v/w) formalin (NBF).
2. Zinc fixation buffer (ZnF): 0.5% (w/v) zinc acetate, 0.5% (w/v) zinc chloride in 0.1 M Tris-based buffer with 0.05% (w/v) calcium acetate at pH 7.4 [5, 6].
3. Ethanol: 100%, 95%, and 70% (v/v) are prepared by diluting in distilled water.
4. Xylene.
5. Paraffin.
6. Quenching buffer: 3% (w/w) Hydrogen peroxide (20 mL 30% (w/w) hydrogen peroxide mixed with 180 mL methanol).
7. Sodium citrate stock solution: 100 mM Sodium citrate in distilled water.
8. Citrate acid stock solution: 100 mM Citric acid in distilled water.

9. Citrate buffer working solution (for 1 L): 82 mL Sodium citrate stock solution, 18 mL citrate acid stock solution, 900 mL distilled water, adjust pH to 6 with 1 N HCl.
10. 25× Phosphate-buffered saline (PBS) for 1 L: 188 g Dipotassium hydrogen phosphate, 33 g sodium phosphate monobasic, 180 g sodium chloride, fill to 1 L, adjust pH to 7.2–7.4 with 1 N HCl, and filtrate with 0.22 μm filter.
11. 1× PBS for 1 L: 40 mL of 25× PBS, 960 mL distilled water.
12. Acetone.
13. Methanol/acetone (50%/50%).
14. 4% (w/v) Paraformaldehyde (PFA) in PBS: 16% or 32% PFA is diluted in PBS (*see* **Note 1**).
15. Permeabilization buffer: 0.25% (v/v) Triton X-100 in PBS.
16. Cupric sulfate buffer: 10 mM Cupric sulfate and 50 mM ammonium acetate in distilled water.
17. Sudan Black buffer: 1% (w/v) Sudan Black in 70% (v/v) methanol diluted with distilled water.
18. Blocking buffer for IHC: 10% (v/v) Normal (goat or horse) serum in PBS.
19. Blocking buffer for IF: 5% (v/v) Goat serum in PBS.
20. Antibody dilution buffer: 0.5% (w/v) Albumin (ovalbumin or bovine serum albumin) in PBS.
21. 0.1% (w/v) 3,3′-Diaminobenzidine (DAB) solution.
22. 4′,6-Diamidino-2′-phenylindole, dihydrochloride (DAPI) solution (1 mg/mL).

2.2 Other Materials

1. Tissue cassettes.
2. Paraffin-embedding station.
3. Cryomold.
4. Optical cutting temperature compound (OCT: Tissue-Tek OCT compound).
5. Rotary Microtome.
6. SuperFrost/Plus glass slides.
7. Glass Coplin jars.
8. Digital decloaking chamber.
9. Cryostat.
10. Immunostain Moisture Chamber.
11. ABC kit (avidin/biotin-based peroxidase system).
12. Mayer's hematoxylin.
13. Mounting solutions (permanent aqueous mounting solution for IHC; liquid anti-fade mounting solution for IF).

3 Methods

3.1 Tissue Preparation

Fixation is a critical procedure in preserving tissue architecture prior to tissue processing and sectioning. Neutral-buffered formalin (NBF) is generally used in histology analysis. However, the cross-linking reaction of the fixation can "mask" the epitope required for antigen recognition. Various techniques for "unmasking" have been developed and are widely used [7]. In certain cases, other fixative reagents like zinc fixative or paraformaldehyde can be used [5, 8]. For example, the detection of T-cell markers (CD4 and CD8) is difficult to detect on NBF-treated tissue sections of mouse origin, but can be detected on zinc fixative-treated samples [5, 6]. Frozen sections offer another technique for avoiding antigen loss with fixation and paraffin embedding. However, frozen tissue is usually fixed after sectioning.

3.1.1 Tissue Preparation for Paraffin Section

1. Tissues are typically cut into 2–3 mm slices and loaded into embedding cassettes. The tissues are submerged and fixed in a solution of NBF (e.g., volume of NBF is more than 20 times cubic volume of tissue slices) for at least 48 h at room temperature. When using zinc fixatives, the same-size tissues (2–3 mm) are fixed in a zinc fixation buffer for 24 h at room temperature.
2. Fixed tissue can be stored in 70% ethanol for a few days, if needed.

3.1.2 Tissue Preparation for Frozen Section

1. Tissues are dissected in thin slices (<5 mm thickness) and placed on OCT in a Cryomold (*see* **Note 2**).
2. Mount entire tissue with OCT compound.
3. Gently place the OCT-embedded Cryomold into liquid nitrogen to freeze the entire tissue in an OCT block (*see* **Note 3**).
4. Keep frozen OCT block in a –80 °C freezer until use.

3.2 Preparation of Tissue Sections from Tissue Blocks

3.2.1 Preparation of Tissue Sections from Paraffin-Infiltrated Tissue Blocks (Dehydration to Antigen Retrieval)

1. Tissues in cassettes are rinsed with tap water for 45 min, and afterwards tissues are dehydrated in a series of steps using 70%, 95%, 100% ethanol and xylene for 45 min each, respectively (*see* **Note 4**).
2. Dehydrated tissues are infiltrated in paraffin at 58 °C for 45 min with Sakura Tissue-Tek IV Embedding center and mounted in embedding cassettes with appropriate-sized paraffin molds forming paraffin-embedded blocks (*see* **Note 5**).
3. Tissue sections are cut from the blocks at 3–5 μm thickness using a Microtome and floated on the water bath at 43 °C.
4. Floated tissue sections are attached on SuperFrost Plus glass slides and dried at room temperature overnight (*see* **Note 6**).

5. Tissue sections have residual paraffin at this stage and need to be hydrated for IHC or IF reactions. To deplete paraffin from sections, samples are soaked in xylene for 2 min using a Coplin jar and replaced into fresh xylene twice more for 2 min (*see* **Notes 7** and **8**).
6. After xylene treatment, tissue slides are rinsed in a series of steps: 100% (twice), 95%, and 70% ethanol for 2 min each to deplete xylene.
7. (Only for IHC) To reduce endogenous peroxidase activity, tissue slides are soaked in quenching buffer for 18 min. Slides are rinsed with tap water for 5 min after the quenching procedure (*see* **Note 9**).
8. To deplete alcohol, tissue slides are soaked in gently running tap water within a Coplin jar for at least 2 min.
9. To enhance accessibility of antibody to antigen, antigen retrieval is routinely performed. In brief, this procedure is performed by placing slides in the citrate buffer in a slide container. This container will be placed in a metal container filled with distilled water in the decloaker before proceeding to the next procedure.
10. The decloaker is heated until the temperature reaches 122 °C, and then it is naturally air cooled to 89 °C followed by opening the lid for further cooling. A steam cooker or steamer is also useful for this procedure; however, it will need optimization because of lower ambient air pressure (*see* **Notes 10** and **11**).

3.2.2 Preparation of Tissue Sections from Frozen OCT Tissue Blocks

1. Set the frozen OCT block inside the cryostat and keep the system at −20 to −30 °C for 10–20 min.
2. Section the OCT block until tissues are facing the surface.
3. Section the tissue-producing sections of 5 μm within the cryostat.
4. Transfer the tissue section onto SuperFrost Plus glass slides. Sections should be kept at −80 °C until use.
5. Tissue sections are dried overnight (O/N) before proceeding to immunostaining.
6. Fix OCT sections with appropriate fixative. Fixatives are decided based on the specificity of the antibody. Usually any of the following methods can be used: ice-cold acetone (−20 °C) for 10 min, ice-cold methanol/acetone (50:50, −20 °C) for 10 min, PFA 4% in PBS for 15 min followed by treating samples with permeabilization buffer for 15 min at room temperature.
7. (For IHC) Proceed to Subheading 3.2.1, **steps 7** and **8**, followed by Subheading 3.4.
8. (For IF) Proceed to Subheading 3.3 if autofluorescence signal is high, or proceed to Subheading 3.4.

3.3 Reducing Autofluorescence from Tissue (Only for IF)

Tissue autofluorescence can interfere with acquiring positive fluorescence signal from IF. Three techniques (photobleaching, cupric sulfate, and Sudan Black) are commonly used to reduce autofluorescence [9]. Alternatively, specialized microscopy and software are available that can be used to digitally subtract autofluorescent signals [10].

1. (a) Photobleaching can be performed by exposing antigen retrieval-treated tissue sections in PBS to sunlight for a day.
   (b) Cupric sulfate treatment can be performed by soaking tissue slides in cupric sulfate buffer for at least 90 min.
   (c) Sudan Black treatment is usually performed after the procedure of IF by soaking slides in Sudan Black buffer for 5 min.
2. Treated slides are rinsed three times with PBS before proceeding to the next procedure.

Figure 1 shows human breast cancer tissues treated with these autofluorescence-reducing procedures and visualized with confocal microscopy to scan variations in autofluorescence. All treatments reduced the levels of autofluorescent signals, with cupric sulfate and photobleaching treatments showing better reduction of autofluorescence (*see* **Note 12**).

3.4 Reducing Nonspecific Antibody Binding in IF and IHC

Reducing nonspecific binding of the antibody in both IHC and IF is a critical procedure. Usually this step uses serum or albumin from animals. However, choosing the appropriate animal species for masking the nonspecific reaction must be carefully done. Since our routine work usually employs mouse- or rabbit-IgG as primary antibody and goat anti-mouse or -rabbit IgG, we use either chicken albumin or serum from goat or horse.

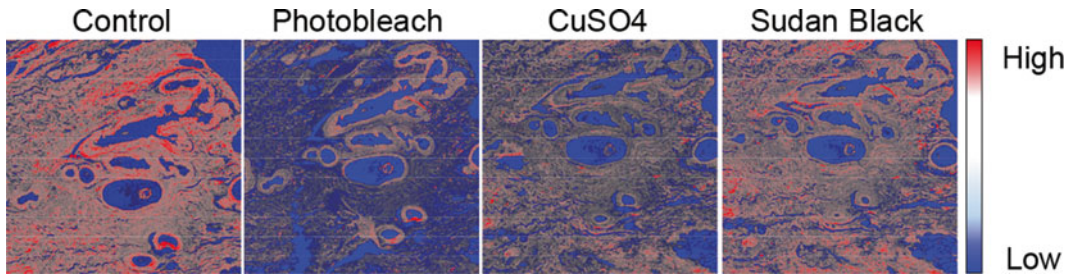

Fig. 1 Reagents to reduce autofluorescence in tissue samples. Images illustrate autofluorescence signals in human breast cancer tissue sections treated or not with Photobleach, $CuSO_4$, and Sudan Black. Images were captured with confocal microscope LSM710 with lambda mode to scan autofluorescence. Images highlight emission at 480 nm and indicated as *blue-red* intensity indicator. The higher level autofluorescent signal is indicated as *red*

1. Tissue slides from the former procedure are rinsed twice in PBS before proceeding to this blocking procedure.
2. (a)For IHC, tissue slides are blocked in 10% (v/v) normal (goat or horse) serum in PBS for at least 20 min.

   (b) For IF, tissue slides are blocked in 5% (v/v) normal goat serum in PBS for O/N at 4 °C (*see* **Note 13**).

3.5 From Antibody Reactions to Visualizing Target Molecule

Both IHC and IF require a specific primary antibody against the target molecule of interest and secondary anti-antibody to visualize the distribution of primary antibody. Although there are several methods to visualize chromogenic dyes for IHC [1] and different fluorophores for IF (e.g., Alexa Fluorophore, Quantum Dot, tyramide), here we discuss a typical IHC process with a catalytic activity of HRP on DAB substrate and IF with fluorophore-conjugated secondary antibody. As a sample case of IHC, we stained for T-lymphocyte markers (CD3, CD4, and CD8) on mouse tissue (Fig. 2). Estrogen receptor and cytokeratin were detected on human breast tissues by IF (Fig. 3).

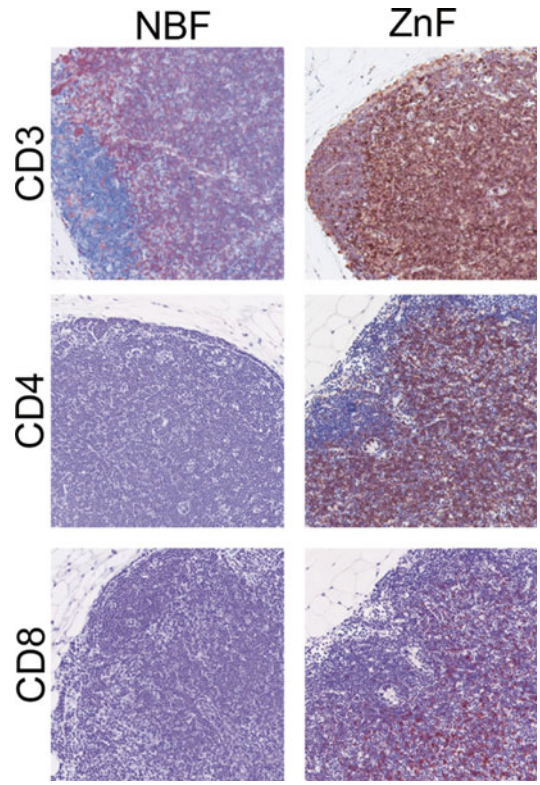

Fig. 2 Comparison of NBF and ZnF fixative on IHC to detect immune cell markers. Images compare NBF- or ZnF-fixed mouse mammary fat pad lymph nodes stained with T-lymphocytic markers (CD3, CD4, and CD8). Whereas CD3 was detected both on NBF- and ZnF fixative-treated tissues, CD4 and CD8 are only detected in ZnF-treated lymph nodes

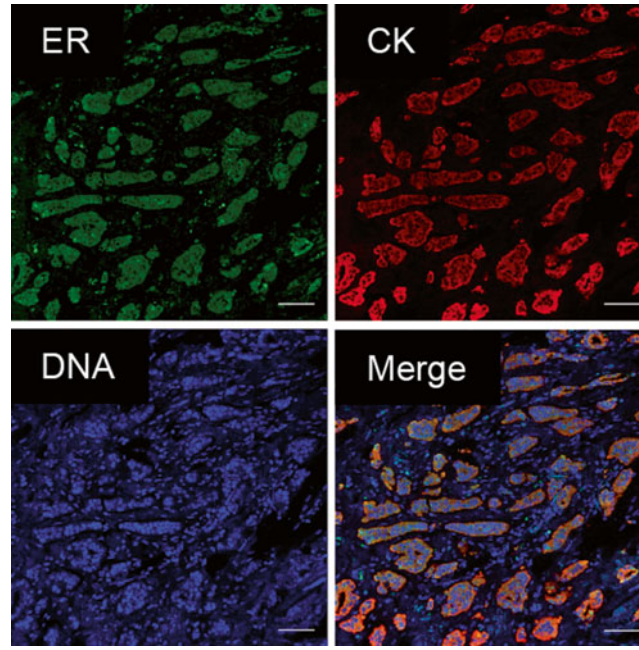

Fig. 3 Detecting estrogen receptor (ER) and cytokeratin (CK) in human breast cancer tissue with IF. Illustration demonstrates IF-stained, ER-positive human breast cancer tissue section. ER was detected with a rabbit monoclonal anti-human ER alpha antibody (clone D8H8; Cell Signaling Technology) visualized with Alexa 488 (*green*) anti-rabbit IgG (Life Technologies). CK was detected with anti-pan keratin mouse monoclonal antibody (clone AE1/AE3 + 5D3; Abcam) and visualized with Alexa 568 (*red*)-conjugated anti-mouse IgG (Life Technologies). DAPI was used to visualize DNA in nuclei (*blue*). Images were captured with a confocal microscopy LSM710 (Zeiss). Scale bar indicates 80 μm

3.5.1 IHC Reactions

1. Blocked tissue slides are incubated with primary antibody diluted in PBS with antibody dilution buffer at room temperature for O/N or the time indicated for each antibody. The volume of primary antibody solution should be enough to cover the tissue on the slide. Usually 500–1000 μL is enough for covering the entire glass slide (*see* **Note 14**).
2. After incubating with the primary antibody, the tissue slides are washed twice with PBS for 5 min.
3. Incubate slides in biotinylated secondary antibody diluted in PBS with 5 % goat serum (same as blocking buffer for IF) for 60 min.
4. Slides are washed twice with PBS for 5 min.
5. Incubate slides in freshly prepared ABC reagent (mixture of avidin DH and biotinylated horseradish peroxidase H: following the manufacturer's protocol) for 30 min.
6. Slides are washed twice with PBS.

7. Incubate slides with 0.1% DAB until desired stain intensity is observed, but usually the incubation time is less than 5 min to prevent a nonspecific reaction (*see* **Note 15**).
8. Slides are rinsed in tap water for 2 min.
9. Rinse slides with deionized water.
10. For counterstaining, slides are incubated in Mayer's hematoxylin. If the antigen is a nuclear protein, the incubation time is 10–20 s. If the antigen is within the cytoplasm or on the membrane, a 30-s incubation will be applied.
11. Rinse slides with tap water at least for 5 min.
12. Dehydrate slides in 70%, 95%, and 100% ethanol for 2 min each.
13. Immerse slides in xylene for 5 min in a glass Coplin jar and change xylene repeating three times.
14. Keep slides in xylene until ready to mount with a cover glass.
15. Mount slides with clear mount and cover glass and dry O/N at room temperature on a flat surface (*see* **Note 16**).

3.5.2 IF Reactions

1. Blocked tissue slides are incubated with primary antibody diluted in PBS with 5% goat serum at 4 °C for O/N using the same procedure as mentioned above (in Subheading 3.5.1, **step 1**). To minimize the usage of antibody and to prevent water evaporation, slides are incubated in a moisture chamber. The volume of primary antibody solution should be enough (500–1000 μL) to uniformly cover the entire glass slide.
2. Tissue slides are washed twice with PBS for 5 min.
3. Incubate tissues on slide with fluorophore-conjugated secondary antibody diluted in PBS with 5% goat serum for 60 min. DAPI is also added at concentration of 1 μg/mL to visualize nucleic acid in each cell. Combinations of fluorophores must be considered before starting the experiment (*see* **Note 17**).
4. Tissue slides are washed twice with PBS for 5 min.
5. Mount slides with approximately 200–300 μL of mounting solution by carefully covering with a cover glass preventing the formation of air bubbles (*see* **Note 18**).
6. Mounted slides are dried at room temperature and kept in the dark to prevent bleaching fluorescent signal.

4 Notes

1. PFA powder is harmful when inhaled or by skin contact. Therefore, we recommend using, pre-dissolved PFA as it is safer to handle. If PFA powder needs to be used, PFA is added to distilled water with mild heating (50–60 °C) and then 1 M

NaOH is added dropwise. Once PFA is dissolved, the reagent is cooled down, the concentration adjusted, and the pH corrected to around 7.2, after being mixed with 10× PBS to produce a 1× PBS solution. The reagent will be kept in the dark at 4 °C for less than a week. Using freshly prepared buffer is desirable.

2. Each Cryomold should be labeled with a chemical-resistant marker. Orientation/geometry of the tissue sample in each OCT block should be recorded in a notebook.
3. The bottom of Cryomold needs to be soaked in liquid nitrogen. However, dropping or floating the Cryomold in liquid nitrogen should be avoided.
4. Xylene might damage plasticwares and remove permanent marker notes written on slides. To prevent damage on container and slides, use glass Coplin jar containers and pencil or xylene-resistant markers. When using NBF as a fixative, use fresh reagents to prevent NBF activity on ZnF-treated tissues.
5. Each laboratory might have its own system for preparing paraffin blocks. These **steps 1** and **2** of Subheading 3.2.1 could be variable in each laboratory.
6. Normal glass slides should not be used, since tissue cannot attach well on non-coated glass.
7. According to Occupational Safety and Health Administration (OSHA: www.osha.gov), xylene is flammable and a toxic carcinogen. For these reasons, it should be handled in a chemical fume hood, and users need to prevent inhalation and exposure to skin by wearing appropriate personal protective equipment (PPE). Used xylene must be kept in a suitable waste combustion chamber.
8. Replacement of xylene is also reported (10).
9. Hydrogen peroxide is a strong oxidizer, which can affect skin or damage eyes when in contact. Handling requires appropriate PPE.
10. Operators of the decloaker or steam cooker need to be cautious of heat and steam. Users should wait until the pressure goes down, particularly for the decloaker.
11. When using a steam cooker, slides are set in a slide holder soaked in citrate buffer in either plastic or metal staining dishes in the steam chamber. The steam cooker is kept at 100 °C for 15 min and cooled down to 50–60 °C by turning off the system.
12. Photobleaching works well on stromal tissue, but not on epithelia in breast cancer tissue, and cupric sulfate reduces autofluorescence signals over entire tissues.
13. To prevent drying the blocking buffer, slides should be kept either in a large amount of blocking buffer in a Coplin jar or

in a moisture chamber with a small amount of blocking buffer on each sample.

14. To minimize the usage of antibody and to prevent water evaporation, slides can be set in an Immunostain Moisture Chamber containing a small amount of distilled water in the bottom of the chamber to retain moisture.
15. The DAB reaction can carefully be monitored by checking the color change on the tissue section. To observe the difference in reaction, include a negative control (such as unstained tissue section or tissue from a gene knockout mice).
16. Bubbles forming between the glass slide and glass cover should be avoided by gently putting the glass cover over approximately 300 μL of the mounting solution to cover the tissue section. Pipetting the mounting solution on the tissue also needs to be done carefully to avoid forming bubbles.
17. There are many good materials available on the market. However, it is better to use fluorophores with a specific excitation and a narrow spectrum in emission, which allows us to observe multiple targets at once as specific signals. To reduce the nonspecific binding of the secondary antibody or to use primary antibodies from the same species, conjugating the fluorophore on primary antibody is often used. Figure 3 shows the human breast tissue stained with an estrogen receptor (Red) and a cytokeratin (green) antibody and DAPI (blue). In this case, Alexa 488 (green) anti-mouse IgG and Alexa 568 (red) anti-rabbit IgG are used as secondary antibodies to visualize each molecule.
18. Usually, a cover slip with 170 μm thickness (#1.5 thickness) is used to acquire the best resolution with most of objective lenses. However, this optimized thickness represents the combined thickness of the glass and the mounting solution (http://www.microscopyu.com/articles/formulas/formulascoverslipcorrection.html). For this reason, using thinner cover slip with 130–160 μm thickness (#1 thickness) might give the best imaging resolution.

Acknowledgements

This work was supported by NCI grants (R33 CA183654, R21 CA183660) and Department of Defense Grant BC132309. We thank the Borowsky laboratory in Center for Comparative Medicine, University of California, Davis, for supporting experiments.

References

1. van der Loos CM (2010) Chromogens in multiple immunohistochemical staining used for visual assessment and spectral imaging: the colorful future. J Histotechnol 33(1):31–40
2. Ranjan AK, Joglekar MV, Atre AN, Patole M, Bhonde RR, Hardikar AA (2012) Cellular detection of multiple antigens at single cell resolution using antibodies generated from the same species. J Immunol Methods 379(1–2):42–47
3. Stack EC, Wang C, Roman KA, Hoyt CC (2014) Multiplexed immunohistochemistry, imaging, and quantitation: a review, with an assessment of Tyramide signal amplification, multispectral imaging and multiplex analysis. Methods 70(1):46–58
4. van de Werken C, Jahr H, Avo Santos M, Eleveld C, Schuilwerve J, Laven JS, Baart EB (2013) A universal method for sequential immunofluorescent analysis of chromatin and chromatin-associated proteins on chromosome spreads. Chromosome Res 21(5):475–489
5. Beckstead JH (1994) A simple technique for preservation of fixation-sensitive antigens in paraffin-embedded tissues. J Histochem Cytochem 42(8):1127–1134
6. Mori H, Soonsawad P, Schuetter L, Chen Q, Hubbard NE, Cardiff RD, Borowsky AD (2015) Introduction of zinc-salt fixation for effective detection of immune cell-related markers by immunohistochemistry. Toxicol Pathol 43(6):883–889
7. Shi SR, Shi Y, Taylor CR (2011) Antigen retrieval immunohistochemistry: review and future prospects in research and diagnosis over two decades. J Histochem Cytochem 59(1):13–32
8. Cardiff RD, Hubbard NE, Engelberg JA, Munn RJ, Miller CH, Walls JE, Chen JQ, Velásquez-García HA, Galvez JJ, Bell KJ, Beckett LA, Li YJ, Borowsky AD (2013) Quantitation of fixative-induced morphologic and antigenic variation in mouse and human breast cancers. Lab Invest 93(4):480–497
9. Schnell SA, Staines WA, Wessendorf MW (1999) Reduction of lipofuscin-like autofluorescence in fluorescently labeled tissue. J Histochem Cytochem 47(6):719–730
10. Buesa RJ, Peshkov MV (2009) Histology without xylene. Ann Diagn Pathol 13(4): 246–256

Chapter 2

Laser Capture Microdissection as a Tool to Study Tumor Stroma

Nicholas R. Bertos and Morag Park

Abstract

Laser capture microdissection (or LCM) allows for isolation of cells from specific tissue compartments, which can then be followed by DNA, RNA, and/or protein isolation and downstream characterization. Unlike other methods for cell isolation, LCM can be directed towards cells situated in specific anatomical contexts, and is therefore of significant value when investigating the tumor microenvironment, where localization is often key to function. Here, we present a summary of ways in which LCM can be utilized, as well as protocols for the isolation of tumor and tumor-associated stromal elements from frozen breast cancer samples, with a focus on preparation of samples for RNA characterization.

Key words Laser capture microdissection, RNA profiling, Quality control, Arcturus PixCell IIe, Cell isolation

1 Introduction

Investigations of tumor stroma, specifically in the field of breast cancer, have been greatly aided by the use of laser capture microdissection (LCM). This technology has been utilized to investigate genomic [1–3], transcriptional [4–14], and protein-level [15, 16] alterations in the human breast cancer microenvironment. Work in our group has principally been carried out using breast tumors from patients and murine models, with a downstream goal of generating mRNA expression profiles and analyzing these to identify stromal influences on breast cancer development, progression, and outcome [11–14]. Importantly, the datasets generated by such experiments constitute key resources for further analyses and validation of findings from other approaches—the datasets generated from some of our studies [12, 14], for example, have been utilized to support multiple additional investigations [17–30].

Laser capture microdissection was first effectively developed in the mid-1990s as a means to rapidly isolate distinct subpopulations of cells from heterogeneous tissues under direct microscopic

Josie Ursini-Siegel and Nicole Beauchemin (eds.), *The Tumor Microenvironment: Methods and Protocols*, Methods in Molecular Biology, vol. 1458, DOI 10.1007/978-1-4939-3801-8_2,

visualization [31, 32]. The underlying principle of the initial infrared (IR) laser-based systems was the placing of a thin thermolabile transparent film over a tissue section placed on a microscope slide. Following visualization of the areas of interest, a short focused laser pulse selectively adheres the film to a small area of tissue; when the film is removed, these tissue regions remain attached and can then be isolated and subjected to downstream assays (Fig. 1). Note that the forces counteracting tissue lifting include both interactions with the slide surface and with neighboring cells; thus, for tissues with very strong intercellular adhesion, other approaches may be needed. These include the use of membrane slides where the area of interest can be cut out using a UV laser which cuts through both the sample and the membrane itself, obviating the

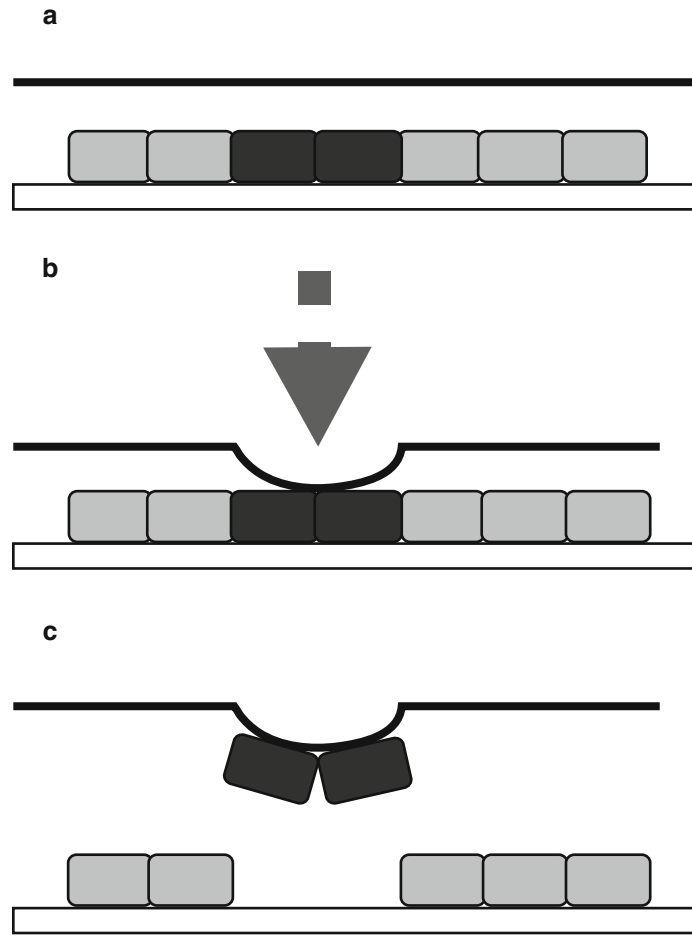

Fig. 1 Schematic image of IR-mediated LCM. (**a**) Thermolabile film (*black line*) is placed above tissue on slide (*bottom*). (**b**) Laser (*dashed line*/*arrowhead*) melts film and causes it to contact cells of interest (*dark grey*), avoiding undesired cells (*light grey*). (**c**) Film bearing cells of interest is lifted, separating these from the remaining cells

need for tissue detachment by lifting from either the slide or the neighboring tissue. A somewhat different technology is used in the laser catapult system (e.g., Zeiss PALM MicroBeam), where a UV laser is used to both cut around the region of interest, and to subsequently "catapult" the excised tissue into a collection cap.

Among existing means for isolating specific cell subpopulations from heterogeneous samples, LCM stands out due to the ability to select cells based on their anatomical context. Fluorescence-activated cell sorting and antibody-bead conjugate-based systems are agnostic with respect to cell localization within a tissue context, while manual microdissection is limited to relatively large areas of interest. Identification of cells for targeted isolation by LCM can be conducted either by standard staining and visual identification or by immunohistochemistry- or immunofluorescence-guided selection.

Since its initial development, various permutations of LCM have been developed, including the use of an ultraviolet (UV) cutting laser either alone or in conjunction with the IR laser. UV lasers are used to ablate unwanted tissue, cut around regions of thick or adherent tissues so that these can be detached using IR laser-mediated adhesion (or isolated separately in the case of sections mounted on membrane slides), and/or to catapult isolated regions into a retrieval container. Semiautomated methods for identification of regions to be isolated are also under development [33].

Candidate materials for LCM include frozen tissue as well as formalin-fixed paraffin-embedded (FFPE) samples—note that staining protocols must be modified for FFPE samples, due to the requirement for deparaffinization. Cytology smears and live cells have also been targeted for this approach. Depending on cell and tissue type and isolation desired, yields can vary widely; pilot experiments should be conducted to determine how much LCM is required to obtain desired target quantities when working with a new experimental system.

Especially for RNA isolation and downstream assays, the importance of maintaining a clean working environment cannot be overstated. The use of dedicated space and equipment, including cryostats for sample preparation, reduces the chances of sample degradation (e.g., by RNase used on adjacent benches) and cross-contamination. In addition, LCM efficacy can be influenced by environmental conditions. Humidity levels above 50% lead to increased adhesion between the tissue section and the slide, which can make it impossible to isolate the selected regions. If room humidity is too high, then the use of a portable dehumidifier may be necessary,

In our experience, the time elapsed between tissue isolation from the organism and initial freezing is key to sample quality and assay success. For human clinical breast tumor samples, we have found that times in excess of 30 min are generally associated with failure to isolate RNA of acceptable quality following LCM;

however, the precise timing is likely to vary between tissues and LCM protocols used, and should be determined experimentally for each experimental condition.

Our standard operating procedure is to immediately place tissue samples obtained in a cryovial (Nalgene) containing ca. 1 mL of Tissue-Tek O.C.T. Compound ("O.C.T.," Sakura Finetek, USA), cover them with additional O.C.T., and then rapidly freeze the vial in liquid nitrogen. Although samples can be frozen directly and later mounted in O.C.T. prior to sectioning, this entails additional manipulation and risks loss of sample morphology. Other approaches that better preserve tissue morphology involve fixation in 4% paraformaldehyde or in ethanol on ice prior to equilibration in O.C.T. and less rapid freezing. However, some RNA degradation may occur with the latter approaches—comparative pilot studies for the tissue and target of interest should be conducted prior to beginning work to achieve the optimal balance of morphology vs. sample preservation required. Samples can then be stored at –80 °C or in liquid nitrogen until use; in our experience, storage times of up to 15 years in liquid nitrogen do not affect RNA integrity.

O.C.T.-embedded samples are then sectioned at 10 μm thickness using a cryostat, taking care to place tissue sections in the central third of the slide. We have found that for breast tumor tissue, this represents an acceptable balance between maximizing LCM yields and ensuring that the area visualized corresponds to what is isolated, since in thicker sections cells lying beneath the visible layer may be co-isolated. For tissue with higher degrees of local heterogeneity, thinner sections may be required; however, these would require more LCM processing to isolate the same amount of tissue. It is important to ensure that samples and sections are kept as cold as possible during this procedure; this entails pre-cooling slide boxes before use, and transferring cut sections into these within the cryostat chamber, as well as always transporting sections in insulated containers with dry ice. To minimize the potential for cross-contamination, the cryostat chamber should be vacuumed between samples, surfaces should be cleaned with acetone, and a fresh blade should be used for each sample. Sections on slides are stored at –80 °C until use. The time for which slides can be stored depends on tissue type and intended use—for human breast tumor samples, 2–3 months is generally the limit for subsequent RNA isolation.

Two key elements in successful LCM-mediated isolation of tissue for downstream analysis are the quality of the input material, and optimization of the protocol to minimize loss of integrity during the procedure. Since LCM is carried out at room temperature, further sample degradation can occur during the procedure; thus, initial sample quality must be carefully assessed, and samples must be followed throughout the procedure.

Our workflow integrates multiple quality control steps designed to avoid additional processing of poor-quality samples. In addition, stepwise assays of sample quality allow for identification of steps leading to sample degradation which may require modification.

First, tissue from four to five slides bearing sectioned samples is manually isolated and subjected to RNA isolation as per the protocol below, followed by quality assessment using the RNA Pico kit on the Agilent Bioanalyzer platform. Next, tissue-bearing slides that have been stained as per the protocol to be used in the study in question are similarly processed to identify samples which deteriorate to an unusable point during the staining step. Samples for which RNA is not of acceptable quality after sectioning or staining are removed from the workflow. As a final step prior to LCM performance, stained sections are exposed to room temperature for times corresponding to expected LCM duration, and similarly processed—this identifies samples for which LCM processing time may require adjustment.

2 Materials

2.1 Total RNA Extraction for Quality Control

1. TRIzol (ThermoFisher).
2. Glycogen (GenHunter).
3. Chloroform.
4. Isopropanol.
5. Ice-cold 75 % ethanol.
6. RNase-free water.
7. 1.5 mL tubes.
8. Pipettor and tips.
9. Vortex mixer.
10. Centrifuge capable of 12,000 × *g* and refrigerated at 4 °C.

2.2 H&E Staining for LCM

Note: Sections should not be allowed to dry out during staining procedures.

1. Harris hematoxylin (Surgipath).
2. Eosin (Surgipath).
3. 70 %, 95 %, and 100 % ethanol.
4. Xylene.
5. RNase-free water.
6. Bluing solution: 0.3 % Ammonium hydroxide.
7. 0.22 μm Filter (Steritop system, Millipore).
8. RNase-free glass surface.
9. RNase-free staining jars.

2.3 HistoGene Staining

Note: Sections should not be allowed to dry out during the procedure.

1. HistoGene staining kit (Life Technologies catalog # KIT0401; this contains all required reagents and consumables).
2. RNase-free glass surface.
3. RNase-free tweezers and forceps to manipulate slides.

2.4 Laser Capture Microdissection

Note: The procedure below is written for the Arcturus PixCell IIe system, which utilizes an IR laser only. Other systems exist which incorporate IR and/or UV lasers; for these, carefully following the manufacturer's directions is recommended.

1. Arcturus PixCell IIe LCM system.
2. CapSure caps.
3. Tissue on slides.
4. 100% Ethanol and lint-free wipes to clean work area.
5. PrepStrips (Arcturus).
6. CapSure cleanup pads (*see* **Note 1**).

3 Methods

3.1 Total RNA Extraction for Quality Control

1. Prepare a 1.5 mL tube with 1 mL of TRIzol (ThermoFisher).
2. Pipette ca. 200 μL of TRIzol onto each section.
3. Pipette TRIzol up and down over the section several times.
4. Transfer material to TRIzol-containing tube.
5. Vortex briefly to homogenize tissue. Samples can now be stored at −80 °C prior to extraction. Prior to proceeding to next step, thaw frozen samples and incubate at room temperature for 5 min.
6. Add 200 μL of chloroform and shake vigorously by hand for 15 s.
7. Incubate at room temperature for 3 min.
8. Centrifuge at 12,000 × *g* for 15 min at room temperature.
9. Transfer upper aqueous phase (400–450 μL) to a new 1.5 mL tube.
10. Precipitate RNA by adding 500 μL of isopropanol and 2 μL of glycogen.
11. Mix by manually inverting ten times, and then incubate for 10 min at room temperature.
12. Centrifuge at 12,000 × *g* for 10 min at 4 °C.
13. Carefully remove and discard supernatant.
14. Add 1 mL ice-cold 75% ethanol (wash step) and shake tube.

15. Centrifuge at 7500 × *g* for 5 min at 4 °C.
16. Carefully remove ethanol and air-dry pellet for 10–15 min at room temperature.
17. Resuspend pellet in 15 μL RNase-free water and incubate at 55 °C for 10 min to dissolve pellet.
18. Proceed to RNA assay, e.g., using the Bioanalyzer platform.

3.2 H&E Staining for LCM

We currently utilize either the Arcturus HistoGene LCM Frozen Section Staining Kit (Applied Biosystems) or an in-house hematoxylin and eosin (H&E)-based procedure for sample staining. Both procedures are listed below; the HistoGene kit has the advantage of not requiring manual preparation of solutions, albeit at higher cost. Also, sections stained using H&E are more easily interpretable for outside experts called in to analyze samples, i.e., pathologists, while the brown staining obtained with the HistoGene kit requires some familiarization.

1. Filter Harris hematoxylin prior to use using a 0.22 μm filter to remove any precipitate.
2. Thaw slides at room temperature on an RNase-free glass surface (to ensure even thawing) for a maximum of 30 s.
3. Fix slides with 70% ethanol for 30 s.
4. Rinse slides with two rapid dips in RNase-free water.
5. Stain slides with hematoxylin for 30 s.
6. Rinse slides with one rapid dip in RNase-free water.
7. Blue in 0.3% ammonium hydroxide solution for 30 s.
8. Dehydrate by placing slides in 70% ethanol (2 × 30 s), followed by 95% ethanol (2 × 30 s).
9. Stain slides with eosin (Surgipath) for 20 s.
10. Dehydrate slides using through 30-s steps in 95% ethanol (2 × 30 s), 100% ethanol (2 × 30 s), and xylene (60 and 90 s).
11. Air-dry slides for 10 min in a fume hood.
12. Use slides immediately for LCM—if multiple slides have been stained and will be used in the same LCM session, the extra sections can be stored in a cold desiccator until use.

3.3 HistoGene Staining

Note: Adapted from the manufacturer's instructions.

1. Thaw slides at room temperature on an RNase-free glass surface for a maximum of 30 s.
2. Fix slides in 75% ethanol for 30 s.
3. Rinse in RNase-free water for 30 s.
4. Apply 100 μL of HistoGene staining solution to each section and place on a glass surface for 20 s.

5. Rinse in RNase-free water for 30 s.
6. Dehydrate slides by dipping in 75 % ethanol for 30 s, 95 % ethanol for 30 s, and 100 % ethanol for 30 s.
7. Clear sections by dipping in xylene for 5 min.
8. Air-dry slides in a fume hood for 5 min.
9. Use slides immediately for LCM—if multiple slides have been stained and will be used in the same LCM session, extra sections can be stored in a cold desiccator until use.

3.4 Laser Capture Microdissection

Note: Adapted from the manufacturer's instructions.

1. Turn on power to the instrument, controller, and computer.
2. If using fluorescence, turn on power to Olympus mercury lamp and close the fluorescence shutter until you are ready to view fluorescent samples (*see* **Notes 2**–**5**).
3. Dust off working surfaces with compressed air and spray with 100 % ethanol. Wipe off excess ethanol with lint-free wipes (e.g., Kimwipes).
4. Load CapSure caps (HS or Macro) in the CapSure cassette module (*see* **Note 6**).
5. Remove possible debris from the section surface using Arcturus PrepStrips.
6. Center the joystick in the vertical position and place the sample slide onto the stage.
7. Identify a region with cells of interest. Place it on the center of the field of view (*see* **Note 7**). Activate the vacuum button on the front of the laser controller (*see* **Note 8**). Make sure that a cap is at the load line position.
8. Without lifting the Cap Placement Arm, rotate it to the cap pickup position. The arm will automatically line up with the cap.
9. Lift the arm with the cap and turn it slowly clockwise until it stops.
10. Lower arm to place the cap on the tissue section, on the region of interest.
11. Adjust the fine focus on microscope and adjust light intensity. Examine the sample, moving around using the joystick.
12. Initiate archiving software. Enter the file name, study name, and slide number, adding notes if necessary.
13. Take "map" (low power, whole section) and "before" (higher power, area to be microdissected) images if desired (Fig. 2) (*see* **Note 9**). Set laser parameters, and then activate laser by turning key clockwise. Once laser interlock check is complete, turn on laser using the "laser enable" button (*see* **Note 10**).

14. To focus the laser, go to the 20× objective, adjust the microscope focus, and decrease the light sufficiently to see the laser spot on the monitor. Move to an open space close to tissue and fire test shots, adjusting laser focus knob until you observe an optimal laser spot (*see* **Note 11**).
15. Reset the pulse number to zero before starting LCM on sample.
16. Position the laser targeting spot over the cells of interest and fire the laser. Move the stage with the joystick and continue firing laser to collect all required material.
17. Raise the Cap Placement Arm with the cap and move it gently to the rest position.
18. Observe remaining tissue on the slide and take "after" images of dissected regions.
19. To observe captured cells, turn off vacuum and remove the slide from stage. Change the objective to low magnification. Gently turn the capping arm clockwise, placing the cap in the center of the field of vision. Examine the cap at low and high magnification, collecting "cap" images, if needed (Fig. 2) (*see* **Note 12**). Using capping tool, transfer the cap with captured cells onto a 1.5 mL tube with appropriate extraction buffer.
20. When finished with LCM procedures, turn off vacuum and laser (turn key counterclockwise), close archiving software, and turn off controller.
21. Remove consumables and cover microscope (*see* **Note 13**).

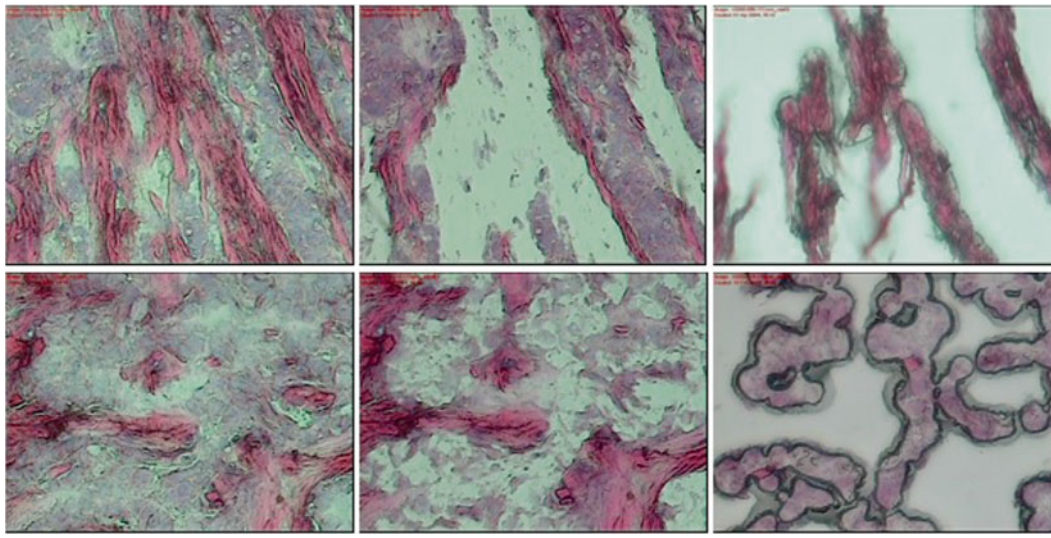

Fig. 2 "Before" (*left*), "after" (*centre*), and "cap" (*right*) images of laser capture microdissection for tumor-associated stroma (*top row*) and tumor epithelium (*bottom row*)

4 Notes

1. These are no longer commercially available; adhesive notes can be used as a substitute.
2. Note that it takes time for the mercury lamp to become stable; turn it on 20–30 min before starting to perform LCM.
3. The fluorescence cube turret is located under the stage. It has four positions for blue, green, and orange filter cubes plus a bright-field position (white light, no color filter cube). Select the position with the appropriate color filter by rotating the cube turret.
4. The cube turret has a built-in shutter. The shutter should always remain closed unless viewing fluorescent samples. Leaving the shutter opened for extended periods will photobleach fluorescent dyes.
5. The "normal" position on the control box is used for routine procedures (no fluorescence or strong fluorescence). For samples with weak fluorescence, it is possible to enhance the signal intensity by increasing the integration time from "normal" to the minimum setting which is needed to observe a good signal from the sample. The white light setting should remain very low.
6. HS caps include a standoff rail that keeps the thermolabile film above the tissue surface, while Macro caps do not. Use of HS caps reduces potential contamination of the film at the expense of reducing total possible yield.
7. Ideal work area should have both open space for laser test firing and cells of interest for dissection.
8. The vacuum acts to hold the slide in place on the stage.
9. Images can be saved in .jpg or .tif formats; saving as .tif files uses more disk space (ca. 1 Mb/image vs. ca. 300 kb for .jpg images).
10. Although each procedure will require individual optimization, a useful set of initial settings for mammary tissue is as follows: spot size 15 μm, target voltage 0.2 V, current 4.4 mA, and power 25 mW.
11. Proper film melting is occurring if you observe a black ring around the spot. If this ring is not observed, adjust laser focus and power until it is observed (Fig. 3).
12. If contamination with non-dissected material is observed on cap, clean it very gently with CapSure pad.
13. In many cases, individuals who have been performing LCM for the first time have reported vertigo and/or nausea following protracted LCM sessions. This is likely an effect of intently

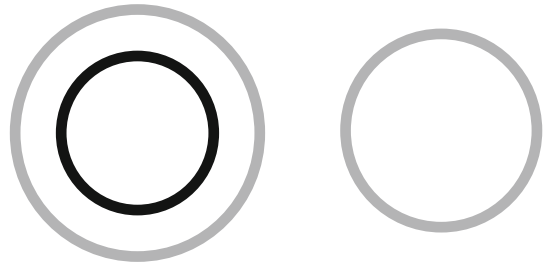

Fig. 3 Schematic images of correct (*left*) and incorrect (*right*) laser pulses. In *the left-hand image*, the thermolabile film is in contact with the tissue below, while in *the right-hand image*, contact has not been achieved

watching the computer screen as it rapidly displays movement across different regions of the specimen. Increased experience with the procedure reduces but does not completely abolish this effect. Taking short breaks every 30 min may be useful.

Acknowledgements

This work was supported by funding from the Database and Tissue Bank Axis of the "Réseau de Recherche sur le Cancer" of the "Fonds de Recherche du Québec-Santé" and the Québec Breast Cancer Foundation to M.P.

References

1. Wernert N, Locherbach C, Wellmann A, Behrens P, Hugel A (2000) Presence of genetic alterations in microdissected stroma of human colon and breast cancers. J Mol Med 78(7):B30
2. Kurose K, Hoshaw-Woodard S, Adeyinka A, Lemeshow S, Watson PH, Eng C (2001) Genetic model of multi-step breast carcinogenesis involving the epithelium and stroma: clues to tumour-microenvironment interactions. Hum Mol Genet 10(18):1907–1913
3. Ellsworth DL, Ellsworth RE, Love B, Deyarmin B, Lubert SM, Mittal V, Shriver CD (2004) Genomic patterns of allelic imbalance in disease free tissue adjacent to primary breast carcinomas. Breast Cancer Res Treat 88(2):131–139. doi:10.1007/s10549-004-1424-7
4. Boersma BJ, Reimers M, Yi M, Ludwig JA, Luke BT, Stephens RM, Yfantis HG, Lee DH, Weinstein JN, Ambs S (2008) A stromal gene signature associated with inflammatory breast cancer. Int J Cancer 122(6):1324–1332. doi:10.1002/ijc.23237
5. Ma XJ, Dahiya S, Richardson E, Erlander M, Sgroi DC (2009) Gene expression profiling of the tumor microenvironment during breast cancer progression. Breast Cancer Res 11(1):R7. doi:10.1186/bcr2222
6. Martin DN, Boersma BJ, Yi M, Reimers M, Howe TM, Yfantis HG, Tsai YC, Williams EH, Lee DH, Stephens RM, Weissman AM, Ambs S (2009) Differences in the tumor microenvironment between African-American and European-American breast cancer patients. PLoS One 4(2):e4531. doi:10.1371/journal.pone.0004531
7. Witkiewicz AK, Kline J, Queenan M, Brody JR, Tsirigos A, Bilal E, Pavlides S, Ertel A, Sotgia F, Lisanti MP (2011) Molecular profiling of a lethal tumor microenvironment, as defined by stromal caveolin-1 status in breast cancers. Cell Cycle 10(11):1794–1809
8. Planche A, Bacac M, Provero P, Fusco C, Delorenzi M, Stehle JC, Stamenkovic I (2011) Identification of prognostic molecular features

in the reactive stroma of human breast and prostate cancer. PLoS One 6(5):e18640. doi:10.1371/journal.pone.0018640

9. Harvell DM, Kim J, O'Brien J, Tan AC, Borges VF, Schedin P, Jacobsen BM, Horwitz KB (2013) Genomic signatures of pregnancy-associated breast cancer epithelia and stroma and their regulation by estrogens and progesterone. Horm Cancer 4(3):140–153. doi:10.1007/s12672-013-0136-z
10. Winslow S, Leandersson K, Edsjo A, Larsson C (2015) Prognostic stromal gene signatures in breast cancer. Breast Cancer Res 17:23. doi:10.1186/s13058-015-0530-2
11. Ponzo MG, Lesurf R, Petkiewicz S, O'Malley FP, Pinnaduwage D, Andrulis IL, Bull SB, Chughtai N, Zuo D, Souleimanova M, Germain D, Omeroglu A, Cardiff RD, Hallett M, Park M (2009) Met induces mammary tumors with diverse histologies and is associated with poor outcome and human basal breast cancer. Proc Natl Acad Sci U S A 106(31):12903–12908. doi:10.1073/pnas.0810402106
12. Finak G, Bertos N, Pepin F, Sadekova S, Souleimanova M, Zhao H, Chen H, Omeroglu G, Meterissian S, Omeroglu A, Hallett M, Park M (2008) Stromal gene expression predicts clinical outcome in breast cancer. Nat Med 14(5):518–527. doi:10.1038/nm1764
13. Pepin F, Bertos N, Laferriere J, Sadekova S, Souleimanova M, Zhao H, Finak G, Meterissian S, Hallett MT, Park M (2012) Gene expression profiling of microdissected breast cancer microvasculature identifies distinct tumor vascular subtypes. Breast Cancer Res 14(4):R120. doi:10.1186/bcr3246
14. Finak G, Sadekova S, Pepin F, Hallett M, Meterissian S, Halwani F, Khetani K, Souleimanova M, Zabolotny B, Omeroglu A, Park M (2006) Gene expression signatures of morphologically normal breast tissue identify basal-like tumors. Breast Cancer Res 8(5):R58. doi:10.1186/bcr1608
15. Hildenbrand R, Schaaf A, Dorn-Beineke A, Allgayer H, Sutterlin M, Marx A, Stroebel P (2009) Tumor stroma is the predominant uPA-, uPAR-, PAI-1-expressing tissue in human breast cancer: prognostic impact. Histol Histopathol 24(7):869–877
16. Reddy LA, Mikesh L, Moskulak C, Harvey J, Sherman N, Zigrino P, Mauch C, Fox JW (2014) Host response to human breast Invasive Ductal Carcinoma (IDC) as observed by changes in the stromal proteome. J Proteome Res 13(11):4739–4751. doi:10.1021/pr500620x
17. Liu S, Umezu-Goto M, Murph M, Lu Y, Liu W, Zhang F, Yu S, Stephens LC, Cui X, Murrow G, Coombes K, Muller W, Hung MC, Perou CM, Lee AV, Fang X, Mills GB (2009) Expression of autotaxin and lysophosphatidic acid receptors increases mammary tumorigenesis, invasion, and metastases. Cancer Cell 15(6):539–550. doi:10.1016/j.ccr.2009.03.027
18. Bronisz A, Godlewski J, Wallace JA, Merchant AS, Nowicki MO, Mathsyaraja H, Srinivasan R, Trimboli AJ, Martin CK, Li F, Yu L, Fernandez SA, Pecot T, Rosol TJ, Cory S, Hallett M, Park M, Piper MG, Marsh CB, Yee LD, Jimenez RE, Nuovo G, Lawler SE, Chiocca EA, Leone G, Ostrowski MC (2012) Reprogramming of the tumour microenvironment by stromal PTEN-regulated miR-320. Nat Cell Biol 14(2):159–167. doi:10.1038/ncb2396
19. Pickup MW, Laklai H, Acerbi I, Owens P, Gorska AE, Chytil A, Aakre M, Weaver VM, Moses HL (2013) Stromally derived lysyl oxidase promotes metastasis of transforming growth factor-beta-deficient mouse mammary carcinomas. Cancer Res 73(17):5336–5346. doi:10.1158/0008-5472.CAN-13-0012
20. Valencia T, Kim JY, Abu-Baker S, Moscat-Pardos J, Ahn CS, Reina-Campos M, Duran A, Castilla EA, Metallo CM, Diaz-Meco MT, Moscat J (2014) Metabolic reprogramming of stromal fibroblasts through p62-mTORC1 signaling promotes inflammation and tumorigenesis. Cancer Cell 26(1):121–135. doi:10.1016/j.ccr.2014.05.004
21. Masiero M, Simoes FC, Han HD, Snell C, Peterkin T, Bridges E, Mangala LS, Wu SY, Pradeep S, Li D, Han C, Dalton H, Lopez-Berestein G, Tuynman JB, Mortensen N, Li JL, Patient R, Sood AK, Banham AH, Harris AL, Buffa FM (2013) A core human primary tumor angiogenesis signature identifies the endothelial orphan receptor ELTD1 as a key regulator of angiogenesis. Cancer Cell 24(2):229–241. doi:10.1016/j.ccr.2013.06.004
22. Shimoda M, Principe S, Jackson HW, Luga V, Fang H, Molyneux SD, Shao YW, Aiken A, Waterhouse PD, Karamboulas C, Hess FM, Ohtsuka T, Okada Y, Ailles L, Ludwig A, Wrana JL, Kislinger T, Khokha R (2014) Loss of the Timp gene family is sufficient for the acquisition of the CAF-like cell state. Nat Cell Biol 16(9):889–901. doi:10.1038/ncb3021
23. Scherz-Shouval R, Santagata S, Mendillo ML, Sholl LM, Ben-Aharon I, Beck AH, Dias-Santagata D, Koeva M, Stemmer SM, Whitesell L, Lindquist S (2014) The reprogramming of tumor stroma by HSF1 is a potent enabler of malignancy. Cell 158(3):564–578. doi:10.1016/j.cell.2014.05.045
24. Ghosh S, Ashcraft K, Jahid MJ, April C, Ghajar CM, Ruan J, Wang H, Foster M, Hughes DC,

Ramirez AG, Huang T, Fan JB, Hu Y, Li R (2013) Regulation of adipose oestrogen output by mechanical stress. Nat Commun 4:1821. doi:10.1038/ncomms2794

25. Wolford CC, McConoughey SJ, Jalgaonkar SP, Leon M, Merchant AS, Dominick JL, Yin X, Chang Y, Zmuda EJ, O'Toole SA, Millar EK, Roller SL, Shapiro CL, Ostrowski MC, Sutherland RL, Hai T (2013) Transcription factor ATF3 links host adaptive response to breast cancer metastasis. J Clin Invest 123(7):2893–2906. doi:10.1172/JCI64410
26. Liu X, Nugoli M, Laferriere J, Saleh SM, Rodrigue-Gervais IG, Saleh M, Park M, Hallett MT, Muller WJ, Giguere V (2011) Stromal retinoic acid receptor beta promotes mammary gland tumorigenesis. Proc Natl Acad Sci U S A 108(2):774–779. doi:10.1073/pnas.1011845108
27. Becker MA, Hou X, Harrington SC, Weroha SJ, Gonzalez SE, Jacob KA, Carboni JM, Gottardis MM, Haluska P (2012) IGFBP ratio confers resistance to IGF targeting and correlates with increased invasion and poor outcome in breast tumors. Clin Cancer Res 18(6):1808–1817. doi:10.1158/1078-0432.CCR-11-1806
28. Luga V, Zhang L, Viloria-Petit AM, Ogunjimi AA, Inanlou MR, Chiu E, Buchanan M, Hosein AN, Basik M, Wrana JL (2012) Exosomes mediate stromal mobilization of autocrine Wnt-PCP signaling in breast cancer cell migration. Cell 151(7):1542–1556. doi:10.1016/j.cell.2012.11.024
29. Wallace JA, Li F, Balakrishnan S, Cantemir-Stone CZ, Pecot T, Martin C, Kladney RD, Sharma SM, Trimboli AJ, Fernandez SA, Yu L, Rosol TJ, Stromberg PC, Lesurf R, Hallett M, Park M, Leone G, Ostrowski MC (2013) Ets2 in tumor fibroblasts promotes angiogenesis in breast cancer. PLoS One 8(8):e71533. doi:10.1371/journal.pone.0071533
30. Garbe JC, Pepin F, Pelissier FA, Sputova K, Fridriksdottir AJ, Guo DE, Villadsen R, Park M, Petersen OW, Borowsky AD, Stampfer MR, Labarge MA (2012) Accumulation of multipotent progenitors with a basal differentiation bias during aging of human mammary epithelia. Cancer Res 72(14):3687–3701. doi:10.1158/0008-5472.CAN-12-0157
31. Emmert-Buck MR, Bonner RF, Smith PD, Chuaqui RF, Zhuang Z, Goldstein SR, Weiss RA, Liotta LA (1996) Laser capture microdissection. Science 274(5289):998–1001
32. Bonner RF, Emmert-Buck M, Cole K, Pohida T, Chuaqui R, Goldstein S, Liotta LA (1997) Laser capture microdissection: molecular analysis of tissue. Science 278(5342):1481–1483
33. Roy Chowdhuri S, Hanson J, Cheng J, Rodriguez-Canales J, Fetsch P, Balis U, Filie AC, Giaccone G, Emmert-Buck MR, Hipp JD (2012) Semiautomated laser capture microdissection of lung adenocarcinoma cytology samples. Acta Cytol 56(6):622–631. doi:10.1159/000342984

Chapter 3

Quantitative Analysis of Human Cancer Cell Extravasation Using Intravital Imaging

Lian Willetts, David Bond, Konstantin Stoletov, and John D. Lewis

Abstract

Metastasis, or the spread of cancer cells from a primary tumor to distant sites, is the leading cause of cancer-associated death. Metastasis is a complex multi-step process comprised of invasion, intravasation, survival in circulation, extravasation, and formation of metastatic colonies. Currently, in vitro assays are limited in their ability to investigate these intricate processes and do not faithfully reflect metastasis as it occurs in vivo. Traditional in vivo models of metastasis are limited by their ability to visualize the seemingly sporadic behavior of where and when cancer cells spread (Reymond et al., Nat Rev Cancer 13:858–870, 2013). The avian embryo model of metastasis is a powerful platform to study many of the critical steps in the metastatic cascade including the migration, extravasation, and invasion of human cancer cells in vivo (Sung et al., Nat Commun 6:7164, 2015; Leong et al., Cell Rep 8, 1558–1570, 2014; Kain et al., Dev Dyn 243:216–28, 2014; Leong et al., Nat Protoc 5:1406–17, 2010; Zijlstra et al., Cancer Cell 13:221–234, 2008; Palmer et al., J Vis Exp 51:2815, 2011). The chicken chorioallantoic membrane (CAM) is a readily accessible and well-vascularized tissue that surrounds the developing embryo. When the chicken embryo is grown in a shell-less, ex ovo environment, the nearly transparent CAM provides an ideal environment for high-resolution fluorescent microcopy approaches. In this model, the embryonic chicken vasculature and labeled cancer cells can be visualized simultaneously to investigate specific steps in the metastatic cascade including extravasation. When combined with the proper image analysis tools, the ex ovo chicken embryo model offers a cost-effective and high-throughput platform for the quantitative analysis of tumor cell metastasis in a physiologically relevant in vivo setting. Here we discuss detailed procedures to quantify cancer cell extravasation in the shell-less chicken embryo model with advanced fluorescence microscopy techniques.

Key words Intravital imaging, Extravasation, Chick embryo, Cancer, Chorioallantoic membrane, Fluorescence, Embryonic vasculature, Cell migration, Metastasis, In vivo, Shell-less, GFP, RFP, Lectin LCA-fluorescein/rhodamine

1 Introduction

The majority of cancer-related deaths are associated with the onset of metastasis [8]. Currently, there is no accurate test to predict metastasis and no effective therapy to prevent it [9, 10]. In order for cancer cells to metastasize successfully, they must undergo local

Josie Ursini-Siegel and Nicole Beauchemin (eds.), *The Tumor Microenvironment: Methods and Protocols*, Methods in Molecular Biology, vol. 1458, DOI 10.1007/978-1-4939-3801-8_3, © Springer Science+Business Media New York 2016

invasion, intravasation, survival in the circulation, extravasation, and colony expansion in distant metastatic sites [11–15]. Of these steps, extravasation is the least understood, partly due to the lack of effective modeling [1, 16, 17]. The difficulty in capturing a cancer cell extravasating in deep solid tissues has limited our ability to closely study the process of extravasation as it is related to metastatic spread of cancer. Here, we discuss an intravital imaging-based approach using the ex ovo chicken embryo model of metastasis to precisely quantify human cancer cell extravasation.

Over the last decade, the chicken embryo model of metastasis has been proven to be a robust and cost-effective research platform to study many aspects of cancer biology. For our purposes, the shell-less chicken embryo model provides a full spectrum of physiologically relevant tissue interactions for studying the metastatic behavior of cancer cells in vivo [7, 18–24]. The easily accessible chick embryo chorioallantoic membrane (CAM), a well-vascularized tissue around the embryo, due to its highly accessible capillary networks, overcomes the deep tissue limitation for microscopic visualization of primary tumor and/or metastatic sites. Intravital imaging in the ex ovo CAM model has shed light on many aspects of the metastasis [25, 26]. Recent advances in "shell-less" embryo preparation coupled with the use of new fluorescent labeling techniques for both host and cancer cells have dramatically enhanced the imaging capabilities of this model in the recent years [2–6, 27–30].

Since the CAM is a translucent and easily accessible tissue, the migratory behavior of fluorescently labeled cancer cells can be readily visualized and recorded longitudinally using various intravital imaging techniques [3, 6, 28] and their migration patterns analyzed by image analysis software. Compared to rodent models, intravital imaging in the CAM requires no anesthesia, surgery, or specialized lenses. These techniques can be achieved with standard upright fluorescent wide-field or confocal microscopy. Temperature control with a local microscope-mounted incubation chamber to provide stable humidity and field of view is suggested for longer term time-lapse imaging. The approach described here allows for an easy-to-use and biophysically relevant in vivo quantitative analysis of human cancer cell extravasation and metastasis.

2 Materials

2.1 Preparation of the Shell-Less Ex Ovo Chicken Embryos

1. Fine-point forceps.
2. Circular cover slips 22 mm.
3. Fertilized white Leghorn eggs, incubated for 12–14 days as described [6, 28, 31].
4. Egg incubator, many commercially available models including 1550E from G.Q.F. MGF Company Inc., Savannah, GA, or

Marsh Farms Roll-X Flowing Air Incubators, Lyon Electric Company Inc., Chula Vista, CA.

5. Avian embryo imaging unit Innovascreen (Halifax, Canada) (Fig. 1): This is a specialized microscope-mounted enclosure that maintains the avian embryo in a humidified (>90% humidity) environment while stabilizing the area of CAM to be imaged using a standard cover slip fixed into the lid of the unit. This allows for short- or long-term noninvasive intravital imaging of the CAM using an upright fluorescence microscope.

2.2 Cancer Cell Line Preparation

1. Use cancer cells either transiently or stably transfected with a construct that constitutively expresses a fluorescent protein such as GFP or RFP, or are otherwise fluorescently labeled (e.g., cell membrane dye, fluorescent nanobeads, or fluorescent fusion protein that labels the nucleus such as H1-mCherry) [32–37] (*see* **Notes 1** and **2**).
2. 1× PBS pH 7.4 [37].
3. 2.5% Trypsin (10×).
4. 15 mL Conical centrifuge tubes.

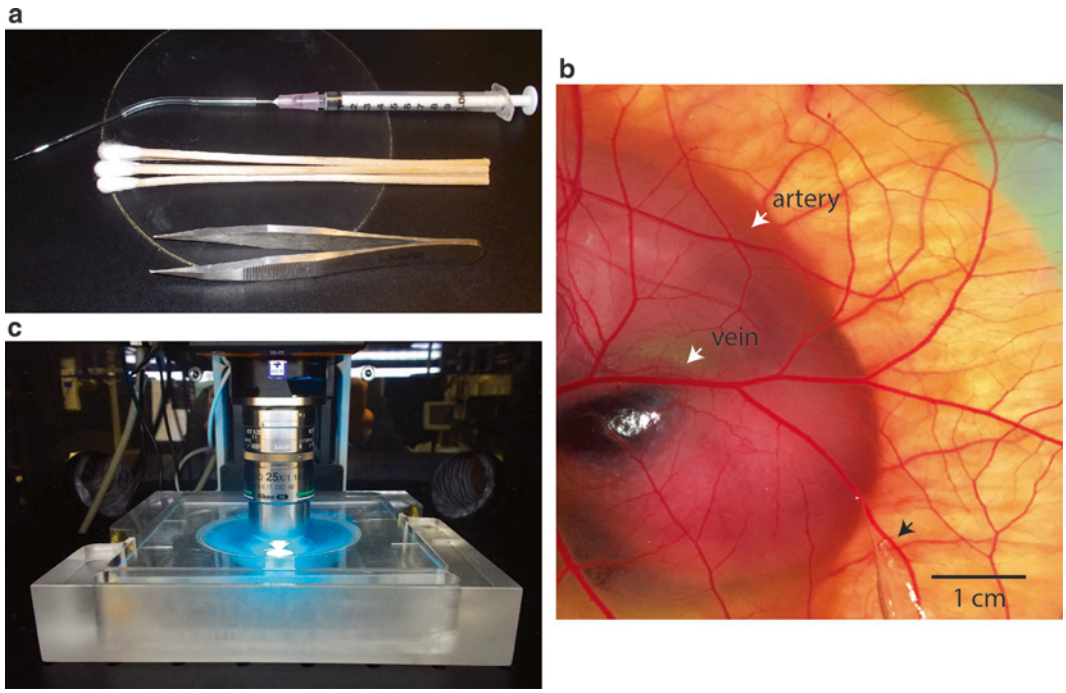

Fig. 1 Overview of the cancer cell intravenous injection. (**a**) Assembled injection apparatus for IV injection of labeling agents and/or cancer cells. (**b**) Typical stereomicroscope eye piece view of an injection site. *Black arrow* points to borosilicate capillary. (**c**) Example of custom-built incubation unit for in vivo fluorescence imaging of shell-less chicken embryos. Incubation unit is shown with a microscope stage encased in a temperature-regulated enclosure

5. 1.5 mL Microfuge tubes.
6. Benchtop centrifuge.
7. Culture media appropriate for the cell lines used.
8. Hemocytometer for cell counting.
9. Trypan blue (0.4% trypan blue).

2.3 Intravenous Injection of Cancer Cells or Agents to Visualize Chicken Embryo Vasculature

1. Lectin *Lens Culinary* Agglutinin (LCA) conjugated with fluorescein or rhodamine (Vector Labs Inc. RL-1042, FL-1041) [38].
2. 1 mL Disposable syringes for injections.
3. 18-gauge disposable hypodermic needles for injections.
4. Tygon R-3603 laboratory tubing, 50 ft, for injections (1/32 in. inner diameter, 3/32 in. outer diameter, 1/32 in. wall thickness).
5. Vertical pipette puller (David Kopf Instruments, Tujunga, CA; Model 720).
6. Sodium borosilicate glass capillary tubes, outer diameter 1.0 mm, inner diameter 0.58 mm, 10 cm length (Sutter Instrument, Novato, CA).
7. Fine-point forceps.
8. Sterile cotton swabs.
9. Fertilized chicken eggs and egg incubator (*see* Subheading 2.1). Appropriate microscope(s) and image analysis software (*see* **Note 3**).

3 Methods

3.1 Cancer Cell Preparation for Injection

1. Culture cancer cell line of interest as required to 80% confluency. Higher confluency can negatively impact tumor take and extravasation efficiency. Routinely check for absence of mycoplasma contamination. (*See* [39] for technical considerations on growth of cancer cell lines for in vivo assays.)
2. To trypsinize cells, wash twice with 1× PBS pH 7.4. Aspirate remaining PBS, then add 0.5% trypsin–EDTA (e.g., 2 mL to 75 cm^2 flask, 3 mL to 175 cm^2 flask, 3 mL to 150 cm^2 culture dish), and incubate at 37 °C for 2–5 min until all cells detach.
3. Add 5 mL of PBS and transfer cell suspension to 15 mL conical centrifuge tube. Centrifuge at room temperature at 200 × *g* for 5 min.
4. Use another 10 mL of PBS to wash cells from unnecessary media components such as antibiotics and centrifuge the cells again as in **step 3**.
5. Discard supernatant and resuspend cells with 1 mL of ice-cold PBS.

6. Take 10 μL of suspension and dilute into 490 μL PBS. Count the number of cells in this diluted suspension using hemocytometer.
7. For intravenous (IV) injection of cells (*see* Subheading 3.2), concentrate cells to 0.5×10^6 to 1.0×10^6 cells/mL. Use ice-cold 1× PBS to dilute/resuspend cell concentrates (*see* **Notes 1** and **4**).

3.2 Intravenous Injection of Cancer Cells for Extravasation Assay

Depending on the experimental setup as many as 20 embryos can be analyzed within 1 day. Plan to inject excess numbers (20%) of embryos to determine the optimal starting time point of cancer cell extravasation and to accommodate for suboptimally injected embryos. Use 12–14-day-old embryos for injection of cancer cells, prepared as described (*see* **Note 5**).

1. When preparing needles for injection of cancer cells (as in Subheading 2.3, **steps 5** and **6**), the needle bore must be slightly wider than the diameter of the cancer cell used in order to avoid shearing of the cancer cells.
2. Maintain a homogenous cell suspension. Between injections, look for cell aggregation and cell lysis. If clumping is observed, remove the borosilicate needle and use the syringe plunger to mix the cell suspension until clumps are dispersed. Ensure that any air bubbles are removed from the syringe and the tubing prior to injection.
3. Depending on the cell type, cell aggregates may form and clog the needle head. If this occurs, replace the needle and tubing. It is generally necessary to change the needle after injection of every 2–4 embryos.
4. Distinguish veins from arteries on surface of CAM using a dissecting scope. The arteries and veins intertwine on the CAM surface (Fig. 1b) terminating in the capillary plexus. The CAM acts as a gas exchange organ and the arteries appear dark red because they deliver deoxygenated blood to the CAM, while veins are bright red because they transport oxygenated blood back to the embryo. Under a dissecting scope, this subtle color difference allows veins or arteries to be easily differentiated. One can also observe the direction of blood flow (blood flows towards the embryo in the veins).
5. Identify the vein to be injected. With a sufficiently tapered microneedle very narrow veins can be injected, which will minimize bleeding during and after injection. Avoid injecting into major vessels, as this will impact embryo viability. It is recommended to target only vessels that are tributaries or secondary tributaries of the major veins. Additionally, it is technically easier to pierce the vascular wall of smaller veins compared to larger veins. In our experience, it is easiest to inject veins that are slightly (10–20%) bigger in diameter than the injection needle tip.

6. Using the assembled injection apparatus (Fig. 1a), press the tip of the borosilicate needle against the surface of a vein and gently press forward in the same direction as blood flow. As you press forward, use your other hand to depress the plunger lightly. When the needle tip successfully enters the vessel lumen, the (clear) solution will stream through the vein away from the tip.
7. Minimize movement of the needle and continue to depress plunger (usually with the cell concentration of 0.5×10^6 cells/mL, 2–10 s is required) until desired volume is injected as indicated by the syringe markings. Injection of a single embryo may take 1–10 min depending on the quality of vessel cannulation. If there is excessive clear fluid buildup at the site of injection, pick another site of injection or use a cotton swab to clear the injection site.
8. After removing needle from CAM, dab the injection site with a cotton swab to remove blood and cancer cells that have spilled onto the surface of the CAM. Cells left behind on the CAM surface may be mistaken as sites of extravasation during imaging.
9. Depending on the user, cancer cells may be injected using either white light or fluorescence stereomicroscope. Use a fluorescence dissection microscope to verify successful injection and to assess uniform distribution of cancer cells throughout the capillary plexus of the CAM. For efficient cancer cell extravasation imaging and quantification approximately 10–30 cells must be present in each imaging field (512×512 μm, 25× objective). If multiple cell lines are injected to access their extravasation efficiency injections should be "stacked" to correct for delay injection time (*see* **Note 4**).
10. Return embryo to incubator.
11. Needles can be reused for multiple injections of the same cell line, but the sharpness will decrease with each injection. If injection becomes difficult, replace the needle.

3.3 Intravenous Injection of Lectin into Chorioallantoic Membrane

Different cell lines may take different times to extravasate out of the vasculature. Additionally, cancer cell extravasation times may vary from one batch of chicken embryos to another. It is recommended to start monitoring embryos for cancer cell extravasation 2–4 h post-injection. Inject lectin into a superfluous embryo to determine if sufficient proportion of cancer cells is extravasated (confocal microscope must be used, see Subheading 3.5). If ~30–50% of the cells per field of image are out of the vasculature in the control condition proceed to the imaging of the rest of the embryos.

1. Smaller needle diameter (10–20 μm) can be used for lectin injection for convenience.
2. Identify the vein to be injected. In our laboratory, we found that it is easier to use the same injection site for lectin as for the tumor cells.

3. Inject lectin using the same technique as for tumor cell injection (*see* Subheading 3.2, **steps 4–10**). It is better to over-inject embryo with lectin than under-inject for ease of cancer cell extravasation imaging and quantification (brighter and sharper signal from vasculature will allow for easier scoring of extravasated cancer cells).
4. After injection, place embryo into the incubator for recovery for 5 min. Inject only one embryo at a time immediately before the imaging.

3.4 Imaging of Cell Extravasation In Vivo

1. Set temperature-regulated microscope chamber to 37 °C ~6 h prior to imaging. This will stabilize temperature and help minimize XYZ drift during imaging.
2. To image cancer cell extravasation a 20× or 25× objective lens is recommended. Allow 10–30 min for imaging of a single embryo (*see* **Note 4**).
3. Apply a thin layer of vacuum grease to underside of the imaging unit lid to create a secure seal with the cover slip. Gently position a cover slip into the lid and wipe away any excess vacuum grease.
4. Position the embryo in the imaging unit such that the cover slip can be lowered down directly onto an open area of the CAM. Slowly lower the lid onto the embryo until the cover slip just makes contact with the CAM. Tighten the screws to secure the lid in place, and ensure that the lid is level and that the cover slip is not putting any downward pressure on the CAM.
5. If longer (time-lapse) imaging is planned, fill the outer jacket of the embryo imaging unit with water heated to 37 °C and place the unit onto the microscope stage (Fig. 1c). For short-term quantitative imaging, no water is necessary. The embryo imaging unit can be fixed to the microscope stage with tape to minimize XY drift.
6. Acquire multiple (~5–10), random 3D (XYZ) fields (25×) from each embryo. Use field-stitching option in the microscope acquisition software, if available. Images must be acquired with such settings (gains/Z-stack thickness, step) such that it is possible to judge intra- or extravascular localization for ~99% cells within each field. We routinely use 25× objective and 3 × 3 or 5 × 5 field stitching with 5–10 μm Z-step, 100 μm total thickness. Image at least 300 cells per condition.

3.5 Quantification of Cancer Cell Extravasation

1. Specialized software can be used to determine the intra- or extravascular location of cancer cells. We suggest software packages such as Nikon Elements, Volocity (Perkin Elmer), or ImageJ (NIH) to assist with this. Outlined below are general steps that will assist in quantitation of cancer cell extravasation.
2. Open the 3D file as a Z-stack using the necessary software. If significant XY movement occurred during the image acquisition

image may be aligned using ImageJ StackReg plug-in (http://bigwww.epfl.ch/thevenaz/stackreg) or similar Nikon Elements and Volocity document alignment protocols (Fig. 2a).

3. Scroll through the XYZ image in the *Z* direction and designate each cancer cell as in or out of the vasculature. We consider a cell extravasated if more than 80 % of the cell body is located out of the blood vessel.
4. Display your data as a percentage of the extravasated cells at a given time point per condition (i.e., particular cancer cell line mutant). Pull together data from several (at least five animals, 300 cells) animals per condition. As mentioned above it may be easier to use differentially labeled cancer cells (i.e., GFP and RFP). This approach provides an internal experiment "control" and decreases number of animals required (Fig. 2b, c and *see* **Note 2**).

4 Notes

1. Cancer cells tend to aggregate in PBS within 1–2 h post-trypsinization and therefore should be prepared immediately before injection. Vital cell cytoplasm or membrane-staining dyes (such as CellTracker or CellMask) tend to diffuse out of the cell within the required incubation times precluding the efficient imaging and should be avoided. Several human cancer cell lines such as LNCaP (prostate cancer) or Saos-2 (osteosarcoma) exhibited decreased survival rates; therefore pilot experiments to increase survival of the cell line used in the experiments may be required.
2. Using differential cancer cell fluorescent labels helps to reduce animal numbers and the time required for each experiment. For example, control cells can be labeled with RFP while mutant tumor cells can be alternatively labeled with GFP. In this case each experiment has a built-in control that corrects for inter-embryo variability. However, careful attention must be paid to ensure equal cell injection and survival of the differentially labeled cells, and that one cell line does not influence the extravasation of the other.
3. For confocal microscopy, we use a Nikon A1r MP confocal microscope. It is equipped with mercury arc lamp four diode-based lasers (405, 491, 561, 647 nm) and tunable (800–1300) Spectra Physics IR laser. For general embryo manipulation and cancer cell injection we use a Zeiss Lumar.V12 stereomicroscope. Less advanced microscope setups can be successfully used for the procedures described in this review. We encourage readers to contact the authors for more detailed recommendations.
4. Depending on the cancer cell type, cells start to extravasate 2–8 h post-injection. Cancer cell extravasation follows a bell-shaped

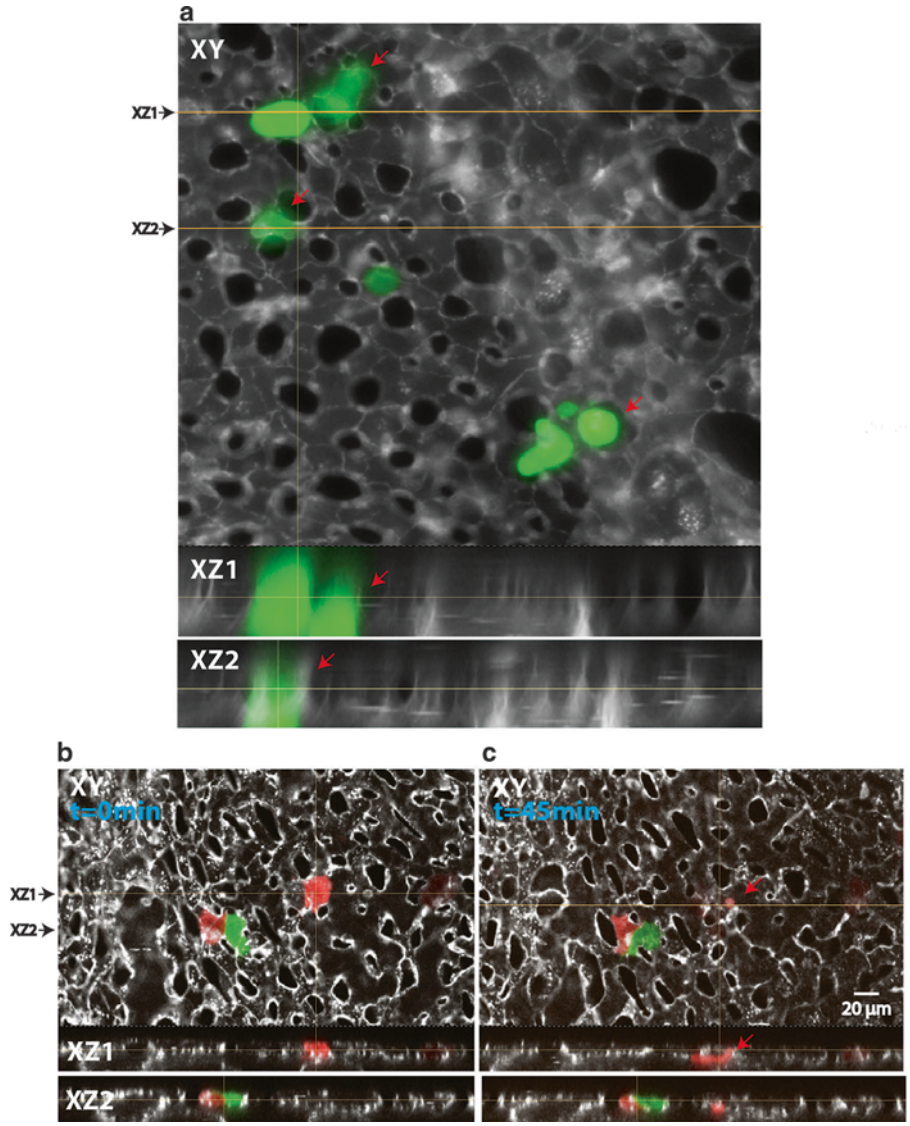

Fig. 2 Tumor cell extravasation analysis. (**a**) Typical 25× optical lens 3D image field used for cancer cell (LNCap GFP, *green*) extravasation analysis. Eight-hour time point is shown. Avian embryo vascular plexus is shown in *white* (Alexa 647). Main panel shows an optical slice that is located approximately in the middle (*Z*-axis) of the vascular plexus. Extravasated cells (*red arrows*) appear dim and below the vascular plexus. *Lower panels* show two separate XZ optical slices used in the analysis of cancer cell extravasation. Note that the extravasated cells appear below the vascular plexus. (**b**, **c**) Typical multi-color cancer cell extravasation analysis (HT1080 RFP and GFP cells). At time = 0, all three cells are located within the vascular plexus (see *lower* XZ panels). At time = 45 min, the red cell on the right (*red arrow*) is out of the vasculature

curve and with the majority of the cells leaving the circulation within 2–4 h after the initial extravasation. To correct for this variation, we recommend offsetting embryo injection and imaging for each condition. For example, if two conditions are being studied the chicken embryos should be injected (and imaged) in

the following order: condition 1 (embryo 1) … condition 2 (embryo 1) … condition 1 (embryo 2) … condition 2 (embryo 2) … and so on.

5. Chicken embryo CAM vessels mature rapidly between 12 and 14 days post-fertilization. Generally, cancer cell extravasation occurs sooner in younger (12–13 days) embryos (2–6 h) than in older (14 days) embryos (4–10 h). If significant (5×) fold difference in extravasation efficiency between cell lines used in the experiments is expected it may be more convenient to use younger embryos. Since older embryos possess more mature vasculature, 14-day-old embryos should be used to discriminate between cell lines with subtle differences in the extravasation efficiency.

Acknowledgments

This work was supported by Canadian Cancer Society Research Institute Grant #702849 to J.D.L. and K.S. L.W. and D.B. hold US Department of Defense Prostate Cancer Research Program Postdoctoral Training Awards. D.B. also holds an Alberta Innovates Health Solutions PDF Award. Dr. Lewis holds the Frank and Carla Sojonky Chair in Prostate Cancer Research supported by the Alberta Cancer Foundation. All experiments were performed in accordance with the regulations and guidelines of the Institutional Animal Care and Use Committee at the University of Alberta. We thank Desmond Pink for his photography.

References

1. Reymond N, d'Agua BB, Ridley AA (2013) Crossing the endothelial barrier during metastasis. Nat Rev Cancer 13:858–870
2. Sung BH, Ketova T, Hoshino D, Zijlstra A, Weaver AM (2015) Directional cell movement through tissues is controlled by exosome secretion. Nat Commun 6:7164
3. Leong HS, Robertson AE, Stoletov K, Leith SJ, Chin CA, Chien AE et al (2014) Invadopodia are required for cancer cell extravasation and are a therapeutic target for metastasis. Cell Rep 8:1558–1570
4. Kain KH, Miller JW, Jones-Paris CR, Thomason RT, Lewis JD, Bader DM et al (2014) The chick embryo as an expanding experimental model for cancer and cardiovascular research. Dev Dyn 243:216–228
5. Leong HS, Steinmetz NF, Ablack A, Destito G, Zijlstra A, Stuhlmann H et al (2010) Intravital imaging of embryonic and tumor neovasculature using viral nanoparticles. Nat Protoc 5:1406–1417
6. Zijlstra A, Lewis J, Degryse B, Stuhlmann H, Quigley JP (2008) The inhibition of tumor cell intravasation and subsequent metastasis via regulation of in vivo tumor cell motility by the tetraspanin CD151. Cancer Cell 13:221–234
7. Palmer TD, Lewis J, Zijlstra A (2011) Quantitative analysis of cancer metastasis using an avian embryo model. J Vis Exp 51:2815
8. Hanahan D, Weinberg RA (2000) The hallmarks of cancer. Cell 100:57–70
9. van't Veer LJ, Dai H, van de Vijver MJ, He YD, Hart AA, Mao M et al (2002) Gene expression profiling predicts clinical outcome of breast cancer. Nature 415:530–536
10. Eccles SA, Welch DR (2007) Metastasis: recent discoveries and novel treatment strategies. Lancet 369:1742–1757
11. Weber GF (2008) Molecular mechanisms of metastasis. Cancer Lett 270:181–190
12. Fidler IJ (2001) Seed and soil revisited: contribution of the organ microenvironment to

cancer metastasis. Surg Oncol Clin N Am 10:257–269

13. Chambers AF, Groom AC, MacDonald IC (2002) Dissemination and growth of cancer cells in metastatic sites. Nat Rev Cancer 2:563–572
14. Pantel K, Brakenhoff RH (2004) Dissecting the metastatic cascade. Nat Rev Cancer 4:448–456
15. Friedl P, Wolf K (2003) Tumour-cell invasion and migration: diversity and escape mechanisms. Nat Rev Cancer 3:362–374
16. Stoletov K, Lewis JD (2015) Invadopodia: a new therapeutic target to block cancer metastasis. Expert Rev Anticancer Ther 15:733–735
17. Leong HS, Chambers AF, Lewis JD (2012) Assessing cancer cell migration and metastatic growth in vivo in the chick embryo using fluorescence intravital imaging. Methods Mol Biol 872:1–14
18. Leighton J (1964) Invasion and metastasis of heterologous tumors in the chick embryo. Prog Exp Tumor Res 4:98–125
19. Locker J, Goldblatt PJ, Leighton J (1969) Hematogenous metastasis of Yoshida ascites Hepatoma in the chick embryo liver: ultrastructural changes in tumor cells. Cancer Res 29:1245–1253
20. McAllister RM, Peer M, Gilden RV, Landing BH (1974) Tumors formed by human rhabdomyosarcoma cells in chorioallantoic membrane of embryonated hens' eggs. Int J Cancer 13:886–890
21. Chambers AF, Shafir R, Ling V (1982) A model system for studying metastasis using the embryonic chick. Cancer Res 42:4018–4025
22. Chambers AF, Wilson S (1985) Cells transformed with a ts viral src mutant are temperature sensitive for in vivo growth. Mol Cell Biol 5:728–733
23. Gordon JR, Quigley JP (1986) Early spontaneous metastasis in the human epidermoid carcinoma HEp3/chick embryo model: contribution of incidental colonization. Int J Cancer 38:437–444
24. Chambers AF, Schmidt EE, MacDonald IC, Morris VL, Groom AC (1992) Early steps in hematogenous metastasis of B16F1 melanoma cells in chick embryos studied by high-resolution intravital videomicroscopy. J Natl Cancer Inst 84:797–803
25. Quigley JP, Armstrong PB (1998) Tumor cell intravasation elucidated: the chick embryo opens the window. Cell 94:281–284
26. MacDonald IC, Schmidt EE, Morris VL, Chambers AF, Groom AC (1992) Intravital videomicroscopy of the chorioallantoic microcirculation: a model system for studying metastasis. Microvasc Res 44:185–199
27. Aguirre-Ghiso JA, Ossowski L, Rosenbaum SK (2004) Green fluorescent protein tagging of extracellular signal-regulated kinase and p38 pathways reveals novel dynamics of pathway activation during primary and metastatic growth. Cancer Res 64:7336–7345
28. Wilson SM, Chambers AF (2004) Experimental metastasis assays in the chick embryo. Curr Protoc Cell Biol Chapter 19:Unit 19 6
29. Pink DB, Schulte W, Parseghian MH, Zijlstra A, Lewis JD (2012) Real-time visualization and quantitation of vascular permeability in vivo: implications for drug delivery. PLoS One 7:e33760
30. Cho CF, Ablack A, Leong HS, Zijlstra A, Lewis JD (2011) Evaluation of nanoparticle uptake in tumors in real time using intravital imaging. J Vis Exp 52:2808
31. Deryugina EI, Quigley JP (2008) Chick embryo chorioallantoic membrane model systems to study and visualize human tumor cell metastasis. Histochem Cell Biol 130:1119–1130
32. Chishima T, Miyagi Y, Wang X, Yamaoka H, Shimada H, Moossa AR, Hoffman RM (1997) Cancer invasion and micrometastasis visualized in live tissue by green fluorescent protein expression. Cancer Res 57:2042–2047
33. Naumov GN, Wilson SM, MacDonald IC, Schmidt EE, Morris VL, Groom AC et al (1999) Cellular expression of green fluorescent protein, coupled with high-resolution in vivo videomicroscopy, to monitor steps in tumor metastasis. J Cell Sci 112:1835–1842
34. Lewis JD, Destito G, Zijlstra A, Gonzalez MJ, Quigley JP, Manchester M et al (2006) Viral nanoparticles as tools for intravital vascular imaging. Nat Med 12:354–360
35. Sahai E (2007) Illuminating the metastatic process. Nat Rev Cancer 7:737–749
36. Hoffman RM (2009) Imaging cancer dynamics in vivo at the tumor and cellular level with fluorescent proteins. Clin Exp Metastasis 26:345–355
37. Hoffman RM (2005) The multiple uses of fluorescent proteins to visualize cancer in vivo. Nat Rev Cancer 5:796–806
38. Jilani SM, Murphy TJ, Thai SNM, Eichmann A, Alva JA, Irula-Arispe ML (2003) Selective binding of lectins to embryonic chicken vasculature. J Histochem Cytochem 51:597–604
39. Welch DR (1997) Technical considerations for studying cancer metastasis in vivo. Clin Exp Metastasis 15:272–306

Chapter 4

Studies on the Tumor Vasculature and Coagulant Microenvironment

Esterina D'Asti, Brian Meehan, and Janusz Rak

Abstract

Angiogenesis represents one aspect in the complex process that leads to the generation of the vascular tumor stroma. The related functional constituents include responses of endothelial, mural, bone marrow-derived, and resident inflammatory cells as well as activation of coagulation and fibrinolytic systems in blood. Multiple molecular and cellular effectors participate in these events, often in a tumor-specific manner and with changes enforced through the microenvironment, genetic evolution, and responses to anticancer therapies. To capture various elements of these interactions several surrogate assays have been devised, which can be mechanistically useful and are amenable to quantification, but are individually insufficient to describe the underlying complexity and are best used in a targeted and combinatorial manner. Below, we present a survey of angiogenesis assays and experimental approaches to analyze vascular events in cancer. We also provided specific examples of validated protocols, which are less described, but enable the straightforward analysis of vascular structures and coagulant properties of cancer cells in vivo and in vitro.

Key words Angiogenesis, Tumor microenvironment, Coagulation, Endothelial cells, Endoglin, Pericytes, Alpha smooth muscle actin, Proliferation, Tissue factor

1 Introduction

The vascular microenvironment defines many essential features of the neoplastic process including metabolic exchange, cellular trafficking, hormonal communication, angiocrine niche effects, metastasis, and paraneoplastic syndromes such as thrombosis and cachexia [1–3]. It is important to consider that vascular responses to tumor growth and dissemination are complex and form a continuum comprising hemostatic, inflammatory, and vessel wall-related mechanisms. While the term "angiogenesis" is often used to describe these events globally, the specific meaning is restricted to vessel formation from pre-existing blood vessels, which is but a fragment of the vascular milieu [3].

The multistep nature of angiogenesis is now understood in considerable molecular detail including the key regulators and cellular events involved [3]. Thus, pre-existing quiescent capillary endothelial

Josie Ursini-Siegel and Nicole Beauchemin (eds.), *The Tumor Microenvironment: Methods and Protocols*, Methods in Molecular Biology, vol. 1458, DOI 10.1007/978-1-4939-3801-8_4,

cells (phalanx cells) receive stimulatory signals exemplified by the gradient of vascular endothelial growth factor (VEGF) surrounding hypoxic or transformed cells. To this stimulus, endothelial cells respond by activation of key signaling pathways involving VEGF receptor 2 (VEGFR2), NOTCH/DLL4, ephrins, integrins, and other effectors resulting in the formation of structures known as angiogenic sprouts. These events begin with structural rearrangements in the capillary vessel wall including enlargement of the vascular diameter resulting in the formation of "mother vessels," followed by dropout of pericytes surrounding the endothelial tube, focal proteolysis of the endothelial basement membrane, and directional invasion of endothelial cell cohorts (sprouts) in the direction of the stimulus [3, 4]. Each of these formations consists of a leading single endothelial tip cell (high expressor of VEGFR2 and DLL4), followed by migrating columns of stalk cells, some of which exhibit mitotic activity. The sprout extension eventually leads to anastomosis with other sprouts/vessels to form a complete loop, a transition mediated by myeloid cell populations, and followed by the establishment of the new lumen, resumption of blood flow, and ultimately an increase in vascular density. Thus endothelial cell division, survival, migration, and morphogenesis involved in different steps of these processes could serve as surrogates of angiogenic activity and frequently represent the basis of the respective assays (Tables 1, 2, and 3) [5–7].

However, several key elements of tumor neovascularisation are not captured by these measurements. For example, tumor cell access to blood vessels may occur through non-angiogenic processes such as vasculogenesis, the recruitment of endothelial progenitor cells to form elements of the endothelial or perivascular milieu. In addition, processes of vessel splitting, vascular cooption, vasculogenic mimicry, endothelial transdifferentiation of cancer cells, and vessel invasion may contribute to the vascular networks in cancer [8]. Components of the circulating blood such as platelets, fibrin, and coagulation factors as well as their receptors such as tissue factor (TF) in perivascular and cancer cells also contribute in various ways to blood vessel formation, and functionality. For example, in human glioblastoma, the high expression of TF coincides with exuberant neovascularisation, intraluminal thrombotic vaso-occlusion, and regions of hypoxia [9–11]. Thus, coagulant properties of cancer and stromal cells may profoundly alter the vascular microenvironment. Moreover, larger vessels, external to the tumor mass, may adapt to and facilitate the demands of the intratumoral vascular networks through processes of arteriogenesis and arterio-venogenesis [4, 12, 13]. Therefore, measurement of angiogenic responses is often insufficient to understand the salient features of the vascular milieu associated with cancer.

Table 1
In vitro angiogenesis assays

Assay	Parameter measured	Principle	Endpoints	References
Endothelial proliferation assay	EC proliferation	Proliferation of ECs in response to angiogenic factors or inhibitors	MTS assay, BrdU or ^{3}H-thymidine uptake, and PCNA or Ki-67 antigen detection	[5, 30]
Endothelial survival assay	EC survival in GF-depleted medium	The ability of exogenous factors to substitute for paracrine EC survival factors	MTS assay, ^{3}H-thymidine incorporation, apoptosis assays, and cell count	[7, 31]
Scratch/stencil ("wounding") assay	EC migration across denuded area	EC motility as element of angiogenesis	Number of cells migrated across the "wound"	[5, 30] [32, 33]
Boyden chamber assay	EC migration across a filter (with or without a matrix coating)	EC motility or invasion reflects elements of angiogenesis	Number of cells migrated across the filter	[5, 30] [34–36]
Tube formation assay	EC morphogenesis on a 2-D or in a 3-D matrix	EC network and tube formation reflect cell functionality	Tube length, number of tubes, and number of branch points	[5, 30] [37–39]
Microfiber co-culture angiogenesis assay	Capillary network formation onto matrix-implanted microfibers	EC network and tube formation resemble angiogenesis	Immunostaining, vessel length, branch points, and volume	[40]
Microfluidic co-culture system	Endothelial cell responses to GF gradients	EC network and tube formation in multicellular context	Immunostaining, visualization of endothelial structures	[5, 41]
Angiogenic sprouting from EC-coated beads	Capillary sprout formation in fibrin gels	EC sprout and tube formation from cell layers exposed to a stimulus	Immunostaining or visualization of endothelial structures	[42]
Embryoid body (EB) assay	Vascular structures of matrix-embedded EBs containing ESCs	Vasculogenesis and angiogenesis are recapitulated by endothelial progenitor cells	Whole-mount immunostaining for EC markers	[7]

Abbreviations: *BrdU* bromodeoxyuridine, *EB* embryoid body, *EC* endothelial cell, *ESCs* embryonic stem cells, *GF* growth factor, *MTS* 3-(4,5-dimethylthiazol-2-yl)-5-(3-carboxymethoxyphenyl)-2-(4-sulfophenyl)-2H-tetrazolium, *PCNA* proliferating cell nuclear antigen

Table 2
In vivo angiogenesis assays

Assay	Parameter measured	Principle	Endpoints	References
Rat mesentery window assay	New blood vessels in the mesentery	Angiogenic tissue implanted into the mesentery triggers angiogenic growth	Vessel count, density, and perfusion	[43]
Chick chorioallantoic membrane (CAM) assay	New blood vessels in CAM	Implantation of angiogenic material (e.g., tumor cells) into CAM triggers chick blood vessel formation	Vessel counts, analysis of structures, and perfusion	[5, 30] [44–46]
Zebrafish model of angiogenesis	Formation of cardinal and connecting vessels	Blood vessels are visualized in transparent fish and through the use of fluorescent tags	Vessel counts, structures, and perfusion	[5, 30] [47, 48]
Corneal micropocket angiogenesis assay	Corneal neovascularization and sprouting	Cornea is avascular and vessel ingrowth is induced by implanting pellets containing angiogenic factors	Vessel counts, length, diameter, density	[5, 49–51]
Matrigel plug angiogenesis assay (matrix invasion assay)	Recruitment of endothelial cells and formation of new blood vessels	Matrigel plugs contain angiogenic growth factors and extracellular matrix that support ingrowth of blood vessels upon subcutaneous implantation into mice	Fixed or frozen sections are stained for EC markers; and plugs can be lysed for hemoglobin content or vascular tracers in the vascular bed, as a measure of the vascular volume	[5, 26, 52, 53]
Angiogenesis chamber assays	New vessel formation between implanted nylon filters	Test substance is sandwiched between nylon mesh layers and vessels are quantified	Vessel counts, diameter, density, and perfusion	[5, 6, 54–62]
Tumor-associated angiogenesis assays	Changes in density and cellular constituents of vascular structures in a growing tumor mass in experimental animals	In situ analysis of the complete neovascularization process is assessed using vascular markers (e.g., ECs, pericytes, basement membrane)	Tumor tissues are immunostained for EC (and other) markers; vascular density, architecture maturation, and perfusion	[5, 30] [13, 63, 64]

(continued)

Table 2
(continued)

Assay	Parameter measured	Principle	Endpoints	References
Tumor-associated EC growth and sprouting assay	Measurement of EC mitogenic activity in the tumor mass	The assay distinguishes between dividing (active) and nondividing ECs	Co-staining for markers of proliferation (PCNA) and ECs (CD31, CD105)	[15]
Endothelial spheroid assay	Sprouting and network formation of EC spheroids grafted into mice	Human EC spheroids are implanted into mice and form vascular structures	Whole-mount immunostaining; or fixed, sectioned, and stained for EC and mural cell markers	[65]
Hollow fiber assay	Vascular network formation to hollow fibers	Hollow fibers containing cancer cells are used as standardized space to attract and quantify the ingrowth of new blood vessels	Microscopic imaging of tumor-associated blood vessels; testing viability of cancer cells	[66]

Abbreviations: *CAM* chorioallantoic membrane assay, *EC* endothelial cell, *PCNA* proliferating cell nuclear antigen

Table 3
Ex vivo angiogenesis assays

Assay	Parameter measured	Principle	Endpoints	References
Aortic ring assay	Vessel outgrowth from aortic explants	Outgrowth of new sprouts from ECs present in the aortic lumen and wall	Microscopic analysis of new sprouts, number of branch points, enhanced by whole-mount immunostaining	[5, 15, 67–71]
Explant angiogenesis assays	Vessel outgrowth from explants of carotid artery, saphenous vein, vena cava, thoracic aorta, fetal or adult metatarsals, placental blood vessels	Assays measure vessel outgrowth from the pre-existing ECs in the vasculature of explanted tissues	Vessel counts, number of branch points, and whole-mount immunostaining	[5, 72–79]
Retina angiogenesis assay	Vessel growth in retinal explants	Vessel growth in mouse retina is visualized microscopically	Sprout formation, vascular structures and architecture, vessel density	[80, 81]

Table 4
Assays measuring non-angiogenic vascular activities in cancer

Assay	Parameter measured	Principle	Endpoints	References
Tumor arteriogenesis and arterio-venogenesis assays	Formation of extra-tumoral "feeding" vessel in mice	Macroscopic blood vessels outside of the tumor mass undergo enlargement to meet the demands of the tumor microcirculation	Diameter of the feeding vessel, blood flow measured by ultrasound, and influx of BM cells in the vessel wall	[4, 13]
Assays for circulating ECs and EPCs	Potential for vasculogenesis	CECs and CEPs and their viability reflect the systemic regulation of tumor neovascularization and antiangiogenic therapies	FACS detection of EPCs and CECs in blood ($VEGFR2^+/CD45^-$ cells)	[82–85]
Tissue factor-dependent coagulation (TF PCA)	Cellular clotting potential	Tumor cell coagulant activity mediated by TF contributes to thrombosis and angiogenesis in cancer	Generation of activated clotting factor X (FXa)	[22, 24]

Abbreviations: *BM* bone marrow, *CEC* circulating endothelial cell, *CEP* circulating endothelial progenitor, *EC* endothelial cell, *EPC* endothelial progenitor cell, *FACS* fluorescence-activated cell sorting, *TF PCA* tissue factor procoagulant activity

While providing detailed experimental protocols for diverse processes involved in tumor neovascularization exceeds the scope of this chapter, we include the synopsis of the relevant literature and methods in Tables 1, 2, 3, and 4, for reference. In this regard, several assays have been generated for in vitro (Table 1), in vivo (Table 2), and ex vivo (Table 3) studies of angiogenesis and of related vascular processes (Table 4), in response to test substances and conditions (e.g., anti-angiogenic and pro-angiogenic factors, or tumor cells). The simplicity of these assays must, however, be balanced with their combinatorial use and careful interpretation, as they capture only small fragments of the underlying biology, and they often do not reflect the distinctive and heterogeneous properties of angiogenic circuits and regulators in different molecular tumor subtypes [14]. The protocols included in this chapter describe immuno-localization of endothelial cells (Subheading 3.1), mural cells/pericytes (Subheading 3.1), and coagulant/tissue factor-expressing cells in tissue sections in situ, as well as quantitative characterization of tissue factor activity of cultured cells.

Immuno-localization of endothelial cells in paraffin sections of tumor tissue can be accomplished using several lineage markers, such as CD31, CD34, vWF, lectin binding, and tumor endothelial

markers (TEMs) [15, 16]. Here, we describe the use of anti-CD105 (endoglin) staining of mouse tumor tissue sections, as a robust and effective strategy to highlight tumor blood vessels [17]. In this protocol, CD105 is combined with staining for Ki-67 to highlight proliferating endothelial cells specifically [13, 15, 18].

The dynamics of the tumor neovascularization process and responses to antiangiogenic therapies can be inferred from staining for markers of endothelial cells (above), basement membrane, and mural cells such as pericytes and smooth muscle cells [19, 20]. In particular, the tight pericyte coverage of endothelial tubes along with structural changes in the vascular pattern often signifies vessel maturation or normalization [3]. Here, we describe the combined use of anti-CD105 (endoglin) staining of endothelial cells and anti-alpha smooth muscle actin (aSMA) staining in mouse tumor tissue sections to reveal the changes in vessel maturation [17].

Tissue factor (TF) is a transmembrane receptor for the coagulation factor VII/VIIa, which is expressed on perivascular cells and is often upregulated by cancer cells, activated endothelium, inflammatory cells, or stroma [21]. TF renders cancer cells pro-coagulant and mediates their angiogenic and metastatic responses through fibrin deposition, or intracellular signaling transduced by protease-activated receptors and integrins [22, 23]. The expression of TF by cancer cells is often reflective of the degree and pathway of malignant transformation as documented in glioblastoma, medulloblastoma, and other malignancies [10, 14, 24]. Here, we describe an effective protocol to stain tumor sections for TF antigen.

The expression of TF by cancer cells is often indicative of their malignant transformation [22] and their ability to respond to stimulation upon exposure to TF ligands such as coagulation factor VII/VIIa. These interactions play a role in the regulation of gene expression [25], as well as pro-angiogenic, pro-inflammatory, invasive, and growth responses of cancer cells upon exposure to effectors of the coagulation system [14, 26]. Detection of tissue factor pro-coagulant activity (TF-PCA) represents a sensitive method to measure the level of biologically active TF on the surface of cancer cells. In this assay, TF is allowed to bind to activated VIIa and convert inactive coagulation factor X to an active form (Xa), which can be measured by conversion of the S-2765 chromogenic substrate. Here, we describe a simple and effective protocol to measure TF PCA using cultured cancer cells.

2 Materials

Reagents may be obtained from a number of suppliers with the exception of specific validated antibodies or products, as indicated. The compatibility with formalin-fixed tissues may differ between different antibodies which may result in high background and low

specificity. High-quality deionized water should be used to prepare all the indicated buffers and solutions. The procedures require access to general wet lab space, basic histology equipment (tissue processing and embedding stations, slides) cell culture and microscopy facilities.

1. *Slide dewaxing reagents*: 100% Xylene and 99% ethanol should be diluted as described for the intended use in immunostaining protocols.
2. *Buffers*: Dulbecco's phosphate-buffered saline (DPBS, used as supplied) and Tris-buffered saline (TBS, pH 7.6) should contain the final concentrations of 20 mM Tris and 150 mM NaCl. For Tris-buffered saline (TBS, pH 7.4), prepare the solution containing 50 mM Tris, 120 mM NaCl, 2.7 mM KCl, and 3 mg/mL BSA.
3. *Tissue permeabilization*, *antigen unmasking*, *and blocking reagents*: For permeabilization 0.3% Triton X-100 is prepared in DPBS. Vector Antigen Unmasking Solution (Vector Labs Burlington, ON) containing 1% citrate is prepared by mixing 2.5 mL of the supplied stock with 247.5 mL of distilled water. Hydrogen peroxide (H_2O_2) should be diluted to 1.5% final concentration in TBS. Bovine serum albumin (BSA) for tissue blocking is prepared at 1% concentration by dissolving 0.1 g of BSA powder in a total final volume of 10 mL DPBS. Blocking rabbit serum is prepared at 10% concentration in DPBS. For blocking tissue normal donkey serum (NDS) is used at the final concentration of 5%, prepared by diluting 200 μL of NDS stock in 4 mL of DPBS.
4. *Primary antibodies*: Immunostaining procedures described herein are sensitive to the antibodies used and we have used the following products: Anti-mouse Endoglin/CD-105 Affinity Purified Goat IgG (AF1320; R&D Systems, Minneapolis, MN, USA; used at 1:100 dilution); Anti-Ki-67 rabbit polyclonal antibody (RM-9106, ThermoFisher, Ottawa, ON, Canada; used at 1:200 dilution); Rabbit Anti-Alpha Smooth Muscle Actin Antibody (ab5694; ABCAM, Toronto, ON, Canada; used at 1:100 dilution); Sheep Anti-human TF Antibody (SATF-IG; Affinity Biologicals, Ancaster, ON, Canada; used at 1:100 to 1:10,000 dilution).
5. *Secondary antibodies*: Chicken Anti-goat, Alexa Flour 488, IgG, H + L (A21467; Life Technologies Inc., Burlington, ON, Canada; dilution 1:200) and Donkey Anti-rabbit Alexa Fluor 594 IgG, H + L (A21207; Life Technologies, Eugene, OR, USA; dilution 1:200).
6. *Immunohistochemistry reagents*, *and slide-mounting media*: Vectastain Elite kit (PK-4006) and ImPACT DAB (SK-4105), VectaMount Mounting Medium (H-5000) from Vector Labs, Burlington, ON, Canada.

7. *TF-PCA reagents and supplies*: The assay requires cell culture supplies (cell culture media, cell culture-grade trypsin/ethylenediaminetetraacetic acid (EDTA) solution, plasticware including 24-well culture plates, pipettes, biosafety cabinet), and a timer. The key assay reagents include Factor VIIa (FVIIa; ADG407act), Factor X (FX; 527), both from Sekisui Diagnostics (Lexington, MA, USA), 2 mM solution of Chromogenic Substrate (S-2765; Chromogenix, Mississauga, ON, Canada), and Rabbit Brain Thromboplastin (RBT) TF activity standard (Sigma, Oakville, ON, Canada; 2 mM/mL solution). In addition, the procedure requires preparation of the anhydrous $CaCl_2$ (100 mM), acetic acid (50%), and protein lysis buffer solutions (0.7 mL basic lysis buffer: 2 mL 10% Triton-X-100; 400 μL 0.5 M EDTA, pH 8.0; 200 μL 1 M Tris–HCl, pH 7.0; 0.175 g NaCl; 6 mL glycerol; 11.4 mL H_2O, supplemented with 170 μL of 7× Mini protease inhibitor, 10 μL of 100 mM phenylmethanesulfonyl fluoride (PMSF), 100 μL of 0.2 M sodium orthovanadate, and 50 μL 1 M sodium fluoride) as well as protein quantification reagents.

3 Methods

3.1 Fluorescent Multicolor Tissue Immunostaining (IF)

Multicolor immunofluorescent staining protocols can be challenging; yet they are increasingly used to reveal complex features of cells in their natural milieu. One practical approach to this question is to employ a three-color procedure, including staining for two different antigens (red and green fluorescence, respectively) and a nuclear counterstain (DAPI-blue). Examples of such protocols compiled in this section are relatively straightforward and amenable to modifications and to imaging by standard fluorescent microscopy (*see* **Note 1**). For practical reasons, a double immunostaining is optimized for a 3-day cycle:

1. (*Day 1*) *Dewaxing and rehydration of tissues*: Processing tissue samples, embedding, and sectioning are described in other sources easily accessible in the literature [27]. Once the sections are cut and mounted on slides the staining begins with the following steps: Place the 5 μm thick paraffin-embedded tissue sections in 100% xylene (histological xylene) in the fume hood for 10 min at room temperature followed by two xylene washes for 5 min each. Remove slides and place in three consecutive washes of 99% ethanol for 5 min each. Sequentially wash the slides in dilutions of ethanol of 95%, 80%, 70%, and 50% and then running tap water to remove any trace of ethanol. For anti-TF staining, the slides are deparaffinized and rehydrated according to a protocol provided by Abcam with slight modification, including the following sequential washes: xylene (3×7 min), xylene 1:1 with 100% ethanol (3 min),

100% ethanol (2 × 3 min), 95% ethanol (3 min), 70% ethanol (3 min), and 50% ethanol (3 min). Rinse under cold tap water.

2. (*Day 1*) *Microwave antigen retrieval*: Place roughly 200 mL of the 1% vector antigen unmasking solution in a glass Coplin jar (250 mL) and heat the solution in a microwave to 95 °C using a thermometer or temperature probe. At 95 °C, place the rack of slides into the antigen retrieval solution. Replace the Coplin jar into the microwave and ensure that the temperature is maintained at 95 °C to 100 °C by periodic heating of the microwave for 15 min. At the end of the 15 min, and using a glove to protect against the hot glass surface, remove the Coplin jar and place on the bench at RT for another 20 min. After 20 min, transfer the slide rack to a clean Coplin jar containing DPBS. Perform three DPBS washes of 5 min each of the slides. For anti-TF staining, antigen retrieval is carried out using antigen unmasking solution for 20 min at 98 °C.
3. (*Day 1*) *Permeabilization*: Prepare a solution of 3% Triton-X in DPBS. Place slides in Triton-X solution for 10 min at RT. At the completion of the permeabilization step, rinse slides in three washes of DPBS for 5 min each. For anti-TF staining, the slides are allowed to cool for 30 min after antigen retrieval and are subsequently washed with running tap water (10 min), TBS (2 × 5 min), and TBS containing 0.025% Triton X-100 (2 × 5 min).
4. (*Day 1*) *Blocking unspecific signal*: Prepare a solution of 1% bovine serum albumin. Mix thoroughly and then filter using a 0.22 μm syringe filter. Remove each slide from DPBS, wipe away excess solution, and place 1% BSA on the entire tissue. Place the slide with 1% BSA in a humidified chamber and incubate for 30 min. For anti-TF staining the slides are blocked for 2 h with 10% rabbit serum in TBS containing 1% BSA.
5. (*Day 1*) *Primary antibody binding—first staining*: While incubating in BSA, make the working solution of the primary antibody (*see* **Note 5**). For Endoglin staining a 1:100 dilution of goat anti-mouse Endoglin/CD105 (AF1320, mouse Endoglin Affinity Purified Goat IgG, R&D Systems, Minneapolis, MN, USA) in DPBS gives strong and specific signal. Maintain the antibody working solution on wet ice (4 °C) until ready for use. When the blocking step is complete, remove a slide from the humidified chamber, remove excess blocking buffer, and wipe the edge of the tissue with blotting paper. Without letting the tissue dry, add enough primary antibody to cover the tissue completely, and place it in the humidified chamber overnight at 4 °C. Complete the same procedure with the other slides. For anti-TF staining, the slides are incubated at 4 °C overnight in a humidified chamber with the TF primary antibody (sheep

anti-human TF, SATF-IG, Affinity Biologicals) at 1:10,000 dilution in TBS containing 1% BSA. While anti-TF staining can be combined with other multicolor protocols, it can also be reduced to a faster immunochistochemical cycle aiming at visualization of TF expression in tumor tissue. In such a case, the slides exposed to the primary antibody are processed through the following steps: the slides are washed (TBS containing 0.025% Triton X-100: 2 × 5 min) and then blocked for endogenous peroxidase activity for 1 h at 4 °C in a H_2O_2 solution; the Vectastain Elite kit for sheep IgG antibody detection is used according to the manufacturer's instructions for incubation with the biotinylated secondary antibody and ABC reagent; and ImPACT DAB (3,3′-diaminobenzidine) peroxidase substrate was used to detect biotinylation prior to counterstaining with hematoxylin or methyl green.

6. (*Day 2*) *Secondary antibody—first staining*: Continue with the double-staining protocol, remove the slides from the humidified chamber, and wash off the primary antibody by placing slides in a Coplin jar of DPBS for 5 min. Repeat the washes three times for 5 min each. Make up a solution of 1:200 dilution of the respective secondary antibodies. This includes the chicken anti-goat Alexa 488 antibody (for anti-CD105 staining). Remove the excess of DPBS by wiping the edge of the tissue and then apply enough of secondary antibody to completely cover the surface of the tissue section. Incubate in the humidified chamber for 45 min. Immediately thereafter, tip the slides to remove the secondary antibody and wash in DPBS in a Coplin jar for a total of five times in DPBS for 5 min each (also *see* **Note 6**). While the slides are still wet, verify the quality of staining under the fluorescent microscope (CD105-positive endothelial cells located around blood vessel lumens should exhibit bright and specific green fluorescence).
7. (*Day 2*) *Blocking tissues for the second staining*: Second stain is intended to reveal the functional states of endothelial cells such as proliferation (Ki67) or association with pericytes/smooth muscle cells (αSMA), the latter a feature of mature blood vessels. For anti-Ki-67 and anti-αSMA antibodies, the blocking buffer consists of 5% normal donkey serum (NDS). Make the solution of 5% NDS (by diluting 200 μL of NDS in 4 mL of DPBS). Wipe excess solution from the edge with a tissue and place enough 5% NDS to cover the tissue completely (*see* also **Notes 2–4**). Place the slide in a humidified chamber for 30 min.
8. (*Day 2*) *Primary antibody binding—second staining*: Make up the working dilutions of the respective primary antibodies for the second staining. For the Ki-67 immunostaining, the primary antibody should be diluted at 1:200 in 0.3% Triton X-100 in DPBS. For the αSMA staining make a 1:100 dilution

using the blocking buffer as diluent. Before applying the antibody solutions, remove the blocking buffer by blotting the excess of liquid and add enough primary antibody to completely cover the tissue section (never wash the slides after the blocking step as the blocking buffer must remain on the tissue to prevent unspecific binding of the antibody). Place the slides in a humidified chamber and place in the refrigerator at 4 °C overnight.

9. (*Day 3*) *Secondary antibody—second staining*: Prepare the solutions of the appropriate secondary antibodies. For staining with anti-Ki-67 and anti-αSMA primary rabbit antibodies, prepare the anti-rabbit secondary antibody (Alexa Fluor donkey anti-rabbit 594 IgG (H + L)) at a dilution of 1:200 in 0.3% Triton X-100 in DPBS. Leave the solution on ice. Remove the slides from the refrigerator and place in 0.3% Triton X-100/DPBS for five washes of 3 min each at room temperature (RT). Add the prepared secondary antibody solution to completely cover the tissue and place the slides in a humidified chamber at RT. Incubate with the secondary antibody for 45 min. When the incubation is complete, remove the slides and place them in 0.3% Triton X-100/DPBS for five washes of 3 min each. Using the fluorescent microscope (while the tissues are still wet), quickly examine whether proper staining has been achieved; for example Ki-67 will appear as bright red nuclear staining in dividing cells, and other patterns of staining such as diffuse or nonnuclear stain may signify lack of specificity.
10. (*Day 3*) *Mounting slides for storage for analysis*: Mount slides by placing the cover slip over the tissue using Vectashield Hard Set Mounting Media with DAPI. This will highlight nuclei with blue fluorescence while protecting the tissue. Maintain slides in the dark and in a cold space (refrigerator, cold room) until used for analysis.
11. *Slide viewing, interpretation, and image analysis*: Stained tissues may be examined visually and micro photographed at different times after completion of the procedure. Image acquisition can be performed using appropriate fluorescent or confocal microscope while ensuring that any unnecessary and protracted exposure to microscope or laser light is avoided, as this may lead to photo-bleaching of the signal. Fluorescent double staining is particularly useful in seeking information as to vascular geometry (e.g., density) and functional state of cells within and around blood vessels. For example, the vascular caliber and density could be combined with the analysis of numbers, percentages, and distribution of proliferating endothelial cells ($CD105^+/Ki67^+$) versus their quiescent counterparts ($CD105^+/Ki67^-$). These features may exhibit regional differences within tumor tissue as shown in Fig. 1. In this

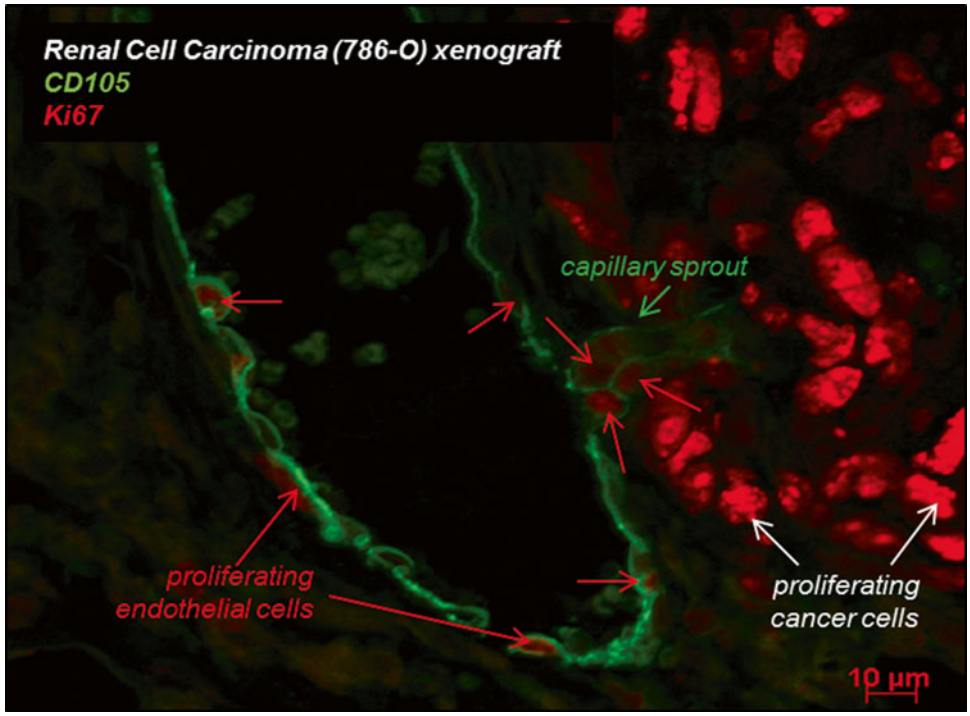

Fig 1 Immunofluorescent staining of tumors for proliferating endothelium. Since normal endothelial cells remain largely quiescent, proliferation of these cells is a hallmark of vascular growth (angiogenesis and arteriogenesis). Human clear cell renal cell carcinoma (ccRCC) cells, 786-O, were injected subcutaneously into immune-deficient SCID mice and the resulting tumors were collected, fixed, sectioned, and co-stained for the endothelial cell marker (CD105, *green*) and proliferation marker (Ki-67, *red*). Nuclei of proliferating endothelial cells within a larger vessels (arteriogenesis) and capillary sprout (angiogenesis) are clearly positive for Ki-67, which also stains CD105-negative tumor cells. Image adapted with permission from [13]

image, proliferating endothelial cells can be found mostly in vascular sprouts, or in tumor regions undergoing vascular remodeling, such as segments within the wall of larger feeding vessels. Of note is the fact that dividing cancer cells surrounding blood vessels exhibit $CD105^{-}/Ki67^{+}$ staining pattern. In Fig. 2, double staining for CD105 and αSMA reveals blood vessels containing pericyte coverage (mature blood vessel). Layers of pericytes or mural cells (smooth muscle cells in larger vessels) are visualized as structures with the $CD105^{-}/aSMA^{+}$ staining pattern located in the outer aspect of the vessel wall. Immunostaining also offers the opportunity to perform some quantification of the features of interest. Using the protocol outlined above, dividing endothelial cells or mature blood vessels may be enumerated under high magnification (400×) and expressed as numbers per high-power field or per number of blood vessels. Such assessment is often performed to compare vascular features under different treatment conditions, in

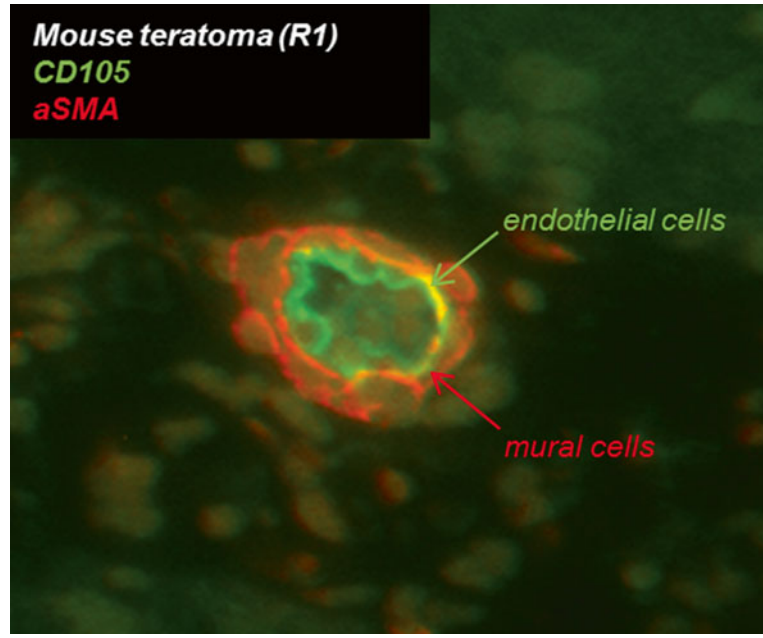

Fig. 2 Immunofluorescent staining of tumors for endothelial and mural cells. Murine embryonic stem cells (R1) were injected into immune-deficient SCID mice to form aggressive teratoma. The tumor tissue was collected, fixed, and stained for markers of endothelial cells (CD105, *green*) and mural cells, such as pericytes and smooth muscle cells (αSMA, *red*). The image depicts the close association of mural and endothelial cells in a small arteriole. Image adapted from [29]

distinct tumor types, or between micro-regions within the same tumor (e.g., center and periphery, or in hypoxic regions). Another aspect of the vascular milieu is revealed by immunohistochemical staining for TF expression. In the protocol, described TF-positive cells are distinguished by brown coloration, often in regions of hypoxia, inflammation, or malignant growth. This signal can be quantified as percent area stained for TF multiplied by average staining intensity, as evaluated by independent blinded observers. The percent area is measured using the ImageJ software, and the staining intensity is assessed on an arbitrary scale of 1–4. However, the specific nature of tissue analysis depends on the underlying research question as described earlier [13, 15, 18, 28].

3.2 Tissue Factor Procoagulant Activity Assay (TF-PCA)

Measurement of TF procoagulant activity of cancer cells is useful and complementary to the aforementioned staining of tissues and cells for the TF antigen. The presence of TF staining does not always correspond to the cellular ability to activate the coagulation cascade as intracellular, encrypted TF, or alternatively spliced TF are inactive in this respect. The simple and effective quantitative TF-PCA can be performed on cultured cancer cells:

1. *Establishing adherent cultures of cancer cells.* Plate each cell line or condition in quadruplicates in a 24-well plate, and grow cells to 70–80% confluence. The cells should be seeded at densities that would not require prolonged culture to achieve these conditions (ideally cells should be grown for 1–3 days) or lead to uneven distribution of cells in wells, altered viability, or other unspecific differentials (*see* **Note** 7).
2. *Preparation of the TF standard curve and stock solutions.* Once cell cultures are at optimal density, the 1-day TF-PCA begins with preparation of the TF standard curve. To accomplish this, serial dilutions of the Rabbit Brain Thromboplastin (RBT; Sigma 44213) standard, a source of TF/thromboplastin activity, are prepared in TBS, pH 7.4, according to Table 5, and 200 µL aliquots of each dilution are added into empty wells of a 24-well plate. Prepare the stock solutions of all reagents in quantities sufficient for all wells containing cells or standard. From these ingredients, prepare the reagent mix containing 281 µL TBS, pH 7.4, 2 µL 5 nM FVIIa, and 2 µL 150 nM FXa per well.
3. *Setting up the TF-PCA reaction:* Wash the cells three times with pre-warmed TBS, pH 7.4. Add 285 µL of reagent mix solution to each well. At 10-s intervals, add 15 µL of 100 mM $CaCl_2$ to each well and incubate the cells with solutions for 30 min at 37 °C (this is important as TF activity reaction is time sensitive).
4. *Developing color reaction*. While the cells are incubating, add 20 µL of chromogenic substrate to wells of 96-well plate. At 10-s intervals in the order as in the previous step, add 200 µL of solution from each well of the 24-well plate to the 20 µL substrate in the 96-well plate. This will mix the activated factor X (FXa) from wells containing cancer cells (or standard) with the chromogenic substrate, the cleavage of which results in a color reaction. This reaction is indicative of the FXa activity, which is quantitatively generated by the TF/VIIa complex on the surface of cancer cells. Incubate for 3–5 min at 37 °C. At 10-s intervals, add 20 µL of 50% acetic acid to stop the reaction.

Table 5
Dilution table

	Dilution			
Component	**1**	**0.5**	**0.25**	**0.125**
RBT standard (µL)	3	450	450	450
TBS, pH 7.4 (µL)	897	450	450	450
Total volume (µL)	900	900	900	900

5. *Reading the TF-PCA reaction*. Place the 96-well plate containing samples and RBT standards in a plate reader and record the absorbance at 405 nm.
6. *Normalization*. Wash the 24-well plate twice with PBS, and lyse the cells for protein quantification. Interpolate the units of TF activity from the RBT standard curve, and normalize to total protein (μg). Additional modification, use of TF-neutralizing antibodies, and related methods to assess the interplay between the coagulation system and the tumor vasculature are reviewed elsewhere [1–3].

4 Notes

1. It is essential to use positive and negative controls with every immunostaining (usually tissue samples known to exhibit the expression of the respective markers). It is also essential to pay attention to subcellular localization of the staining, e.g., membrane/cytoplasmic for CD105 or nuclear for Ki67.
2. Do not place the slides in direct contact with running water but rather allow water to flush over the slides.
3. When applying the primary antibody completely cover the surface of tissue sections and never wash the slides after the blocking step, as the blocking buffer must remain on the tissue to prevent unspecific binding.
4. When removing the blocking buffer, wipe the edge of the tissue with blotting paper and never let tissue dry.
5. For double staining, carefully select the antibodies. For example, the secondary antibody of the second stain must be devoid of any cross-reactivity against all the primary and secondary antibodies used in the first stain. It must also be matched to the species and class of the primary immunoglobulin in the second stain, and carry a fluorophore that has non-overlapping emission spectra with the first staining cycle. It is also practical to avoid antibodies reactive with host tissue immunoglobulins (e.g., anti-mouse antibodies to stain mouse tumors), as blocking off these signals often complicates the protocol.
6. After incubation with the secondary antibody and washing, and while slides are still wet, check one slide to verify, under fluorescence, if the staining was successful (vessels will appear bright green).
7. For TF-PCA, having a proper cell culture and control cells and especially timing the reaction using 10-s intervals, as indicated, are essential as FXa generation and substrate cleavage are dynamic processes.

Acknowledgements

Financial support: This work was supported by the operating grants from Canadian Institutes for Health Research (CIHR Foundation grant; CIHR; MOP 102736, MOP 111119), Cancer Research Society (CRS), and Canadian Cancer Society Innovation to Impact (CCSRI) to J.R., who is also a recipient of the Jack Cole Chair in Pediatric Hematology/Oncology. Studentship support for E.D. and infrastructure funds were provided by Fonds de Recherche du Québec en Santé (FRQS). E.D. was also supported by the Piccoli 401 Bike Challenge Fund.

References

1. Folkman J (2007) Angiogenesis: an organizing principle for drug discovery? Nat Rev Drug Discov 6:273–286
2. Rak J (2009) Ras oncogenes and tumour vascular interface. In: Thomas-Tikhonenko A (ed) Cancer genome and tumor microenvironment. Springer, New York, pp 133–165
3. Carmeliet P, Jain RK (2011) Molecular mechanisms and clinical applications of angiogenesis. Nature 473:298–307
4. Nagy JA, Dvorak HF (2012) Heterogeneity of the tumor vasculature: the need for new tumor blood vessel type-specific targets. Clin Exp Metastasis 29:657–662
5. Irvin MW, Zijlstra A, Wikswo JP, Pozzi A (2014) Techniques and assays for the study of angiogenesis. Exp Biol Med (Maywood) 239: 1476–1488
6. Jain RK, Schlenger K, Hockel M, Yuan F (1997) Quantitative angiogenesis assays: progress and problems. Nat Med 3:1203–1208
7. Goodwin AM (2007) In vitro assays of angiogenesis for assessment of angiogenic and anti-angiogenic agents. Microvasc Res 74:172–183
8. Welti J, Loges S, Dimmeler S, Carmeliet P (2013) Recent molecular discoveries in angiogenesis and antiangiogenic therapies in cancer. J Clin Invest 123:3190–3200
9. Brat DJ, Van Meir EG (2004) Vaso-occlusive and prothrombotic mechanisms associated with tumor hypoxia, necrosis, and accelerated growth in glioblastoma. Lab Invest 84:397–405
10. Magnus N, Gerges N, Jabado N, Rak J (2013) Coagulation-related gene expression profile in glioblastoma is defined by molecular disease subtype. J Thromb Haemost 11:1197–1200
11. Tehrani M, Friedman TM, Olson JJ, Brat DJ (2008) Intravascular thrombosis in central nervous system malignancies: a potential role in astrocytoma progression to glioblastoma. Brain Pathol 18:164–171
12. Yu JL, Rak JW (2003) Host microenvironment in breast cancer development: inflammatory and immune cells in tumour angiogenesis and arteriogenesis. Breast Cancer Res 5:83–88
13. Meehan B, Dombrovsky A, Magnus N, Rak J (2015) Arteriogenic expansion of extratumoral macrovessels—impact of vascular ageing. Neoplasma 62:372–383
14. D'Asti E, Kool M, Pfister SM, Rak J (2014) Coagulation and angiogenic gene expression profiles are defined by molecular subgroups of medulloblastoma: evidence for growth factor-thrombin cross-talk. J Thromb Haemost 12:1838–1849
15. Klement H, St CB, Milsom C, May L, Guo Q, Yu JL, Klement P, Rak J (2007) Atherosclerosis and vascular aging as modifiers of tumor progression, angiogenesis, and responsiveness to therapy. Am J Pathol 171:1342–1351
16. Weidner N, Semple JP, Welch WR, Folkman J (1991) Tumor angiogenesis and metastasis—correlation in invasive breast carcinoma. N Engl J Med 324:1–8
17. Meehan B, Garnier D, Dombrovsky A, Lau K, D'Asti E, Magnus N, Rak J (2014) Ageing-related responses to antiangiogenic effects of sunitinib in atherosclerosis-prone mice. Mech Ageing Dev 140:13–22
18. Meehan B, Appu S, St CB, Rak-Poznanska K, Klotz L, Rak J (2011) Age-related properties of the tumour vasculature in renal cell carcinoma. BJU Int 107:416–424
19. Benjamin LE, Golijanin D, Itin A, Pode D, Keshet E (1999) Selective ablation of immature blood vessels in established human tumors follows vascular endothelial growth factor withdrawal. J Clin Invest 103:159–165

20. Mancuso MR, Davis R, Norberg SM, O'Brien S, Sennino B, Nakahara T, Yao VJ, Inai T, Brooks P, Freimark B, Shalinsky DR, Hu-Lowe DD, McDonald DM (2006) Rapid vascular regrowth in tumors after reversal of VEGF inhibition. J Clin Invest 116:2610–2621
21. Contrino J, Hair G, Kreutzer DL, Rickles FR (1996) In situ detection of tissue factor in vascular endothelial cells: correlation with the malignant phenotype of human breast disease. Nat Med 2:209–215
22. Yu JL, May L, Lhotak V, Shahrzad S, Shirasawa S, Weitz JI, Coomber BL, Mackman N, Rak JW (2005) Oncogenic events regulate tissue factor expression in colorectal cancer cells: implications for tumor progression and angiogenesis. Blood 105:1734–1741
23. van den Berg YW, Osanto S, Reitsma PH, Versteeg HH (2012) The relationship between tissue factor and cancer progression: insights from bench and bedside. Blood 119:924–932
24. Magnus N, Garnier D, Rak J (2010) Oncogenic epidermal growth factor receptor up-regulates multiple elements of the tissue factor signaling pathway in human glioma cells. Blood 116: 815–818
25. Albrektsen T, Sorensen BB, Hjorto GM, Fleckner J, Rao LV, Petersen LC (2007) Transcriptional program induced by factor VIIa-tissue factor, PAR1 and PAR2 in MDA-MB-231 cells. J Thromb Haemost 5:1588–1597
26. Magnus N, Garnier D, Meehan B, McGraw S, Lee TH, Caron M, Bourque G, Milsom C, Jabado N, Trasler J, Pawlinski R, Mackman N, Rak J (2014) Tissue factor expression provokes escape from tumor dormancy and leads to genomic alterations. Proc Natl Acad Sci U S A 111:3544–3549
27. Erickson HS, Gillespie JW, Emmert-Buck MR (2008) Tissue microdissection. Methods Mol Biol 424:433–448
28. D'Asti E, Huang A, Kool M, Meehan B, Chan JA, Jabado N, Korshunov A, Pfister SM, Rak J (2016) Tissue factor regulation by miR-520g in primitive neuronal brain tumor cells: a possible link between oncomirs and the vascular tumor microenvironment. Am J Pathol 186:446–459
29. Yu J, May L, Milsom C, Anderson GM, Weitz JI, Luyendyk JP, Broze G, Mackman N, Rak J (2008) Contribution of host-derived tissue factor to tumor neovascularization. Arterioscler Thromb Vasc Biol 28:1975–1981
30. Staton CA, Reed MW, Brown NJ (2009) A critical analysis of current in vitro and in vivo angiogenesis assays. Int J Exp Pathol 90:195–221
31. Rak J, Mitsuhashi Y, Bayko L, Filmus J, Shirasawa S, Sasazuki T, Kerbel RS (1995) Mutant ras oncogenes upregulate VEGF/VPF expression: implications for induction and inhibition of tumor angiogenesis. Cancer Res 55:4575–4580
32. Liang CC, Park AY, Guan JL (2007) In vitro scratch assay: a convenient and inexpensive method for analysis of cell migration in vitro. Nat Protoc 2:329–333
33. Ashby WJ, Wikswo JP, Zijlstra A (2012) Magnetically attachable stencils and the non-destructive analysis of the contribution made by the underlying matrix to cell migration. Biomaterials 33:8189–8203
34. Boyden S (1962) The chemotactic effect of mixtures of antibody and antigen on polymorphonuclear leucocytes. J Exp Med 115:453–466
35. Alessandri G, Raju K, Gullino PM (1983) Mobilization of capillary endothelium in vitro induced by effectors of angiogenesis in vivo. Cancer Res 43:1790–1797
36. Albini A, Benelli R, Noonan DM, Brigati C (2004) The "chemoinvasion assay": a tool to study tumor and endothelial cell invasion of basement membranes. Int J Dev Biol 48:563–571
37. Arnaoutova I, Kleinman HK (2010) In vitro angiogenesis: endothelial cell tube formation on gelled basement membrane extract. Nat Protoc 5:628–635
38. Lawley TJ, Kubota Y (1989) Induction of morphologic differentiation of endothelial cells in culture. J Invest Dermatol 93:59S–61S
39. Kanzawa S, Endo H, Shioya N (1993) Improved in vitro angiogenesis model by collagen density reduction and the use of type III collagen. Ann Plast Surg 30:244–251
40. Weinandy S, Laffar S, Unger RE, Flanagan TC, Loesel R, Kirkpatrick CJ, Van ZM, Hermanns-Sachweh B, Klee D, Jockenhoevel S (2014) Biofunctionalized microfiber-assisted formation of intrinsic three-dimensional capillary-like structures. Tissue Eng Part A 20:1858–1869
41. Shin Y, Han S, Jeon JS, Yamamoto K, Zervantonakis IK, Sudo R, Kamm RD, Chung S (2012) Microfluidic assay for simultaneous culture of multiple cell types on surfaces or within hydrogels. Nat Protoc 7:1247–1259
42. Nakatsu MN, Hughes CC (2008) An optimized three-dimensional in vitro model for the analysis of angiogenesis. Methods Enzymol 443:65–82. doi:10.1016/S0076-6879(08)02004-1
43. Norrby KC (2011) Rat mesentery angiogenesis assay. J Vis Exp 52:pii: 3078
44. Ribatti D, Nico B, Vacca A, Presta M (2006) The gelatin sponge-chorioallantoic membrane assay. Nat Protoc 1:85–91
45. Ausprunk DH, Knighton DR, Folkman J (1975) Vascularization of normal and neo-

plastic tissues grafted to the chick chorioallantois. Role of host and preexisting graft blood vessels. Am J Pathol 79:597–618

46. Vogel HB, Berry RG (1975) Chorioallantoic membrane heterotransplantation of human brain tumors. Int J Cancer 15:401–408
47. Weinstein BM, Stemple DL, Driever W, Fishman MC (1995) Gridlock, a localized heritable vascular patterning defect in the zebrafish. Nat Med 1:1143–1147
48. Serbedzija GN, Flynn E, Willett CE (1999) Zebrafish angiogenesis: a new model for drug screening. Angiogenesis 3:353–359
49. Kenyon BM, Voest EE, Chen CC, Flynn E, Folkman J, D'Amato RJ (1996) A model of angiogenesis in the mouse cornea. Invest Ophthalmol Vis Sci 37:1625–1632
50. Gimbrone MA Jr, Leapman SB, Cotran RS, Folkman J (1973) Tumor angiogenesis: iris neovascularization at a distance from experimental intraocular tumors. J Natl Cancer Inst 50:219–228
51. Gimbrone MA Jr, Cotran RS, Leapman SB, Folkman J (1974) Tumor growth and neovascularization: an experimental model using the rabbit cornea. J Natl Cancer Inst 52:413–427
52. Akhtar N, Dickerson EB, Auerbach R (2002) The sponge/Matrigel angiogenesis assay. Angiogenesis 5:75–80
53. Passaniti A (2004) In vivo angiogenesis assays. In: Augustin H (ed) Methods in endothelial cell biology. Springer, Berlin, pp 207–222
54. Oikawa T, Sasaki M, Inose M, Shimamura M, Kuboki H, Hirano S, Kumagai H, Ishizuka M, Takeuchi T (1997) Effects of cytogenin, a novel microbial product, on embryonic and tumor cell-induced angiogenic responses in vivo. Anticancer Res 17:1881–1886
55. Sandison JC (1924) A new method for the microscopic study of living growing tissues by the introduction of transparent chamber in the rabbit's ear. Anat Rec 28:281–287
56. Clark ER, Kirby-Smith HT, Rex RO, Williams RG (1930) Recent modifications in the method of studying living cells and tissues in transparent chambers inserted in the rabbit's ear. Anat Rec 47:187–211
57. Clark ER, Clark EL (1932) Observations on living preformed blood vessels as seen in transparent chamber inserted into the rabbit's ear. Am J Anat 49:441–477
58. Ide AG, Baker NH, Warren SL (1939) Vascularization of the Brown Pearce rabbit epithelioma transplant as seen in the transparent ear chamber. Am J Roentgenol 42:891–899
59. Algire GH (1943) An adaptation of the transparent-chamber technique to the mouse. J Natl Cancer Inst 4:1–11
60. Papenfuss HD, Gross JF, Intaglietta M, Treese FA (1979) A transparent access chamber for the rat dorsal skin fold. Microvasc Res 18:311–318
61. Endrich B, Asaishi K, Gotz A, Messmer K (1980) Technical report—a new chamber technique for microvascular studies in unanesthetized hamsters. Res Exp Med (Berl) 177:125–134
62. Lehr HA, Leunig M, Menger MD, Nolte D, Messmer K (1993) Dorsal skinfold chamber technique for intravital microscopy in nude mice. Am J Pathol 143:1055–1062
63. Baluk P, McDonald DM (2008) Markers for microscopic imaging of lymphangiogenesis and angiogenesis. Ann N Y Acad Sci 1131:1–12. doi:10.1196/annals.1413.001
64. Benjamin LE, Hemo I, Keshet E (1998) A plasticity window for blood vessel remodelling is defined by pericyte coverage of the preformed endothelial network and is regulated by PDGF-B and VEGF. Development 125:1591–1598
65. Laib AM, Bartol A, Alajati A, Korff T, Weber H, Augustin HG (2009) Spheroid-based human endothelial cell microvessel formation in vivo. Nat Protoc 4:1202–1215
66. Phillips RM, Pearce J, Loadman PM, Bibby MC, Cooper PA, Swaine DJ, Double JA (1998) Angiogenesis in the hollow fiber tumor model influences drug delivery to tumor cells: implications for anticancer drug screening programs. Cancer Res 58:5263–5266
67. Nicosia RF, Tchao R, Leighton J (1982) Histotypic angiogenesis in vitro: light microscopic, ultrastructural, and radioautographic studies. In Vitro 18:538–549
68. Aplin AC, Fogel E, Zorzi P, Nicosia RF (2008) The aortic ring model of angiogenesis. Methods Enzymol 443:119–36. doi:10.1016/S0076-68796879(08)02007-7
69. Burbridge MF, West DC (2001) Rat aortic ring: 3D model of angiogenesis in vitro. Methods Mol Med 46:185–204
70. Zhu WH, Nicosia RF (2002) The thin prep rat aortic ring assay: a modified method for the characterization of angiogenesis in whole mounts. Angiogenesis 5:81–86
71. Reed MJ, Karres N, Eyman D, Vernon RB (2007) Culture of murine aortic explants in 3-dimensional extracellular matrix: a novel, miniaturized assay of angiogenesis in vitro. Microvasc Res 73:248–252
72. Nicosia RF, Zhu WH, Fogel E, Howson KM, Aplin AC (2005) A new ex vivo model to study venous angiogenesis and arterio-venous anastomosis formation. J Vasc Res 42:111–119
73. Stiffey-Wilusz J, Boice JA, Ronan J, Fletcher AM, Anderson MS (2001) An ex vivo angiogenesis assay utilizing commercial porcine

carotid artery: modification of the rat aortic ring assay. Angiogenesis 4:3–9

74. Lamfers ML, Aalders MC, Grimbergen JM, de Vries MR, Kockx MM, Van HV, Quax PH (2002) Adenoviral delivery of a constitutively active retinoblastoma mutant inhibits neointima formation in a human explant model for vein graft disease. Vascul Pharmacol 39:293–301
75. Bardy N, Karillon GJ, Merval R, Samuel JL, Tedgui A (1995) Differential effects of pressure and flow on DNA and protein synthesis and on fibronectin expression by arteries in a novel organ culture system. Circ Res 77:684–694
76. Deckers M, van der Pluijm G, Dooijewaard S, Kroon M, van HInsbergh V, Papapoulos S, Lowik C (2001) Effect of angiogenic and anti-angiogenic compounds on the outgrowth of capillary structures from fetal mouse bone explants. Lab Invest 81:5–15
77. Cackowski FC, Anderson JL, Patrene KD, Choksi RJ, Shapiro SD, Windle JJ, Blair HC, Roodman GD (2010) Osteoclasts are important for bone angiogenesis. Blood 115:140–149
78. Brown KJ, Maynes SF, Bezos A, Maguire DJ, Ford MD, Parish CR (1996) A novel in vitro assay for human angiogenesis. Lab Invest 75:539–555
79. Jung SP, Siegrist B, Wade MR, Anthony CT, Woltering EA (2001) Inhibition of human angiogenesis with heparin and hydrocortisone. Angiogenesis 4:175–186
80. Gerhardt H, Golding M, Fruttiger M, Ruhrberg C, Lundkvist A, Abramsson A, Jeltsch M, Mitchell C, Alitalo K, Shima D, Betsholtz C (2003) VEGF guides angiogenic sprouting utilizing endothelial tip cell filopodia. J Cell Biol 161:1163–1177
81. Rezzola S, Belleri M, Gariano G, Ribatti D, Costagliola C, Semeraro F, Presta M (2014) In vitro and ex vivo retina angiogenesis assays. Angiogenesis 17:429–442
82. Asahara T, Murohara T, Sullivan A, Silver M, van der Zee R, Li T, Witzenbichler B, Schatteman G, Isner JM (1997) Isolation of putative progenitor endothelial cells for angiogenesis. Science 275:964–967
83. Lyden D, Hattori K, Dias S, Costa C, Blaikie P, Butros L, Chadburn A, Heissig B, Marks W, Witte L, Wu Y, Hicklin D, Zhu Z, Hackett NR, Crystal RG, Moore MA, Hajjar KA, Manova K, Benezra R, Rafii S (2001) Impaired recruitment of bone-marrow-derived endothelial and hematopoietic precursor cells blocks tumor angiogenesis and growth. Nat Med 7:1194–1201
84. Bertolini F, Shaked Y, Mancuso P, Kerbel RS (2006) The multifaceted circulating endothelial cell in cancer: towards marker and target identification. Nat Rev Cancer 6:835–845
85. Basile DP, Yoder MC (2014) Circulating and tissue resident endothelial progenitor cells. J Cell Physiol 229:10–16

Chapter 5

A Microfluidic Method to Mimic Luminal Structures in the Tumor Microenvironment

José A. Jiménez-Torres, David J. Beebe, and Kyung E. Sung

Abstract

Microscale 3D in vitro systems have attracted significant interest as tools for cancer research because the microscale systems offer better organization of the cellular microenvironment and enhance throughput of the systems by lowering costs and reducing the amount of reagents and cells. Lumens (i.e., tubular structures) are ubiquitous in vivo being present in blood vessels, mammary ducts, prostate ducts, and the lymphatic system. Lumen structures of varying size and geometry are involved in key normal and disease processes including morphogenesis, angiogenesis, cancer development, and drug delivery. Therefore, there is a need for practical methods that create various lumen structures having different size and geometries to investigate how cells in the lumen structure respond to certain microenvironmental conditions during cancer development and progression. Here, we present a method to create multiple three-dimensional (3D) luminal structures, where parameters, such as size, geometry, and distance, can easily be controlled using simple poly-dimethylsiloxane (PDMS) micro-molds.

Key words Microfluidics, Organotypic model, 3D cell culture, Luminal structure, Tumor microenvironment

1 Introduction

Some types of cancers including breast, kidney, and prostate cancers usually arise from tubular structures known as lumens. Blood or lymphatic vessel lumens are universally used when cancer cells metastasize to secondary sites. For many years, scientists have been using animal models or two-dimensional (2D) in vitro models to study these types of cancer. Even though those traditional models have significantly enhanced our understanding of cell signaling mechanisms involved during tumor progression, the simplicity of 2D models does not faithfully recapitulate complex in vivo conditions and often exclude cell-ECM interactions. Animal models provide the complexity but to a level where it is difficult to isolate specific cell-cell and cell-ECM interactions. To overcome these limitations, we certainly need better in vitro systems that are more biologically relevant and allow the comprehensive investigation of

Josie Ursini-Siegel and Nicole Beauchemin (eds.), *The Tumor Microenvironment: Methods and Protocols*, Methods in Molecular Biology, vol. 1458, DOI 10.1007/978-1-4939-3801-8_5,

complex interactions of different components in the tumor microenvironment.

Biomimetic in vitro culture systems that recapitulate tissue structure and functions have recently been introduced and highlighted as enhanced 3D in vitro systems that capture in vivo-like structures and functions. One example of such biomimetic systems is lumen-based in vitro systems that generate tubular tissues within unique microenvironments, such as mammary ducts and blood vessels. It has been shown that the 3D spatial organization of epithelial cells in a lumen system affects the proliferation and migration of epithelial cells [1–5]. More interestingly, we have recently observed a considerable change in the levels of cytokines secreted by endothelial and epithelial cells that are cultured in in vivo-like tubular structures (i.e., a lumen) compared to the same cells cultured in 2D and simple 3D conditions [6, 7]. As lumens are ubiquitous in vivo, being present in many physiological structures including blood vessels, lymphatic vessels, mammary, renal, and prostate ducts [8–14], regulating key biological processes, there is a substantial need for practical in vitro tools that can create various lumen structures to advance our understanding of complex interactions in the tumor microenvironment.

Here, we present a poly-dimethylsiloxane (PDMS) micromolding method to fabricate 3D-embedded lumens where the size and structure of each lumen along with inter-lumen distance are highly controllable [15]. This method enables fabrication of multiple lumen structures in an ECM gel placed within a single microfluidic chamber. The multiple lumens generated in the micro chamber can be lined with different types of cells, such as endothelial cells and cancerous epithelial cells, allowing the investigation of biophysical and biochemical signaling between the cells lined in different luminal compartments (e.g., blood vessels adjacent to organ ducts or tumors). This user-friendly in vitro lumen method will facilitate the investigation of cell-cell and cell-ECM interactions in a more in vivo-like environment.

2 Materials

All solutions are prepared using autoclaved deionized (DI) water. Sterilize the reagents and handle them inside a biosafety cabinet. Sterilize the microfluidic devices using UV light for 20 min before adding any solutions to them. Store all reagents at 4 °C. Follow the biohazard disposal regulation for cell materials and waste.

2.1 Device Fabrication Components

1. SU-8 silicon mold: Silicon wafer, SU-8 100. SU-8 developer (propylene glycol methyl ether acetate (PGMEA)), iso-propyl alcohol, and DI water.

2. PDMS mixture: PDMS (Sylgard 184 silicon elastomer base) is mixed with curing agent (Sylgard 184 silicone elastomer curing agent) at a w/w ratio of 10:1, respectively.
3. Desiccator.
4. Transparency films and 10 lb flat weights.
5. Hypodermic needles (25G for lumens with a diameter of approximately 300 μm). Lumen diameter can be adjusted by using different gauge needles.
6. Glass-bottom dishes.
7. Plasma cleaner for bonding: Oxygen (O_2) plasma is used in a plasma cleaner (Femto, Thierry Corp., Royal Oak, MI) to oxidize PDMS and glass surfaces for creating an irreversible seal.
8. Device coating solution: 2% (v/v) of poly(ethyleneimine) (PEI) diluted in DI water and 0.1% (v/v) of glutaraldehyde (GA) diluted in DI water. Prepare approximately 1 ml of both reagents every time when coating the surface of devices (*see* **Note 1**).

2.2 Collagen Preparation

1. Collagen dilution buffer: Five times concentrated phosphate-buffered solution (5× PBS) in 80 ml DI water: 4 g NaCl, 0.1 g KCl, 0.72 g, and 0.12 g. Adjust pH to 7.4 with HCl and finally adjust volume to 100 ml DI water. In a biosafety cabinet, filter the solution using a 0.22 μm filter. Aliquot and store at 4 °C.
2. Collagen neutralization buffer: 0.5 N Sodium hydroxide (NaOH). For 0.5 N NaOH solution, weigh 1 g of NaOH and dilute in 50 ml of DI water. In a biosafety cabinet, filter the solution using a 0.22 μm filter. Aliquot and store at 4 °C.
3. High-concentration collagen type 1 from rat tail (approximately 10 mg/ml).

2.3 Sample Fixation and Staining

1. Fixation solution: 4% Paraformaldehyde. Dilute 10 ml 16% paraformaldehyde in 10 ml of 2× PBS for a concentration of 8% paraformaldehyde in 1× PBS. Dilute again with 20 ml of 1× PBS for a final concentration of 3% paraformaldehyde.
2. Washing buffer: Prepare 1× PBS with 0.1% Tween-20.
3. Cell permeabilization buffer: 0.1% Triton X-100. Add 10 μl of Triton X-100 in 100 ml of 1× PBS.
4. Blocking buffer: 3% (w/v) Bovine serum albumin with 0.1% Tween-20.
5. Cell staining: Dilute appropriate stain or antibodies following the manufacturer's recommended dilution ratio in the blocking buffer.

3 Methods

Device assembly can proceed under non-sterile conditions. Following device sterilization, all experimental procedures should be performed in a sterile biosafety cabinet. Carry out all methods at room temperature unless otherwise indicated.

3.1 SU-8 Mold Preparation

1. Fabricate two separate SU-8 molds for the top and bottom halves of the microfluidic channels following soft lithography steps listed below (*see* Fig. 1).
2. Design the mold masks (*see* Fig. 1d) using the drawing software of your preference (*see* **Note 2**) and print them on a transparency sheet using a high-resolution printer (*see* **Note 3**).
3. Spin the layers of SU-8 100 photoresist on a silicon wafer according to the manufacturer's specifications (*see* Fig. 1b).
4. Soft-bake the photoresist on a hot plate following the SU-8 100 manufacturer's specifications. Subsequently, place the mask over the SU-8 on the wafer and expose to UV light to

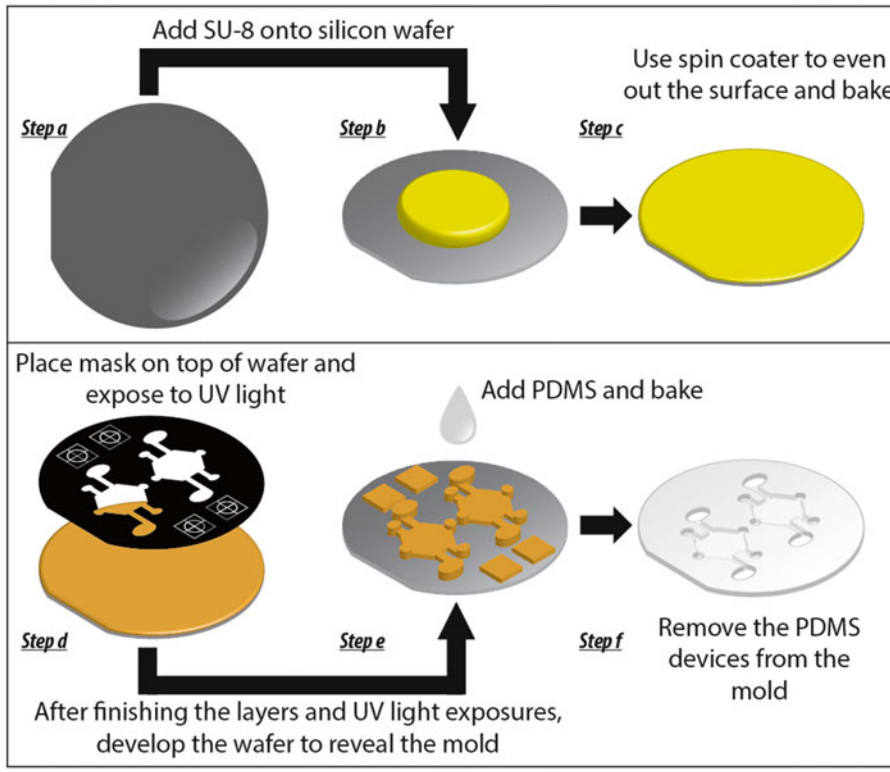

Fig. 1 Soft-lithography procedure to create molds for PDMS devices. We illustrate the steps to create the mold used to make PDMS devices. The colors and scales are not representative. A single wafer can contain many devices. For example, a 3 in. wafer can hold around 48 devices. The illustration only contains two to aid visibility

transfer the mask pattern to the photoresist (use the UV intensity value suggested in the SU-8 manufacturers specifications) (*see* Fig. 1c, d).

5. Perform a post-exposure hard-baking step as specified by the manufacturer.
6. Repeat step (b) through step (d) illustrated in Fig. 1 for the subsequent layers (*see* **Note 4**).
7. Upon completing all necessary layers, allow the mold to develop for 2 h in SU-8 developer to remove the unexposed photoresist (*see* **Note 5**).
8. To clean the mold after the developing step, rinse it with PGMEA solution, followed by three rinses of isopropyl alcohol and DI water each time (*see* **Note 6**).

3.2 PDMS Device Fabrication

1. Prepare PDMS mixture at a ratio of 1:10 curing agent and PDMS base, respectively, and degas it in a desiccator for 30 min.
2. Pour the PDMS mixture over the SU-8 silicon mold on a hot plate and cover with a transparency film.
3. Place two of 10 lb flat weights on the mold to evenly spread PDMS mixture on the SU-8 mold and bake at 80 °C for 4 h.
4. After baking, let the mold cool down to room temperature and carefully remove the PDMS devices from the mold.
5. Use a pair of tweezers to remove any remaining PDMS film that may block the ports and the bottom-layer chamber opening.
6. Place the PDMS devices in 70% ethanol for 30 min to clean the devices.
7. Remove from ethanol and let the devices dry.

3.3 PDMS Rod Fabrication

1. Fabricate circular cross-sectional PDMS rods by filling hypodermic needles (25G) with PDMS solution and baking the needle on a hot plate or in an oven at 100 °C for 2 h (*see* ref. 15).
2. After baking, carefully remove the PDMS rods from the needle by breaking the needle tip with a pair of needle-nose pliers, using a back-and-forth motion to expose a part of the rod, and pulling the rod out using tweezers.
3. Alternatively, the PDMS rods can be created by using micromachining. PDMS rod molds can be fabricated via CNC milling of thin (1.2 mm or smaller thickness) polystyrene sheets. Design the molds using SOLIDWORKS. After milling the molds, clamp the pieces together and fill them with PDMS solution. After filling the entire mold, place the mold on a hot plate or in an oven at 100 °C for 2 h. After baking in the oven, separate the mold pieces and collect the PDMS rods (*see* **Note 7**).

3.4 Microfluidic Device Setup

1. Bond the top and bottom halves of the PDMS microfluidic channels, resulting in the PDMS device.
2. Place the PDMS device upside down on a flat surface. Using fine-tip tweezers, place the PDMS rods in the rod placeholder channels, located near the bottom surface of the device, that connect the lumen input and output ports (*see* Figs. 2 and 3).
3. In order to tightly bond the PDMS devices to a glass surface and to create hydrophilic surfaces inside the chamber, treat the surfaces of the PDMS devices and glass dishes that are going to be bonded in a plasma chamber (*see* **Note 8**).
4. To sterilize, place the devices under UV light inside a biosafety cabinet for 10 min. From this point onward, every step needs to be performed using sterile solutions and sterile cell-culture techniques.
5. Coat the devices in 2% poly(ethyleneimine) diluted in DI water for 10 min, followed by 0.1% glutaraldehyde diluted in DI water for 30 min (*see* **Note 9**). Wash the remaining poly(ethyleneimine) and glutaraldehyde thoroughly with at least three washes of DI water (*see* **Note 10**).

3.5 Collagen Gel Preparation

1. Carry out the following steps on ice to halt the polymerization of collagen. For a collagen solution with a final concentration of 6 mg/ml, combine 80 μl of rat-tail collagen type 1 10 mg/ml with 10 μl of 10 × PBS and 3 μl of 0.5 N sodium hydroxide for a final pH of 7.4 (*see* **Note 11**).
2. Incubate the mixture on ice for 20 min (*see* **Note 12**). Finally, add 40 μl of PBS for a final collagen concentration of 6 mg/ml and a pH of 7.4. For other desired collagen concentrations, adjust the amount of PBS in the previous step to obtain a different final concentration (*see* **Note 13**).

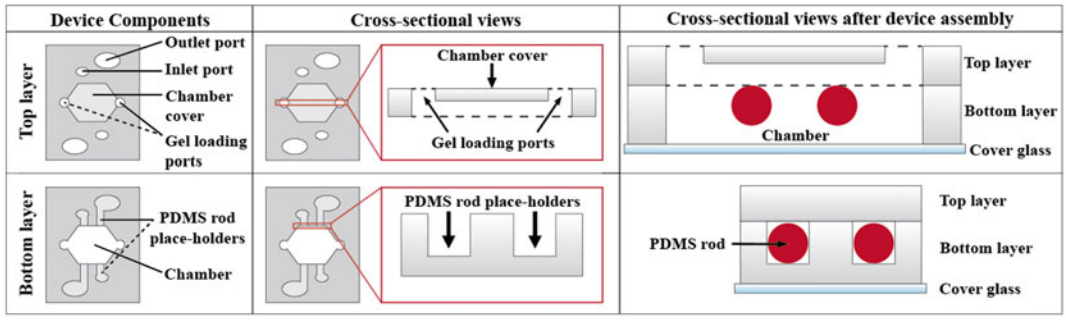

Fig. 2 Device components and cross-sectional views before and after bonding layers together. We illustrate the important components of the top and bottom layers of the device. In addition, we included cross-sectional views to show the placement of the PDMS rods

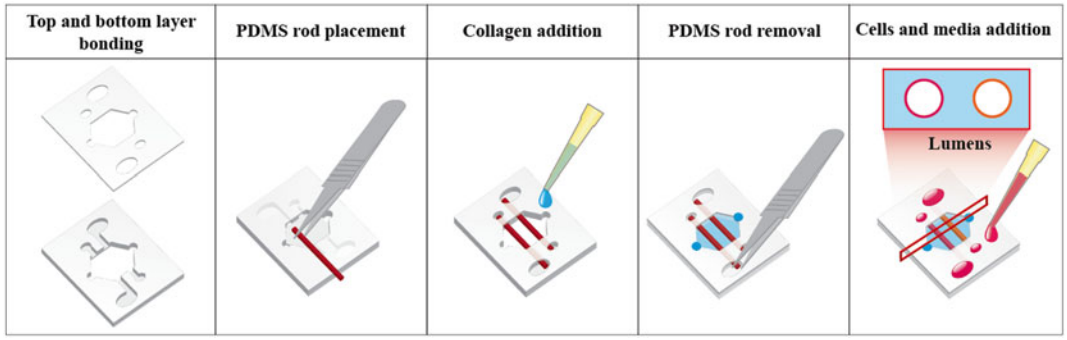

Fig. 3 Device assembly. First the device top and bottom layers are bonded together, followed by PDMS rods placement in the chamber. After performing the coatings described in Subheading 3.3, **step 5**, ECM gel is added and polymerized. PDMS rods are removed revealing the lumens that are lined with cells

3.6 Creating Lumens

1. After completing the device-coating process, load the collagen gel mixture in the chamber using one of the devices' gel-loading ports (*see* Fig. 2) (*see* **Note 14**). If handling more than one device, place the dish on ice while loading the chambers with collagen (*see* **Note 15**). After loading collagen in the chamber, incubate the device for 20 min at 37 °C to polymerize the collagen (*see* **Note 16**).
2. After incubation, pull the PDMS rods out of the polymerized collagen gel via the output port using fine tweezers, resulting in a lumen structure in the collagen gel as illustrated in Fig. 3 (*see* **Note 17**).

3.7 Cell Seeding (Blood Vessel Next to Tumor Example)

1. After removing the PDMS, fill the lumens with cells to create the biomimetic models (*see* Fig. 4).
2. For a biomimetic blood vessel, fill the lumen with 2 μl of a cell suspension of 50,000 cells/μl. Using a rotation device, rotate the dish at 2 RPM for 45 min at 37 °C to allow cell attachment uniformly throughout the lumen (*see* **Note 18**).
3. For a tumor model, a cell suspension of approximately 250,000 cells/μl in collagen (same concentration that was used to fill the chamber) is recommended. These cells are not used to line the lumen but to fill the lumen with a 3D suspension of the cells to create a tumor model.
4. Feed cell-lined lumens with 6 μl of EGM-2 medium every 24 h (*see* **Note 19**).
5. This microfluidic device is tubeless and pump free. The cell media flow through the lumen is driven by passive pumping (*see* ref. 16).

3.8 Cell Fixation and Immunofluorescent Staining

1. For cell fixation, add 4% paraformaldehyde solution inside the lumens at room temperature for 15 min (*see* **Note 20**). Remove and wash the paraformaldehyde with 0.1% Tween-PBS three times.

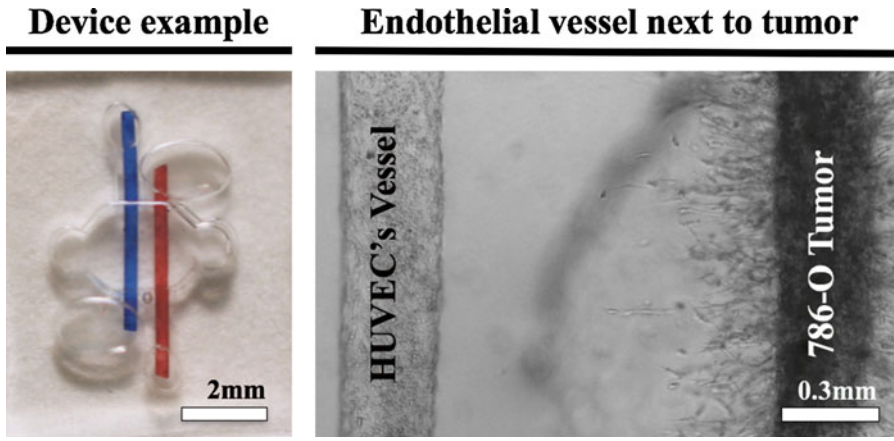

Fig. 4 A double-lumen device for co-culture. The *left-side* image shows a picture of a double-lumen device, and the *right-side* image shows an endothelial cell (HUVEC)-lined lumen and 786-O kidney cancer cell-filled lumen next to each other. The 786-O cells in co-culture invaded into the surrounding ECM gel. This model can be use to study tumor cell migration and intravasation into a biomimetic blood vessel in vitro.

2. For cell permeabilization, add 0.2% Triton® X-100 solution in the lumens for 30 min at an ambient temperature. Wash the lumens three times with 0.1% Tween-PBS.
3. As a blocking step, add 3% bovine serum albumin (BSA) and leave the solution in the lumens overnight. Next day, wash the lumens three times with 0.1% Tween PBS.
4. For staining, dilute primary antibodies in blocking buffer following the distributor-recommended dilution (*see* **Note 21**). Add the primary antibody solution in the lumens and leave it overnight at 4 °C. Wash out the primary antibodies thoroughly with 0.1% Tween-PBS every 30 min three times. Use the same procedure when adding the secondary antibodies.
5. Prior to imaging, wash the lumens thoroughly with 0.1% Tween PBS every 30 min three times to remove the dyes and minimize nonspecific background signal.

4 Notes

1. When the solution is prepared fresh every time, it works better and is more consistent than stored stock solutions.
2. To draw soft lithography masks, use the software of your preference.
3. Many companies provide the high-resolution photo plotting printing service, but some are limited in the types of files that can be processed. Some will provide file conversion for an extra fee and others are restricted to a specific file format.

Communicate with the vendor and make sure that they can process your file, and if it needs to be converted, ask for the converted file and verify that nothing has changed before printing it.

4. Each PDMS layer (top and bottom) of the device described in this protocol requires two photoresist layers and two masks. The bottom layer of the device contains an SU-8 layer of 400 μm for the first mask followed by a layer of 250 μm for the second mask. The bottom layer is constructed upside down to create the placeholder features on the silicon wafer mold (*see* Fig. 2). The top layer of the device contains an SU-8 layer of 250 μm for the first mask and a second layer of 250 μm for the second mask (*see* Fig. 2). The number of layers will be determined by the device requirements.
5. The developing time will vary depending on the amount of SU-8 to be removed. We recommend that if you are doing this for the first time, you should look at your developing mold every 30 min to make sure that you are developing the mold for the right amount of time. Over development can lead to deterioration of the mold features.
6. At this step, it is important that the silicon wafer is cleaned very well. If you do not get a mirror-clean wafer, place it back in PGMEA solution for some extra time or try to repeat the washing step with acetone and isopropanol.
7. When using needles, the dimensions of the PDMS rod are limited to the commercially available needle dimensions. For more specific dimensions and shapes, we recommend using a micromachining method to create a mold that can provide the lumen dimensions and design you need.
8. Oxygen plasma treatment of both the device and the glass bottom dish will modify the surface chemistry to make the PDMS hydrophilic and to create reactive species on the surfaces (PDMS is hydrophobic and adding solutions in the chamber is difficult without making the surfaces hydrophilic) as well as the glass, allowing covalent bonding between the two pieces. If this step is not performed, the devices will not bond to the glass and the solution will leak out of the chamber.
9. If this step is not performed, the collagen can fracture the moment the PDMS rod is pulled out. More information about this procedure can be found in ref. 17.
10. Removing the two coating solutions is very important as they can affect cell viability if present at the moment of culturing cells in the lumen.
11. You can use other collagen neutralization protocols.
12. Low-temperature incubation of neutralized collagen gels helps in the formation of bigger collagen fibers (*see* ref. 18).

13. Because of the nature of pulling the PDMS rod out of a soft hydrogel like collagen type 1, the minimum collagen concentration for which this method works successfully is 3 mg/ml. Lower concentrations can result in gel fracturing when pulling the rod out.
14. Figure 2 illustrates the device's four main ports. Two are the inlet and outlet luminal ports (access to the lumen), and the other two are the gel-loading ports. Any of the two gel-loading ports can be used to fill the chamber. The remaining gel-loading port will be an exit to air while the chamber is being loaded with gel. Without this port, air bubbles can form inside the chamber. The chamber dimensions are 2.2 mm wide and 2 mm height.
15. When handling a dish or plate with devices, it is important to keep the dish on ice the entire time to avoid differences in collagen polymerization rates in the different chambers, as collagen starts polymerizing when the device is removed from ice.
16. For better fibers, the collagen in the devices can be pre-incubated at room temperature for 10 min and then placed in an incubator at 37 °C for 10 min to complete the collagen polymerization.
17. When pulling the PDMS rod out, it is important to do it in a straight motion parallel to the rod orientation. If the rod is pulled out in any other direction, it can result in disfigurement of the collagen lumen shape.
18. For this step, we use a rotisserie in a temperature-controlled chamber (37 °C). The lumens must be parallel to the axis of rotation. An alternative way to line the lumen with cells would be to place the dish inside an incubator at 37 °C and flip the dish 90° every 15–20 min four times.
19. Since cells are seeded at high densities, it is important to change media frequently to sustain cell viability. We have seen that some cells require media change more frequently. If the cells do not survive over 48 h, try changing media every 12 h. From our observation, cell-lined lumens will be optimal after 24–48 h depending on the cell type. As long as media is replaced frequently, the experiments are viable for over 6 days. The termination of experiment depends on the endpoint that it is being studied. For example, cell migration and morphogenesis will require longer culture time.
20. Longer exposure to paraformaldehyde can affect the adherence of antibodies.
21. If the region to be stained is small, we recommend using twice the concentration recommended by the antibody distributor to achieve a better staining.

Acknowledgements

David J. Beebe holds equity in Bellbrook Labs, LLC, Tasso, Inc., Salus Discovery, LLC, and Stacks for the Future, LLC.

This work was supported by NIH R01 EB010039, University of Wisconsin Carbone Cancer Center Cancer Center Support Grant NIH P30 CA014520, and the University of Wisconsin Graduate Engineering Research Scholars.

References

1. Mori H, Gjorevski N, Inman JL, Bissell MJ, Nelson CM (2009) Self-organization of engineered epithelial tubules by differential cellular motility. Proc Natl Acad Sci U S A 106: 14890–14895
2. Bissell MJ, Radisky D (2001) Putting tumours in context. Nat Rev Cancer 1(1):46–54
3. Cukierman E, Pankov R, Stevens DR, Yamada KM (2001) Taking cell-matrix adhesions to the third dimension. Science 294(5547):1708–1712
4. Wolf K, Alexander S, Schacht V, Coussens LM, von Andrian U, van Rheenen J, Deryugina E, Friedl P (2009) Collagen-based cell migration model in vitro and in vivo. Semin Cell Dev Biol 20(8):931–941
5. Blobel CP (2010) 3D trumps 2D when studying endothelial cells. Blood 115(25): 5128–5130
6. Gjorevski N, Nelson CM (2010) Endogenous patterns of mechanical stress are required for branching morphogenesis. Integr Biol 2:424–434
7. Griffith LG, Swartz MA (2006) Capturing complex 3D tissue physiology in vitro. Nat Rev Mol Cell Biol 7(3):211–224
8. Bischel LL, Sung KE, Jiménez-Torres JA, Mader B, Keely PJ, Beebe DJ (2014) The importance of being a lumen. FASEB J 28(11): 4583–4590
9. Bryant DM, Mostov KE (2008) From cells to organs: building polarized tissue. Nat Rev Mol Cell Biol 9:887–901
10. Nelson CM, van Duijn MM, Inman JL, Fletcher DA, Bissell MJ (2006) Tissue geometry determines sites of mammary branching morphogenesis in organotypic cultures. Science 314(5797):298–300
11. Tan T, Shah S, Thomas A, Ou-Yang HD, Liu Y (2013) The influence of size, shape and vessel geometry on nanoparticle distribution. Microfluid Nanofluidics 14(1–2):77–87
12. Kim HY, Nelson CM (2014) Epithelial engineering: from sheets to branched tubes. Bioinspired Mater Biome Eng 1:161–171
13. Wang X, Hao J, Zhou R, Zhang X, Yan T, Ding D, Shan L, Liu Z (2013) Collecting duct carcinoma of the kidney: a clinicopathological study of five cases. Diagn Pathol 8:96
14. Roberts JA, Zhou YWP, Ro JY (2013) Intraductal carcinoma of prostate: a comprehensive and concise review. Korean J Pathol 47(4):307–315
15. Jiménez-Torres JA, Peery SL, Sung KE, Beebe DJ (2015) LumeNEXT: a practical method to pattern luminal structures in ECM gels. Adv Healthc Mater 5(2):198–204. doi:10.1002/adhm.201500608
16. Walker GM, Beebe DJ (2002) A passive pumping method for microfluidics devices. Lab Chip 2:131–134
17. Tran CNB, Walt DR (1989) Plasma modification and collagen binding to PTFE grafts. J Colloid Interface Sci 132:373–381
18. Sung KE, Su G, Pehlke C, Trier SM, Eliceiri KW, Keely PJ, Friedl A, Beebe DJ (2009) Control of 3-dimensional collagen matrix polymerization for reproducible Human Mammary Fibroblast cell culture in microfluidic devices. Biomaterials 30(27):4833–4841

Chapter 6

Measuring Vascular Permeability In Vivo

Eelco F.J. Meijer, James W. Baish, Timothy P. Padera, and Dai Fukumura

Abstract

Over the past decades, in vivo vascular permeability measurements have provided significant insight into vascular functions in physiological and pathophysiological conditions such as the response to pro- and anti-angiogenic signaling, abnormality of tumor vasculature and its normalization, and delivery and efficacy of therapeutic agents. Different approaches for vascular permeability measurements have been established. Here, we describe and discuss a conventional *2D* imaging method to measure vascular permeability, which was originally documented by Gerlowski and Jain in 1986 (Microvasc Res 31:288–305, 1986) and further developed by Yuan et al. in the early 1990s (Microvasc Res 45:269–289, 1993; Cancer Res 54:352–3356, 1994), and our recently developed *3D* imaging method, which advances the approach originally described by Brown et al. in 2001 (Nat Med 7:864–868, 2001).

Key words Vascular permeability, Intravital fluorescence microscopy, Vascular normalization, Multiphoton microscopy

1 Introduction

Measurements of transvascular transport have been proven invaluable in studying numerous in vivo processes and their regulation, including pro- and anti-angiogenic signaling, as well as vascular abnormalities and their putative normalization in disease states like cancer and inflammation [5]. It has been shown that abnormal tumor vasculature can be remodeled towards a more normal phenotype ("normalization") by restoring the proper balance of pro- and anti-angiogenic signaling pathways, improving vascular function [6], and delivery of therapeutics [7]. There are two different types of transport for molecules to extravasate across the blood vessel wall—convection and diffusion [5]. Convection is an active transport defined by a driving force–pressure gradient and a resistance–hydraulic conductivity such that $\text{Convection} = L_p S\left[\left(P_v \quad P_i\right) \quad s\left(p_v \quad p_i\right)\right]$, where L_p = hydraulic conductivity of vessel ($cm^4/s\text{-}mmHg$); S = surface area per unit volume (cm^2/cm^3), P_v; P_i = vascular and interstitial

Josie Ursini-Siegel and Nicole Beauchemin (eds.), *The Tumor Microenvironment: Methods and Protocols*, Methods in Molecular Biology, vol. 1458, DOI 10.1007/978-1-4939-3801-8_6, © Springer Science+Business Media New York 2016

pressures; s = osmotic reflection coefficient, p_v; and p_i = vascular and interstitial osmotic pressures (mmHg). On the other hand, diffusion is a passive transport defined by concentration gradients and permeability such that Diffusion = $PS\left(C_v \quad C_i\right)$, where P = vascular permeability (cm/s); S = surface area per unit volume (cm^2/cm^3), C_v; and C_i = concentrations in vascular and interstitial space (mol/cm^3). Tumor vessels are leaky which elevates tumor interstitial fluid pressure. While the extravagated fluid can escape (ooze out) from the tumor periphery, it builds up inside the tumor mass. Therefore, the pressure gradient across a vessel wall is diminished in tumors making convective transport less important and diffusion the dominant transport mechanism in solid tumors [8]. In this chapter, we discuss tumor transvascular transport measurements which is referred to as the effective permeability. It includes the dominant diffusive component (intrinsic permeability) as well as the less important convective component [5]. Effective permeability is a principal parameter to understand functionality of blood vessels and especially in tumors, one of the most important parameters [5, 6].

Early methods for estimating vascular permeability using *2D* imaging data were formulated by Gerlowski and Jain in 1986 [1] and further developed in the early 1990s by Yuan et al. [2, 3]. This approach relies on the estimates derived from temporal alteration in total fluorescence intensity as well as vascular morphologies obtained from superficial aspects of tissue using intravital fluorescence microscopy. Around a decade later, a *3D* approach was developed by Brown et al. [4] using multiphoton microscopy [9]. This advanced optical technique allows determining fluorescence intensity gradients surrounding *individual* vessels to calculate local permeability with high spatial resolution.

Both the *2D* and *3D* vascular permeability measurement methods are based on the same general principles. If pressure-driven transport can be neglected in a region of interest (ROI), as is often the case in disease states such as tumors, the apparent vascular permeability P may be calculated from $P = J / S \quad C$, where J is the rate at which a solute material is transported across a membrane of area S due to the concentration difference across the membrane ΔC. The most common approaches to measuring J, S, and ΔC involve three related but distinct steps. The first is establishment of a known concentration difference between the inside and outside of one or more blood vessels (ΔC). Image-based methods are used to observe the concentrations inside and outside of the vessel wall where the concentration is taken to be proportional to the observed fluorescence level. Right after injecting fluorescent material, the concentration outside the vessel wall should be zero. Secondly, the surface area of the blood vessel must be estimated (S). Estimates of the surface area are derived from the analysis of the vascular architecture in the image. If the vessel can be assumed to be cylindrical,

the surface can be estimated from the length and diameter of the vessel. Alternatively, a pixel or voxel counting technique can be employed to estimate the surface area if the vascular architecture is identified in *3D*. Thirdly, the transport rate is determined from changes in the fluorescence intensity of the tissue over time. Typically, the intravascular and extravascular spaces are taken to be different control volumes separated by the membrane. If we assume that all of the fluorescent material leaving the blood vessel through the vessel wall can be observed in the extravascular space of the ROI,

we can represent flux as $J = \frac{d}{dt}\int_{V_{ex}} C_{ex}\, dV$. However, for this equation to be strictly valid the boundary of the ROI must not offer an alternative route in or out. Such conditions might be well approximated if the blood vessels are relatively distant from the ROI boundary, or the boundary is sufficiently typical of adjacent ROIs such that material loss at the boundary is balanced by material gain. Accurately determining the flux has proven the biggest challenge.

The *2D* approach from Yuan et al. has proven valuable for measuring vascular permeability using the principles described above (*see* Table 1 for examples of *2D* permeability measurements). This technique, however, has several limitations because of its many assumptions. Because this method is in *2D*, the surface area-to-volume ratio of vessels collected from a single defocused plane on the surface is used to approximate the ratio of vessels in the entire ROI that is being imaged. Also, in a fluorescence image, the vessel diameter will appear larger than its true value because of light scattering, which needs to be corrected for. The actual in vivo tissue depth of the ROI being measured may also vary per tissue and tumor, depending on the cellular content and fluorescent material used. In addition, the vessels are assumed to be of cylindrical shape to be able to estimate the surface area of the blood vessels. Lastly, any fluorescent material leaking out from tissue surrounding the ROI and residing on top of the tissue will incorrectly increase calculated vascular permeability value, leading to measurement error in some samples.

The *3D* method using multiphoton microscopy—which can achieve greater imaging depths when compared to single-photon intravital imaging techniques—described in Brown et al. addressed many of the issues described above, but has some disadvantages on its own (*see* Table 1 for examples of *3D* permeability measurements). This method requires an accurate vessel mask and the quality of the multiphoton microscopy images dominates how accurate the vessel masking is at greater tissue depths. However, the actual tissue depth where light is collected is known using this method and the surface area-to-volume ratio is more realistic than the *2D* method. In addition, light scattering adjustments as well as hematocrit value and

Table 1
Examples of *2D* and *3D* method permeability measurements in the E.L. Steele Laboratories

Site	Tumor/model	Animal	Treatment/manipulation	Probes	*2D* methods	*3D* method	References
Brain (cranial window)	U87	Nude/SCID	Anti-VEGF/R2/Ang2/PlGF	BSA	$0.7–3.8\times10^{-7}$ cm/s	$0.4–2.5\times10^{-7}$ cm/s	[14–19]
	U87/MCaIV	SCID	VEGF-GFP imaging	100 and 500 nm QD-NP	NP and VEGF co-localize		[20]
	U87/GL261	*Rag-1-/-/-* SCID	nNOS KD/nNOS inhibitor	BSA	$0.3–7.8\times10^{-7}$ cm/s		[21]
	HGL21	SCID	VEGF		$0.11–4.3\times10^{-7}$ cm/s		[14, 22]
	HCaI/Shionogi/MCaIV	SCID		100–550 nm NP	HCaI 210-380, Shionogi 100–380, MCaIV 380–550 nm		[23]
	MCaIV	C3H/SCID		BSA	$1.9–2.9\times10^{-7}$ cm/s		[14]
	R3230AC	Fisher Rat			1.7×10^{-7} cm/s		[14]
	MDA-MB-361HK	SCID	Anti-HER2		$2.7–8.0\times10^{-7}$ cm/s		[24]
	ZR75-1	SCID			1.2×10^{-7} cm/s		[25]
	Tissue-engineered vessels	SCID	HUVEC, CB-EPC + 10T1/2		$0.5–4.4\times10^{-7}$ cm/s		[26–28]
			hiPSC-EC + 10T1/2			$0.2–15\times10^{-7}$ cm/s	[29]
	Normal cranium				$0.2–0.8\times10^{-7}$ cm/s		[22, 26]
Cerebellum window	D283-MED	SCID	Anti-PlGF	BSA		$1.2–3.1\times10^{-7}$ cm/s	[30]
Breast (mammary fat pad window)	E0771/4T1	SCID	Low dose anti-VEGFR2	12, 60, 125 nm Qd NP		0.01–0.45 μm/s Transvascular flux	[31, 32]
	E0771	SCID		Rod, sphere-shape Qd NP		0.04–0.17 μm/s Transvascular flux	[33]
	E0771/MCaIV	SCID		Neutral and negative charge Qd NPs		$0.3–5.0\times10^{-4}$ μm/s Transvascular flux	[34]
	4T1	Nude	VE-PTP inhibitor	BSA		0.1–1.8-fold	[35]
	ZR75-1	SCID		BSA	3.2×10^{-7} cm/s		[25]

Liver (acute)	LS174T	SCID		BSA	4.8×10^{-7} cm/s		[36]
	Normal liver				0.27×10^{-7} cm/s		
Pancreas (abdominal wall window)	Panc-1	SCID		BSA	3.1×10^{-7} cm/s		[37]
	Normal pancreas				0.5×10^{-7} cm/s		
Skin (dorsal skin chamber)	LS174T	SCID	Anti-VEGF, NOS inhibitor	BSA	$1.2–6.0\times10^{-7}$ cm/s		[2, 3, 15, 36, 38]
				90 nm NP	0.2×10^{-7} cm/s		[3]
				Mr. 24,000 (Fc) to 160,000 (IgG)	$1.5–5.7\times10^{-7}$ cm/s		[39]
				BSA	Single vessel permeability		[40]
	MCaIV	C3H/SCID	NOS inhibitor, anti-VEGFR2, PDT		$1.3–2.6\times10^{-7}$ cm/s	3.5×10^{-7} cm/s	[4, 38, 41, 42]
	Shionogi	SCID	Castration		$0.6–3.4\times10^{-7}$ cm/s		[43]
	HCaI/Shionogi/ MCaIV			100–2000 nm NP	HCaI 380-550, Shionogi 200–380, MCaIV 1200–2000 nm		[23]
	Mu89 melanoma			12, 60, 125 nm QD-NP		10–250 μm penetration	[44]
	T241		VEGF-C, anti-VEGFR2, VFGF-null	BSA	$0.5–4.4\times10^{-7}$ cm/s		[45]
	hES-teratoma		VEGF KO/HIF-1 KO		$1.3–3.1\times10^{-7}$ cm/s		[46]
	Normal skin				$0.3–0.7\times10^{-7}$ cm/s		[22]
Ear (*in situ*)	Spontaneous SCC	*Pol η−/−*		BSA	$1.2–9.4\times10^{-7}$ cm/s		[47]

4T1 murine breast cancer, *Ang2* angiopoietin 2, *BSA* bovine serum albumin, *CB-EPC* cord blood endothelial progenitor cell, *D283-MED* human medulloblastoma, *E0771* murine breast cancer, *GL261* murine glioma, *HCaI* murine hepatoma, *HER2* human epidermal growth factor receptor 2, *hES* human embryonic stem ells, *hiPSC* human induced pluripotent stem cell, *HUVEC* human umbilical vein endothelial cell, *LS174T* human coon cancer, *Mu89* human melanoma, *nNOS* neuronal nitric oxide synthase, *Panc-1* human pancreatic cancer, *PDT* photodynamic therapy, *PlGF* placenta growth factor, *QD-NP* quantum dot-nanoparticle, *R3230AC* rat breast cancer (rat mammary), *SCC* squamous cell carcinoma, *SCID* severe combined immunodeficient mice, *Shionogi* murine androgen-dependent cancer, *T241* murine fibrosarcoma, *U87* human glioma, *VEGF* vascular endothelial growth factor, *VEGFR2* VEGF receptor 2, *VE-PTP* vascular endothelial protein tyrosine phosphatase, *ZR75-1* human breast cancer

cylindrical vessel shape assumptions are not needed. Fluorescent material residing on top of the tissue can also be selectively avoided.

The formula used by Brown et al. calculates vascular permeability (P) in cm/s as $P = \lim_{t \to 0} \frac{\delta}{\delta t} \frac{\int_{r=R}^{\infty} F(r) r \, dr}{(F_v - F_i) R}$. Derivatives should be d/dt not lower case delta. This formula, however, is not strictly correct except under fairly restrictive conditions that may not be generally met. Correct use of this method requires that a roughly cylindrical region exists around a vessel that is influenced only by the vessel of interest during the time that is used for permeability calculation. In vivo, however, this cylindrical region is generally not present because the ROI may include multiple—tortuous—vessels in close vicinity. Vessels may also be present near the edges of the ROI. Altogether, this *3D* method yields a more realistic measurement of vascular permeability.

A recommended alternative approach would be to use a box-shaped ROI, using $P = \frac{\frac{\delta}{\delta t} \int_{Vext} F(\vec{r}) dV}{S(F_v - F_i)}$ Derivatives should be d/dt as used in Kesler et al. [10]. In this approach, the voxels are segmented into three categories, namely those inside the vessel, those on the vessel wall, and those outside the vessel. For calculating vascular permeability, all vessels are mathematically considered as a single vessel. A downside of this approach is that permeability differences among single vessels cannot be estimated. However, the mean over all vessels should be very well estimated if the vessel masking is adequate.

The experimental setup of the *2D* method developed by Yuan et al. and our recommended alternative *3D* approach to measure vascular permeability in vivo are discussed in detail below. If executed properly, our recommended *3D* approach should yield more accurate and reliable in vivo vascular permeability measurements than the other methods discussed. The *3D* permeability measurements, however, rely heavily on an accurate vessel masking and while our vessel masking described below is fairly accurate in a range of tissues with high signal-to-noise ratio and low auto-fluorescence, a different approach for vessel masking may be more practically robust if images are obtained with lower signal-to-noise ratio or if there is high auto-fluorescence. Comparison between permeability measurements obtained with the same method can be safely made. However, the comparison of permeability measurements between different methods should be made with caution. There should be a common comparator such as measurements performed in the same tumor model with the same condition

(i.e., size, control treatment) in order to interpret the data properly. As discussed above, the difference in surface area-to-volume ratio estimation of multiple vessels in a similar ROI between the *2D* and *3D* methods will tend to result inherently lower calculated permeability values in the *2D* method as compared to that in the *3D* method. Hence, for the comparison purpose, the *3D* measurement raw data should be converted to *2D* data before the analysis. Finally, examples of vascular permeability measurements from the E.L. Steele Laboratories using *2D* and *3D* methods described by Yuan et al. and Brown et al., respectively, are summarized in Table 1.

2 Materials

1. General materials: Heating pad or similar device.
2. Ketamine/xylazine mixture 90 mg/9 mg per kg body weight.
3. Fluorescent molecules: 1% 2,000,000 mol. wt. fluorescein isothiocyanate (FITC)-dextran, 1% tetramethylrhodamine-bovine serum albumin (BSA), and 1% FITC-BSA.
4. $30^{1/2}$ gauge needles.
5. PE10 Polyethylene Tubing.
6. ½ cc U-100 $28^{1/2}$ gauge insulin syringes.
7. Graticule slides.

2.1 Microscope Setup Measuring Vascular Permeability in Mice Using 2D Method

1. The tracer molecules used in this method are 100 μL per 25 g body weight 1% 2,000,000 mol. wt. FITC-dextran and 1% tetramethylrhodamine-BSA.
2. A fluorescence intravital microscope (*see* Fig. 1) is used with a long-working-distance 20 × 0.40 NA objective and a fluorescence filter set suitable for FITC and rhodamine, connected to an intensified charge-coupled device (CCD) video camera and photomultiplier tube.
3. A computer is used to capture the output.
4. The microcirculation is epi-illuminated by a 100-W mercury lamp.
5. A 50% neutral density filter and a heat absorption filter were put in the epi-illumination pathway to prevent overheating of tissue.

2.2 Microscope Setup Measuring Vascular Permeability in Mice Using 3D Method

1. The tracer molecule used in this method is 100 μL per 25 g body weight 1% FITC-BSA.
2. The multiphoton microscope (*see* Fig. 1) consists of a mode-locked Ti:sapphire laser and an x–y laser scanner purchased as described previously [4]. A Pockels cell is used to allow for rapid modulation of laser intensity.

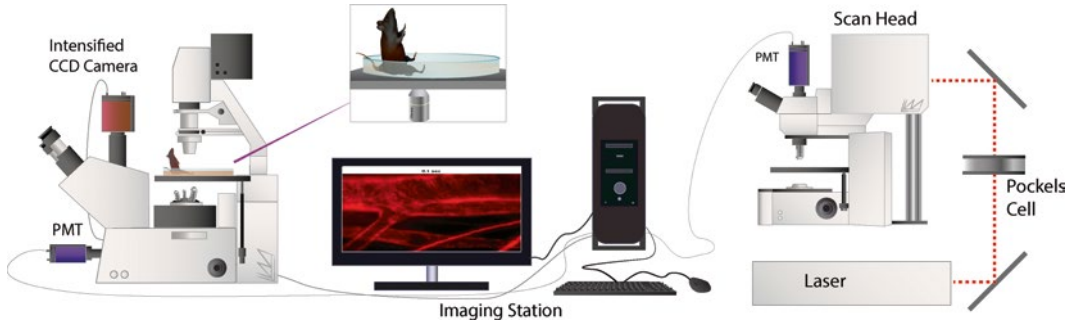

Fig. 1 Schematic representation of the fluorescence intravital microscope (*left*) and multiphoton microscope (*right*) setups. Fluorescence intravital microscopy and multiphoton microscopy are used for *2D* and *3D* method permeability measurements, respectively. Inverted microscope (*left*) with popliteal lymph node/lymphatics imaging setup is shown. Both inverted and upright (*right*) microscope with appropriate animal models can be used for the permeability measurements. *CCD* cooled coupled device, *PMT* photomultiplier tube. This figure was generously drawn by Dr. Lance L. Munn, E.L. Steele Laboratories, Boston, MA

3. The system also requires non-descanned photomultiplier tubes (PMT), a dichroic beam splitter, a digital image and analysis station, and a computer with image acquisition software. We use a 20×0.95 NA or 25×1.05 NA water-immersion objective (Olympus) and a 525DF100 filter (Chroma) suitable for FITC.

3 Methods

3.1 Measuring Vascular Permeability in Mice Using 2D Method

General comment: Make sure that the microscope is in complete darkness when imaging.

1. Anesthetize the mouse with a ketamine/xylazine mixture 90 mg/9 mg per kg body weight. Maintain the animal's core body temperature using a heating pad or similar device.
2. Insert a $30^{1/2}$ gauge needle into a tail vein, connected to PE10 Polyethylene Tubing and a ½cc U-100 $28^{1/2}$ gauge insulin syringe filled with 100 μL per 25 g body weight 1% 2,000,000 mol. wt. FITC-dextran. Also prepare an insulin syringe filled with 100 μL per 25 g body weight 1% tetramethylrhodamine-BSA.
3. Inject the FITC-dextran (MW 2,000,000 or more). Flush the Polyethylene Tubing with a small amount of physiologic saline for intravenous infusion and leave the needle in the tail vein (*see* **Note 1**). FITC-dextran is used for vessel marking (*see* **step 10**). It does not easily extravasate into the surrounding tissue due to its large molecular weight.
4. Place the mouse and the area to be studied under the intravital fluorescence microscope, equipped with the fluorescence fil-

ter set for rhodamine and FITC and a 100-W mercury lamp (*see* **Note 2**).

5. Acquire an image of the vessels in the area to be studied using the CCD camera. Do this by using the fluorescence filter for FITC (*see* **Note 3**). It is important to settle the location of permeability measurement and focus target blood vessels using FITC-dextran image as there is little room of adjustment once the permeability measurements start (*see* **step 7**).
6. Set the fluorescence filter to rhodamine. Use the photomultiplier tube to acquire background signal for several seconds and make sure that the system is fully operational.
7. Attach the insulin syringe containing tetramethylrhodamine-BSA. Start measuring the tissue fluorescence using the PMT and subsequently inject the tetramethylrhodamine-BSA. Flush the Polyethylene Tubing with a small amount of physiologic saline for intravenous infusion. Do not exceed 10 s of measuring to avoid photo-damage of the tissue and photo-bleaching of the fluorescent molecules (*see* **Note 4**). Tetramethylrhodamine-BSA will start leaking out into the surrounding tissue immediately. By using narrow band-pass filters the PMT, fluorescence of tetramethylrhodamine-BSA, and FITC-dextran are clearly separated. Different combinations of two different fluorophores can be used for permeability measurements as long as fluorescence spectra are reasonably separated and with the proper sets of band-pass filters. In general, longer wavelength is preferred for permeability measurement due to reduced auto-fluorescence and tissue penetration.
8. Repeat 10 s of signal acquisition every 2 min for up to 20 min.
9. After the last signal acquisition, acquire a second image of the vessels in the area studied using the fluorescence filter for FITC and the CCD camera. Compare with the image taken at **step 5** and confirm the tissue had no x, y, or z shift.
10. Using the images and measurements gathered, vascular permeability (P) can be calculated in cm/s as $P=(1-\mathrm{HT})V/S(1/(I_0-I_b)\cdot dI/dt+1/K)$, where HT is the tissue hematocrit estimated to be 0.19 in tumors [3, 11] and 0.46 in the systemic circulation [12], I is the average fluorescence intensity of the whole image, I_0 is the value of I immediately after the filling of all vessels by tetramethylrhodamine-BSA, I_b is the background fluorescence intensity, and K is the time constant of plasma clearance estimated to be 9.1×10^3 s for BSA [3]. The slope of the measurements plotted over time should be normalized, where dI/dt becomes $(dI/dt)/(I_0-I_b)$. V and S are the total volume and surface area of vessels within the tissue volume covered by the surface image, respectively. The volume-to-sur-

face ratio is calculated as $\frac{V}{S} = \sum_{n=1}^{M} L_n d_n^2 / \sum_{n=1}^{M} 4 d_n L_n$ where *dn* is the diameter of the *n*th vessel and *Ln* is the length of the *n*th vessel corrected by a factor of 0.79 for light scattering in the tissue [3]. These vessel diameters and lengths can be manually calculated from the acquired image of the vessels in the area to be studied after injecting FITC-dextran (*see* **Note 5**).

3.2 Measuring Vascular Permeability in Mice Using 3D Method

General comment: Make sure that the microscope is in complete darkness when imaging.

1. Make sure that your multiphoton setup is working correctly before you anesthetize your mouse. Use fluorescence filters adequate for the material you will be using, in this case FITC-BSA. We use a 525DF100 filter. Set Ti-sapphire laser wavelength to 780 nm. Set laser power to 60 mW.
2. Anesthetize the mouse with a ketamine/xylazine mixture 90 mg/9 mg per kg body weight. Maintain the animal's core body temperature using a heating pad or similar device.
3. Insert a $30^{1/2}$ gauge needle into a tail vein, connected to PE10 Polyethylene Tubing and a ½cc U-100 $28^{1/2}$ gauge insulin syringe filled with 100 µL per 25 g body weight 1% FITC-BSA.
4. Place the mouse and the area to be studied under the multiphoton microscope objective. We use a 20×0.95 NA or 25×1.05 NA water-immersion objective. Set the focus on the most superficial vasculature you can find in the area of interest and make sure that the water between tissue and objective is not leaking.
5. Inject the FITC-BSA. Flush the Polyethylene Tubing with a small amount of physiologic saline for intravenous infusion (*see* **Note 6**).
6. Start imaging 30 s after injecting FITC-BSA. Arteries show fluorescence within seconds after injection; veins can take somewhat longer. We use the slowest acquisition to get best quality images, 256×256 voxels, 74 *z* slices, and steps of 1.84 µm obtained with a 25× water-immersion objective. For a 20× objective, use *z* steps of 2.76 µm (*see* **Note 7**).
7. Acquire *z* stacks for up to 20 min (*see* **Note 8**).
8. For image analysis, we recommend a box-shaped ROI approach containing multiple vessels. Use software to segment voxels into three categories: those inside the vessel, those on the vessel wall, and those outside the vessel (*see* Fig. 2). Calculate vas-

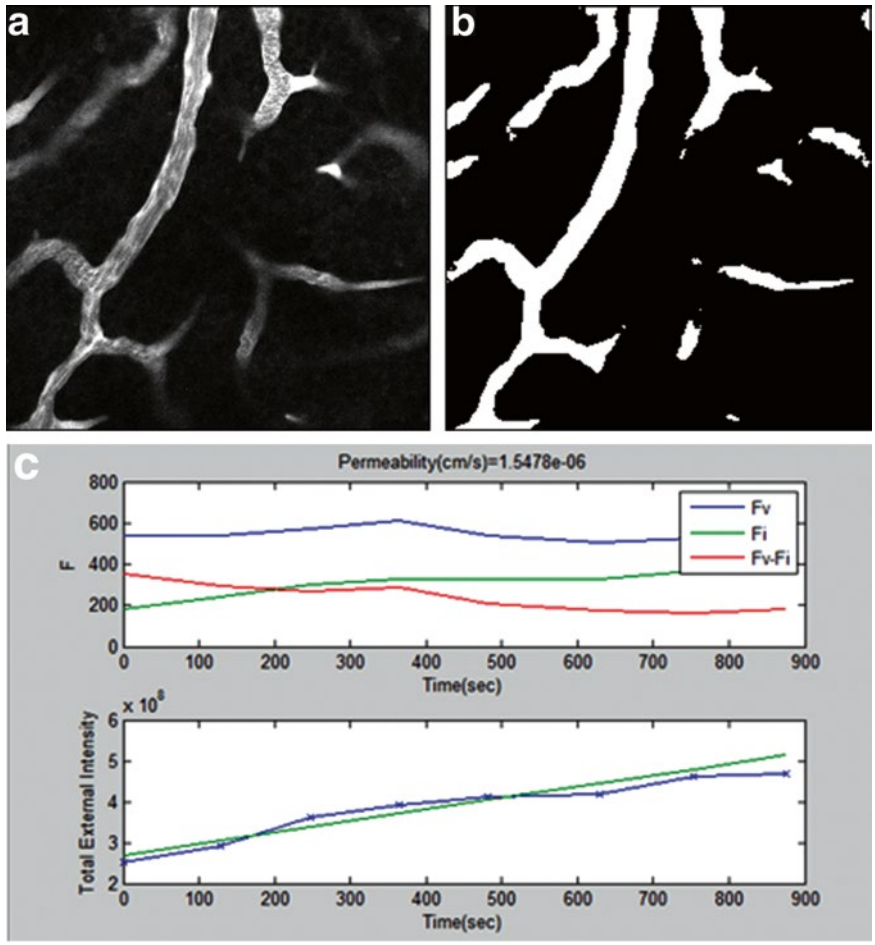

Fig. 2 Example of *3D* method data analysis. (**a**) Single slice from a multiphoton image *z* stack of tumor vasculature. (**b**) Vessel masking from slice presented at **a** using method "*Li*" thresholding in ImageJ. (**c**) *Right-top graph* shows MATLAB results from the same *z* stack (44 out of 74 slices, $z \approx 81$ μm, 8 time points over 15 min, images not shown) showing a vascular permeability of 1.55×10^{-6} cm/s. *Right-bottom graph* depicts the total external intensity (F_e, *blue line*) being the total fluorescence from all exterior points including those on the wall and the straight line (*green line*) being the slope estimated from the first 6 time points to which the *blue line* theoretically should closely adhere to. *F* fluorescence intensity, F_v mean fluorescence from the interior voxels, F_i mean fluorescence from the vessel wall voxels

cular permeability (P) as

$$P = \frac{(\text{voxel size}) \times \text{Slope of } F_e \text{ over time}}{(n_{wall}) \times \text{Mean of } (F_v - F_i)}$$

where n_{wall} is the number of voxels making up the vessel walls, F_e is the total fluorescence from all exterior points including those on the wall, F_v is the mean fluorescence from the interior voxels, and F_i is the mean fluorescence from the vessel wall voxels (*see* **Note 9**).

4 Notes

1. Insulin syringes are precise and have little syringe dead space.
2. We prefer using a chronic window to keep the area to be studied in place and allow for chronic imaging without serial laparotomies and breathing artifacts [13].
3. Take an image with maximum gain that the camera can handle without damaging it or before switching off. Do not adjust offset or other settings; you can do this later with image processing software.
4. Leave the needle in the tail vein attached to the tubing and syringe to prevent blood loss.
5. Use a graticule slide to know the actual size of the area and vessels you are measuring. Use μm for V/S and K in seconds.
6. Make sure that the area you are imaging is clean. If you are using imaging windows with a cover slip, replace the glass cover slip before imaging if needed. If there is water leakage, check if the cover slip is intact and well secured or replace the cover slip. Also, be particularly careful to prevent collision between your objective and anything that can damage it.
7. Do not adjust the gain, offset, etc. Similar modifications can be done after imaging with off-line processing while keeping the best quality raw data. We would recommend gathering more z slices than you need to be able to correct for any z shift you might experience over time. Moreover, check your data for pixel saturation. If you are seeing saturation in the fluorescence intensity in your data, lower the photomultiplier tube power or alternatively lower laser power in future experiments; your data will be incorrect and hence (partly) useless otherwise.
8. Stay alert for xy shifts during imaging; you can manually adjust these in between data acquisition or use off-line processing to correct for this later. If you are seeing intensity loss of the vessels in the field of view, make sure that there is enough water between the tissue and the objective. We recommend leaving a syringe with water in the vicinity of your objective.
9. We use ImageJ (1.47v, *NIH*) for vessel masking and MATLAB (R2015b, *MathWorks*) for further data analysis. Use earliest data stacks acquired for vessel masking to obtain the most accurate mask. Data stacks are converted to binary (ImageJ > Process > Binary > Make Binary > Method "Li") and a median filter (Process > Filter > Median > Radius 1 pixel) is subsequently used to remove noise and smoothen blood vessel lumen but not the vessel wall. The *MATLAB* script is not added here due to page limitations but is available upon request.

Acknowledgements

We would like to thank Echoe Bouta, Cheryl Cui, Nir Maimon, Lance L. Munn, and Rakesh K. Jain from the E.L. Steele Laboratories and Cedric Blatter and Benjamin Vakoc from the Wellman Center for Photomedicine (Massachusetts General Hospital, USA) for insightful discussions and intellectual input. We would like to thank Lance L. Munn for his help with illustrations and Cedric Blatter for his tremendous help with vessel masking and MATLAB coding for the *3D* method. This study was supported by the National Institutes of Health grants P01-CA 080124 (DF), DP2-OD008780 (TPP) and R01-HL128168 (TPP, JWB).

References

1. Gerlowski LE, Jain RK (1986) Microvascular permeability of normal and neoplastic tissues. Microvasc Res 31:288–305
2. Yuan F, Leunig M, Berk DA, Jain RK (1993) Microvascular permeability of albumin, vascular surface area, and vascular volume measured in human adenocarcinoma LS174T using dorsal chamber in SCID mice. Microvasc Res 45:269–289
3. Yuan F, Leunig M, Huang SK, Berk DA, Papahadjopoulos D, Jain RK (1994) Microvascular permeability and interstitial penetration of sterically stabilized (stealth) liposomes in a human tumor xenograft. Cancer Res 54:352–3356
4. Brown EB, Campbell RB, Tsuzuki Y, Xu L, Carmeliet P, Fukumura D, Jain RK (2001) In vivo measurement of gene expression, angiogenesis and physiological function in tumors using multiphoton laser scanning microscopy. Nat Med 7:864–868
5. Jain RK (1987) Transport of molecules across tumor vasculature. Cancer Metastasis Rev 6:559–593
6. Jain RK, Munn LL, Fukumura D (2002) Dissecting tumour pathophysiology using intravital microscopy. Nat Rev Cancer 2:266–276
7. Chauhan VP, Jain RK (2013) Strategies for advancing cancer nanomedicine. Nat Mater 12:958–962
8. Baxter LT, Jain RK (1989) Transport of fluid and macromolecules in tumors. I. Role of interstitial pressure and convection. Microvasc Res 37:77–104
9. Denk W, Strickler JH, Webb WW (1990) Two-photon laser scanning fluorescence microscopy. Science 248:73–76
10. Kesler CT, Pereira ER, Cui CH, Nelson GM, Masuck DJ, Baish JW, Padera TP (2015) Angiopoietin-4 increases permeability of blood vessels and promotes lymphatic dilation. FASEB J 29:3668–3677
11. Brizel DM, Klitzman B, Cook JM, Edwards J, Rosner G, Dewhirst MW (1993) A comparison of tumor and normal tissue microvascular hematocrits and red cell fluxes in a rat window chamber model. Int J Radiat Oncol Biol Phys 25:269–276
12. Schuler B, Arras M, Keller S, Rettich A, Lundby C, Vogel J, Gassmann M (2010) Optimal hematocrit for maximal exercise performance in acute and chronic erythropoietin-treated mice. Proc Natl Acad Sci U S A 107:419–423
13. Brown E, Munn LL, Fukumura D, Jain RK (2010) In vivo imaging of tumors. Cold Spring Harbor Protoc 2010(7):pdb.prot5452
14. Yuan F, Salehi HA, Boucher Y, Vasthare US, Tuma RF, Jain RK (1994) Vascular permeability and microcirculation of gliomas and mammary carcinomas transplanted in rat and mouse cranial windows. Cancer Res 54:4564–4568
15. Yuan F, Chen Y, Dellian M, Safabakhsh N, Ferrara N, Jain RK (1996) Time-dependent vascular regression and permeability changes in established human tumor xenografts induced by an anti-vascular endothelial growth factor/vascular permeability factor antibody. Proc Natl Acad Sci U S A 93:14765–14770
16. Winkler F, Kozin SV, Tong RT, Chae SS, Booth MF, Garkavtsev I et al (2004) Kinetics of vascular normalization by VEGFR2 blockade governs brain tumor response to radiation: role of oxygenation, angiopoietin-1, and matrix metalloproteinases. Cancer Cell 6:553–563

17. Xu L, Cochran DM, Tong RT, Winkler F, Kashiwagi S, Jain RK, Fukumura D (2006) Placenta growth factor overexpression inhibits tumor growth, angiogenesis, and metastasis by depleting vascular endothelial growth factor homodimers in orthotopic mouse models. Cancer Res 66:3971–3977
18. Kamoun WS, Ley CD, Farrar CT, Duyverman AM, Lahdenranta J, Lacorre DA et al (2009) Edema control by cediranib, a vascular endothelial growth factor receptor-targeted kinase inhibitor, prolongs survival despite persistent brain tumor growth in mice. J Clin Oncol 27:2542–2552
19. Chae SS, Kamoun WS, Farrar CT, Kirkpatrick ND, Niemeyer E, de Graaf AM et al (2010) Angiopoietin-2 interferes with anti-VEGFR2-induced vessel normalization and survival benefit in mice bearing gliomas. Clin Cancer Res 16:3618–3627
20. Stroh M, Zimmer JP, Duda DG, Levchenko TS, Cohen KS, Brown EB et al (2005) Quantum dots spectrally distinguish multiple species within the tumor milieu in vivo. Nat Med 11:678–682
21. Kashiwagi S, Tsukada K, Xu L, Miyazaki J, Kozin SV, Tyrrell JA et al (2008) Perivascular nitric oxide gradients normalize tumor vasculature. Nat Med 14:255–257
22. Monsky WL, Fukumura D, Gohongi T, Ancukiewcz M, Weich HA, Torchilin VP et al (1999) Augmentation of transvascular transport of macromolecules and nanoparticles in tumors using vascular endothelial growth factor. Cancer Res 59:4129–4135
23. Hobbs SK, Monsky WL, Yuan F, Roberts WG, Griffith L, Torchilin VP, Jain RK (1998) Regulation of transport pathways in tumor vessels: role of tumor type and microenvironment. Proc Natl Acad Sci U S A 95:4607–4612
24. Izumi Y, Xu L, di Tomaso E, Fukumura D, Jain RK (2002) Tumour biology: herceptin acts as an anti-angiogenic cocktail. Nature 416:279–280
25. Monsky WL, Mouta Carreira C, Tsuzuki Y, Gohongi T, Fukumura D, Jain RK (2002) Role of host microenvironment in angiogenesis and microvascular functions in human breast cancer xenografts: mammary fat pad versus cranial tumors. Clin Cancer Res 8:1008–1013
26. Fukumura D, Gohongi T, Kadambi A, Izumi Y, Ang J, Yun CO et al (2001) Predominant role of endothelial nitric oxide synthase in vascular endothelial growth factor-induced angiogenesis and vascular permeability. Proc Natl Acad Sci U S A 98:2604–2609
27. Koike N, Fukumura D, Gralla O, Au P, Schechner JS, Jain RK (2004) Tissue engineering: creation of long-lasting blood vessels. Nature 428:138–139
28. Au P, Daheron LM, Duda DG, Cohen KS, Tyrrell JA, Lanning RM et al (2008) Differential in vivo potential of endothelial progenitor cells from human umbilical cord blood and adult peripheral blood to form functional long-lasting vessels. Blood 111:1302–1305
29. Samuel R, Daheron L, Liao S, Vardam T, Kamoun WS, Batista A et al (2013) Generation of functionally competent and durable engineered blood vessels from human induced pluripotent stem cells. Proc Natl Acad Sci U S A 110:12774–12779
30. Snuderl M, Batista A, Kirkpatrick ND, Ruiz de Almodovar C, Riedemann L, Walsh EC et al (2013) Targeting placental growth factor/neuropilin 1 pathway inhibits growth and spread of medulloblastoma. Cell 152:1065–1076
31. Chauhan VP, Stylianopoulos T, Martin JD, Popovic Z, Chen O, Kamoun WS et al (2012) Normalization of tumour blood vessels improves the delivery of nanomedicines in a size-dependent manner. Nat Nanotechnol 7:383–388
32. Chauhan VP, Martin JD, Liu H, Lacorre DA, Jain SR, Kozin SV et al (2013) Angiotensin inhibition enhances drug delivery and potentiates chemotherapy by decompressing tumour blood vessels. Nat Commun 4:2516
33. Chauhan VP, Popovic Z, Chen O, Cui J, Fukumura D, Bawendi MG, Jain RK (2011) Fluorescent nanorods and nanospheres for real-time in vivo probing of nanoparticle shape-dependent tumor penetration. Angew Chem 50:11417–11420
34. Han HS, Martin JD, Lee J, Harris DK, Fukumura D, Jain RK, Bawendi M (2013) Spatial charge configuration regulates nanoparticle transport and binding behavior in vivo. Angew Chem 52:1414–1419
35. Goel S, Gupta N, Walcott BP, Snuderl M, Kesler CT, Kirkpatrick ND et al (2013) Effects of vascular-endothelial protein tyrosine phosphatase inhibition on breast cancer vasculature and metastatic progression. J Natl Cancer Inst 105:1188–1201
36. Fukumura D, Yuan F, Monsky WL, Chen Y, Jain RK (1997) Effect of host microenvironment on the microcirculation of human colon adenocarcinoma. Am J Pathol 151:679–688
37. Tsuzuki Y, Mouta Carreira C, Bockhorn M, Xu L, Jain RK, Fukumura D (2001) Pancreas microenvironment promotes VEGF expression and tumor growth: novel window models for pancreatic tumor angiogenesis and microcirculation. Laboratory investigation. J Tech Methods Pathol 81:1439–1451
38. Fukumura D, Yuan F, Endo M, Jain RK (1997) Role of nitric oxide in tumor microcirculation. Blood flow, vascular permeability,

and leukocyte-endothelial interactions. Am J Pathol 150:713–725
39. Yuan F, Dellian M, Fukumura D, Leunig M, Berk DA, Torchilin VP, Jain RK (1995) Vascular permeability in a human tumor xenograft: molecular size dependence and cutoff size. Cancer Res 55:3752–3756
40. Lichtenbeld HC, Yuan F, Michel CC, Jain RK (1996) Perfusion of single tumor microvessels: application to vascular permeability measurement. Microcirculation 3:349–357
41. Dolmans DE, Kadambi A, Hill JS, Waters CA, Robinson BC, Walker JP et al (2002) Vascular accumulation of a novel photosensitizer, MV6401, causes selective thrombosis in tumor vessels after photodynamic therapy. Cancer Res 62:2151–2156
42. Tong RT, Boucher Y, Kozin SV, Winkler F, Hicklin DJ, Jain RK (2004) Vascular normalization by vascular endothelial growth factor receptor 2 blockade induces a pressure gradient across the vasculature and improves drug penetration in tumors. Cancer Res 64:3731–3736
43. Jain RK, Safabakhsh N, Sckell A, Chen Y, Jiang P, Benjamin L et al (1998) Endothelial cell death, angiogenesis, and microvascular function after castration in an androgen-dependent tumor: role of vascular endothelial growth factor. Proc Natl Acad Sci U S A 95:10820–10825
44. Popovic Z, Liu W, Chauhan VP, Lee J, Wong C, Greytak AB et al (2010) A nanoparticle size series for in vivo fluorescence imaging. Angew Chem 49:8649–8652
45. Kadambi A, Mouta Carreira C, Yun CO, Padera TP, Dolmans DE, Carmeliet P et al (2001) Vascular endothelial growth factor (VEGF)-C differentially affects tumor vascular function and leukocyte recruitment: role of VEGF-receptor 2 and host VEGF-A. Cancer Res 61:2404–2408
46. Tsuzuki Y, Fukumura D, Oosthuyse B, Koike C, Carmeliet P, Jain RK (2000) Vascular endothelial growth factor (VEGF) modulation by targeting hypoxia-inducible factor-1alpha→hypoxia response element→VEGF cascade differentially regulates vascular response and growth rate in tumors. Cancer Res 60:6248–6252
47. Hagendoorn J, Tong R, Fukumura D, Lin Q, Lobo J, Padera TP et al (2006) Onset of abnormal blood and lymphatic vessel function and interstitial hypertension in early stages of carcinogenesis. Cancer Res 66:3360–3364

Chapter 7

Hydroxylation-Dependent Interaction of Substrates to the Von Hippel-Lindau Tumor Suppressor Protein (VHL)

Pardeep Heir and Michael Ohh

Abstract

Oxygen-dependent hydroxylation of critical proline residues, catalyzed by prolyl hydroxylase (PHD1-3) enzymes, is a crucial posttranslational modification (PTM) within the canonical hypoxia-inducible factor (HIF)-centric cellular oxygen-sensing pathway. Alteration of substrates in this way often leads to proteasomal degradation mediated by the von Hippel-Lindau Tumor Suppressor protein (VHL) containing E3-ubiquitin ligase complex known as ECV (Elongins B/C, CUL2, VHL). Here, we outline in vitro protocols to demonstrate the ability of VHL to bind to a prolyl-hydroxylated substrate.

Key words In vitro hydroxylation, In vitro binding assay, Proline, VHL, PHD, HIF1α

1 Introduction

The ability of oxygen-dependent PTM to govern protein stability plays a central role in the cellular response to compromised oxygen availability. Specifically, HIF1α is hydroxylated on conserved proline residues by PHD1-3 and rapidly eliminated by the ECV complex under normoxia [1–5]. In hypoxia, HIF1α cannot be efficiently hydroxylated due to the absence of oxygen. Consequently, HIF1α accumulates and heterodimerizes with HIFβ to form an active transcription factor to promote the expression of numerous genes that help the cell adapt to hypoxia [6].

Several proteins have been shown to bind to VHL specifically after hydroxylation [4, 5, 7]. Here, we describe feasible in vitro methods that take advantage of the ability of VHL to bind to hydroxylated substrates (Fig. 1). Compared to protocols published previously, we have eliminated the use of radioactive isotopes [8]. These methods produce robust results using inexpensive reagents and represent an early step in confirming or validating potential novel prolyl-hydroxylated substrates of VHL. In addition, we were able to demonstrate that disease-associated point mutation on VHL alters its binding properties towards the substrate. Notably,

Josie Ursini-Siegel and Nicole Beauchemin (eds.), *The Tumor Microenvironment: Methods and Protocols*, Methods in Molecular Biology, vol. 1458, DOI 10.1007/978-1-4939-3801-8_7,

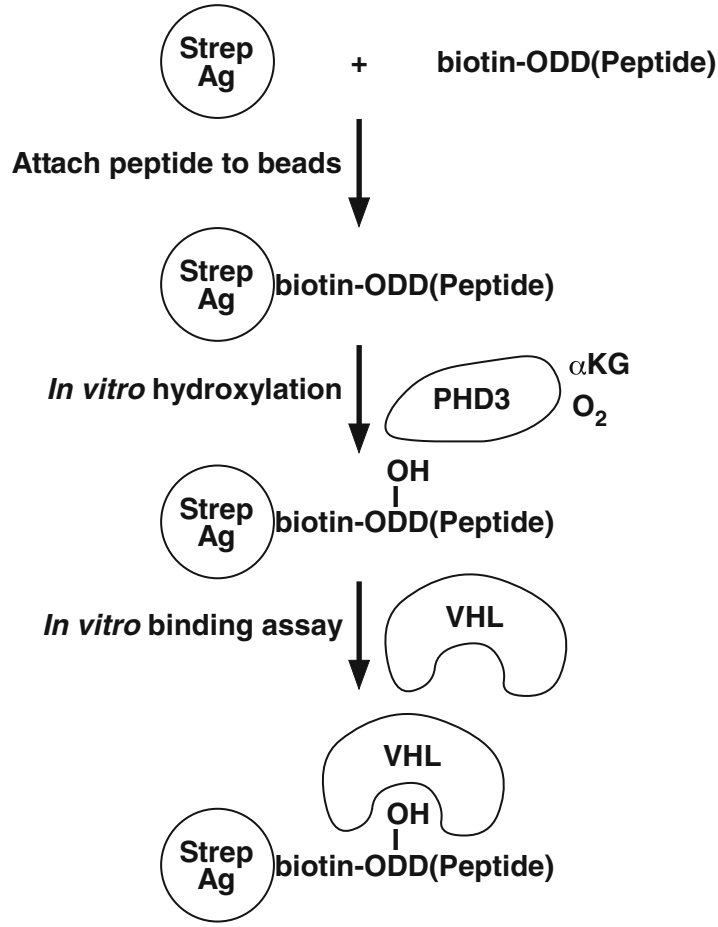

Fig. 1 Schematic of workflow. The biotinylated peptide is first attached to streptavidin agarose. Once bound, an in vitro hydroxylation reaction is performed using PHD3, α-ketoglutaric acid, and oxygen. After catalysis, binding to VHL is used to functionally assess hydroxylation

inclusion of a catalytically dead form of the PHD enzyme in our assay reduced concerns over spurious chemical oxidation taking place in an in vitro hydroxylation protocol.

2 Materials

All chemicals are prepared in ultrapure water.

2.1 In Vitro Binding Assay

1. Rabbit reticulocyte lysate quick-coupled in vitro transcription/translation kit.
2. Plasmids: pRc/CMV-HA-VHL, pRc/CMV-HA-VHL (Y112N), pRc/CMV-HA-VHL (R64P), and pRc/CMV-HA-VHL (V84L) [1, 9]. Although pRc/CMV is no longer

manufactured, pRc/CMV-HA-VHL can be purchased from Addgene.

3. Peptides corresponding to 20 amino acids of HIF1α were synthesized by Genscript. Peptides were N-terminally biotinylated through an aminohexanoic acid (Ahx) linker. Lyophilized peptides were reconstituted to a final concentration of 1 μg/μL. The following is the amino acid sequence of the indicated peptides.

   Unhydroxylated ODD Peptide: DLDLEMLAPYIPMDD DFQLR.

   Hydroxylated ODD Peptide (ODD-OH): DLDLEMLAP(OH) YIPMDDDFQLR.

4. Phosphate-buffered saline (PBS): 137 mM NaCl, 2.7 mM KCl, 4.3 mM Na_2HPO_4, 1.47 mM KH_2PO_4, pH 7.4.
5. Streptavidin agarose.
6. EBC buffer: 50 mM Tris–HCl, pH 8.0, 120 mM NaCl, 0.5% NP-40.
7. Protease inhibitor (PI).
8. HiNETN buffer: 20 mM Tris–HCl, pH 8.0, 300 mM NaCl, 1 mM ethylenediaminetetraacetic acid (EDTA), 0.5% NP-40.
9. NETN buffer: 20 mM Tris–HCl, pH 8.0, 100 mM NaCl, 1 mM EDTA, 0.5% NP-40.
10. 3× Sample buffer: 187.5 mM Tris–HCl, pH 6.8, 6% sodium dodecyl sulfate (SDS), 30% glycerol, 0.03% bromophenol blue, 0.3 M dithiothreitol (DTT).
11. Anti-HA antibody (Cell Signaling Technology #3724): Please note that in our experience, this HA antibody is superior to others tested in this assay.

2.2 In Vitro Hydroxylation Reagents

All components used in the in vitro binding assay in addition to:

1. Plasmids: pcDNA3, pcDNA3-HA-PHD3 [10], pcDNA3-HA-PHD3 (H196A) [10], pcDNA3-3x-FLAG-VHL.
2. 10× Prolyl hydroxylation assay (PHA) buffer: 400 mM HEPES, pH 7.4, 800 mM KCl.
3. α-Ketoglutaric acid, dissolved to 50 mM in water, pH 7.4.
4. 20 mM in water ascorbic acid, pH 7.4.
5. 10 mM in water iron (II) chloride tetrahydrate.
6. Anti-FLAG antibody (M2) (Sigma-Aldrich F1804): Please note that in our experience, this FLAG antibody is superior to others tested in this assay.

3 Methods

3.1 In Vitro Binding Assay

1. In vitro translate 1 μg of HA-VHL, HA-VHL(Y112N), HA-VHL(R64P), and HA-VHL(V84L) constructs using rabbit reticulocyte lysate quick-coupled in vitro transcription/translation kit. Supplement the reaction with non-radioactive methionine as indicated in the manufacturer's instructions. The reaction is allowed to proceed for 90 min by incubating at 30 °C.
2. In four separate 1.5 mL tubes (one tube for each form of VHL), incubate 1 μg of hydroxylated ODD peptide with 30 μL of streptavidin agarose slurry (*see* **Note 1**) in 500 μL of PBS and incubate at 4 °C for 1 h on a rocking platform. Set up an additional tube using 1 μg of unhydroxylated ODD peptide to use as a negative control.
3. Spin down the tubes containing streptavidin agarose bound to peptide at maximum speed for 15 s in a tabletop centrifuge.
4. Aspirate the PBS, being careful not to disturb the bead pellet.
5. Resuspend the beads in approximately 1.25 mL EBC buffer.
6. Repeat the procedure outlined in **steps 3–5** for two more washes.
7. Resuspend the beads in 500 μL EBC buffer + PI.
8. Incubate the indicated in vitro-translated HA-VHL constructs with beads bound to hydroxylated ODD peptides (*see* **Notes 2** and **3**). Incubate the beads bound to unhydroxylated ODD peptide with wild-type HA-VHL (*see* **Note 4**). The mixtures are incubated on a rocking platform for 2 h at 4 °C.
9. A 50% input (a quantity that is half the amount used for binding in **step 8**) of the in vitro-translated HA-VHL protein products should be removed to a new tube. 3× Sample buffer is added so that its final concentration is 1×.
10. Wash beads four times in HiNETN buffer.
11. Wash beads once in NETN buffer.
12. Aspirate all residual NETN buffer.
13. Add 50 μL of 1× sample buffer to the beads and incubate at 95 °C for 5 min to elute the protein off the beads. Perform the same incubation on the inputs.
14. Run a 10% SDS-PAGE gel and perform immunoblotting (*see* **Note 5**). Use anti-HA antibody to detect a band at approximately 30 kDa (Fig. 2).

3.2 In Vitro Hydroxylation Reaction

1. In vitro translate 1 μg pcDNA3, HA-PHD3, and HA-PHD3 (H196A) (*see* **Note 6**) constructs using rabbit reticulocyte lysate quick-coupled in vitro transcription/translation kit. Supplement the reaction with non-radioactive methionine as

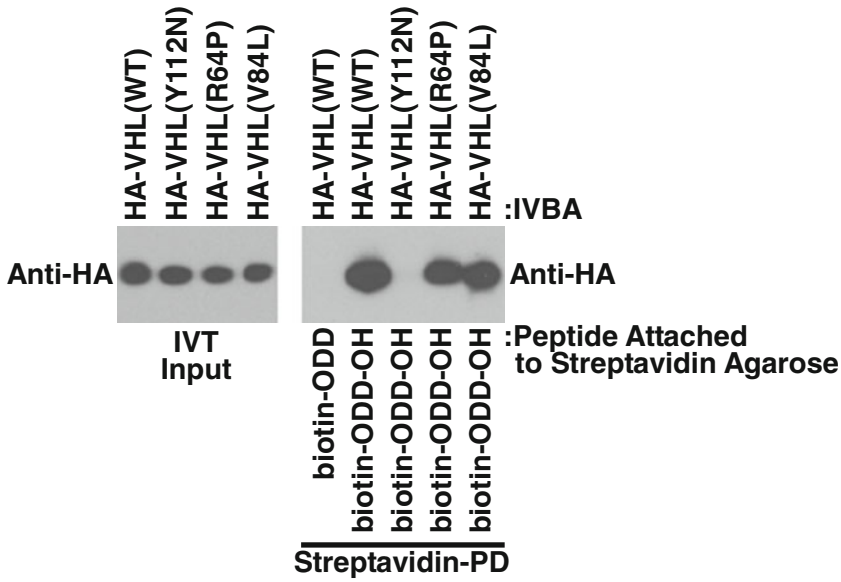

Fig. 2 In vitro binding of HA-VHL to hydroxylated ODD peptides. HA-VHL and the indicated HA-VHL mutants were in vitro translated. In vitro binding to hydroxylated peptides was then performed. Anti-HA immunoblotting was used to detect HA-VHL. *IVT* in vitro translated, *IVBA* in vitro binding assay, *PD* pulldown

indicated in the manufacturer's instructions. The reaction is allowed to proceed for 90 min by incubating at 30 °C.

2. In three separate 1.5 mL tubes incubate 1 μg of unhydroxylated ODD peptide with 30 μL of streptavidin agarose slurry (*see* **Note 1**) in 500 μL of PBS at 4 °C for 1 h on a rocking platform. Set up an additional tube using 1 μg of hydroxylated ODD peptide to use as a positive control for VHL binding. The positive control will not be undergoing in vitro hydroxylation and will be used in **step 12**.
3. Spin down the streptavidin agarose bound to peptide at maximum speed for 15 s in a tabletop centrifuge.
4. Aspirate the PBS being careful not to disturb the bead pellet.
5. Wash the beads twice in PBS.
6. Wash the beads once in 1× PHA buffer.
7. Aspirate all residual 1× PHA buffer.
8. Resuspend beads to a final volume of 200 μL comprised of 1× PHA supplemented with 5 mM α-ketoglutaric acid, 2 mM ascorbic acid, 0.1 mM $FeCl_2$ and 10 μL of rabbit reticulocyte lysate programmed with the desired enzyme.
9. Incubate at room temperature for 2 h with mixing end over end.
10. Set aside a 10% input of the above programed rabbit reticulocyte lysate to validate by immunoblotting that an equivalent amount of enzyme was used for catalysis.

11. In vitro translate 3× FLAG-VHL from pcDNA3-3xFLAG-VHL plasmid by incubation at 30 °C for 90 min.
12. Wash beads from in vitro hydroxylation reaction and positive control in NETN buffer four times.
13. Wash beads once in EBC buffer.
14. Aspirate residual EBC buffer.
15. Resuspend beads in 500 μL EBC buffer + PI. Incubate in the presence of 10 μL of in vitro-translated 3× FLAG-VHL on a rocking platform at 4 °C for 2 h.
16. Wash beads four times in 1.25 mL of HiNETN buffer.
17. Wash beads in 1.25 mL of NETN buffer once.
18. Aspirate all residual NETN buffer.
19. Add 50 μL of sample buffer to the beads and incubate at 95 °C for 5 min.
20. Apply samples on a 10% SDS-PAGE gel and run electrophoresis. Transfer samples onto membrane for immunoblotting. Use the anti-FLAG antibody or the anti-HA antibody to detect bands at approximately 30 kDa corresponding to VHL or approximately 26 kDa corresponding to PHD3, respectively (Fig. 3).

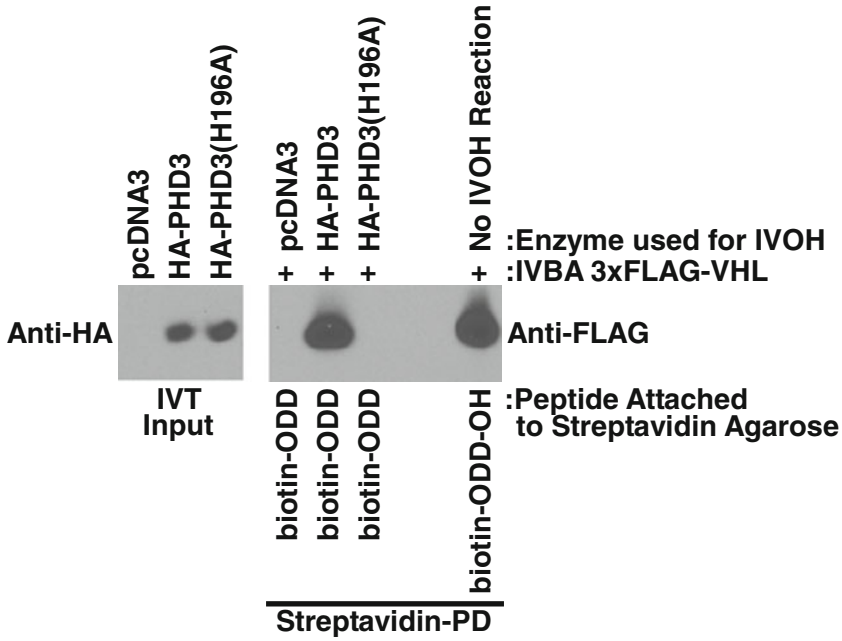

Fig. 3 In vitro hydroxylation of unhydroxylated ODD peptides. Empty pcDNA3 plasmid and plasmids encoding HA-PHD3 or catalytically inactive HA-PHD3 (H196A) were in vitro translated in rabbit reticulocyte lysate. In vitro hydroxylation was then performed on unhydroxylated ODD peptides and an *in* vitro binding assay to in vitro-translated 3xFLAG-VHL was performed. Anti-HA and anti-FLAG immunoblotting was performed to detect HA-PHD3 and FLAG-VHL, respectively. *IVT* in vitro translated, *IVBA* in vitro binding assay, *IVOH* in vitro hydroxylation, *PD* pulldown

4 Notes

1. Using a clean razor blade to cut the pipette tip, thus making the opening wider so it is easier to remove an accurate amount of bead slurry.
2. Depending on the efficiency of in vitro translation and the strength of the interaction to the substrate, samples of 2–10 μL can be used.
3. Leftover in vitro-translated protein product can be stored in a −80 °C freezer and reused for additional binding assays.
4. Aliquots of HA-VHL from one in vitro translation reaction are used in separate binding assays on hydroxylated and unhydroxylated ODD peptides. This ensures that a lack of binding in the negative control reaction is not due to inadvertent poor quality of in vitro translation or misfolding.
5. The SDS-PAGE gel is transferred onto polyvinylidene fluoride membrane. Next the membrane is blocked in 4% nonfat milk dissolved in TBST (10 mM Tris–HCl, pH 7.5, 150 mM NaCl, 0.05% Tween-20) for 1 h on a rocking platform at room temperature. The blot is then washed in TBST five times for 5 min. Anti-HA antibody is diluted 1:1000 in TBST and applied to the membrane overnight at 4 °C on a rocking platform. The next day the blot is washed in TBST five times for 5 min. HRP-conjugated secondary antibody is diluted to 1:7500 in 2% milk-TBST and is applied to the membrane for 1 h at room temperature. The membrane is then washed in TBST five times for 5 min. The membrane is developed using enhanced chemiluminescence (ECL).
6. The use of catalytically inactive PHD3 reduces concerns of spurious chemical oxidation of the ODD peptide as being the cause of VHL binding to ODD peptide after hydroxylation by active PHD3.

Acknowledgements

This work was supported by funds from the Canadian Institutes of Health Research.

References

1. Ohh M, Park CW, Ivan M, Hoffman MA, Kim TY, Huang LE et al (2000) Ubiquitination of hypoxia-inducible factor requires direct binding to the beta-domain of the von Hippel-Lindau protein. Nat Cell Biol 2:423–427
2. Bruick RK, McKnight SL (2001) A conserved family of prolyl-4-hydroxylases that modify HIF. Science 294:1337–1340
3. Epstein AC, Gleadle JM, McNeill LA, Hewitson KS, O'Rourke J, Mole DR et al (2001) *C. elegans* EGL-9 and mammalian homologs define a family of dioxygenases that regulate HIF by prolyl hydroxylation. Cell 107:43–54
4. Ivan M, Kondo K, Yang H, Kim W, Valiando J, Ohh M et al (2001) HIFalpha targeted for

VHL-mediated destruction by proline hydroxylation: implications for O_2 sensing. Science 292:464–468

5. Jaakkola P, Mole DR, Tian YM, Wilson MI, Gielbert J, Gaskell SJ et al (2001) Targeting of HIF-alpha to the von Hippel-Lindau ubiquitylation complex by O_2-regulated prolyl hydroxylation. Science 292:468–472
6. Semenza GL (2011) Oxygen sensing, homeostasis, and disease. N Engl J Med 365:537–547
7. Xie L, Xiao K, Whalen EJ, Forrester MT, Freeman RS, Fong G et al (2009) Oxygen-regulated beta(2)-adrenergic receptor hydroxylation by EGLN3 and ubiquitylation by pVHL. Science Signal 2:ra33
8. Ivan M, Haberberger T, Gervasi DC, Michelson KS, Gunzler V, Kondo K et al (2002) Biochemical purification and pharmacological inhibition of a mammalian prolyl hydroxylase acting on hypoxia-inducible factor. Proc Natl Acad Sci U S A 99:13459–13464
9. Hoffman MA, Ohh M, Yang H, Klco JM, Ivan M, Kaelin WG Jr (2001) von Hippel-Lindau protein mutants linked to type 2C VHL disease preserve the ability to downregulate HIF. Hum Mol Genet 10:1019–1027
10. Lee S, Nakamura E, Yang H, Wei W, Linggi MS, Sajan MP et al (2005) Neuronal apoptosis linked to EglN3 prolyl hydroxylase and familial pheochromocytoma genes: developmental culling and cancer. Cancer Cell 8:155–167

Chapter 8

Analyzing the Tumor Microenvironment by Flow Cytometry

Yoon Kow Young, Alicia M. Bolt, Ryuhjin Ahn, and Koren K. Mann

Abstract

Flow cytometry is an essential tool for studying the tumor microenvironment. It allows us to quickly quantify and identify multiple cell types in a heterogeneous sample. A brief overview of flow cytometry instrumentation and the appropriate considerations and steps in building a good flow cytometry staining panel are discussed. In addition, a lymphoid tissue and solid tumor leukocyte infiltrate flow cytometry staining protocol and an example of flow cytometry data analysis are presented.

Key words Tumor microenvironment, Solid tumor, Immune cell infiltrate, Flow cytometry (FCM), Staining panel, Intracellular staining, Fluorescence-activated cell sorting (FACS), Multi-parameter, Isotype control, Spillover, Compensation, Fluorescence minus one (FMO)

1 Introduction to Flow Cytometry

1.1 General Information on Flow Cytometry

The tumor microenvironment consists of the basement membrane, extracellular matrix, immune cells, fibroblasts, and capillaries that form an intricate network at the primary tumor and metastatic niche to play an important role in tumor progression and metastasis. Flow cytometry is a quantitative tool that has been successfully used to characterize and isolate the heterogeneous components of the tumor microenvironment in clinical patient and cancer animal model samples. For example, using flow cytometry, researchers have identified increased levels of CD4+ CD25+ regulatory T-cells in the peripheral blood, tumor, and lymph nodes of breast and pancreatic cancer patients [1]. Using a mouse model of colorectal cancer, flow cytometry was used to determine increased levels of Gr1+ CD11b+ myeloid-derived suppressor cells in the tumor and spleen of animals, which played a role in enhanced angiogenesis and tumor growth [2]. In addition, researchers have used flow cytometry to characterize the infiltration of bone-marrow-derived myeloid and natural killer cells in the pre-metastatic niche in breast and melanoma cancer models [3]. In this chapter, we discuss flow cytometry

Josie Ursini-Siegel and Nicole Beauchemin (eds.), *The Tumor Microenvironment: Methods and Protocols*, Methods in Molecular Biology, vol. 1458, DOI 10.1007/978-1-4939-3801-8_8,

methodology and how to design and run a multi-parameter flow cytometry panel to characterize the tumor microenvironment at the site of primary tumor and metastatic niche.

Flow cytometry technology is an attractive tool for studying the tumor microenvironment, because it is a rapid and quantitative means to assess multiple markers (called parameters) in several cell populations from a cell suspension at single-cell resolution. Since its conception in the 1960s, there have been several major technological advances [4, 5]. Of these, the increase in the number of parameters that can be evaluated per sample has greatly advanced our understanding of cellular biology. Building and analyzing a multi-parameter flow cytometry staining panel can be challenging. However, smaller, more user-friendly instruments and software have made this technology more accessible.

Flow cytometers measure physical and fluorescent parameters of particles in suspension, which are termed "events." Examples of events could include cells, bacteria, organelles, or latex beads. Samples can be labeled with fluorescent probes or markers that include fluorescent dyes, fluorescent reporter genes, and fluorophores conjugated to antibodies or other proteins. Different fluorescent conjugates and dyes are commercially available and have excitation and emission characteristics that span the whole visible spectrum.

As mentioned, the power of flow cytometry rests on four main qualities. (1) *Data are acquired rapidly*. Analysis of thousands of events per second is routine. Due to the rapid speed at which data can be acquired, a large sample size can be analyzed, often in the order of millions of events. Having a large sample size effectively increases the statistical power of the data. (2) *Data are quantitative*. The fluorescence intensity observed is quantitative and therefore, the intensity for each probe compared to control can be directly related to the abundance of the parameter probed (protein content, DNA/RNA content, metabolites, etc.). (3) *Analyses can be multi-parametric*. Flow cytometry has the capability of simultaneously analyzing multiple fluorescent probes with each probe measuring a unique cellular parameter. Increasing the number of parameters increases the number of different populations and/or functions that can be analyzed simultaneously. Multiplexing multiple types of assays into one flow cytometry staining panel can increase the amount of data that can be acquired using a relatively small sample size. (4) *Every event is analyzed individually*. This allows us to simultaneously characterize multiple cell populations from a single sample. In addition, having a large number of events collected per sample makes it possible to focus on very rare cell populations by removing or "gating out" populations that are not of interest and "drill down to" or "gate into" a rare population of interests, even down to a single cell.

There are however several limitations in using flow cytometry. Flow cytometers can only analyze cells in suspension. Therefore, anatomical location of each cell within whole tissue is lost. Once

cultured cells are enzymatically treated (trypsinized) or organs mechanically dissociated, virtually all morphological parameters of the cell are altered. The cells retract their protrusions and extensions and become rounded. As we will see below, forward scatter (size) and side scatter (granularity) measurements are the only two physical parameters that are collected. Enzymes are often used to digest tissue into a single-cell suspension. These enzymes also have the potential of cleaving surface proteins of interest [6, 7]. In addition, when immunophenotyping, the antibody used to tag the cells can potentially activate them. This may alter the metabolism and expression of markers of interest. As is the case for immunofluorescent microscopy, cell fixation and permeabilization are required for intracellular immunophenotyping. This limitation impacts our ability to isolate live cells by fluorescence-activated cell sorting that differ in intracellular epitope properties.

1.2 Instrumentation

There are two main types of flow cytometers: flow cytometry analyzers and fluorescence-activated cell sorters (FACS). Both have the same analysis capability, but FACS has the additional ability to physically separate targeted populations into separate tubes for further downstream applications, such as in vitro culture or RNA, DNA, and protein isolation. Despite this added function, flow cytometers are based on the same components. There are three main components of a flow cytometer: fluidics, optics, and electronics (Fig. 1). The fluidics drives the instrument. In a large majority of instruments, pressurized sheath fluid hydrodynamically focuses the sample through the flow cells. At the interrogation point, fluidics and optics meet. High-power lasers are the excitation source of choice, since laser light is coherent and sample illumination time is extremely short. As a particle strikes the laser, light is scattered and excited fluorescent probes emit florescent light. Light-focusing and steering optics direct the scattered and fluorescent photons to detectors. Light detection optics, such as photodiodes and photomultiplier tubes (PMT), amplify and convert photon signals into electrical pulses. The electronics digitize each pulse in three integrations: pulse height, width, and area. Pulse height is the peak intensity of the pulse or the highest intensity measured. The width of the pulse is the time it takes for the event to pass through the laser or the time of flight. The area under the pulse is the sum of all heights. The area of the pulse is the preferred parameter to use for analysis, as it reflects the average intensity of each event.

The light deflection or scattering properties of each event allow for the detection of two physical parameters. Forward scatter (FSC) refers to the light deflected in front of or in line with the laser, which can tell us about the particle size. Larger events will scatter more light, increasing the FSC value. It is also important to note that other factors, such as refractive index and light absorption of the event, can also affect the FSC parameter readout by

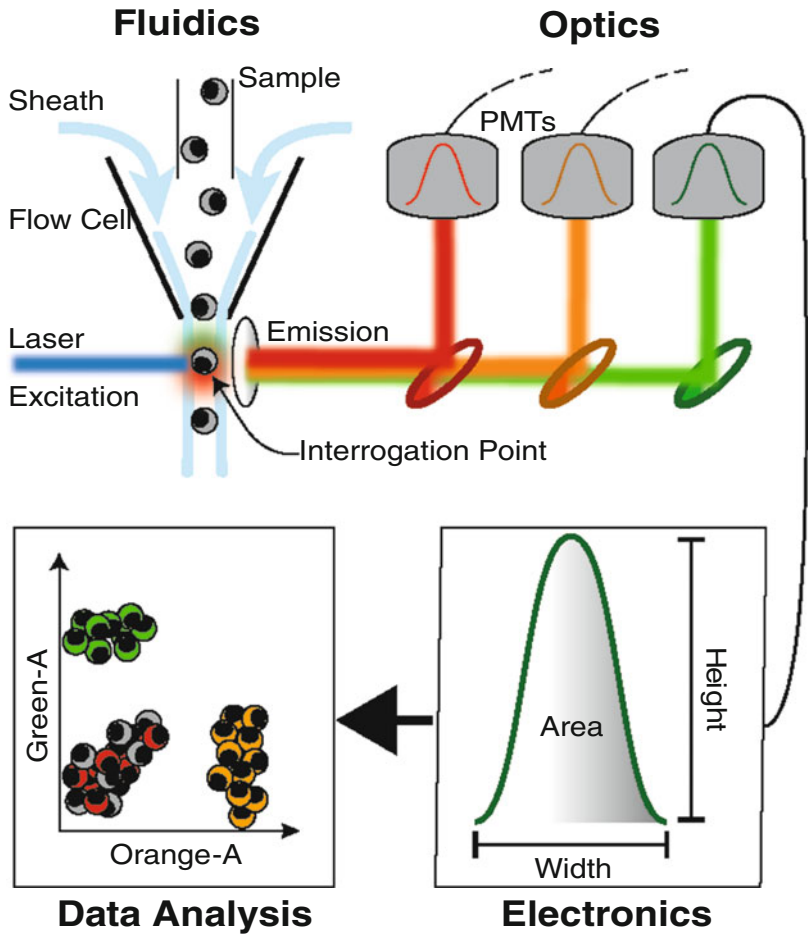

Fig. 1 Flow cytometry workflow. Flow cytometers are composed of three components: fluidics, optics, and electronics. Signals processed by the electronics are analyzed using flow cytometry software

about 2–5% [8]. The second physical parameter is side scatter (SSC), commonly referred to as granularity. Cells that have a rough outer membrane, granular vesicles, or an irregular internal structure scatter more light at right angles to the illumination source. The FSC and SSC parameters provide a rough estimate of the size and granularity of each cell, but also allow us to discriminate noise, debris, dead cells, and aggregates from the cells of interest.

Fluorescence emission is also measured at roughly right angles to the laser excitation source. Several optical components, such as lenses, fiber optics, dichroic mirrors, and band-pass filters, are used to steer and filter the emitted light, which is sent to the PMT. Each PMT is essentially collecting a discrete range of light wavelengths. The available excitation laser and the arrangement of the emission optics are highly customizable. The instrument layout of the optical components is referred to as the instrument optical configuration. It is important to note that the choice of probes must match

not only the assay, but also the instrument configuration. Improper fluorescence probe panel designs will negatively affect the sensitivity of the experiment; thus, it is recommended to consult with your flow cytometry core manager to determine your site's machine specifications, if applicable.

1.3 Panel Design

Immunophenotyping is a very common flow cytometry assay in which fluorophore-conjugated antibodies are used as probes to stain target cells with high avidity and affinity. This allows for rapid and easy phenotyping of each cell type in a heterogeneous sample according to the presence or absence of a combination of proteins. The epitope density of each event is also measured by assessing the intensity of the fluorescence, thus providing not only information on the presence or absence of an epitope, but also a quantitative measure of how many epitopes are present.

In the study of the tumor microenvironment, many researchers are interested in studying immune infiltrates, which can include, but are not limited to, lymphocytes (both T and B), macrophages, and myeloid derived-suppressor cells. These primary samples are heterogeneous, and thus it is important to be able to discriminate and identify different cell subpopulations within each sample. As mentioned, the probes must not only match the assay, but also the instrument configuration. Each fluorophore must be excitable by the available laser(s) and its emission must be detectable by one of the available emission filters.

With the right cocktail of probes, it is possible to affix each cell type with a unique set of fluorescent markers. Care must be taken to choose fluorochromes that are distinct. If two cellular proteins were stained with different probes conjugated to fluorophores with similar light excitation and emission spectra, the cytometer may not be able to differentiate them from one another. The emission profile of each fluorophore should be as spectrally separate as possible. Many manufacturers have spectra viewers to help choose the most compatible fluorophores when designing a new staining panel. However, in multi-parameter flow cytometry, the emission spectra of two distinct probes may overlap slightly and spill over into adjacent filters. Fluorescence spillover can be visually mitigated by compensation, but should be avoided or minimized as much as possible since it introduces error in the measurement [9, 10]. Spillover is seen as a spreading of the data or swelling of the negative population into affected parameters. Compensation helps to separate overlapping fluorescence so that respective populations can be more easily analyzed and gated. Adding compensation does not introduce measurement error into the data. It is the fluorescence spillover itself that causes data spread and decreases the sensitivity of the affected parameters [11]. Therefore, choosing two fluorophores that overlap increases background and decreases our ability to resolve dim double positives. The negative effect of

spillover is more apparent for very bright fluorescent signals and in turn, will decrease the sensitivity of fluorescence measured by adjacent detectors [10].

There are other important considerations when choosing fluorochromes. Fluorochromes differ in their intensity. Brilliant Violet™ 421 (BV421), phycoerythrin (PE), and allophycocyanin (APC) for example are amongst the brightest fluorophores currently available. Tagging the least abundant markers with these fluorochromes will increase our ability to visualize these events. In addition, considering the stability of the fluorophore is also important. APC and the GFP reporter proteins are large and more labile to formaldehyde and especially alcohol fixation. If a fixation step is required (intracellular staining), lower molecular weight fluorophores, such as Alexa Fluor 488, Cyanin 5 (Cy5), and Alexa Fluor 647, are more resistant to denaturation [12]. Tandem dyes consist of two dyes that are covalently coupled, so the light emission of the first excites the second by fluorescence resonance energy transfer (FRET) [13]. PE-Cy5 and APC-Cy7 dyes are common tandem dyes used in flow cytometry. For example, when PE (FRET donor) is excited by a laser, its emission can in turn excite Cy5 (FRET acceptor) and in turn emits a red shifted light (higher Stokes shift). This expands the range of fluorescence that can be emitted with a single excitation laser. However, tandem dyes are unstable and must be kept at 4 °C and protected from light [13]. The donor and acceptor can decouple causing the probes to fluoresce at the donor wavelength and the acceptor to aggregate, introducing false positive and artifacts. As in immunofluorescent microscopy, a secondary detection system, such as fluorescent-conjugated secondary antibody or avidin-biotin detection system, can be employed. Unconjugated primary antibodies can be easily labeled with a fluorescent secondary antibody, which has binding affinity to the primary antibody. Commercial kits are also available to directly conjugate primary antibody in-house. Biotinylated primary antibody coupled to a fluorescently coupled avidin secondary detection system is advantageous where there is low expression of epitopes. Since several fluorescent avidin can bind to each biotin, the signal is greatly amplified [14].

Primary samples, especially digested tissue, contain a lot of dead cells, cellular debris, and cells that are not of interest. It is sometimes very difficult to distinguish cells from dead cells and debris. Adding a live and dead discrimination marker will eliminate most of the debris and dead cells from the analysis. In addition, dead cells are highly autofluorescent and sticky and nonspecifically bind to dyes and antibodies, introducing false positives. Propidium iodide (PI) is often used because it is inexpensive and easy to use, but it cannot be used for fixed samples and its broad fluorescence emission is prohibitive. Several other live/dead dyes exist, including some that are amenable to fixation. In addition, introducing a marker of nucleated hematopoietic cells when studying immune infiltrates in a digested tumor sample is also wise (i.e.,

CD45). Teasing out these cells from all other events (debris, dead cells, and all other non-hematopoietic cells) simplifies the analysis of the target cells. These strategies can be adapted for any flow cytometry panel.

All flow cytometers are not alike and differ in their optical configuration. Thus, fluorescence measurements obtained from one instrument to another might differ greatly. It is recommended to perform a titration assay of all the fluorescent markers, even when using published assays. The background fluorescence and the positive signal should fit the linear reading range of the PMT. Several protocols have been published on how to titrate fluorescent markers properly [15, 16]. At an optimal titer, the signal-to-noise ratio is at maximum and the separation between the positive and negative populations will be at its greatest (making it easier to identify your positive population). A sample that is stained above or below the optimal titer will have lower signal-to-noise ratio. When the sample is stained with increasing number of reagents, the negative cells will start nonspecifically binding these markers, increasing background fluorescence and decreasing the separation between negative and positive fluorescence values. On the other hand, as we decrease staining reagent, the negative signal stays low but the positive signal will decrease until it merges with the negative.

1.4 Flow Cytometry Controls

A flow cytometry experiment is only as good as its controls. Three main groups of controls should be run during each assay: instrument controls, sensitivity controls, and biological controls [17]. Instrument controls include the negative or unstained controls and compensation controls. Sensitivity controls are the gating controls, which help to identify the positive cell populations. Biological controls are also gating controls with the added advantage of being biologically relevant. These three controls are an integral part of every flow cytometry experiment, stained the same day and acquired at the same time as the experimental samples. Here is a brief overview of each of these controls.

1.4.1 Instrument Controls

Unstained Control

Any unstained particle that is excited by a laser emits a baseline amount of fluorescence, autofluorescence. Cells typically show higher autofluorescence in the green spectrum. The unstained control allows us to adjust the PMT voltage gain for each detector, with the goal of adjusting the PMT gain to place the autofluorescence above the noise of the instrument. Some labs prefer to adjust the autofluorescence to three standard deviations above noise and others will set the population at a fixed intensity (above noise) for each parameter being read. Positive signal will clear the autofluorescence threshold and still be within the reading range (dynamic range) of the detector. If it is too bright, the PMT gain can be readjusted lower, putting the positive population in range. If possible, it would be wise to decrease the intensity of the positive signal for the next experiment by decreasing the titration of fluorescent label.

Compensation Control

The second set of necessary instrument controls are compensation controls. In conventional digital cytometers, compensation is an algorithm that is used to correct fluorescence spillover. For example, a flow cytometry experiment is set up to analyze the level of GFP transfection and PE antibody-labeled cells. The cytometer is equipped with a blue laser to excite both fluorophores and green and orange emission filters to collect GFP and PE fluorescence, respectively. While most of the light emitted from GFP-labeled cells is in the green spectrum, GFP-positive cells will also emit orange fluorescence in lesser intensity. The GFP green emission filter will collect most of the GFP green spectrum. However, portions of the light emitted by GFP cells will also spill over into the orange emission filter. All GFP cells will also be PE positive. With a GFP compensation control sample tube, the fluorescence spillover into PE can be properly compensated.

In order to calculate the correct fluorescence spillover compensation value, each compensation control sample tube must meet the three golden rules [18]. First, each compensation tube must contain a single positive signal, stained with the same fluorochrome as the experimental panel. Second, the autofluorescence of the negative and positive population must be identical. Third, the positive portion of the control must be as bright or brighter than the experimental sample.

The sample used for the compensation controls can be different from the test sample as long as the golden rules are met. For example, splenocytes can be a source of T-cells to prepare compensation sample tubes instead of precious tumor T-cell infiltrates. In addition, for low-expressing epitopes or rare cell types, compensation beads stained with the test-conjugated antibody are an excellent substitute. Compensation beads are engineered to capture the test antibody. It is important that the positive signal is as least as bright as the test sample, because the compensation value is more accurately calculated with a brighter fluorescence signal. A dimly stained compensation control will most often result in an underestimation of the compensation value (under-compensation). It is strongly recommended to use software automated compensation tools, because performing compensation manually will often result in overcompensation.

1.4.2 Sensitivity Controls

Sensitivity controls are negative controls. They are guides to determine the boundary between autofluorescence and positive specific antibody-binding fluorescence. There are three sensitivity controls: isotype control, fluorescence minus one (FMO) control, and antibody competition control [17].

Isotype Control

An isotype control antibody is an antibody of the same isotype as the test antibody, but has no affinity for antigen being tested. Thus, this antibody has the same constant region, but not the same variable region. In addition, if the primary test antibody is conjugated to a

fluorochrome, the isotype control is also conjugated with the same fluorochrome. Traditionally, isotype controls have been used as absolute gating controls. However, there are strong arguments that refute the validity of using this type of control as a gating control [9, 17, 19, 20]. Isotype controls can be useful in certain situations. For example, cultured primary cells may show increased nonspecific binding and an isotype control can help evaluate the increased level of background staining. When performing an intracellular stain with a conjugated primary antibody, it is difficult to wash off nonspecific antibody trapped in the cell. The isotype control can show how effective the washing steps were. Some immune cell types have high levels of Fc receptors, which can bind the staining antibody. When staining these cells, the Fc receptors need to be blocked adequately. In this case, an increase in isotype control staining will show incomplete Fc receptor blocking. Once a complete Fc receptor blocking protocol is determined, the isotype control can be omitted. However, as mentioned, the increase in background shown using isotype controls is inaccurate and only qualitative.

Fluorescence Minus One Control

Background fluorescence is affected in large multi-parameter staining assays, because increasing the number of fluorescent markers increases the inevitable fluorescence spillover. As mentioned above, fluorescence spillover increases spread of the data, increases background, and decreases sensitivity of the parameter(s) affected by spillover. This is visualized as a swelling of the background fluorescence. FMO is a very good gating guide, because it helps to determine the threshold between autofluorescence and positivity [17, 19]. An FMO control sample is stained with all the fluorescent markers within a given panel with the exception of one. Some laboratories spike in the isotype control matching the omitted test antibody marker. However, as mentioned above, this is not recommended, because isotype controls do not accurately delineate the background fluorescence boundary. With proper panel design, the amount of spillover can be minimized. FMOs account for the combined spillover effect of all other markers onto the parameter for which the stain has been omitted. They are especially important in samples where there is not a clear delimitation between background and positive fluorescence. Even when the fluorescence spillover compensation is miscalculated, FMOs can help gate for the real positive events. It is strongly recommended to do all FMOs for the first few flow cytometry assays. The use of FMOs can then be re-evaluated or even omitted for the parameters that can be easily gated. Please keep in mind that FMOs are not perfect, as we will see below.

Antibody Competition Control

To access the specificity of the antibody, the sample can be stained with a fluorescently labeled antibody with the addition of increasing amounts of a competing unlabeled antibody. If the antibody is specific, there will be a decrease of positive events with increasing unlabeled antibody. This control is useful when the specificity of the test antibody is in doubt or you are validating a new antibody.

1.4.3 Biological Controls

A biological control sample lacks the target protein or has a baseline amount of this protein of interest. This control sample is stained with the full staining panel. It allows identification and gating of positive events with certainty. It takes into account all the spillover effects just like in the FMO controls, but it is biologically relevant to the assay, for example, if we were to study the level of pSTAT1 in cancer cells. In this assay, the FMO control would not do justice because all cells express some pSTAT1. The FMO would show that the cells have no pSTAT1, which is improbable. A fully stained, unstimulated cancer cell sample will serve as a much more accurate baseline biological control. Cancer cells stimulated with IFNγ, which would increase pSTAT1, can also serve as a positive biological control. An increase or decrease in fluorescent intensity compared to baseline in pSTAT1 can then be accessed when treated.

2 Materials

2.1 Sample Preparation

1. 50 mL Conical tubes.
2. 1.5 mL Eppendorf tubes.
3. Centrifuge.
4. RPMI or DMEM Media.
5. FBS.
6. 1× Phosphate-buffered saline (PBS).
7. 1.5 or 2 mL Rubber pestles.
8. EDTA/PBS.
9. Chemical dissociates: DNase I (final concentration at 0.3 mg/mL) and collagenase B (final concentration at 2.4 mg/mL).
10. 70 μm Nylon cell strainers.
11. 37 °C Plate shaker.
12. Hemocytometer or automated cell counter.

2.2 Staining

External/Internal Staining

1. Centrifuge.
2. Cold 1× PBS.
3. Cold FACS buffer: 500 ml 1× PBS, 5% sodium azide, 5% FBS.
4. 1.5 mL Eppendorf tubes.
5. 5 mL Polystyrene round-bottom "FACS" tubes.
6. 96-Well V-bottom, clear, polystyrene microplates.
7. Live/Dead Marker.
8. Live/Dead Fixable Aqua Dead Cell Stain Kit, for 405 nm excitation.

9. Live/Dead Fixable Near-IR Dead Cell Stain Kit, for 633 or 635 nm excitation.
10. Fc block: Purified Rat Anti-Mouse CD16/CD32 (Mouse BD Fc Block).
11. Fluorescently-conjugated primary antibodies.
12. Vortex.
13. Fixation/permeabilization buffer (*see* **Note 1**).
14. Normal rat or mouse serum.

3 Methods

3.1 Sample Preparation

This protocol will focus on characterizing the immune cell infiltrates in primary tumors, although other cell types could certainly be incorporated into a staining panel. Analysis can also be performed in lymphoid tissues where it serves as a good control of the immune cell infiltrates in the primary tumor. This type of analysis also helps to distinguish systemic versus tumor-specific activation of immune cells.

The sample preparation will obviously depend upon the type of tissue. In general, solid tumors will need to be enzymatically digested in order to acquire a single-cell suspension. Other organs, particularly lymphoid tissues, can be dissociated through mechanical means.

3.1.1 Solid tumor

1. Dissect primary tumor and cut into small pieces in ice-cold 1× PBS.
2. Chemically dissociate tumor samples by incubating tumor in a 50 mL conical tube with 10 mL media supplemented with 5% FBS and 2.4 mg/mL collagenase B (*see* **Note 2**).
3. Incubate for 1.5–2 h at 37 °C on a shaker.
4. Monitor frequently and only allow reaction to continue until all the tissue is dissociated.
5. After incubation, put in 20 mL of PBS. Pipet up and down four times to dissociate tissue.
6. Centrifuge samples for 7 min at 300 × *g* at room temperature.
7. Remove supernatant, add 6 mL media containing 0.3 mg/mL DNase I, and dissociate pellet (*see* **Note 2**).
8. Incubate for 15–30 min at 37 °C on a shaker.
9. Centrifuge samples for 7 min at 300 × *g* at 4 °C.
10. Remove supernatant and resuspend in 10 mL of 1 mM EDTA/PBS. Pipet up and down to dissociate tissue.
11. Pass dissociated cells through a 70 μm filter, and rinse filter with PBS.

12. Count cells using hemocytometer or automated cell counter.

(Protocol optimized in Dr. Josie Ursini-Siegel's Laboratory, McGill University.)

3.1.2 Spleen or Other Lymphoid Tissues

1. Dissect spleen and dissociate tissue using a rubber pestle in a 1.5 mL tube with 1× PBS.
2. Pass dissociated cells through a 70 μm filter, and rinse filter with 1× PBS.
3. Count cells.

3.2 Staining Protocol

Once a single-cell suspension is obtained, cells can be stained for multiple parameters. In general, staining to detect external or cell surface antigen is performed first, followed by fixation/permeabilization steps, and staining for intracellular antigens.

3.2.1 External Staining

1. Resuspend $2–10 \times 10^6$ cells (depending on cell populations that you want to analyze and the cell type you are measuring; *see* **Note 3**) per sample in 25 μL PBS and place into staining tubes/plate (*see* **Note 4**).
2. Add 25 μL of pre-titrated Live/Dead stain mix to each sample.
3. Incubate for 30 min on ice in the dark.
4. Add 100 μL PBS per sample; spin at 350 × *g*, 4 °C, for 5 min; and decant (*see* **Note 5**).
5. Add 25 μL Fc block mix to each sample.

   Purified Rat Anti-Mouse CD16/CD32 (Mouse BD Fc Block): 2 μL per sample diluted in 23 μL FACS buffer.
6. Incubate for 30 min on ice in the dark.
7. Add 25 μL of antibody mix, already titrated antibody concentrations (*see* **Note 6**).
8. Incubate for 30 min on ice in the dark.
9. Add 100 μL FACS buffer per well; spin at 350 × *g*, 4°C, for 5 min; and decant.
10. For samples stained with only fluorescently conjugated primary antibodies against cell surface markers, add 100 μL of FACS buffer to each well and transfer to FACS tubes containing ~300 μL FACS buffer. These are ready for analysis. For samples that require a fluorescently conjugated secondary antibody, follow **steps 7–10** again.

3.2.2 Internal Staining

11. For samples that require staining of internal cell markers, stain all external markers first by following **steps 1–10**, and then continue on with **steps 12–20**.

12. Add 100 μL FACS buffer to each sample and transfer to a FACS tube containing 900 μL fixation/permeabilization buffer and vortex.
13. Incubate at 4 °C for 30 min in the dark.
14. Add 2 mL FACS buffer, spin at 300 × *g* for 5 min, and decant.
15. Resuspend in 100 μL FACS buffer.
16. Add 2 μL normal mouse/rat serum.
17. Incubate for 15 min at room temperature.
18. Add titrated internal antibodies for 30 min at room temp in the dark.
19. Add 2 mL FACS buffer, spin at 300 × *g* for 5 min, and decant.
20. Resuspend in 400 μL FACS buffer. These samples are ready for analysis.

3.3 Sample Analysis and Gating Strategies

For analysis of immune cell infiltrates within the tumor tissue, it is important to isolate the immune cells from the tumor cells at the beginning of the analysis. A helpful tip is to use a marker of nucleated hematopoietic cells to pull out the immune cell populations from the tumor cells. The leukocyte-specific marker CD45 was chosen for this analysis. Aggregates were gated out using FSC-A vs. FSC-H and SSC-A vs. SSC-H and live cells were selected. T- and B-cells were quantified using CD3 and B220, respectively. CD3– and B220– cells were then further subdivided using myeloid cell markers. The granulocytic MDSC population is CD11b+ and Gr1+. The other portion of the CD11b+ population that is Gr1– can be further subdivided by F4/80 staining. Gr1– CD11b+ F4/80– cells are monocytes and Gr1– CD11b+ F4/80+ cells are macrophages (Fig. 2). Separate FMO controls should be performed on the tumor cells to know where to place positive cell population gates for each cell type analyzed.

4 Notes

1. The fixation/permeabilization buffer is often recommended by the supplier, which is optimized for their antibody and should be used when possible. If no buffer is supplied, the fixation/permeabilization buffer will need to be optimized for each antibody [21]. In our experience, we prefer the Foxp3 Fix/Perm Staining Buffer from eBioscience for this step.
2. Some chemicals used to dissociate tumor tissue have been reported to alter cell surface marker expression on immune cells [6, 7]. Make sure to validate your specific protocol to determine how the chemical dissociation process affects surface marker expression on the cell types you are planning on analyzing in your panel before performing your experiments.
3. You should also consider how many cells you should stain per sample. In the context of analyzing immune cell components,

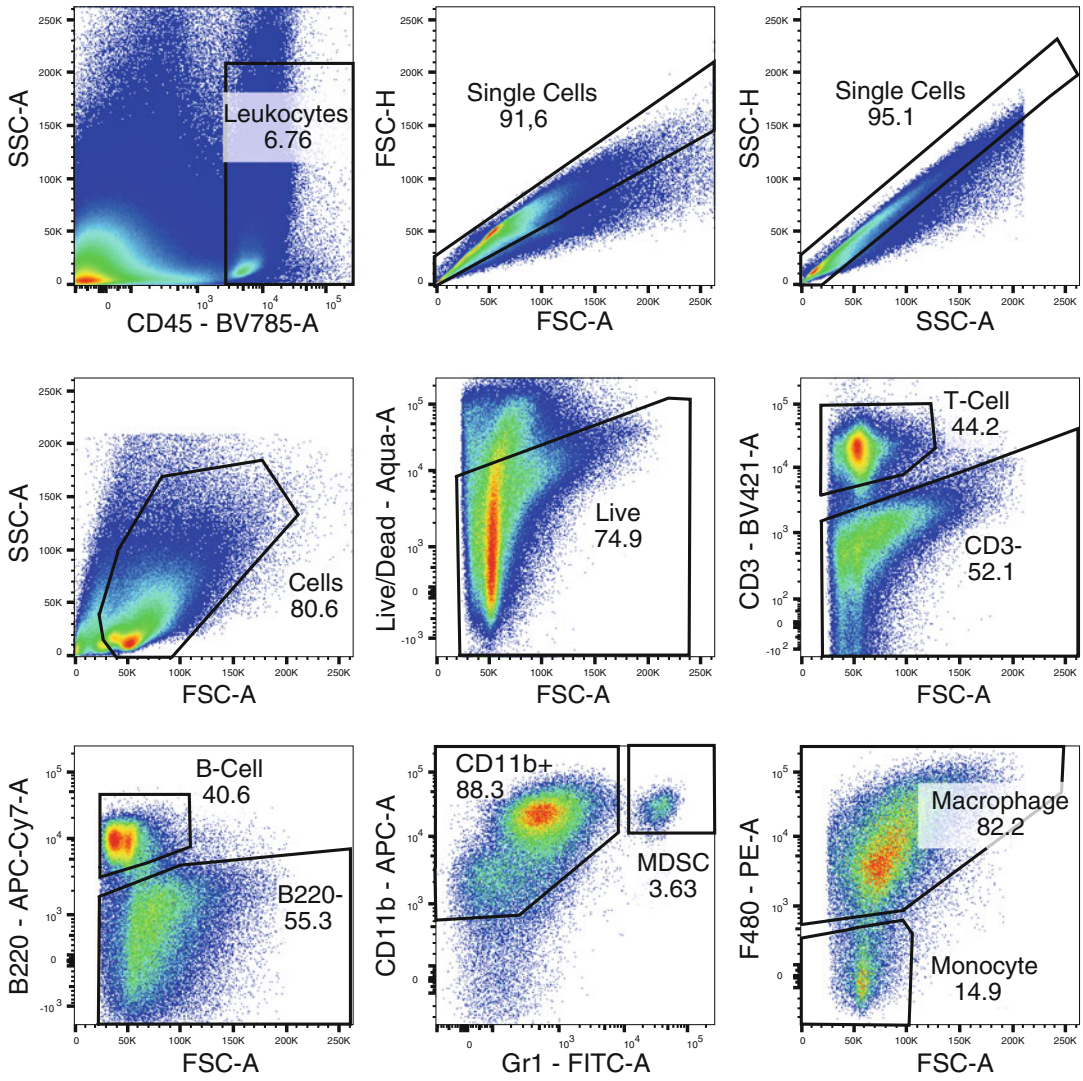

Fig. 2 Example of gating schematics to characterize the immune cell infiltrates in a primary tumor sample. A primary mouse mammary tumor was dissociated and cells were stained with fluorescently conjugated antibodies specific for immune cell subpopulations. The following markers were used in this analysis: Fixable Live/Dead Aqua, CD45 BV785, CD3 BV421, B220 APC-Cy7, CD11b APC, Gr1 FITC, and F4/80 PE

cell types from lymphoid tissues, such as spleen or thymus in which almost all the cells are lymphoid in origin, require a fewer number of cells to analyze than a more heterogeneous tissue type, such as a tumor where the number of immune cells in the total cell population is lower.

4. Samples can either be stained in tubes (FACS tubes) or 96-well microplates (with V-bottom) depending on sample volume. Staining in microplates is recommended for larger experiments to facilitate washing.
5. It is important to optimize centrifuge speed conditions in order to reduce the amount of sample lost in the wash steps.

6. All antibody concentrations within a given panel should be titrated for each cell type analyzed, taking into account the total number of cells you plan to stain per sample in your experimental design.
7. New technologies, such as imaging cytometry and mass cytometry, are bridging the gap between different technological fields and allow for more data parameters to be acquired at a single-cell resolution. Imaging cytometry allows for simultaneous visualization of the cells [22]. Mass cytometry, flow cytometry in tandem with mass spectroscopy, has brought multi-parameter analysis to a whole new level [23]. In mass cytometry, rare earth metals are used instead of fluorochromes, which eliminate fluorescence spillover, a major hurdle when combining several fluorescent probes in one staining panel. It is challenging to build panels exceeding 12 fluorescent parameters, but with mass cytometry, simultaneous detection of 30 or more parameters is possible. Since the instrumentation cost and/or availability of these young technologies are still limited, we focused the previous protocol on using classical flow cytometers to analyze components in the tumor microenvironment.

Acknowledgements

We acknowledge grant support from the Canadian Institutes of Health Research (MOP115000 to K.K.M.) and Jewish General Hospital Foundation's continued support of the LDI Flow Cytometry Facility. R.A. is supported by a fellowship from the Fonds de Recherche du Québec-Santé.

References

1. Liyanage UK, Moore TT, Joo HG, Tanaka Y, Herrmann V, Doherty G et al (2002) Prevalence of regulatory T cells is increased in peripheral blood and tumor microenvironment of patients with pancreas or breast adenocarcinoma. J Immunol 169:2756–2761
2. Yang L, DeBusk LM, Fukuda K, Fingleton B, Green-Jarvis B, Shyr Y et al (2004) Expansion of myeloid immune suppressor Gr+ CD11b+ cells in tumor-bearing host directly promotes tumor angiogenesis. Cancer Cell 6:409–421
3. Sceneay J, Chow MT, Chen A, Halse HM, Wong CS, Andrews DM et al (2012) Primary tumor hypoxia recruits CD11b+/Ly6Cmed/Ly6G+ immune suppressor cells and compromises NK cell cytotoxicity in the premetastatic niche. Cancer Res 72:3906–3911
4. Hulett HR, Bonner WA, Barrett J, Herzenberg LA (1969) Cell sorting: automated separation of mammalian cells as a function of intracellular fluorescence. Science 166:747–749
5. Kamentsky LA, Melamed MR, Derman H (1965) Spectrophotometer: new instrument for ultrarapid cell analysis. Science 150:630–631
6. Ford AL, Foulcher E, Goodsall AL, Sedgwick JD (1996) Tissue digestion with dispase substantially reduces lymphocyte and macrophage cell-surface antigen expression. J Immunol Methods 194:71–75
7. Autengruber A, Gereke M, Hansen G, Hennig C, Bruder D (2012) Impact of enzymatic tissue disintegration on the level of surface molecule expression and immune cell function. Eur J Microbiol Immunol 2:112–120

8. Shapiro HM (2005) Practical flow cytometry, 4th edn. Wiley, New York, p 736
9. Hulspas R, O'Gorman MR, Wood BL, Gratama JW, Sutherland DR (2009) Considerations for the control of background fluorescence in clinical flow cytometry. Cytometry B Clin Cytom 76:355–364
10. Maecker HT, Frey T, Nomura LE, Trotter J (2004) Selecting fluorochrome conjugates for maximum sensitivity. Cytometry A 62:169–173
11. Roederer M (2001) Spectral compensation for flow cytometry: visualization artifacts, limitations, and caveats. Cytometry 45:194–205
12. Schmid I, Dagarag MD, Hausner MA, Matud JL, Just T, Effros RB, Jamieson BD (2002) Simultaneous flow cytometric analysis of two cell surface markers, telomere length, and DNA content. Cytometry 49:96–105
13. Hulspas R, Dombkowski D, Preffer F, Douglas D, Kildew-Shah B, Gilbert J (2009) Flow cytometry and the stability of phycoerythrin-tandem dye conjugates. Cytometry A 75:966–972
14. Kaplan D, Smith D (2000) Enzymatic amplification staining for flow cytometric analysis of cell surface molecules. Cytometry 40:81–85
15. Hulspas R (2001) Titration of fluorochrome-conjugated antibodies for labeling cell surface markers on live cells. Curr Protoc Cytom Chapter 6:Unit 6.29
16. Stewart CC, Stewart SJ (2003) Titering antibodies. Wiley, New York, pp 4.1.1–4.1.13
17. Maecker HT, Trotter J (2006) Flow cytometry controls, instrument setup, and the determination of positivity. Cytometry A 69:1037–1042
18. Roederer M (2002) Compensation in flow cytometry. Curr Protoc Cytom Chapter 1:Unit 1.14
19. Herzenberg LA, Tung J, Moore WA, Herzenberg LA, Parks DR (2006) Interpreting flow cytometry data: a guide for the perplexed. Nat Immunol 7:681–685
20. O'Gorman Maurice RG, Thomas J (1999) Isotype controls—time to let go? Cytometry 38:78–80
21. Holmes K, Lantz LM, Fowlkes BJ, Schmid I, Giorgi JV (2001) Preparation of cells and reagents for flow cytometry. Curr Protoc Immunol Chapter 5:Unit 5.3
22. McGrath KE, Bushnell TP, Palis J (2008) Multispectral imaging of hematopoietic cells: where flow meets morphology. J Immunol Methods 336:91–97
23. Giesen C, Wang HA, Schapiro D, Zivanovic N, Jacobs A, Hattendorf B et al (2014) Highly multiplexed imaging of tumor tissues with subcellular resolution by mass cytometry. Nat Methods 11:417–422

Chapter 9

Detecting Secreted Analytes from Immune Cells: An Overview of Technologies

Kelly A. Pike, Caitlyn Hui, and Connie M. Krawczyk

Abstract

The tumor microenvironment is largely shaped by secreted factors and infiltrating immune cells and the nature of this environment can profoundly influence tumor growth and progression. As such, there is an increasing need to identify and quantify secreted factors by tumor cells, tumor-associated cells, and infiltrating immune cells. To meet this need, the dynamic range of immunoassays such as ELISAs and ELISpots have been improved and the scope of reagents commercially available has been expanded. In addition, new bead-based and membrane-based screening arrays have been developed to allow for the simultaneous detection of multiple analytes in one sample. Similarly, the optimization of intracellular staining for flow cytometry now allows for the quantitation of multiple cytokines from either a purified cell population or a complex mixed cell suspension. Herein, we review the rapidly evolving technologies that are currently available to detect secreted analytes. Emphasis is placed on discussing the advantages and disadvantages of these assays and their applications.

Key words Cytokine, ELISA, ELISpot, Cytokine array, Intracellular cytokine staining (ICS)

1 Introduction

Secreted analytes such as cytokines, chemokines, and growth factors mediate intercellular communication within the tumor microenvironment (TME), driving tumor growth, angiogenesis, and metastasis [1, 2]. These factors impact the number, type, and functional state of immune cells present in the TME, all of which can be indicators of a patient's prognosis [3–5]. Furthermore, immune cells are a significant source of secreted analytes, and the presence of immune cell-derived cytokines is indicative of the type of inflammation present. As such, characterizing the network of analytes present in a given tumor is necessary to define the TME, which has diagnostic, prognostic, and therapeutic implications [5, 6].

Cytokines can be broadly grouped into those that promote (pro-inflammatory) or those that diminish (suppressive) antitumor immune activity [7, 8]. Perhaps some of the most

Josie Ursini-Siegel and Nicole Beauchemin (eds.), *The Tumor Microenvironment: Methods and Protocols*, Methods in Molecular Biology, vol. 1458, DOI 10.1007/978-1-4939-3801-8_9,

well-known cytokines that promote antitumor activity are IL-12, IL-2, IFNγ, and type 1 IFNs [9]. These cytokines promote the cytolytic activity of $CD8^+$ and NK cells and also promote the differentiation of macrophages and $CD4^+$ T helper (TH)cells to acquire an "M1" and "Th1" phenotype, respectively. "Suppressive" cytokines, such as IL-10 and TGFβ, are known for their ability to limit effector and cytolytic responses of many immune cells including cytolytic cells, T_H cells, and innate cells. These cytokines are thought to play a particularly important role in instructing the antitumor response. Specifically, they have been shown to induce changes in gene expression and activity of signaling pathways that can impair the ability of immune cells to respond to pro-inflammatory signals [10]. For example, IL-10 is known to suppress the cytotoxic capacity of $CD8^+$ T cells, modulate macrophage polarization, and decrease the ability of dendritic cells to respond to and produce pro-inflammatory factors [11, 12].

Cytokine secretion is one of the primary features defining the functional state of immune cells. For example, polyfunctional $CD8^+$ T cells are described as producing TNFα, IFNγ, and IL-2 and are thought to have greater capacity to protect against infections and cancer. Among $CD4^+$ T T_H cells, T_H1 cells are characterized by their ability to produce IFNγ, and are known for their ability to promote the cytolytic activity of $CD8^+$ T cells and NK cells, whereas T_H2 cells secrete cytokines including IL-4, IL-5, and IL-13 that are associated with poor prognosis in certain cancers. Dendritic cells and macrophages that secrete pro-inflammatory cytokines such as IL-12, IL-6, or TNFα are capable of mounting an antitumor response, while partially matured IL-10-secreting DCs or macrophages are regulatory and can instruct T cells to be unresponsive [13, 14]. Therefore, identifying cytokines produced by immune cells provides information about their function along with insight regarding the nature of the inflammatory milieu present in any given tumor.

Perhaps one of the most widely used techniques to measure secreted analytes is the enzyme-linked immunosorbant assay (ELISA). By enabling efficient detection and quantification of secreted factors, such as peptides, proteins, antibodies, and hormones, the ELISA is a powerful tool to measure the presence of specific analytes within a crude preparation. As such, the ELISA can provide an accurate and sensitive measurement of cytokine production within the TME. However, while highly sensitive, the traditional ELISA can only measure one analyte at a time, and cannot provide any information on the cell from which it is derived (unless the cells are purified). Several other related techniques have been designed in recent years to overcome these limitations and provide a more comprehensive overview of the cytokine network present in the TME. Supernatant-based multiplex assays come in many forms and allow the simultaneous quantification of multiple proteins. These screening strategies provide a

Table 1
A comparison of supernatant-based assays

	Supernatant-based technologies		
	ELISA	**Cytokine bead arrays**	**Cytokine membrane array**
Format	Coated multi-well plates	Antibody-coated beads	Nitrocellulose membrane
Volume	50–100 µL	25–50 µL	200–700 µL (cell culture supernatant), 50–200 µL (serum and plasma samples)
Sample dilution	√	√	√
# of analytes detected	1 (up to 16 by multiplexing)	30–100 analytes	5–100 analytes
Time	1 day	3–3.5 h	1 day
Principle of detection	Colorimetric	Fluorescence	Chemiluminescence
Detection device	Spectrophotometric plate reader	Single- or dual-laser analyzers	X-ray film, digital imagers
Detection limit	1 pg/mL	Nanogram range	1 pg
Advantage(s)	Quick way to analyze large number of samples	Option to multiplex large number of analytes	Low cost, straightforward, screen large number of analytes
Disadvantage(s)	Costly multiplexing, narrow dynamic range	Cost and need for specialized detection instrumentation	High background
Customization	√	√	√

more global overview of the cytokine network and do not require any prior knowledge of the immune compartment present in the TME.

Alternatively, cell-based assays have been developed to provide more information regarding the cells producing the cytokines under investigation. For example, the enzyme-linked immunospot (ELISpot) assay was developed to detect the number of cells secreting a particular protein of interest, rather than quantifying the amount of analyte produced. Such information is critical for assessing the frequency of cells capable of engaging in an antitumor response. In addition, intracellular cytokine staining (ICS) detects the production and accumulation of cytokines within the cell, on a single-cell basis, rather than secreted products from a cell population.

Considering the wide range of detection assays now available, it is important for researchers to assess the strengths and weaknesses of each assay in order to select the most suitable technique

for answering their scientific question (Table 1). The following overview is therefore designed to compare and contrast these technologies.

2 Supernatant-Based Technology

2.1 ELISA

2.1.1 Key Principles

The ELISA is a plate-based immunoassay that measures the concentration of secreted analytes in solution. While four ELISA variants exist, all ELISAs are based on the same principle: the detection of an antigen by an antibody-enzyme conjugate (Fig. 1). An enzyme-matching substrate is transformed into a colored reaction product and the optical density of the reaction product is proportional to the analyte. To quantify the amount of analyte present within the sample, a standard curve is generated by preparing serial dilutions of a standard of known concentration and plotting absorbance against known concentration. The concentration of the samples is then calculated by interpolation.

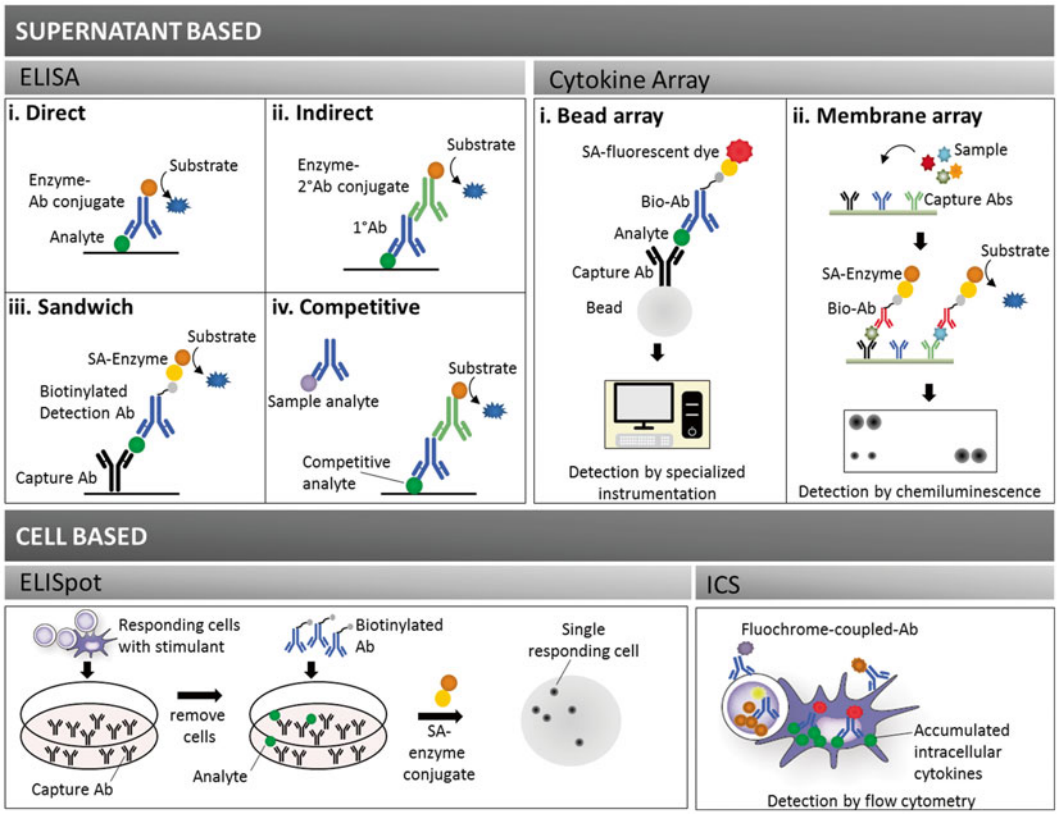

Fig. 1 An overview of analyte-detecting immuno-assays. Schematics illustrating the components of supernatant-based assays and cell-based assays are shown. *Ab* antibody, *Bio-Ab* biotinylated antibody, *1°Ab* primary antibody, *SA* streptavidin

2.1.2 Overview of Methodology

Direct ELISA

The direct ELISA is considered the simplest of the four techniques. It involves the addition of the analyte to a high-binding plate. All other binding sites are then blocked by the addition of an irrelevant protein, such as bovine serum albumin (BSA). Next, an enzyme-linked antibody specific for the analyte is added to the reaction.

Indirect ELISA

The indirect ELISA follows a similar methodology as the direct ELISA; however, it depends on a two-step process to amplify the signal. A primary antibody specific to the protein of interest is first added to the ELISA plate pre-coated with the analyte. This antibody-analyte complex is then detected with an enzyme-coupled secondary antibody that is specific to the primary antibody. Multiple washing and blocking steps (often with BSA) reduce the possibility of nonspecific signals that may arise from cross reactions between antibodies.

Sandwich ELISA

In contrast to the direct and indirect ELISAs, the sandwich ELISA requires plates to be first coated with a capture antibody specific for the analyte of interest. Samples are then added to each well, followed by the addition of a biotinylated detection antibody specific for an alternate site on the analyte. An avidin-coupled enzyme is then added, followed by the enzyme substrate. If the detection antibody is not biotinylated, a secondary enzyme-coupled antibody, specific for the detection antibody, can be used. The multiple layers of the sandwich ELISA necessitate extensive washing to prevent the production of nonspecific signals.

Of the four techniques, the sandwich ELISA tends to provide the highest level of sensitivity and is the most widely available in commercial kits. Although the assay may pose challenges to optimize—the capture and detection antibody must recognize different epitopes on the target protein to prevent cross-reactivity—many companies now sell commercial sandwich ELISA kits that are pre-optimized and designed to detect low-abundant cytokines. ELISA-optimized antibody-matched pairs, standards, detection reagents, and wash and coating buffers can be purchased as kits or sometimes as stand-alone products.

Competitive ELISA

The competitive ELISA is performed on crude samples and as such does not require sample processing and is therefore highly reproducible. This approach is based on competitive binding between the sample analyte and an add-in purified analyte bound to a microtiter plate. First, a primary antibody is incubated with the sample to allow for the formation of analyte-Ab complexes. Second, the sample is added to plates pre-coated with purified analyte. Following an incubation period, the sample is removed, and a secondary enzyme-coupled antibody is added to detect the primary antibody, and finally the enzyme substrate. As an alternative, the primary antibody can be directly linked to the enzyme. The higher the concentration of analyte in the sample, the less free antibody

will be available to bind the purified analyte coated on the well. As such, the substrate product is inversely proportional to the concentration of the sample analyte.

2.1.3 Detection Limit

Commercial ELISA kits, which are generally more sensitive than homemade ELISA reagents, typically having a lower detection limit of 1 pg/mL. However, there is currently a range of companies selling high-sensitivity ELISA kits, which are specifically designed to detect low-abundant cytokines. These kits enable accurate analyte quantification lower than conventional ELISA limits (<1 pg/mL), where some kits are as sensitive as 0.01 pg/mL.

2.1.4 Sample Volume

ELISAs typically require 50–100 μL of sample or standard per well in a 96-well plate. Depending on the abundance of the analyte of interest, samples may be added directly or require subsequent dilution. Therefore, optimization is required for each analyte and experimental condition.

2.1.5 Multiplexing

Multiplexed arrays based on ELISA technology can be commercially purchased to detect multiple analytes in one well. These assays rely on capture antibodies for different analytes being spotted on specific regions in each well. Detectors specific to the technology are generally required to detect signals from each region of the well.

2.1.6 Time and Cost

Although incubation times may vary between ELISA variants and commercial kits, typically one full day or two half days are required. Furthermore, sandwich ELISA kits often necessitate a pre-coating step 1 day prior to conducting the assay, where the capture antibody is added to the high-binding plates. To increase efficiency, some sandwich ELISA kits are sold with pre-coated plates, thereby eliminating the extra day. These plates are typically more expensive.

2.1.7 Advantages and Disadvantages

The main advantage of the ELISA are the cost and the range of assays available. Homemade ELISA can be performed by purchasing commercial antibodies and detection reagents separately. However, for rapid analysis, more sensitive detection, and improved quality control, commercial kits can be purchased at a wide range of prices. The disadvantage of the ELISA is that typically only one analyte can be detected per sample (aside from costly multiplex assays). In addition, ELISAs performed on supernatants harvested from mixed populations or kinetic assays in which analytes can accumulate can be difficult to interpret for mixed populations and should therefore be avoided.

2.2 Cytokine Bead Arrays

2.2.1 Key Principles

Collectively, bead assays use spectrally distinct beads coated with capture antibodies to quantify secreted analyte proteins in cell culture supernatant, serum, and plasma. While bead assays can be used for the detection of a single analyte, they are primarily used in an array format that simultaneously quantifies multiple

analytes in a single sample. While all bead arrays follow a similar protocol, several distinct bead arrays are available: cytometric bead arrays, color-coded polystyrene bead arrays, and superparamagnetic bead arrays.

2.2.2 Overview of Methodology

Cytometric Bead Array

The cytometric bead array utilizes hard-dyed polystyrene-based microspheres, with distinct fluorescence intensities coated with capture antibodies of differing specificities. A combination of different beads is then mixed with the sample followed by the addition of a detection antibody coupled to a fluorescence protein such as phycoerythrin (PE). Similar to the sandwich ELISA, the capture and detection antibodies recognize distinct epitopes. The intensity of the PE fluorescence is proportional to the concentration of analyte. The cytometric bead array can be read on any flow cytometer equipped with 488 nm or 532 nm and 633 nm lasers.

The cytometric bead array requires a recombinant protein standard to provide an internal control, in addition to generating a standard curve for subsequent quantitative analysis.

Polystyrene and Superparamagnetic Bead Array

Polystyrene and superparamagnetic bead arrays follow a similar methodology to the cytometric bead array. First, the sample is added to a mixture of color-coded polystyrene or magnetic beads that are pre-coated with antibodies specific for the analytes of interest. Next, biotinylated detection antibodies are added to the reaction. These antibodies are also specific to the analytes of interest, and, in conjunction with the capture antibody, form an antibody-antigen sandwich. Finally, PE-conjugated streptavidin is added, which binds the biotinylated detection antibodies (Fig. 1). The assay can then be read on a variety of technology-specific instruments that classify the beads according to analyte specificity, and detect the magnitude of the PE-derived signal as a measure of analyte abundance.

2.2.3 Detection Limit

Cytometric Bead Array

The cytometric bead array has the capacity to measure up to 30 different analytes within a sample. Furthermore, enhanced sensitivity cytometric bead array assays are available that enable the detection of as low as 0.274 pg/mL of protein in the multiplexed assay.

Polystyrene and Superparamagnetic Bead Array

Polystyrene and superparamagnetic bead arrays are capable of quantifying up to 100 different target analytes per sample. Companies are constantly expanding their libraries and improving detection limits in the nanogram range.

2.2.4 Sample Volume

In comparison to more conventional techniques, such as the ELISA, the cytometric bead array requires a reduced sample volume (Table 1). Specifically, the assay can be completed with only 25–50 μL of sample. The polystyrene and superparamagnetic bead arrays also require 50 μL of sample or standard per assay. While

both bead arrays and ELISAs utilize 50 μL sample volume per experiment, the bead arrays have the capacity to measure more than one analyte in a single assay. Therefore, techniques like the cytometric bead array and the polystyrene bead array reduce the overall sample volume necessary to measure multiple analytes.

2.2.5 Time and Cost

The cytometric bead array is available in two formats: Flex Sets and Kits. In the Flex Sets, companies allow researchers to build their own multiplex of secreted analytes of interest. In contrast, cytometric bead array kits are optimized to consistently measure a predetermined multiplex of cytokines based on routine panels. Assay cost, therefore, depends on both the format of the cytokine bead array and the number of analytes examined. Generally, Flex Sets are more expensive than the Kits as they are customizable. Furthermore, the greater the number of analytes measured, the more expensive the Flex Set or the Kit. Regardless of format, the cytometric bead array requires approximately 3.5 h to complete.

Superparamagnetic and polystyrene arrays take approximately 3 h to conduct. Similar to the cytometric bead array, these assays can be purchased in a pre-mixed kit or custom ordered. While the assay has the capacity to quantify up to 100 target analytes, many kits are optimized to screen a lower number of analytes per sample. Furthermore, costs vary depending on the number of analytes of interest and whether or not the kit is pre-mixed. Generally, the greater the number of analytes measured, the higher the cost. Premixed kits are also less expensive than custom-designed arrays.

2.2.6 Advantage and Disadvantages

The main advantage of the bead assays is that a large number of analytes can be detected in a small volume of sample within a short period of time and over a large dynamic range. Though some technologies can be read on a standard flow cytometer, the main limitations are the need for specialized detection instrumentation, the incompatibility between different commercialized products, and the cost.

2.3 Cytokine Membrane Arrays

2.3.1 Key Principles

Similar to the bead arrays, cytokine membrane arrays are used to screen a panel of cytokines. They are based on the sandwich immunoassay principle, which involves spotting capture antibodies onto nitrocellulose membranes. Analytes within cell culture supernatants, cell lysates, tissue lysates, serum, or plasma samples may be measured using this methodology.

2.3.2 Overview of Methodology

Membranes are purchased ready for use, spotted with a panel of capture antibodies. Currently, membrane arrays can be purchased to detect 5–100 cytokines, grouped by biological function or customized. Membranes are exposed to diluted samples, after which the membrane is processed in the same manner as western blotting. In brief, the membrane is incubated with a cocktail of biotinylated antibodies, which are then detected with an enzyme-linked

streptavidin. Once the enzyme substrate is added, the reaction product can be visualized using film or a digital imaging system (Fig. 1).

2.3.3 Detection Limit

The detection limit of the cytokine membrane array depends on the chemiluminescent substrate utilized to detect the protein sample. The most commonly used detection reagents are enhanced chemiluminescence (ECL) with horseradish peroxidase (HRP), which may be captured with film or a CCD imager. These reagents are available in varying forms with enhanced sensitivity, detecting approximately 1 pg or less of protein sample.

2.3.4 Sample Volume

The recommended volume for membrane cytokine arrays depends on the type of sample. For example, while the array recommends 200–700 μL sample volume of cell culture supernatant, it only requires 50–200 μL of serum and plasma samples.

2.3.5 Time and Cost

The cytokine arrays are a fast technology to screen a large panel of cytokines. Typically, the protocol can be completed within 1 day. As well, given that no specialized equipment is required, membrane arrays are a relatively inexpensive technology.

2.3.6 Advantages and Disadvantages

The clear advantages of the membrane arrays are the low cost and straightforward protocol. In addition, the membrane arrays are reported to have a wider range of detection than traditional ELISAs (25–250,000 pg/mL for IL-2) and to have lower inter-array variation. However, the need for sample dilution, the high background typically observed, and the reliance on densitometry for quantitation are limitations that need to be considered when choosing to use a membrane array.

2.4 Commercial Services

Commercial services are available for the purpose of discovery or routine analysis. The technologies used are generally ELISA- or bead-based assays. The researcher pays on a per analyte/per sample basis to measure custom or predetermined sets of secreted factors. For discovery assays, while commercial services or multiplex may be costly up front, a specific panel of analytes can be focussed on in future experiments. Most companies will make custom arrays to suit your experimental needs.

3 Cell-Based Technologies

3.1 ELISpot

3.1.1 Key Principles

The enzyme-linked immunospot (ELISpot) assay is a variant of the ELISA technique and is frequently used to quantify the number of cytokine-secreting cells. It is an antibody-based method that depends on both a capture and detection antibody, similar to the sandwich ELISA technique (Table 2).

Table 2
A comparison of cell-based assays

	Cell-based technologies	
	ELISpot	**ICS**
Format	Nitrocellulose membrane	Multi-well plate, round-bottom FACS tube
Cell number	Cell type/experiment dependent	Cell type/experiment specific
# of analytes detected	2	Dependent of flow cytometry laser configuration
Time	3 days	1 day
Principle of detection	Colorimetric	Fluorescence
Detection device	ELISpot plate reader	Flow cytometer
Detection limit	1 in 100,000 cells	Avg: 2000 molecules, lower limit: 100 molecules
Advantage(s)	Sensitivity	Compatible with complex cell preparation
Disadvantage(s)	Need to optimize cell number	Need for stimulation and secretion blocking reagents
Customization	√	√
Applications	Detection of the number of cytokine secreting antigen-specific immune cells	Identification of distinct immune cell subsets and the cytokine(s) they produce within a mixed cell population

3.1.2 Overview of Methodology

Nitrocellulose or PVDF membrane-bottomed 96-well plates are pre-coated with a capture antibody specific to the secreted analyte of interest. Cells are then added to this surface in the presence or absence of stimuli, the latter of which serves as a negative control for spontaneous cytokine production. During a defined incubation period, analytes secreted by the cells are immobilized by the capture antibodies. The plate is then washed to remove the cells and an enzyme-conjugated or biotinylated detection antibody is added. As with the sandwich ELISA technique, this antibody recognizes a different epitope from the capture antibody. The enzyme's substrate is then added, generating a colored precipitate that is visible on the surface of the membrane (Fig. 1). Each spot corresponds to an individual analyte-secreting cell. The membrane is then analyzed manually by counting the spots or is read by an automated reader specific for ELISpot assays.

3.1.3 Detection Limit

Generally, the limit of detection of an ELISpot assay is 1 in 100,000 cells; however, several companies claim that the assays are now sensitive enough to accurately quantitate cytokine-secreting cells that fall below this frequency. This high sensitivity makes

the ELISpot an attractive choice for measuring T and B cell responses, in addition to investigating cytokine production by small populations of immune cells. ELISpot assays are typically available in single- and dual-color kits. Dual-color kits are designed to measure the number of single cells that secrete one or both cytokines specified in the kit.

3.1.4 Sample Volume

The ELISpot assay typically requires 100 μL of sample or standard per well; however, slight variations exist between protocols.

3.1.5 Time and Cost

The ELISpot protocol is simple and efficient, consisting of primarily of washing and incubation steps. However, due to the long incubations necessary to conduct this assay, the entire protocol requires at least 3 days. The assay may however be stopped at certain points in the protocol and stored for up to 2 weeks.

3.1.6 Advantages and Disadvantages

The advantage of the ELISpot is that it allows the evaluation of the number of cytokine-producing cells rather than the amount of analyte in the supernatant. It can also be scaled up for high-throughput screening. However, as with ELISAs, ELISpots are reliant on the availability of two quality antibodies that recognize separate sites on the cytokine of interest.

3.2 Intracellular Cytokine Staining

3.2.1 Key Principles

Intracellular cytokine staining (ICS) is an alternative strategy that detects cytokine production at the single-cell level. It is a flow cytometry-based assay designed to simultaneously phenotype immune cells and detect the cytokines they produce (Fig. 1). This approach has allowed for the identification of immune cells capable of secreting multiple cytokines simultaneously.

3.2.2 Overview of Methodology

In vitro stimulation is required to promote cytokine production. During stimulation, the addition of a protein secretion inhibitor retains cytokines within responding cells. Brefeldin A (BFA) and monensin are two common inhibitors used for this purpose. While monensin inhibits trans-Golgi function, BFA inhibits transport between the endoplasmic reticulum and the Golgi [15]. Although monensin can be more toxic to certain cell types, BFA can affect the surface expression of activation markers such as CD69 on T cells [16, 17]. As such, the choice of transport inhibitor is dependent on the cytokine to be detected and the cell type being analyzed. At the end of the stimulation, cells are washed and stained for extracellular markers by following a typical immunofluorescence protocol. To detect intracellular molecules, cells are then fixed and permeabilized for antibodies to gain access to the interior of the cell.

3.2.3 Detection Limit

The sensitivity of ICS is dependent on the flow cytometer setup, the quality of the reagents used, and the optimization of the protocol. Optimization of the protocol requires the identification

of the appropriate secretion inhibitor, activation conditions, permeabilization/fixation solutions, and incubation times. The detection limit of most flow cytometry protocols is 2000 molecule antigens per cell, which is sufficient for common immune-associated antigens such as CD4 and CD8 (expressed at 20,000–100,000 molecule antigens per cell). However, protocols optimized for sensitivity can detect as few as 100 molecule antigens per cell [18].

3.2.4 Sample Volume

In contrast to the other techniques discussed, ICS does not require a fixed sample volume. The cells can be distributed in microwell plates or plastic tubes, and the sample size is largely dependent on the parameters of the individual experiment.

3.2.5 Time and Cost

ICS involves two incubations of a minimum of 30–60 min, one for the extracellular and the other for the intracellular stain. The duration of the assay, therefore, is largely dependent on the number of samples and the time it takes to collect and analyze the results with the flow cytometer. ICS is easily completed in a day.

3.2.6 Advantages and Disadvantages

Unlike the other assays discussed so far, ICS can be used to discriminate the contribution of each cell type to the pool of cytokines present in the microenvironment. Moreover, cytokine production is detected on a single-cell level but millions of cells can be analyzed in a timely fashion. Significantly, ICS enables simultaneous multi-parameter phenotyping including analysis of cytokine production, surface markers, other intracellular proteins, and transcription factors. The disadvantage, however, is that cells often have to be "restimulated" prior to analysis to enable detection of the intracellular protein. As well, the use of drugs to block secretion can affect the surface expression of critical activation markers and cytokine production itself.

4 Discussion

The technologies reviewed here will allow for a greater understanding of the abundance and functionality of immune cells present in the TME. Generally, it is thought that type 1 immunity favors tumor clearance by cytolytic means and the presence of type 2 immunity favors tumor progression, either directly or through inhibition of cytolytic and pro-inflammatory cell function. However, this model is greatly simplified and more comprehensive studies are necessary to fully appreciate extent to which the "nature" (type 1, type 2, regulatory, suppressive) of the immune component in the TME regulates tumor control. While many studies have been performed that describe the presence of immune-related factors within the TME, these factors are seldom divided into functional groups. Furthermore, presence of mRNA transcripts (expression profiling) does not indicate

that the cytokine is being produced at that moment; the capacity to produce a cytokine (mRNA expression) and the actual production of that cytokine are not equivalent. Therefore, detection of cytokine production is necessary to infer function and/or regulatory role of the cells within the TME.

In the future, it will be critical to correlate these findings with the localization of cytokine-producing immune cells within the TME. This approach will distinguish between tumor subtypes capable of activating antitumor effector cells that are unable to migrate to the target tumor cells, from tumor subtypes which contain suppressed and exhausted effector cells throughout the TME.

Acknowledgements

We acknowledge the support of the Leukemia and Lymphoma Society of Canada and the Canadian Cancer Society Research Institute to K.A.P., and the CIHR and NSERC for funding to C.K.

References

1. McAllister SS, Weinberg RA (2014) The tumour-induced systemic environment as a critical regulator of cancer progression and metastasis. Nat Cell Biol 16:717–727
2. Chai EZ, Siveen KS, Shanmugam MK, Arfuso F, Sethi G (2015) Analysis of the intricate relationship between chronic inflammation and cancer. Biochem J 468:1–15
3. Gajewski TF, Schreiber H, Fu YX (2013) Innate and adaptive immune cells in the tumor microenvironment. Nat Immunol 14:1014–1022
4. Mahmoud S, Lee A, Ellis I, Green A (2012) CD8(+) T lymphocytes infiltrating breast cancer: a promising new prognostic marker? Oncoimmunology 1:364–365
5. Galon J et al (2012) The immune score as a new possible approach for the classification of cancer. J Transl Med 10:1
6. Motz GT, Coukos G (2013) Deciphering and reversing tumor immune suppression. Immunity 39:61–73
7. Landskron G, De la Fuente M, Thuwajit P, Thuwajit C, Hermoso MA (2014) Chronic inflammation and cytokines in the tumor microenvironment. J Immunol Res 2014:149185
8. Wang D, DuBois RN (2015) Immunosuppression associated with chronic inflammation in the tumor microenvironment. Carcinogenesis 36:1085–1093
9. Floros T, Tarhini AA (2015) Anticancer cytokines: biology and clinical effects of interferon-alpha2, interleukin (IL)-2, IL-15, IL-21, and IL-12. Sem Oncol 42:539–548
10. Wu AA, Drake V, Huang HS, Chiu S, Zheng L (2015) Reprogramming the tumor microenvironment: tumor-induced immunosuppressive factors paralyze T cells. Oncoimmunology 4:e1016700
11. Mittal SK, Roche PA (2015) Suppression of antigen presentation by IL-10. Curr Opin Immunol 34:22–27
12. Dennis KL, Blatner NR, Gounari F, Khazaie K (2013) Current status of interleukin-10 and regulatory T-cells in cancer. Curr Opin Oncol 25:637–645
13. Liu J, Cao X (2015) Regulatory dendritic cells in autoimmunity: a comprehensive review. J Autoimmun 63:1–12
14. Benencia F, Muccioli M, Alnaeeli M (2014) Perspectives on reprograming cancer-associated dendritic cells for anti-tumor therapies. Front Oncol 4:72
15. Schuerwegh AJ, Stevens WJ, Bridts CH, De Clerck LS (2001) Evaluation of monensin and brefeldin A for flow cytometric determination of interleukin-1 beta, interleukin-6, and tumor necrosis factor-alpha in monocytes. Cytometry 46:172–176

16. Nylander S, Kalies I (1999) Brefeldin A, but not monensin, completely blocks CD69 expression on mouse lymphocytes: efficacy of inhibitors of protein secretion in protocols for intracellular cytokine staining by flow cytometry. J Immunol Methods 224:69–76
17. O'Neil-Andersen NJ, Lawrence DA (2002) Differential modulation of surface and intracellular protein expression by T cells after stimulation in the presence of monensin or brefeldin A. Clin Diagn Lab Immunol 9:243–250
18. Zola H (2004) High-sensitivity immunofluorescence/flow cytometry: detection of cytokine receptors and other low-abundance membrane molecules. Curr Prot Cytom Chapter 6:Unit 6.3

Chapter 10

Purification of Immune Cell Populations from Freshly Isolated Murine Tumors and Organs by Consecutive Magnetic Cell Sorting and Multi-parameter Flow Cytometry-Based Sorting

Camilla Salvagno and Karin E. de Visser

Abstract

It is well established that tumors evolve together with nonmalignant cells, such as fibroblasts, endothelial cells, and immune cells. These cells constantly entangle and interact with each other creating the tumor microenvironment. Immune cells can exert both tumor-promoting and tumor-protective functions. Detailed phenotypic and functional characterization of intra-tumoral immune cell subsets has become increasingly important in the field of cancer biology and cancer immunology. In this chapter, we describe a method for isolation of viable and pure immune cell subsets from freshly isolated murine solid tumors and organs. First, we describe a protocol for the generation of single-cell suspensions from tumors and organs using mechanical and enzymatic strategies. In addition, we describe how immune cell subsets can be purified by consecutive magnetic cell sorting and multi-parameter flow cytometry-based cell sorting.

Key words Tumor microenvironment, Immune cells, Myeloid cells, Magnetic cell sorting, Enrichment, Fluorescence-activated cell sorting (FACS), Solid tumor, Preclinical mouse model

1 Introduction

It is now well established that immune cells present in the tumor microenvironment play a critical role in tumor development and progression [1]. Most human and experimental tumors are abundantly infiltrated with various immune cell types. The presence of some of these immune cells, including regulatory T cells, macrophages, and myeloid-derived suppressor cells, is frequently associated with a poor prognosis [2–4], while other immune cells, including $CD8^+$ T cells and NK cells, frequently correlate with good prognosis [5, 6]. Experimental studies using transgenic mouse models for de novo tumorigenesis have been instrumental in identifying the functional significance of the various immune cell subsets in tumor development, progression, and therapy response [4, 7–11].

Josie Ursini-Siegel and Nicole Beauchemin (eds.), *The Tumor Microenvironment: Methods and Protocols*, Methods in Molecular Biology, vol. 1458, DOI 10.1007/978-1-4939-3801-8_10,

In these transgenic tumor models, tumors develop spontaneously in their natural microenvironment and immune cells evolve together with tumor cells, thus closely recapitulating tumor development in the human setting [12]. For these reasons, careful phenotypic and functional characterization of the complexity of the inflammatory tumor microenvironment has been increasingly important.

There are various methods for the assessment of the type, the phenotype, and/or the activation status of immune cells in tumors and other organs. It is possible to either directly analyze freshly generated single-cell suspension by multi-parameter flow cytometry or isolate specific immune cell population by flow cytometry-based cell sorting for further culturing, protein, or RNA extraction analyses. Regardless of which of these techniques will be performed, single-cell suspensions need to be generated from tumor and organs. Here, we describe a protocol to mechanically and enzymatically process tumors and other organs to generate single-cell suspensions and to prepare the samples for flow cytometry analysis. Flow cytometry-based sorting is the ultimate method for the isolation of specific cell populations. However, depending on the number and percentage of the immune cells of interest, the actual sorting procedure might be time consuming. In order to accelerate the sorting procedure and to obtain a high purity of the desired cells, we have described a two-step

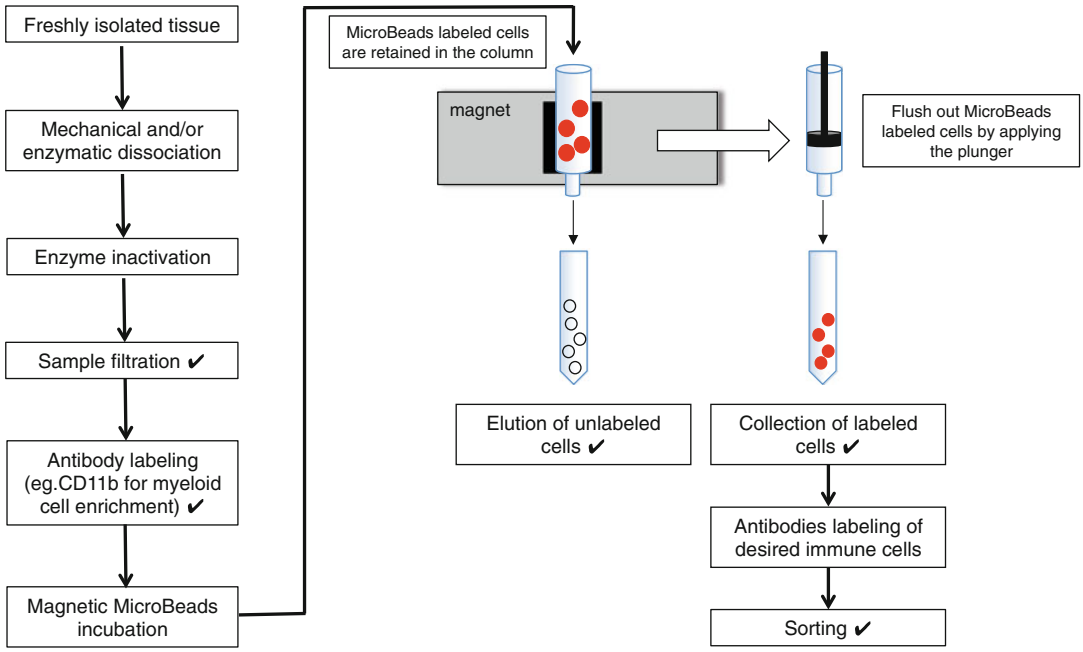

Fig. 1 Schematic workflow of the immune cell subset isolation by magnetic cell sorting and multi-parameter flow cytometry-based cell sorting. Ticks (✓) indicate steps to collect a small sample of cells that will be analyzed by flow cytometry at the end of the protocol

method for isolation of several myeloid cell subsets from tumors. Briefly, we first enrich the samples for myeloid immune cells by the use of magnetic cell sorting; then, we isolate immune cell subpopulations by flow cytometry-based sorting. A schematic overview of the protocol is depicted in Fig. 1. Although here we focus on the isolation of myeloid immune cells, researchers can adapt this protocol for the isolation of other type of cells, such as lymphocytes.

2 Materials

2.1 Generation of Single-Cell Suspensions from Freshly Isolated Solid Tumors and Organs

1. McIlwain Tissue Chopper (Ted Pella, Inc.) (*see* **Note 1**).
2. Enzyme digestion mix 1: 3 mg/mL Collagenase A in DMEM (serum free) (*see* **Notes 2** and **3**).
3. Enzyme digestion mix 2: 100 μg/mL Liberase in DMEM (serum free).
4. DMEM medium supplemented with 8% fetal bovine serum (FBS), 100 IU/mL penicillin, 100 μg/mL streptomycin (P/S), and 0.5 mM EDTA.
5. DMEM medium supplemented with 8% FBS, P/S.
6. Sorting buffer: IMDM, 2% FBS, 0.5% β-mercaptoethanol, 0.5 mM EDTA.
7. Erylysis buffer: 155 mM NH_4Cl, 10 mM $KHCO_3$, 0.1 mM EDTA in H_2O, pH 7.2–7.4.
8. 5000 U.I./mL Heparin sulfate.
9. Deoxyribonuclease I from bovine pancreas (DNase) dissolved to 10 μg/μL in 1× PBS.
10. FACS buffer: 0.5% BSA in 1× PBS.
11. Plunger from a 2 mL syringe.
12. Water bath or MACSmix™ tube rotator from Miltenyi Biotec.

Table 1
Example of an antibody panel for the purification of several myeloid cell populations by consecutive magnetic cell sorting and flow cytometry-based cell sorting

Antigen	Marker for	Fluorochromes/dye
CD11b	Myeloid cells	APC
F4/80	Macrophages	PE
Ly6G (1A8)	Neutrophils	FITC
Ly6C	Monocytes and neutrophils	eFluor450
	Live/dead	405 excitation

2.2 Purification of Immune Cell Subsets by Consecutive Magnetic Cell Sorting and Multi-parameter Fluorescence-Activated Cell Sorting (FACS)

1. AutoMACS™ Rinsing Solution supplemented with 0.5% BSA from Miltenyi Biotec (*see* **Note 4**).
2. Magnetic Micro Beads (Miltenyi Biotec) conjugated to an antibody with specificity for the fluorochrome of the antibody used in Subheading 3.3, **step 3** (*see* **Notes 4** and **5**).
3. QuadroMACS™ separator from Miltenyi Biotec (*see* **Notes 4** and **6**).
4. LS columns from Miltenyi Biotec (*see* **Notes 4** and **7**).

Table 2
Examples of antibody panels for the quantitative and phenotypic characterization of myeloid and lymphoid cell populations

Antigen	Marker for	Fluorochromes/dye
Lymphoid panel		
CD45	Immune cells	eFluor605NC
CD11b	Myeloid cells	APC-Cy7 eFluor780 (damp channel)
CD3	Lymphocytes	PE-Cy7
CD19	B cells	FITC
CD4	$CD4^+$ T cells	PE-Cy5
CD8	$CD8^+$ T cells	PerCP
CD49b	NK cells	APC
Granzyme B[a]	Lymphocyte activation	PE
IFNγ[a,b]	Lymphocyte activation	eFluor450
	Live/dead	Dye eFluor780
Antigen	Marker for	Fluorochromes and dye
Myeloid panel		
CD45	Immune cells	PerCP
CD11b	Myeloid cells	APC-Cy7 eFluor780
CD3	Lymphocytes	PE-Cy7
Ly6G (1A8)	Neutrophils	FITC
Ly6C	Monocytes and neutrophils	eFluor450
F4/80	Macrophages	PE
	Live/dead	Dye 405 excitation

[a]These are intracellular markers. For intracellular staining, we have good experience with BD Cytofix/Cytoperm Fixation/Permeabilization kit from BD Bioscience. Follow the manufacturer's instruction for the intracellular staining
[b]For IFNγ staining, before starting with Subheading 3.2, **step 3**, cells need to be stimulated with 50 ng/mL PMA, 1 μM ionomycin and GolgiPlug in IMDM, 8% FBS, and 0.5% β-mercaptoethanol for 3 h in the incubator at 37 °C

5. Antibodies: For the antibody combination used to isolate different myeloid cell populations, see Table 1 (*see* **Notes 8** and **9**).

2.3 Other Materials

1. 96-Well U-bottom plates.
2. 70 μm Filter cell strainers that fit on top of a 50 mL tube.
3. 15 and 50 mL Polypropylene tubes (*see* **Note 19**).
4. 5 mL Polypropylene tubes.
5. Antibodies: For the antibody combination used for quantitative and/or phenotypic characterization of immune cells, see Table 2 (*see* **Note 9**).
6. Flow cytometer (*see* **Note 10**).
7. Sorter (*see* **Note 11**).

3 Methods

Throughout the protocol, it is important to keep the samples on ice as much as possible, unless stated otherwise. Freshly harvested tissues should be collected in 1× PBS on ice and immediately processed. Single-cell suspensions are prepared as follows.

3.1 Tissue Digestion and Single-Cell Suspension

1. Mammary gland and mammary gland tumors: Chop the sample in a tissue chopper three times or until the tumor is dissociated (*see* **Note 1**). It is recommended to cut the tissues in smaller pieces with a scalpel before chopping to facilitate the procedure. Once chopped, incubate the sample in 10 mL enzyme digestion mix 1 with 25 μg/mL DNase in a 50 mL tube for 1 h at 37 °C in a shaking water bath (*see* **Notes 2**, **3**, and **12**).

   After digestion, stop the reaction by adding 20 mL DMEM, 8% FBS, P/S, and 0.5 mM EDTA and filter the sample through a 70 μm cell strainer in a 50 mL tube at 4 °C. Wash the cell strainer with 5 mL of DMEM, 8% FBS, P/S, and 0.5 mM EDTA to collect residual cells, centrifuge 300×*g* for 10 min at 4 °C, and discard supernatant. Immediately continue through Subheading 3.2 or 3.3.
2. Lungs: Chop the lungs three times in a tissue chopper (*see* **Note 1**) and incubate the sample in 2 mL digestion mix 2 in a 15 mL tube for 30 min at 37 °C in a shaking water bath (*see* **Note 12**). Stop the reaction by adding 5 mL DMEM, 8% FBS, and P/S and filter the sample through a 70 μm cell strainer in a 50 mL tube at 4 °C. Wash the cell strainer with 5 mL DMEM, 8% FBS, and P/S to collect residual cells, centrifuge at 300×*g* for 10 min at 4 °C, and discard supernatant. Immediately continue through Subheading 3.2 or 3.3.
3. Spleen and lymph nodes: Disperse the tissue through a 70 μm cell strainer (pre-wetted with 1× PBS) in a 50 mL tube by smashing it with a plunger while adding 1× PBS. Wash the cell

strainer with 5 mL 1× PBS in order to collect residual cells. Centrifuge at 300 × *g* for 10 min at 4 °C and discard supernatant. Resuspend the pellet of the spleen in 5 mL erylysis buffer for 5–10 min at RT in order to eliminate erythrocytes that might interfere with flow cytometry analyses. Filter the cells through a 70 μm cell strainer, centrifuge at 300 × *g* for 10 min, and discard supernatant. Immediately continue through Subheading 3.2 or 3.3.

4. Blood: Collect 1 mL of blood in 50 μL heparin sulfate. Add 5 mL erylysis buffer and incubate for 5–10 min at RT in a 15 mL tube. Centrifuge at 300 × *g* for 10 min at 4 °C and pour off the supernatant. Add again 5 mL erylysis buffer for 5–10 min at RT, centrifuge at 300 × *g* for 10 min at 4 °C, and pour off the supernatant. Immediately continue through Subheading 3.2.

Once the single-cell suspensions have been prepared, the samples can either be directly analyzed by flow cytometry in order to quantitatively and phenotypically characterize cell populations (*see* Subheading 3.2) or prepared for cell sorting (*see* Subheading 3.3).

3.2 Quantitative and/or Phenotypic Characterization of Immune Cells by Multi-parameter Flow Cytometry

1. Resuspend single cells in 5–10 mL FACS buffer (for a small tumor and for one lymph node we recommend 5 mL; for large tumors, spleen, and lung, we recommend 10 mL) and count the cells. Plate ≈ 2×10^6 cells per antibody combination in a 96-well plate U-bottom shape.
2. Centrifuge the plate in a cold plate—centrifuge at 300 × *g* for 2 min and flick out supernatant.
3. Add 50 μL of antibody mix (*see* **Note 9**), gently mix by pipetting, and incubate the cells for 30 min at 4 °C in the dark. In Table 2, an example of an antibody combination for myeloid and lymphoid cells is shown.
4. Wash the wells twice with 150 μL of FACS buffer, centrifuge the plate at 300 × *g* for 2 min, and flick out supernatant. Resuspend in 50–100 μL of FACS buffer and analyze the sample with a flow cytometer (*see* **Notes 9** and **10**).

Although immune cell subsets can be directly sorted by flow cytometry from the prepared single-cell suspensions, it is our experience that a better yield and purity can be obtained by a two-step process involving pre-enrichment for total myeloid immune cells by magnetic cell sorting, followed by purification of the desired immune cell subset(s) by multi-parameter flow cytometry-based cell sorting. Throughout the protocol, we advise to collect small samples of cells for analysis by flow cytometry at the end of the procedure to check the enrichment by the column and the purity of the sorted cells.

3.3 Immune Subset Purification by Consecutive Magnetic Cell Sorting (See Note 4) and Multi-parameter Flow Cytometry-Based Cell Sorting

1. Resuspend single cells in 5–10 mL of sorting buffer (for a small tumor and for one lymph node we recommend 5 mL; for large tumors, spleen, and lung, we recommend 10 mL) and count cells.
2. Centrifuge cells at 300×*g* for 10 min at 4 °C and discard supernatant.
3. To enrich the sample for myeloid cells, we use the marker CD11b (*see* **Note 8**). Resuspend the sample in sorting buffer containing the fluorochrome-conjugated CD11b antibody (e.g.: CD11b-APC) and incubate for 30 min at 4 °C in the dark. Use 50 µL of antibody mix per 10^7 cells (*see* **Note 13**). We advise to collect a small sample (≈50,000 cells) and store it in the 96-well plate at 4 °C. This sample will be used later for flow cytometry analyses and will be referred to as the "labeled" fraction.
4. Wash cells with 1–2 mL of sorting buffer per 10^7 cells (*see* **Note 13**). Centrifuge the cells at 300×*g* for 10 min at 4 °C and discard supernatant.
5. Resuspend cell pellet in 80 µL of sorting buffer per 10^7 cells (*see* **Note 13**). Add 20 µL per 10^7 cells of magnetic Micro Beads conjugated with an antibody against the CD11b-fluorochrome used in Subheading 3.3, **step 3** (e.g.: anti-APC Micro Beads) (*see* **Notes 5**, **13**, and **14**). Incubate for 20 min on ice in the dark.
6. Wash cells by adding 1–2 µL of sorting buffer per 10^7 cells (*see* **Note 13**). Centrifuge the cells at 300×*g* for 10 min at 4 °C and discard supernatant.
7. Resuspend up to 10^8 cells in 500 µL of AutoMACS™ Rinsing Solution and filter the cell suspension through a 70 µm cell strainer on a 50 µL tube to eliminate clumps that might obstruct the column (*see* **Note 15**). Wash the cell strainer with 100 µL of AutoMACS™ Rinsing Solution to collect residual cells.
8. Depending on the number of labeled cells, choose the appropriate column, and place it in the magnetic field of a MACS separator (*see* **Notes 6** and **7**). Prepare empty 15 mL tubes underneath the column in order to collect the flow-through.
9. After rinsing the column with 3 mL of AutoMACS™ Rinsing Solution, apply cell suspension once the flow-through has stopped. Let the column empty by gravity.
10. Wash column three times with 3 mL of AutoMACS™ Rinsing Solution and collect the flow-through that contains the CD11b– cells. Add new buffer only when column reservoir is empty.
11. Remove the column from the magnetic field and place it into a new 15 mL tube. Pipette 6 mL of AutoMACS™ Rinsing Solution into the column and immediately flush out the CD11b+ cells by firmly pressing the plunger into the column (*see* **Note 16**).

12. Count both CD11b+ and CD11b– cell fractions. We advise to collect a small sample (≈50,000 cells) to put in the 96-well plate at 4 °C. These samples will be used later for flow cytometry analyses and will be referred to as "CD11b–" and "CD11b+" fractions.
13. Spin down CD11b+ cells at 300×*g* for 10 min at 4 °C and discard supernatant.
14. Resuspend the CD11b+ cell fraction in the AutoMACS™ Rinsing Solution containing antibodies specific for the immune cell populations of interest. An example can be found in Table 1. Calculate 50 µL antibody mix per 10^7 cells (*see* **Notes 9** and **13**). If the number of cells is low, use at least 5 µL of antibody mix. Incubate cells for 30 min on ice in the dark.
15. Wash cells by adding 1–2 mL of AutoMACS™ Rinsing Solution per 10^7 cells (*see* **Note 13**). Centrifuge the cells at 300×*g* for 10 min at 4 °C and discard supernatant. Resuspend cells in AutoMACS™ Rinsing Solution at a concentration of 20×10^6 cells per mL (*see* **Notes 17** and **18**), add live/dead marker if necessary, and take it to the sorter (*see* **Note 11**). Collect sorted cells in 5 ml DMEM and 8% FBS in polypropylene tubes (*see* **Note 19**).
16. An example of a gating strategy to sort macrophages, neutrophils, and monocytes with markers described in Table 1 is shown in Fig. 2. After gating out duplets and gating on live cells, plot CD11b and F4/80. After gating on the CD11b+ F4/80– population, plot Ly6G and Ly6C. CD11b+ F4/80+ cells are macrophages; Ly6G+ Ly6C+ cells are neutrophils; Ly6G– Ly6C+ cells are monocytes.
17. We advise to collect a small sample of each sorted cell type (≈50,000 cells) and put it in the 96-well plate at 4 °C. These samples will be used for flow cytometry analysis.
18. Analyze the samples collected in Subheading 3.3, **steps 3**, **12**, and **17** by flow cytometry. These samples will give an estimation of the CD11b enrichment by the column and the sorting purity. *See* Fig. 3 for an example.

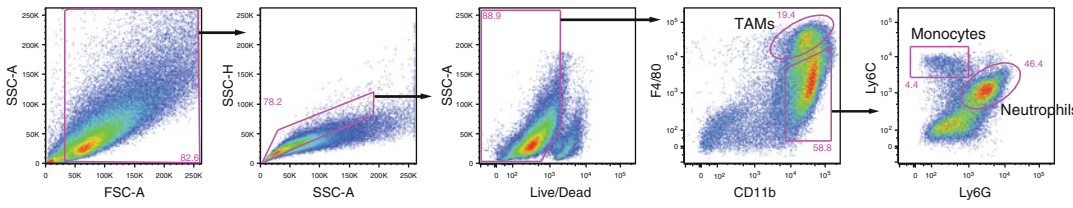

Fig. 2 Dot plots of a murine mammary gland tumor illustrating the flow cytometry gating strategy. After gating out duplets and dead cells, the macrophage population is gated as CD11b+ F4/80+. In the CD11b+ F4/80– fraction, neutrophils are Ly6G+ Ly6C+ and monocytes are Ly6C+ Ly6G–

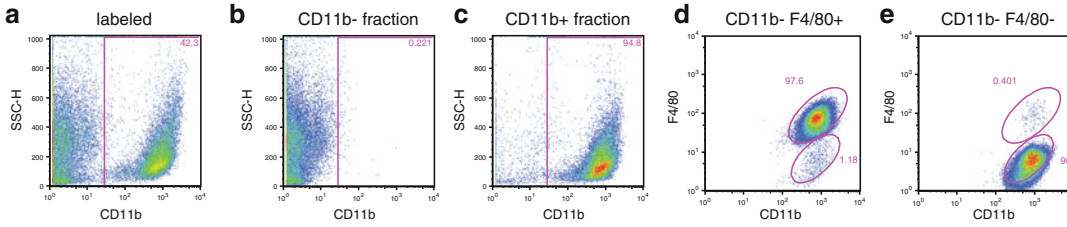

Fig. 3 Dot plots of murine mammary gland tumor samples collected during the pre-enrichment procedure for myeloid immune cells by magnetic cell sorting and after the isolation by flow cytometry-based sorting. In this example, F4/80+ and F4/80– cells were isolated from the tumor. (**a**) Panel **a** depicts the dot plot and gating of CD11b+ myeloid cells before the magnetic column pre-enrichment. (**b**) and (**c**) show the CD11b– and CD11b+ fractions, respectively, obtained after the magnetic column pre-enrichment procedure. The comparison between (**a**) and (**c**) shows the enrichment of CD11b+ cells by the magnetic column. (**d**) and (**e**) show the purity of F4/80+ and F4/80– cells, respectively, after isolation by flow cytometry-based sorting

4 Notes

1. Researchers can adjust cutting speed, blade force, and blade travel on the tissue chopper. We have good experience with maximum cutting speed and blade force, and 5–10 μm blade travel. As an alternative to the tissue chopper, researchers can use razor blades, scissors, or scalpels to chop the tumors into very small fragments.
2. We have optimized the digestion mix for mammary tumors. For other tumor types, different composition of the enzyme digestion mix and different incubation time might be needed. An example for prostate cancer and subcutaneous B16 melanoma can be found in [13].
3. If the sample is not properly digested, it is also possible to add trypsin at the final concentration of 1.5 mg/mL to the digestion mix. Trypsin might cleave some surface markers that can be of interest for sorting or other type of analysis. For this reason, before proceeding with the experiment, it should be established if the marker of interest is cleaved by trypsin.
4. We have good experience with the MACS cell separation reagents from Miltenyi Biotec. However, researchers can also purchase magnetic separation columns from other vendors.
5. This protocol describes an indirect method for magnetically labeling the cells of interest. Researchers should select the Micro Beads based on the fluorochrome conjugated to the antibody used for column enrichment. For example, if the antibody is conjugated with allophycocyanin (APC), researchers are advised to use anti-APC Micro Beads.

6. MACS separators are strong magnets with holders for columns. Since there are different column sizes, researchers should match the correct separator with the correct column holder (*see* **Note 7**).
7. Based on the number of expected magnetically labeled cells, researchers should select the correct column capacity. For example, LS columns from Miltenyi Biotec can hold up to 10^8 magnetically labeled cells from up to 2×10^9 total cells. Make sure to match the correct MACS separator format (*see* **Note 6**).
8. We have good experience with the pan-myeloid marker CD11b conjugated to APC for column enrichment. However, it is also possible to use other markers for immune cells, like CD45, or CD3 for the isolation of lymphocytes.
9. According to the immune cell populations of interest, researchers should design their own antibody combinations. The choice of the fluorochromes conjugated to the antibodies is dependent on the flow cytometer used. Make sure that the flow cytometer contains the right lasers and detectors to excite and read the fluorochromes. An overview of our frequently used antibody combinations can be found in Tables 1 and 2.
10. We have good experience with BD LSRII Flow Cytometer with DIVA software (BD Biosciences, USA). Other machines can be used as long as they can detect the antibody combination used (*see* **Note 9**).
11. We have good experience with BD FACSARIA II sorter with DIVA software (BD Biosciences, USA). Other machines can be used as long as they can detect the antibody combination used (*see* **Note 9**).
12. Alternatively, we also have good experience using the MACSmix™ tube rotator from Miltenyi Biotec located in an incubator at 37 °C.
13. Round up the number of counted cells and use this value to calculate the amount of antibodies, sorting buffer or Micro Beads in order to ensure that all cells are labeled. For example, if the researcher counts 1.2×10^6 cells, round it up to 2×10^6.
14. Prior to use, resuspend the Micro Beads by vortexing.
15. Scale up the volume of sorting buffer according to the total number of cells.
16. Miltenyi Biotec provides the correct plunger together with the column.
17. This is the optimal concentration for cell sorting for the BD FACSARIA II in our facility. We suggest asking your FACS facility for optimal cell concentration. In case of very few cells, do not add less than 500 µL of AutoMACS™ Rinsing Solution in order for the sorter to have enough volume.

18. Use AutoMACS™ Rinsing Solution for sorting because it is colorless. Phenol red in medium may interfere with fluorochromes.
19. Cells easily attach to the wall of polystyrene tubes. To avoid this, polypropylene tubes are recommended for collection of sorted cells. Researchers should choose the size of the polypropylene tube accordingly to the tube holder of the sorter machine.

Acknowledgements

We thank Kim Vrijland and Tisee Hau for insightful comments on the manuscript. Work in the lab is supported by grants from the European Union (FP7 MCA-ITN 317445 TIMCC), the European Research Council (ERC consolidator award INFLAMET 615300), the Beug Foundation for Metastasis Research, and the Dutch Cancer Society (2011-5004).

References

1. Quail DF, Joyce JA (2013) Microenvironmental regulation of tumor progression and metastasis. Nat Med 19:1423–1437
2. Bates GJ, Fox SB, Han C, Leek RD, Garcia JF, Harris AL, Banham AH (2006) Quantification of regulatory T cells enables the identification of high-risk breast cancer patients and those at risk of late relapse. J Clin Oncol 24:5373–5380
3. Chevolet I, Speeckaert R, Schreuer M, Neyns B, Krysko O, Bachert C et al (2015) Clinical significance of plasmacytoid dendritic cells and myeloid-derived suppressor cells in melanoma. J Transl Med 13:9
4. DeNardo DG, Brennan DJ, Rexhepaj E, Ruffell B, Shiao SL, Madden SF et al (2011) Leukocyte complexity predicts breast cancer survival and functionally regulates response to chemotherapy. Cancer Discov 1:54–67
5. Ishigami S, Natsugoe S, Tokuda K, Nakajo A, Che X, Iwashige H et al (2000) Prognostic value of intratumoral natural killer cells in gastric carcinoma. Cancer 88:577–583
6. Mahmoud SM, Paish EC, Powe DG, Macmillan RD, Grainge MJ, Lee AH et al (2011) Tumor-infiltrating CD8+ lymphocytes predict clinical outcome in breast cancer. J Clin Oncol 29:1949–1955
7. Coffelt SB, Kersten K, Doornebal CW, Weiden J, Vrijland K, Hau CS et al (2015) IL-17-producing gammadelta T cells and neutrophils conspire to promote breast cancer metastasis. Nature 522:345–348
8. Coussens LM, Raymond WW, Bergers G, Laig-Webster M, Behrendtsen O, Werb Z et al (1999) Inflammatory mast cells up-regulate angiogenesis during squamous epithelial carcinogenesis. Genes Dev 13:1382–1397
9. Lin EY, Nguyen AV, Russell RG, Pollard JW (2001) Colony-stimulating factor 1 promotes progression of mammary tumors to malignancy. J Exp Med 193:727–740
10. Ciampricotti M, Hau CS, Doornebal CW, Jonkers J, de Visser KE (2012) Chemotherapy response of spontaneous mammary tumors is independent of the adaptive immune system. Nat Med 18:344–346
11. Bald T, Quast T, Landsberg J, Rogava M, Glodde N, Lopez-Ramos D et al (2014) Ultraviolet-radiation-induced inflammation promotes angiotropism and metastasis in melanoma. Nature 507:109–113
12. Junttila MR, de Sauvage FJ (2013) Influence of tumour micro-environment heterogeneity on therapeutic response. Nature 501:346–354
13. Watkins SK, Zhu Z, Watkins KE, Hurwitz AA (2012) Isolation of immune cells from primary tumors. J Vis Exp 64:e3952

Chapter 11

Viral Engineering of Chimeric Antigen Receptor Expression on Murine and Human T Lymphocytes

Joanne A. Hammill*, Arya Afsahi*, Jonathan L. Bramson, and Christopher W. Helsen

Abstract

The adoptive transfer of a bolus of tumor-specific T lymphocytes into cancer patients is a promising therapeutic strategy. In one approach, tumor specificity is conferred upon T cells via engineering expression of exogenous receptors, such as chimeric antigen receptors (CARs). Here, we describe the generation and production of both murine and human CAR-engineered T lymphocytes using retroviruses.

Key words Chimeric antigen receptor, T lymphocytes, CAR-T cell, Gamma-retrovirus, Lentivirus

1 Introduction

Cancer immunotherapy aims to utilize or bolster the immune system's antitumor capabilities to regress or cure malignancies. One such strategy sees cancer patients treated with a bolus of their own T cells possessing specificity against their tumor. These adoptive T cell therapies have seen significant clinical success in a variety of malignancies [1–5]. Obtaining tumor-specific T cells on a per-patient basis is afforded through either the expansion of endogenously occurring tumor-specific T cells or by genetically engineering peripheral T cells to express receptors with specificity for tumor targets. Both of these strategies require the generation of large numbers of tumor-specific T cells prior to treatment through an ex vivo culture period. Chimeric antigen receptors (CARs) are recombinant proteins composed of an extracellular antigen recognition domain and an intracellular activation domain, which trigger T cell activation and cytotoxicity upon binding of target antigen [6]. Here, we focus on the production of both murine and human T cells engineered to express a CAR for preclinical evaluation.

*Authors contributed equally to this work.

Josie Ursini-Siegel and Nicole Beauchemin (eds.), *The Tumor Microenvironment: Methods and Protocols*, Methods in Molecular Biology, vol. 1458, DOI 10.1007/978-1-4939-3801-8_11,

Genetic engineering of recombinant receptors in T lymphocytes is most commonly accomplished using retroviruses. Retroviruses, members of the *Retroviridae* family of enveloped viruses, have the natural capacity to integrate their genetic information into the genome of infected host cells. As such, a retrovirus engineered to encode a CAR can permit the production of T cells which stably express the tumor-specific receptor. *The protocol described herein details the production of two different retroviruses and their use for the production of CAR-T cells: a gamma-retrovirus with tropism for murine cells (used for the generation of murine CAR-T cells) and a lentivirus with tropism for human cells (used for the generation of human CAR-T cells).*

Production of a gamma-retrovirus [7] is accomplished by combining a retroviral vector (encoding the CAR in a retroviral genomic backbone) with a packaging plasmid and/or packaging cell line (both of which contain the *gag*, *pol*, and *env* genes required for production of functional viral particles). By providing the viral packaging genes *gag*, *pol*, and *env* in *trans* (not encoded in the viral genome), the resultant gamma-retroviruses are non-replicative, increasing the safety profile of the system. Here, we co-transfect the Platinum-E (Plat-E) packaging cell line [8] with our retroviral vector and the packaging plasmid pCL-Eco [9] to generate gamma-retroviruses.

Similar to the gammaretrovirus used for transduction of murine cells, the lentivirus utilized for transduction of human T cells is prepared using a conditional, split-genome packaging system that is based off of the HIV-1 backbone [10]. This platform dispenses with all virulent and non-essential genes, and uses complementation of *gag, pol, rev*, and the vesicular stomatitis virus envelope protein in *trans* to generate a self-inactivating, non-replicative virion. In this protocol, we utilize the pRSV-REV and pCCL packaging and transfer vectors, respectively.

2 Materials

2.1 Tissue Culture Considerations

All methods should be conducted in a BSL2 certified biological safety cabinet to ensure sterility and safety. Use filter tips anytime you are pipetting retroviruses (gamma-retrovirus or lentivirus) or retrovirally transduced cells to prevent contamination of pipettes with viral particles. Tissue culture incubation conditions are 37 °C, 5% CO_2 and ambient O_2. Reagents for tissue culture and virus work should all be stored at 4 °C and preheated in a 37 °C water bath prior to use.

2.2 Common Materials and Reagents

1. BSL2-certified biological safety cabinet.
2. Tabletop centrifuge.
3. 1× phosphate buffered saline (PBS).

4. T cell media: RPMI 1640, 10% heat-inactivated fetal bovine serum (hiFBS), 2 mM L-glutamine, 10 mM HEPES, 0.5 mM sodium pyruvate, 1× nonessential amino acids, 55 μM β-mercaptoethanol, 100 U/mL penicillin + 100 μg/mL streptomycin.

2.3 Gamma-Retrovirus Preparation

1. T-75 tissue culture coated flasks.
2. Platinum-E (Plat-E) cells.
3. Plat-E maintenance media: Dulbecco's Modified Eagle Medium (DMEM), 10% hiFBS, 2 mM L-glutamine, 10 mM HEPES, 10 μg/mL blasticidin, 1 μg/mL puromycin, 0.1 mg/mL normocin.
4. Plat-E transfection media: DMEM, 10% hiFBS, 2 mM L-glutamine, 10 mM HEPES, 0.1 mg/mL normocin.
5. 15 mL Falcon tubes.
6. Opti-MEM media.
7. Retroviral plasmids; packaging (pCL-Eco [9]) and transfer plasmid (e.g., pRV2011 and pRV100G, however, other retroviral transfer vectors may be substituted) engineered to contain your gene of interest (CAR).
8. Lipofectamine 2000 (Life Technologies) (*see* **Note 1**).
9. 15 mL 100K NMWL centrifugal filter.
10. 10 mL syringe.
11. 0.45 μm syringe filter.

2.4 Murine CAR-T Cell Preparation

1. Murine donor.
2. Tweezers.
3. Small, sharp scissors.
4. 70% ethanol.
5. 6 cm petri dishes.
6. Microscope slides, with frosted glass tips.
7. Transfer pipettes.
8. 24-well, tissue culture coated plates.
9. ACK lysis buffer: 0.15 M NH_4Cl, 10 mM $KHCO_3$, 0.1 mM EDTA (prepared with autoclaved Milli-Q water).
10. Recombinant human IL-2.
11. Anti-murine CD3e, clone: 145-2C11.
12. Anti-murine CD28, clone: 37.51.
13. Polybrene.

2.5 Lentivirus Preparation

1. HEK293T cells.
2. HEK293T maintenance media: DMEM, 10% heat-inactivated fetal bovine serum, 10 mM HEPES, 2 mM L-glutamine, 100 U/mL penicillin + 100 μg/mL streptomycin.

3. HEK293T transfection media: DMEM, 10% heat-inactivated fetal bovine serum, 10 mM HEPES, 2 mM L-glutamine, 0.1 mg/mL normocin (*see* **Note 1**).
4. T-150 tissue culture coated flasks.
5. 15 cm dish.
6. 1× trypsin–EDTA solution (0.05%), no phenol red.
7. Lentiviral transfection plasmids: pRSV-Rev, pMDLg-pRRE, pMD2.G, pCCL/pRRL transfer plasmid.
8. Lipofectamine 2000.
9. Opti-MEM media.
10. 1 M sodium butyrate.
11. 150 mL 0.45 μm cellulose acetate or polyenersulfone (PES) Filter.
12. Ultracentrifuge with appropriate rotor and tubes suitable for ~130k RCF and ~40 mL (such as the Beckman Coulter SW-32 Ti Swinging Bucket Rotor and 38.5 mL Ultracentrifuge tubes).
13. 24-well, tissue culture coated plates.

2.6 Human CAR-T Cell Generation

1. PBMCs isolated from healthy donors.
2. Recombinant hIL-2.
3. Recombinant hIL-7.
4. Gibco Dynabeads Human T cell Activator CD3/CD28 beads and necessary magnets (e.g., Gibco Dynabeads and Dynabeads® MPC®-S) (Magnetic Particle Concentrator).
5. 1× PBS + 0.1% BSA + 2 mM EDTA.
6. 96-well round bottom, tissue culture coated plates.
7. 24-well, tissue culture coated plates.
8. T-25 and T-75 tissue culture coated flasks.

3 Methods

3.1 Murine CAR-T cells

3.1.1 Gamma-Retrovirus Generation

Note: Protocols 3.1.1 and 3.1.2 are interconnected in that the retrovirus generated in Subheading 3.1.1 will be used to transduce the murine T cells in Subheading 3.1.2; as such, the timelines used are consistent between the two protocols. Refer to Fig. 1 for a timeline of gamma-retrovirus production.

Preparation:

1. Seed a T-75 flask with retrovirus packaging Plat-E cells (*see* **Note 2**) in transfection media (*see* **Note 3**) such that the cells will be ~70% confluent at the time of transfection (*see* **Note 4**).

Day 1—transfect Plat-E cells:

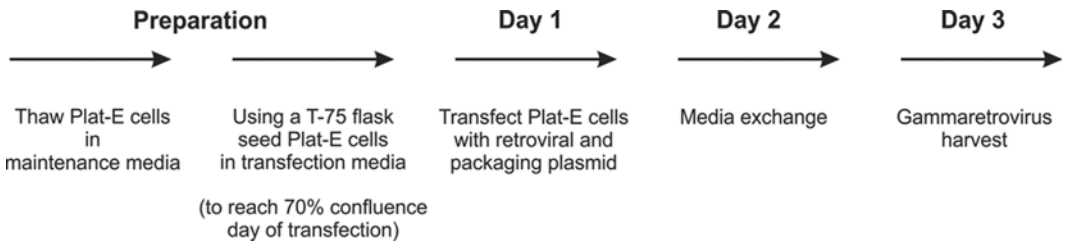

Fig. 1 Timeline of gammaretrovirus preparation. A visual representation providing a broad overview of the steps required/timeline for preparation of a CAR-encoding gammaretrovirus. The timeline of preparation steps may vary depending on density of Plat-E cell seeding and is thus unspecified

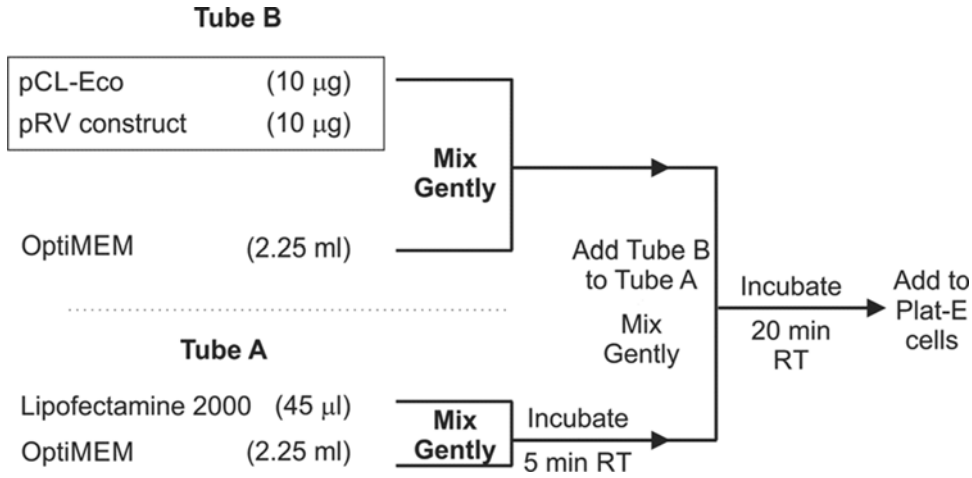

Fig. 2 Plat-E cell transfection. Flowchart indicating amounts and procedures for transfection of Plat-E cells for the generation of gammaretrovirus. To be completed on day 1 of the gammaretrovirus/murine CAR-T cell production process

2. Transfection should be conducted in the afternoon (*see* Fig. 2 for a visual summary). Prepare two 15 mL Falcon tubes each containing 2.25 mL of room temperature Opti-MEM media. To the first, Tube A, add 10 µg of retroviral plasmid DNA and 10 µg of packaging plasmid (pCL-Eco) DNA. To the second, Tube B, add 45 µL Lipofectamine 2000, vortex gently to mix, and allow to rest at room temperature for 5 min (*see* **Note 5**). Add Tube B to Tube A, vortex gently to mix, and incubate at room temperature for 20 min. Add the 4.5 mL of DNA/Lipofectamine Opti-MEM solution to the T-75 Plat-E flask; mix by gently rocking the flask front-to-back and side-to-side (*see* **Note 6**). Incubate at 37 °C and 5% CO_2 overnight.

Day 2—change media:

3. The next morning, carefully aspirate off the 14.5 mL of media from the transfected Plat-E flask. Replace with 10 mL of fresh,

pre-warmed transfection media being cautious not to disturb the cell layer.

Day 3—harvest viral supernatants:

4. The next morning, wash an Amicon Ultra 100K centrifugal filter; add 5 mL of PBS to the upper chamber and centrifuge at 2000 × *g* for 5 min. Aspirate flow through from the lower chamber. You will require one filter per Plat-E flask.
5. Collect supernatant from T-75 Plat-E flask. Load into a 10 mL syringe. Pass through a 0.45 μm syringe filter and into the upper chamber of a washed centrifugal filter. Concentrate viral supernatants 10× by centrifuging filters at 2000 × *g* for ~7–9 min; concentrate 10 mL of supernatant down to 1 mL.

3.1.2 Murine CAR-T Cell Generation

Refer to Fig. 3 for a visual summary of murine CAR-T cell production steps.

Day 2—activate splenocytes:

1. Harvest donor spleen as a source of murine T cells (*see* **Note** 7), working in a biological safety cabinet to ensure sterility. Saturate all instrumentation and the fur on the left side of the mouse with 70% ethanol. Using tweezers, lift the skin approximately midway between the front and hind limbs and make a long incision with sharp scissors. Locate the spleen beneath the peritoneum (a deep red organ with an elongated kidney shape). Cut into the peritoneal cavity. Use tweezers to carefully lift the spleen whilst using scissors to liberate the organ, cutting away any fatty material. Once removed, place the spleen in ~8 mL of T cell media in a 15 mL Falcon tube and keep on ice.
2. Decant Falcon tube contents (spleen and media) into a 6 cm petri dish. Using two scored microscope slides (use one microscope slide to score the frosted area of the other slide in a rough crosshatch pattern and vice versa), sandwich the spleen between the scored areas, using pressure and swirling one slide against the other to compress the spleen. Complete this step above the Petri dish, rinsing the slides with the media in the petri dish as necessary, to collect splenocytes. Continue rinsing and squishing until all that remains of the spleen is a small amount of white pulp, which can be discarded.
3. Eliminate large debris. Use a transfer pipette to collect the ~8 mL of media containing the liberated splenocytes into a 15 mL Falcon tube. Allow contents to settle for ~1 min. Transfer the supernatant (to avoid any sediment leave ~0.5 mL of media behind) into a fresh 15 mL Falcon tube.
4. Pellet cells (splenocytes) via centrifugation; 500 × *g*, 5 min. Aspirate the supernatant, being careful not to disturb the cell pellet.

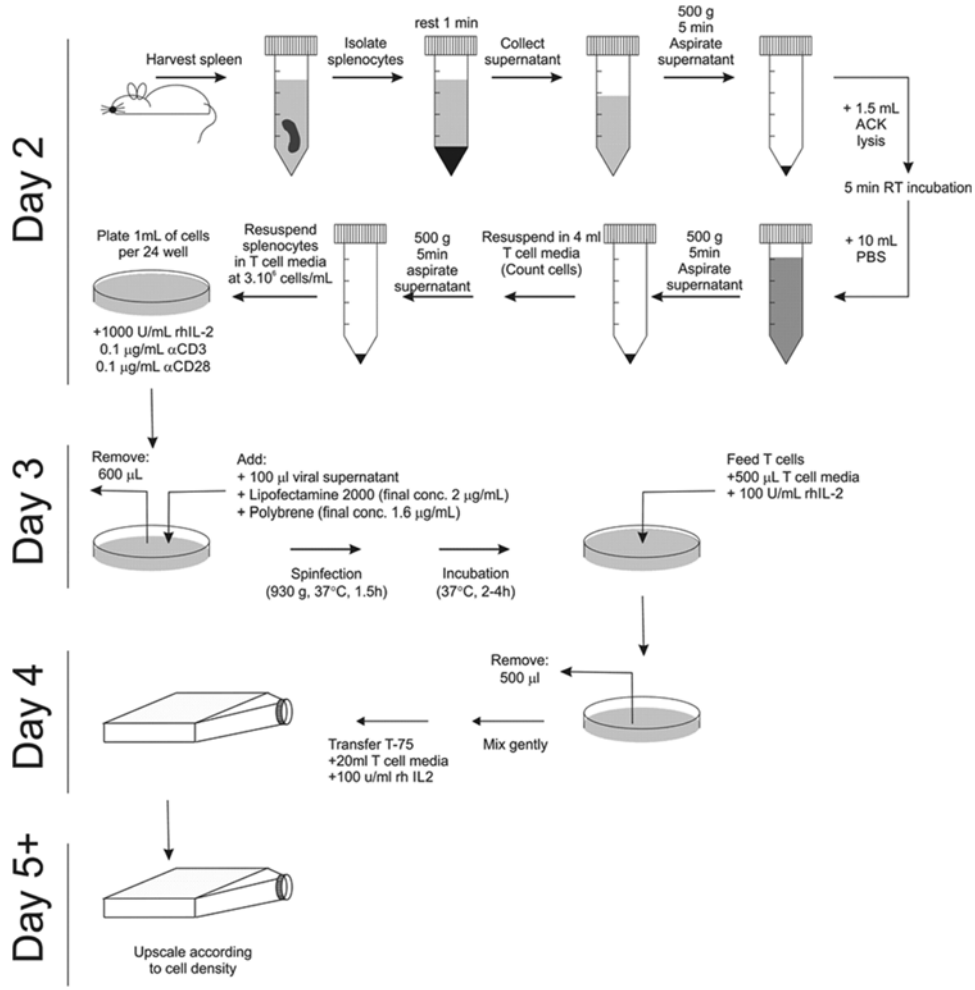

Fig. 3 Murine CAR-T cell generation. A flowchart which visually summarizes the steps/timeline required for the generation of CAR-engineered murine T cells; details are provided in the text

5. To lyse red blood cells, resuspend the pellet in 1.5 mL of ACK buffer. Incubate at room temperature for 5 min. Add 10 mL of PBS and pellet (500 × *g*, 5 min). Aspirate the supernatant.
6. Resuspend cell pellet in 4 mL of T cell media. Count cells.
7. Rinse: pellet cells (500 × *g*, 5 min), aspirate supernatant, and resuspend in T cell media as desired.
8. Plate splenocytes in a 24-well tissue culture dish; 3×10^6 splenocytes per well in 1 mL T cell media containing 100 IU/mL recombinant human IL-2, 0.1 µg/mL anti-CD3, and 0.1 µg/mL anti-CD28 (*see* **Notes 8** and **9**).
9. Incubate for 22–24 h at 37 °C and 5% CO_2.

Day 3—transduce splenocytes:

10. Remove 600 µL of media per well, being careful not to disturb the cell pellet.
11. Per well, add 100 µL of viral supernatant concentrate (from Subheading 3.1.1), Lipofectamine 2000 to 2 µg/mL, and Polybrene to 1.6 µg/mL.
12. Spinfection: centrifuge the 24-well plate at 930 × *g*, 37 °C, for 1.5 h.
13. Remove plate from centrifuge and incubate at 37 °C, 5% CO_2 for 2–4 h.
14. Add 500 µL of T cell media (return to 1 mL total volume per well) supplemented with recombinant human IL-2 at 100 IU/mL (use the same concentration as in **step 8**).

Day 4—expand T cell cultures:

15. Remove 500 µL of media from each well. Transfer remaining 500 µL (*see* **Note 10**) (pipette up and down gently to mix) into 20 mL of T cell media supplemented with recombinant human IL-2 (100 IU/mL, as in **steps 8** and **14**) in a T-75 flask (*see* **Note 11**).
16. Lay flask flat and incubate at 37 °C and 5% CO_2.

Ongoing—feed T cells:

17. As necessary, add T cell media supplemented with recombinant human IL-2 (100 IU/mL, as in **steps 8**, **14**, and **15**), keeping T cells at a concentration of 1–1.5 × 10^6 cells/mL (*see* **Notes 12** and **13**).
18. It is recommended to verify successful CAR-T cells generation by appropriate analytical methods, such as flow cytometric analysis of reporter genes encoded within the retrovirus (*see* **Notes 14–16**).

3.2 Human CAR-T Cells

3.2.1 Lentivirus Preparation

Refer to Fig. 4 for timeline of lentivirus production. Ideally, the transfer plasmid used to encode your CAR will also contain some form of transduction marker, such as a fluorescent protein (e.g., GFP) or a truncated receptor (e.g., nerve growth factor receptor), as this is needed for titrating the number of transducing units of lentivirus for the transduction of T cells.

Day –3—Thaw HEK293T cells for seeding:

1. Thaw cryopreserved HEK293T cells in 37 °C water bath (*see* **Note 18**) and seed roughly 1.5–2 × 10^6 cells in 20 mL HEK293T maintenance media per T-150 flask. On average, two confluent T-150 flasks are required to obtain enough cells for one viral batch.

Day 0—Harvest HEK293T cells for plating:

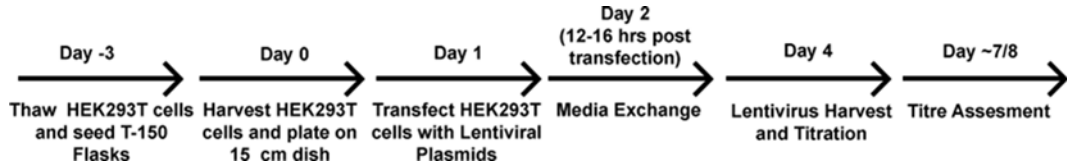

Fig. 4 Timeline of lentivirus preparation. A visual representation providing a broad overview of the steps required/timeline for preparation of a CAR-encoding lentivirus

2. Once HEK293T cells are ~90% confluent in the flask (after ~3 days), harvest HEK293T cells from flasks by first carefully aspirating media. Then flush residual media by gently washing cells with 5 mL pre-warmed 1× PBS (*see* **Note 19**).
3. Add 3 mL pre-warmed 1× trypsin–EDTA (0.05%) per T-150 flask and ensure coverage of cells. Incubate in a 37 °C incubator for 5 min (*see* **Note 20**). Add 7 mL HEK293T maintenance media to inactivate the trypsin–EDTA and combine cells from flasks.
4. Count cells by hemocytometer and resuspend HEK293T cells at 8×10^6 cells/mL in HEK293T maintenance media. Plate 1 mL of cells (i.e., 8×10^6) + 19 mL HEK293T culture media per 15 cm dish, for a total of three 15 cm dishes. Seed one T-150 flask with 0.5×10^6 cells to be used for titration purposes later on. Place flask and dishes into 37 °C incubator overnight (*see* **Note 21**).

Day 1—Transfect HEK293T cells:

5. One hour prior to transfection (*see* **Note 22**), replace the media on each plate carefully (*see* **Note 23**) with 12 mL of HEK293T transfection media containing an antibiotic suitable for your transfection reagent.
6. Transfection with Lipofectamine 2000 (*see* Fig. 5 for a visual summary) utilizes 60 μg DNA with 2 μL Lipofectamine per μg DNA. Prepare two series of 15 mL screw cap tubes for each plate as outlined in Fig. 2 (*see* **Note 24**). Once the Lipofectamine with DNA is added, gently swirly the dish to evenly distribute transfection reagents. Place the dish into the 37 °C incubator (*see* **Note 25**).

Day 2—Media Change:

7. Following transfection, roughly 12–16 h later, change the media on each dish carefully (see Note 23) with 12 mL HEK293T maintenance media supplemented with sodium butyrate (1 mM final). Place the dishes back into the 37 °C incubator to incubate for 48 h.

Day 4—Lentivirus Harvest:

8. Prior to viral harvest, precool ultracentrifuge buckets and rotor to 4 °C (*see* **Note 26**).
9. Harvest the media from the three 15 cm dishes into a 50 mL screw cap tube and centrifuge at 2000 RCF_{max} for 10 min to sediment any collected HEK293T cellular debris.
10. Filter the supernatant through a 0.45 μm PES filter (*see* **Note 27**) and add the filtrate to ultracentrifuge tubes, toping up with enough cold 1× PBS to bring within 0.5 cm of the tube (*see* **Note 28**).
11. Create any necessary balance tubes and pellet the lentivirus at RCF_{max} of 130,000 for 1 h 40 min, 4 °C, with minimal deceleration (*see* **Note 29**).
12. During the ultracentrifugation, harvest HEK293T cells from the T-150 flask seeded on day 1 as previously laid out. Plate 30,000 cells in 0.5 mL HEK293T maintenance medium (6×10^4 cells/mL) per well of a 24-well plate (*see* **Note 30**) for the purposes of lentivirus titration, and place in a 37 °C incubator to adhere for 3 h.
13. Once centrifuged, dispense supernatant into a bleach bucket. Keeping the ultracentrifuge tube inverted, place onto several layers of paper towel for 2 min to remove residual supernatant (*see* **Note 31**).
14. Add 60 μL ice-cold 1× PBS to the ultracentrifuge tube and place on ice for 10 min (*see* **Note 32**).
15. Begin resuspension by slowly and gently scraping the bottom of the ultracentrifuge tube using a micropipettor (*see* **Note 33**). Continue doing so until the pellet is mostly taken off, then begin slowly pipetting up and down gently to resuspend (*see* **Note 34**).

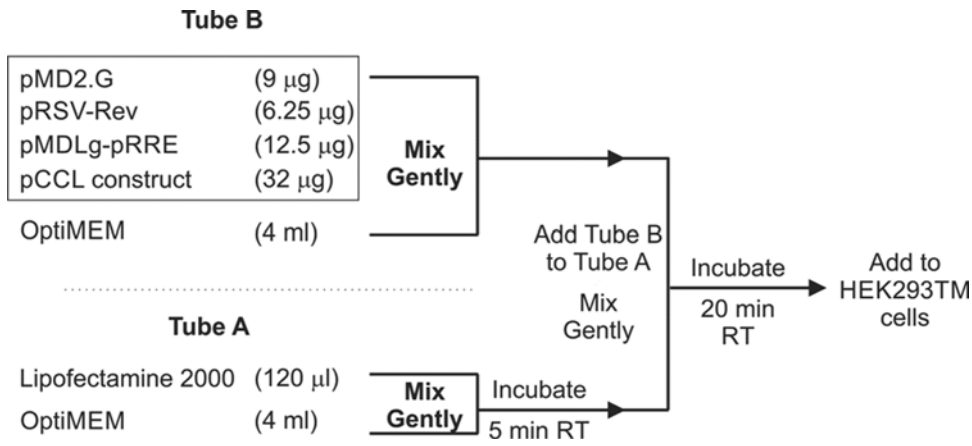

Fig. 5 HEK293T cell transfection. Flowchart indicating amounts and procedures for transfection of HEK293T cells for the generation of lentivirus. To be completed on day 1 of the lentivirus/human CAR-T cell production process

16. Once the pellet has begun to dissolve add more ice-cold 1× PBS (*see* **Note 19**) and transfer to a 1.5 mL microcentrifuge tube and resuspend until adequately homogenous (*see* **Note 35**).
17. Make aliquots into 1.5 mL microcentrifuge tubes, making sure to make a separate aliquot of 3 μL for the purposes of titration (*see* **Note 36**). Place aliquots into −80 °C and proceed to decontaminate centrifuge buckets and anything that has come into contact with virus with 70% ethanol.
18. Once HEK293T cells have adhered for at least 3 h, prepare a series of dilutions using the virus aliquot frozen for titration (refer to Table 1 and *see* **Note 38**).
19. Add 500 μL of dilution to a corresponding well of the 24-well plate. Two wells will receive only HEK293T maintenance media to act as either the unstained control, or stained non-transduced control. Allows cells to grow for 2–3 days.

Day 7/8—Titer Determination:

20. Harvest HEK293T cells from wells into 5 mL polystyrene tubes using a micropipettor with filter tips.
21. Stain cells using a fluorochrome-conjugated antibody specific for the transduction marker included in the transfer plasmid, or if the vector encodes a fluorescent molecule such as GFP simply run cells on the flow cytometer (*see* **Notes 39** and **40**).
22. Calculate the titer based on the dilution resulting in ~10% positive cells. Your flow data should be gated on the marker$^+$ population by histogram on your stained non-transduced cells. Then subtract the %marker$^+$ of the stained non-transduced from the rest of your samples.

    (a) Calculation: $30{,}000 \times \text{positive fraction} \times \text{dilution factor} = \text{virus titer in TU/mL}$.

    For example, for 17% marker$^+$ in 10^{-5} dilution.

    $30{,}000 \times 0.17 \times 100{,}000 = 5.1 \times 10^8$ TU/mL.

3.2.2 Human CAR-T Cell Generation

In general, T cell culture media is to be supplemented with 100 U/mL IL-2 and 10 ng/mL IL-7 immediately before use with primary T cells (*see* **Note 40**). Refer to Fig. 6 for a visual summary of human CAR-T cell production steps.

1. Human PBMCs isolated from healthy individuals should be acquired before beginning this protocol. These cells can be bought from commercial vendors (e.g., Normal LeukoPack; HemaCare Corporation) or derived from donors on site using various established methods (e.g., Ficoll-Paque Plus gradient separation [11]). Such protocols are readily available online through the manufacturer website.

Table 1
Example dilutions for lentiviral titration

Final dilution (after addition to cells)	Volume of virus (μL)	Diluent to add (μL)
1×10^{-3}	2 of stock	998
1×10^{-4}	70 of previous dilution	630
1×10^{-5}	70 of previous dilution	630
1×10^{-6}	70 of previous dilution	630

Frozen and thawed lentiviral stocks are diluted in HEK293T maintenance media as below; 500 μL of each dilution is added to HEK293T cells plated in 500 μL in 24-well plates, resulting in final dilutions. Other dilutions may be utilized to provide greater accuracy as per your individual virus

2. Thaw human PBMCs in 37 °C water bath, then slowly add cells drop wise to 7 mL T cell media (with no cytokine supplementation) (*see* **Note 41**). Mix gently and remove 10 μL to count cells by trypan exclusion on a hemocytometer. In parallel, spin the remaining cells at 500 × *g* for 5 min.
3. Carefully aspirate media by tilting tube horizontal so as not to disturb pellet. Resuspend cells to a final concentration of 1×10^6 cells/mL.
4. If you desire to use isolated total T cells, or CD8 or CD4 only T cells, use an appropriate means of sorting such as FACS or column purification. We suggest negative selection sorting columns.
5. To begin cultures start with 100,000 PBMCs per well of a round bottom 96-well plate. Take 100 μL of the PBMCs prepared in **step 3**, with one additional well for security (*see* **Notes 42**).
6. anti-CD3/anti-CD28-coated Dynabeads are utilized to activate T cells within the PBMC mixture and begin their proliferation (*see* **Note 43**). Following the manufacturer guidelines, briefly vortex the beads for 30 s and transfer 2 μL beads per well to a 1.5 mL microcentrifuge tube (*see* **Note 44**). Add 1 mL PBS + 0.1 % BSA + 2 mM EDTA to beads, vortex for 5 s.
7. Place beads on MPC-S magnet for 1 min, then aspirate the supernatant with care taken to not disrupt the beads gathered on the side of the 1.5 mL tube.
8. Remove 1.5 mL tube from the magnet and resuspend the beads with 100 μL T cell media supplemented with 2× cytokine (200 U/mL IL-2 and 20 ng/mL IL-7), referred to as activation media (2×), per 2 μL beads.
9. Aliquot 100 μL PBMC (100,000 cells) per well of a round-bottom 96-well dish. Combine with 100 μL of Dynabead activator solution previously made, per well. This results in the

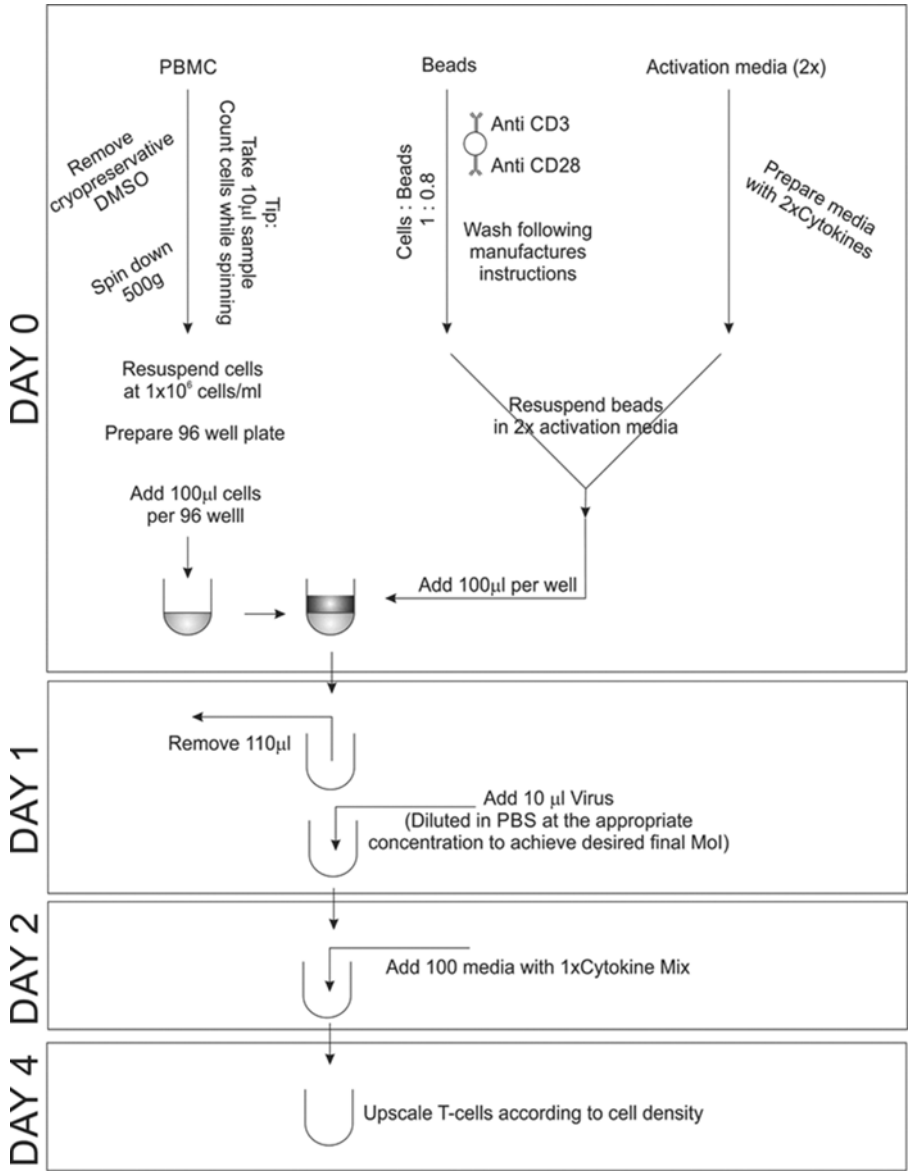

Fig. 6 Human CAR-T cell generation. A flowchart which visually summarizes the steps/timeline required for the generation of CAR-engineered human T cells, details of which are provided in the text

final cytokine concentration of 100 U/mL IL-2 and 10 ng/mL IL-7. Place into 37 °C incubator overnight.

10. After 18–24 h of incubation use the titer of the virus previously created and transduce the culture at the desired MOI (*see* **Note 45**). To do so, remove 110 µL from each well carefully (*see* **Note 46**). Take necessary amount of virus for desired MOI, bring up to 10 µL with PBS if below 10 µL, and add to cells gently without disturbing the pellet. Place into 37 °C incubator overnight.

11. The following day, supplement the wells with 100 μL T cell media supplemented with IL-2 and IL-7.
12. Check cells every day to assess growth. T cells will appear as a white halo surrounding a small red core of beads. When the halo reaches ~2–2.5 mm in diameter, the cells are ready to scale up (*see* **Note 47**).
13. Add 900 μL cytokine supplemented T cell medium per well of a 24-well plate corresponding to the number of the wells used at the 96-well stage. Transfer the ~200 μL cells into 900 μL cytokine supplemented (*see* **Note 48**).
14. Continue to culture the T cells in the 24-well plate until the wells are ~90–95% confluent (*see* **Note 49**). At this point, combine two wells and transfer to a T25 flask laying down, bringing up to 5 mL with fresh cytokine supplemented T cell media (*see* **Note 50**).
15. From this point on, cells should be given fresh media with cytokine every 2–3 days. Attention should be paid to the color of the media, as well as cell density. Thus, cells should be counted every 2–3 days and fed accordingly to maintain a density of ~1.0×10^6 cells/mL. If cells are growing well, the media will begin to turn yellow and will need to be supplemented with fresh media.
16. Cells can be scaled to larger flasks as they increase in number. While maintaining roughly ~$0.1–2 \times 10^6$ cells/cm^2 and 1.0×10^6 cells/mL, when the cells reach sufficient number increase the flask size (*see* **Note 51**).

4 Notes

1. There are many commercial transfection reagents available. We recommend Lipofectamine as a high efficiency reagent. Others may be substituted in place, however the DNA to transfection reagent ratios must be optimized. When Lipofectamine 2000 reagent is utilized, penicillin/streptomycin interferes with the transfection processes. In place of penicillin/streptomycin, either normocin antibiotic or no antibiotic should be used during transfection. Other reagents, such as Lipofectamine 3000, may be less susceptible to this problem. However, we are not experienced with such reagents.
2. We keep Plat-E cells in culture for a maximum of 2 weeks before thawing a fresh batch. Decreased transduction efficiencies may be observed if gamma-retroviruses are generated from Plat-Es that have been in culture for extended periods.
3. When thawing and over extended periods in culture, Plat-E cells should be passaged in maintenance media. The puromycin

and blasticidin contained therein ensure Plat-E cells retain expression of the viral packaging genes *gag*, *pol*, and *env*. However, due to potential toxicities associated with increased cellular permeability to antibiotics during transfection, Plat-Es should be cultured in transfection media (containing normacin in lieu of puromycin and blasticidin) during this time.

4. In order to generate a T-75 flask of 70% confluent PLAT-E cells, a T-75 flask may be seeded with 1.15×10^6 Plat-E cells three d before, 2.3×10^6 Plat-E cells two d before, or 5.6×10^6 Plat-E cells the day before transfection. Alternatively, frozen vials of 2.8×10^6 Plat-E cells will generate a 70% confluent T-75 in 3 days post-thaw.
5. In our experience, efficiency of retrovirus generation is decreased if Opti-MEM DNA and Lipofectamine solutions are scaled up; prepare one set of two tubes (DNA and Lipofectamine solutions) per each T-75 flask of Plat-E cells being transfected.
6. One transfected Plat-E flask is sufficient to generate enough gamma-retrovirus for transduction of ten wells of T cells.
7. One spleen from a 6–8-week-old C57BL/6 or Balb/c mouse typically yields ~100 million splenocytes.
8. Gamma-retroviruses require actively dividing cells for efficient transduction; thus, the purified retrovirus is added to T cells 24 h post-activation with anti-CD3 and anti-CD28.
9. Altering the type and amount of cytokines in the T cell growth media can impact on the phenotype, and thus functionality, of T cells grown in vitro [12]; different cytokine compositions to yield a desired phenotype are available in the literature.
10. When observing the 24-well plate under a microscope, post-activation, you should expect to see dense clusters of T cell growth rather than a homogenous dispersion of cells throughout the well. In our experience these clusters are desirable for optimal T cell growth.
11. If preparing multiple wells of murine T cells simultaneously, three wells transduced with the same virus and grown under the same conditions can be expanded into 60 mL of appropriately supplemented T cell media in a T-150 flask laid flat.
12. In our experience, CAR-T cells are generally usable for in vitro assays/in vivo experiments from 4 to 7 days post-activation. After this point, viability of T cell cultures begins to rapidly decline.
13. Starting from 3×10^6 splenocytes, one well can yield upwards of 10^8 cells after expansion, depending on growth conditions. For example, we have observed yields of between 10 and 95×10^6 T cells 6 days after activation when growing splenocytes in 100 IU/mL rhIL-2. It should also be noted that in some cases, T cell growth rate may be dependent on the contents of your gamma-retrovirus.

14. We have observed that T cell cultures expanded from bulk splenocytes are between 80 and 95% pure for $CD4^+ + CD8^+$ cells; the distribution between $CD4^+$ and $CD8^+$ cells can range, for example, from 78.6% $CD8^+$ and 6.19% $CD4^+$ to 47.8% $CD8^+$ and 38.9% $CD4^+$ (generally $CD8^+$ T cells always dominate), depending on experimental variation and growth conditions.
15. It should be noted that it is possible to begin with a purified population of $CD4^+$ or $CD8^+$ T cells, rather than bulk PBMCs, if having an enriched final population of either is desirable for your purposes. We have found that magnetic negative selection kits work well for this purpose.
16. In our experience using this protocol, one can expect a transduction efficiency anywhere from 40 to upwards of 80%. This is generally dependent on the gamma-retrovirus used as well as experimental variability.
17. We have found that with our own HEK293T cells, usage of freshly thawed cultures of low passage, rather than older cultures, enhance lentiviral yield.
18. In our experience, HEK293T cells are weakly bound to the culture flask and so will lift off quite easily. Because of this, it is recommended that the media be removed carefully and the PBS wash to be done gently to prevent unnecessary loss of cells. To facilitate this, we suggest standing the flask up and aspirating the media away from the cells. Additionally, when adding PBS, add the volume to the flask upside down and then slowly rotate the flask so the PBS gently washes over the cells once. This is sufficient to remove residual media.
19. Although HEK293T cells can easily come off by mechanical means, the cells remain clumpy. Trypsin–EDTA is used to prevent clumping and facilitate accurate cell counting and even spreading on the 15 cm dish.
20. It is important that the dishes are level to ensure an even coverage of the dish with cells. We have found that three 15 cm dishes per viral batch are sufficient to yield high titer. However, this is optimized for the Beckman Coulter SW32Ti rotor and tubes capable of holding 38 mL. This may be adjusted per your needs and ultracentrifuge.
21. We suggest performing the transfection in the evening, such as 4 or 5 pm, to easily time the post-transfection media exchange, and lentivirus harvest.
22. It is important to be very gentle with exchanging media in the 15 cm dish. The HEK293T cells are easily lifted, thus we suggest removing and adding media using a pipette aid set to a slow setting if possible.
23. We have found that preparing a master mix of DNA with Lipofectamine reduces the efficiency of transfection. It is

therefore better to prepare a series of tubes for each dish. To increase productivity, you may make a master mix of the DNA to aliquot per tube.

24. At this point, the HEK293T cells will begin producing lentivirus upon transfection. It is important to follow all biosafety guidelines for BSL2 viruses that are in place in your institution.
25. It is essential that lentivirus be kept at 4 °C or on ice throughout the harvest once it has been pelleted, we have found this improves lentiviral titer.
26. A filter smaller than 0.45 μm, such as the commonly used 0.2 μm filter, has a pore size that is very close to the diameter of a lentivirus and will likely filter out virus. Similarly, cellulose acetate or PES membrane filters are recommended as nitrocellulose membranes will bind proteins on the lentivirus and bind up virions.
27. This is to ensure that the ultracentrifuge tube does not collapse during centrifugation.
28. Max deceleration may disrupt the lentivirus pellet and no brake requires a considerable period of time to fully stop that is not efficient.
29. Accurate counting is very important here as the math behind titration relies on the accuracy of plating 30,000 cells. Titration requires 6–7 wells per virus; however, it is beneficial to make spare wells in case of user error.
30. At this point, it is essential that the virus does not dry out and is kept at 4 °C to maintain a high titer of infective lentiviral particles. Thus, it is critical to ensure the tube is only kept inverted a minimal period of time and then promptly placed on ice.
31. From this point on, the virus should be on ice at all times to maintain stability during the resuspension process.
32. The ultracentrifugation process will have created a gel-like pellet. Scraping gently will assist in the resuspension by dislodging this gel. The micropipettor will naturally take up a small amount of liquid by doing this. It is important to be aware of this when resuspension by pipetting begins as it can introduce bubbles. The pellet will often resist complete resuspension and an emulsion is the best scenario at this point.
33. It is very important to avoid generating bubbles at any point during this step. We have found that exposure of lentivirus to bubbles will negatively impact yield. To prevent this from happening, we suggest setting the micropipettor to a lower volume.
34. The amount of 1× PBS added is up to the users' discretion and experience with assessing whether the yield is high titer or not. We find the best metric to follow is the turbidity of the resuspended solution. Increased turbidity suggests higher yield. Depending on your desired number of aliquots, volume per

aliquot, and titer, users can add from 40 to 100 μL more 1 × PBS. We suggest starting with 40 μL for the first batch.

35. Often there is a white "fluff" that is very difficult to fully resuspend, we have found that it does not impact the lentiviral efficacy if this is not fully homogeneous.
36. The volume of the aliquots is dependent on the titer of the virus. Thus, it is at your discretion and experience with the individual lentivirus being produced. We suggest 15 μL as a good middle ground.
37. When pipetting 2 μL, it is important to utilize an appropriate micropipettor to ensure high accuracy and low margin of error, such as a P2.
38. It should be noted that these cells have been exposed to lentivirus and as such should be handled accordingly under the necessary guidelines for your institution and state. Transduced cells are fixed with 4% glutaraldehyde to a final concentration of 2% for 20 min to inactivate lentivirus [13].
39. In addition to staining for the transduction marker, it may be beneficial to probe for expressed genes as well if compatible fluorochromes are available to determine the ability of the CAR to reach the cell surface.
40. The choice of cytokines is the determinant for much of the T-cell properties. It is a crucial choice that should be tailored to the scientists and experiments needs. For review, see DiGiusto and Cooper [14]. IL-2 and IL-7 aliquots should be frozen to −20 °C to maintain stability, and thawed just prior to use in fresh T cell medium.
41. Thawing cells rapidly at 37 °C enhances viability over a slower thaw. As the cryopreserved cells are stressed and have been maintained with DMSO, exposing cells to media slowly reduces osmotic shock.
42. We have found that starting with two wells (i.e., 200,000 cells) is sufficient to reach $15–100 \times 10^6$ cells by day 14 of culture, pending your specific construct. The limit of 100,000 cells is due to the limitations of lentivirus production. With higher titer virus, it may be possible to scale this step, however, we have not experimented with such a protocol. It should be noted that growth is highly construct-dependent, and is further affect by the MOI (higher results in slower growth).
43. VSV-G pseudotyped lentivirus is an excellent platform for transduction and gene insertion into non-dividing cells [15]. In regard to T cells, expression of the VSV-G receptor, LDL-receptor [16], is low until activation through the TCR, affecting the potential of LV to transduce T cells in vitro [17]. In the case of CAR-T cell

production, this is not an issue as cultures are first activated with activator beads.

44. Beads settle very quickly, thus to ensure accurate transfer of the correct number of beads, pipette the required amount immediately after resuspension. Although the manufacturer recommends a ratio of 1:1 bead–T cell ratio, we utilize a slightly lower ratio of 0.8:1. However, the literature has used ratios as high as 3:1 [18], although it should be noted that these cultures utilize a slightly different cytokine cocktail.
45. Often a MOI of 1–10 is sufficient to achieve transduction efficiencies of >60%. This is dependent on the individual virus batch and should be titrated on T cell cultures to determine optimal MOI. We have found that the number of transducing units (as determined by the MOI) added can have a significant impact on T-cell growth. Reporter genes that show no impact on T-cell behavior or growth have demonstrated reduced T-cell proliferation at high MOI's. In our hands, MOI's of 10 and below have consistently shown to have no significant impact.
46. To avoid disturbing the PBMC pellet, tilt the plate slightly forward and remove media carefully from the lower edge. As previously mentioned, cell disruption impacts cell proliferation. Especially in early stages of T-cell growth, a 20–30% reduction in cell proliferation was observed if pellets were disrupted.
47. We have found with this protocol, almost universally the cell pellets are sufficiently large the second day following addition of 100 μL media. In the case that they are not ready by this point, carefully replace half media with fresh cytokine-supplemented media.
48. This step is best completed by bringing a 100 μL micropipettor close to the T cell pellet and gently aspirating. This process maintains the general structure of the pellet and allows you to transfer it over. We have found that minimal disruption is important to the growth of the T cells and we believe at this stage they are interacting with each other and the activator beads. You may use some of the 900 μL media to wash the remainder of the well for any remaining cells.
49. This metric is slightly dependent on the state of the pellet when it was originally transferred to the 24-well plate. That is to say, should the pellet remain completely whole, it will not spread as quickly if the pellet was transferred in several pieces. We have found that on average this takes 2 days. Cells should be given fresh media every 2–3 days, if you deem a well not ready by this point, simply add 1 mL cytokine-supplemented T cell media.
50. We have found as a general rule of thumb that 100,000 cells /cm^2 is a low point for cell density over surface area. Below this number, we have found the proliferation of the T-cells is impacted

negatively. With two wells at ~90% confluence, this is about $2–2.5 \times 10^6$ cells and is sufficient. If you are unsure, it is best to resuspend cells thoroughly and count. However, to promote growth it is still optimal to not disturb cells at this point.

51. Cell densities exceeding 300,000 cells/cm^2 may prove problematic for nutrient and oxygen exchange, thus we recommend maintaining within 100,000–200,000 cells/cm^2. It is important to have the appropriate volume of media within a flask of certain size. This is to maintain optimal oxygenation of the T cells. We have found that media for the T-25, T-75, and T-150 should not exceed 6 mL, 15 mL, and 25 mL, respectively.

Acknowledgements

We would like to kindly thank Dr. Megan Levings for providing the original lentiviral generation protocol and her guidance with which to proceed in lentiviral preparation. We would also like to extend thanks to Dr. Brian Rabinovich for providing both help and plasmids in the generation of retroviruses used for engineering of murine T cells.

References

1. Maude SL, Frey N, Shaw PA, Aplenc R, Barrett DM, Bunin NJ, Chew A, Gonzalez VE, Zheng Z, Lacey SF, Mahnke YD, Melenhorst JJ, Rheingold SR, Shen A, Teachey DT, Levine BL, June CH, Porter DL, Grupp SA (2014) Chimeric antigen receptor T cells for sustained remissions in leukemia. N Engl J Med 371(16):1507–1517. doi:10.1056/NEJMoa1407222
2. Lee DW, Kochenderfer JN, Stetler-Stevenson M, Cui YK, Delbrook C, Feldman SA, Fry TJ, Orentas R, Sabatino M, Shah NN, Steinberg SM, Stroncek D, Tschernia N, Yuan C, Zhang H, Zhang L, Rosenberg SA, Wayne AS, Mackall CL (2015) T cells expressing CD19 chimeric antigen receptors for acute lymphoblastic leukaemia in children and young adults: a phase 1 dose-escalation trial. Lancet 385(9967):517–528. doi:10.1016/S0140-6736(14)61403-3
3. Maude SL, Teachey DT, Porter DL, Grupp SA (2015) CD19-targeted chimeric antigen receptor T-cell therapy for acute lymphoblastic leukemia. Blood 125(26):4017–4023. doi:10.1182/blood-2014-12-580068
4. Kochenderfer JN, Dudley ME, Kassim SH, Somerville RP, Carpenter RO, Stetler-Stevenson M, Yang JC, Phan GQ, Hughes MS, Sherry RM, Raffeld M, Feldman S, Lu L, Li YF, Ngo LT, Goy A, Feldman T, Spaner DE, Wang ML, Chen CC, Kranick SM, Nath A, Nathan DA, Morton KE, Toomey MA, Rosenberg SA (2015) Chemotherapy-refractory diffuse large B-cell lymphoma and indolent B-cell malignancies can be effectively treated with autologous T cells expressing an anti-CD19 chimeric antigen receptor. J Clin Oncol 33(6):540–549. doi:10.1200/JCO.2014.56.2025
5. Grupp SA, Kalos M, Barrett D, Aplenc R, Porter DL, Rheingold SR, Teachey DT, Chew A, Hauck B, Wright JF, Milone MC, Levine BL, June CH (2013) Chimeric antigen receptor-modified T cells for acute lymphoid leukemia. N Engl J Med 368(16):1509–1518. doi:10.1056/NEJMoa1215134
6. Curran KJ, Brentjens RJ (2015) Chimeric antigen receptor T cells for cancer immunotherapy. J Clin Oncol 33(15):1703–1706. doi:10.1200/JCO.2014.60.3449
7. Maetzig T, Galla M, Baum C, Schambach A (2011) Gammaretroviral vectors: biology,

technology and application. Viruses 3(6):677–713. doi:10.3390/v3060677

8. Morita S, Kojima T, Kitamura T (2000) Plat-E: an efficient and stable system for transient packaging of retroviruses. Gene Ther 7(12):1063–1066. doi:10.1038/sj.gt.3301206
9. Naviaux RK, Costanzi E, Haas M, Verma IM (1996) The pCL vector system: rapid production of helper-free, high-titer, recombinant retroviruses. J Virol 70(8):5701–5705
10. Dull T, Zufferey R, Kelly M, Mandel RJ, Nguyen M, Trono D, Naldini L (1998) A third-generation lentivirus vector with a conditional packaging system. J Virol 72:8463–8471
11. Fuss IJ, Kanof ME, Smith PD, Zola H (2009) Isolation of whole mononuclear cells from peripheral blood and cord blood. Curr Protoc Immunol Chapter 7:Unit 7.1. doi:10.1002/0471142735.im0701s85
12. Crompton JG, Sukumar M, Restifo NP (2014) Uncoupling T-cell expansion from effector differentiation in cell-based immunotherapy. Immunol Rev 257(1):264–276. doi:10.1111/imr.12135
13. Hanson PJ, Gor D, Jeffries DJ, Collins JV (1989) Chemical inactivation of HIV on surfaces. BMJ 298(6677):862–864
14. DiGiusto D, Cooper L (2007) Preparing clinical grade Ag-specific T cells for adoptive immunotherapy trials. Cytotherapy 9(7):613–629. doi:10.1080/14653240701650320
15. Cronin J, Zhang XY, Reiser J (2005) Altering the tropism of lentiviral vectors through pseudotyping. Curr Gene Ther 5(4):387–398. doi:10.2174/1566523054546224
16. Finkelshtein D, Werman A, Novick D, Barak S, Rubinstein M (2013) LDL receptor and its family members serve as the cellular receptors for vesicular stomatitis virus. Proc Natl Acad Sci U S A 110(18):7306–7311. doi:10.1073/pnas.1214441110
17. Amirache F, Lévy C, Costa C, Mangeot PE, Torbett BE, Wang CX, Nègre D, Cosset FL, Verhoeyen E (2014) Mystery solved: VSV-G-LVs do not allow efficient gene transfer into unstimulated T cells, B cells, and HSCs because they lack the LDL receptor. Blood 123:1422–1424. doi:10.1182/blood-2013-11-540641
18. Barrett DM, Singh N, Liu X, Jiang S, June CH, Grupp SA, Zhao Y (2014) Relation of clinical culture method to T-cell memory status and efficacy in xenograft models of adoptive immunotherapy. Cytotherapy 16(5):619–630. doi:10.1016/j.jcyt.2013.10.013

Chapter 12

Methods to Evaluate the Antitumor Activity of Immune Checkpoint Inhibitors in Preclinical Studies

Bertrand Allard, David Allard, and John Stagg

Abstract

Immune checkpoint inhibitors (ICI) are a new class of drugs characterized by their ability to enhance antitumor immune responses through the blockade of critical cell surface receptors involved in the maintenance of peripheral tolerance. The recent approval of ICI targeting CTLA-4 or PD-1 for the treatment of cancer constitutes a major breakthrough in the field of oncology and demonstrates the potential of immune-mediated therapies in achieving durable cancer remissions. The identification of new immune regulatory pathways that could be targeted to reactivate or boost antitumor immunity is now a very active field of research. In this context, the use of syngeneic mouse models and immune monitoring techniques are the cornerstone of proof-of-concept studies. In this chapter, we describe the general methodology to evaluate antitumor activity of ICI in immunocompetent mice. We outline protocols to reliably establish tumors in mice and generate lung metastasis through tail vein injections with the aim of testing the efficacy of ICI. We also present methods to analyze the composition of the tumor immune-infiltrate by multicolor flow cytometry.

Key words Immune-checkpoint, PD-1, PD-L1, Immuno-oncology, Cancer

1 Introduction

Over the last decade, the discovery of the main pathways involved in the control and in the resolution of immune responses has enabled a better understanding of the chronic inflammation process occurring in auto-immune disorders, infectious diseases and in cancer. In the case of cancers, the activation of immune inhibitory receptors is a critical mechanism by which tumors evade immunosurveillance [1]. As a consequence, the targeted blockade of pivotal components of these inhibitory pathways, commonly referred as immune checkpoints, has emerged as a ground-breaking approach for cancer therapy [2–4]. The first generation of biological therapeutics capable of blocking immune checkpoints, also called immune checkpoint inhibitors or ICI, have been recently approved for the treatment of metastatic melanoma or non-small-cell lung cancers (NSCLC).

Josie Ursini-Siegel and Nicole Beauchemin (eds.), *The Tumor Microenvironment: Methods and Protocols*, Methods in Molecular Biology, vol. 1458, DOI 10.1007/978-1-4939-3801-8_12,

The first ICI, ipilimumab (Yervoy), was marketed in 2011 and consists of a monoclonal antibody (mAb) targeting the inhibitory receptor CTLA-4 [5, 6]. CTLA-4 is expressed at the surface of T lymphocytes and transmits inhibitory signals when interacting with CD80 or CD86 expressed by antigen presenting cells (APC). The binding of ipilimumab on CTLA-4 blocks its interaction with CD80 and CD86 which prevents immunosuppressive signaling and promotes antitumor immune responses [7]. Ipilimumab is currently approved for the treatment of metastatic melanoma and several clinical trials are ongoing to evaluate its clinical efficacy in patients with prostate cancer, NSCLC and bladder cancers. While the exact mechanism of action of ipilimumab is still unclear, there are evidence that it blocks the interaction of CTLA-4 with CD80 and CD86 and that it can deplete CTLA-4-expressing T regulatory cells (Tregs) through antibody-dependent cellular cytotoxicity (ADCC) [8–10]. Notably, transcriptome analysis of tumor-specific CD8+ T cells following CTLA-4 blockade revealed increased T cell proliferation and effector memory function [11].

The second ICI that has been developed and approved in cancer patients targets the PD-1/PD-L1 pathway [12]. PD-1 is an inhibitory receptor mainly expressed by activated and exhausted lymphocytes. Engagement of PD-1 by its ligand PD-L1 or PD-L2 expressed on APC, myeloid cells or tumor cells inhibits T cell activation [13] and restrains their antitumor functions [14]. In both preclinical models and cancer patients, PD-1/PD-L1 blockade promotes antitumor immunity [12, 14–16]. From a mechanistic point of view, blocking PD-1 promotes antitumor effector functions and T cell metabolism [11]. Notably, PD-1/PD-L1 blockade modulates glucose availability in the tumor microenvironment, thereby restoring glucose metabolism in activated T cells present in the tumor microenvironment, thus favoring differentiation into effector T cells [11, 17]. A recent report also suggested that anti-PD-1/PD-L1 mAb therapies could be modulated by Fc receptor function [18].

In the past 2 years, anti-PD-1 and anti-PD-L1 mAbs have benefited from accelerated evaluation by the FDA through the "breakthrough therapy" designation. This has led to the approval of two anti-PD-1 mAbs, pembrolizumab (Keytruda™, Merck) and nivolumab (Opdivo™, Bristol-Myers Squibb), for the treatment of melanoma and NSCLC. Importantly, both pembrolizumab and nivolumab showed greater clinical benefit and less side-effects than ipilimumab alone in melanoma patients, and this observation may apply to other types of cancers [19]. With this favorable efficacy and toxicity profile, inhibitors of PD-1/PD-L1 are now the backbone for clinical trials involving immune-mediated therapies [20].

Given the clinical successes of ICI, the search for new immune checkpoints contributing to tumor immune evasion is rising and the list of immunomodulatory targets with antitumor activities is rapidly expanding [20]. Many of these "second-generation" immune checkpoints are currently evaluated in preclinical and clinical trials [20].

Preclinical testing of new compounds is a critical step in the drug development process. It enables the demonstration of therapeutic activity in vivo and the selection of lead compounds that will be evaluated in phase I clinical trial. Hence, choosing the right preclinical models to test a drug candidate is of outmost importance [21]. In the field of oncology, a large variety of preclinical cancer models are available and can be divided into two categories: immune-deficient and immune-competent models. For preclinical testing of ICI, immune-competent models are required as treatments are meant to stimulate the immune system to attack tumors in a MHC-matched manner. The most common immunocompetent models involve subcutaneous transplantation of syngeneic tumor cells in mice. Although these models present clear limitations, they are still important tools to test the antitumor activity of drug candidates. Intrinsic limitations of these models can be circumvented, at least in part, by testing compounds against multiple tumor cell lines to better recapitulate tumor heterogeneity in patients or by performing orthotopic injections. In this chapter, we describe the methods [22–32] we reliably use in syngeneic transplantable mouse models of cancer to test the antitumor activity of ICI.

2 Materials

2.1 Cell Culture Before the Injection of Tumor Cells

1. Tumor cell lines (*see* American Type Culture Collection website).
2. Cell culture medium; usually RPMI 1640 or DMEM, supplemented with 5% FBS.
3. Fetal bovine serum.
4. Antibiotics for cell culture: penicillin/streptomycin.
5. Trypsin 0.25%.
6. 1× phosphate buffer saline, without calcium and magnesium (PBS).
7. Trypan blue solution.
8. Sterile cell culture plastics: 100 mm petri dishes, 15 mL or 50 mL polypropylene tubes, pipets.
9. Sterile filter tips.
10. Sterile 1.5 mL microtubes.
11. 40 μm cell strainers.
12. Hemocytometer.
13. Tabletop centrifuge.

2.2 Subcutaneous Injections

1. Syngeneic mice; C57BL/6 or Balb/c.
2. Small animal clipper.
3. Ear tags.
4. Ear tags applier.
5. Sterile 1 mL syringe.

6. Sterile 26G 5/8 or 26G 3/8 needles.
7. Alcohol pads.
8. Digital caliper.
9. Immune checkpoint blocking mAbs (BioXcell; anti-PD1, clone RPM4-14; anti-CTLA4, clone 9H10).
10. Euthanyl.
11. Dissection instruments and dissection board.
12. Precision scale.

2.3 4T1 Tumor Model

1. 4T1 cell line (ATCC # CRL-2539).
2. Balb/c mice.
3. RPMI 1640 medium supplemented with 5% FBS.
4. Same material as in Subheading 2.2.
5. 10 mL syringes.
6. Pipet tips of 200 and 10 μL.
7. India ink.
8. 1× phosphate buffer saline.
9. Fekete's solution: 100 mL 70% ethanol, 10 mL formalin, 5 mL glacial acetic acid.

2.4 Experimental Metastasis Through Tail Vein Injections

1. Tumor cell line.
2. Syngeneic mice.
3. Ear tags.
4. Ear tags applier.
5. Heating lamp.
6. Tail vein restrainer (Braintree Scientific).
7. Alcohol pads.
8. 0.5 mL 28G ½ needles.
9. Dissection instruments and dissection board.
10. 10 mL syringes.
11. Pipet tips of 200 and 10 μL.
12. India ink.
13. 1× phosphate buffer saline.
14. Fekete's solution.
15. Bouin's solution (if using the B16F10 tumor model).

2.5 Analysis of Tumor Immune Infiltrate by Flow Cytometry

1. EDTA solution.
2. Collagenase IV.
3. DNAse I.
4. 1× PBS.
5. RPMI 1640.

6. Dissection instruments.
7. Incubator.
8. Tabletop centrifuge.
9. 40 μm cell strainers.
10. Strainer-cap FACS tubes.
11. Percoll Solution.
12. FACS buffer: 1× PBS containing 2% FBS and 5 mM EDTA.
13. Digestion buffer: RPMI 1640 containing 2% FBS, 1 mg/mL collagenase IV, 20 μg/mL DNAse I.
14. Fluorochrome-labeled antibodies compatible with cytometry (*see* Table 1).

Table 1

List of fluorochrome-labeled antibodies compatible with cytometry

Panel 1		Panel 2	
Antibody	**Dilution**	**Antibody**	**Dilution**
Anti-CD16/CD32 (BD)	1/100	Anti-CD16/CD32	1/100
Viability dye eFluor 506 (eBioscience)	1/500	Viability dye eFluor 506	1/500
Anti-CD45-BUV395 (BD)	1/100	Anti-CD45-BUV737 (BD)	1/200
Anti-CD3-BV786 (BD)	1/500	Anti-CD11b-BUV395 (BD)	1/500
Anti-CD4-BUV737 (BD)	1/1000	Anti-CD11c-V450 (BD)	1/200
Anti-CD8-BV650 (BD)	1/500	Anti-F4/80-BV605 (BioLegend)	1/400
Anti-NK1.1-Alexa 700 (BD)	1/200	Anti-merTK-biotin (Miltenyi)	1/25
Anti-CD19-PerCPCy5.5 (Tonbo)	1/500	Anti-Ly6C-BV711 (BioLegend)	1/500
Anti-CD44-APC-Cy7 (BD)	1/100	Anti-Ly6G-APC-Cy7 (BD)	1/500
Anti-CD62L-PECF594 (BD)	1/100	Anti-SiglecF-PE (BD)	1/200
Anti-ckit-BB515 (BD)	1/200	Anti-MHCII-BV650 (BD)	1/1000
Anti-FcERIa-PECy7 (eBioscience)	1/100	Anti-B220-BV786 (BD)	1/500
Anti-CD49b-BV421 (BD)	1/400	Anti-PDCA1-FITC (BioLegend)	1/100
Anti-Foxp3-PE (eBioscience)	1/400	Anti-CD19-PerCPCy5.5	1/500
Anti-Eomes-eFluor 660 (eBioscience)	1/400	Anti-Nkp46-PerCPCy5.5 (BD)	1/200
		Anti-CD3-PerCPCy5.5 (Tonbo)	1/200
		Anti-CD206-PECy7 (BioLegend)	1/100
		Anti-NOS2-eFluor 660 (eBioscience)	1/400

3 Methods

3.1 Preparation of the Tumor Cells Before Subcutaneous or Intravenous Injections

1. Tumor cells are thawed rapidly by adding 1 mL of warm medium to the cryovial and resuspended carefully. Alternately, the cryovial can be incubated in a 37 °C water bath for 1–2 min to rapidly thaw the cells.
2. The cell suspension is then transferred into a 15 mL tube containing 10 mL of warm medium, homogenized and dispensed into a 100 mm petri dish (*see* **Note 1**).
3. Cells are incubated overnight in an incubator at 37 °C with 5 % CO_2.
4. The following day, cells are rinsed with PBS and fed with fresh medium.
5. When the cells reach 80–90 % confluency, the cells are detached using trypsin and split into several petri dishes for expansion (*see* **Note 2**).
6. The day before the in vivo injection, cells are rinsed with PBS and fresh medium is added.
7. The day of the injection, the cells are rinsed with PBS and detached by adding 3 mL of trypsin per 100 mm petri dish and incubating for 2 min at 37 °C (*see* **Note 3**).
8. When the cells are all floating, trypsin is neutralized by adding 7 mL of medium containing FBS.
9. The cell suspension is then transferred into a 15 mL tube and centrifuged at 280 × *g* for 5 min. If several petri dishes/flasks are used, cells can be pooled in one/several 50 mL tubes.
10. The supernatant is discarded and the cell pellet is resuspended carefully with a micropipette in 1 mL of PBS. Then, 9 mL of PBS (19 mL for a 50 mL tube) are added and the suspension is homogenized with a 10 mL pipette.
11. The cell suspension is then passed through a 40 μm cell strainer adapted on a 50 mL tube. The cell strainer is wetted with 5 mL PBS before dispensing the cell suspension. The strainer is rinsed with 10 mL PBS after passing the cell suspension (*see* **Note 4**).
12. The cells are centrifuge at 1200 rpm for 5 min.
13. Repeat **step 10** and **12**.
14. The supernatant is discarded and the cell pellet is resuspended in 1 mL of PBS per petri dish/T75 flask used at the beginning of the procedure (increase the volume of PBS accordingly if larger dishes are used). Measure the exact volume of the cell suspension.

15. Collect 10 μL of the cell suspension and dilute it in 1 m of PBS containing 20% (v/v) of trypan blue to count viable and dead cells. During the counting step, place the cell suspension on ice to maintain a good viability.
16. Cells are counted with a Malassez's hemocytometer using 10 μL of the cell solution diluted in trypan blue (*see* **Note 5**).
17. Adjust the volume of the cell suspension with PBS to obtain the desired concentration of cells for injections. If the cells are too diluted, centrifuge and resuspend in a smaller volume.
18. Split the cell suspension in several tubes (one tube par cage to be injected). Add more cells than needed as there will be some loss in the syringe (three doses more than needed is enough).
19. Until the injection, keep the cells on ice.

3.2 Subcutaneous Injections of Syngeneic Tumor Cell Lines, Monitoring of Tumor Growth and Treatment with Immune Checkpoint Inhibitors

1. Before performing a large experiment with many mice and many treatments, use the injection procedure described below (**steps 2–13**) to determine the optimal number of tumor cells to inject in vivo (*see* **Note 6**).
2. One day before the injections, shave the mice on their right flank and identify them with an ear-tag or an ear-punch.
3. Prepare the cells as described in Subheading 3.1 and keep them on ice until the injection.
4. We usually prepare one tube of cells per cage; a cage contains five mice.
5. At the animal facility, under a laminar flow hood, make sure the cell suspension is homogeneous by flicking and inverting the tube of cells.
6. Using a needle-free 1 mL syringe, aspirate 0.7 mL of the cell suspension (*see* **Note 7**).
7. Attach a 26G 5/8 needle to the syringe and get rid of air bubbles; adjust the syringe volume to 0.5 mL to inject five mice (*see* **Note 8**).
8. Wipe the needle tip with an alcohol pad.
9. Grab a mouse and make sure it is well restrained (*see* **Note 9**).
10. Insert the needle under the skin, on the flank, and locate the tip of needle between the third and fourth mammary gland (as shown in Fig. 1, *see* **Note 10**).
11. Slowly inject 100 μL of the cell suspension; a bump should appear under the skin (*see* **Note 11**).

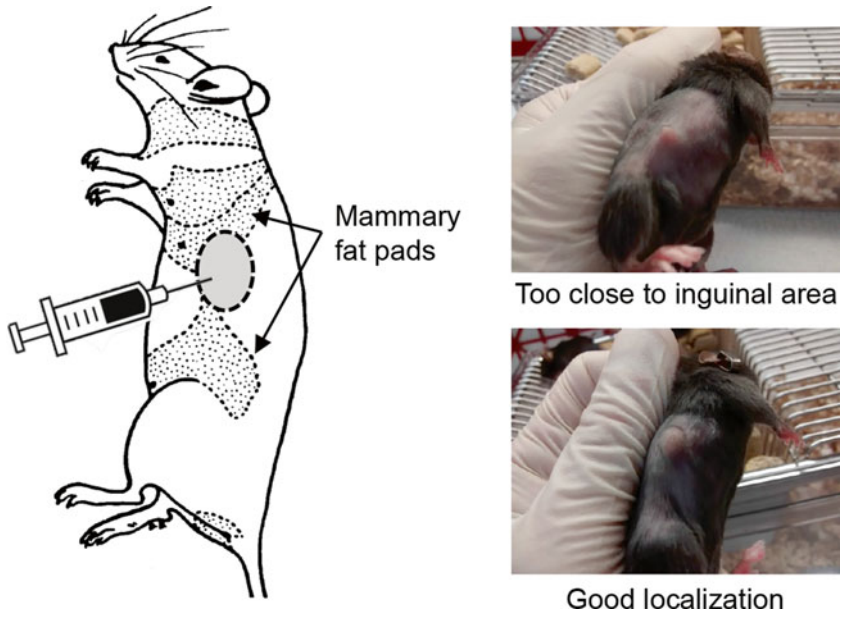

Fig. 1 Technique for subcutaneous injection of cancer cells. *Left Hand Panel*: Schematic diagram illustrating the location of the third and fourth mammary glands in rodents along with the optimal area for subcutaneous injection between both glands. *Right Hand Panel*: A representative example of proper versus improper injection techniques based on the distance from the inguinal (fourth) mammary gland

12. Slowly withdraw the needle and replace the mouse in its cage.
13. Repeat this procedure to inject the other mice (wipe the needle with an alcohol pad for each mouse, *see* **Note 12**).
14. 3 days after the injection, check the presence of a visible tumor mass in mice. Sometimes nothing is visible before day 7. On the contrary, with some tumor models, it is already possible to perform a first measurement of tumor size after 3 days.
15. Monitor tumor growth, two or three times per week, by measuring the size of the tumors using a digital caliper (*see* **Note 13**).
16. When the average tumor size reaches 20–30 mm^2, start the first treatment with immune checkpoint inhibitors (*see* **Note 14**).
17. Treat mice with immune checkpoint inhibitors (e.g., 100 μg twice per week i.p. for a total of 4–6 injections), while continuing to monitor tumor size.
18. Sacrifice mice at the end of the experiment using CO_2 or a lethal injection of pentobarbital (*see* **Note 15**).
19. Dissect subcutaneous tumors and weigh them.

3.3 Spontaneous Lung Metastasis Model Using the 4T1 Tumor Cell Line

3.3.1 Tumor Growth and Treatment with Immune Checkpoint Blockers

1. Prepare the 4T1 cell line as described in Subheading 3.1 (*see* **Note 16**).
2. Inject mice subcutaneously as described in Subheading 3.2 (*see* **Note 17**); subcutaneously inject 1×10^5 cells per mouse in 100 μL PBS.
3. Small tumors should be visible and measurable within 3–5 days.
4. When tumors reach 20–30 mm^2 (7–10 days after tumor inoculation), start treatments with immune checkpoint inhibitors as described in **steps 16** and **17** of Subheading 3.2.
5. Sacrifice mice at the end of the experiment (3–4 weeks after tumor inoculation) using CO_2 or a lethal injection of pentobarbital (*see* **Note 18**).
6. Dissect subcutaneous tumors and weigh them.

3.3.2 Evaluation of Lung Metastasis Tumor Burden

1. After collecting and weighing the subcutaneous tumors, open the thoracic cavity being careful not to damage the lungs; completely remove the rib cage to expose the heart and the lungs (Fig. 2a).

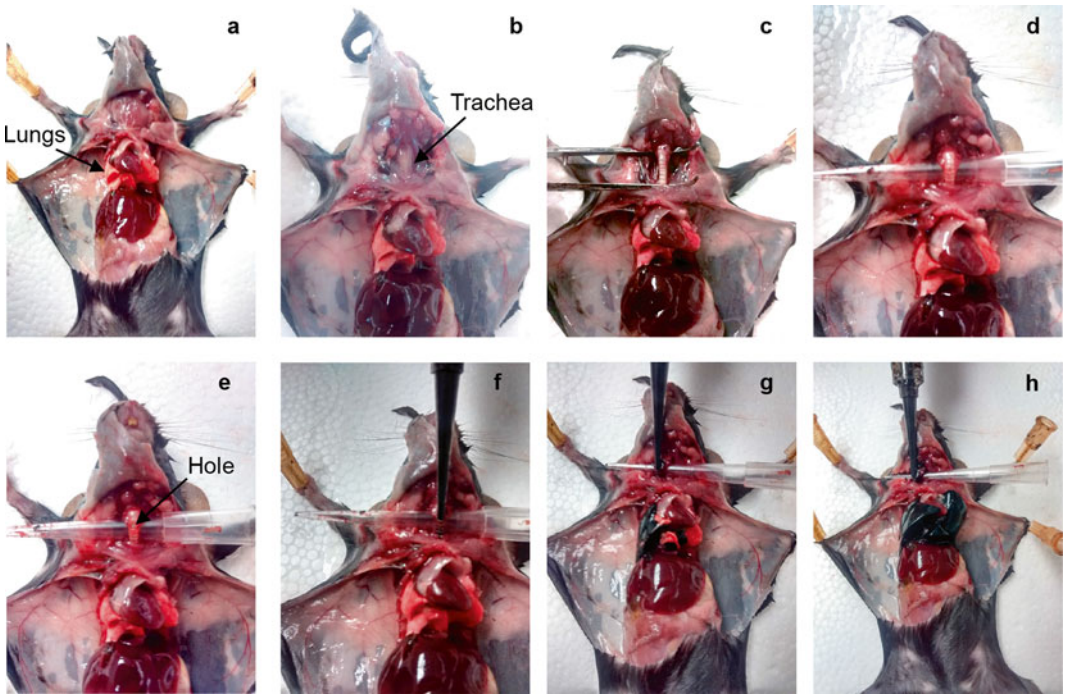

Fig. 2 Method to evaluate lung metastatic tumor burden in mice. (**a**) Open the thoracic cavity being careful not to damage the lungs; completely remove the rib cage to expose the heart and the lungs. (**b**) Expose the trachea over 1 cm, by removing the salivary glands and the muscle layer surrounding the trachea. (**c**) Gently insert the tip of a curved tweezer under the trachea to detach it from the underlying tissues. (**d**) Insert a 200 μL pipet tip under the trachea through the space created with the tweezer. (**e**) Partially cut the trachea so that a small hole is visible. (**f**, **g**) Perfuse the lungs, through the trachea, with 2–3 mL of the 20 % India ink solution. Lungs should swell progressively and turn black. (**h**) When all the pulmonary lobes are black, remove the syringe and dissect out the lungs keeping the heart attached to them

2. Expose the trachea over 1 cm, by removing the salivary glands and the muscle layer surrounding the trachea (Fig. 2b).
3. Gently insert the tip of a curved tweezer under the trachea to detach it from the underlying tissues and create a small space under the trachea (Fig. 2c).
4. Insert a 200 µL pipet tip under the trachea through the space created with the tweezer (Fig. 2d).
5. Using a small and sharp pair of scissors half-cut the trachea; be careful not to completely cut the trachea; a small hole should be visible (Fig. 2e).
6. Insert the tip of a 5 mL syringe adapted onto a 10 µL pipet tip, and loaded with a 20% India ink solution in PBS, into the trachea (Fig. 2f).
7. Perfuse the lungs, through the trachea, with 2–3 mL of the 20% India ink solution. Lungs should swell progressively and turn black (Fig. 2g).
8. When all the pulmonary lobes are black, remove the syringe and dissect out the lungs keeping the heart attached to them.
9. Wash the lungs in a beaker containing PBS to remove excess ink.
10. Fix the lungs immersing them in Feketes's solution. At this step, metastatic foci should appear as white dots on the lung surface (Fig. 2h). Lungs can remain in this solution until the tumor nodules are enumerated.
11. Enumerate macroscopic metastatic nodules on the lung surface.

3.4 Immune Checkpoint Inhibitors Testing in Experimental Lung Metastasis Models

1. Perform a preliminary experiment to select the optimal number of cells to inject (*see* **Note 19**).
2. One day before the injections identify the mice with an ear-tag or an ear-punch.

3.4.1 Tail Vein Injections

3. Prepare the cells as described in Subheading 3.1; one tube of cells per cage with an excess volume of three doses (one dose is usually 100 µL for intravenous injections).
4. At the animal facility, under a laminar flow hood, place one cage of five mice under a heating lamp for 5 min (*see* **Note 20**).
5. Make sure the cell suspension is homogeneous by flicking and inverting the tube of cells.
6. Using a 0.5 mL syringe with 28G ½ needle, slowly aspirate 0.4 mL of the cell suspension (*see* **Note 21**).
7. Get rid of air bubbles (*see* **Note 8**); adjust the syringe volume to 0.3 mL to inject three mice in a row (*see* **Note 22**).
8. Wipe the needle tip with an alcohol pad.

9. Grab a mouse and place it in a tail-vein injection restrainer (*see* **Note 23**).
10. Keep the tail out of the restrainer and clean the injection site with an alcohol pad.
11. Gently pull the tail and localize the lateral tail veins (located on each side of the tail).
12. With the bevel of the needle facing upward and the needle almost parallel to the vein, slide the needle into the tail vein (*see* **Note 24**).
13. Slowly press the plunger to inject the cell suspension (*see* **Note 25**).
14. Remove the needle and apply firm pressure to the injection site to prevent backflow of the injected cell suspension and/or blood.
15. At the same time rapidly remove the plug from the restrainer and extract the animal from the restrainer.
16. Keep pressure on the injection site for 15–20 s and release the animal in its cage.
17. Inject the following animals.

3.4.2 Evaluation of Lung Metastasis Tumor Burden

1. 14–21 days after tumor cell inoculation, sacrifice the animals using an overdose of pentobarbital.
2. Follow **steps 2–9** of the Subheading 3.3.2, except for the B16F10 model.
3. If using the B16F10 melanoma model, do not perfuse lungs with India ink. Directly collect the lungs and fix them in Bouin's solution (*see* **Note 26**) before counting the tumor nodules.

3.5 Analysis of the Tumor Immune Infiltrate by Flow Cytometry

3.5.1 Tumor Disaggregation and Isolation of Tumor Infiltrating Leukocytes

1. Euthanize mice by CO_2 asphyxiation or with an overdose of pentobarbital.
2. Dissect subcutaneous tumors and place them in a 1.5 mL microtube filled with 0.5 mL of medium containing 2% of FBS.
3. Keep the samples on ice while collecting the tumors.
4. With a small and sharp dissection scissor, finely cut the tumor directly in the microtube.
5. Using a 1 mL pipet, transfer the tumor homogenate into a 15 mL tube filled with 5 mL of digestion buffer.
6. Incubate the tumor homogenate at 37 °C with vigorous agitation for 30–60 min (*see* **Note 27**).
7. After 30 min, check the digestion efficiency; if there are no tumor pieces left proceed to next step; otherwise, incubate the sample for 15–30 min more.

8. Once tumor pieces are completely digested, place the tubes on ice and add 5 mL of FACS buffer containing EDTA to stop the digestion process.
9. Pipet the cell suspension up and down with a 10 mL pipette and pass it through a 40 μm cell strainer placed on a 50 mL falcon tube. Gently mash remaining aggregates with the plunger of a 5 mL syringe. Keep the tubes on ice.
10. Add 10 mL of FACS buffer through the filter to rinse it.
11. Spin 5 min at 1200 rpm and discard supernatant.
12. Resuspend the pellet in 2.5 mL of FACS buffer and pass through a 40 μm strainer capped FACS tube (*see* **Note 28**).
13. Rinse the strainer with 1 mL of FACS buffer.
14. Spin 5 min at 1200 rpm, discard supernatant.
15. Resuspend the pellet in 2 mL of PBS containing 30% of Percoll.
16. Gently layer the cell suspension onto a 70% Percoll solution (2 ml in a FACS tube).
17. Centrifuge at 1200 rpm, at 4 °C for 30 min with no brake.
18. Collect the tumor infiltrating leukocytes located at the interface.
19. Rinse twice with a large excess of FACS buffer (*see* **Note 29**).

3.5.2 Staining for Flow Cytometry Analysis

1. Resuspend in 50 μL of FACS buffer containing Fc blocking antibodies (anti-CD16/CD32) and the fixable viability dye. Incubate on ice for 15 min (*see* **Note 30**).
2. Add 50 μL of the cell surface antibody cocktail (*see* Table 1) and incubate for 30 min on ice, protected from light.
3. Rinse twice with FACS buffer.
4. If no intracellular staining is performed, samples can be analyzed directly on the flow cytometer or fixed with formaldehyde and acquired later on (*see* **Note 31**).
5. If performing intracellular stainings, fix and permeabilize the samples using the fix/perm kit.
6. Add 100–200 μL of the fix/perm solution and incubate samples on ice for 30 min.
7. Rinse twice using the perm/wash buffer (*see* **Note 32**).
8. Add 100 μL of the intracellular antibody mix (diluted in perm/wash buffer) and incubate for 30–60 min on ice.
9. Rinse twice with perm/wash buffer.
10. Resuspend samples in FACS buffer before acquisition.

4 Notes

1. At this step, cells can be directly plated or centrifuged once to completely remove the DMSO contained in the freezing medium. For most cells, diluting the freezing medium at least ten times with complete medium and plating the cells immediately will not affect cell viability, even if some DMSO is remaining (1% or less depending on the concentration used in the freezing medium). Depending on the number of cells contained in the cryovial, the appropriate dish is used. It is common to freeze 1–10 million cells/cryovial/mL. If the cell recovery after thawing is good (over 70%), plating the cells in a 100 mm petri dish or T75 flask should be OK to have a confluent dish a few days after thawing.
2. The number of flask/petri dish to use for expansion depends on the number of cells needed for the experiment. Always plan to have more cells than needed, as a significant fraction of the cells will be lost during the procedure and during the injections.
3. On the day of injection, the cells should be in the log phase of their proliferation curve (confluency around 70%). Cells can be detached with trypsin 0.25%, trypsin 0.05% or with nonenzymatic solutions such as Versene buffer (PBS—8 mM EDTA) or Accutase. Most of the cells will support trypsin treatment very well and the time required to detach the cells should be optimized for each cell type (usually a few minutes).
4. The cells are passed through the 40 μm cell strainer to remove cell aggregates and to have a uniform single-cell suspension. Some cells are lost during this step, but this will improve the reproducibility of tumor growth in vivo. This step is very important for intravenous injection as it will prevent mice dying from a pulmonary embolism that could arise from big cell aggregates.
5. Be sure that the cell suspensions were well homogenized before pipetting the 10 μL needed for the dilution in trypan blue and for loading the hemocytometer cell. Using the resuspension volume and the dilution mentioned in **step 14** and **15** respectively; there should be more than 100 and less than 500 cells to count. Do not count less than 100 cells. Count the bright refringent cells (viable) and also the ones colored in blue (dead cells) located on the grid. If there are not many cells (100–250), count the cells present on the whole grid (10 columns divided in 10 rows = 100 small squares). If there are a lot of cells, just count 10 or 20 small squares amongst the 100. To obtain the concentration in your cell suspension, divide the number of cells counted by the number of columns included in the count (if you counted the whole grid divide by 10; if you counted 20

small squares, which represents 2 columns, divide by 2) and multiply by the dilution factor used in **step 15** (here 100) and by 10,000. The number obtained will be your number of cells per mL of solution. Do this calculation for both viable and dead cells. The dead cells should not represent more than 10% of the cells. If there are too many dead cells, the tumor growth could be altered. A high number of dead cells could result from an over-incubation with trypsin. Some cell lines are more sensitive to trypsin; the use of a diluted (0.05%) trypsin or a nonenzymatic detaching solution could improve cell viability.

6. Before starting an experiment to test the antitumor efficacy of immune checkpoint inhibitors (or other antitumor compounds), it is recommended to titrate the dose of tumor cells to inject in vivo. We have frequently tried to use the same dose as described in reference papers and found that the number of cells injected was too high or too low. Tumor growth is affected by numerous factors, including the housing temperature of the mouse facility, microbiota of the mice, and the in vitro conditions used to culture tumor cell lines. As a consequence, variations in the growth of the same tumor cell line in vivo can be observed from lab to lab and titrating the dose of tumor cells to inject when testing a new model is highly recommended. To perform a titration experiment, inject three groups of five mice with three different concentrations of tumor cells according to doses reported in the literature. Select the cell concentration that generates similar size tumors in every mouse with the following properties: (1) tumors should be visible, measurable with a caliper within 3–7 days, (2) 7 days after tumor injection the average tumor size should not exceed 30 mm^2, (3) ideally, tumors should reach a size of 20–30 mm^2 within 7–12 days after inoculation. To observe the antitumor activity of immune checkpoint inhibitors or immunomodulatory compounds, an immune response against the tumor is often required. In mice, it takes approximately 7–10 days to elicit a cellular immune response against an antigen; therefore, ICI treatments such as anti-PD1 or anti-CTLA4 are routinely initiated within 1 or 2 weeks after tumor cell inoculation (7 days at the earliest for subcutaneous tumors) [22–24]. Furthermore, those treatments are far less effective in vivo when tumors are too big (over 40 mm^2).
7. Avoid aspirating cells with the needle attached to the syringe as it could damage the cells. If the syringe needs to be reloaded remove the needle.
8. To eliminate air bubbles attached to the plunger, maintain the syringe vertically, needle up, and flick it once to make air bubbles going up just below the needle entry. Still maintaining the syringe vertically, slowly expulse air bubbles through the nee-

dle. If the cell suspension is precious, collect the droplets of liquid expulsed during the procedure by placing a tube close to the needle exit. Experienced manipulators can inject five mice in less than 2 min which means that the cell suspension usually remains homogeneous in the syringe along the procedure. If it takes more time to inject, or if the cell suspension is highly concentrated (more than 10^7 cells/mL), it is better to reload the syringe between each mouse or each two mice to be sure that the cells are not pelleting in the syringe during the injections.

9. Some strains such as Balb/c mice are calm and usually do not move once restrained. On the contrary, C57Bl/6 are more nervous and a really good contention is required; in addition, when restraining C57Bl/6 mice, we usually hold the back leg with one finger as those mice most often try to kick out the needle.
10. The needle should be visible under the skin, easy to insert and the tip should be able to move. If there is resistance, the needle may be located in the dermis instead of the subcutaneous space (which corresponds to the hypodermis). Try not to inject too close to the fourth mammary fat pad as the tumor may be difficult to measure and to discriminate from the bump created by the inguinal lymph node once inflamed. If using a 26G 5/8 needle, do not insert the needle completely (insert a little more than half of the length) as tumor cells could implant in the needle path once the needle is removed and generate elongated tumors or several tumor nodules that will be more difficult to measure.
11. If there is resistance during the injection, you are probably located in the dermis rather than in the subcutaneous space. We observed that tumors growing too close to the skin surface are more susceptible to ulceration.
12. If you have more than 40 mice to inject, make two groups and inject in two sessions.
13. Usually, the tumors have an ellipsoid shape. Measure the largest diameter of the tumor (L) and the larger distance perpendicular to L (W). Then calculate tumor area multiplying L by W. Alternately, tumor volume can be calculated using the following formula: $V=(L\times W^2)/2$.
14. Prepare treatments in a physiological solution (usually PBS for immune checkpoint blocking monoclonal antibodies) and administer treatments in the peritoneal cavity. Use a 26G 3/8 needle for intraperitoneal injections and inject 100 or 200 µL of treatment (for anti-PD-1 and anti-CTLA4 mAbs the dose is usually 5 or 10 mg/kg, which corresponds to 100 or 200 µg per mouse (an 8–12 week old female C57Bl/6 or Balb/c mouse weighing approximately 20 g). Alternately, depending on the compound, treatment can be administered by oral gavage, by intra-tumor injections or by intravenous injections.

15. Before starting an experiment with animals, submit a protocol to your local animal ethic committee and wait for approval. Determine end points beyond which animals should be treated or euthanized. For subcutaneous tumor models, tumor size exceeding 2500 mm^3 and ulceration of the tumor are endpoints requiring euthanasia of animals.
16. The 4T1 cell line is cultured is RPMI supplemented with 5 % serum. We routinely inject 1×10^5 cells per mouse in 100 μL of PBS.
17. The 4T1 cell line is syngeneic to Balb/c mice. When injected subcutaneously into Balb/c mice, 4T1 cells spontaneously metastasize to the lung, liver, lymph nodes and brain while the primary tumor is still growing in situ. Increased metastatic potential can be achieved by injecting the 4T1 cells orthotopically in the mammary fat pad. The primary tumor does not have to be removed to induce the growth of the metastatic lesions. The metastatic spread of 4T1 cells in Balb/c mice closely mimic what can be observed with human breast cancer. The 4T1 model is a relevant animal model for stage IV human breast cancer and triple negative breast cancer. Subclones of the 4T1 parental line, with specific metastatic tropism have been isolated (the 4T1.2 subclone is used as a model of breast cancer metastasis to bones).
18. Tumors should be around 150 mm^2 in size to observe a significant number of lung metastatic nodules (average of 20–30 nodules per lung) [22].
19. Inject three groups of five mice with three different doses of cells according to the literature. In experimental lung metastasis models the number of cells to inject usually range between 1 and 5×10^5 cells. Select a dose of cells that will generate at least 100 and less than 400 tumor nodules per lung in 2–3 weeks. With such a tumor burden, mice should not present clinical signs during the experiment (but this latter point depends on each tumor model).
20. Placing mice under a heating lamp is required to dilate the tail vein before the injections. Be very careful with heating lamp as different heating capacities can be observed depending on the lamp. Overheating mice could kill or severely injure them so make sure that the temperature is not too high.
21. The syringes we use for i.v. injections have permanent needles attached. Therefore the cell suspension has to be pipetted with the needle attached to the syringe. To limit the pressure applied to cells passing through the needle and thus limit cell damage, a slow pipetting is required.
22. We usually inject a cage in two steps; three mice in a row and then two mice. This prevents cells from pelleting into the

syringe due to the time required for injections and limits the pipetting of the cells with the needle to twice. An experimented person can inject 30 mice/h.

23. Be careful not to restrain mice too much with the plug as it could prevent them from breathing properly.
24. When inserting the needle in the tail vein there should be no resistance. Moreover, you should be able to see the needle penetrating in the vein as lateral tail vein are superficial. Do not insert the needle too proximal as you will not be able to try a second time immediately after a failure. If the first trial fails, it is also possible to try with the second lateral tail vein.
25. If the needle is correctly inserted in the vein there should be no resistance while injecting the cell suspension and the vein will blanch temporarily. If the needle is not in the vein, the fluid will be difficult to inject and will cause blanching around the vein or a subcutaneous bleb.
26. The Bouin's solution will color the lungs in yellow making black B16F10 tumor nodules easier to visualize and count.
27. Place the tubes horizontally to have a good agitation of the tumor pieces.
28. If there is a lot of blood in the pellet, lyse red blood cells resuspending the pellet in 2 mL of ACK buffer for 1 min at room temperature; then add 1 mL of FACS buffer to stop the lysis and pass the cell suspension through a 40 μm strainer-capped FACS tube.
29. Add a large excess of FACS buffer to dilute the Percoll and to efficiently pellet the cells.
30. At this step, samples can be transferred in a V-shaped 96-well plate.
31. Cell viability is decreasing over time even if samples are kept on ice. Hence, if you have a lot of samples, viability of the cells can be negatively affected due to the acquisition time. To avoid this problem, samples can be fixed in 1 or 2% paraformaldehyde for 15 min at room temperature prior the acquisition. If fixing the samples, be careful of overfixation as it could damage the fluorochromes used to stain the cells.
32. It is critical to use the perm/wash buffer for rinsing and diluting intracellular antibodies. The kit used here contains saponin as permeabilizing agent which means that permeabilization is not permanent unless saponin-containing buffer are used. After rinsing the fix/perm solution, cells can be stored overnight in perm/wash buffer and intracellular stainings performed the following day.

Conflict of Interest

J. Stagg was a paid consultant for MedImmune, Palobiofarma, and Surface Oncology, has received research grants from MedImmune, Palobiofarma, and Surface Oncology, and is a member of the Scientific Advisory Board of Surface Oncology.

References

1. Schreiber RD, Old LJ, Smyth MJ (2011) Cancer immunoediting: integrating immunity's roles in cancer suppression and promotion. Science 331:1565–1570. doi:10.1126/science.1203486
2. Pardoll DM (2012) The blockade of immune checkpoints in cancer immunotherapy. Nat Rev Cancer 12:252–264. doi:10.1038/nrc3239
3. Sharma P, Allison JP (2015) Immune checkpoint targeting in cancer therapy: toward combination strategies with curative potential. Cell 161:205–214. doi:10.1016/j.cell.2015.03.030
4. Topalian SL, Drake CG, Pardoll DM (2015) Immune checkpoint blockade: a common denominator approach to cancer therapy. Cancer Cell 27:450–461. doi:10.1016/j.ccell.2015.03.001
5. Hodi FS, O'Day SJ, McDermott DF et al (2010) Improved survival with ipilimumab in patients with metastatic melanoma. N Engl J Med 363:711–723. doi:10.1056/NEJMoa1003466
6. Schadendorf D, Hodi FS, Robert C et al (2015) Pooled analysis of long-term survival data from phase II and phase III trials of ipilimumab in unresectable or metastatic melanoma. J Clin Oncol. doi:10.1200/JCO.2014.56.2736
7. Leach DR, Krummel MF, Allison JP (1996) Enhancement of antitumor immunity by CTLA-4 blockade. Science 271:1734–1736. doi:10.1126/science.271.5256.1734
8. Simpson TR, Li F, Montalvo-Ortiz W et al (2013) Fc-dependent depletion of tumor-infiltrating regulatory T cells co-defines the efficacy of anti-CTLA-4 therapy against melanoma. J Exp Med 210:1695–1710. doi:10.1084/jem.20130579
9. Selby MJ, Engelhardt JJ, Quigley M et al (2013) Anti-CTLA-4 antibodies of IgG2a isotype enhance antitumor activity through reduction of intratumoral regulatory T cells. Cancer Immunol Res 1:32–42. doi:10.1158/2326-6066.CIR-13-0013
10. Romano E, Kusio-Kobialka M, Foukas PG et al (2015) Ipilimumab-dependent cell-mediated cytotoxicity of regulatory T cells ex vivo by nonclassical monocytes in melanoma patients. Proc Natl Acad Sci U S A 112:6140–6145. doi:10.1073/pnas.1417320112
11. Gubin MM, Zhang X, Schuster H et al (2014) Checkpoint blockade cancer immunotherapy targets tumour-specific mutant antigens. Nature 515:577–581. doi:10.1038/nature13988
12. Brahmer JR, Drake CG, Wollner I et al (2010) Phase I study of single-agent anti-programmed death-1 (MDX-1106) in refractory solid tumors: safety, clinical activity, pharmacodynamics, and immunologic correlates. J Clin Oncol 28:3167–3175. doi:10.1200/JCO.2009.26.7609
13. Freeman GJ, Long AJ, Iwai Y et al (2000) Engagement of the PD-1 immunoinhibitory receptor by a novel B7 family member leads to negative regulation of lymphocyte activation. J Exp Med 192:1027–1034
14. Hirano F, Kaneko K, Tamura H et al (2005) Blockade of B7-H1 and PD-1 by monoclonal antibodies potentiates cancer therapeutic immunity. Cancer Res 65:1089–1096
15. Brahmer JR, Tykodi SS, Chow LQM et al (2012) Safety and activity of anti-PD-L1 antibody in patients with advanced cancer. N Engl J Med 366:2455–2465. doi:10.1056/NEJMoa1200694
16. Topalian SL, Hodi FS, Brahmer JR et al (2012) Safety, activity, and immune correlates of anti-PD-1 antibody in cancer. N Engl J Med 366:2443–2454. doi:10.1056/NEJMoa1200690
17. Chang C-H, Qiu J, O'Sullivan D et al (2015) Metabolic competition in the tumor microenvironment is a driver of cancer progression. Cell 162:1229–1241. doi:10.1016/j.cell.2015.08.016
18. Dahan R, Sega E, Engelhardt J et al (2015) FcγRs modulate the anti-tumor activity of antibodies targeting the PD-1/PD-L1 axis. Cancer

Cell 28:285–295. doi:10.1016/j.ccell.2015.08.004

19. Postow MA, Chesney J, Pavlick AC et al (2015) Nivolumab and ipilimumab versus ipilimumab in untreated melanoma. N Engl J Med 372:2006–2017. doi:10.1056/NEJMoa1414428
20. Mahoney KM, Rennert PD, Freeman GJ (2015) Combination cancer immunotherapy and new immunomodulatory targets. Nat Rev Drug Discov 14:561–584. doi:10.1038/nrd4591
21. Gould SE, Junttila MR, de Sauvage FJ (2015) Translational value of mouse models in oncology drug development. Nat Med 21:431–439. doi:10.1038/nm.3853
22. Stagg J, Divisekera U, McLaughlin N et al (2010) Anti-CD73 antibody therapy inhibits breast tumor growth and metastasis. Proc Natl Acad Sci U S A 107:1547–1552. doi:10.1073/pnas.0908801107
23. Stagg J, Loi S, Divisekera U et al (2011) Anti-ErbB-2 mAb therapy requires type I and II interferons and synergizes with anti-PD-1 or anti-CD137 mAb therapy. Proc Natl Acad Sci U S A 108:7142–7147. doi:10.1073/pnas.1016569108
24. Allard B, Pommey S, Smyth MJ, Stagg J (2013) Targeting CD73 enhances the antitumor activity of anti-PD-1 and anti-CTLA-4 mAbs. Clin Cancer Res 19:5626–5635. doi:10.1158/1078-0432.CCR-13-0545
25. Stagg J, Divisekera U, Duret H et al (2011) CD73-deficient mice have increased antitumor immunity and are resistant to experimental metastasis. Cancer Res 71:2892–2900. doi:10.1158/0008-5472.CAN-10-4246
26. Stagg J, Beavis PA, Divisekera U et al (2012) CD73-deficient mice are resistant to carcinogenesis. Cancer Res 72:2190–2196. doi:10.1158/0008-5472.CAN-12-0420
27. Stagg J, Sharkey J, Pommey S et al (2008) Antibodies targeted to TRAIL receptor-2 and ErbB-2 synergize in vivo and induce an antitumor immune response. Proc Natl Acad Sci U S A A105:16254–16259. doi:10.1073/pnas.0806849105
28. Beavis PA, Divisekera U, Paget C et al (2013) Blockade of A2A receptors potently suppresses the metastasis of CD73+ tumors. Proc Natl Acad Sci U S A 110:14711–14716. doi:10.1073/pnas.1308209110
29. Loi S, Pommey S, Haibe-Kains B et al (2013) CD73 promotes anthracycline resistance and poor prognosis in triple negative breast cancer. Proc Natl Acad Sci U S A 110:11091–11096. doi:10.1073/pnas.1222251110
30. Allard B, Turcotte M, Spring K et al (2014) Anti-CD73 therapy impairs tumor angiogenesis. Int J Cancer 134:1466–1473. doi:10.1002/ijc.28456
31. Beavis PA, Milenkovski N, Henderson MA et al (2015) Adenosine receptor 2A blockade increases the efficacy of anti-PD-1 through enhanced antitumor T-cell responses. Cancer Immunol Res 3:506–517. doi:10.1158/2326-6066.CIR-14-0211
32. Mittal D, Young A, Stannard K et al (2014) Antimetastatic effects of blocking PD-1 and the adenosine A2A receptor. Cancer Res 74:3652–3658. doi:10.1158/0008-5472.CAN-14-0957

Chapter 13

Isolation and Characterization of Low- vs. High-Density Neutrophils in Cancer

Jitka Y. Sagiv, Sandra Voels, and Zvi Granot

Abstract

Neutrophils are the most abundant of all white blood cells in the human circulation and serve as the first line of defense against microbial infections. Traditionally, neutrophils were viewed as a homogeneous population of myeloid cells. However, in recent years accumulating evidence has suggested that neutrophils are heterogeneous and that distinct neutrophil subsets may play very different roles. Here, we describe the methodology for isolation of high- and low-density neutrophils from the murine and human circulation using a density gradient and antibody based enrichment. We further describe the methodology for functional characterization of these different neutrophil subsets in the context of cancer.

Key words Neutrophils, Cancer, Isolation, Density, Enrichment, Flow cytometry, Cytotoxicity

1 Introduction

Neutrophils are the most abundant of all white blood cells in the human circulation and make the largest component of the innate immune system. They are short-lived myeloid cells with phagocytic properties and are usually associated with fighting microbial infections and with inflammation. In recent years, neutrophils have been shown to play additional roles in various pathologies including cancer. Intriguingly, in the context of cancer, neutrophil function remains a matter of debate as they were shown to posses both pro-tumor and antitumor properties. Neutrophils were shown to promote tumor growth [1], promote tumor angiogenesis [2], enhance tumor cell dissemination and metastasis [3], mediate immune suppression [4] and play a role in priming of the premetastatic niche [5]. On the other hand, neutrophils are capable of killing disseminated tumor cells either directly [6, 7] or through antibody-dependent cellular cytotoxicity (ADCC), thereby limiting metastatic seeding and tumor spread [8].

Neutrophils are commonly perceived as a homogeneous population of terminally differentiated effector cells with limited

Josie Ursini-Siegel and Nicole Beauchemin (eds.), *The Tumor Microenvironment: Methods and Protocols*, Methods in Molecular Biology, vol. 1458, DOI 10.1007/978-1-4939-3801-8_13,

versatility and plasticity [9]. However, our recent study [10] together with other reports [11–14] suggests that rather than being a homogeneous population neutrophils indeed consist of distinct subsets. In cancer, neutrophils can be roughly divided to two subsets according to their density where high-density neutrophils provide antitumor protection and low-density neutrophils are tumor-permissive and promote immune suppression [10]. Accordingly, the ratio between high- and low-density neutrophils determines the net contribution of neutrophils.

Here, we describe the methodology for isolation and functional characterization of high- and low-density neutrophils in the context of cancer. This includes the methodology for collection and purification of circulating neutrophils from human donors and tumor-bearing mice. We further describe the experimental strategies for functional characterization of these neutrophil subsets in the context of cancer.

2 Materials

Neutrophils are easily activated by a wide variety of bacterially derived molecules. It is therefore crucial to minimize potential contaminations. Thus, all solutions are prepared using autoclaved HPLC grade ddH_2O. Once prepared, the reagents used for neutrophil experimental procedures are filter-sterilized before use and are maintained at 4 °C if not indicated otherwise.

2.1 Materials and Reagents for Cancer Cell Injection

1. Isoflurane Anesthesia Apparatus, equipped with induction chamber and nose cone.
2. Isoflurane.
3. 0.3 ml syringe with a 30G×8 mm needle (BD Micro-Fine™), forceps.
4. Breast Cancer Cell Line as 4T1 (ATCC), E0771 (Ross Levine, Memorial Sloan Kettering Cancer Center, New York, NY, USA) or AT-3 (Scott Abrams, Buffalo, NY, USA).
5. Cell Culture Medium: 10% DMEM—Dulbecco's modified Eagle medium (DMEM) containing 4.5 g/L d-glucose supplemented with 10% heat-inactivated fetal bovine serum (FBS), 2 mM d-glutamine, 100 U/ml penicillin G, and 100 μg/ml streptomycin sulfate.
6. 1× PBS (no Ca^{2+}, no Mg^{2+}).
7. Trypsin.
8. Female Balb/C or C57BL/6 mice, 7–8 week old.
9. 70% EtOH in spray bottle.

Table 1
Antibodies for FACS analysis

Antibody	Clone	Working concentration (μg/ml)
Ly6G	1A8	2
Ly6C	HK1.4	2.5
CD11b	M1/70	2

2.2 Reagents for Low- and High-Density Neutrophil Isolation

1. 25G × 5/8′ needle, 1 ml syringe.
2. Human Blood Extraction Kit (Green top, Lithium-Heparin tubes).
3. 20 mg/ml heparin solution: dissolve 100 mg heparin in 5 ml 1 x PBS and filter sterilize using a syringe filter (0.2 μm).
4. Stock solution of 5% (w/v) bovine serum albumin (BSA, Sigma) in 10× phosphate-buffered saline (PBS): Weigh 25 g BSA and add to 500 ml 10× PBS, put solution on shaker at RT until BSA is completely dissolved and filter sterile using a bottle top filter (0.2 μm).
5. Working solution of 2.5% BSA/5 × PBS and 0.5% BSA/1 × PBS: Dilute stock solution of 5% BSA/10 × PBS 1:1 with ddH_2O to make 2.5% BSA/5 × PBS. Dilute 2.5% BSA/5% PBS 1:5 with ddH_2O to make 0.5% BSA/1 × PBS.
6. Histopaque®-1119 and Histopaque®-1077 (Sigma), sterile filtered using bottle top filters (0.2 μm). Keep covered with aluminum foil to protect from light.
7. 3% dextran/saline: Dissolve 15 g Dextran T500 (Sigma, Cat. No. 31392) in 500 ml saline (0.9% NaCl). Filter sterile using a bottle top filter (0.2 μm).
8. NaCl 1.6% and 0.2% (in ddH2O).
9. Quality of ddH2O is crucial.

2.3 Antibodies for FACS Analysis

See Table 1.

2.4 Neutrophil Enrichment

1. Buffer: 0.5% BSA/PBS × 1 and 2 mM EDTA. Prepared solution should be passed through 0.20 μm vacuum-driven filtration system for sterilization and for degassing (*see* **Note 1**). Keep working solution at 4 °C.
2. Biotinylated mouse anti-Ly6G antibody/human anti-CD66b antibody.
3. Anti-biotin-coated magnetic microbeads.

4. Magnetic separation column (determine column size according to cells count), for best results should be kept at 4 °C.
5. Magnet holder and magnetic stand.

2.5 Cytotoxicity Assay

1. Luciferase-expressing tumor cell line.
2. Optimized reduced serum medium (Opti-MEM).
3. Fetal bovine serum (FBS).
4. 1 x PBS.
5. Passive Cell Culture Lysis Reagent (Promega, E153A).
6. Luciferase assay solution: Add 110 μl of 10 mM d-luciferin and 75 μl of 0.2 M ATP to 10 ml luciferase buffer (100 mM tris-acetate, pH 7.8, 10 mM MgAc, and 1 mM EDTA).
7. Luminescence plate reader equipped with injector.
8. White, flat bottom 96-well tissue culture plate.

2.6 Modified Winn Assay

1. Saline.
2. Tumor cells.
3. Purified neutrophils.

2.7 Phagocytosis Assay

1. Optimized reduced serum medium.
2. PMA (Stock Solution 100 nM or 1 μM), fMLP (Stock Solution 100 μM).
3. Latex beads coated with fluorescently labeled rabbit IgG.
4. 0.5% BSA/1 × PBS.
5. Trypan Blue Quenching Solution.

2.8 Chemotaxis Assay

1. Polystyrene 24-well plate with 5-μm-pores hanging cell culture inserts.
2. Optimized reduced serum medium.
3. FBS.
4. Breast cancer cell line (*see* Subheading 2.1).

2.9 Oxidative Burst Assay

1. Hank's balanced salt solution without phenol red (HBSS).
2. White 96-flat-bottom well plate.
3. Luminescence plate reader with injector.
4. 500 μM Luminol solution in HBSS (stock 50 mM Luminol: 8.8 mg Luminol (5-amino-2,3-dihydro-l,4-phthalazinedione in 1 ml DMSO). Aliquots are stored at −20 °C protected from light.
5. PMA (phorbol myristate acetate).
6. fMLP (*N*-formylmethionyl-leucyl-phenylalanine).
7. HRP - Horse Radish Peroxidase (400u/ml).

3 Methods

3.1 Orthotopic Injection of Mammary Tumor Cell Lines

1 Seed at least 5×10^5 breast carcinoma cells in 10% DMEM in a 10 cm dish and grow until approx. 80% confluent (*see* **Note 2**).

2 Aspirate medium, wash once with PBS and incubate with 2 ml trypsin until cells detach from the plate.

3 Stop trypsin by adding 10 ml medium containing 10% FBS and spin down cells at $300 \times g$ for 5 min, RT.

4 Wash once more in PBS and resuspend in PBS for counting (*see* **Note 3**).

5 Resuspend cells at a final concentration of 2×10^7 cells/ml in PBS. Keep cells on ice.

6 Fill a 30G × 8 mm syringe with the cell suspension and tap to eliminate air bubbles before injection.

7 Anesthetized the mice in an induction chamber receiving isoflurane (3–5%) in oxygen under a slow flow rate.

8 Confirm proper anesthesia by pinching the paw and transfer the mouse to a surgical pad.

9 Lay the mouse on the back and place head inside the nose cone to provide continuous flow of isoflurane. Spray lower abdomen with 70% EtOH.

10 Using forceps gently grab the inguinal teat of the mouse (located in the lower left quarter of the abdomen). Lift it up to get a tent-like structure of the skin.

11 Insert tip of the needle into the middle of the triangular skin flap and slowly inject 50 µl of the cell suspension. Wait a moment before slowly pulling out the needle (Fig. 1).

12 Place the mouse back in the cage and monitor until it regains consciousness.

13 After 3–4 weeks, the primary tumor will have reached a size of about 2 cm^3 and the mice have to be euthanized. Neutrophil populations can be analyzed at various time points.

3.2 Isolation of Circulating Mouse Neutrophils

1. Sacrifice mice under slow flow of CO_2. Immediately after the mouse stops breathing, check reflex by pinching the mice paw and draw blood by cardiac puncture using a 25G × 5/8′ needle pretreated with heparin.

2. Lay the mouse on its back, spray the area around the sternum with 70% ethanol. Insert the needle under the right side of the sternum at an angle of approx. 20°. Insert the needle approx. ¾ of the way to penetrate the heart and gradually pull the plunger to draw blood. If no blood is coming out, try to adjust the needle with small movements penetrating deeper, pulling the needle out a bit or by slightly rotating the needle's opening.

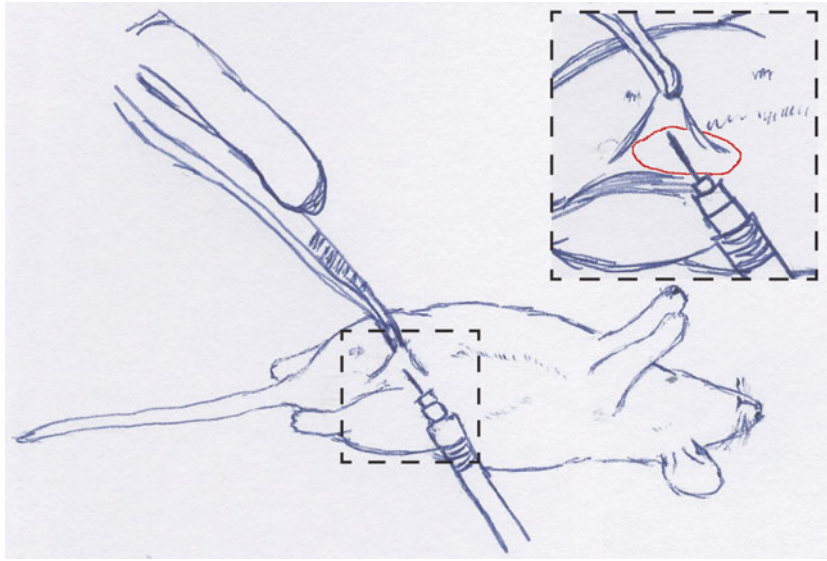

Fig. 1 Mammary fat pad injection. Lay the anesthetized mouse on its back and pull the inguinal nipple upwards using forceps. Insert the needle into the tent shaped structure and into the mammary fad pad (*red circle* in *inset*). Slowly and gradually inject up to 50 μl of cell suspension

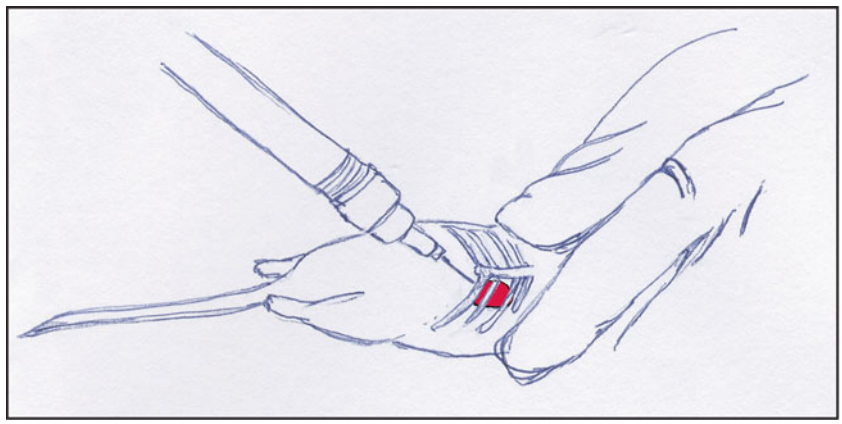

Fig. 2 Collection of murine blood via cardiac puncture. The mouse was euthanized under slow CO_2 flow. Immediately after the mouse has taken its terminal breath, it is laid on its back and a 1 ml heparinized syringe is inserted at the base of the sternum (to the right) until reaching the heart. Slowly pull on the plunger to aspirate the blood

Make sure not to take the needle out of the thoracic cavity. The plunger has to be pulled slowly to avoid collapse of the heart chambers. If air bubbles appear, stop pulling the plunger and try to readjust the needle. When done, push the plunger slightly back in to avoid sucking in air when pulling out the needle from the thoracic cavity (Fig. 2 and *see* **Note 4**).

Important—All following steps are carried out inside a tissue culture hood.

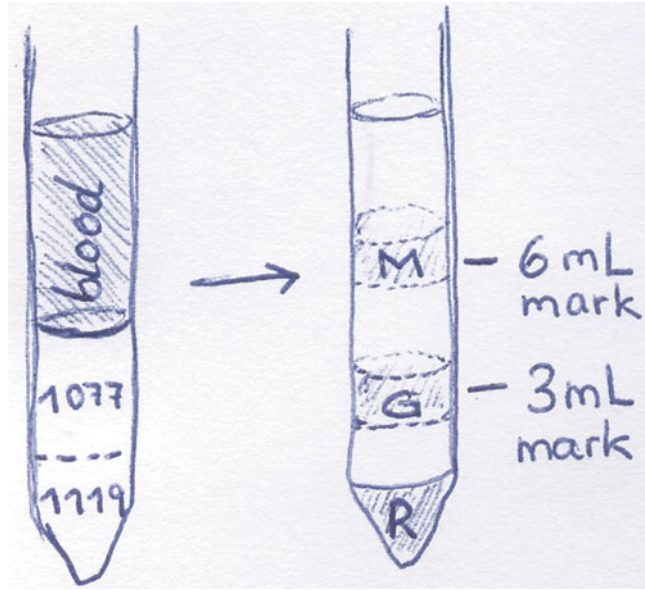

Fig. 3 Gradient isolation of mouse neutrophils. *Left*: Layer 3 ml of Histopaque 1077 slowly on top of 3 ml Histopaque 1119 in a 15 ml tube. Layer the diluted blood (6 ml) slowly on top of the Histopaque gradient. *Right*: Following centrifugation the blood is fractionated to red blood cells (R) in the pellet, a granulocytic fraction (G) containing high-density neutrophils and a mononuclear fraction (M) containing low-density neutrophils

3. Transfer the blood into a conical 15 ml tube and adjust the volume to 6 ml with 0.5 % BSA/1 × PBS (*see* **Note 5**).
4. Prepare the Histopaque® gradient in a 15 ml conical tube. Pipette 3 ml of Histopaque®-1119 and carefully overlay with 3 ml of Histopaque®-1077 to avoid any perturbations (*critical step*!). Overlay gradient very slowly with 6 ml of blood–BSA mixture.
5. Centrifuge at 700 × *g* for 30 min at RT with no brake (*critical*, *see* **Note 6**).
6. Carefully remove the gradient from the centrifuge (*see* **Note 7**) and aspirate overlaying BSA/PBS until 5 mm above the ring of low-density cells. Use 1 ml pipette to collect cells of low-density ring (*see* **Note 8**) and transfer into 10 ml 0.5 % BSA/1 × PBS in a fresh conical 15 ml tube. Aspirate until reaching 5 mm above the high-density cell ring. Collect high-density cells (*see* **Note 9**) and transfer to 10 ml 0.5 % BSA/1 × PBS in a fresh 15 ml tube. Invert collection tubes at least two times. Spin down collected cells at 400 × *g*, 10 min, RT (Fig. 3).
7. Aspirate supernatant and lyse red blood cells by resuspending the pellet in 8 ml ddH_2O. Pipette five times up and down and incubate for no longer than 25 s (altogether) before adding

2 ml of 2.5% BSA/5×PBS and invert 2–3 times to regain isotonicity. Centrifuge for 10 min, 400×*g*, RT.

8. Resuspend cells in 10 ml 0.5% BSA/1×PBS and count with hemocytometer. Often a pre-dilution of 1:4 or higher, including trypan blue to check viability, is required due to the high number of cells.

3.3 Neutrophil Isolation of Human Blood Samples

1. Human blood is collected in green top Lithium-Heparin tubes (*see* **Note 10**). Start by mixing the blood with equal volume of 3% dextran in saline by inverting at least 20 times in a 50 ml tube. Incubate at RT for 20 min to let the red blood cells sediment to the bottom of the tube. Collect leukocyte-rich supernatant.
2. Prepare a 50 ml conical tube with Histopaque®-1077 (same volume as collected leukocyte-rich supernatant) and carefully overlay the leukocyte suspension (*critical step*, *see* **Note 11**). Centrifuge for 30 min without brake, 400×*g*, RT (Fig. 4).
3. Aspirate till 5 mm above the interface between BSA/PBS and Histopaque®-1077. Collect ring of low-density cells using a 1 ml pipette and transfer into 10 ml 0.5% BSA/1×PBS. Aspirate the remaining supernatant without perturbing the pellet. Resuspend the pellet in 12 ml 0.5% BSA/1×PBS (*see* **Note 12**) and centrifuge for 10 min, 160×*g*, RT (Fig. 4).

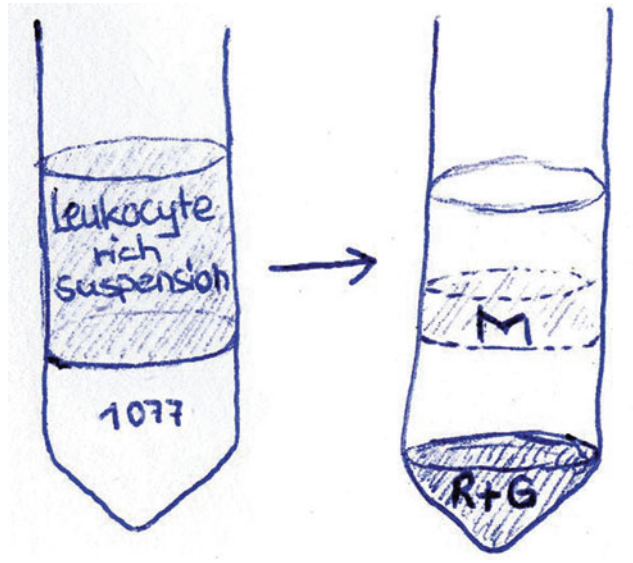

Fig. 4 Gradient isolation of human neutrophils. *Left*: Layer the leukocyte rich supernatant slowly on an equal volume of Histopaque 1077 in a 50 ml tube. *Right*: Following centrifugation the blood is fractionated to give a mix of red blood cells and granulocytes containing high-density neutrophils (R+G) in the pellet and a mononuclear fraction (M) containing low-density neutrophils

4. Aspirate supernatant and lyse contaminating RBC by adding 10 ml NaCl 0.2% to the cell pellet. Pipette five times up and down and incubate for no longer than 25 s. Stop lysis by adding 10 ml NaCl 1.6%. Spin down at 160×*g*, 10 min, RT and resuspend in 10 ml 0.5% BSA/1×PBS for counting.

3.4 Analysis of Neutrophil Purity in the Low- and High-Density Fractions Using Flow Cytometry

1. Take 0.2–1×10⁶ cells from each fraction and spin down at 400×*g* (for mouse neutrophils) or 160 x g (for human neutrophils), 10 min, RT.
2. Resuspend cells in 50 µl 0.5% BSA/1×PBS containing FcR blocker and incubate for 5 min.
3. Prepare antibody staining dilutions in 0.5% BSA/1×PBS.
4. Add 50 µl of antibody solution (Ly6G, Ly6C, and CD11b for mouse; CD15, CD66b, and CD11b for human) and incubate for 15 min at RT. Add 1 ml 0.5% BSA/1×PBS to wash samples and spin down 400×*g* (for mouse neutrophils) or 160 x g (for human neutrophils), 10 min, RT (*see* **Notes 13** and **14**).
5. Resuspend cells in 200 µl 0.5% BSA/1×PBS and analyze with flow cytometer (Fig. 5 and *see* **Note 15**).

3.5 Neutrophil Enrichment

For functionality assays, neutrophils isolated on a density gradient are further enriched for Ly6G/CD66b positive cells only. While the high-density fraction purity in tumor-bearing mice is usually above 95% the low-density fraction consists of less than 50%

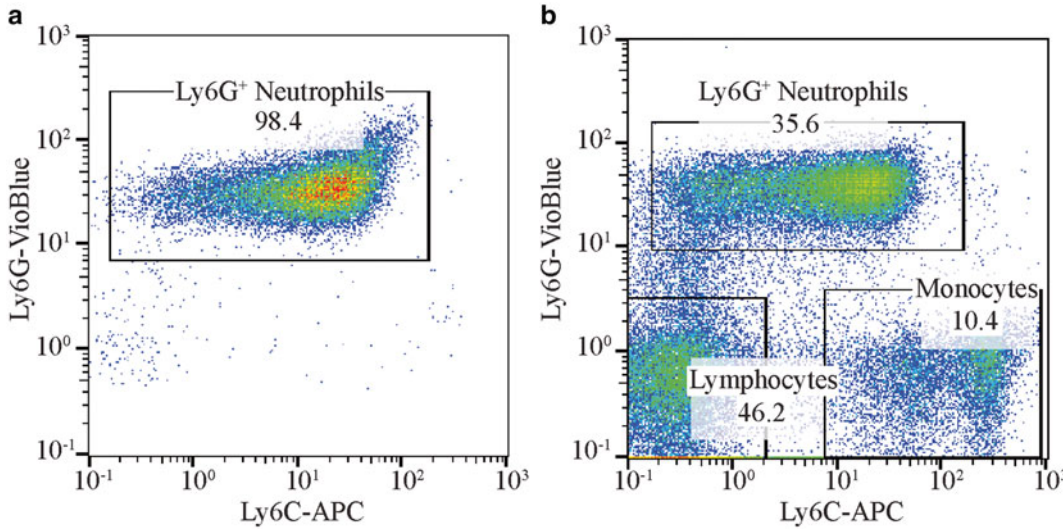

Fig. 5 Flow cytometry analysis of neutrophils in high- and low-density fractions. High-density granulocytic fraction and low-density mononuclear fraction were isolated from the circulation of a Balb/C mouse 3 weeks after 4T1 tumor injection into the mammary fat pad. (**a**) The granulocytic fraction consists almost exclusively (>98%) of Ly6G^{high}Ly6C^{int} neutrophils. (**b**) The mononuclear fraction contains Ly6G^{high}Ly6C^{int} neutrophils as well as Ly6G^{neg}Ly6C^{high} monocytes and Ly6G^{neg}Ly6C^{neg} lymphocytes

neutrophils. In human samples, the purity is even lower. Nevertheless, both fractions should go through the same enrichment process to eliminate any potential bias. There are several protocols for neutrophil enrichment and here, we will describe positive selection using neutrophil specific antibodies, magnetic beads, and separation columns.

1. Centrifuge cells of low- and high-density fraction (Subheadings 3.2 and 3.3) at 400 × *g* for 10 min, RT. Aspirate supernatant completely.
2. Resuspend cell pellet in 200 µl of buffer per 10^8 total cells (*see* **Note 16**).
3. Add 50 µl of biotinylated anti-Ly6G/CD66b antibody. Mix well and incubate for 10 min (2–8 °C, *see* **Note 16**).
4. Resuspend cells by adding 150 µl of buffer per 10^8 total cells. Pipette gently.
5. Vortex the anti-biotin-coated magnetic microbeads stock solution. Add 100 µl of the microbead solution to the cell suspension. Mix well and incubate for 15 min (2–8 °C).
6. Wash cells by adding 10 ml of buffer per 10^8 total cells and centrifuge at 300 × *g* for 10 min, RT.
7. Aspirate supernatant completely, and gently resuspend cells in 500 µl buffer. Insert a magnetic separation column (*see* **Note 17**) into the magnetic holder and rinse it with 500 µl of cold buffer.
8. Apply the cell suspension onto the column. The flow-through contains Ly6G/CD66b^{neg} cells. Wait until the column stops dripping.
9. Rinse the column gently by adding 500 µl of buffer. Additional Ly6G/CD66b^{neg} cells will be in the flow-through.
10. Repeat the washing step once more.
11. Remove the column from the magnet and place it on a 15 ml collection tube. Add 1 ml buffer, and flush out the magnetically labeled cells by firmly pushing the plunger into the column. Enriched neutrophils are released from the column. Count the cells. Once the purity of the isolated neutrophils is determined by flow cytometry, they can be used for in vitro and in vivo functional assays.

3.6 Functional Assays

3.6.1 Cytotoxicity Assay

1. Seed 5×10^3 luciferase-labeled (transduced with a luciferase expression vector) tumor cells (*see* Subheading 3.1, **steps 1** and **2**) in 100 µl optimized reduced serum medium containing 0.5–2% FBS (*see* **Note 18**), in each well of a white 96-flat-bottom tissue-culture well plate.
2. Prepare a neutrophil cell suspension with a density of 2×10^6 cells/ml. Control wells should get 50 µl medium without

neutrophils (see Note 19). Following 4 h of incubation, add 1×10^5 neutrophils from Subheading 3.5, **step 11** in 50 µl optimized reduced serum medium containing 0.5–2% FBS and incubate overnight.

3. On the next day, gently aspirate the supernatant and wash each well with 200 µl PBS. Aspirate the PBS and add 50 µl of luciferase assay lysis buffer (*see* **Note 20**).
4. Cover the plate with aluminium foil and incubate while shaking at 150 rpm for 20 min, RT.
5. Place the plate in an injector equipped luminescence plate reader. Inject well-wise 50 µl luciferase assay solution, and read the chemiluminescence for 10 seconds per well.
6. Cytotoxicity of neutrophils should be calculated as the decrease in luminescence in wells where tumor cells were cocultured with neutrophils (high or low density) compared with tumor cells cultured alone.

3.6.2 Modified Winn Assay

1. Prepare column purified neutrophils (12×10^7/ml) (high or low density, Subheading 3.5) and cancer cells (40×10^6/ml) (Subheading 3.1) in saline in separate vials, keep on ice.
2. Shave the flank prior to tumor engraftment to allow accurate measurements of tumor size.
3. Mix the neutrophils and cancer cells solutions right before injection in the ratio of 1:1 and inject final volume of 50 µl/mouse. (1×10^6 tumor cells (25 µl) and 3×10^6 neutrophils (25 µl)).
4. Inject the cells subcutaneously to the flank of 6–8 week old naïve Balb/C mice.
5. Measure tumor size daily, starting on day 5 post-engraftment (*see* **Note 21**).

3.6.3 Neutrophil Chemotaxis Assay

1. Culture 5×10^5 tumor cells in 7 ml optimized reduced serum medium supplemented with 0.5% FBS in a 25 cm^2 tissue culture flask and incubate for 24 h at 37 °C.
2. Collect the conditioned media and centrifuge at $700 \times g$ 5 min to pellet unwanted cells and cell debris. Transfer 800 µl of the supernatant to the bottom chamber of a 24-well plate equipped with 5 µm pore hanging inserts.
3. Resuspend 2×10^5 of purified low/high-density neutrophils (Subheading 3.5) in 400 µl of optimized reduced serum medium supplemented with 0.5% FBS. Apply the cell suspension to the top chamber and incubate for 2 h at 37 °C.
4. At the end of incubation, remove the top chamber (be careful to do it gently and uniformly to all samples to avoid contaminations) and count the number of neutrophils that have

migrated to the bottom chamber. Image wells at the end of the assay. Migrating cells can be quantified manually (analysis of cell number in well images) or using FACS ($Ly6G^+$ cells in the lower chamber).

3.6.4 Neutrophil Oxidative Burst

1. Prepare a 1.1×10^6/ml purified neutrophil suspension (low or high density, Subheading 3.5) in Hank's balanced salt solution without phenol red. Plate 180 µl of the suspension (2×10^5 neutrophils/well) in a white 96-flat-bottom well plate.
2. Place the plate in a luminescence plate reader. Inject well-wise 20 µl of a 500 µM Luminol solution (10 µl Luminol 50mM, 100 µl HRP 400 U/ml, 890 µl HBSS)to each well to get a final concentration of 50 µM. Read the basal chemiluminescence for 1 second in a time course of 5 min with 10 second intervals.
3. Prepare a 10× concentrated solution of stimulant in Hank's balanced salt solution without phenol red (e.g., PMA working concentration 100 nM or 1 µM; final concentration 10 or 100 nM, fMLP working concentration of 100 µM; final concentration, 10 µM). Add 22 µl of the concentrated stimulant to the respective wells. To control wells add 22 µl HBSS.
4. Measure the chemiluminescence in the plate reader in a short (every 10 seconds for 5 min) and a long (every minute for 1 hour) time course to monitor both immediate and long term responses.

3.6.5 Phagocytosis Assay

1. Prepare a 1×10^6 cells/ml neutrophil suspension in optimized serum free medium. Neutrophils may also be stimulated with PMA or fMLP prior (see above) to performing the assay.
2. Place 100 µl of the suspension in a 1.5 ml tube.
3. Add Rabbit IgG-FITC Latex Beads directly to each tube to a final dilution of 1:100.
4. Incubate cells at 37 °C for 1 hour or more.
5. To assess degree of phagocytosis, centrifuge the cells at $400 \times g$ for 10 min, RT. Remove the supernatant, and resuspend the cells in 100 µl of FACS buffer for further staining with neutrophil markers or live/dead dyes (such as propidium iodide). Process the samples in dark to prevent changes in the FITC fluorescence. Cells are analyzed by flow cytometry or by a fluorescence microscope capable of measuring FITC fluorescence. Cells may also be visualized by cytospin centrifugation and nuclear staining with DAPI.
6. To distinguish cells which have phagocytosed the beads from those simply binding the beads at the surface, a short (1–2 min) incubation with Trypan Blue Quenching Solution, followed by a wash with 5% BSA/PBS, will quench surface FITC fluorescence.

4 Notes

1. Buffer and solutions used for column separation have to be free of bubbles as these decrease column efficiency. Buffer can be degassed by prolonged vacuum filtration or by centrifugation. Cell suspension to be loaded has to be pipetted gently without creating bubbles. Dead cells in the suspension also decrease efficiency and should be avoided. The process of neutrophil enrichment has to be done quickly as neutrophils may be activated by antibodies used.
2. Other breast carcinoma cell lines like AT-3 and E0771 are also cultivated in 10% DMEM. The different carcinoma cell lines have different growth kinetics in vitro and in vivo with 4T1 showing the most rapid tumor growth, E0771 moderate growth and AT-3 the slowest. The extent of LDN mobilization corresponds with tumor size [10]. Due to their origin, 4T1 are injected to Balb/C mice and E0771 and AT-3 to C57BL/6 mice.
3. Contaminating serum could lead to additional immune responses.
4. Usually 800 µl to 1 ml blood can be withdrawn from a tumor-bearing mouse. For healthy control mice it is around 700 µl.
5. Working reagents as BSA solutions and Histopaque have to be taken out of 4 °C before starting the isolation protocol as cold reagents may affect downstream procedures.
6. Be careful when handling the tube with the prepared gradient (transfer to centrifuge and back) to avoid any perturbations.
7. At the bottom of the tube a pellet of red blood cells (RBC) will be visible. In a conical 15 ml tube, the ring of granulocytes will be around the 3 ml mark at the interface between the 1.119 g/ml and the 1.077 g/ml layers, the ring of mononuclear cells (including lymphocytes, monocytes, low-density neutrophils) is at the 6 ml mark, the interface between 1.077 g/ml sucrose and 0.5% BSA/1× PBS.
8. Usually 1.5–2 ml is collected.
9. High-density fraction is often contaminated with RBC, whereas low-density fraction barely contains RBC. Nevertheless the osmotic shock in the following step has to be done for both samples, as the treatment needs to be exactly the same.
10. A blood sample volume of 10 ml from a healthy donor usually contains around 20×10^6 neutrophils in the high-density fraction.
11. As the volume of the leukocyte suspension often exceeds 10 ml the gradient is prepared in a conical 50 ml tube.

12. Pellet contains high-density neutrophils and RBCs. Be very careful when discarding the interface between low- and high-density fraction while remaining cells from the low-density fraction may stick and slide on the walls of the tube and contaminate the high-density fraction.
13. If the staining is done the first time, single stains must be included to adjust compensation matrix.
14. PI (propidium iodide) staining (or other viable staining) may be included to exclude damaged/dead cells.
15. The high-density fraction usually is pure to 95% and higher. The percentage of neutrophils in the low-density fraction depends on the stage of the tumor and typically lies between 20 and 60%.
16. All the separation process should be done using cold buffer (4 °C) and the incubation in all steps is done in the fridge. Using ice is not recommended. As cells tend to sediment quickly during the incubation, the solution may be gently mixed from time to time.
17. During the enrichment process, the column should be kept wet, anyhow between every new loading all the liquid has to enter from the reservoir into the column itself. Avoid loading neutrophil suspension that contains any clots, as this will occlude the column. If having such a problem, the solution should be passed through single cell mesh.
18. The amount of FBS (0.5–2%) needs to be adjusted for each cell line used.
19. Luciferase assay is "noisy" and therefore each experimental setting should be repeated multiple times.
20. For easily detaching cells (such as AT-3 cells), do not wash in PBS. Add the lysis buffer immediately after aspirating the growth medium.
21. Winn assays may also include cytotoxic T-cells towards evaluating the immune suppressive properties of high or low-density neutrophils.

References

1. Pekarek LA, Starr BA, Toledano AY, Schreiber H (1995) Inhibition of tumor growth by elimination of granulocytes. J Exp Med 181(1):435–440
2. Nozawa H, Chiu C, Hanahan D (2006) Infiltrating neutrophils mediate the initial angiogenic switch in a mouse model of multistage carcinogenesis. Proc Natl Acad Sci U S A 103(33):12493–12498
3. De Larco JE, Wuertz BR, Furcht LT (2004) The potential role of neutrophils in promoting the metastatic phenotype of tumors releasing interleukin-8. Clin Cancer Res 10(15):4895–4900
4. Youn JI, Nagaraj S, Collazo M, Gabrilovich DI (2008) Subsets of myeloid-derived suppressor cells in tumor-bearing mice. J Immunol 181(8):5791–5802

5. Yan HH, Pickup M, Pang Y, Gorska AE, Li Z, Chytil A, Geng Y, Gray JW, Moses HL, Yang L (2010) Gr-1+CD11b+ myeloid cells tip the balance of immune protection to tumor promotion in the premetastatic lung. Cancer Res 70(15):6139–6149
6. Granot Z, Henke E, Comen EA, King TA, Norton L, Benezra R (2011) Tumor entrained neutrophils inhibit seeding in the premetastatic lung. Cancer Cell 20(3):300–314
7. Lopez-Lago MA, Posner S, Thodima VJ, Molina AM, Motzer RJ, Chaganti RS (2013) Neutrophil chemokines secreted by tumor cells mount a lung antimetastatic response during renal cell carcinoma progression. Oncogene 32(14):1752–1760
8. Sionov RV, Fridlender ZG, Granot Z (2014) The multifaceted roles neutrophils play in the tumor microenvironment. Cancer Microenviron 8(3):125–158
9. Galdiero MR, Bonavita E, Barajon I, Garlanda C, Mantovani A, Jaillon S (2013) Tumor associated macrophages and neutrophils in cancer. Immunobiology 218(11):1402–1410
10. Sagiv JY, Michaeli J, Assi S, Mishalian I, Kisos H, Levy L, Damti P, Lumbroso D, Polyansky L, Sionov RV, Ariel A, Hovav A-H, Henke E, Fridlender ZG, Granot Z (2015) Phenotypic diversity and plasticity in circulating neutrophil subpopulations in cancer. Cell Rep 10(4): 562–573
11. Brandau S, Trellakis S, Bruderek K, Schmaltz D, Steller G, Elian M, Suttmann H, Schenck M, Welling J, Zabel P, Lang S (2011) Myeloid-derived suppressor cells in the peripheral blood of cancer patients contain a subset of immature neutrophils with impaired migratory properties. J Leukoc Biol 89(2): 311–317
12. Cloke T, Munder M, Taylor G, Muller I, Kropf P (2012) Characterization of a novel population of low-density granulocytes associated with disease severity in HIV-1 infection. PLoS One 7(11):e48939
13. Denny MF, Yalavarthi S, Zhao W, Thacker SG, Anderson M, Sandy AR, McCune WJ, Kaplan MJ (2010) A distinct subset of proinflammatory neutrophils isolated from patients with systemic lupus erythematosus induces vascular damage and synthesizes type I IFNs. J Immunol 184(6):3284–3297
14. Morisaki T, Goya T, Ishimitsu T, Torisu M (1992) The increase of low density subpopulations and CD10 (CALLA) negative neutrophils in severely infected patients. Surg Today 22(4):322–327

Chapter 14

Analysis of Extracellular Vesicles in the Tumor Microenvironment

Khalid Al-Nedawi and Jolene Read

Abstract

Extracellular vesicles (ECV) are membrane compartments shed from all types of cells in various physiological and pathological states. In recent years, ECV have gained an increasing interest from the scientific community for their role as an intercellular communicator that plays important roles in modifying the tumor microenvironment. Multiple techniques have been established to collect ECV from conditioned media of cell culture or physiological fluids. The gold standard methodology is differential centrifugation. Although alternative techniques exist to collect ECV, these techniques have not proven suitable as a substitution for the ultracentrifugation procedure.

Key words Exosome, Microvesicle, Ultracentrifugation, Tumor microenvironment

1 Introduction

Extracellular vesicles (ECV) are membrane compartments shed from all types of cells in a variety of physiological and pathological states [1, 2]. There are two main types of extracellular vesicles, namely microvesicles, and exosomes. Microvesicles are generated from the direct outward budding and vesiculation of the plasma membrane into the extracellular milieu [3]. Exosomes, on the other hand, are generated by invagination of the limiting membrane of a multivesicular body (MVB) to form intraluminal vesicles (ILV) [4]. Upon fusion of the MVB with the plasma membrane, ILV are released into the extracellular environment, where they are termed exosomes [4]. In general, microvesicles have average diameters of 200–1000 nm, whereas exosomes range from 50 to 200 nm. The molecular cargo of both classes of ECV comprises proteins, mRNAs [5], miRNAs [6], and even DNAs [7, 8]. In recent years, ECV have garnered much attention for their role in modulating the tumor microenvironment through their role as mediators of intercellular communication [9–12]. Furthermore, ECV have been shown to affect tumor growth by horizontal transfer of oncogenic molecules or tumor

Josie Ursini-Siegel and Nicole Beauchemin (eds.), *The Tumor Microenvironment: Methods and Protocols*, Methods in Molecular Biology, vol. 1458, DOI 10.1007/978-1-4939-3801-8_14,

suppressor proteins among tumor cells and possibly stromal cells [13]. The transfer of such receptors to indolent cells via ECV confers oncogenic and angiogenic phenotypes to target cells [9, 14]. In addition, ECV can transfer mRNA transcripts that can be translated into functional proteins in recipient cells [5], or miRNAs that can regulate translation of target proteins [6].

Further to their role in the tumor microenvironment, ECV are considered a novel source for diagnostic and predictive biomarkers in bodily fluids [15]. Circulating ECV in blood provide a simple, noninvasive platform to look for biomarkers of cancer and other pathologies. Herein, we describe optimal procedures for collection of ECV from cell culture, serum, or plasma samples. In addition, we also describe how to treat cells with ECV and study their effects on a variety of acceptor cells.

2 Materials

2.1 Cell Culture

1. Cell lines. Almost all cell types produce ECV, including primary and immortalized cell lines; therefore ECV can be harvested from the conditioned medium of any cell line of interest.
2. Cell medium. The type of medium and supplements added will be dependent on the cell line used.
3. Tissue culture grade vented flasks (e.g., 75 cm^2).
4. Biosafety cabinet, pipet aids, etc. used for basic mammalian cell culture.
5. Hemocytometer.

2.2 Isolation of ECV

1. Centrifuges. Refrigerated low speed centrifuge, refrigerated high-speed centrifuge, and ultracentrifuge with fixed angle rotor.
2. Centrifuge tubes. 50 mL centrifuge tubes and appropriately sized ultracentrifuge tubes for rotor being used.
3. Phosphate-buffered saline (PBS), pH 7.4.
4. 0.2 μm low-protein-binding filter.

2.3 Quantification of ECV Concentration

1. 2× Protein Sample Buffer (65.8 mM Tris–HCl, pH 6.8, 26.3% (w/v) glycerol, 2.1% sodium dodecyl sulfate).
2. DC BioRad Protein Assay or CBQCA Protein Assay.
3. Microplate reader.
4. Nanoparticle Tracking Analysis such as NanoSight LM10.

2.4 Purity Assessment of ECV Preparation

1. Scanning electron microscope (SEM).
2. 0.1 M phosphate buffer, (pH 7.4).
3. 2.5% glutaraldehyde in 0.1 M phosphate buffer.

4. 0.1 M cacodylate buffer (4.28 g sodium cacodylate, 25 g $CaCl_2$, 2.5 mL 0.2 N hydrochloric acid, diluted to 200 mL with ultrapure water, pH 7.4).
5. 1 % osmium tetraoxide.

2.5 Analyzing Transport of ECV-Associated Proteins to Recipient Cells

1. Cell lines.
2. Complete growth medium and serum-free growth medium (components will vary depending on the cell type employed).
3. Tissue culture grade dishes (e.g., 100 mm^2).
4. Biosafety cabinet, pipet aids, etc. used for basic mammalian cell culture.

3 Methods

3.1 Cell Culture

1. Grow the mammalian cells using recommended cell culture protocol for the given cell type. Complete growth medium should contain suitable supplements and bovine serum (BS; *see* **Note 1**). Grow cells in an incubator with a fixed temperature of 37 °C and 5 % CO_2.
2. Examine cells daily for growth estimation. For adherent cells, estimate the percentage of confluence. For cells growing in suspension, mix the cell suspension well, remove 100 μL of the cell suspension, and estimate the cell number by hemocytometer or automated cell counter.
3. When cells reach 70 % confluence (adherent cells) or approximately 0.5×10^6 cells/mL (suspension cell lines), replace the growth medium with ECV-depleted growth medium (*see* **Note 2**).
4. Grow cells for 24–48 h in the ECV-depleted medium. Then collect the conditioned medium in appropriately sized conical tubes and store on ice.

3.2 Isolation of ECV

Samples should be kept on ice and all centrifugations should be done at 4 °C. The workflow of this procedure is summarized in Fig. 1.

1. Cell debris and large vesicles are removed by passing conditioned medium through a low protein-binding 0.2 μm filter. Centrifuge the filtrate at $300 \times g$ for 10 min, collecting the supernatant and discarding the pellet.
2. Transfer the supernatant to a fresh centrifuge tube and centrifuge the sample at $12{,}000 \times g$ for 20 min to remove any remaining cellular debris or large vesicles.
3. Collect the supernatant and transfer sample to fresh ultracentrifuge tubes. Pellet ECV by centrifuging at $100{,}000 \times g$ for 2 h in ultracentrifuge (*see* **Note 3**). Carefully remove supernatant,

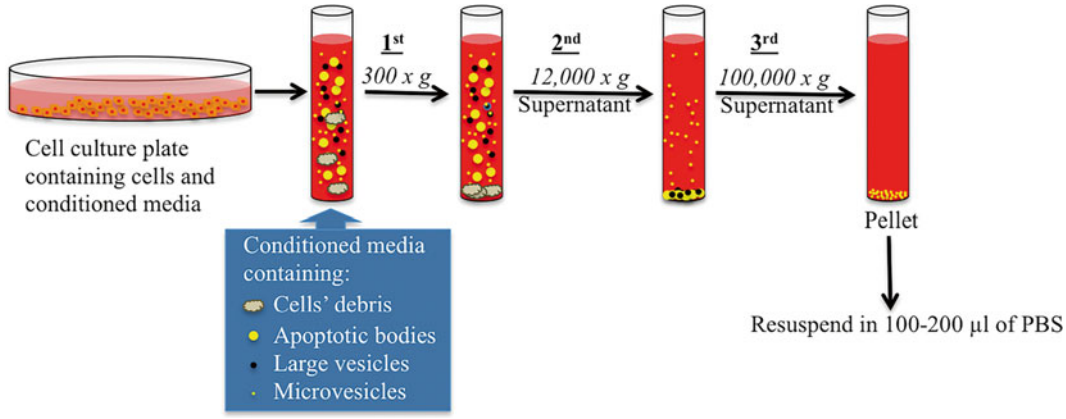

Fig. 1 Collection of extracellular vesicles (ECV) from cells' conditioned media. Cells were grown in suitable growth media supplemented with ECV-depleted FBS. Conditioned media containing cell debris, apoptotic antibodies, large vesicles, and microvesicles were collected and subjected to sequential centrifugation steps to collect ECV. First, conditioned media were subjected to 300 × *g* centrifugation for 5 min to eliminate cell debris. Second, Supernatants from the first step were subjected to 12,000 × *g* centrifugation for 20 min in a high-speed refrigerated centrifuge to remove apoptotic antibodies and large vesicles. Third, the supernatants from the second step were collected and subjected to 100,000 × *g* centrifugation for 2 h at 4 °C in an ultracentrifuge to pellet the ECV. The pelleted ECV were resuspended in 100–200 µL of cold PBS

taking care not to disturb the pellet. Resuspend the pellet (ECV) in a limited volume (100–200 µL) of phosphate-buffered saline (PBS) or serum-free cell culture medium (*see* **Note 4**).

4. Transfer ECV-suspension into a sterile microfuge tube. Reserve a small aliquot of the sample to determine protein concentration.

3.3 Quantification of ECV Concentration

There are different procedures to quantify ECV; here we list the most popular ones.

1. Quantification of Total Protein Concentration. Mix the ECV suspension by pipetting, and withdraw 20 µL for protein assay. Mix sample with an equal volume (i.e., 20 µL) of 2× protein sample buffer lacking bromophenol blue. Boil the mixture for 5 min at 95 °C to lyse ECV. Protein concentration may be determined using a colorimetric method or a fluorimetric method; *see* **Note 5**.
2. Nanoparticle Tracking Analysis (NTA). This is a light scattering technique that is useful for rapid assessment of ECV size and number (*see* **Note 6**). This procedure has been criticized for the lack of standardization, but generally provides acceptable measurement of the size and number of ECV [16]. The potential causes of error related to size assessment include inaccurate measurement of temperature, incorrect assessment of viscosity and external vibration. The ECV concentration

assessment is dependent on factors such as camera, laser wavelength, depth of laser beam, cleanliness/wear of the metallized glass optical flat surface, duration of measurements, optical alignment, vibration, and operator proficiency. Take the precautions necessary for the specific NTA instrument available for your laboratory to get sustainable results from the different measurements.

3.4 Purity Assessment of ECV Preparation

To assess the purity of ECV preparations, you will require continuous access to a scanning or transmission electron microscope (*see* **Note 7**). To prepare ECV for scanning electron microscopy (SEM), use the following procedure. Immunoblotting can also achieve assessment of ECV purity (*see* **Note 8**).

1. Collect ECV from conditioned media, blood plasma, or serum using the multistep centrifugation procedure as described in Subheading 3.2.
2. Spread 50 μL of the ECV suspension on a cover slip.
3. Fix with 2% glutaraldehyde in 0.1 M sodium cacodylate buffer, pH 7.4.
4. Rinse 2× in 0.1 M sodium cacodylate buffer, pH 7.4, then post-fixed in 1% osmium tetroxide in 0.1 M sodium cacodylate buffer for 1 h.
5. Dehydrate the sample through a graded ethanol series (50, 70, 70, 95, 95, 100%), 10–15 min for each step.
6. Expose the sample to critical point drying (*see* **Note 9**). Keep the samples immersed in 100% EtOH, then place the samples in wire baskets and transfer to a precooled (18 °C) chamber of the critical point dryer (Ladd Research Industries, Williston, VT). Seal the chambers and flush several times with liquid CO_2. Heat the CO_2 filled chamber to 39 °C and increase the pressure in the chamber to above 1100 psig to change CO_2 from liquid phase to gaseous phase. The gas should then to be vented slowly from the chamber until atmospheric pressure is reached; in this stage, the samples were dehydrated without surface tension damage.
7. Mount the coverslips onto SEM stubs with double-sided carbon tape and silver paste.
8. Expose the samples to sputter-coating with gold. The coating is achieved by placing the stubs in the chamber of a Polaron Model E5100 sputter coater (Polaron Equipment Ltd., Watford, Hertfordshire) and deposit approximately 20 nm of gold onto the stubs.
9. Inspect the specimens with the SEM. Verify the size of ECV under different magnifications to assess the homogeneity of your preparation. Take photographs for your reference (*see* **Note 10**).

3.5 Uptake of ECV by Recipient Cells

This protocol may be used to assess in vitro uptake of ECV by recipient cells. The functional outcome of ECV-treatment may be measured by western blotting, microscopy, cellular proliferation assays, or real-time PCR.

1. Grow recipient cells to 60% confluency in complete growth medium.
2. Wash cells three times with sterile, warmed PBS. Replace medium with serum-free medium for 24 h.
3. Add desired ECV concentration to fresh, pre-warmed serum-free medium (*see* **Notes 11** and **12**). Add directly to cell culture.
4. Perform a time course to determine optimal incubation time. In our experience, 24 h post-treatment works well, although this will depend on the functional assays being used.

4 Notes

1. The percentage of FBS is dependent on the cell type. The generally accepted percentage is 10%, but some cells grow better in 5% (see the data sheet for the cell line) or perform a simple experiment to find out the optimal concentration for your cells.
2. FBS is known to contain ECV, which may affect the yield and purity of ECV harvested from the conditioned medium. Using sterile technique, centrifuge FBS at 100,000 × *g* (ultracentrifuge) for 16 h to remove all ECV. Use the depleted FBS to supplement your media.
3. Special precautions and training for the use of the ultracentrifuge are required, as any misuse of this equipment may result in personal injury or damage to this expensive machine.
4. For maximum ECV-retrieval, resuspend the ECV pellet repeatedly in a small volume (i.e., 3 × 50 μL).
5. The advantage of the latter assay includes a lower detection threshold and greater tolerance for high phospholipid concentrations.
6. A ratio of protein content determined from a protein assay and particle number determined by Nanoparticle Tracking Analysis may be used as a straightforward protocol for determining ECV purity [17]. A ratio of 1×10^{10} to 3×10^{10} particles per μg protein has been proposed. This ratio helps provide information on the amount of contaminating protein that is co-pelleted throughout the ECV isolation procedure.
7. Preparations for scanning electron microscopy are easier and less time consuming than the transmission electron microscopy preparation.

8. Purity of exosome preparations should be assessed using a panel of marker antibodies. Common marker proteins include CD9, CD63, CD81, Hsp70, Alix, TSG101, and Flotillin-1.
9. This procedure helps to preserve ECV surface morphology better than air dehydration. In this procedure, the water within the specimen will be replaced with an exchange fluid such as ethanol or acetone. The exchange fluid then will be replaced with liquid CO_2. The liquid CO_2 is then exposed to its critical point (31 °C and 74 bar) to be converted to the gaseous phase by decreasing the pressure at constant critical point temperature.
10. Although this procedure seems to be time consuming, in fact it is not, and if you have access to a reasonably good EM facility, this is one of their daily procedures. You need to use this procedure at least once when you begin collecting the ECV from the given specimen to familiarize yourself with the morphology and structure of ECV.
11. We recommend performing a quantitative dose–response curve to determine the optimal working concentration for your system.
12. It is important to use systematic negative controls to validate data obtained. For example, "mock ECVs" (e.g., culture medium that has not been conditioned by cells of interest) provide a baseline of background functional activity. ECVs from BS contain functional miRNAs and proteins that may impact measurements [18].

Acknowledgments

This work was supported by a Movember Foundation/Prostate Cancer Canada Discovery Grant # D-2014-1 for Dr. K. Al-Nedawi.

References

1. Raposo G, Stoorvogel W (2013) Extracellular vesicles: exosomes, microvesicles, and friends. J Cell Biol 200:373–383
2. Lo Cicero A, Stahl PD, Raposo G (2015) Extracellular vesicles shuffling intercellular messages: for good or for bad. Curr Opin Cell Biol 35:69–77
3. Muralidharan-Chari V, Clancy JW, Sedgwick A, D'Souza-Schorey C (2010) Microvesicles: mediators of extracellular communication during cancer progression. J Cell Sci 123:1603–1611
4. Thery C, Zitvogel L, Amigorena S (2002) Exosomes: composition, biogenesis and function. Nat Rev Immunol 2:569–579
5. Valadi H, Ekstrom K, Bossios A, Sjostrand M, Lee JJ, Lotvall JO (2007) Exosome-mediated transfer of mRNAs and microRNAs is a novel mechanism of genetic exchange between cells. Nat Cell Biol 9:654–659
6. Montecalvo A, Larregina AT, Shufesky WJ, Stolz DB, Sullivan MLG, Karlsson JM et al (2012) Mechanism of transfer of functional microRNAs between mouse dendritic cells via exosomes. Blood 119:756–766
7. Thakur BK, Zhang H, Becker A, Matel I, Huang Y, Costa-Silva B et al (2014) Double-stranded DNA in exosomes: a novel biomarker in cancer detection. Cell Res 24:766–769

8. Montermini L, Meehan B, Garnier D, Lee WJ, Lee TH, Guha A, Al-Nedawi K, Rak J (2015) Inhibition of oncogenic epidermal growth factor receptor kinase triggers release of exosome-like extracellular vesicles and impacts their phosphoprotein and DNA content. J Biol Chem 290:24534–24546
9. Al-Nedawi K, Meehan B, Micallef J, Lhotak V, May L, Guha A, Rak J (2008) Intercellular transfer of the oncogenic receptor EGFRvIII by microvesicles derived from tumour cells. Nat Cell Biol 10:619–624
10. Al-Nedawi K, Meehan B, Rak J (2009) Microvesicles: messengers and mediators of tumor progression. Cell Cycle 8:2014–2018
11. Al-Nedawi K (2014) The yin-yang of microvesicles (exosomes) in cancer biology. Front Oncol 4:172
12. Lee TH, D'Asti E, Magnus N, Al-Nedawi K, Meehan B, Rak J (2011) Microvesicles as mediators of intercellular communication in cancer—the emerging science of cellular 'debris'. Semin Immunopathol 33:455–467
13. Costa-Silva B, Aiello NM, Ocean AJ, Singh S, Zhang H, Thakur BK et al (2015) Pancreatic cancer exosomes initiate pre-metastatic niche formation in the liver. Nat Cell Biol 17:816–826
14. Al-Nedawi K, Meehan B, Kerbel RS, Allison AC, Rak J (2009) Endothelial expression of autocrine VEGF upon the uptake of tumor-derived microvesicles containing oncogenic EGFR. Proc Natl Acad Sci U S A 106:3794–3799
15. Melo SA, Luecke LB, Kahlert C et al (2015) Glypican-1 identifies cancer exosomes and detects early pancreatic cancer. Nature 523(7559): 177-182. doi: 10.1038/nature14581
16. Soo CY, Song Y, Zheng Y et al (2012) Nanoparticle tracking analysis monitors microvesicle and exosome secretion from immune cells. Immunology 136(2):192–197. doi:10.1111/j.1365-2567.2012.03569.x
17. Webber J, Clayton A (2013) How pure are your vesicles?. J Extracell Vesicles 2:10. 3402/jev.v2i0.19861. eCollection 2013. doi:10.3402/jev.v2i0.19861
18. Shelke GV, Lasser C, Gho YS et al (2014) Importance of exosome depletion protocols to eliminate functional and RNA-containing extracellular vesicles from fetal bovine serum. J Extracell Vesicles 3:10.3402/jev.v3.24783.eCollection 2014. doi:10.3402/jev.v3.24783

Chapter 15

Visualizing the Tumor Microenvironment of Liver Metastasis by Spinning Disk Confocal Microscopy

Liane Babes and Paul Kubes

Abstract

Intravital microscopy has evolved into an invaluable technique to study the complexity of tumors by visualizing individual cells in live organisms. Here, we describe a method for employing intravital spinning disk confocal microscopy to picture high-resolution tumor–stroma interactions in real time. We depict in detail the surgical procedures to image various tumor microenvironments and different cellular components in the liver.

Key words Spinning disk confocal microscopy, Liver, Intravital imaging, Metastasis, Mouse models, Transgenic mice, Imaging, Tumor microenvironment

1 Introduction

Intravital microscopy has made a tremendous impact in the field of cancer biology [1]. It is a powerful technique to pursue in real-time the relationship of subpopulations of stromal cells and cancer cells in whole organs of living animals. High-resolution imaging techniques such as confocal and two-photon microscopy are used to perform intravital microscopy of fluorescently labeled objects [2–4]. Two-photon microscopy is extensively used to conduct intravital imaging of different tumor environments deep into tissues (300–500 μm) with high resolution [5, 6]. However, high sensitivity to tissue movement restricts detailed observation of fast moving objects.

In confocal microscopy, lasers are used to excite fluorophores with a single photon in a small area on the specimen. Fluorescence in the specimen is generated at different depths because fluorochromes are activated in different focal planes. The fluorescence emitted from

Electronic supplementary material: The online version of this chapter (doi:10.1007/978-1-4939-3801-8_15) contains supplementary material, which is available to authorized users. Videos can also be accessed at http://link.springer.com/chapter/10.1007/978-1-4939-3801-8_15

Josie Ursini-Siegel and Nicole Beauchemin (eds.), *The Tumor Microenvironment: Methods and Protocols*, Methods in Molecular Biology, vol. 1458, DOI 10.1007/978-1-4939-3801-8_15,

the specimen is focused back from the confocal plane due to the use of pinholes. The narrow aperture of the lens and pinholes exclude fluorescent light emitted outside of the confocal plane thereby increasing spatial resolution [7]. In spinning disk confocal microscopy, the instrument is equipped with a rotating disk (Nipkow disk) containing approximately 20,000 pinholes. Multiple light beams excite the specimen as the disk rotates and allows simultaneous illumination of the entire field of view leading to increased temporal resolution and reduced motion artifacts during image acquisition [8]. This permits long-term imaging with reduced photobleaching. Fluorescent light passing the pinhole is then focused through a dichroic mirror and is directed to a digital camera. The resolution depth of a spinning disk confocal microscope is smaller than 100 μm. Limitation in speed occurs when fluorochromes with weak fluorescence are used because prolonged exposure is needed.

Spinning disk confocal microscopy has been substantially used to visualize the tumor microenvironment in mouse breast cancer models in order to investigate tumor and stromal cell interactions and the effect of therapeutic agents [1, 9–11]. Our liver metastasis mouse model allows monitoring the tumor microenvironment in the liver of various cancers that have the capability to grow in the liver [12]. The model permits the use of miscellaneous fluorescent reporter mice which evades the requirement of expensive antibodies or lack of antibodies to label certain cell populations.

We present here our in vivo protocol using confocal spinning disk microscopy, to visualize dynamic cellular interactions and cellular functions with high resolution in the tumor microenvironment of the liver.

2 Materials

We use a customized inverted spinning disk confocal microscope equipped with xyz-stage (Applied Scientific Instrumentation, MS-2000 with piezo-z insert) for and EM-CCD cameras. Our image acquisition software is Velocity (PerkinElmer). For image analysis, we use Velocity (PerkinElmer) and ImageJ (National Institute of Health).

2.1 Microscope Setup

1. Turn on Multichannel Spinning Disk Confocal Microscope system: main power switch, computer, laser keys for lasers that will be used, and open acquisition software (Velocity) (Fig. 1).
2. Clean the heating stage with 70% ethanol and fix microscope cover glass (thickness 0.12–0.19 mm) with transparent tape on the imaging port of the heating stage.
3. Place a gauze compress on the stage and a cotton tip applicator (Fig. 2a).
4. Turn on the stage (set for 37 °C).

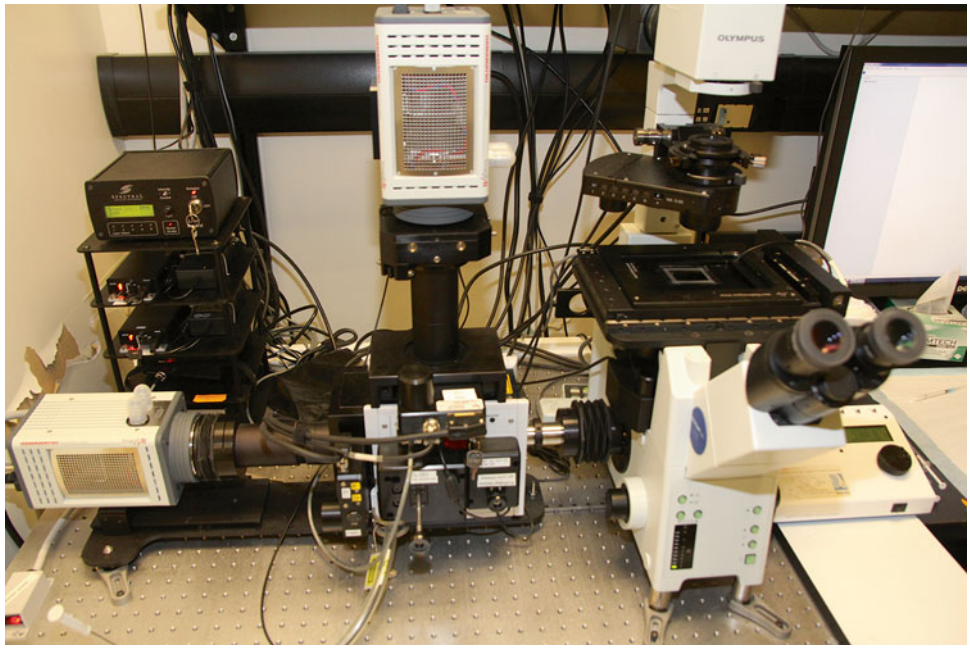

Fig. 1 Spinning disk confocal microscope for intravital microscopy. The inverted microscope is connected with the Yokogawa spinning disk scanner and two CCD cameras. The system is equipped with four lasers for multicolor imaging. The motorized stage is placed over the objective and can be moved in *xy* and *z* direction

2.2 Anesthesia and Catheter Preparation

1. Prepare anesthetic solution in 0.9% saline mixture of ketamine (final concentration: 200 µg/g mouse) and xylazine (final concentration: 10 µg/g mouse).
2. For the catheter buildup, use a 1 ml syringe, polyethylene tubing (Ø 0.28 mm, length 15 cm) and a 30G×1/2 in. needle.
3. Fill the above syringe with 100 U heparin in saline and clip the needle on the syringe.
4. Slip tubing over the needle and fill tubing with heparin containing saline. Avoid air bubbles in the catheter (Fig. 2b).

2.3 Surgical Tools and Other Instruments

1. Sterile (autoclaved) scissors and two small forceps with butt bent tip (Fig. 2c).
2. Black braided silk. Prepare three short (7–8 cm) silks (black braided, size 3-0) and one long (12 cm) silk with a loop in the middle (Fig. 2e).
3. Surgical board (Fig. 2d, clean with 70% ethanol before use).
4. Small vessel cauterizer.
5. Transparent tape (Fig. 2h),
6. Kimwipes.
7. Mineral oil.
8. 30G×1/2 in. needle (Fig. 2g).

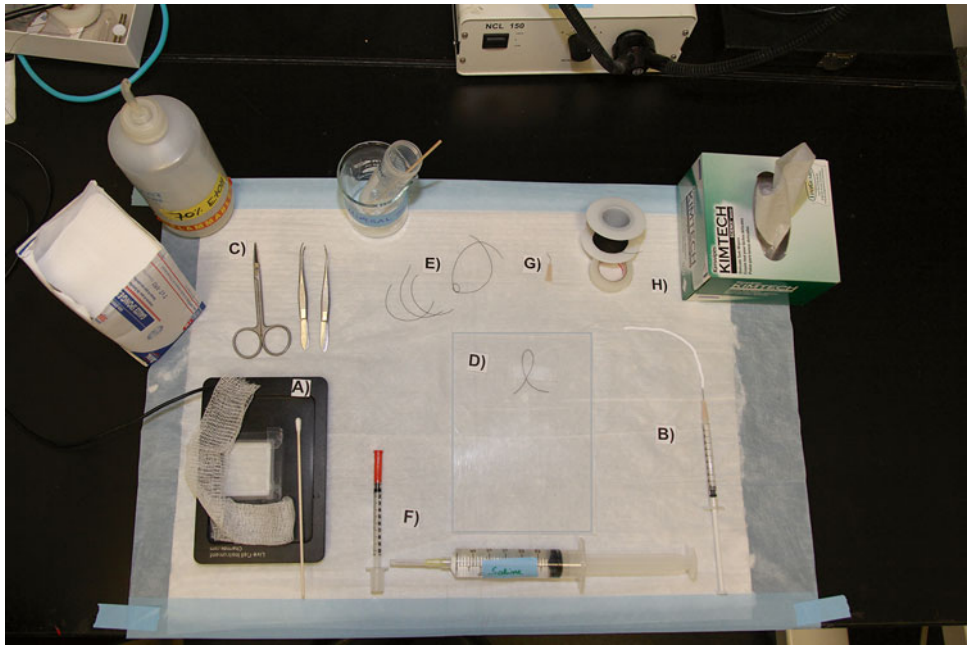

Fig. 2 Instruments for animal surgery. (**a**) Heated stage with fixed microscopy cover glass, gauze compress and cotton tip applicator. (**b**) Catheter (syringe with false colored tubing in white). (**c**) Scissors and forceps. (**d**) Surgical board with silk and transparent tape for position of animal head. (**e**) Short silks (three) and one long silk with loop. (**f**) Insulin syringe and 30 ml syringe with saline. (**g**) Needle with bent tip for cannulation. (**h**) Black silk, transparent tape, and Kimwipes. In addition, ethanol 70 % is prepared, mineral oil and gauze compresses

9. 30 mL syringe filled with sterile saline.
10. Insulin syringe (Fig. 2f).

3 Methods

We have collated procedures for visualizing metastases and their interaction with various immune cells in the microenvironment of the liver using an inverted spinning disk confocal microscope (*see* **Note 1**).

3.1 Preparation of Tumor Cells for Transplantation

Our lab uses an experimental metastasis model for transplantation of tumor cells into the liver. We label tumor cells with fluorescent membrane dyes (suitable for experiments up to 5 days; e.g., *see* legend to Movie 1) or use genetic manipulations in established cell lines to express fluorescent proteins constitutively. Another option is to isolate tumor cells from transgenic reporter mice. Before tumor cell transplantation, wash cells several times in balanced salt solution (PBS or HBSS). Dilute appropriate number of tumor cells in 100 μL volume of balanced salt solution and store cells on ice until use.

3.1.1 Anesthesia of Mice

1. Inject mice intraperitoneal (i.p.) with ketamine–xylazine mix (*see* Subheading 2.2) using an insulin syringe or a syringe with a $29Gx_{1/2}$ needle.
2. Place the mouse back into the cage and after 10 min, check reflexes (toe-pinch withdrawal reflex) by pinching (with your fingertips or forceps) the footpad of the mouse. Do not start the surgery as long as the mouse shows reflexes (*see* **Note 2**).

3.2 Catheter Placement (5 min)

1. Place mouse onto its dorsum with the head pointing towards yourself and use surgical tape to fix the front feet onto the surgical board. Next, hook the short silk into the front upper teeth. Carefully stretch the neck and fix the head in this position by taping the silk on the board (Fig. 3a).
2. Dip the cotton tip into the mineral oil and apply some oil onto the right ventral side of the neck up to the lower jaw.
3. Lift the skin on the right hand side of the mouse lower jaw and make an incision along the neck up to the clavicle. Separate the skin from the viscera and expose right sublingual lymph node and the external jugular vein by removing the surrounding fat tissue. Do not rupture the vein!
4. Now gently lift the lymph node and pull with a second forceps a short silk below the external jugular vein. Very carefully tighten the vein and fix the ends of the silk with tape on the surgical board (Fig. 3b).
5. Take two additional short silks and place them below the external jugular vein at the site before the external jugular vein anastomoses into the subclavian vein (Fig. 3b).
6. Take a $30G \times 1/2$ in. needle and bend it with your scissors so that the tip has a 45° angle (Figs. 2g and 3b).
7. Hold needle in your left hand and the tip of the catheter tubing with a forceps in your right hand.
8. Puncture the exposed external jugular vein by inserting the needle 2–3 mm into the vein and next slide the tubing along the needle into the vein. As soon as the tip of the tubing is in the lumen of the vein, gently remove the needle. Once the catheter is placed (4–6 mm) into the vein, tie the silk around the tubing and make a knot (Fig. 3c) and slowly try to aspirate blood in order to check the flow through catheter (*see* **Note 3**).
9. Take the silk tightening the vein from **step 4** and tie it as well around the catheter. Last, cut all silks used to fix the catheter short (Fig. 3d).
10. Additional anesthesia (10–50 μL max. i.v.) can now be injected via the catheter. Antibodies and fluorescent probes can be administered to label cell surface molecules and other objects for visualization (*see* **Note 4**).

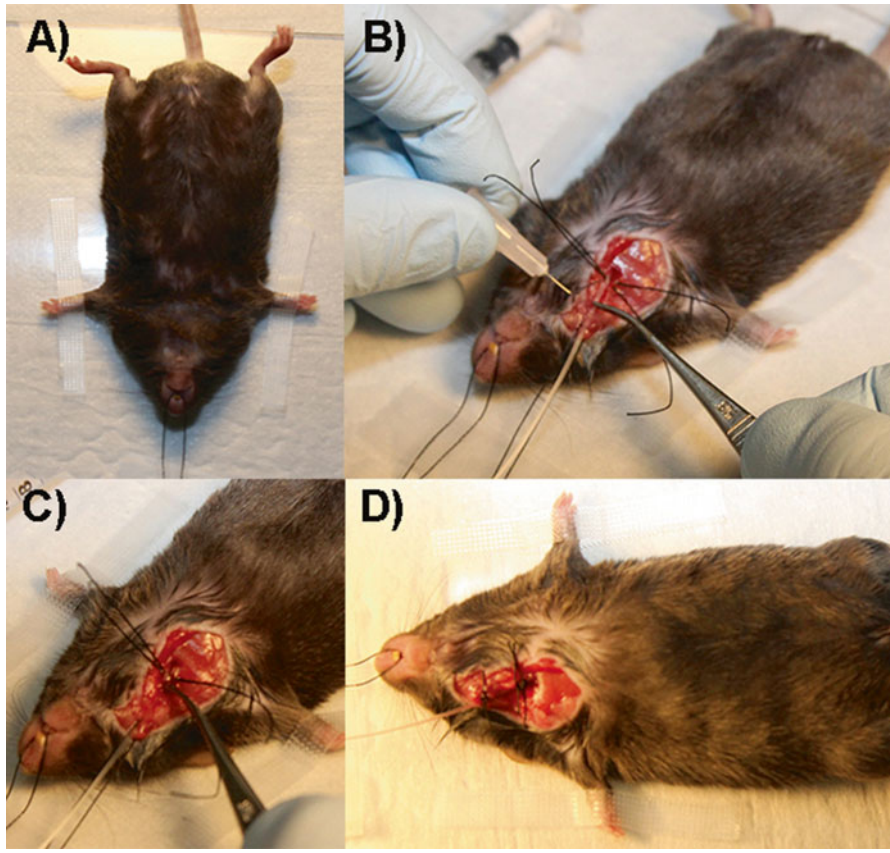

Fig. 3 Catheter placement. (**a**) The anesthetized mouse is fixed on the surgical board with transparent tape. The neck is placed into a stretched position and fixed with black silk. (**b**) Short silks are placed underneath the external jugular vein. The silk close to the right sublingual lymph node is used to hold the vein stretched so that the catheter can be easily introduced into the vein. (**c**) The two silks are tied around the tubing to retain tubing in the vessel. (**d**) The third silk is also tied around the tubing and afterwards silks were cut short

3.3 Abdominal Surgery for Intravital Imaging (10–12 min)

Continuously check vitals while performing the surgery. Always have additional anesthetic solution prepared.

1. Turn the surgical board so that the head of the mouse is facing away from you and apply mineral oil onto the abdomen.
2. Lift with your forceps the skin on the top of the bladder and make an incision along the midline of the abdomen up to the sternum with scissors.
3. Separate the skin on the left and right side from abdominal muscles using your scissors and cauterize the veins on the inside of both skin flaps. Avoid any bleeding (Fig. 4a).
4. Cauterize the blood vessels on both skin flaps.
5. Make a cut through the cauterization point to remove the skin flaps on both sides (Fig. 4b).

6. Now make an incision along the linea alba of the abdomen and expose the xiphoid cartilage.
7. Use the cauterizer to remove abdominal muscles starting from the xiphoid cartilage along the left rib cage to the lower abdomen and do the same for the right side (Fig. 4c). Use cauterizer instead of scissors to avoid any bleeding. Also always use cauterizer to stop bleeding if bleeding reoccurs.
8. Take the long silk (12 cm) and tie it around the xiphoid cartilage.
9. Lift the thorax with the silk so that you can see the transparent ligament that connects the gall bladder with the diaphragm and sever it with your scissors (Fig. 4d).
10. In this step, tumor cells will be injected into the spleen. If tumor cells had already been injected intrasplenically by using

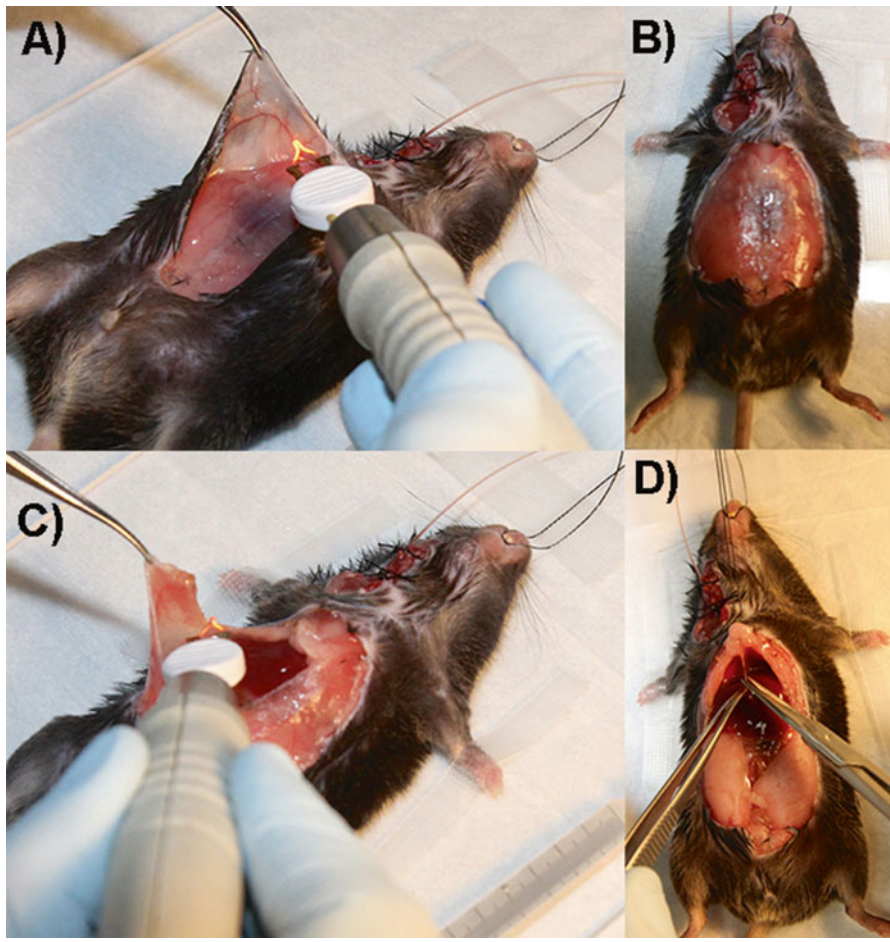

Fig. 4 Abdominal surgery. (**a**) Skin is cut along the midline and separated from the peritoneal skin. Blood vessels on the inside of the left and right skin flap are cauterized. (**b**) Left and right skin flaps are then removed. (**c**) Peritoneal skin around the abdomen is removed with a cauterizer. (**d**) The ligament between the gall bladder and the diaphragm is cut without touching the liver

isoflurane for long-term experiments (*see* **Note 5**), proceed with **step 11**. Gently lift the spleen with your forceps and inject tumor cells. Within 1 min tie the blood vessels (lineal vein and artery) and remove the spleen. Avoid bleeding.

11. Moisturize the gauze with saline on the heated stage (37 °C) and place the mouse lying on the right hand side onto the stage (Fig. 5a). Do not forget to move the catheter with the mouse.
12. Move the right front paw behind the head and moisturize the cotton tip applicator with saline.
13. Pull the ends of the silk tied around the xiphoid cartilage and stretch it parallel to the upper body.
14. Carefully use the cotton tip to move the intestine away from the stomach.
15. Next, the ventral side of the liver must be gently flipped onto the microscope cover glass. The stomach will be used to flip the liver. Use the cotton tip to guide the stomach (Fig. 5b). Never touch the liver with the cotton tip.
16. After you have flipped the liver, gently move the stomach close to the intestine and cut the small transparent ligament that connects the liver with the stomach (Fig. 5c, white arrow). This reduces movement caused by breathing. Be very careful not to touch the liver lobe.
17. Now wrap the moisturized gauze around stomach and intestine. This will avoid contact and weight on top of the liver by internal organs, which would cause increased movement and irregular blood flow in the liver.
18. Cut a small piece (double the size of the mouse liver) from the Kimwipes and slowly cover the liver with it. Moisturize Kimwipes with saline and gently pull the liver away from the abdomen so that the liver does not touch the abdomen (Fig. 5d). This will also reduce movement (*see* **Note 6**).
19. Move heated stage to the microscope and start the imaging of the liver.
20. Check vitals (toe-pinch withdrawal reflex and breathing) every 5–10 min and keep Kimwipes moist and start the imaging.
21. After imaging is finished the mouse receives an overdose of the anesthetic (100 μL) and 2 min later, cervical dislocation is performed to ensure that the mouse has been euthanized.
22. Turn off the microscope: (a) turn the laser keys off, (b) turn off main power, (c) copy imaging data and turn off computer.
23. Clean all instruments with 70% ethanol and autoclave surgical tools.

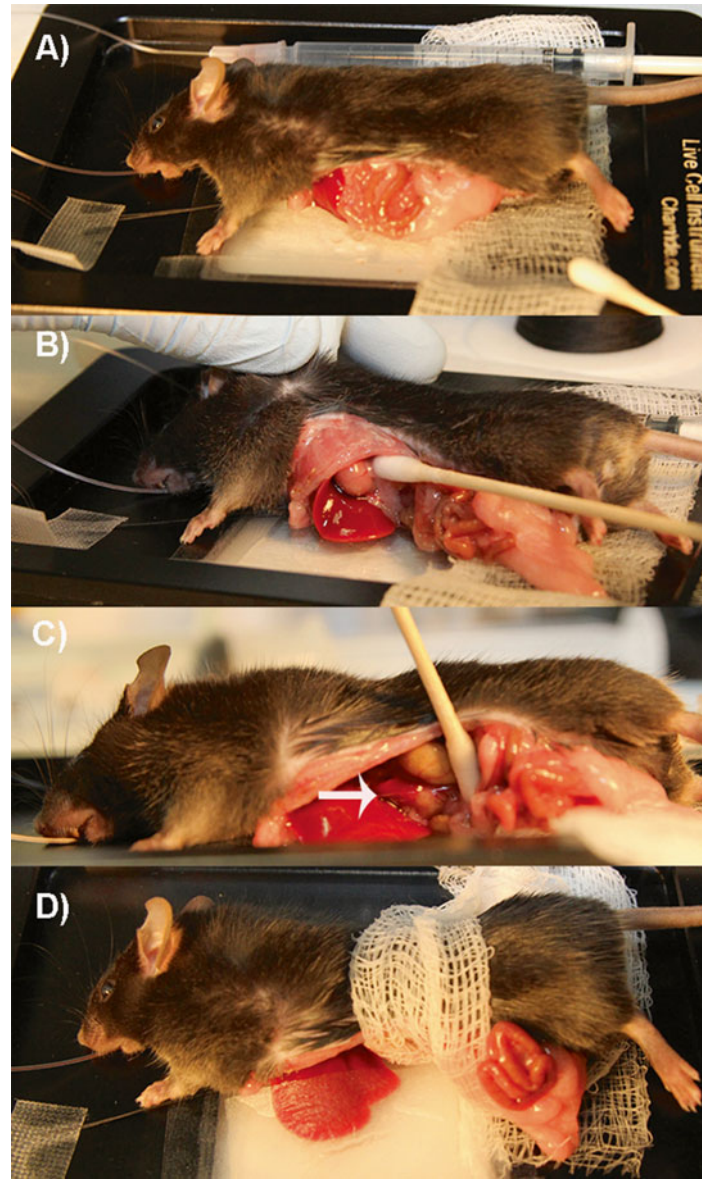

Fig. 5 Animal setup on stage. (**a**) Place the mouse on its right hand site and lean the mouse with its belly towards the cover glass so that the liver is touching the glass. (**b**) Use the cotton tip applicator to move intestine and fat tissue onto the gauze compress and move the stomach with the tip to flip the liver. (**c**) Hold the stomach with the cotton tip and cut the thin ligament (*arrow* indicates the position of the ligament) without cutting into the liver. (**d**) Wrap the gauze around the inner organs and away from the liver. Use a small piece of Kimwipes to place it on top of the liver and moisturize with saline

4 Results

Intravital imaging of the liver using spinning disk confocal microscopy permits visualizing the tumor microenvironment of the liver. Our multichannel system allows capture of up to four different fluorophores. This is beneficial for imaging multiple cell populations in the tumor microenvironment. Due to very rapid image acquisition through spinning-disk technology, we can track cell dynamics of fast moving cells in the vasculature at high spatial and lateral resolution. This reveals detailed information about cell dynamics, different cell–cell interactions, and alterations in blood flow and morphological changes in the tumor microenvironment. Image acquisition is not limited to one field of view. We can acquire images along the *x*-/*y*-axes and align them together to obtain an overview image of the organ, what we call a "stitched image." Figure 6 is a representative picture of a stitched image of the liver recorded 10 days after intrasplenic colon adenocarcinoma cell transplantation.

The resolution obtained by spinning disk confocal microscopy in vivo is dependent on the depth of imaging. High-resolution images can be obtained up to 20 μm (Movie 1). Image acquisition deeper into the tissue beyond 20 μm minimizes resolution due to light aberrations induced by tissue absorption and scattering which leads to weak detectable signal.

One of the advantages of using spinning-disk confocal for intravital imaging is the ability to capture high resolution images very fast, which reduces breathing artifacts and photobleaching of fluorescently labeled objects over long-term periods (Movies 2, 3, and 4).

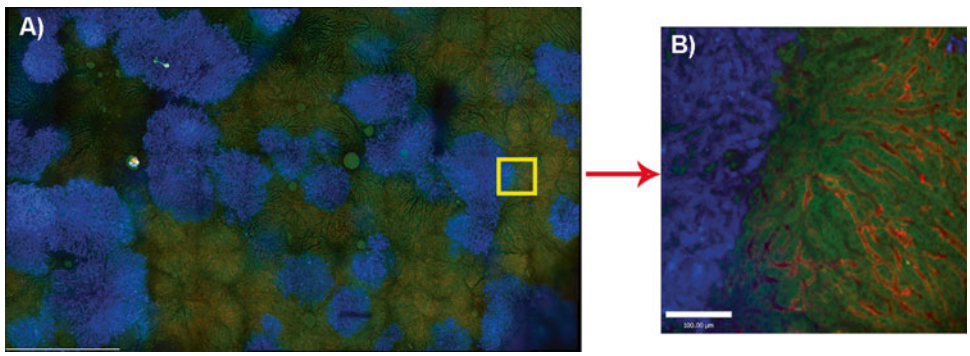

Fig. 6 Tumor microenvironment in the liver of live mice. Murine colon carcinoma cells expressing iRFP (*blue*) were injected intrasplenically and visualized 10 days later in the liver. Liver vasculature is pictured with an antibody against CD31 (*red*) and autofluorescent liver tissue appears in *dark green*. (**a**) Single images (10× lens) were recorded with an electronic computer-controlled stage and subsequently joined together (10% overlap). *Yellow rectangle* depicts a single image. Scale bar represents 1 mm. (**b**) Enlarged single image. Scale bar represents 100 μm. The images have been modified to improve contrast and brightness

Movie 2 shows high magnification (20× lens) cell dynamics of Kupffer cells (which were visualized with fluorescently labeled antibody) and NKT cells (reporter mice) during basal conditions in liver sinusoids.

In the environment of colon carcinoma metastases, NKT cells retain their dynamic behavior and interact vigorously with tumor cells (Movie 3).

After melanoma cell transplantation into LysM-eGFP transgenic mice, neutrophils and tumor cells were observed over 3.5 h in the liver (Movie 4). Tumor cell death was detected with propidium iodide. No photobleaching was detected within this time span.

5 Notes

1. The procedures for the conducted experiments were approved by the Animal Care Committee of the University of Calgary and were in compliance with the Canadian Council for Animal Care.
2. If the mouse still has the toe-pinch withdrawal reflex 30 min after the initial injection of anesthetic, inject additional 50 μL i.p., and wait for 5–10 min. If necessary repeat injection and wait for 5–10 min. Note that overdosing of anesthetic can cause death of the animal.
3. While testing the flow through the catheter, be careful not to inject air bubbles and test if the injection of saline operates smoothly. This ensures that the catheter is placed in the vessel lumen and the vessel wall was not punctured. It can happen that quick aspiration makes the tubing become stuck to the vessel wall, therefore draw slowly.
4. Additional dosage of anesthesia intravenously should not exceed 50 μL due to high sensitivity which would lead to animal death. Right antibody dosage used to label cells and fluorophores have to be tested separately. Liver tissue can have very high autofluorescence depending on the genetic background of the mouse used. Injection (i.v.) of 2.5 mM propidium iodide can be used to visualize cell death in vivo. Injections of 10 μL/25 g mouse should be repeated every 2 h.
5. For long-term observation of tumors in the liver intrasplenic, transplantation of tumor cells can be performed using isoflurane. The procedure involves laparotomy of the upper left abdomen and exteriorization of the spleen. Tumor cells are then injected into the spleen. Splenectomy is carried out after blood vessels, which connect to the spleen, are tied off. The incision is then sutured. Mice are treated with buprenorphine to reduce pain and can be imaged at any desired time point after tumor transplantation.

6. Avoid air bubbles when placing Kimwipes on top of the liver. Keep it moist during the entire imaging period. Also continuously moisturize gauze compress that holds organs.

Acknowledgements

This work was supported by the Alberta Innovates Health Solutions graduate studentship (201400345). We would like to acknowledge Caitlyn MacDonald for her assistance in acquiring images during surgical procedures.

Video Captions

Movie 1: 3D reconstitution of liver metastasis. Melanoma cells (B16F10) were labeled in vitro with lipophilic membrane dye DiI (*red*) and intrasplenically transplanted into genetically engineered LysM-eGFP mice. Neutrophils (rounded cell morphology) are depicted in *bright green* and reside inside the vasculature (AF647-albumin, *blue*). Kupffer cells are located in the vasculature and labeled with anti-F4/80 (*white*). Hepatic stellate cells (*bright green*) can be distinguished from neutrophils by their elongated cell shape situated outside of hepatic vasculature. Autofluorescent hepatocytes are represented in dark green. 5 days after melanoma cell injection confocal *z* planes (20× lens) were recorded every 1 μm and reconstructed into a movie. Scale bar: 200 μm. Images were corrected for contrast and brightness (AVI 533219 kb)

Movie 2: Visualizing immune cells in liver vasculature by spinning disk confocal microscopy. NKT cells (*bright green*) in the liver are visualized in CXCR6-GFP transgenic mice. Kupffer cells (*red*) are labeled with anti-F4/80. Autofluorescent hepatocytes are shown in *dark green*. Representative picture (20× lens) of a 30 min long image sequence with 10 s between frames. Scale bar: 68 μm. Images were corrected for contrast and brightness (AVI 41511 kb)

Movie 3: Visualizing NKT cell dynamics in the liver tumor microenvironment. CXCR6-GFP transgenic mice were injected with colon adenocarcinoma cells (C26 cells labeled with DID membrane dye). 3 days later, metastases (*blue*) and NKT cells (*bright green*) are pictured in the liver. Autofluorescent hepatocytes are shown in *dark green*. The 1 h image sequence was recorded with 15 s between frames. Scale bar: 140 μm. Images were corrected for contrast and brightness (AVI 68991 kb)

Movie 4: Long-term imaging of liver tumors. Neutrophils are visualized in LysM-eGFP transgenic mice. Image acquisition was performed right after tumor cells (B16F10 labeled with DID membrane dye (*blue*)) were intrasplenically injected. Dying tumor cells were

detected with propidium iodide (*red*). Autofluorescent hepatocytes are shown in *dark green*. The movie over 3.5 h was recorded with 30 s between frames. Scale bar: 140 μm (MP4 26154 kb)

References

1. Ellenbroek SI, van Rheenen J (2014) Imaging hallmarks of cancer in living mice. Nat Rev Cancer 14:406–418
2. Zomer A, Beerling E, Vlug EJ, van Rheenen J (2011) Real-time intravital imaging of cancer models. Clin Transl Oncol 13:848–854
3. Lohela M, Werb Z (2010) Intravital imaging of stromal cell dynamics in tumors. Curr Opin Genet Dev 20:72–78
4. Masedunskas A, Milberg O, Porat-Shliom N, Sramkova M, Wigand T, Amornphimoltham P, Weigert R (2012) Intravital microscopy: a practical guide on imaging intracellular structures in live animals. Bioarchitecture 2:143–157
5. Dunn KW, Young PA (2006) Principles of multiphoton microscopy. Nephron Exp Nephrol 103:e33–e40
6. Helmchen F, Denk W (2005) Deep tissue two-photon microscopy. Nat Methods 2:932–940
7. Smith, C.L. (2008) Basic confocal microscopy. In: Ausubel FM et al (eds) Current protocol in molecular biology. Chapter 14:Unit 14.11
8. Tanaami T, Otsuki S, Tomosada N, Kosugi Y, Shimizu M, Ishida H (2002) High-speed 1-frame/ms scanning confocal microscope with a microlens and Nipkow disks. Appl Optics 41:4704–4708
9. Ewald AJ, Werb Z, Egeblad M (2011) Dynamic, long-term in vivo imaging of tumor-stroma interactions in mouse models of breast cancer using spinning-disk confocal microscopy. Cold Spring Harbor Protocols 2011(2):pdb top97. doi:10.1101/pdb.top97
10. Nakasone ES, Askautrud HA, Kees T, Park JH, Plaks V, Ewald AJ et al (2012) Imaging tumor-stroma interactions during chemotherapy reveals contributions of the microenvironment to resistance. Cancer Cell 21:488–503
11. Nakasone ES, Askautrud HA, Egeblad M (2013) Live imaging of drug responses in the tumor microenvironment in mouse models of breast cancer. J Vis Exp 73:e50088
12. Gul N, Babes L, Siegmund K, Korthouwer R, Bogels M, Braster R et al (2014) Macrophages eliminate circulating tumor cells after monoclonal antibody therapy. J Clin Invest 124:812–823

Chapter 16

Intravital Microscopy for Imaging the Tumor Microenvironment in Live Mice

Victor Naumenko, Craig Jenne*, and Douglas J. Mahoney*

Abstract

The development of intravital microscopy has provided unprecedented capacity to study the tumor microenvironment in live mice. The dynamic behavior of cancer, stromal, vascular, and immune cells can be monitored in real time, in situ, in both primary tumors and metastatic lesions, allowing treatment responses to be observed at single cell resolution and therapies tracked in vivo. These features provide a unique opportunity to elucidate the cellular mechanisms underlying the biology and treatment of cancer. We describe here a method for imaging the microenvironment of subcutaneous tumors grown in mice using intravital microscopy.

Key words Tumor microenvironment, Intravital microscopy, Multiphoton imaging, Confocal imaging, Mouse models, Subcutaneous tumors

1 Introduction

The tumor microenvironment (TME) is a complex structure comprising both malignant and non-malignant cells, often supported by a dense matrix of extracellular protein and a disorganized network of blood vessels [1–3]. Indeed, cancer biology is increasingly being viewed through the lens of the TME as a tissue. Within the TME, various behaviors of noncancer cells such as inflammatory and immune cells and their interactions with malignant cells are now recognized as "hallmarks of cancer" [4]. Increasingly, new treatments are being developed to target noncancer cells within the TME, such as the antiangiogenesis and immunotherapy classes of medicines [5–8]. Developing these

Douglas J. Mahoney and Craig Jenne contributed equally to this chapter.

Electronic supplementary material: The online version of this chapter (doi:10.1007/978-1-4939-3801-8_16) contains supplementary material, which is available to authorized users. Videos can also be accessed at http://link.springer.com/chapter/10.1007/978-1-4939-3801-8_16

Josie Ursini-Siegel and Nicole Beauchemin (eds.), *The Tumor Microenvironment: Methods and Protocols*, Methods in Molecular Biology, vol. 1458, DOI 10.1007/978-1-4939-3801-8_16,

therapies effectively, however, is predicated upon a deep appreciation of how cancer and noncancer cells function and interact within the TME. Unfortunately, until recently, our ability to study cellular behavior within the TME was limited to snapshots in time provided by biochemical or histological analyses.

Microscopic imaging of the TME in vivo using intravital microscopy (IVM) represents a powerful new technique for overcoming this limitation [9–11]. IVM enables the visualization of fluorescently labeled cells within the TME over space and time. With IVM, individual cancer and noncancer cells can be tracked, their interactions with one another analyzed, and their behavior studied—all in live mice [12, 13]. IVM can reveal cellular responses within the TME relevant to most, if not all hallmarks of cancer, from deregulated cell growth to metastasis to angiogenesis to the recruitment of inflammatory cells [14]. Treatment responses can be monitored at the cellular level, and indeed many therapies themselves can be labeled and tracked at high resolution [15]. Moreover, as Turnkey systems are now available from a variety of commercial venders, IVM is an accessible technique for most modern cancer biology laboratories [16].

The general principle behind IVM is that cells labeled with fluorescent reporters, typically conjugated to an antibody injected into the mouse or genetically expressed in a reporter mouse strain, can be visualized in situ by exciting fluorophores within the tumor and collecting and separating the specific fluorescence signal from the out-of-focus light. Accomplishing this with sufficient spatial and temporal resolution to observe individual moving cells, without damaging the tissue, is typically achieved using a scanning or spinning-disk confocal fluorescence microscope or a multiphoton fluorescence microscope, equipped with a variety of detectors and filters. In general, confocal platforms are cheaper, easier to use, and more amenable to multiplexing (visualizing multiple markers in the same animal), but limited by an imaging depth of approximately 70–100 μm in most tumors. Thus, although the tumor surface, its vasculature and the leukocytes within are easily imaged using a confocal platform, limitations in imaging depth prevent clear visualization of the TME much beyond the surface. In contrast, multiphoton microscopes provide an imaging depth of 300–500 μm in most tumors, which enables deeper and more complete imaging of the TME. The downside of this platform, however, is its expense and operational complexity.

Below we provide a detailed method for performing IVM of the microenvironment in transplantable tumors established subcutaneously in mice. While we have developed our protocol in the CT26 model system, we have validated it in B16, 4T1, and EMT6 tumors and feel confident that it can be applied to most other subcutaneous models. Moreover, while we do not provide a method for imaging orthotopic, visceral tumors by IVM, others have imaged cancers growing in the liver, brain, and lung, amongst

other places, demonstrating that IVM can be used to image primary and metastatic lesions in most organs.

2 Materials

2.1 Tumor Cell Implantation

1. Tumor-derived cell line.
2. Phosphate buffered saline (NaCl 9 g/L, KH_2PO_4 144 mg/L, Na_2HPO_4 795 mg/L).
3. Insulin syringe (0.3 cc 31G).
4. Gauze.
5. Single-edged razor.

2.2 Intravital Imaging System Set-Up

1. Inverted confocal fluorescence microscope, preferentially resonant scanning with spectral detection and multiphoton laser (*see* **Note 1**).
2. Computer with appropriate microscope drivers and image capture software (*see* **Note 2**).
3. Heated microscope stage.
4. Glass coverslip (thickness 0.12–0.19 mm).
5. Blenderm® tape.

2.3 Anesthesia and Tail Vein Catheter Insertion

1. Ketamine.
2. Xylazine.
3. 0.9% saline.
4. 100 U heparin solution in 0.9% saline.
5. 1 mL slip tip syringe.
6. Polyethylene tubing (Ø 0.28 mm, 15–20 cm length).
7. 30G × 1/2 in. needles (×2).
8. Hemostat.
9. Heat lamp.
10. 70% ethanol.
11. Gauze.
12. Transpore® tape.

2.4 Surgical Tools and Other Instruments

1. Sterile (autoclaved) scissors.
2. Small sterile (autoclaved) forceps with blunt, bent tip (×2).
3. Surgical board (20 cm × 20 cm plastic board).
4. Needle holder.
5. Sutures (PERMA-HAND silk 5-0, c-31 reverse cutting).
6. Small vessel cauterizer.

7. Fiber-optic positionable surgical lamp.
8. 30G × 1/2 in. needles.
9. Transpore® tape.
10. 35 mm petri dish.
11. Glass slides (25 × 75 mm).
12. Mineral oil.
13. Cotton swabs.
14. 30 mL syringe filled with sterile 0.9% saline.
15. 70% ethanol.
16. Kimwipes® tissues, gauze.

2.5 Injection of Labeling Antibodies

1. 1 mL slip-tip syringe.
2. Pipette, filter tips (2–20 μL).
3. 1.5 mL microfuge tube.
4. Desired fluorescently conjugated antibodies.

3 Methods

3.1 Establishing the Tumor

1. Shave the hair around the injection site (*see* **Note 3** and Fig. 1a, b) using a single-edge razor.
2. Wash and resuspend the tumor cells in cold PBS at the desired concentration (*see* **Note 4**). Keep the cells on ice until the injection.
3. Slowly draw up 50 μL of cell suspension into an insulin syringe.
4. Inject the cell suspension into the animal's flank at the desired location (*see* **Note 3** and Fig. 1a, b). Pinch the skin between your index finger and thumb, and gently pull it away from the mouse's body. Inject the cell suspension slowly and evenly into the pouch created by your fingers. This should lead to a single bubble of cells beneath the skin.
5. Begin measuring the tumor's size 4 days after injection, using skin calipers. Tumors are ready for IVM when they reach 4 × 4 mm–6 × 6 mm which, depending on the tumor cell line used and the number of cells injected, is usually between 5 and 10 days post-implantation (*see* **Note 5**).

3.2 Setting Up the Imaging System

1. Turn on the Compact Supply Unit, Metal-Halide Power Supply, confocal imaging components and computer. Open the software (*see* **Note 6**).
2. Fix a microscope cover glass (thickness 0.12–0.19 mm) using surgical Blenderm® tape so that it overlays the imaging port located within the heating stage.

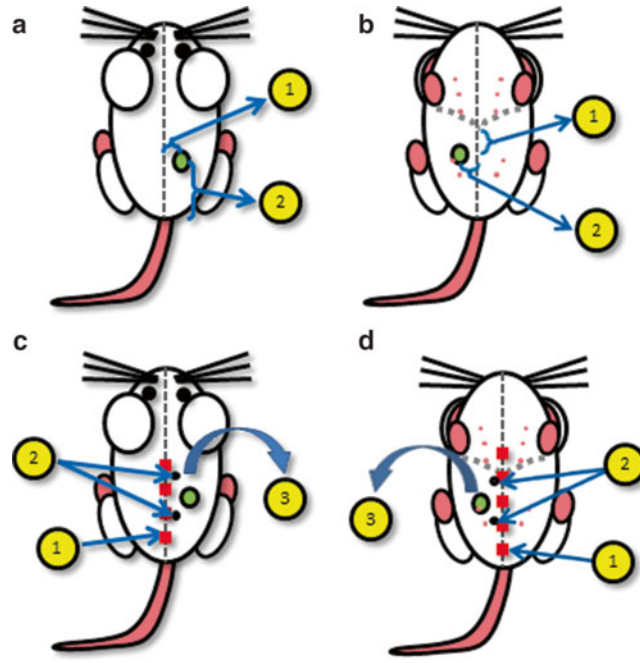

Fig. 1 Schematics for the location of tumor implantation and surgery. (**a**) Schematic for tumor cell injection into the dorsal flank at a location (**1**) 5–10 mm lateral to midline and (**2**) 20–30 mm cranial to base of tail. (**b**) Schematic for tumor cell injection into the fourth mammary fat pad at a location (**1**) 10–20 mm caudal to xyphoid process of sternum and (**2**) 5–10 mm lateral to midline. (**c**) Surgical schematic for dorsal tumors: (**1**) midline incision from 5 mm above base of tail to near apex of shoulder, (**2**) location of two suture attachment points along midline incision used to stabilize the tissue, (**3**) separation skin flap from underlying tissue and reflection. (**d**) Surgical schematic for ventral tumors: (**1**) midline incision from 5 mm above pubic symphysis to 10 mm above xyphoid process of sternum, (**2**) location of two suture attachment points along midline incision used to stabilize the tissue, (**3**) separation skin flap from underlying tissue and reflection

3. Turn on the heated stage power supply. Set the temperature to 37 °C.

3.3 Anesthetizing the Mouse and Inserting Tail Vein Catheter (See Note 7)

1. Prepare the anesthetic solution in saline (0.9%): a mixture of ketamine (final concentration 200 μg/g mouse) and xylazine (final concentration 10 μg/g mouse).
2. Inject the anesthetic mix into the intraperitoneal (i.p.) cavity using an insulin syringe.
3. After 10 min, verify the depth of anesthesia by checking the animal's reflexes (toe-pinch withdrawal reflex—pinching with your fingertips or forceps the footpad of the mouse). The catheter insertion and surgery should not be started until the

animal is deeply anesthetised and no longer demonstrates the toe-pinch withdrawal reflex.

4. To assemble the venous catheter, a 1 mL syringe, polyethylene tubing (Ø 0.28 mm, length 15 cm) and two 30G×1/2 in. needles are required. Using a hemostat, bend one of the needles back and forth until it cleanly breaks off from the hub. Insert the blunt end of the needle into one end of the catheter tubing. The needle insertion is aided by holding it with a hemostat or forceps. Fill a 1 mL slip-tip syringe with 100 U heparin in 0.9% saline and attach the second 30G needle. Slip the tubing over the second needle and dispense the contents of the syringe to fill the tubing with heparin containing saline and remove air bubbles.
5. Position the anesthetised mouse on its side so the tail vein (located laterally on the tail) is positioned facing up. Clean the tail with 70% alcohol.
6. Warm the tail using a heating lamp or warm water, to dilate the vein.
7. Using your dominant hand to hold the catheter, grasp the tail between the thumb and index finger of your other hand, thumb on top, then pull back slightly so the tail is taut. Using forceps, hold the catheter needle bevel up and pierce the skin at a flat angle. Advance the needle ahead several mm into the vein.
8. To verify the catheter was properly inserted and the vein was not perforated, draw back on the syringe to check for a "flash" of blood entering the catheter. If blood is observed, dispense a small amount of saline into the tail vein. The plunger will move easily and the dark colored vein will become clear if the catheter was positioned correctly.
9. Secure the catheter in place with Transpore® tape.

3.4 Preparing the Tumor for Imaging

1. Place the mouse onto the surgical board. Turn the surgical board so that the head of the mouse is facing away from you. Use surgical tape to fix the front and back feet (*see* **Note 8**). Check the mouse's vital signs. Administer anesthetic as needed to ensure the maintenance of an appropriate level of sedation.
2. Disinfect the surgical area by cleaning with gauze soaked in 70% alcohol. Dip a cotton tip swap into mineral oil and apply oil onto the surgical area to coat the animal's fur. This will help prevent hair from contaminating the surgical incision.
3. Make an initial incision through the skin:
   (a) For dorsal surgery, follow the animal's spine, starting about 0.5 cm from the base of the tail to the top curve of the spine (Fig. 1c).

(b) For ventral surgery, follow along the linea alba from 0.5 cm above pubic symphysis to 1 cm above xyphoid process (Fig. 1d).

4. Using forceps and scissors carefully separate the skin and tumor from the underlying tissues. Ensure this "skin flap" remains attached, laterally, to maintain blood supply (*see* **Note 9**).
5. Fix the tissue stabilization pedestal (35 mm petri dish or customer-built Plexiglas platform) with Transpore® tape alongside of the mouse at the position of the tumor.
6. Extend the skin flap with the tumor over the tissue stabilization pedestal and secure it along the edge using 5.0 sutures with a needle holder and tape (Fig. 2).
7. Carefully remove the connective tissue overlaying the tumor without disrupting or damaging the vasculature. To do this, gently loosen the tension placed on the sutures stretching and securing the skin, lift the connective tissue immediately adjacent to the

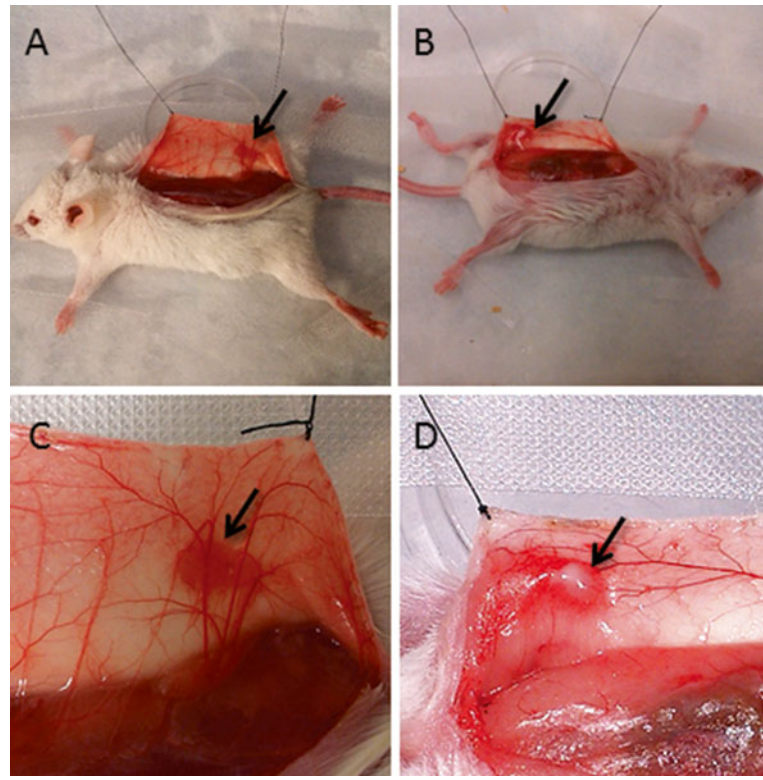

Fig. 2 Tumor preparation for imaging. *Arrow* indicates dorsal tumor implants (**a**, **c**), and ventral tumor implants (**b**, **d**). Reflected skin flaps are stretched over a pedestal (an overturned 35 mm petri dish) and secured using the attached sutures. This positioning of the skin flap allows for surgical removal of connective tissue overlaying the tumor. Once the tumor area has been prepared, the sutures are released (not removed) and the animal is transferred to the microscope stage

tumor with forceps, and carefully dissect out the membrane-like connective tissue with scissors. Ensure that no vessels are damaged or cut during this process. (*see* **Notes 10** and **11**).

8. Check tumor vasculature for bleeding and cauterize vessels as needed. Rinse the tumor with 0.9% saline and remove excess saline with Kimwipes® tissues.
9. Remove the tape securing the animal to the surgical board and transfer the mouse to the microscope stage.
   (a) For dorsal tumors, place the mouse on its back with the skin flap reflected out sideways so that the subcutaneous surface of the tumor is in contact with the microscope stage (Fig. 3a, c).
   (b) For ventral tumors, place the mouse on its abdomen with the skin flap reflected out sideways so that the subcutane-

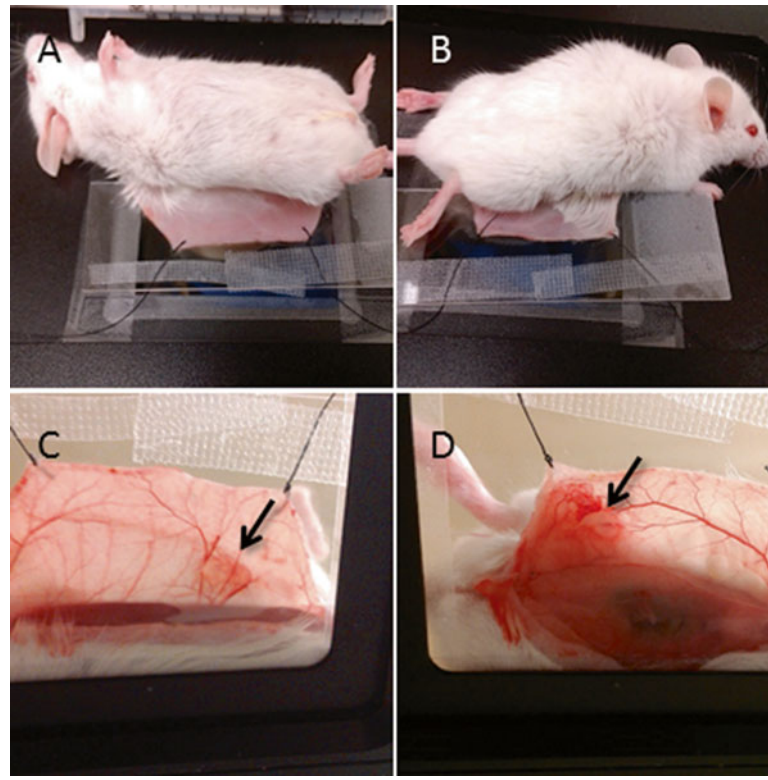

Fig. 3 Tumor positioning on the microscope stage for imaging. Dorsal (**a**) and ventral (**b**) tumor preparation, top view. Dorsal (**c**) and ventral (**d**) tumor preparation, viewed from underneath the microscope stage to illustrate the positioning of the skin flap, *arrow* indicates tumor. Once the animal is placed on the stage, the skin flap is extended and secured/stabilized using the attached sutures. A glass microscope slide is placed over the outside of skin flap to slightly flatten the tissue and to further stabilize the preparation

ous surface of the tumor is in contact with the microscope stage (Fig. 3b, d).

10. Take a glass microscope slide and position it over the skin flap so that it overlays the outside of the skin and is in direct contact with the fur. This should slightly flatten the tumor surface against the microscope stage. The slide itself should not contact the hind limbs (*see* **Note 12** and Fig. 3). Make sure the tumor feeding vessels are adequately perfused and not restricted by the pressure of the microscope slide. This is accomplished by looking at blood flow through the microscope, which is approximated by visualizing the shadows of red blood cells and leukocyte.

3.5 Injecting Antibodies and Imaging

1. Prepare a mixture of antibodies in a 1.5 mL microfuge tube using pipette and filter tips (*see* **Notes 13–17**).
2. Draw back the plunger of a slip-tip 1 mL insulin syringe to get a 200 μL air space and then load antibody mix into the tip syringe using a pipette. The antibody mix will remain as a single volume of liquid held by surface tension within the tip of the syringe.
3. Connect the syringe containing you antibodies to the tail vein catheter. Slowly push the plunger until the antibodies are injected into the catheter, stopping once the preloaded air space located behind the antibody mixture reaches the needle supporting the catheter. Remove the syringe used for administering the antibodies and replace it with a syringe containing heparinized 0.9% saline. Avoid the introduction of air bubbles. Dispense 100 μL of saline to flush the antibody mix out of the catheter tubing to ensure the animal receives the full administration of labeling antibodies.
4. Make sure the surgical preparation is stable. If necessary, tighten the stabilization sutures or reposition the glass slide flattening the tissue. Ensure the animal is continually anesthetised. Additional anesthesia can be injected via the catheter.
5. Image the TME using the appropriate microscope settings (*see* **Notes 2** and **14**; Figs. 3 and 4; Supplemental Videos 1, 2, and 3).
6. Optimal imaging strategies and microscope configuration is dependent on the specific questions being addressed with IVM and the desired data to be obtained.
   (a) Some tumors have a high degree of background autofluorescence. In these tumors, it may be essential to select labeling fluorophores and reporter dyes that are spectrally distinct and separate from the wavelength(s) associated with the observed autofluorescence. As this phenomenon is tissue-specific, empirical determination of autofluorescence spectrums must be completed for each new tumor imaged.

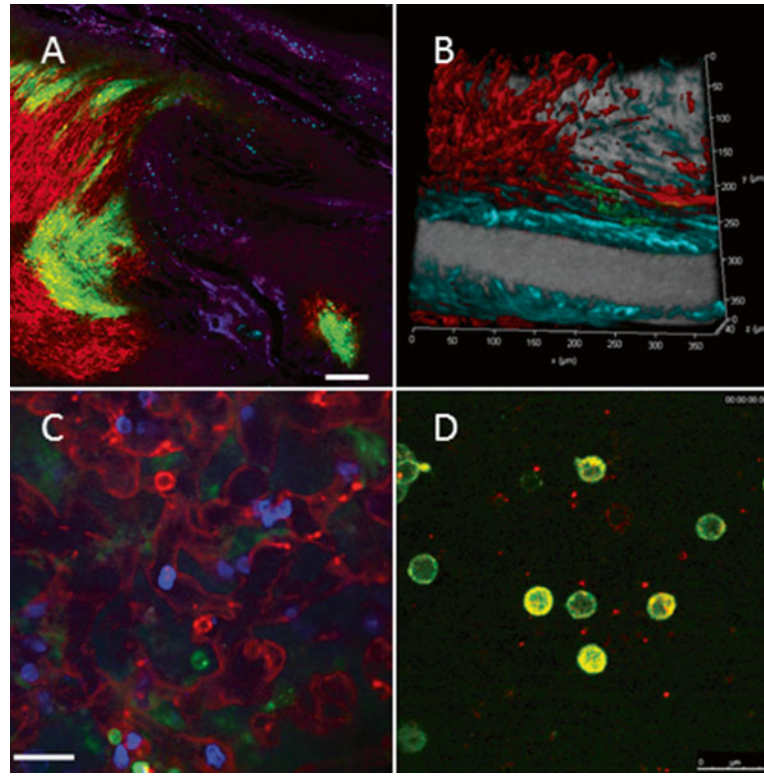

Fig. 4 Representative imaging of tumor microenvironment. (**a**) Low magnification image of vesicular stomatitis virus (VSV) infection (*green*) of tumor (*red*), Ly6G+ (*cyan*), F4/80+ (*blue*) cells, and the tumor vasculature (*magenta*), scale bar 200 μm. Image is a composite of 25 higher magnification images tiled and stitched. (**b**) 3D-reconstruction of tumor microenvironment: tumor cells (*red*), vessels (*gray*), VSV infection (*green*), collagen/second harmonic (*cyan*). Image is composed of a z-stack of ten optical sections (8 μm per section) (also suppl. Video 1). (**c**) IVM of lymphocyte populations within the tumor vasculature: CD4 (*green*), CD8 (*blue*) and NK cells (*red*), scale bar 30 μm (also suppl. Video 2). (**d**) IVM of CD11b (*red*) and Ly6G (*green*) stained cells within tumor vasculature, scale bar 25 μm, (also suppl. Video 3)

(b) Imaging fast moving cells/processes (such as cells within a tumor vessel) requires rapid image acquisition (high frame rate). To achieve this, platforms such as resonant scanners or spinning-disk are required. Rapid image acquisition requires extensive exposure of fluorophores to excitation lasers resulting in the potential for photo-bleaching. As such, care must be taken to select stable fluorophores (*see* **Note 16**).

(c) Extended, time-lapsed imaging can be used to document slower processes (cell migration within the TME, cellular recruitment to a tissue following treatment). Imaging processes that occur over hours allows for much slower image acquisition rates (one frame every few minutes). This approach

allows for smaller data files and protects photo-sensitive dyes, allowing for longer optimal imaging windows.

(d) Visualizing deep within the TME is optimally achieved with an MP imaging platform. Several factors must be considered and controlled. Increasing laser power is required as imaging progresses deeper through a tissue. Increased laser power has the potential to cause thermal damage to the tissue resulting in cellular death and sterile inflammation. Optimal deep imaging is achieved with fluorophores that excite/emit towards the near-IR range of the spectrum as these wavelengths are less susceptible to absorption/scattering by the tissue.

(e) Capturing multiple focal planes (z-stacks) and reassembling them into a single image allows for the generation of 3D reconstructions of the TME. To ensure optimal 3D model generation, rapid image acquisition is required so that the cells within the TME do not move during capture of the focal planes. Additionally, the use of MP imaging generally results in higher resolution 3D models as this imaging modality captures thinner optical sections at each focal plane with less out-of-focus light originating from above or below the imaging plane.

4 Notes

1. For the described experiments, we used a Leica SP8 inverted microscope (Leica Microsystems, Concord, Ontario, Canada), equipped with 405-, 488-, 552-, and 638-nm excitation lasers, 8 kHz tandem scan head, and spectral detectors (conventional PMT and hybrid HyD detectors) for superficial imaging (up to 100 μm). This platform is also equipped with a tuneable multiphoton (MP) laser (700–1040 nm) (Newport Corporation, Irvine, CA) and external PMT and HyD detectors (Leica) for imaging deeper into the tumors (up to 500 μm). Spectral detection combined with resonant scanning confocal allows for multicolor imaging of moving cells (both in simultaneous and sequential mode). This permits the study of interactions between tumor cells and different populations of host immune and non-immune cells within the TME.
2. For the described experiments we used Leica Application System X Version 1.8.1.0.13370. The dye separation software is useful for 5–6 color imaging.
3. For most subcutaneous tumor model systems, inject the cells directly under the skin of the right or left hind flank, 10–15 mm lateral to the midline, 20–30 mm superior to the base of the animal's tail (Fig. 1a). For orthotopic models of breast cancer, inject the cells into the right or left mammary fat pad, 5–10 mm

lateral to the midline, 20–30 mm caudal to xyphoid process (Fig. 1b). This specific location is crucial for optimal surgical access and intravital imaging.

4. Tumor cell concentration depends on the aggressiveness of the cell line and the rate of tumor growth. To get palpable tumors within 5 days, we use 2×10^6 cells/mL for 4T1 and EMT6 and 2×10^7 cells/mL for B16 and CT26 cell lines.
5. Many tumors are not sufficiently vascularized for high-quality IVM before 4–5 days post-implantation. After 10 days post-implantation, the thick capsule established by many tumors impedes clear visualization of the TME.
6. For MP imaging, specific equipment start-up procedures must be followed to ensure optimal performance. The Electro-Optical Modulator must be switched on first as it requires at least 15 min to "warm up" before achieving full modulation depth. The super-HyD detector's power and cooling unit should be turned on before the Compact Supply Unit to protect the circuitry.
7. A jugular vein catheter can be substituted for tail vein cannulation.
8. Place the mouse onto its dorsum for imaging tumors growing in mammary fat pad or onto its abdomen for imaging tumors growing on the back.
9. A stable surgical preparation depends upon a clean separation of tumor from the muscles and other underlying tissues. For best results:
   (a) The tumors should be smaller than ~6 × 6 mm, as larger tumors are more likely to grow into deeper tissues, which makes the tumor preparation more difficult;
   (b) The tumor cells should be injected at the specific anatomical sites outlined in Fig 1a, b, to allow for ease of surgical access.
10. Dissecting away the connective tissue from the tumor is crucial for successful imaging. For best results:
    (a) The tumors should be smaller than ~6 × 6 mm, as larger tumors develop a thick capsule.
    (b) Use a dissecting microscope to visualize the overlaying connective tissue that must be removed.
    (c) Frequently moisten the surface with 0.9% saline to preserve tissue health and aid in removal of connective tissue.

11. Dissecting the connective tissue overlaying the mammary fat pads is more surgically challenging than from tumors grown on the flank, due to increased vasculature and propensity for bleeding.
12. The application of a microscope slide helps to gently flatten the tumor, which increases the imageable area and allows for deeper imaging. Additionally, this approach helps stabilize the surgical preparation, reducing movement in the tissue being imaged. Optimal imaging is dependent on injecting tumor cells at specific anatomical location (*see* **Note** 7), as cells injected too proximal or distal to the mid-line will establish tumors that are more challenging to surgically prepare. Additionally, Transpore® tape can be used to stabilize the microscope slide, but care must be taken to ensure that tumor feeding blood vessels are not restricted by the additional pressure. Tumors should not be bigger than ~6×6 mm post-implantation as it is more challenging to "flatten" larger solid tumors without blocking at least some blood vessels.
13. Although the antibody concentration should be adjusted individually, 5–10 μg per mouse can be used as a starting point.
14. The selection of fluorophores will depend upon the microscope configuration and imaging conditions. In our system, we can use up to 6 colors on the confocal platform and four colors by MP imaging. For confocal IVM, we have found that combining BV421 (BD Biosciences), QD655 (Life Technologies) (excited by 405 laser), Alexa 488, phycoerythrin (PE), PerCP-Cy 5.5 (excited by 488 laser), and Alexa 647 (excited by 638-laser) provides excellent 6-color imaging. Four-color MP imaging at 980 nm-excitation wavelength can be achieved using BV421, Alexa 488, PE and QD655 together with the following filter sets; dichroic 560 nm followed by light path 1—dichroic 495 nm followed by a 460/50 nm filter for BV421 and a 525/50 nm filter for Alexa 488, and light path 2—620 nm dichroic followed by a 575/15 nm filter for PE and a 661/20 nm filter for QD 655.
15. Administration of fluorophore-conjugated antibodies for in vivo labeling of cells has the potential for biological effects (blocking the function of specific proteins (i.e., adhesion molecules), cellular activation through Fc-receptors, complement activation, cellular depletion). As such, each antibody used for in vivo labeling must be fully characterized and vetted in carefully controlled experiments prior to drawing conclusions from IVM.
16. Care must be taken when selecting fluorophores to ensure adequate photo-stability and limit quenching during periods of extended imaging. Some fluorophores, such as PE, are susceptible to photo-bleaching. Such fluorophores are not amendable to the repeated and extended excitation associated with long-term time-lapsed imaging. Better alternatives include the

broad class of sulfonated dyes (e.g., Alexa Fluor®) or nanocrystal based dyes (e.g., Qdots®). These fluorophores demonstrate remarkable photo-stability and intense brightness making them optimal for IVM. Additionally, when multiplexing imaging, selection of dyes that are spectrally distinct and with limited emission overlap is important for efficient separation of individual fluorescent signals.

17. The use of fluorescently conjugated antibodies to label cells and structures in vivo is dependent on permeability of the tissue to the labeling antibody. Poorly perfused or dense tumors, or tumors with a thick, impenetrable capsule frequently afford poor access for vascular-administered antibodies resulting in suboptimal (or complete absence of) labeling of desired targets. Some of these limitations can be overcome by using cells expressing genetically encoded fluorescent reporter proteins although this approach has its own potential limitations (changes in expression level of reporter genes following a specific treatment, lack of cell-lineage specificity).

References

1. Elinav E, Nowarski R, Thaiss CA, Hu B, Jin C, Flavell RA (2013) Inflammation-induced cancer: crosstalk between tumours, immune cells and microorganisms. Nat Rev Cancer 13:759–771
2. Cook J, Hagemann T (2013) Tumour-associated macrophages and cancer. Curr Opin Pharmacol 13:595–601
3. Turley SJ, Cremasco V, Astarita JL (2015) Immunological hallmarks of stromal cells in the tumour microenvironment. Nat Rev Immunol 15:669–682
4. Hanahan D, Weinberg RA (2011) Hallmarks of cancer: the next generation. Cell 144:646–674
5. Pardoll DM (2012) The blockade of immune checkpoints in cancer immunotherapy. Nat Rev Cancer 12:252–264
6. Topalian SL, Weiner GJ, Pardoll DM (2011) Cancer immunotherapy comes of age. J Clin Oncol 29:4828–4836
7. Norden AD, Drappatz J, Wen PY (2009) Antiangiogenic therapies for high-grade glioma. Nat Rev Neurol 5:610–620
8. Smyth MJ, Ngiow SF, Ribas A, Teng MWL (2015) Combination cancer immunotherapies tailored to the tumour microenvironment. Nat Rev Clin Oncol 13:143–158. doi:10.1038/nrclinonc.2015.209
9. Moalli F, Proulx ST, Schwendener R, Detmar M, Schlapbach C, Stein JV (2015) Intravital and whole-organ imaging reveals capture of melanoma-derived antigen by lymph node subcapsular macrophages leading to widespread deposition on follicular dendritic cells. Front Immunol 6:114
10. Zal T, Chodaczek G (2010) Intravital imaging of anti-tumor immune response and the tumor microenvironment. Semin Immunopathol 32:305–317
11. Mempel TR, Bauer CA (2009) Intravital imaging of CD8+ T cell function in cancer. Clin Exp Metastasis 26:311–327
12. Lohela M, Werb Z (2010) Intravital imaging of stromal cell dynamics in tumors. Curr Opin Genet Dev 20:72–78
13. Deguine J, Breart B, Lemaître F, Di Santo JP, Bousso P (2010) Intravital imaging reveals distinct dynamics for natural killer and CD8(+) T cells during tumor regression. Immunity 33:632–644
14. Ellenbroek SIJ, van Rheenen J (2014) Imaging hallmarks of cancer in living mice. Nat Rev Cancer 14:406–418
15. Breart B, Lemaître F, Celli S, Bousso P (2008) Two-photon imaging of intratumoral CD8+ T cell cytotoxic activity during adoptive T cell therapy in mice. J Clin Invest 118:1390–1397
16. Phan TG, Bullen A (2010) Practical intravital two-photon microscopy for immunological research: faster, brighter, deeper. Immunol Cell Biol 88:438–444

Chapter 17

Development of a Patient-Derived Xenograft Model Using Brain Tumor Stem Cell Systems to Study Cancer

Chirayu Chokshi*, Manvir Dhillon*, Nicole McFarlane, Chitra Venugopal, and Sheila K. Singh

Abstract

Patient-derived xenograft (PDX) models provide an excellent platform to understand cancer initiation and development in vivo. In the context of brain tumor initiating cells (BTICs), PDX models allow for characterization of tumor formation, growth, and recurrence, in a clinically relevant in vivo system. Here, we detail procedures to harvest, culture, characterize, and orthotopically inject human BTICs derived from patient samples.

Key words Patient-derived xenograft (PDX), Brain tumor-initiating cell (BTIC), Flow cytometry, In vitro self-renewal assay, In vitro proliferation assay, Lentivirus, Intracranial injections, Immunohistochemistry, NOD-SCID

1 Introduction

Current cancer treatments are largely unsuccessful in preventing disease progression, relapse, and overall survival of the patient. A rare fraction of cells with stem cell-like properties, known as cancer stem cells (CSCs), may be responsible for maintaining neoplastic clones and contributing to treatment failure [1, 2]. In addition, current treatments are challenged by extensive intratumoral heterogeneity across multiple solid tumors [3]. The development of novel therapeutic treatments that target CSCs may reduce relapse rate and mortality in cancer patients.

Intratumoral heterogeneity is characterized by the presence of several malignant stem cell-like subpopulations, with corresponding phenotypic diversity. Cell surface markers that identify tumor-initiating cells include CD133 [4–7], stem cell antigen 1 (Sca1) [8–11], CD44 [12, 13], CD24 [14, 15], and epithelial-specific antigen (ESA) [14, 16]. Several studies demonstrate that a fraction

Authors contributed equally to this chapter.

Josie Ursini-Siegel and Nicole Beauchemin (eds.), *The Tumor Microenvironment: Methods and Protocols*, Methods in Molecular Biology, vol. 1458, DOI 10.1007/978-1-4939-3801-8_17, © Springer Science+Business Media New York 2016

of CD133+ cancer cells within brain tumors are capable of multilineage differentiation, clonal tumorsphere formation in vitro, and serial tumor transplantation in vivo [7, 17–19]. This stem cell-like subpopulation, termed brain tumor-initiating cells (BTICs), is resistant to current therapeutic regimens and may be responsible for relapse in many pediatric and adult brain tumors [19–21].

Xenograft mouse models of brain tumors are an excellent platform to study BTICs in a living system. These models allow for investigation of in vivo BTIC tumorigenicity, interaction of BTIC populations with the surrounding microenvironment, and the role of BTICs in causing tumor relapse after treatment [7, 20, 22]. Some of the first patient-derived xenograft models of human brain malignancy involved the injection of human brain tumor cells into the brains of both immune-competent and immune-deficient mice [23–25]. However, recent xenograft models typically take advantage of newer immune-deficient mouse strains such as NOD SCID, NRG, and NSG mice, which carry combinations of mutations in RAG1/2 (recombination activating genes), VDJ recombination machinery, IL2 receptor gamma chain, and the *SCID* (severe combined immune deficiency) gene [26]. The efficiency of tumor engraftment is increased due to minimal rejection of human tissue by a compromised murine immune system.

Here, we detail methods to develop a patient-derived murine xenograft model for brain cancer studies. First, a primary human brain tumor is dissociated into single cells and cultured in conditions that enrich for BTICs. This initial cell culture can be characterized using flow cytometry and sorted for specific cell populations based on surface markers. These cell populations can be injected intracranially into immune-deficient mice. Resulting tumors can be harvested for immunohistochemistry (IHC), examination of vascularity and size, flow cytometric analysis of marker expression, or serial tumor transplantation in vivo.

2 Materials

2.1 Patient Brain Tumor Processing and Primary Cell Culturing

1. 1× Dulbecco's phosphate-buffered saline (PBS).
2. 100 mm glass petri dish.
3. Surgical forceps and scissors.
4. RNA*later*® stabilizing reagent.
5. Liberase TM (Roche).
6. Ammonium chloride solution (0.8% NH_4Cl, 0.1 mM EDTA in water; STEMCELL Technologies).
7. Falcon® 70 μm nylon mesh cell strainer.
8. Neural stem cell (NSC) complete media: 1% N_2 supplement (Invitrogen), 0.2% 60 μg/mL *N*-acetylcystine (Sigma), 2% neural survival factor-1 (Lonza), 1% HEPES (Wisent), 6 mg/

mL glucose (Invitrogen) in 1:1 Dulbecco's Modified Eagle Medium and F12 media (Invitrogen), supplemented with 1× antibiotic–antimycotic (Wisent), 20 ng/mL human epidermal growth factor (Invitrogen), 20 ng/mL basic fibroblast growth factor (Invitrogen), and 10 ng/mL leukemia inhibitory factor (Chemicon) (*see* **Note** 7).

9. Grenier Bio-One CELLSTAR® cell-repellent surface 50 or 100 mm dish.

2.2 Tumorsphere Dissociation for In Vitro and In Vivo Assays

1. PBS.
2. Liberase TM.
3. DNAse I (Worthington Biochemical Corporation).
4. Trypan blue.
5. BD Falcon® 12 × 75 mm tubes with 35 μm cell strainer cap.

2.3 Flow Cytometry

1. BD Falcon® 12 × 75 mm tubes.
2. Antibodies to the desired cell marker and matched isotype controls (where available).
3. PBS + 2 mM EDTA (PBS–EDTA).
4. Viability dyes: 7-amino-actinomycin D (7-AAD) excitation 488/emission 655 (Beckman Coulter) and Live/Dead® Fixable Near-IR Dead Cell Stain Kit (Life Technologies).
5. BD Cytofix/Cytoperm™ Fixation/Permeabilization Kit (BD Biosciences):
   - Fixation/Permeabilization solution, ready to use.
   - 10× BD Perm/Wash™ buffer, dilute 1:10 with sterile ddH_2O before use.

2.4 Intracranial Injections

1. PBS.
2. Rodent gas anesthesia instrument equipped with a vaporizer, isoflurane, oxygen tank, charcoal scavenger filters, induction chambers, and nose cones.
3. Refresh Lacri-Lube (56.8% Petrolatum, 42.5% mineral oil).
4. Surgical detergent and povidone–iodine surgical scrub.
5. Size 24 disposable safety scalpel.
6. Hamilton® 10 μL Model 1701 RN Neuros Syringe.
7. 17 mm Vicryl-coated absorbable suture; violet, braided.
8. 3 M Vetbond Tissue adhesive.
9. 3 μg/mL buprenorphine/PBS.
10. Sterile 0.9% sodium chloride for injection/injectable USP.

2.5 Mouse Brain Harvesting

1. 2.5% 2,2,2-tribromoethanol (Avertin): Dissolve 5 g of Avertin powder in 5 mL of tert-amyl alcohol (*see* **Note 1**). Add 2.5 mL of Avertin-*tert*-amyl alcohol solution to 97.5 mL of pre-

warmed PBS. Filter through 0.22 μm filter and aliquot into glass Vacutainer tubes. Wrap the tubes in foil and store at 4 °C.

2. 1-in sharp-ended scissors, 3-in sharp-ended scissors, 3-in blunt-ended scissors.
3. 6-in sharp-ended forceps, 8-in blunt-ended forceps.
4. One 1cc syringe and one ½ cc insulin syringe per mouse.

2.6 Mouse Brain Immunohistochemistry

1. 21G needles to attach to saline and formalin lines.
2. 1000 USP units/mL heparin sodium injection.
3. Saline solution.
4. 0.9% sodium chloride 1000 mL bag.
5. 10% formalin.
6. 1.0 mm coronal mouse brain slicer matrix and two razor blades.
7. 50 % and 70% ethanol.
8. One tissue-embedding cassette per mouse brain.

3 Methods

Ensure that all tools, equipment and reagents are sterile to prevent contamination. All procedures must be performed in a Biosafety Level 2 cabinet, unless otherwise stated.

3.1 Patient Brain Tumor Processing and Primary Cell Culturing

1. Place 15 mL of PBS and 200 μL of Liberase TM into a 50 mL Falcon tube. Incubate in a 37 °C water bath (for use in **step 6**).
2. Place the patient brain tumor sample in the 100 mm glass petri dish.
3. Gently pipette 5–10 mL of PBS onto the sample to wash away red blood cells (RBCs) and other fluids. Discard these fluids.
4. Using surgical scissors and forceps, dissociate the tumor sample into a homogenous consistency (*see* **Note 2**).
5. Aliquot and freeze a small amount of tumor sample (~1 mm^3) in 1 mL of RNA*later* at −30 °C for gene expression analysis (*see* **Note 3**).
6. Transfer the tumor suspension into the pre-warmed 50 mL Falcon tube prepared in **step 1**. Incubate at 37 °C for 15 min in an incubator-shaker (30 rpm) (*see* **Note 4**).
7. After incubation, filter the tissue lysate through a 70 μm nylon mesh cell strainer into another 50 mL Falcon tube to remove undigested tissue (*see* **Note 5**).
8. Centrifuge filtrate at 300 × *g* for 5 min. Remove supernatant carefully and resuspend pellet in 1 mL of PBS.

9. Add 4–12 mL of ammonium chloride solution and incubate at room temperature for 5 min (*see* **Note 6**).
10. Add the same amount of PBS as lysis buffer in **step 9** to the cell suspension. Centrifuge at 300 × *g* for 5 min.
11. Remove supernatant, resuspend cell pellet in 1 mL of NSC complete media (*see* **Note 7**). Transfer the cell suspension to either a 50 mm or a 100 mm ultra-low binding tissue culture dish, with final volumes of 3 mL and 7 mL NSC complete media, respectively (*see* **Note 8**).
12. When cell culture media changes from red to orange, add 2–4 mL of NSC complete media to the cell culture dish. Change cell culture media completely when media color turns slightly yellow (*see* **Note 9**).

3.2 Tumorsphere Dissociation for In Vitro and In Vivo Assays

1. Observe cell culture under microscope for the presence of tumorspheres (Fig. 1). In the absence of tumorspheres, clumps, and aggregates, proceed to **step 5**.
2. Transfer cell culture to an appropriate size Falcon tube. Collect any remaining cells by rinsing the culture dish with 4–5 mL of PBS, and add it to the same Falcon tube. Centrifuge cell suspension at 300 × *g* for 5 min.
3. Remove supernatant carefully and resuspend cell pellet in 1 mL of PBS. Add 10 μL of Liberase TM and 10 μL of DNase I. Incubate in a 37 °C water bath for 5 min (*see* **Note 4**).
4. After incubation, triturate gently using a micropipette to facilitate complete cell dissociation.
5. Add 5–10 mL of PBS to the cell suspension. Centrifuge at 300 × *g* for 5 min. Remove supernatant and resuspend cell pellet in 500–1000 μL of PBS.
6. Filter the cell suspension into a 12 × 75 mm tubes with 35 μm cell strainer cap.
7. Determine cell number and viability using Trypan Blue solution. Adjust cell count as required for specific assays.

3.3 Flow Cytometry: Surface Staining

1. Using the tumorsphere dissociation protocol (Subheading 3.2), obtain a single cell suspension with live cell concentration of 1.0×10^6 cells/mL.
2. Label the required number of 12 × 75 mm tubes and add appropriate amount of antibody or isotype control (as predetermined by antibody titration) (*see* **Notes 10** and **11**). Add 100 μL cell suspension to each tube.
3. Incubate cell suspension for 15 min at room temperature.
4. Wash cells by adding 1 mL of PBS + 2 mM EDTA (PBS-EDTA) to each sample and centrifuge at 300 × *g* for 3 min. Remove

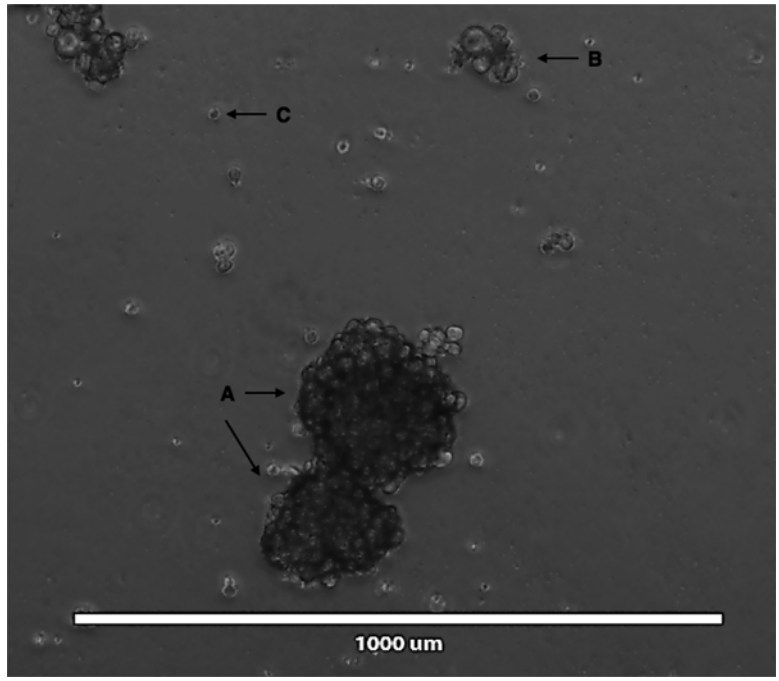

Fig. 1 BTIC populations form tumorspheres in culture. Dissociated brain tumor cells plated in NSC complete media form (**a**) tumor spheres, (**b**) cell aggregates, and (**c**) cellular debris

supernatant by decant and blot method (*see* **Note 12**). Gently tap tubes to loosen pellets.

5. Resuspend pellets in 250 µL PBS–EDTA with 2% 7AAD for 10 min at room temperature.

3.4 Flow Cytometry: Internal Staining

1. Using the tumorsphere dissociation protocol (Subheading 3.2), obtain single cell suspension with live cell concentration of 1.0×10^6 cells/mL.
2. Add 1 µL of Live/Dead® fixable dead cell stain to every 1 mL of cell suspension and incubate on ice for 20 min.
3. Add an equal volume of PBS–EDTA and centrifuge at 300 × *g* for 3 min. Carefully remove supernatant and resuspend pellet well.
4. Add 250–300 µL of Fixation/Permeabilization solution, gently swirl tube to resuspend and incubate on ice for 20 min.
5. Label the required number of 12 × 75 mm tubes, and add antibodies and isotype controls (as predetermined by titration).
6. Add 1 mL Perm/Wash™ buffer to the fixed cell suspension and centrifuge at 300 × *g* for 3 min. Carefully remove supernatant.

7. Resuspend cell pellet in sufficient Perm/Wash™ buffer to add 2×10^5 live cells per 100 µL of cell suspension to every tube prepared in **step 5**. Incubate on ice for 30–45 min.
8. Add 1 mL Perm/Wash™ buffer to each test tube and centrifuge at 300 × *g* for 3 min. Carefully remove supernatant.
9. Resuspend in 250 µL of PBS–EDTA.

3.5 Flow Cytometry: Combined Surface and Internal Staining

1. Follow **steps 1–3** from the internal staining procedure, i.e., addition, incubation and washing of Live/Dead® fixable dead cell stain. Resuspend cells in sufficient PBS–EDTA to add 100 µL to each staining tube required, then follow surface staining **steps 2–4**, resuspending pellets well after washing.
2. Fix each test tube of stained cells by adding 250 µL Fixation/Permeabilization solution and incubating on ice for 20 min.
3. Add 750 µL Perm/Wash™ buffer to each tube and centrifuge at 300 × *g* for 3 min. Carefully remove supernatant.
4. Add appropriate amounts of internal antibodies/isotype controls and incubate on ice for 30–45 min.
5. Follow wash **steps 8** and **9** from internal staining procedure (Subheading 3.4).

3.6 Flow Cytometry Acquisition and Sorting

1. Use the negative control sample to establish cytometer settings: adjust forward and side scatter to view all cells and create a gating region around the cells of interest (Fig. 2a) (*see* **Notes 13** and **14**). Adjust required fluorescence detectors to position negatives within the first decade and a half (Fig. 2b).
2. Create a second gating region around the viable cells (i.e., cells that are negative for the viability dye) (Fig. 2c). Both the forward-side scatter and the viability of gating regions should be applied to all fluorescence plots before establishing statistical regions which will define the positives (Fig. 2d, e).
3. If more than one fluorophore is used, run single stained controls and establish color compensation values (Fig. 3).

3.7 Intracranial Injections

Immunodeficient mice must be used for engraftment of patient derived cells. All procedures must be performed in a BSL 2 cabinet, within a clean room.

1. Follow **steps 1–6** from Subheading 3.2.
2. Resuspend desired number of patient-derived cells in 10 µL of PBS, and keep cell suspension on ice.
3. Assemble and turn on the rodent anesthesia instrument.
4. Weigh mouse and place in gaseous induction chamber. After 2–3 min, the mouse should be unresponsive to a toe pinch (*see* **Note 15**).

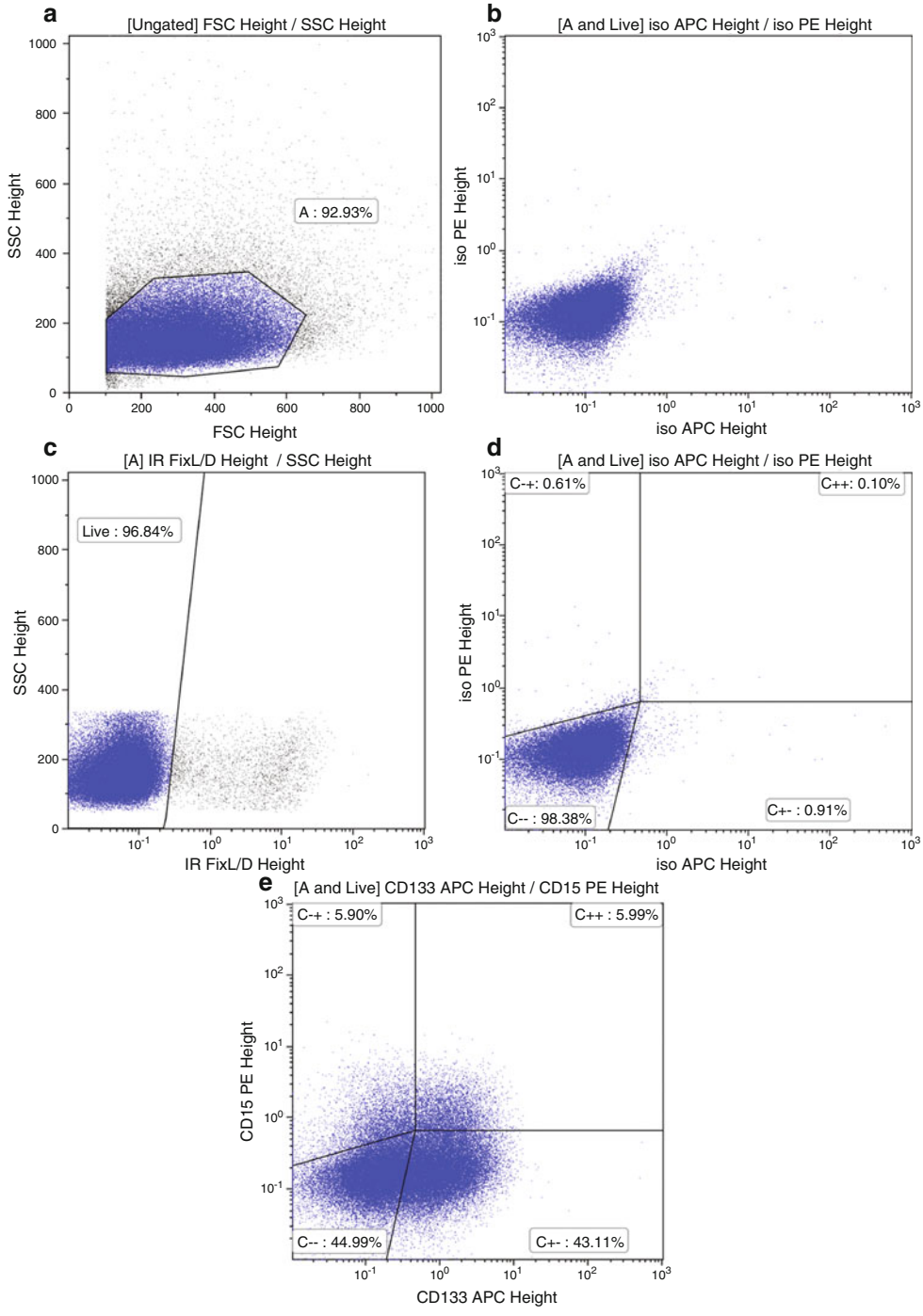

Fig. 2 Flow cytometric analysis of BTIC population. (**a**) Light scatter plot providing an image of all cells, including debris. A region has been drawn around potential cell population based on size (FSC) and granularity (SSC). (**b**) Required fluorescence detectors are adjusted to position negatives within the first decade and a half. (**c**) Dead cells that stain with viability dye (7-AAD or IR) are eliminated from further analysis. (**d**) Matched isotype control is used to position the statistical quadrants. (**e**) Glioblastoma BTICs are stained and quantified with surface markers CD133-APC and CD15-PE

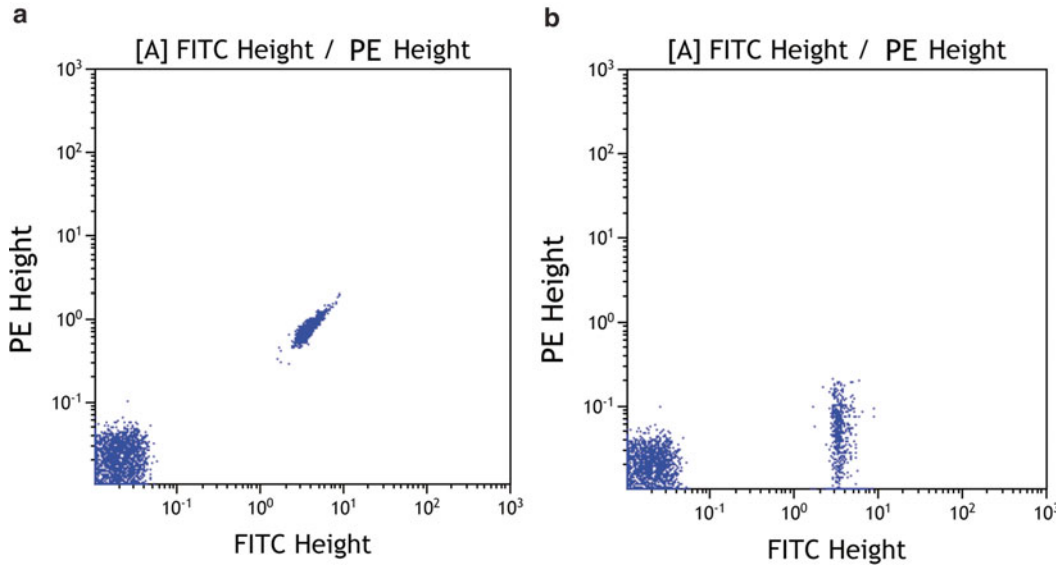

Fig. 3 Color compensation between PE and FITC. (**a**) Uncompensated signal overlap between phycoerythrin (PE) and fluorescein (FITC). (**b**) Compensation subtracts the FITC signal from the PE signal

5. Place the mouse on a platform, and insert its nose properly into the maintenance tube of the rodent anesthesia instrument. Gently secure the mouse to a stereotactic frame (*see* **Note 16**).
6. Use a cotton swab to clean the top of the mouse head with surgical detergent, followed by sterile water and then a povidone–iodine surgical scrub.
7. Use a scalpel to make a cut down the midline of the mouse's head, between the eyes to the ears (Fig. 4).
8. Spread the skin to locate the sagittal and coronal sutures, and identify the point located 2 mm behind the coronal suture, and 3 mm to the right of the sagittal suture. Drill a burr hole by tapping the drill bit lightly against the skull. Drill until a reddish area is visible, or until a Hamilton syringe can penetrate through the remaining skull (*see* **Note 17**).
9. Using a 10 μL Hamilton syringe filled with 10 μL of cell suspension, insert the syringe 3 mm into the burr hole at either 90° or 60° from the horizontal plane.
10. Inject the 10 μL of cell suspension in one slow, smooth, and uninterrupted motion into the mouse right frontal lobe. Gently tap the end of the syringe 2–3 times before removing it to ensure that cell suspension remains in the brain.
11. Clean any spilled blood with gauze, and suture the cut with 2–3 stitches using a simple interrupted technique. Add two

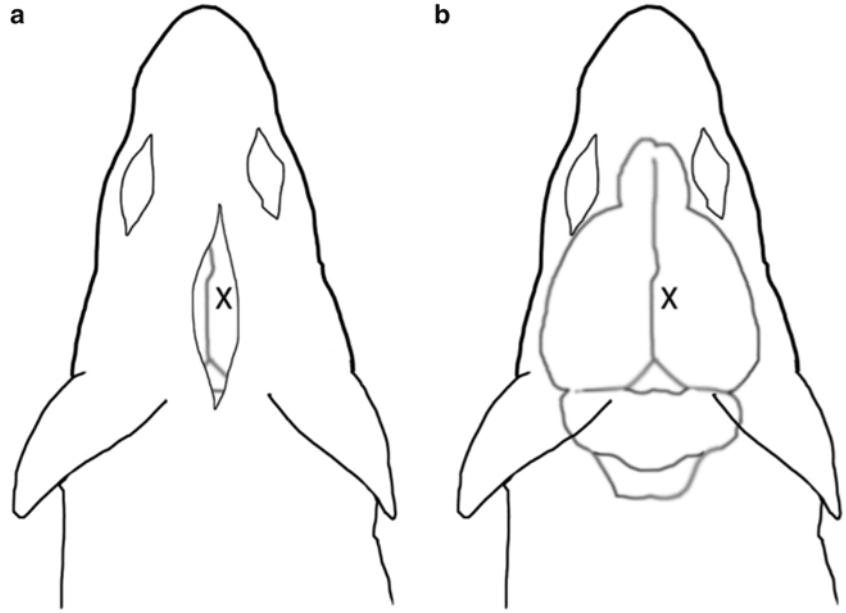

Fig. 4 Representative anatomical landmarks of mouse skull. The main anatomical landmarks are outlined. The approximate location of burr hole and site of injection is marked by *X*

extra throws after the initial knot has been tied and cut off any excess suture thread.

12. Apply a small amount of tissue adhesive to the sutured cut and mark the mouse as necessary (i.e. tail mark or ear notch).
13. Inject 1 mL of sterile 0.9% sodium chloride and 0.5 mL of buprenorphine (Temgesic) subcutaneously.
14. Place mouse in a recovery cage on a piece of gauze, and position part of the cage near a heat source (heat lamp or heat pad) until the mouse is awake (*see* **Note 18**).
15. Repeat **step 13**, 24 h after surgery.
16. Observe mouse for required length of time or until experimental endpoint.

3.8 Preparation of Mouse Brain for Harvesting

1. Retrieve and weigh the mouse. Administer 18 μL of 2.5% Avertin per gram weight by intraperitoneal injection using a 1 cc syringe.
2. Return the animal to its cage and, after 3–4 min, it should be unresponsive to a toe pinch.
3. Perform cervical dislocation as instructed by your animal facility.
4. Decapitate the mouse at the site of dislocation and remove the skin from the base of the head to the nose, exposing the scalp.
5. Using small sharp-ended scissors, pierce the skull at the base of the head and carefully cut the ridge between the eyes.

6. Using sharp-ended forceps, remove the skull by carefully pulling it away from the brain until all of the brain is exposed (*see* **Notes 19** and **20**).
7. Carefully lift the brain out of the skull in a scooping manner.
8. Place it in 15 mL of sterile PBS and culture the mouse brain as mentioned previously in Subheading 3.1.

The cultured cells could be reinjected (follow steps from Subheading 3.7) for serial transplantation, or reanalyzed by flow cytometry (follow steps from Subheading 3.3–3.6).

3.9 Preparation of Mouse Brain for Immunohistochemistry

1. Follow **steps 1** and **2** from Subheading 3.8.
2. Place the anesthetized mouse on an inclined surface with abdomen facing up. Spread the paws as wide as possible and secure with tape.
3. Using blunt-ended forceps, grab skin at the level of the diaphragm and cut with blunt-ended scissors to expose the liver and heart. Cut laterally and then through the ribs. Ensure that organs are not damaged to avoid unnecessary interference with the circulation (*see* **Note 21**).
4. Inject 20 μL of heparin using ½ cc syringe into the left ventricle. After 10–12 heart beats, hold the heart gently with forceps and insert the saline needle 2–3 mm into the left ventricle (~2 mL/min). Immediately cut the right ventricle. Let the blood drain from the right ventricle until the liver changes color to light brown.
5. Replace the saline needle with 10 mL of 10% formalin (~2 mL/min) into the same hole (*see* **Note 22**).
6. Decapitate and remove the mouse brain as detailed in **steps 3**–**7** from Subheading 3.8. Put brain in 10 mL of 10% formalin.
7. Store brain at 4 °C for at least 48 h for fixation.
8. Place the mouse brain in a 1 mm coronal mouse brain sliver matrix, and slice the brain at every other channel using sharp razor blades (Fig. 5). This procedure does not need to be performed in a BSL2 hood.
9. Place mouse brain slices in cassettes and dehydrate in 50% ethanol for 5 min, followed by 70% ethanol for at least 24 h. This step prepares the brain slices for paraffin embedding. Hematoxylin and eosin staining is performed to visualize tumor size and immunohistochemistry may now be performed for analysis of specific marker expression (Fig. 6).

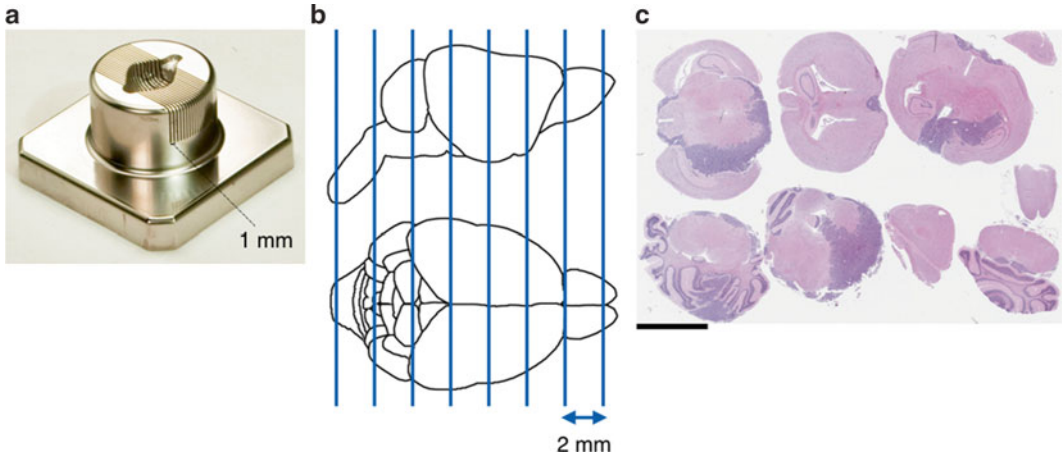

Fig. 5 Preparation of excised mouse brain for immunohistochemistry. (**a**) 10 % formalin-fixed mouse brain is placed on the 1 mm coronal mouse brain sliver matrix. (**b**) The mouse brain is sliced at every other channel using razor sharp blades. (**c**) Following dehydration using ethanol, hematoxylin and eosin staining is performed to visualize tumor size (5 mm black scale bar)

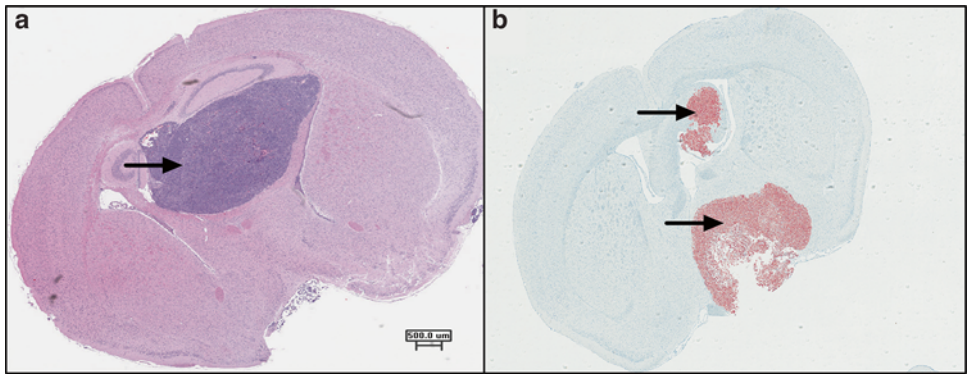

Fig. 6 Representative H&E and IHC-stained mouse xenograft. (**a**) H&E staining of coronal section of mouse brain reveals large tumor masses (*arrow*). (**b**) COX-IV IHC staining identifying human xenograft within the mouse brain (*arrows*)

4 Notes

1. Dissolution of Avertin is aided by vigorous stirring and placing the mixture in an incubator-shaker (30 rpm) set at 50 °C.
2. Minimize exposure of brain tumor tissue to air for extended periods of time to prevent cell death.
3. Ensure that the RNA*later* aliquot of the dissociated tumor sample contains the tumor itself rather than fatty tissue surrounding the tumor.
4. Prolonged incubation with Liberase TM is toxic to cells; do not extend incubation beyond 5 min.

5. To increase yield, withdraw additional filtrate from the bottom side of the nylon mesh cell strainer without puncturing it.
6. The Ammonium Chloride solution used for RBC lysis is very gentle on all other cells.
7. Neurocult™ NS-A Proliferation Kit (Human) from STEMCELL Technologies can be used to replace NSC complete media for patient brain tumor processing and primary cell culturing.
8. Increased growth of patient-derived tumor cells has been observed when initial cell density is high. Therefore, use a 50 mm culture dish with 3 mL of NSC complete media when the cell pellet is less than 1 mm thick. However, when the thickness is greater than 1 mm, use the 100 mm culture dish with 7 mL of NSC complete media.
9. Growing cells at high-density with few passages may lead to a signaling environment similar to the original tumor microenvironment, facilitating robust growth and viability. Cells may develop as free-floating clusters of spheroid bodies called tumorspheres (Fig. 1). Many tumorspheres are clonal colonies derived from a single brain tumor initiating cell or progenitor cell, and are enriched for stem-cell-like populations. However, cultures from different patients may behave differently due to intertumoral and intratumoral heterogeneity. Thus, careful inspection and evaluation of each sample is necessary.
10. Always consult antibody technical data sheets provided by the supplier for recommended incubation times, temperatures and amount of antibody. Starting with the recommended amount, prepare a serial dilution of decreasing antibody concentrations and add each dilution to 100 μL of sample. Select the antibody dilution that delivers the greatest separation between positive and negative cells.
11. The emission spectra of some fluorochromes spill over into other detectors and must be subtracted. We use BD™ CompBeads in order to determine the appropriate compensation values.
12. After centrifugation of the cell suspension, decant the supernatant by turning the tube upside down over a waste container. Carefully blot the edge of the tube to remove excess liquid, then turn the tube upright and gently resuspend. Do not turn the tube upside down again as the resuspended cell pellet may be lost.
13. This scatter pattern allows end users to view live and dead cells in the sample, including debris.
14. The specifics of acquisition, analysis, and sorting are instrument-dependent.

15. The vaporizer of the isoflurane anesthetic machine can be set between 3 and 5% when the mouse is in the induction chamber.
16. The mouse must be kept under maintenance anesthesia (vaporizer dial at 2.5%) to ensure that the mouse does not feel pain or wakes during surgery.
17. We have found that a burr hole is usually achieved after approximately ten gentle taps of the drill bit against the mouse skull.
18. While placing the mouse on gauze, make sure that its air passages are unobstructed to allow for proper respiration. This promotes better recovery post-surgery.
19. The skull can be removed in small pieces to prevent damage to the brain.
20. Be careful around the olfactory bulbs as they are easy to damage. Make sure that the entire skull is removed around the olfactory bulbs to prevent damage while removing the brain.
21. Free the heart by tearing any connective tissue with forceps and not scissors.
22. A good indication of how well the animal is being fixed is to test tail flexibility, which should be stiff.

References

1. Reya T, Morrison SJ, Clarke MF, Weissman IL (2001) Stem cells, cancer, and cancer stem cells. Nature 414:105–111
2. Pardal R, Clarke MF, Morrison SJ (2003) Applying the principles of stem-cell biology to cancer. Nat Rev Cancer 3:895–902
3. Swanton C (2012) Intratumor heterogeneity: evolution through space and time. Cancer Res 72:4875–4882
4. Cox CV, Diamanti P, Evely RS, Kearns PR, Blair A (2009) Expression of CD133 on leukemia-initiating cells in childhood ALL. Blood 113:3287–3296
5. Hermann PC, Huber SL, Herrler T, Aicher A, Ellwart JW, Guba M et al (2007) Distinct populations of cancer stem cells determine tumor growth and metastatic activity in human pancreatic cancer. Cell Stem Cell 1:313–323
6. O'Brien CA, Pollett A, Gallinger S, Dick JE (2007) A human colon cancer cell capable of initiating tumour growth in immunodeficient mice. Nature 445:106–110
7. Singh SK, Hawkins C, Clarke ID, Squire JA, Bayani J, Hide T et al (2004) Identification of human brain tumour initiating cells. Nature 432:396–401
8. Collins AT, Berry PA, Hyde C, Stower MJ, Maitland NJ (2005) Prospective identification of tumorigenic prostate cancer stem cells. Cancer Res 65:10946–10951
9. Xin L, Lawson DA, Witte ON (2005) The Sca-1 cell surface marker enriches for a prostate-regenerating cell subpopulation that can initiate prostate tumorigenesis. Proc Natl Acad Sci U S A 102:6942–6947
10. Batts TD, Machado HL, Zhang Y, Creighton CJ, Li Y, Rosen JM (2011) Stem cell antigen-1 (sca-1) regulates mammary tumor development and cell migration. PLoS One 6:e27841
11. Seigel GM, Campbell LM, Narayan M, Gonzalez-Fernandez F (2005) Cancer stem cell characteristics in retinoblastoma. Mol Vis 11:729–737
12. Du L, Wang H, He L, Zhang J, Ni B, Wang X et al (2008) CD44 is of functional importance for colorectal cancer stem cells. Clin Cancer Res 14:6751–6760
13. Patrawala L, Calhoun T, Schneider-Broussard R, Li H, Bhatia B, Tang S et al (2006) Highly purified CD44+ prostate cancer cells from xenograft human tumors are enriched in

tumorigenic and metastatic progenitor cells. Oncogene 25:1696–1708

14. Li C, Heidt DG, Dalerba P, Burant CF, Zhang L, Adsay V et al (2007) Identification of pancreatic cancer stem cells. Cancer Res 67:1030–1037
15. Baumann P, Cremers N, Kroese F, Orend G, Chiquet-Ehrismann R, Uede T et al (2005) CD24 expression causes the acquisition of multiple cellular properties associated with tumor growth and metastasis. Cancer Res 65:10783–10793
16. Dalerba P, Dylla SJ, Park IK, Liu R, Wang X, Cho RW et al (2007) Phenotypic characterization of human colorectal cancer stem cells. Proc Natl Acad Sci U S A 104:10158–10163
17. Hemmati HD, Nakano I, Lazareff JA, Masterman-Smith M, Geschwind DH, Bronner-Fraser M, Kornblum HI (2003) Cancerous stem cells can arise from pediatric brain tumors. Proc Natl Acad Sci U S A 100:15178–15183
18. Singh SK, Clarke ID, Terasaki M, Bonn VE, Hawkins C, Squire J, Dirks PB (2003) Identification of a cancer stem cell in human brain tumors. Cancer Res 63:5821–5828
19. Galli R, Binda E, Orfanelli U, Cipelletti B, Gritti A, De Vitis S et al (2004) Isolation and characterization of tumorigenic, stem-like neural precursors from human glioblastoma. Cancer Res 64:7011–7021
20. Bao S, Wu Q, McLendon RE, Hao Y, Shi Q, Hjelmeland AB et al (2006) Glioma stem cells promote radioresistance by preferential activation of the DNA damage response. Nature 444:756–760
21. Liu G, Yuan X, Zeng Z, Tunici P, Ng H, Abdulkadir IR et al (2006) Analysis of gene expression and chemoresistance of CD133+ cancer stem cells in glioblastoma. Mol Cancer 5:67
22. Calabrese C, Poppleton H, Kocak M, Hogg TL, Fuller C, Hamner B et al (2007) A perivascular niche for brain tumor stem cells. Cancer Cell 11:69–82
23. Kaye AH, Morstyn G, Gardner I, Pyke K (1986) Development of a xenograft glioma model in mouse brain. Cancer Res 46:1367–1373
24. Rana MW, Pinkerton H, Thornton H, Nagy D (1977) Heterotransplantation of human glioblastoma multiforme and meningioma to nude mice. Proc Soc Exp Biol Med 155:85–88
25. Shapiro WR, Basler GA, Chernik NL, Posner JB (1979) Human brain tumor transplantation into nude mice. J Natl Cancer Inst 62:447–453
26. Shultz LD, Brehm MA, Bavari S, Greiner DL (2011) Humanized mice as a preclinical tool for infectious disease and biomedical research. Ann N Y Acad Sci 1245:50–54

Chapter 18

Modeling Breast Tumor Development with a Humanized Mouse Model

Lisa M. Arendt

Abstract

The tumor microenvironment plays a critical role in breast cancer growth and progression to metastasis. Here, we describe a method to examine stromal–epithelial interactions during tumor formation and progression utilizing human-derived mammary epithelial cells and breast stromal cells. This method outlines the isolation of each cell type from reduction mammoplasty tissue, the culture and genetic modification of both epithelial and stromal cells using lentiviral technology, and the method of humanizing and implantation of transformed epithelial cells into the cleared mammary fat pads of immunocompromised mice. This model system may be a useful tool to dissect signaling interactions that contribute to invasive tumor behavior and therapeutic resistance.

Key words Human-in-Mouse model, Human mammary epithelial cells, Breast cancer, Stroma, Mammary gland, Stromal–epithelial interactions

1 Introduction

Breast cancer is a complex disease, resulting from pathogenic genetic changes that occur in epithelial cells leading to unregulated epithelial cell proliferation. Tumor growth is supported through the recruitment of a reactive stroma, comprised of cancer associated fibroblasts and adipocytes, recruited immune cells, endothelial and lymphatic networks, and extracellular matrix. Functionally, this stromal compartment can promote tumor growth through increased angiogenesis, secretion of immunomodulating cytokines, and creation of niches for cancer stem-like cells [1–3]. An increasing body of evidence suggests that formation of the tumor stroma is a major regulator of tumor progression [4–7]. However, since many xenograft models recapitulate advanced disease, understanding the signaling interactions between epithelial and stromal cells during early tumor development is challenging. Here, we describe a xenograft model to study tumor progression. Both the breast epithelial cells and

Josie Ursini-Siegel and Nicole Beauchemin (eds.), *The Tumor Microenvironment: Methods and Protocols*, Methods in Molecular Biology, vol. 1458, DOI 10.1007/978-1-4939-3801-8_18,

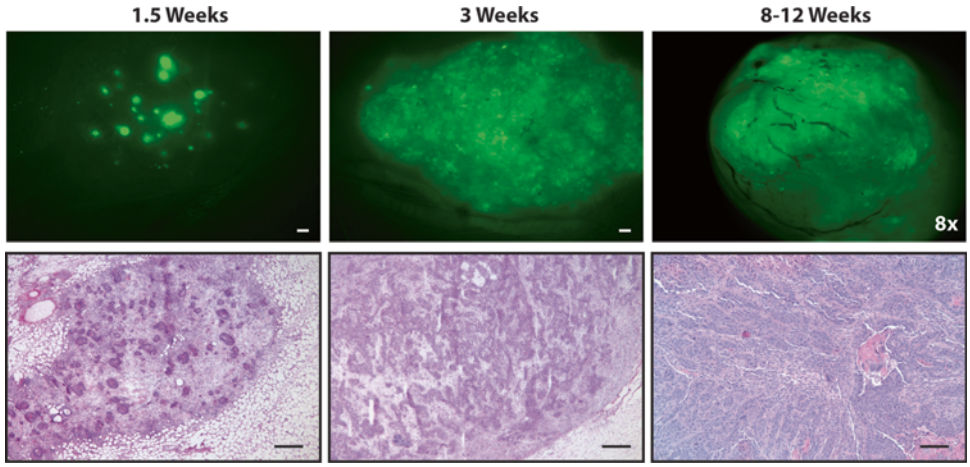

Fig. 1 Tumor progression utilizing the Human-in-Mouse (HIM) model. Following transplant of genetically modified mammary epithelial cells into humanized mammary fat pads, epithelial cells form hyperplasias which can be detected using green fluorescent protein (GFP) within 1.5 weeks. The tumors grow from approximately 1–2 mm in diameter at 3 weeks to large masses (1 cm in diameter) within 8–12 weeks. This timeline for growth may be altered due the oncogenes used to induce tumor formation as well as genetic variation in the epithelial cells utilized. Scale bar = 100 μm

stromal cells are of human origin, and these human-derived cells can be genetically modified in order to model genetic changes observed in human breast tumors then transplanted into the mammary fat pads of immunocompromised mice. This method allows for the stepwise progression of breast tumors from circumscribed hyperplasias to disorganized tumors (Fig. 1).

For this model, human mammary epithelial cells (HMEC) and stromal cells are isolated using collagenase digestion of breast tissue from reduction mammoplasty surgeries (Fig. 2). Stromal cells can be immortalized with lentiviruses encoding human telomerase (hTERT) and genetically modified to express growth factors or other proteins of interest [8]. These stromal cells are then transplanted into the cleared mammary fat pads of NOD/SCID mice in order to generate connective tissue to support the growth of HMEC. HMEC can be transduced with lentiviruses encoding oncogenes observed in breast cancer subtypes to generate breast tumors [9, 10]. As the tumors develop, the human-derived stromal cells are replaced by immune cells and myofibroblasts from the recipient mouse [11]. This protocol outlines the methods for the isolation of epithelial and stromal cells used in this model, the surgical procedures for clearing and humanizing the mouse mammary gland, and the transplant of transformed epithelial cells into humanized mammary glands in order to generate tumors.

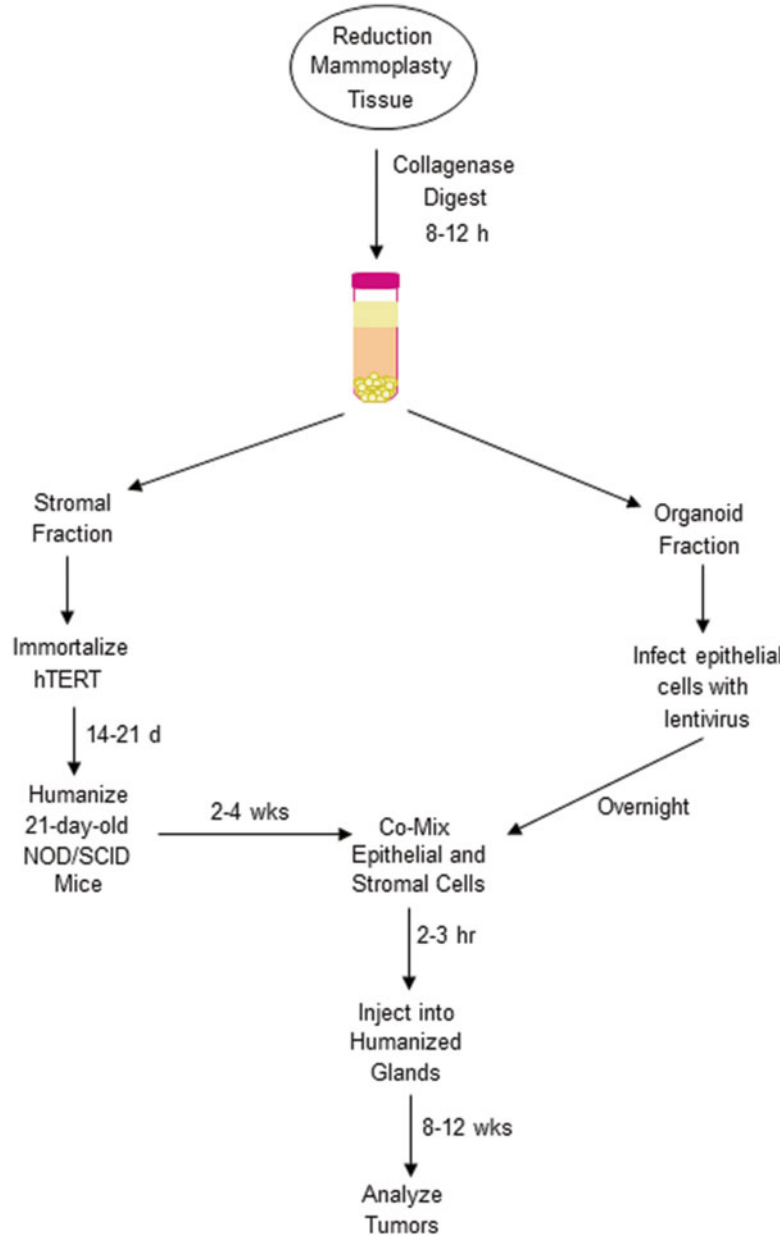

Fig. 2 Human-in-Mouse (HIM) model flowchart. Breast tissue from a reduction mammoplasty surgery is minced and digested overnight in collagen. The resulting suspension can be separated into a stromal fraction and organoids for use in culture or frozen in aliquots in liquid nitrogen for later use. The stromal fraction can be immortalized using lentivirus encoding human telomerase (hTERT) and then further genetically modified using additional lentiviral particles to express other genes of interest. The resulting stromal cell lines are used to humanize the cleared mammary fat pads of NOD/SCID mice. Two to three weeks later, epithelial cells from the organoid fraction can be dissociated into single epithelial cells, transduced with lentiviruses encoding oncogenes, co-mixed with stromal cells and implanted into the humanized glands for breast tumor formation

2 Materials

2.1 Equipment

1. Biosafety cabinet.
2. 37 °C incubator with tube rotator.
3. Tissue culture incubator held at 37 °C and 5 % CO_2.
4. Water bath set to 37 °C.
5. Centrifuge.
6. Isofluorane vaporizer, induction chamber, anesthesia circuits with nose cone, heating pad.
7. Hemocytometer.
8. Heat lamp.
9. Hair clipper.

2.2 Reagents

1. Reduction mammoplasty tissue (*see* **Notes 1** and **2**).
2. 21-day-old NOD/SCID (NOD.CB17-Prkdcscid/J) female mice (*see* **Notes 3** and **4**).
3. Mayo scissors or razor blades.
4. 15 and 50 mL conical tubes (*see* **Note 5**).
5. 100 mm × 20 mm tissue culture plates.
6. Cryovials.
7. Plastic aspirating pipettes (*see* **Note 6**).
8. Dulbecco's Modified Eagle's medium.
9. DMEM–F12 medium.
10. 0.05 % trypsin–EDTA.
11. Calf serum.
12. Antibiotic–antimycotic.
13. Epidermal growth factor (EGF).
14. Insulin.
15. Hydrocortisone.
16. Collagenase A.
17. Hyaluronidase.
18. Red blood cell lysis buffer: (0.15 M NH_4Cl, 0.01 M $KHCO_3$, 0.03 mM EDTA).
19. 1× phosphate buffered saline (PBS).
20. Dimethyl sulfoxide (DMSO).
21. DNAse I.
22. Lentiviral particles encoding human telomerase (hTERT; *see* **Notes 2** and **7**).
23. Lentiviral particle encoding oncogene of interest (*see* **Note 8**).

24. Protamine sulfate (*see* **Note 9**).
25. Bleomycin sulfate (2 mU/mL).
26. 0.1% bovine serum albumin (BSA) in PBS, filter sterilized.
27. Growth factor-reduced Matrigel.
28. Rat tail type I collagen.
29. 0.1 N NaOH.
30. 0.01 N glacial acetic acid.
31. 40 μm basket filter.
32. Low adherence 24-well plates.
33. 10 mL syringes and 18 g needles.
34. pH indicator paper.
35. Parafilm.

2.3 Media

1. Epithelial Cell Media: Mammary epithelial cell basal media supplemented with 52 μg/mL bovine pituitary extract, 0.5 μg/mL hydrocortisone, 10 ng/mL human EGF, 5 μg/mL insulin.
2. Organoid Media: DMEM–F12 media supplemented with 5% calf serum, 10 μg/mL insulin, 10 ng/mL EGF, 0.5 μg/mL hydrocortisone, and 1% antibiotic–antimycotic.
3. Digestion Media: Organoid Media supplemented with 3 mg/mL collagenase and 600 μg/mL hyaluronidase.
4. Fibroblast Media: DMEM supplemented with 10% calf serum and 1% antibiotic–antimycotic.
5. Wash Buffer: PBS + 5% calf serum.

2.4 Surgical Supplies

1. Analgesic (*see* **Note 10**).
2. Ophthalmic lubricant (such as Dechra NDC).
3. Betadine solution (1% iodine).
4. Cotton tip applicators.
5. Alcohol wipes (70% ethanol).
6. 9 mm Autoclips.
7. Autoclip applicator.
8. Autoclip remover.
9. Hamilton syringe 100 μL size.
10. Hamilton syringe needles 22G, 2″, point style 2.
11. 1 mL syringes and 27G needles.
12. Surgical scissors.
13. Surgical forceps.

3 Methods

3.1 Dissociation of Reduction Mammoplasty Tissue

1. Transfer tissue into a biosafety cabinet, and mince the sample with sterile razor blades or Mayo scissors until tissue pieces measure approximately 5 mm^3 (*see* **Notes 11** and **12**).
2. Fill a 15 mL conical tube with 10 mL of Digestion Media. Add minced tissue to fill the tube to the 15 mL marker (approximately 2 g of tissue). Cover the tube and seal with Parafilm. Invert the tube to make sure that the tissue can mix with the media. If the tissue does not mix, remove tissue from the top of the tube to create more space (*see* **Note 12**).
3. Incubate filled 15 mL tubes at 37 °C with rotation for approximately 8–10 h.
4. Remove the tubes from the incubator, then centrifuge the tubes for 1 min at 9 × *g* to separate the Digestion Media into an oil/fat layer, middle aqueous layer enriched for stromal cells, and bottom organoid pellet.
5. Remove oil/fat layer (*see* **Note 13**).
6. Separate the stromal and organoid fractions into 50 mL conical tubes. Centrifuge the tubes for 5 min at 300 × *g*. Aspirate the supernatant.
7. Resuspend the organoid and stromal cell pellets in 2 mL of red blood cell lysis buffer. Incubate at room temperature for 2–5 min.
8. Add 10 mL of Wash Buffer and centrifuge for at 300 × *g* for 5 min.
9. Repeat **step 8** three times.
10. The fractions can be used for further experiments now or frozen for later use. Centrifuge cells at 300 × *g* for 5 min, and remove supernatant. Resuspend the stromal fraction in Fibroblast Media + 10% DMSO; resuspend the organoid fraction in Organoid Media supplemented with an additional 5% calf serum and 10% DMSO (*see* **Note 14**).

3.2 Generation of Immortalized Stromal Cells

1. Thaw or use the stromal fraction pellet as generated in Subheading 3.1 (*see* **Note 15**).
2. Plate cells onto 100 mm × 20 mm plates in Fibroblast Media and allow stromal cells to adhere to the plastic overnight. Cells should be grown in a tissue culture incubator.
3. Culture cells in Fibroblast Media, feeding every other day, until they approach 80% confluence.
4. To split the cells, aspirate the media from the plate. Add trypsin, and incubate the cells at 37 °C for 5 min. Gently tap the plate to dislodge remaining adherent cells. Quench the trypsin with Fibroblast Media, collect the cells into a conical tube, and centrifuge at 300 × *g* for 5 min. Aspirate the supernatant.

5. Resuspend the cells in Fibroblast Media and count the number of cells using a hemocytometer.
6. Plate and infect the cells using lentivirus encoding hTERT, according to the manufacturer's instructions, and subsequently select the cells using a mammalian selection marker or by fluorescence activated cell sorting (FACS) depending on the viral construct backbone (*see* **Note 7**).
7. Expand the number of fibroblasts in culture prior to humanizing. Each mammary gland that is humanized will require 2.5×10^5 untreated and 2.5×10^5 bleomycin-treated fibroblasts. The fibroblasts should not reach confluence during growth as this may have a negative effect on the engraftment during humanization (*see* **Note 16**).
8. 24 h prior to surgery, add 2 mU/mL bleomycin sulfate to the media of half of the fibroblasts to be used for humanizing. Incubate the cells for 30 min at 37 °C, then aspirate off the media, wash the cells with PBS, and add fresh Fibroblast Media.
9. On the day of the surgery, wash the cells with PBS, trypsinize and count cells (*see* Subheading 3.2 **step 4**). Prepare enough cells to inject at least four extra glands for both bleomycin-treated and untreated fibroblasts. Pool the correct number of treated and untreated cells, centrifuge at $300 \times g$ and resuspend in 25 μL Fibroblast Media per gland prepared. Keep the cells on ice until the mice are ready for humanizing.

3.3 Humanizing Mammary Fat Pads

1. Clean surgical area with disinfectant and sterilize surgical instruments. Inject mice with analgesic prior to the start of surgery (*see* **Note 10**).
2. Place a mouse in the induction chamber of the anesthesia machine, and induce anesthesia using 1–3% isofluorane with an O_2 flow rate of 1–2 L/min. When the mouse no longer withdraws its foot in response to pinching its toes, the mouse is in a surgical plane of anesthesia. Apply ophthalmic ointment to its eyes and place the mouse in lateral recumbency with a nose cone to supply anesthesia.
3. Shave a 2–3 cm area extending from the rib cage to the leg. Disinfect the shaved area completely with betadine applied with a cotton tip applicator, and then wash the skin with 70% ethanol wipes. The lymph node should be visible though the skin as a small, dark oval at the level of the kneecap.
4. Make a 1 cm incision in the skin over the surface of the mammary gland at the level of the lymph node. Expose the lymph node, and with forceps, lift the lymph node and cut the mammary gland dorsal to the lymph node. Retract the mammary gland gently from the skin with the forceps, and excise the mammary gland ventrally toward the nipple. This will remove the lymph node and the endogenous mammary epithelium.

5. Using forceps gently retract the remaining mammary fat pad. Using a Hamilton syringe and needle, slowly inject 25 μL of immortalized fibroblasts into the remaining mammary fat pad. Insert the needle deeply enough into the fat pad to prevent leakage around the needle. Slowly withdraw the needle, and twist the syringe upon removal to prevent leakage.
6. Pull the skin together and tent over the injection site to avoid puncturing the injected mammary gland. Apply wound clips to close skin incision.
7. Turn mouse over and repeat **steps 3–6** on the contralateral mammary gland.
8. Place mice in clean cage with an area of the cage under a heat lamp, and monitor the mice until they are able to walk on their own. Continue to monitor mice daily post-surgically. Surgical clips can be removed after 10–14 days (*see* **Note 17**).

3.4 Preparation of Human Mammary Epithelial Cells

1. Injections of epithelial cells for both tumor studies and normal outgrowths should be made 2–4 weeks following humanization for the best results.
2. Expand fibroblasts for co-injection with epithelial cells. For this injection 2.5×10^5 fibroblasts are co-mixed with epithelial cells at the time of the injection.
3. 24 h before injection, thaw a vial of collagenase pellet generated in Subheading 3.1 in a 37 °C water bath. Resuspend the pellet in 10 mL of Fibroblast Media and plate on a 100 mm × 20 mm plate. Incubate in a tissue culture incubator for 1–2 h (*see* **Note 18**).
4. Decant the non-adherent cells into a 50 mL conical tube with a pipette, and wash the plate with 10 mL PBS to remove any remaining organoids (*see* **Note 19**). Centrifuge cells at 300 × *g* for 5 min. Aspirate and discard the supernatant.
5. Add 10 mL of 0.1 % BSA in PBS, and resuspend the pellet by it passing though an 18 g needle attached to a 10 mL syringe 8–10 times. Centrifuge at 300 × *g* for 5 min. Aspirate and discard the supernatant.
6. Resuspend the pellet in 2 mL trypsin. Triturate the solution with a 1 mL pipette for 1 min to break up the organoids. Incubate the tube in a 37 °C water bath for 5 min. Triturate the solution again, and then continue the incubation in the water bath for an additional 5 min.
7. Add 10 mL of Fibroblast Media to quench the trypsin and 100 μL of DNAse to remove cellular clumping due to cell death. Mix thorough with a 10 mL pipette until the cell clumps disperse, then filter through a 40 μm basket filter into a 50 mL conical tube. Wash the filter with an additional 10 mL of Fibroblast Media.

8. Centrifuge cells at 300 × *g* for 5 min and resuspend the pellet in Epithelial Cell Media. Count cells with a hemocytometer. Centrifuge cells at 300 × *g* for 5 min and resuspend the cells in Epithelial Cell Media at a concentration of 1×10^6 cells/mL.
9. Aliquot 500 mL of the resuspended epithelial cells into each well of a 24-well non-adherent plate. Add lentivirus encoding oncogenes to the cells in the presence of 5 μg/mL protamine sulfate (see **Note 20**). Incubate the epithelial cells with the lentivirus in a tissue culture incubator overnight.
10. Using a 200 μL pipette tip, triturate the transduced mammary epithelial cells to break up clumps that formed overnight. Collect the epithelial cells into a conical tube. Wash each well with 1 mL Wash Buffer, and collect the wash fraction with the infected cells in the conical tube. Centrifuge at 300 × *g* for 5 min.
11. Aspirate off the supernatant and wash cell pellet with 10 mL of Wash Buffer. Centrifuge at 300 × *g* for 5 min. Aspirate the supernatant and repeat the wash step two additional times.
12. Resuspend cells in 5 mL Epithelial Cell Media and count the cells. The target number of cells for injection to make tumors is between 1 and 2×10^5 cells/gland. Remove the number of cells necessary to complete the injections, including enough cells for at least four additional injections, and put the cells in a conical tube on ice until the fibroblasts and matrix components have been prepared.
13. Aspirate off media from fibroblasts, wash with PBS, and trypsinize as described in Subheading 3.2 **step 4**. Count fibroblasts using a hemocytometer and remove the number of cells necessary for the injections. The total number for each gland is 2.5×10^5, and enough fibroblasts should be prepared to inject four additional glands. Place the correct number of fibroblasts in a 15 mL conical tube on ice until the matrix has been prepared.
14. The fibroblasts and epithelial cells are mixed in a mixture of collagen and Matrigel for injection. Matrigel should be thawed and maintained on ice, because it will gel at 37 °C. For tumor growth, use a 1:1 mixture of collagen and Matrigel. Dilute stock collagen to a concentration of 2 mg/mL with 0.01 N glacial acetic acid, then add 0.1 N NaOH dropwise until the pH reaches approximately 5.0 when measured with pH paper.
15. Combine collagen and Matrigel together. The mixture will turn yellow/clear due to the low pH of the collagen. Keep on ice. Check the pH of the mixture using pH paper. Add 0.01 N NaOH to the mixture dropwise, mixing well, and check the pH frequently until it reaches approximately 7–7.5. The color of the matrix mix should be pale rose pink.
16. Combine fibroblast and epithelial cells into one conical tube and centrifuge at 300 × *g* for 5 min. Aspirate the supernatant

and resuspend the cell pellet in collagen–Matrigel. The amount of matrix used for each injection is 30 μL. Keep the cells in matrix on ice until surgery.

3.5 Injection into Humanized Glands

1. Prepare the surgical area and induce anesthesia as in Subheading 3.3 **steps 1** and **2**.
2. Re-shave the area from the humanization surgery, scrub with Betadine, and wash with 70% ethanol wipes.
3. Make a small incision dorsal to the scar formed from the previous humanization incision. Gently retract the skin from the mammary gland with a forceps. The area of humanization will be evident as a whitish, striated area in the gland.
4. Redistribute the cells in the collagen–Matrigel mixture by flicking the tube, and draw 30 μL into a Hamilton syringe.
5. Inject the 30 μL bolus slowly in the same area that was used to humanize. Turn the needle while withdrawing to prevent leakage from the gland.
6. Close the wound as described in Subheading 3.3 **step 6**. Repeat Subheading 3.3 **steps 2–5** on contralateral gland. Recover the mice and monitor as described in Subheading 3.3 **step 8**.
7. Monitor mice weekly for tumor formation. Tumors may be palpable (approximately 2 mm in diameter) within 3 weeks following epithelial cell injection.

4 Notes

1. Human breast tissue for these studies is obtained from patients undergoing elective breast reduction mammoplasty surgeries. All studies should be performed in accordance with guidelines for human research subjects and institutional policies.
2. Working with cells from human breast tissue and lentiviruses requires the utilization of biosafety containment procedures. Human breast tissue may be a source of blood-borne pathogens. Risk assessments should be carried out in conjunction with institutional guidelines for biosafety prior to starting any procedures.
3. All animal procedures must be conducted in accordance with institutional animal care and use committees and ethical guidelines. All surgeries should be conducted under sterile conditions with aseptic technique.
4. We typically use 21-day-old NOD/SCID females that weigh between 8 and 10 g of body weight. If a pup weighs less than 7 g, it is advisable to wait until the pup gains weight in order to improve viability following surgery. Mice greater than 12 g of body weight should be avoided, because they might be older than suspected. The mammary ductal epithelium

continues to grow allometrically, and increasing age may reduce the ability to remove the endogenous epithelium by clearing the fat pad.

5. We recommend using polypropylene centrifuge tubes with a plug cap. This type of tube is less likely to leak or crack during rotation, reducing the potential for laboratory contamination from the human breast tissue.
6. The use of plastic aspirating pipettes greatly reduces the possibility of sharp injuries from glass potentially contaminated with blood-borne pathogens.
7. Lentiviral particles are available from a number of commercial sources. Lentivirus is particularly good for generating stable lines from primary stromal cells, because the virus infects both proliferating and non-proliferating cells. Alternatively, vectors encoding hTERT for generation of lentivirus or retrovirus as well as packaging and envelope plasmids are available from Addgene. For generation of viruses in the laboratory, 293T packaging cells can be obtained from ATCC (CRL-3216). After selection, the immortalized stromal cells can be further modified to overexpress other genes, growth factors and proteases, such as transforming growth factor beta, hepatocyte growth factor, or vascular endothelial growth factor. Lentiviruses can also be purchased to create stable cell lines encoding these genes. When selecting a second lentiviral construct, it is necessary to choose lentiviruses that encode a second selectable target, such as resistance to a different antibiotic or expression of a separate fluorescent protein.
8. In order to generate tumors, our laboratory routinely uses lentivirus for SV40 T antigen and mutant KRas G12V, which are both commercially available (abm and GenTarget, Inc, respectively). Other oncogenes may be utilized and are available from other commercial vendors. Alternatively, constructs for oncogenes in lentivirus plasmids as well as packaging and envelope plasmids can be obtained from Addgene and 293T cells from ATCC (CRL-3216) for generation of lentivirus in the laboratory.
9. We have found that protamine sulfate is less toxic to primary epithelial cells than polybrene (hexadimethrine bromide). Polybrene can be used in place of protamine sulfate at a concentration of 8 μg/mL.
10. For analgesia, we treat mice with ketoprofen at a dose of 2–5 mg/kg subcutaneously every 12–24 h. Alternatively, buprenorphine may be administered subcutaneously or intraperitoneally at a dose of 0.05–0.1 mg/kg. However, buprenorphine is a controlled substance and has strict regulations for its usage. The institutional laboratory animal veterinarian can provide guidance for analgesia as necessary.

11. After clearance with Surgical Pathology, the tissue should remain in a closed specimen cup on ice until mincing and collagenase digestion. Recovery of viable cells is maximal if the tissue is processed on the same day as the surgery.
12. Following incubation, if the digestion media contains tissue pieces >2 mm^3, the tissue may not have been minced enough in Subheading 3.1 **step 1** or the tubes were filled with too much tissue which inhibited collagenase digestion (Subheading 3.1 **step 2**).
13. The oil/fat layer is enriched for mature adipocytes, although the cells that grow in culture will not be a pure population of adipocytes. This layer can be plated in Fibroblast Media on tissue culture plates, and adipocytes without lipid droplets will grow within 3–7 days.
14. To aliquot cells for freezing, we usually freeze one vial for each 15 mL digestion tube. Although this method usually results in $2–3 \times 10^6$ epithelial cells in each vial, the number of epithelial cells isolated from organoids can be variable depending on the patient tissue sample. To enhance viability after thawing, each vial of cells should be cooled to −80 °C in an isopropanol-based cooling chamber, then transferred to liquid nitrogen for long-term storage.
15. Thaw vials of cells quickly in 37 °C water bath. Immediately after the media in the cryovial is thawed, dilute the cells in Fibroblast Media and plate on tissue culture 100 mm × 20 mm plates.
16. Immortalized fibroblasts grow quickly and may become confluent in several days. We recommend expanding the fibroblasts following selection and freezing back stocks for storage in liquid nitrogen. Immortalized fibroblasts may grow poorly and need to be replaced by a different stock if the cells are grown too sparsely or confluently. During passaging, the cells will optimally be split at a 1:3 or 1:4 dilution. To minimize genetic variations between experiments, we maintain a culture of fibroblasts for ten passages, and then replace them with frozen stocks. Generally, an 80–90 % confluent 150 mm × 25 mm plate will yield $2–4 \times 10^6$ cells.
17. Surgical clips should be removed at least 1–2 days prior to the next surgery for implanting mammary epithelial cells. This allows any remaining swelling in the tissue to reduce prior to the next surgical procedure.
18. The organoid pellet is enriched for mammary epithelial cells. However, there are still fibroblasts present in the pellet. Plating the cells in Fibroblast Media for 2 h depletes the fibroblasts in our experience by approximately 50 %, although this may be patient sample-dependent or dependent upon the collagenase digestion efficiency.

19. The fibroblasts depleted from the organoid fraction can be maintained by feeding the cells that adhered to the plate with Fibroblast Media. The fibroblasts grow faster than any remaining epithelial cells, leading to a pure culture of stromal cells within a couple of passages. Fibroblasts cannot be easily differentiated from adipocytes growing in this culture, since adipocytes grown in culture lose their lipid droplets.
20. We generally add 1×10^6 colony forming units of lentiviral particles to 5×10^5 epithelial cells for a multiplicity of infection of 3. However, depending on the size of the target gene, it may be necessary to titer the appropriate amount of the virus needed to obtain acceptable infections. In planning the number of epithelial cells to infect for each experiment, we plate and infect 2–3 times more cells than the number that we will need for the injections the following day. Dissociation of cryopreserved organoids and overnight infection with lentiviruses decreases epithelial cell viability. By plating at least twice the number of cells that we need for our experiment, we will have an acceptable yield of viable cells the following day.

Acknowledgements

The author would like to thank Victoria Thompson for helpful discussions. This work is supported by the Susan G. Komen Foundation.

References

1. Kalluri R, Zeisberg M (2006) Fibroblasts in cancer. Nat Rev Cancer 6:392–401
2. Korkaya H, Liu S, Wicha MS (2011) Regulation of cancer stem cells by cytokine networks: attacking cancers inflammatory roots. Clin Cancer Res 17:6125–6129
3. Chiarugi P (2013) Cancer-associated fibroblasts and macrophages: friendly conspirators for malignancy. Oncoimmunology 2:e25563
4. Bhowmick NA, Neilson EG, Moses HL (2004) Stromal fibroblasts in cancer initiation and progression. Nature 432:332–337
5. Pickup MW, Mouw JK, Weaver VM (2014) The extracellular matrix modulates the hallmarks of cancer. EMBO Rep 15:1243–1253
6. Clark AG, Vignjevic DM (2015) Modes of cancer cell invasion and the role of the microenvironment. Curr Opin Cell Biol 36:13–22
7. Klemm F, Joyce JA (2015) Microenvironmental regulation of therapeutic response in cancer. Trends Cell Biol 25:198–213
8. Arendt LM, McCready J, Keller PJ, Baker DD, Naber SP, Seewaldt V et al (2013) Obesity promotes breast cancer by CCL2-mediated macrophage recruitment and angiogenesis. Cancer Res 73:6080–6093
9. Proia TA, Keller PJ, Gupta PB, Klebba I, Jones AD, Sedic M et al (2011) Genetic predisposition directs breast cancer phenotype by dictating progenitor cell fate. Cell Stem Cell 8:149–163
10. Keller PJ, Arendt LM, Skibinski A, Logvinenko T, Klebba I, Dong S et al (2012) Defining the cellular precursors to human breast cancer. Proc Natl Acad Sci U S A 108:7950–7955
11. Arendt LM, Rudnick JA, Keller PJ, Kuperwasser C (2010) Stroma in breast development and disease. Semin Cell Dev Biol 21:11–18

Chapter 19

CRISPR/Cas9 Genome Editing as a Strategy to Study the Tumor Microenvironment in Transgenic Mice

Yojiro Yamanaka

Abstract

Development of engineered site-specific endonucleases like zinc finger nucleases (ZFNs), transcription activator-like effector nucleases (TALENs), and CRISPR/Cas9 has been revolutionizing genetic approaches in biomedical research fields. These new tools have opened opportunities to carry out targeted genome editing in mouse zygotes without the need for manipulating embryonic stem cells, which have a higher technical burden and many constraints in strain availability. Specific genetic modifications can be directly generated in working genetic backgrounds. This new approach saves time and costs associated with generation and backcrossing of genetically modified animals and will facilitate their use in various cancer research fields.

Key words CRISPR/Cas9, Double strand DNA breaks (DSBs), Nonhomologous end joining (NHEJ), Homology directed repair (HDR), Mouse zygotes, Blastocysts, sgRNAs

1 Introduction

Cancer is not a simple disease caused by abnormally proliferating cells but rather a complex disease generated by the interaction between abnormal cancer cells and the host noncancerous microenvironment [1–3]. The host microenvironment can initiate immunological reactions that reject cancer cells. But it can also facilitate cancer growth, invasion and even metastasis. Thus, the tumor microenvironment created by interactions between cancer and host cells has been a recognized critical factor in cancer progression. Many cancer research laboratories use mouse animal models, particularly genetically modified mice. However, the majority of these studies focus on the mutations causing cancer instead of the permissive host microenvironment facilitating cancer progression. Alternatively, there are isograft and xenograft cancer models used to study invasion and metastasis but once again, most studies using these models focus on the changes in cancer cells and not in the host. Since the cancer-host interactions are

Josie Ursini-Siegel and Nicole Beauchemin (eds.), *The Tumor Microenvironment: Methods and Protocols*, Methods in Molecular Biology, vol. 1458, DOI 10.1007/978-1-4939-3801-8_19,

so important for cancer progression, and thus for patient survival, a strategy to study genes important for cancer progression in normal host cells is much needed.

Engineered site-specific endonucleases like ZFNs/TALENs/CRISPR/Cas9 are a novel genome manipulation tool [4]. They can be engineered to recognize a specific DNA sequence in the genome to introduce DNA double strand breaks (DSBs). Since ZFNs and TALENs use a protein–DNA interaction for DNA sequence recognition, designing and assembling them to target new DNA loci requires considerable expertise and intensive molecular biology work. However, the CRISPR/Cas9 system, which was originally identified as a bacterial adoptive immune system [5], is significantly easier to design and construct for targeting new loci due to its RNA-DNA based interaction; demanding a lower threshold for biotechnology expertise and time commitment. The ease of making highly specific and efficient genome targeting tools makes the CRISPR/Cas9 system an appealing option in various medical research fields [6]. The current CRISPR/Cas9 system often used in eukaryotic cells, consists of two components: a codon-optimized Cas9 endonuclease, derived from *Streptococcus pyogenes*, fused with nuclear localization signal (NLS), and a small guide RNA (sgRNA) which forms a complex with the Cas9 protein (Fig. 1). The protospacer adjacent motif (PAM) sequence is the minimum sequence requirement for target site selection in the genome, but is usually managed without significant tradeoffs due to its small sequence (e.g., the PAM sequence for *Streptococcus pyogenes* Cas9 is 5′-NGG-3′). Generally, the 19–20 nt sequence upstream of the PAM sequence is used as a guide sequence to design specific sgRNAs. The last 10–12 nt adjacent to the PAM sequence, called the seed sequence, is critical for sgRNA specificity.

When the sgRNA/Cas9 complex is reconstituted in cells, it efficiently introduces DSBs at a specific DNA locus. This activates the DNA repair mechanisms in cells (Fig. 2) [4, 6]. When homologous donor DNA is not available, the nonhomologous

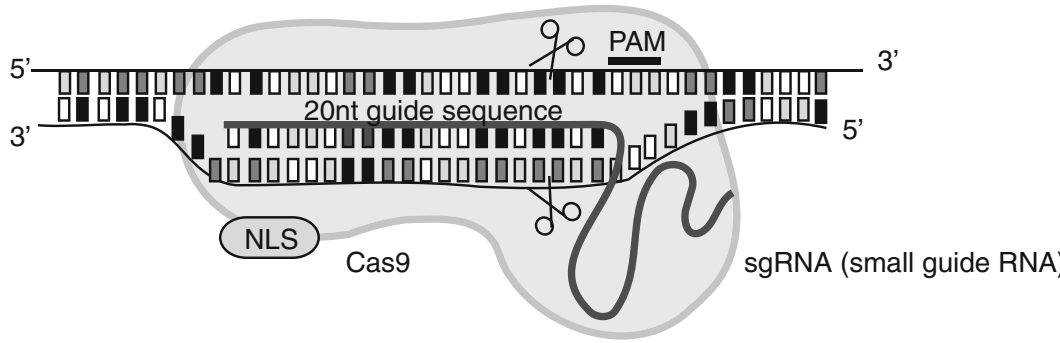

Fig. 1 Diagram of a sgRNA/Cas9 complex recognizing a targeting DNA sequence. A 19–20 nt guide sequence at the 5′ end of sgRNA is used for DNA sequence recognition. DNA double strand breaks are generated 3–4 bp upstream of the PAM sequence. *PAM* protospacer adjacent motif, *NLS* nuclear localization signal, *sgRNA* small guide RNA

end-joining (NHEJ) pathway, which is generally considered to be error-prone, is activated. The two break ends are directly ligated, but a small indel (insertion or deletion) mutation is often created during ligation. Alternatively, when homologous donor DNA is available, the homology-directed repair (HDR) pathway is activated. Similar to homologous recombination in ESCs, this process allows making precise specific genome modifications.

In this chapter, we focus on two experimental approaches to use the CRISPR/Cas9 system in mice: NHEJ-based mutagenesis to study loss of function of genes and HDR-based introduction of small genome modifications with single strand oligo DNAs. There are no mouse strain restrictions to use these approaches. Desired genetic modifications can be directly generated in researchers' working genetic backgrounds (e.g., C57/B6, FVB and NOD-SCID).

2 Materials

2.1 sgRNA and Cas9

1. pX330-U6-Chimeric_BB-CBh-hSpCas9: encoding codon-optimized Cas9 endonuclease and U6 promoter-driven sgRNA cassette (Addgene).
2. Cas9 mRNA (Millipore-Sigma).

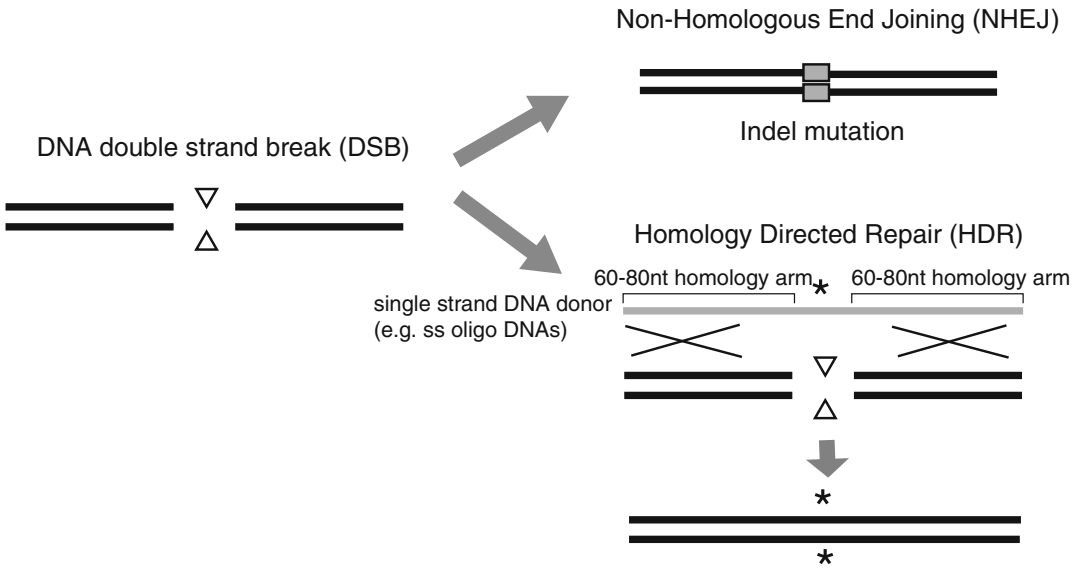

Fig. 2 Two DNA repair mechanisms activated by DNA double strand breaks. DNA-DSBs can activate two DNA repair mechanisms in a cell. (*Top*) When there is no homologous donor DNA, the nonhomologous end-joining (NHEJ) pathway is activated. The two break ends are directly ligated, but a small indel (insertion or deletion) mutation is often created during ligation. (*Bottom*) Single strand oligo (ssOligo) DNA can be the donor DNA for the homology directed repair (HDR) pathway. Specific sequence modifications can be introduced in ssOligo DNAs. Homology arms of 60–80 nt at both ends of the modification are required for efficient HDR events

2.2 sgRNAs Synthesis

1. PCR primers:

   T7-$N_{1–20}$-sgRNA scaffold: (60 nt, 5′-TTAATACGACTCACTATAGG—$N_{1–20}$—GTTTTAGAGCTAGAAATAGC-3′).

   sgRNA-R: (20 nt, 5′-AAAAGCACCGACTCGGTGCC-3′).
2. 10× PCR buffer (100 mM Tris–HCl, pH 8.3, 500 mM KCl, 15 mM $MgCl_2$).
3. TAE buffer (40 mM Tris, 20 mM acetic acid, 1 mM EDTA).
4. Taq DNA polymerase or high stringency DNA polymerase.
5. Gel/PCR DNA fragments extraction kit (Geneaid or equivalent).
6. MAXIscript T7 kit (Thermo Fisher) or equivalent.

2.3 Genotyping

1. A pair of genomic PCR primers for a targeting site.
2. REDExtract-N-Amp™ Tissue PCR kit (Millipore-Sigma).
3. T7 endonuclease I (New England Biolabs).
4. 10× NEBuffer 2 (New England Biolabs; 500 mM NaCl, 100 mM Tris–HCl, pH7.9, 100 mM $MgCl_2$, 10 mM DTT).

2.4 Mouse Embryo Culture

1. KSOM/M2/mineral oil (Zenith Biotech).

3 Methods

3.1 Selecting Genome Targeting Sites and Designing sgRNAs

1. The gene information and genomic structure of a gene of interest are retrieved from the MGI database (http://www.informatics.jax.org/).
2. Potential targeting areas (250–500 bp) are selected based on project goals, its intron–exon structure and protein functional domains (*see* **Note 1**).
3. Identify potential targeting sites using Web-based sgRNA designing platforms (*see* **Note 2**).
4. Select 2–3 potential targeting sites based on predicted specificity and efficiency (*see* **Note 3**).
5. Order 60 nt T7-N_{1-20}-sgRNA scaffold and sgRNA-R primers.

3.2 sgRNA Synthesis

3.2.1 PCR Generation of T7 Promoter-Attached sgRNA DNA Templates

1. PCR reaction solution (20 μL/tube × 4 tubes/single sgRNA reaction):

5 μL	2 μM T7-$N_{1–20}$-sgRNA scaffold primer
5 μL	2 μM sgRNA-R primer
2 μL	10× PCR buffer

0.2 μL	20 mM dNTPs
1 μL	pX330 (40 ng/μL)
6.55 μL	H_2O
0.25 μL	Taq polymerase

2. PCR condition:

5 min	94 °C	
30 s	94 °C	30 cycles
40 s	58 °C	
40 s	72 °C	
5 min	72 °C	
Hold	12 °C	

3. After the PCR reaction, purify the PCR product with a PCR purification kit (Geneaid or equivalent) following the instruction of the kit.
4. Transfer and combine the reaction product (~80 μL) to a new 1.5 mL tube.
5. Following the kit's instruction, add 400 μL of DF buffer and mix well.
6. Transfer the sample mixture to a column.
7. Centrifuge at 20K×*g*, 30 s and discard the flow-through.
8. Add 600 μL of washing buffer and centrifuge again.
9. Centrifuge at 20K×*g*, 3 min to dry the column matrix.
10. Elute the PCR product with 30 μL of the elution buffer (10 mM Tris–HCl, pH 8.5).
11. Measure DNA concentration and check the integrity of the product on a 2% agarose gel run in 1× TAE buffer.

3.2.2 In Vitro RNA Transcription for sgRNA

1. T7 RNA polymerase reaction is performed with the MAXIscript T7 kit, following the kit's instruction (20 μL/tube):

10 μL	30–50 ng/μL purified T7-sgRNA PCR-amplified template
2 μL	10× T7 reaction buffer
4 μL	2.5 mM NTPs
2 μL	H_2O
2 μL	T7 RNA polymerase

2. Incubate at 37 °C for 1–2 h.
3. Add 1 μL of DNaseI and incubate at 37 °C for 15 min.
4. Add 115 μL of RNase-free water and 15 μL of 5 M Ammonium acetate.
5. Add an equal volume of phenol and $CHCl_3$ and mix vigorously.
6. Centrifuge at 20K×*g* for 10 min and transfer the aqueous phase to a new 1.5 mL tube.
7. Add an equal volume of isopropanol and mix well. Store at −20 °C for 30 min or overnight.
8. Centrifuge at 20K×*g* for 10 min and discard the supernatant. Rinse the pellet twice with 70% ethanol.
9. Completely remove the liquid with a 20 μL pipette. Do not let the pellet dry (*see* **Note 4**).
10. Add 5–10 μL of RNase-free water and dissolve the RNA pellet completely.
11. Measure the RNA concentration.
12. Store at −20 °C.

3.3 Designing and Validation of a Pair of Genomic PCR Primers for Genotyping

It is very important to design a pair of genomic PCR primers and validate if they can generate a single PCR product from mouse tissue DNA samples before microinjection experiments.

1. Using Primer3Plus (http://www.bioinformatics.nl/cgi-bin/primer3plus/primer3plus.cgi/), a pair of genomic PCR primers are designed such that the size of a PCR product is 300–800 bp encompassing the CRISPR targeting site.
2. Test and optimize PCR conditions with genomic DNA from mouse tissues (e.g., tails, ear punches, or blastocysts).

3.4 Microinjection, Embryo Culture, and Implantation

Microinjection of sgRNA/Cas9 mRNA solutions into zygotes is performed as traditional pronuclear or cytoplasmic microinjections. You may need to discuss this with the technicians responsible for such microinjections in your core facility.

1. Prepare 10 μL sample solution in a 1.5 mL tube (*see* **Note 5**).

   10–100 ng/μL of sgRNAs

   10–100 ng/μL of Cas9 mRNA

   1 μM of ssOligo DNA for HDR with ssOligo DNA in RNase-free H_2O (or in 10 mM KCl).
2. Centrifuge at 20K×*g* for 15 min to remove small debris potentially clogging the microinjection pipets.
3. Gently transfer 7 μL of the supernatant to a new 1.5 mL tube.
4. Proceed with microinjection.

The injected zygotes are cultured overnight in KSOM droplets under mineral oil in a 35 mm dish at 37 °C in a 5% CO_2 incubator. The embryos developed to the 2-cell stage are transferred to oviducts of pseudopregnant females. Some injected embryos can be cultured for another 3–4 days for blastocyst genotyping (*see* **Note 6**).

3.5 Blastocyst Genotyping [7]

3.5.1 Genomic DNA Preparation from Blastocysts

1. 3–4 days after injection, the cultured injected embryos should become blastocysts.
2. Each embryo is transferred into DNA extraction solution (4.4 μL of extraction solution + 1.1 μL of tissue preparation solution/tube) in a PCR tube using a mouth pipette under a dissecting microscope.
3. Run the program below on a PCR machine.

20 min	25 °C	1 cycle
30 min	56 °C	
5 min	95 °C	
Hold	12 °C	

4. Add 4.4 μL of neutralizing solution and mix well. Store in a −20 °C freezer.

3.5.2 Genomic PCR from Single Blastocysts

1. PCR reaction solution (20 μL/tube)

10 μL	REDExtract-N-Amp PCR Ready Mix (Millipore-Sigma or equivalent)
1 μL	10 μM forward primer
1 μL	10 μM reverse primer
5.5 μL	H_2O
2.5 μL	DNA extract from single blastocysts

2. PCR condition

5 min	94 °C	
30 s	94 °C	40 cycles
40 s	54–65 °C	
45 s	72 °C	
5 min	72 °C	
Hold	12 °C	

3. The PCR product can be used for the T7E1 assay, restriction fragment length polymorphism (RFLP) assay and Sanger sequencing to analyze mutations (*see* **Note 7**)

3.6 T7 Endonuclease I Assay

1. Denature and reanneal the PCR product.

PCR machine conditions:		
3 min	95 °C	
5 min	90 °C	RAMP at −0.1 °C/s
5 min	85 °C	RAMP at −0.1 °C/s
5 min × 11 steps	every −5 °C	
5 min	25 °C	RAMP at −0.1 °C/s
Hold	12 °C.	

2. T7E1 assay (10 μL/tube)

10× NEBuffer 2	1 μL
Annealed PCR product	7 μL
H_2O	1.9 μL
T7E1 enzyme	0.1 μL

3. Incubate at 37 °C for 20–30 min (*see* **Note 8**).
4. Run samples on a 2% agarose gel in 1× TAE buffer with controls (i.e., no T7E1 enzyme).

4 Notes

1. Selecting targeting genome areas

   1.1 *For NHEJ-based mutagenesis* [8]

   A protein coding exon should be targeted. Theoretically, two thirds of indel mutations would be frame-shift mutations, but one third would be in-frame mutations. Depending on targeting sites, in-frame mutations could generate fully functional proteins, reduced functions (hypomorph) or dominant-negative proteins.
   We consider three points for successful sgRNAs design for NHEJ based mutagenesis:

   1. Targeting an early exon:

      Advantage: when a frame-shift mutation is introduced, the chance of introducing a nonsense mutation early on is high and it is more likely to create a null allele. Nonsense-mediated mRNA decay would be also induced.
      Risk: an in-frame mutation would create a fully functional protein.

2. Targeting an exon coding a highly conserved functional domain:

   Advantage: Unlike targeting an early exon, even an in-frame mutation will yield a functionally compromised protein due to the relative importance of eliminating key catalytic/structural amino acids within the domain.
   Risk: Partial products or dominant-negative forms might be inadvertently created.

3. Targeting a splice donor/acceptor:

   Advantage: A proper exon–intron structure could be destroyed. The number of indel sizes is not an issue.

   A general limitation of NHEJ-based mutagenesis is that, if a targeting gene has alternative start sites or splicing variants, the effect of mutations would be limited.

1.2 For HDR-based genome modification with ssOligo DNAs [9, 10]

The HDR-based genome modification with ssOligo DNAs is a very powerful strategy to introduce sequence-specific genome modifications (e.g., introducing SNPs, inserting a tag sequence and a loxP site, and deleting transcriptional factor recognition sites). 60–80 nt homology arms at the both end of modification are often used (Fig. 2). To have efficient HDR events, DSB and a modification site should be closer (less than 50 bp is recommended) [11]. If the selection of sgRNAs is limited in specificity, double Nickase approaches could be considered [12].

2. Web-based sgRNA designing platforms

   There are many useful sites to design sgRNAs with various selection criteria. We often use the following three sites and compare their outcomes.

   - CHOPCHOP (https://chopchop.rc.fas.harvard.edu/index.php) [13]. This site is useful to select sgRNAs for NHEJ mutagenesis. By entering a gene of interest, the site will provide potential targeting sites with its exon–intron structure and ranking of specificity.
   - CRISPR/Resources (MIT Zhang lab. http://crispr.mit.edu/).To use this site, a targeting area (smaller than 250 bp) in the genome should be selected. By submitting the sequence of interest, the site will provide potential targeting sites with potential off-targeting sites and ranking of specificity. In this site, sgRNAs targeting intronic and noncoding genomic regions can

be designed. This site also provides information for double Nickase approaches.

- Sequence Scan for CRISPR (http://crispr.dfci.harvard.edu/SSC/) [14].This site provides predictive values of targeting efficiency of sgRNAs. It has been recognized as a variation of targeting efficiency in sgRNAs. Xu et al. identified preferential seed sequence patterns in sgRNAs efficiently cutting targeting sites [14]. By entering a potential targeting sequence, the site provides potential sgRNAs with positive and negative predictive values of targeting efficiency.

3. It is worthwhile generating 2–3 sgRNAs to a single targeting area and testing their efficiency in embryos (e.g., blastocyst genotyping) or in cultured cells to select the best one.
4. RNA pellets need to be fully dissolved in water for microinjection. Don't let them dry. It is very difficult to fully dissolve dried RNA pellets.
5. The microinjection conditions can be modified depending on the efficiency/specificity of sgRNAs, lethality of target gene modifications and goals of experiments. For example, if the goal is to recover homozygous mutants in high frequency in the F0 generation, the concentration of sgRNA/Cas9 mRNA can be set higher. However, if the goal is to recover heterozygous mutants, it can be lower.
6. It is important to check the targeting efficiency of each sgRNA in blastocysts before setting up larger experiments to establish mouse lines.
7. Sanger sequencing can be performed directly on PCR products or after subcloning. For precise characterization of mutations, sequencing after subcloning is recommended. Due to the timing of DNA repair events, more than three alleles could be identified (i.e., the repair events happen after the S-phase of the zygote). In this case, the embryo/mouse becomes genetically mosaic.
8. To minimize false positives, the T7E1 assay is performed with fresh PCR products. Do not exceed 40 min for the T7E1 reaction. Longer incubation would cause nonspecific digestion and generate false positives.

Other useful websites:

CRISPR/Cas9 Plasmids and Resources (Addgene, https://www.addgene.org/crispr/).
E-CRISP (German Cancer Research Center, http://www.e-crisp.org/E-CRISP/).
OMIC Tools (http://omictools.com/crispr-cas9-c1268-p1.html).

Acknowledgements

I thank Aaron Kwong and Nobuko Yamanaka for valuable comments. I also thank the past and present members of Yamanaka lab and the Goodman Cancer Research Centre Transgenic facility for optimizing our protocols. Y.Y. is supported by CIHR (MOP111197) and NSERC (RGPIN418720).

References

1. Egeblad M, Nakasone ES, Werb Z (2010) Tumors as organs: complex tissues that interface with the entire organism. Dev Cell 18(6):884–901
2. Joyce JA, Pollard JW (2009) Microenvironmental regulation of metastasis. Nat Rev Cancer 9(4):239–252
3. Quail DF, Joyce JA (2013) Microenvironmental regulation of tumor progression and metastasis. Nat Med 19(11):1423–1437
4. Gaj T, Gersbach CA, Barbas CF III (2013) ZFN, TALEN, and CRISPR/Cas-based methods for genome engineering. Trends Biotechnol 31(7):397–405
5. Barrangou R (2015) The roles of CRISPR-Cas systems in adaptive immunity and beyond. Curr Opin Immunol 32:36–41
6. Hsu PD, Lander ES, Zhang F (2014) Development and applications of CRISPR-Cas9 for genome engineering. Cell 157(6):1262–1278
7. Stephenson RO, Yamanaka Y, Rossant J (2010) Disorganized epithelial polarity and excess trophectoderm cell fate in preimplantation embryos lacking E-cadherin. Development 137(20):3383–3391
8. Wang H, Yang H, Shivalila CS, Dawlaty MM, Cheng AW, Zhang F et al (2013) One-step generation of mice carrying mutations in multiple genes by CRISPR/Cas-mediated genome engineering. Cell 153(4):910–918
9. Yang H, Wang H, Shivalila CS, Cheng AW, Shi L, Jaenisch R (2013) One-step generation of mice carrying reporter and conditional alleles by CRISPR/Cas-mediated genome engineering. Cell 154(6):1370–1379
10. Chen F, Pruett-Miller SM, Huang Y, Gjoka M, Duda K, Taunton J et al (2011) High-frequency genome editing using ssDNA oligonucleotides with zinc-finger nucleases. Nat Methods 8(9):753–755
11. Inui M, Miyado M, Igarashi M, Tamano M, Kubo A, Yamashita S et al (2014) Rapid generation of mouse models with defined point mutations by the CRISPR/Cas9 system. Sci Rep 4:5396
12. Ran FA, Hsu PD, Lin CY, Gootenberg JS, Konermann S, Trevino AE et al (2013) Double nicking by RNA-guided CRISPR Cas9 for enhanced genome editing specificity. Cell 154(6):1380–1389
13. Montague TG, Cruz JM, Gagnon JA, Church GM, Valen E (2014) CHOPCHOP: a CRISPR/Cas9 and TALEN web tool for genome editing. Nucleic Acids Res 42(Web Server Issue):W401–W407
14. Xu H, Xiao T, Chen CH, Li W, Meyer CA, Wu Q et al (2015) Sequence determinants of improved CRISPR sgRNA design. Genome Res 25(8):1147–1157

Chapter 20

Metabolomics Analyses of Cancer Cells in Controlled Microenvironments

Simon-Pierre Gravel, Daina Avizonis, and Julie St-Pierre

Abstract

The tumor microenvironment is a complex and heterogeneous milieu in which cancer cells undergo metabolic reprogramming to fuel their growth. Cancer cell lines grown in vitro using traditional culture methods represent key experimental models to gain a mechanistic understanding of tumor biology. This protocol describes the use of gas chromatography–mass spectrometry (GC-MS) to assess metabolic changes in cancer cells grown under varied levels of oxygen and nutrients that may better mimic the tumor microenvironment. Intracellular metabolite changes, metabolite uptake and release, as well as stable isotope (^{13}C) tracer analyses are done in a single experimental setup to provide an integrated understanding of metabolic adaptation. Overall, this chapter describes some essential tools and methods to perform comprehensive metabolomics analyses.

Key words Metabolomics, Microenvironment, Hypoxia, Nutrients, Stable isotope, Methoximation, Silylation, GC-MS

1 Introduction

Tumor cells evolve in a complex and multifaceted microenvironment. In addition to the influence of stromal cells, immune infiltrates, extracellular matrix, cytokines, and growth factors [1], tumors experience substantial variations in oxygen and nutrient levels that may limit their capacity to grow and proliferate. It is now appreciated that cancer cells have the ability to adapt to nutrient stress by modulating or rerouting various metabolic pathways to meet their survival and biosynthetic needs [2–6]. This biological adaptation is known as metabolic reprogramming, an emerging hallmark of cancer. The tumor microenvironment, especially in solid tumors, is limited in oxygen levels [7, 8]. Cancer cells deprived of oxygen or exhibiting mitochondrial dysfunctions rely on compensatory mechanisms to support ATP synthesis and fuel their growth. Increased reliance on glycolysis and reductive carboxylation of glutamine are examples of such metabolic adaptations [9, 10].

Josie Ursini-Siegel and Nicole Beauchemin (eds.), *The Tumor Microenvironment: Methods and Protocols*, Methods in Molecular Biology, vol. 1458, DOI 10.1007/978-1-4939-3801-8_20,

Ultimately, cancer cells shape their microenvironment and promote structural changes such as angiogenesis to promote their growth. A proper understanding of cancer metabolic reprogramming can reveal metabolic vulnerabilities of cancer cells and therefore help find novel therapeutic targets to fight cancer [11, 12].

Cancer cells have been classically grown in adapted growth media that contain, but are not limited to, D-glucose, essential and nonessential amino acids, cofactor precursors, salts, buffering systems, and optional pH indicators, as well as less well-defined components such as animal serum or pituitary extracts [13]. Cells are placed in a temperature-, CO_2-, and humidity-controlled incubator and monitored on a daily basis for the presence of sufficient growth media and optimal confluency. Since standard tissue culture conditions cannot recapitulate the three-dimensional (3D) complexity of a tumor, 3D-cultures or spheroid models have been developed in an attempt to better mimic cells evolving in a complex tumor microenvironment [14, 15].

Furthermore, cultured cells are usually grown under oxygen and nutrient levels that are much higher than those found in tumors. Increasing media nutrient concentrations is convenient to lighten maintenance labor and eliminate the need for continuous media replacement devices (such as the Nutrostat [16]). Nevertheless, traditional 2D cell culture techniques under low oxygen or nutrient conditions remain an important and attractive research tool due to the high plasticity of culture conditions, the setup of large-scale experiments at low expense, and easy monitoring of cell survival and growth properties. In simplified 2D tissue culture systems, strictly controlled environmental experiments allow for a hypothesis-driven approach that may provide more physiologically relevant data.

Metabolomics is a continuously evolving research field that permits the metabolite profiling of virtually any biological system (model organisms, cells in culture, tissue samples, patient materials, and bio fluids). Metabolomics approaches have been successfully applied in cancer research using cultured cells [17, 18]. Given the diverse nature of metabolites, ranging from molecular size, charge, and polarity, there is no unique methodology to precisely study all metabolites in a given sample. The extraction procedure and chromatography conditions dictate which class of metabolites can be measured with optimal accuracy. Although the combination of sequential extraction procedures coupled with the use of multiple chromatographic columns allows to broaden metabolite coverage, simple methodologies using only one extraction procedure and one chromatographic method are most commonly used for targeted analysis of specific metabolite classes. There are numerous methodologies available depending on the pathway of interest. One common experimental approach is the GC-MS methods for methoxime-TBDMS (*tert*-butyldimethylsilyl) derivatized samples.

They have been applied successfully to amino acids and small metabolites of central metabolic pathways (glycolysis, citric acid cycle) in a variety of studies [19–21]. This methodology involves two sequential reactions. First, labile α-ketoacid species, such as pyruvate and α-ketoglutarate, are converted to methoximes, improving their stability and limiting the number of potential chromatographic peaks that can result from enolization reactions. Second, silylation with MTBSTFA (*N-tert*-butyldimethylsilyl-*N*-methyltrifluoroacetamide) increases the volatility of compounds and greatly improves resistance to hydrolysis. Metabolite identification requires knowledge of derivatized metabolite structures and fragmentation pattern (for electron ionization MS), as well as comparison with known MS patterns from publicly available or homemade libraries and authentic standards.

In addition to permitting metabolite quantification in culture media or inside cells, the GC-MS methods for methoxime-TBDMS derivatized samples allow researchers to study the fate of substrates into metabolic pathways using stable isotope tracers. Stable isotopes are nonradioactive atoms that possess extra mass units due to the presence of supernumerary neutrons. Commonly used stable isotope tracers are nutrients, such as D-glucose, L-glutamine, or cell-permeable metabolites where carbons (^{12}C) or nitrogens (^{14}N) are replaced with ^{13}C ($^{12}C+1$ atomic mass) or ^{15}N ($^{14}N+1$ atomic mass), respectively. Tracer molecules where deuterium is replaced by hydrogen can also be used, but great care must be taken to ensure that there is no hydrogen–deuterium exchange under the experimental conditions used, and no effect on metabolism due to the heavy deuterium atom replacement. The choice of labeling pattern (specific atoms or all atoms) within a tracer compound is an essential part of the experimental design. Cells will use the stable isotope tracer indistinctly from unlabeled counterparts (except for the potential case when deuterium labeling is used). The tracer will progressively fill the metabolic pathways until saturation of metabolite pools where additional mass units ($m+1$, +2, etc.) can be monitored by MS. Importantly, two types of analyses can be made from these experiments. First, detailed kinetics analyses of metabolite labeling allow an estimation of the speed at which metabolite pools are being labeled within a metabolic pathway. Second, labeling to saturation (isotopic steady state) allows for the determination of the fraction of metabolite being labeled from a given tracer (fractional contribution) [22, 23]. Before undertaking stable isotope tracer analysis, it is important that the pathways and pathway branch points be studied to select for the most informative labeled compound. Also, many preliminary studies are required to determine tracer exposure time and dose as well as detection by GC-MS or other techniques. Therefore, this technique requires extensive planning and pilot studies to ensure that the global experimental setup is optimal for the desired information.

The GC-MS methods for methoxime-TBDMS analysis outlined in this chapter allow for the quantification of intracellular metabolite levels as well as culture media analysis for uptake or release studies. We provide only select modified cell culture conditions of the many that are possible to mimic the complex tumor microenvironment. These serve only as an avenue to provide some advice for successful experimental planning. Finally, the fundamental steps of stable isotope tracer experiments are based on a detailed and recent comprehensive review written by leaders in metabolomics [24]. With proper experimental planning, as outlined here, it is possible to set up all of the necessary cell culture conditions to perform the following three experimental analyses (Figs. 1 and 2): (1) Media dynamics (uptake/release of metabolites); (2) Cellular steady-state metabolite levels; and (3) Stable isotope tracer analysis for specified pathways. Together, these analyses will provide a comprehensive understanding of the metabolic reprogramming of cancer cells under conditions that aim to better mimic the tumor microenvironment.

2 Materials

2.1 Culture of Human Cancer Cells and Tumor Microenvironment Mimicry

1. BT-474 human breast cancer cell line (*see* **Note 1**).
2. Basal culture media: add 50 mL fetal bovine serum (FBS) and 5 mL of a 100× penicillin/streptomycin solution to a 500 mL sterile bottle of DMEM containing 25 mM (4.5 g/L) d-glucose, 4 mM (584 mg/L) L-glutamine, sodium bicarbonate, 1 mM (110 mg/L) sodium pyruvate, and phenol red. All components should be certified sterile, otherwise filter the prepared media into an autoclaved bottle using a 0.2 μm bottle-top filter under a certified tissue culture hood.
3. Tumor microenvironment mimicry media (*see* **Note 2**): this media consists of D-glucose, L-glutamine, and sodium pyruvate deficient DMEM in which the following components are added (1/7 of the basal media concentration): 3.57 mM D-glucose, 571.4 μM L-glutamine (*see* **Note 3**), 1.43% dialyzed FBS, and 1× penicillin/streptomycin. All components should be certified sterile, otherwise filter the prepared media in an autoclaved bottle using a 0.2 μm bottle-top filter under a certified tissue culture hood.
4. Normoxic incubator: for basal conditions, use a water-jacketed incubator set at 5% CO_2 and 37 °C. Follow the manufacturer's instructions for CO_2 and humidity control.
5. Hypoxic incubator set at 3% O_2, 5% CO_2 and 37 °C, with nitrogen tank. Follow manufacturer's instructions for N_2/O_2, CO_2, and humidity control.

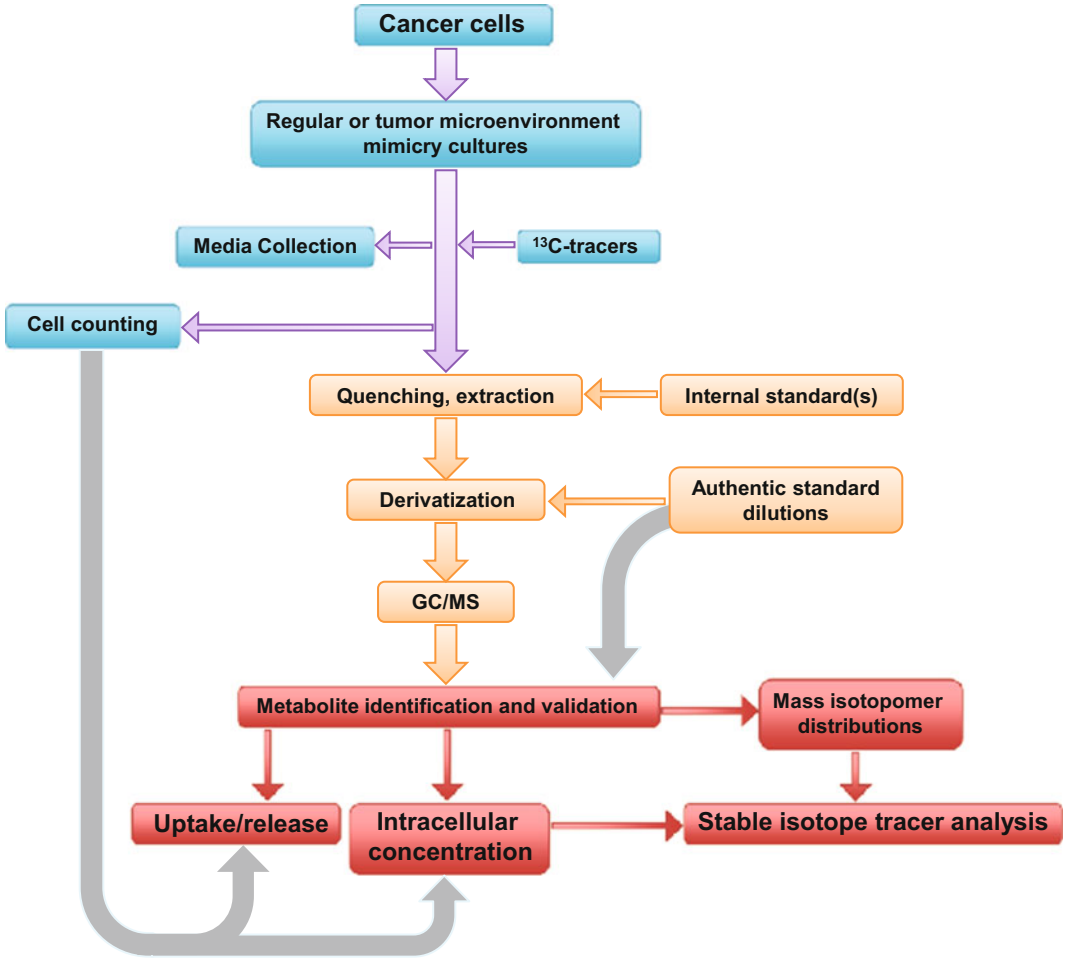

Fig. 1 Experimental workflow. *Blue*: steps involving handling of cancer cells. These steps are performed in a laboratory equipped with certified laminar flow hoods and cell incubators (normoxia and hypoxia). All steps are performed under sterile conditions, except endpoint assessment of cell counts. *Orange*: steps involving manipulation of cell extracts. Samples should always be kept at 4 °C before derivatization steps. *Red*: Steps involving data analysis and calculations. Cell counts are necessary to calculate metabolite exchanges with media as well as intracellular metabolite levels. Stable isotope tracer analysis (SITA) allows for the determination of the fraction of a labeled metabolite at a given time and the maximal labeling of the pool. To determine the absolute amount of labeled metabolite, it is essential to take into account the metabolite pool size, previously calculated using cell counts

6. Certified laminar hood (HEPA filters).
7. 37 °C water bath to warm up media.
8. Aspiration device.
9. Sterile Pasteur pipets and serological pipets (i.e., 5, 10, 25 mL).
10. Sterile phosphate buffer saline (PBS 1×, commercial).
11. Sterile 0.25 % trypsin in 0.53 mM EDTA solution.

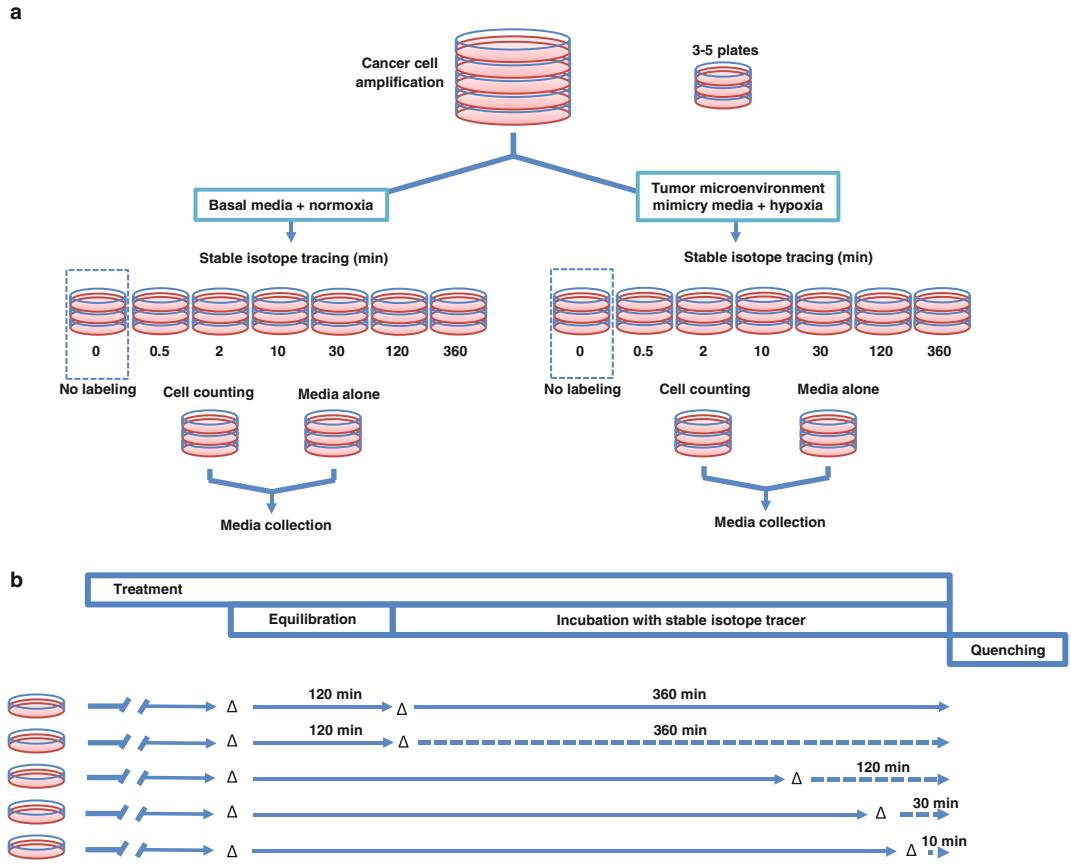

Fig. 2 Schematic depicting a typical experimental setup that permits the quantification of intracellular and extracellular metabolite amounts and the execution of stable isotope tracer experiments. (**a**) Cancer cells can be amplified using multiple 10 or 15 cm plates. Smaller dishes (e.g., 35 mm) are suitable for GC-MS studies. All datasets are minimally composed of biological triplicates. The number of replicates required will depend on the expected biological differences between groups. The setup shown is for 1 day of treatment. Long-term experiments require more plates and daily media changes. (**b**) Typical experimental setup for a stable isotope tracing experiment. *Solid lines* represent unlabeled conditions, *dashed lines* represent incubation with stable isotope tracer. *Open triangle* represents media change. Time is in min

12. Tabletop centrifuge that can accommodate 15 mL tubes.
13. Pipets (i.e., 20 µL, 200 µL, 1 mL) and sterile tips.
14. Stable isotope tracer: D-$^{13}C_6$-glucose (*see* **Note 4**).
15. Analytical balance.
16. 35 mm individual plates or 6-well plates, 10 cm plates, 15 cm plates.
17. Hemocytometer or an automated cell counting device.
18. 70% (v/v) ethanol in water to sterilize surfaces and glassware.
19. Sterile Pyrex bottles with caps.

2.2 Quenching, Extraction, and Derivatization

1. Ice-cold saline (9 g/L NaCl in HPLC-grade water).
2. 80% (v/v) HPLC-grade methanol in HPLC-grade water.
3. 25 mm cell scrapers.
4. Fume hood.
5. Aspiration device.
6. −80 °C freezer.
7. Ultrasonic bath, kept in a cold room.
8. Benchtop vacuum concentrator and pump. The vacuum centrifuge must be able to control the temperature of the samples at 4 °C or colder during the drying process.
9. Chemicals: acetone (ACS grade); methoxyamine hydrochloride (≥98%); anhydrous pyridine (99.8%); *N-tert*-butyldimethylsilyl-*N*-methyltrifluoroacetamide (MTBSTFA); 800 ng/μL myristic acid-D_{27} (C/D/N stable isotopes) in anhydrous pyridine (*see* **Note 5**).
10. Gas-tight syringes (10, 50, 100, 500 μL).
11. Heat-plate set at 70 °C and suitable for GC-MS injection vials.
12. Amber glass injection vials, 200 μL glass inserts, and gas-tight caps.
13. Hand crimper.
14. Sonicator, held at room temperature.
15. 1.5 or 2 mL polystyrene tubes.
16. Refrigerated benchtop centrifuge that accommodates 1.5 or 2 mL tubes.
17. Tube holders.
18. Analytical balance.

2.3 GC-MS Instrumentation

1. Agilent 5975C series GC-MSD with Triple-Axis HED/EM Detector coupled to a 7890A gas chromatograph, equipped with a 7693 auto sampler. Other vendor equivalent instruments can also be used.
2. DB-5MS + DG capillary column, 30 m length, 10 m Duraguard deactivated fused silica tubing, 0.25 mm internal diameter, 0.25 μm film thickness.
3. Ultra-inert liners, splitless, single tapered.
4. Helium (He) tank.
5. Chemicals: Hexanes (≥98.5%), ethyl acetate (99.9%).

3 Methods

Although individual experimental procedures are divided into subsections, all the following steps can be performed in a single experimental setup (Fig. 2).

3.1 Growth of Cancer Cells and Media Collection

1. Plate 200,000–500,000 BT-474 cells (*see* **Note 1**) per well in 35 mm plates in 2 mL basal growth media, such that cells are at 10–25% confluence the next day. Ensure that enough plates are prepared for the whole experimental procedure (Fig. 2). Let the plates sit undisturbed in a normoxic incubator for 24 h.
2. After the 24 h period, aspirate media and replenish with 2 mL of fresh, pre-warmed basal growth media or mimicry media (*see* **Note 6**).
3. Place cell plates growing in basal media in a normoxic incubator, and cell plates growing in mimicry media in a hypoxic incubator. Let sit undisturbed for 24 h.
4. The same day, generate control plates by adding 2 mL of basal or mimicry media to empty dishes and place them in their respective incubators (*see* **Note 6**).
5. The next day, assess the confluency of cells by estimating the surface occupied by cells in the dish.
6. Collect 5–10 μL of media from cell plates that will be used for cell counting and cell-free control dishes with control media alone. Transfer to a prechilled 1.5 mL tube on ice. Add 600 μL 80% (v/v) methanol–HPLC water solution to each tube. For further handling of media samples, proceed immediately to Subheading 3.3, **step 10**.
7. For cell counting, aspirate media from wells and carefully rinse cells with 2 mL room temperature PBS 1×.
8. Aspirate PBS 1× completely and add 250 μL trypsin EDTA solution. Ensure the surface is entirely covered and place the dishes in the normoxic incubator until cell detachment from the plate is visible. Gently tap the plate when only 10% or less of the cells are remaining attached to the plate.
9. Add 250 μL basal growth media and pipet up and down using a pipet while rinsing the well with the cell suspension. Visually inspect that cells are single cells and not clusters of cells under the microscope. Transfer the cell suspension (approx. 0.5 mL) in a 1.5 mL tube.
10. Rinse the empty well with an additional 0.5 mL basal media and pool with the previous suspension such that the volume is now close to 1 mL.
11. Count cells with a hemocytometer or an automated counting device.
12. Repeat **steps 2–11** as many times as needed to generate a cell growth curve (*see* **Note 7**).
13. Generate a cell growth curve for each culture condition by plotting the number of cells (million cells) as a function of time (days).

3.2 Incubation with Stable Isotope Tracers

1. The next day following the beginning of treatment, aspirate media from plates, replace with pre-warmed unlabeled media (basal or mimicry), and allow cells to equilibrate in their respective incubator for at least 2 h (*see* **Note 6** and Fig. 2b).
2. Weigh powdered stable isotope tracer into an empty 1.5 mL tube using an analytical balance.
3. For the two environmental conditions described here weigh enough $^{13}C_6$-glucose to generate sufficient 25 mM (basal) and 3.57 mM (tumor mimicry) solutions for the full experiment. This is achieved by solubilizing the powder in a small amount of glucose-free media using a 1 mL pipet and pipetting up and down. This is then added to the full volume required for the experiment and the tube is rinsed twice to ensure that no concentrated stable isotope tracer is left in the tube and that the desired final concentration is reached.
4. Pre-warm the tracing media in a 37 °C water bath.
5. Aspirate media from wells and replace with 1–2 mL tracing media.
6. Leave cells in the corresponding incubator for time periods ranging from seconds to hours (i.e., 30 s, 2 min, 10 min, 30 min, 2 h, 6 h (*see* **Note 8**)), by changing media in retrograde fashion starting with media for the longest time points (Fig. 2b).
7. Additional cell plates where standard glucose or glutamine (or other non-labeled tracer) is used instead of the isotopically labeled compounds are also prepared. They serve as control plates to validate metabolite detection and quantitation (*see* **Note 9**).
8. Stop the experiment by following the instructions in Subheading 3.3.

3.3 Sample Collection, Quenching, Extraction, and Storage

Rinsing and quenching of cells must be done as quickly as possible after plate retrieval from incubators. Prepare a workspace in advance that has all of the necessary equipment and prechilled solutions handy. Work consistently and keep samples cold at all times. Select plates from the incubator at random to minimize bias. All samples/plates should be extracted at once.

1. Prechill labeled 1.5 mL tubes and 80% (v/v) methanol–water solution on crushed dry ice.
2. Aspirate media, place tissue culture plates on ice, and rinse twice with 2 mL ice-cold saline solution, being careful not to dislodge cells from the plate.
3. Add 300 μL 80% (v/v) methanol–water per plate or well and thoroughly scrape off cells using a cell scraper.
4. Transfer the slurry (liquid and precipitate) to the prechilled tubes.

5. Repeat **steps 3** and **4** one additional time to ensure complete sample collection.
6. Close the 1.5 mL tubes and let sit for a minimum of 10 min on dry ice.
7. At this stage, tubes can be transferred for storage in a −80 °C freezer, or immediately used for extraction. If extraction is to continue, turn on the vacuum centrifuge system to prepare the cold solvent trap and chill the sample vacuum centrifuge area.
8. Fill the ultrasonic bath with a mixture of crushed ice and cold water.
9. Sonicate the tubes following the manufacturer's recommendation and using time and power settings optimized for maximal metabolite recovery.
10. Centrifuge the tubes for 10 min at $\geq 13{,}000 \times g$ at ≤ 4 °C.
11. Prechill labeled 1.5 mL tubes on ice while samples are in the centrifuge (**step 10**).
12. Transfer supernatants to prechilled labeled tubes taking care not to disturb the pellets.
13. Under a fume hood, carefully add 1 μL of myristic acid-D_{27} solution per tube. It is unnecessary to mix at this stage.
14. Quick spin the tubes to ensure that no solution remains in the cap, then transfer the opened tubes, in the vacuum centrifuge at −4 °C.
15. When tubes are completely dry (few hours to overnight—depending on the vacuum centrifuge), these can be stored in a −80 °C freezer or immediately used for derivatization (Subheading 3.4).

3.4 Methoximation and Derivatization

1. If the tubes were stored in a −80 °C freezer, allow them to equilibrate at room temperature for 10–20 min, otherwise proceed immediately to **step 2**.
2. Prepare GC-MS vials by inserting 200 μL glass insert into each vial, capping and labeling the vials.
3. Dissolve 10 mg methoxyamine (MOX) hydrochloride per mL in anhydrous pyridine (*see* **Note 5**). Vortex to ensure complete dissolution, quick spin.
4. Add 30 μL MOX/pyridine solution to each tube using a gas-tight syringe. Vortex tubes for 30 s and sonicate for 30 s in a room temperature sonicator bath.
5. Centrifuge for 10 min at room temperature.
6. Carefully transfer supernatants to GC-MS vials containing glass inserts and incubate for 30 min at 70 °C in a dry bath.
7. Add to each vial 70 μL MTBSTFA (*see* **Note 5**). Vortex briefly.
8. Incubate for 1 h at 70 °C in a dry bath.

9. Samples are ready to be loaded onto the GC-MS auto-sampler (Subheading 3.5).

3.5 GC-MS Method

The GC-MS analyses can be performed on instruments from various suppliers. We present essential parameters for methoxime-TBDMS-derivatized sample analysis using the Agilent system previously described (Subheading 2.3).

1. For consistent retention times, use myristic acid-D_{27} as an internal standard, set the He carrier gas flow rate such that myristic acid-D_{27} has a retention time of 18 min. Note that the helium flow and pressure will need to be adjusted each time the column is cut. The flow and pressure will be instrument- and column-dependent.
2. Set the injector to 280 °C and the auxiliary heater to 300 °C.
3. Set the run so that the GC temperature starts at 60 °C for 1 min followed by an increase of 10 °C/min up to 320 °C.
4. Set Bake-out at 320 °C for 9 min.
5. Operate in full scan mode with a range of 50–700 Da (2.28 scan/s or faster).
6. Set the ion source chamber to 230 °C.
7. Perform the standard tune procedure using gain factor 1 (=1600 V) in EMV mode. Electron energy is set at 69.9 eV.
8. Inject 1 μL of MOX/TBDMS-derivatized samples (splitless). Start acquiring data after a solvent delay of 8.6 min. A sample run lasts around 40 min including bake-out. Samples should be run in a random order to minimize bias. A blank should be run every three or four sample run. Plan derivatization and data collection such that all sample data are collected within a 48 h period, or preferably a 24 h period. Samples are susceptible to oxidation over time.
9. Ensure to program GC syringe washes with ethyl acetate and hexanes before and after each sample.
10. Run blanks (methoximation and derivatization reactions alone) before, throughout and after the run.
11. Ensure that the instrument is tuned and calibrated before the start of the study.

3.6 Standard Curve Preparation

1. For assessment of metabolite levels present in media, prepare dilutions of the metabolites of interest in the corresponding tissue culture media (following **steps 2–4**).
2. Prepare a 30 mM solution of the desired metabolite in cold cell culture media on ice.
3. Prepare serial-fold dilutions (e.g., 10, 3, 1, 0.3, 0.1, 0.03 mM) of the 30 mM solution in cold cell culture media. Mix well between each step.

4. Remove 5 μL of each dilution and proceed to metabolite extraction as done for media samples from tissue culture dishes (Subheading 3.3).
5. For assessment of intracellular metabolite levels, perform standard addition to cell extracts.
6. After derivatization (Subheading 3.4) and GC-MS analysis (Subheading 3.5), plot the ratio of the area under the curve for the metabolite of interest to the area under the curve of the internal standard myristic acid-D_{27} as shown for lactate in Fig. 3a. For all calibrated metabolites, identify the linear range as well as limits of detection where the lower limit of detection is defined as peak signal to noise of 2 and limit of quantitation is defined as a peak having signal to noise of 10 (*see* **Note 10**).

3.7 Metabolite Identification and Quantification

1. Identify metabolites by matching retention time, mass spectrum from previously run standards under the same GC-MS conditions. Select the M-57 (loss of t-butyl group) as the quantifying ion and other unique qualifying ion(s) (Table 1). Ensure that the integrations are within detection limits (Subheading 3.6, *see* **Note 10**).
2. Report metabolite and internal standard (myristic acid-D_{27}) integrations for the quantifying ions.

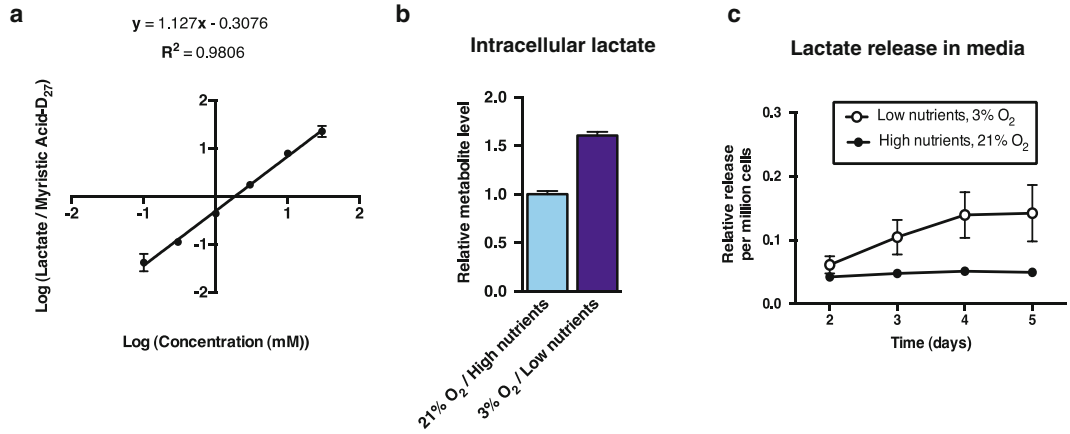

Fig. 3 Typical GC-MS analyses using lactate as an example. (**a**) Lactate standard curve prepared by serial-fold dilutions in basal growth media. This experiment shows that lactate integration is in the linear range between 0.1 and 30 mM. Such tests are performed at least three times independently over a period of time to ensure reproducibility of the curve. (**b**) Intracellular lactate level from BT-474 cells grown for 24 h under normal conditions or tumor microenvironment mimicry conditions (3 % O_2 and reduced nutrient concentrations). Integration values for the $m+0$ from unlabeled cell extracts have been divided by integrations for the internal standard myristic acid-D_{27} and by cell number. Values are reported as fold change over normal conditions that are set at 1. Such results are usually obtained using 3–5 biological replicates per experiment, and each experiment is repeated at least three times independently. (**c**) Lactate release by BT-474 cells. In this example, cells were counted every day and media was collected, diluted in dry ice cold 80 % (v/v) methanol–HPLC-grade water and stored in a −80 °C freezer until all samples were collected. The samples were analyzed together by GC-MS. Such experiment has to be performed at least three times independently

Table 1
Identification features of selected glycolytic and citric acid cycle metabolites typically found in cell extracts

Metabolite	MOX-TBDMS M-57 fragment formula	Quantifying ion	Qualifying ion	Typical Rt (min)
Internal standard myristic acid-D_{27}	$C_{16}D_{27}H_6O_2Si$	312	132	17.986
Dihydroxyacetone phosphate (DHAP)	$C_{18}H_{43}N_1O_6P_1Si_3$	484	383	20.365
Pyruvate oxime	$C_6H_{12}NO_3Si_3$	174	115	8.958
Lactate	$C_{11}H_{25}O_3Si_2$	261	233	11.777
Citrate	$C_{20}H_{39}O_6Si_3$	459	431	22.459
α-ketoglutarate oxime	$C_{14}H_{28}N_1O_5Si_2$	346	258	17.349
Succinate	$C_{12}H_{25}O_4Si_2$	289	331	14.852
Fumarate	$C_{12}H_{23}O_4Si_2$	287	329	15.225
Malate	$C_{18}H_{39}O_5Si_3$	419	287	18.279

3. For metabolite concentration measurements, divide the metabolite quantifier integration by the internal standard quantifier integration (*see* **Note 11**). Further divide the result by cell count (million cells) (Subheading 3.1) (Fig. 3b).
4. For metabolite concentration in media for uptake/release experiments, divide the metabolite quantifier integration by the internal standard quantifier integration for both spent cell media and cell-free media. Subtract ratio values of spent cell media from ratio values from cell-free media. Positive values represent uptake, while negative values indicate release.
5. Divide the values by cell number for relative uptake/release quantification (Fig. 3c).
6. For absolute measurements, calculate the metabolite uptake or release using equations derived from standard curves (Subheading 3.6).

3.8 Stable Isotope Tracer Analysis

1. For a given metabolite, report integration values for quantifier ($m+0$) and all possible isotopomers ($m+1$, $m+2$, $m+3$, etc.).
2. Sum up all the previous integrations to obtain the total amount of metabolite detected in a sample.
3. Divide $m+0$ and all isotopomers individually by the sum obtained in 2 to obtain the uncorrected mass isotopomer distribution (MID) vector [25]. All isotopomers are expressed as a fraction of the total metabolite pool.
4. Remove the contribution of naturally occurring stable isotopes (*see* **Note 12**) to obtain the corrected MID. Express $m+0$ and

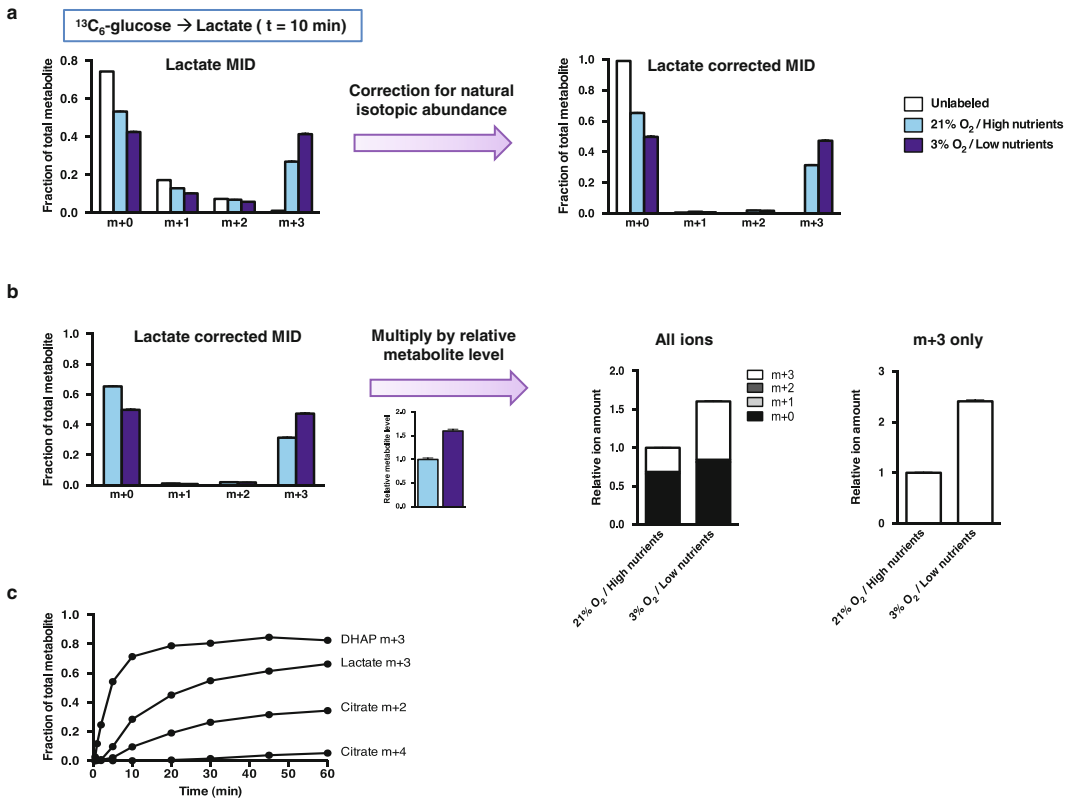

Fig. 4 Stable isotope tracer analysis using lactate as an example. (**a**) Mass isotopomer distribution (MID) [25] of lactate has to be corrected for the presence of naturally occurring isotopomers. BT-474 cells were incubated with $^{13}C_6$-glucose for 10 min (dynamic range) following a 24 h incubation period under normal or tumor environment mimicry (3 % O_2 and reduced nutrient concentrations) conditions. (**b**) Multiplying corrected MID by relative metabolite amounts permits the evaluation of the absolute metabolite labeling. Data can be presented by stacking $m+0$ and isotopomers so that changes in specific isotopomer amounts are easily discernable. Alternatively, specific isotopomer enrichments can be shown. (**c**) Example of various dynamic ranges for selected metabolites. Incubation with $^{13}C_6$-glucose leads to a quick saturation (isotopic steady state) of DHAP (dihydroxyacetone phosphate), a glycolytic intermediate, while citrate $m+2$ (generated from labeled acetyl-CoA) has a longer dynamic range. Citrate $m+4$ is discernable at even longer time points and reflects a second cycling within the citric acid cycle

all isotopomers as fractions of total metabolite pool, as done in **steps 2** and **3**. (Fig. 4a).

5. Multiply the corrected MID by the relative metabolite amount present in a sample (Subheading 3.8) to take into account the metabolite pool size (Fig. 4b).

4 Notes

1. This method has been adapted for the HER2+ luminal B breast cancer cell line BT-474. These cells were chosen for their slow growing rate that allows working under pseudo-constant nutri-

ent supply when they are maintained at low densities. This method can be adapted to virtually any cell line, as far as their growth profile has been well characterized (*see* Subheading 3.1). For other cell lines, follow the supplier's recommendations for media formulations and culture protocols.

2. Specific media formulations are obtained through numerous manufacturers. Common formulations are D-glucose- and/or L-glutamine-depleted, but virtually any compound can be excluded for the formulation (phenol red, sodium bicarbonate, specific amino acids, etc.) and then replenished to the desired concentration using labeled or unlabeled metabolite. Prior knowledge of in vivo specific metabolite concentration is definitively of great help in designing media composition. A good starting point for determining metabolite concentrations in different bio fluids can be found in the human metabolome database [26].
3. We recommend the use of L-glutamine powder. L-glutamine is a photosensitive amino acid that rapidly degrades into pyroglutamate (or 2-oxoproline) and ammonia. Commercial or homemade L-glutamine solutions that have experienced temperature changes are not reliable.
4. The choice of tracer and/or stable isotope is dictated by the research hypothesis and/or interest in a specific metabolic pathway. For example, stable isotope tracers of L-glutamine can include $^{13}C_5$-glutamine. ^{15}N-glutamine, and $^{13}C_5$, $^{15}N2$-glutamine. ^{15}N-tracers are often used to follow transamination reactions. For example, serine biosynthesis involves a transamination step that can be monitored using ^{15}N-glutamine.
5. Chemicals and samples used for methoximation and derivatization must be free of water. Water can compete for derivatization, resulting in poor detection of metabolites. Place stock solutions in a desiccator and use sealed bottles whenever possible. When removed from 4 °C storage, allow bottles to fully equilibrate at room temperature to prevent condensation.
6. Ensure that any media is equilibrated at 37 °C using a water bath prior to media change. Alternatively, equilibrate media for a few hours or overnight in the CO_2 incubator used for cultured cells. This will allow pH equilibration and avoid any metabolic disturbance.
7. For experiments performed over numerous days, it is crucial to change media daily. As cells grow to higher densities, nutrient depletion from media will increase, as well as metabolic side products accumulation. Undesirable metabolic stresses occur due to complete loss of essential nutrients thus skewing and potentially confusing results.
8. It is required to perform detailed labeling kinetics experiments in order to evaluate dynamic range and steady isotopic labeling (saturation). Each metabolite will have a unique labeling

kinetics. For example, glycolytic intermediate pools will be labeled rapidly in cells fed with ^{13}C-glucose, while citric acid cycle intermediates will show slower labeling (Fig. 4c). Thus, one single time-point cannot be chosen for the study of both glycolytic and citric acid cycle intermediates, as the former will be at isotopic steady state while the latter will still be in a dynamic state.

9. When cells are allowed to equilibrate in fresh media prior to labeling kinetic experiments, the intracellular metabolite amounts from unlabeled and labeled samples should be as close as possible. If significant differences occur between unlabeled and labeled samples, optimize the pre-incubation time (more than 2 h), and ensure proper calculations for tracers and unlabeled counterparts. Make sure that the same basic components are used for all media preparation (e.g., do not use media that were prepared on distinct days and in which components such as L-glutamine or pH may differ). If dialyzed FBS is used, make sure it is used for both unlabeled and labeled samples. The use of dialyzed FBS should be done days in advance to ensure that cells are able to adapt and reach steady state metabolite levels.
10. The dynamic range of metabolites measured by GC-MS can be very large. Intracellular glutamate and lactate are usually highly abundant species, while alpha-ketoglutarate and isocitrate display low abundance. Above the limit of detection, integration of peak areas is invalid and samples should be diluted (dilute dried samples in larger volumes of MOX/pyridine, and then take only a fraction of this solution for subsequent steps). Below limit of detection, integration of peaks areas is imprecise and close to background values. This can be fixed by working with cells at higher densities, grown on larger surfaces, or by performing single ion monitoring (SIM). Alternatively, methoximation and derivatization temperatures and incubation times can be optimized for specific metabolites. Note that if one opts to use a split configuration for GC-MS sample introduction, all calibration curves must be collected under the same injection conditions.
11. For quantitation of endogenous metabolites, the gold standard is to use stable isotope dilution where each endogenous metabolite is compared to its isotopically labeled standard. While this technique is recognized as the best approach for MS-based quantitation, the availability of isotopically labeled standards and their costs are prohibitive. As an alternative, other internal standards can be used. The ideal internal standard will have similar retention time and chemical properties to the metabolite of interest. Note that when using myristic acid-D_{27} as a general internal standard, its extraction may vary with sample pH. To ensure the most consistent extraction, adjust sample pH such that all samples have the same pH.

12. Any metabolite fragment analyzed by MS has its specific proportion of naturally occurring stable isotopes (^{2}H, ^{13}C, etc.) Although changes in isotopomer enrichments upon labeling with a stable isotope tracer can be measured from raw data, they do not reflect the actual tracer contribution, since any isotopomer has its own naturally occurring isotopic distribution. For this reason, removal of unlabeled sample values for $m+1$, $m+2$, etc. from labeled samples is not correct, as it will give erroneous values. For the same reason, expressing raw (uncorrected) isotopic enrichments as ratio to $m+0$ (i.e., $m+3/m+0$) is incorrect. Given the potential infinite possibilities of labeling patterns within a metabolite pool, it is essential to correct for natural isotopic abundances using metabolite-specific correction matrices. Such matrices are prepared using dedicated software based on proper mathematical modeling [22, 27, 28].

Acknowledgements

This work was supported by a Program Project Grant from the Terry Fox Research Institute (grant number TFF-116128 to J.S.-P.) and a grant from the Canadian Institutes of Health Research (CIHR, MOP-106603 to J.S.-P.). The Rosalind and Morris Goodman Cancer Research Centre Metabolomics Core Facility is supported by the Canada Foundation of Innovation, The John R. and Clara M. Fraser Memorial Trust, the Terry Fox Foundation (TFF-116128) and McGill University. J.S.-P is a FRQS research scholar.

References

1. Descot A, Oskarsson T (2013) The molecular composition of the metastatic niche. Exp Cell Res 319:1679–1686
2. Boroughs LK, DeBerardinis RJ (2015) Metabolic pathways promoting cancer cell survival and growth. Nat Cell Biol 17:351–359
3. Sullivan LB, Chandel NS (2014) Mitochondrial reactive oxygen species and cancer. Cancer Metab 2:17
4. Ferreira LM, Hebrant A, Dumont JE (2012) Metabolic reprogramming of the tumor. Oncogene 31:3999–4011
5. Hanahan D, Weinberg RA (2011) Hallmarks of cancer: the next generation. Cell 144:646–674
6. Sciacovelli M, Gaude E, Hilvo M, Frezza C (2014) The metabolic alterations of cancer cells. Methods Enzymol 542:1–23
7. Helmlinger G, Yuan F, Dellian M, Jain RK (1997) Interstitial pH and pO2 gradients in solid tumors in vivo: high-resolution measurements reveal a lack of correlation. Nat Med 3:177–182
8. Vaupel P, Kallinowski F, Okunieff P (1989) Blood flow, oxygen and nutrient supply, and metabolic microenvironment of human tumors: a review. Cancer Res 49:6449–6465
9. Wise DR, Thompson CB (2010) Glutamine addiction: a new therapeutic target in cancer. Trends Biochem Sci 35:427–433
10. Mayers JR, Vander Heiden MG (2015) Famine versus feast: understanding the metabolism of tumors in vivo. Trends Biochem Sci 40:130–140
11. Kroemer G, Pouyssegur J (2008) Tumor cell metabolism: cancer's Achilles' heel. Cancer Cell 13:472–482
12. Joyce JA (2005) Therapeutic targeting of the tumor microenvironment. Cancer Cell 7:513–520
13. Sato JD, Kan M (2001) Media for culture of mammalian cells. Curr Protoc Cell Biol Chapter 1:Unit 1.2
14. Chambers KF, Mosaad EM, Russell PJ, Clements JA, Doran MR (2014) 3D Cultures of prostate cancer cells cultured in a novel

high-throughput culture platform are more resistant to chemotherapeutics compared to cells cultured in monolayer. PLoS One 9:e111029

15. Antoni D, Burckel H, Josset E, Noel G (2015) Three-dimensional cell culture: a breakthrough in vivo. Int J Mol Sci 16:5517–5527
16. Birsoy K, Possemato R, Lorbeer FK, Bayraktar EC, Thiru P, Yucel B et al (2014) Metabolic determinants of cancer cell sensitivity to glucose limitation and biguanides. Nature 508:108–112
17. Halama A (2014) Metabolomics in cell culture—a strategy to study crucial metabolic pathways in cancer development and the response to treatment. Arch Biochem Biophys 564:100–109
18. Patel S, Ahmed S (2015) Emerging field of metabolomics: big promise for cancer biomarker identification and drug discovery. J Pharm Biomed Anal 107:63–74
19. Hur H, Paik MJ, Xuan Y, Nguyen DT, Ham IH, Yun J et al (2014) Quantitative measurement of organic acids in tissues from gastric cancer patients indicates increased glucose metabolism in gastric cancer. PLoS One 9:e98581
20. Grassian AR, Parker SJ, Davidson SM, Divakaruni AS, Green CR, Zhang X et al (2014) IDH1 mutations alter citric acid cycle metabolism and increase dependence on oxidative mitochondrial metabolism. Cancer Res 74:3317–3331
21. Morita M, Gravel SP, Chenard V, Sikstrom K, Zheng L, Alain T et al (2013) mTORC1 controls mitochondrial activity and biogenesis through 4E-BP-dependent translational regulation. Cell Metab 18:698–711
22. Nanchen A, Fuhrer T, Sauer U (2007) Determination of metabolic flux ratios from 13C-experiments and gas chromatography-mass spectrometry data: protocol and principles. Methods Mol Biol 358:177–197
23. Fendt SM, Bell EL, Keibler MA, Olenchock BA, Mayers JR, Wasylenko TM et al (2013) Reductive glutamine metabolism is a function of the alpha-ketoglutarate to citrate ratio in cells. Nat Commun 4:2236
24. Buescher JM, Antoniewicz MR, Boros LG, Burgess SC, Brunengraber H, Clish CB et al (2015) A roadmap for interpreting (13)C metabolite labeling patterns from cells. Curr Opin Biotechnol 34:189–201
25. Fan TW, Yuan P, Lane AN, Higashi RM, Wang Y, Hamidi AB et al (2010) Stable isotope-resolved metabolomic analysis of lithium effects on glial-neuronal metabolism and interactions. Metabolomics 6:165–179
26. Wishart DS, Jewison T, Guo AC, Wilson M, Knox C, Liu Y et al (2013) HMDB 3.0—the human metabolome database in 2013. Nucleic Acids Res 41(Database issue):D801–D807
27. Fernandez CA, Des Rosiers C, Previs SF, David F, Brunengraber H (1996) Correction of 13C mass isotopomer distributions for natural stable isotope abundance. J Mass Spectrom 31:255–262
28. Jennings ME 2nd, Matthews DE (2005) Determination of complex isotopomer patterns in isotopically labeled compounds by mass spectrometry. Anal Chem 77:6435–6444

Chapter 21

Analysis of the Tumor Microenvironment Transcriptome via NanoString mRNA and miRNA Expression Profiling

Marie-Noël M'Boutchou and Léon C. van Kempen

Abstract

Gene expression analysis in the tumor microenvironment using archived clinical samples is challenging because of formalin fixation, RNA degradation, and limiting sample volume. NanoString gene expression profiling is a RNA–DNA hybrid capture technology that does not require PCR and can accurately quantify the expression of to 800 transcripts in a single reaction. The technology requires 50–100 ng of RNA, which can be degraded (EDITOR: is this correct?) to a 200 bp fragment size. In contrast to amplification technologies, nanoString counts the actual numbers of transcripts that are captured with transcript-specific and fluorescently-barcoded probes. This chapter describes protocols for RNA extraction, quantification, mRNA and miRNA profiling and data analysis.

Key words NanoString, mRNA and miRNA expression profiling

1 Introduction

Analysis of gene expression profiles in formalin-fixed and paraffin-embedded (FFPE) tissues was challenging in the past. PCR-based expression analysis technologies require good quality RNA and a correct design of the assay as described in the MIQE guidelines [1]. After validation of the PCR assay, the analysis of multiple targets in a series of samples remains labor intensive and prone to technical errors when sample processing is not automated. The introduction of nCounter gene-expression profiling (also known as "nanoString") has significantly contributed to the accurate analysis of gene expression up to 800 different genes in a single experiment with as little as 100 ng of total RNA [2]. NanoString profiling is based on RNA–DNA hybrid capture technology using a biotinylated capture probe and a fluorescently labeled detection probe for each target of interest (Fig. 1). The two juxtaposed probes cover a 100 nt region of the gene of interest, and array of six fluorescent molecules (red, green, yellow, blue) functions as a target specific barcode. The small target that is required for hybridization makes

Josie Ursini-Siegel and Nicole Beauchemin (eds.), *The Tumor Microenvironment: Methods and Protocols*, Methods in Molecular Biology, vol. 1458, DOI 10.1007/978-1-4939-3801-8_21,

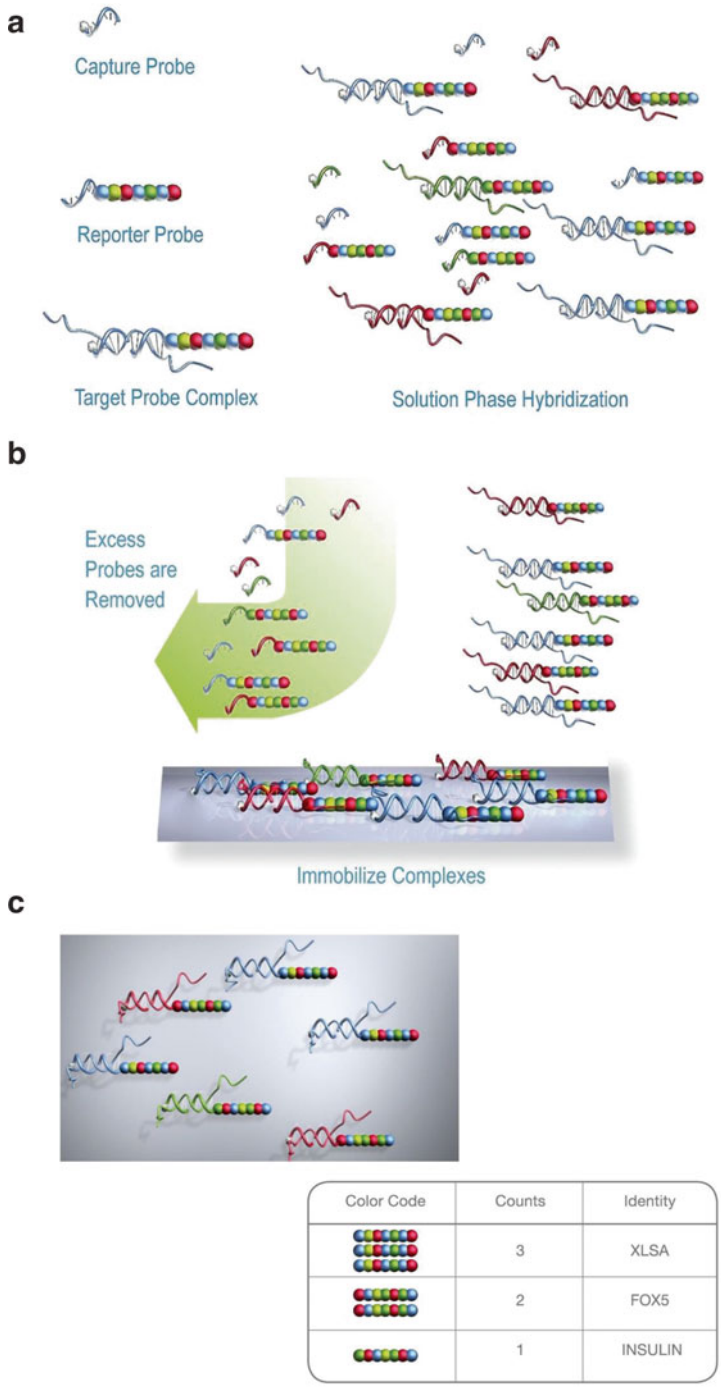

Fig. 1 Schematic overview over the nanoString technology. (**a**) Targets of interest are hybridized with two juxtapositioned probes: a biotinylated capture probe and uniquely fluorescently-labeled reporter probe for each target. A target–probe complex is formed during hybridization with a RNA sample. (**b**) After removal of excess probes, the target–probe complexes are immobilized and aligned on the surface of a flow cell. These steps are automated on a liquid handler. (**c**) Images of nonoverlapping fields on the flow cell are taken. The unique sequences of the reporter probes are counted and translated into the number of counts per target.

nanoString profiling an excellent expression analysis tool using RNA extracted from formalin-fixed and formalin-embedded material in which fragmentation of RNA is common. The absence of a PCR step allows for an accurate counting of fluorescent barcodes, which directly correlates with the amount of RNA molecules in the sample. With exception of preparing the RNA–probe mixtures and overnight hybridization, all subsequent procedures are performed on a liquid handler. A scanner is used to count the fluorescent barcodes in each sample. NanoString profiling is an excellent method for targeted gene expression profiling for a large number of genes in single sample.

NanoString profiling on formalin-fixed tissues demonstrates excellent reproducibility when comparing matched frozen and FFPE tissues. Regardless of the differences in quality of RNA extracted from snap-frozen, cryopreserved or FFPE liver samples, a very good concordance is observed between the expression profile of 96 genes in frozen and matched FFPE tissues (Fig. 2a, b). These data demonstrate that source and quality of RNA does not strongly impact an accurate quantification of RNA molecules in a given samples. A direct comparison of gene expression analysis in frozen and FFPE tissue confirmed that the nanoString method achieves superior gene expression quantification results when compared to qPCR (SYBR Green) in archived samples [3]. This has opened doors for measuring the expression of mRNAs and miRNAs in FFPE sections [4]. The ability to use small FFPE samples is an important attribute of this technology for tumor microenvironment research because material obtained with laser microdissection will yield sufficient amounts of RNA for multiplex profiling of gene expression by tumor stromal cells [5, 6].

The nanoString company (http://www.nanoString.com/) offers off-the-shelf CodeSets (i.e., a collection of probes) for the for expression analysis of mRNAs, microRNAs, and long noncoding RNAs of mouse and human origin, as well as CodeSets for single cell gene expression analysis and copy number variation analysis. Custom codes sets can be prepared to include the researcher's genes of interest (up to 800 genes). A recent feature is the ability to analyze the expression of 30 cell surface proteins and 770 genes (RNA–protein) that are involved in immune responses in a single sample of cryopreserved intact cells (e.g., PBMC or cell lines). Whereas nanoString has established a protocol for RNA–protein profiling in cell lines, there is not yet a validated protocol for (laser microdissected) formalin-fixed and paraffin-embedded or frozen tissue samples. Therefore, this chapter only describes the protocols for mRNA and miRNA nanoString expression profiling, because these are currently most relevant to study the dynamic immune responses in disease.

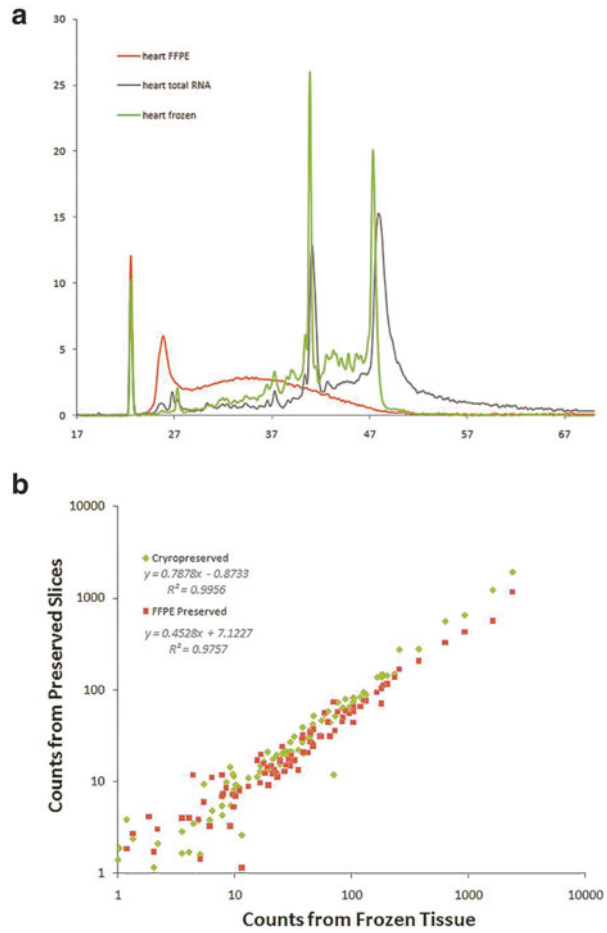

Fig. 2 Variation in pre-analytical variables does not negatively affect nanoString counts. (**a**) A bioanalyzer profile reveals that strong degradation of RNA isolated from FFPE heart (*orange line*) compared to RNA isolate from fresh (*grey line*) or frozen (*green line*) heart. (**b**) Despite these difference in RNA integrity, highly similar target counts were obtained from matched frozen and FFPE heart tissue.

2 Materials

2.1 RNA Extraction from FFPE (Crude Lysate)

Any RNA extraction method can be used to purify 100 ng of RNA (*see* **Note 1**) from frozen or FFPE samples (whole sections or microdissected fragments; *see* **Note 2**). However, it is advisable to use the same extraction method for all samples in one experiment. Alternatively, any tissue lysate can be used directly in a profiling experiment without the need for RNA purification (crude lysate). A drawback of using lysates is that equal loading of RNA into the

experiment is not possible without RNA quantification. For miRNA profiling, RNA purification is required.

1. Microtome with clean blade in an RNAse-free environment (*see* **Note 3**).
2. Xylene.
3. 100% ethanol.
4. 10 mM 2-(*N*-morpholino)ethanesulfonic acid (MES), pH 6.5 containing 0.5% SDS.
5. 20 mg/mL Proteinase K.

2.2 RNA Quantification (Qubit)

RNA concentrations measured by Qubit are more accurate than by NanoDrop because of the saturating dye that binds to RNA specifically rather than optical properties of nucleic acids. In order to minimize the variation in content normalization (*see* Subheading 3.5, Analysis, **step 10**), it is recommended to accurately measure the RNA concentration.

1. RNA sample obtained with an extraction of choice (*see* **Note 4**).
2. QuBit RNA HS Buffer provided with the kit (Invitrogen).
3. RNA dye provided with the kit.
4. RNA Standards (STDs) #1 and #2 provided with the kit.
5. RNA samples at a concentration of approximately 50 ng/μL as measured by NanoDrop.
6. 0.5 mL microtubes (1/sample + 2 for standards).
7. 1 × 15 mL tubes.

2.3 mRNA Profiling

1. nCounter XT gene expression assay Capture probe set and Reporter CodeSet.
2. RNase Free water (not DEPC treated) in 1.5 mL tubes.
3. 100 ng of total RNA per sample normalized to 20 ng/μL.
4. nCounter Prep Pack: Tips, tip sheaths, strip tubes (0.2 mL), hybridization buffer, and adhesives, all stored at room temperature. Cartridge (*see* **Note 5**; in sealed pouch stored at −20 °C), two 96 well reagent plates (Prep Plates, stored a 4 °C).
5. Picofuge (for 1.5 mL tubes and 6-strip tubes).
6. Rack for strip tubes.
7. Thermocycler (with heated lid).
8. Filter tips for P2.5 and P10, P20, P200.

2.4 miRNA Profiling

1. nCounter Human miRNA Expression Assay kit.
2. nCounter Human miRNA sample preparation kit.
3. RNase Free water (NOT DEPC-treated) in 2 × 1.5 mL tubes.

4. 100 ng of total RNA per sample normalized to 33 ng/μL (*see* **Note 6**).
5. nCounter Prep Pack: Tips, tip sheaths, strip tubes (0.2 mL), hybridization buffer, and adhesives, all stored at room temperature. Cartridge (*see* **Note 7**; in sealed pouch stored at −20 °C), two 96-well reagent plates (Prep Plates stored a 4 °C).
6. Sterile microcentrifuge tubes (1.5 mL) RNAse-free. Three tubes are needed and are labeled: (1) miRNA ctrl, (2) Ann MM, (3) Lig MM.
7. Picofuge (for 1.5 mL tubes and 6-strip tubes).
8. Two Racks for strip tubes.
9. Thermocycler (with heated lid).
10. Filter tips for P2.5 and P10, P20, P200.

3 Methods

3.1 RNA Extraction from FFPE (Crude Lysate)

1. Cut two 10 μm FFPE sections (0.2–1 cm^2 each, *see* **Note 8**) with a new blade in an RNAse-free environment.
2. Collect the curls in a 1.5 mL microcentrifuge tube (*see* **Note 9**).
3. Add 1 mL of xylene and vortex for 10 s.
4. Centrifuge 4 min at maximum speed in a benchtop microcentrifuge at room temperature.
5. Remove supernatant by pipetting, leaving 100 μL of supernatant behind. Be careful not to disturb pellet.
6. Add 1 mL of 100% ethanol. Vortex. Spin down the pellet at maximum speed for 2 min in benchtop microcentrifuge.
7. Repeat **steps 4** and **5**.
8. Remove as much supernatant as possible without disturbing pellet. Let dry at room temperature for 30 min with the tube open. Make sure all ethanol has evaporated.
9. Resuspend the pellet in 45 μL 10 mM MES, pH 6.5, 0.5% SDS, and 5 μL Proteinase K (20 mg/mL) (*see* **Note 10**). Vortex briefly.
10. Incubate at 55 °C for 15 min.
11. Flick tubes and incubate at 80 °C for 15 min to inactivate the proteinase K.
12. Centrifuge maximum speed for 30 s in a benchtop microcentrifuge.
13. Remove and keep supernatant (50 μL). Discard the pellet.
14. Store the supernatant containing the RNA at −80 °C. Use 5 μL of supernatant per nCounter hybridization (*see* **Note 11**). RNA aliquots can be made accordingly.

3.2 RNA Quantification (Qubit)

1. Touch the QuBit to turn it on.
2. Calculate how much of the working solution (WS) is needed.
   (a) For every 200 µL of HS buffer, add 1 µL of dye.
   (b) Calculate the total volume needed for *x* number of samples plus 2 STDs + 1 dead volume sample.
3. Mix the WS by pipetting up and down without bubbles.
4. Samples: Pipet 199 µL of WS in each tubes. Add 1 µL of RNA sample (conc of ≈50 ng/µL).
   Standards: Pipet 190 µL of WS in each of the two tubes. Add 10 µL of STD #1 or #2.
5. Vortex. Spin down.
6. On the QuBit:
   (a) Choose RNA (NOT "RNA broad range").
   (b) Read new standards? YES.
   (c) Put STD #1 in the QuBit. Read.
   (d) Put STD #2 in the QuBit. Read.
   (e) Insert sample tubes. Read.
   (f) Calculate stock conc (volume of sample used): 1 µL.
   (g) Choose units: ng/µL.
   (h) Record the RNA concentration.
   (i) Read next sample (*see* **Note 12**).

3.3 mRNA Profiling

3.3.1 mRNA Sample Preparation Protocol

1. Remove one tube of both the Reporter CodeSet (green cap) and Capture probe set reagent (silver cap) from the freezer (−80 °C) and thaw on ice (*see* **Note 13**).
2. Thaw RNA samples on ice.
3. Invert all tubes several times to mix well. Do NOT vortex or pipet vigorously! Briefly spin down reagent with picofuge (*see* **Note 14**).
4. Create a master mix: Add 70 µL of hybridization buffer directly to the Reporter CodeSet tube.
5. Invert to mix and spin down with the picofuge.
6. Label a provided 12 tube strip and cut in half so it will fit in a picofuge.
7. Add 8 µL of master mix to each of the 12 tubes. Use a fresh tip for each pipetting.
8. Add total RNA sample, maximum 5 µL for a total of 100 ng (5 µL of 20 ng/µL). Total volume per tube is 13 µL.
9. Preheat the thermocycler to 65 °C (*see* **Note 15**).
10. Add 2 µL of Capture probe set, cap the tubes, and mix by inverting several times and flicking with your finger.

11. Briefly spin down.
12. Place the tubes immediately in the PCR block at 65 °C (*see* **Note 16**).
13. Incubate hybridization assays for at least 12 h. Max incubation time should not exceed 30 h because it will increase the background signal (*see* **Note 17**).
14. After hybridization, remove the tubes from the PCR block and allow cooling down to room temperature. Do NOT store the samples at 4 °C.
15. Proceed immediately with binding sample to the nCounter flow cell on the nCounter Prep Station.

3.3.2 Processing of the Samples on the nCounter Prep Station (See **Note 18***)*

1. Before the end to the hybridization (**step 14**), remove the cartridge from the freezer and reagents plates from the fridge and allow to reach room temperature before using (*see* **Note 19**).
2. Centrifuge the plates at 2000 × *g* for 2 min.
3. Turn on the Prep Station and press 'Start processing' on the touch screen.
4. Select the plate type that is provided with the CodeSet.
5. Select the desired sensitivity (standard or high) when asked (*see* **Note 20**).
6. The next screen is the sample selection screen: select the number of samples that are to be processed (*see* **Note 21**).
7. The next screen prompts the user to place the Prep plates (without the clear lids, but with intact foil cover) on the deck at the indicated positions.
8. Load the tips and foil piercers onto the aluminum carrier and place the loaded tip carrier back onto the Prep station and forward to the next screen.
9. Place the tip sheaths on the deck and press firmly into place and forward to the next screen.
10. Place an empty 12-strip tube (supplied with the CodeSet) on the deck and close the aluminum cover securely.
11. The next screen instructs to load to cartridge on the deck and to secure the electrode fixtures over the cartridge (*see* **Note 22**).
12. Place the sample strip on the deck and confirm that tube 1 aligns with position 1 on the sample holder (*see* **Note 23**). Remove all caps and make sure that all tubes are seated fully and evenly in the rack (*see* **Note 24**).
13. Close the door of the liquid handler.
14. When the system is connected to the Internet, the user can enter his e-mail address. The user will receive and e-mail after completion of the run.

15. Start the run.
16. When processing is complete, it is important to immediately close the wells of the cartridge with the cartridge well seal to prevent evaporation. Do not leave the cartridge in direct sunlight or at temperatures higher than room temperature. The cartridge can be stored in the pouch at 4 °C for up to 3 week with minimal loss of signal if it cannot be scanned within 1 h after the run.

3.3.3 Scanning of the Cartridge on the nCounter Digital Analyzer (See **Note 25***)*

1. If the cartridge is stored at 4 °C, let the pouch come to room temperature before removing the cartridge to minimize condensation.
2. Turn on the nCounter digital analyzer.
3. In the main menu, select upload files and upload the RLF file (Reporter Library File) onto the digital analyzer. The RLF file is located on the USB key that is delivered with the CodeSet and contains the information required to convert fluorescent bar code counts into gene counts (*see* **Note 26**).
4. Select 'start counting'.
5. The Select Stage Position screen appears.
6. On the screen, select the position where the cartridge is placed.
7. In the next screen, enter the cartridge information: cartridge ID and Fields Of View (FOV) counts (*see* **Note 27**).
8. Place the cartridge in one of the six available positions (*see* **Note 28**) and close the magnetic clips gently to secure the cartridge in position.
9. Shut the instrument door and press start the Initiate Imaging screen (*see* **Note 29**)**.**
10. Once imaging begins, the Counting Cartridge ID screen will appear with current time, time left for scanning the current cartridges, time left for scanning all cartridges and expected finish time.
11. After the run, insert the USB key provided by nanoString with the CodeSet and press download RCC (Reporter Code Count) data (*see* **Note 30**).
12. Proceed with Subheading 3.5 Data analysis.

3.4 miRNA Profiling

3.4.1 miRNA Sample Preparation Protocol

1. Verify the different protocols on the Bio-Rad C1000 PCR machine: Annealing Protocols, Ligation Protocol, Purification Protocol, and Hybridization at 65 °C (*see* Tables 1 and 2).
2. Remove RNA, miRNA Assay Controls (clear cap) from the −80 °C freezer and the Annealing Buffer (clear cap) and nCounter miRNA Tag Reagent (clear cap), Ligase buffer (red cap), Ligase (blue cap), and PEG from the −20 °C freezer.

3. Thaw all tubes on ice.
4. Let PEG and Ligase equilibrate to room temperature.
5. Normalize RNA samples to 33 ng/μL using RNAse-free ddH_2O.
6. Prepare a 1:500 dilution of the miRNA Assay Controls (clear cap) (−80) in a 1.5 mL tube: 499 μL of RNAse-free ddH_2O + 1 μL of miRNA Assay Controls.
7. Vortex for 1 min (time it), spin down in picofuge, and store on ice.
8. Prepare an annealing master mix: 13 μL of Annealing Buffer + 26 μL of nCounter miRNA Tag Reagent + 6.5 μL of the 1:500 miRNA Assay Controls dilution (prepared in **step 6**).
9. Mix well by pipetting up and down. Do NOT vortex.
10. Cut strip of 12 tubes (0.2 mL strip tubes) in half with scissors so it will fit in the picofuge. Number the tubes.
11. Aliquot 3.5 μL of the annealing master mix (**step 8**) into each tube. Use clean tip for each tube.
12. Add 3 μL (100 ng) of RNA sample to the corresponding tube.
13. Cap tubes and flick gently to mix. Spin down briefly in picofuge.
14. Place strip in thermocycler and initiate Annealing protocol (6.5 μL total volume) *See* Table 1.
15. Prepare a ligation master mix by combining: 16 μL of Ligase Buffer + 24 μL PEG (*see* **Note 31**).

Table 1
Annealing and ligation protocols

Temperature	Time
94 °C	1 min
65 °C	2 min
45 °C	10 min
48 °C	Hold
48 °C	3 min
47 °C	3 min
46 °C	3 min
45 °C	5 min
65 °C	10 min
4 °C	Hold
Total time	37 min

Table 2
Purification protocol

Temperature	Time
37 °C	2 h
70 °C	10 min
4 °C	Hold
Total time	2 h 10 min

16. Mix well by pipetting up and down. Keep at room temperature.
17. Following completion of the Annealing protocol (approx. 15 min), when the thermocycler has reached 48 °C: Pause the thermocycler to keep the temperature at 48 °C.
18. Remove tubes from the machine and remove the caps.
19. Add 2.5 μL of the ligation master mix (prepared in **step 15**) to each tube. Cut a new strip of lids in two (6-6) and place on tube.
20. Flick gently to mix. Spin down.
21. Return tubes to 48 °C thermocycler, close lid, and incubate at 48 °C for 5 min (9 μL total).
22. Open thermocycler. At this point, do NOT remove the tubes from the 48 °C heat block.
23. Carefully remove caps from tubes, leaving strips in place in the heat block add 1.0 μL of Ligase (*see* **Note 32**) directly in the bottom of each tube while incubating at 48 °C.
24. Check the pipette tip to make certain all of the ligase was added to the reaction. Do not pipet up and down. Recap tubes with new caps while leaving the tubes in the block (*see* **Note 33**).
25. Immediately after addition of the Ligase to the final tube (10 μL total volume), close thermocycler lid, and continue with the Annealing and Ligation Protocol (*see* Table 1).
26. After completion of Ligation Protocol, add 1.0 μL Ligation Clean-Up Enzyme to each reaction. Tubes can be removed from the heat block.
27. Flick gently to mix. Spin down in picofuge.
28. Return tubes to thermocycler and initiate Purification Protocol (11 μL total volume). *See* Table 2.
29. After completion of Purification Protocol (*see* **Note 34**), remove tubes and set thermocycler to 85 °C forever for the miRNA Hybridization Protocol (*see* Subheading 3.4.2).

30. Add 40 µL of RNAse-free ddH_2O to each sample (51 µL total). Mix well and spin down. Proceed immediately with the miRNA CodeSet Hybridization Protocol (*see* Subheading 3.4.2).

3.4.2 miRNA CodeSet Hybridization Protocol (See **Note 35***)*

1. Thaw the Reporter CodeSet (green cap) and Capture probe set reagent (silver cap) on ice.
2. Invert the Reporter CodeSet (green cap) and Capture probe set reagent (silver cap) several times to mix well and briefly spin down reagent with picofuge.
3. Create a Master Mix containing: 130 µL of the Reporter CodeSet + 130 µL of hybridization buffer. Add the hybridization buffer to the tube containing the Reporter CodeSet (*see* **Note 36**).
4. Invert to mix and spin down in picofuge.
5. Label a provided 12-tube strip and cut in half so it will fit in a picofuge.
6. Add 20 µL of Master Mix (**step 3**) to each of the 12 tubes. Use a new tip for each pipetting step.
7. Denature samples from the miRNA sample prep protocol (Subheading 3.4.1, **step 30**) at 85 °C for 5 min.
8. Place the samples on ice.
9. Add 5 µL denature RNA (**step 8**) to each tube (25 µL total volume) (*see* **Note 37**).
10. Preheat thermocycler to 65 °C (*see* **Note 38**).
11. Add 5 µL of Capture probe set to each tube immediately before placing at 65 °C.
12. Cap tubes and mix by inverting several times and flicking with your finger.
13. Briefly spin down in picofuge.
14. Place in the center block of the thermocycler at 65 °C (*see* **Note 39**).
15. Incubate hybridization assays for at least 12 h but it should not exceed 30 h (*see* **Note 40**).
16. After hybridization, do not store at 4 °C, but continue with the nCounter Prep Station.

The processing of samples on the nCounter Prep Station is identical for mRNA or miRNA profiling: *See* Subheading 3.3.2.

The scanning of the cartridge on the nCounter digital analyzer is identical for mRNA or miRNA profiling: *See* Subheading 3.3.3.

3.5 Data Analysis

nSolver is a software package designed by nanoString for the analysis of counts generated by the nCounter digital analyzer. The current version (2.6) includes graphical presentation of the data in a heat map, scatter plot, violin plot, box plot and histograms.

1. Install and open the nSolver analysis software from a work station (*see* **Note 41**).
2. Import the CodeSet RLF File (*see* **Note 42**).
3. Import the RCC Files from the USB key (*see* **Note 43**).
4. The RCC files are automatically sorted to the correct RLF files (*see* **Note 44**).
5. Create a new study and within this study create a new experiment.
6. This will open up the Experiment design wizard. By selecting the RLF file under which the RCC files are collected, the samples can be highlighted for analysis (*see* **Note 45**).
7. Samples can now be annotated if necessary (*see* **Note 46**).
8. Background subtraction. Every CodeSet contains eight negative controls (*see* **Note 47**). The mean of negative controls plus a desired amount of standard deviations will be subtracted from the experimental counts (*see* **Note 48**). Alternatively a blank lane can be selected as the negative control (*see* **Note 49**).
9. Next, normalization parameters are identified. Each CodeSet contains 6 positive controls at different concentrations that are not homologous to any known organism. The mean value of these positive controls is used to calculate a normalization factor that correct for inter-sample variability of hybridization efficiency.
10. A second normalization can be performed on CodeSet content. Every CodeSet contains a set of genes that have been identified as reference of housekeeping genes. These are selected by the nSolver software automatically for normalization. However, true reference genes (those whose expression does not change with experimental conditions) are rare. Therefore whole content normalization is preferred. This can be done by selecting all genes in the CodeSet.
11. If desired, the next step allows for the selection of the reference sample(s) against which a fold difference in expression will be calculated for each sample (*see* **Note 50**).

When completed, the data set will be built and results in four files collected within the experiment (raw data, normalized data, grouped data, ratio data, and analysis data).

3.5.1 Quality Control (QC) of the Raw and Normalized Data Must Be Performed to Determine Data Quality

1. Highlight all samples in the Raw data folder and run the QC analysis by pressing the QC button. Standard values for imaging, binding density, positive control linearity and positive control limit of detection are set automatically but can be changed upon the user's preference for stringency. If this analysis results in a QC issue, then the sample will be flagged with the specific QC problem. Caution needs to be taken with the interpretation of that specific sample.

2. In the Normalized data folder, values for positive normalization and content normalization can be found (*see* **Note 51**). The positive normalization factors will fluctuate closely around one and indicates comparable probe hybridization efficiency for each sample. The whole content normalization factors are commonly more variable, but should be between 0.8 and 1.2 when RNA input in the assay was normalized. A sample with a normalization flag should be interpreted with caution as this indicates a problem with hybridization efficiency or total counts (i.e., RNA input).

3.5.2 Data Visualization

nSolver is a great tool for the visualization of data, but lacks a statistical analysis component. Heat maps, scatter plots, violin plots, box plots, and histograms can be generated from both the raw or normalized data.

1. Select the samples of interest and click the Analysis button (*see* **Note 52**).
2. Within the analysis menu select the graph type and subsequent the samples for which the data needs to be presented graphically (Fig. 3).

3.5.3 Data Analysis

The graphical presentation of data results in the visualization of RNA counts, but without information of statistically relevant differences in expression. To this end, the data can be analyzed by the user-preferred statistical analysis software. A script in R (NanoStringNorm) has been made available to the scientific community [7] (*see* **Note 53**). NanoStriDE [8] (*see* **Note 54**) is a Web-based analysis program to calculate differential expression from RCC files. With the release of the Mouse PanCancer Immunology and Human PanCancer Immunology CodeSet, nanoString also released a comprehensive advanced analysis tool for pathway analysis. These advanced analysis tools can be downloaded from the nanoString website (*see* **Note 55**).

4 Notes

1. 100 ng of RNA when analyzing <400 transcripts and 50 ng of RNA when analyzing >400 transcripts. The amount of RNA needs to be reduced for large CodeSets because of the possibility to saturate the flow cells. With the lowering of the amount of RNA, an increase in the variation of counts for genes that are expressed at low levels (<200 counts) must be anticipated.
2. The number of sections or area of microdissected tissue that is required to yield 100 ng of total RNA depends on different variables such as cellularity, cell type and tissue type. This required amount of tissue needs to be established empirically.

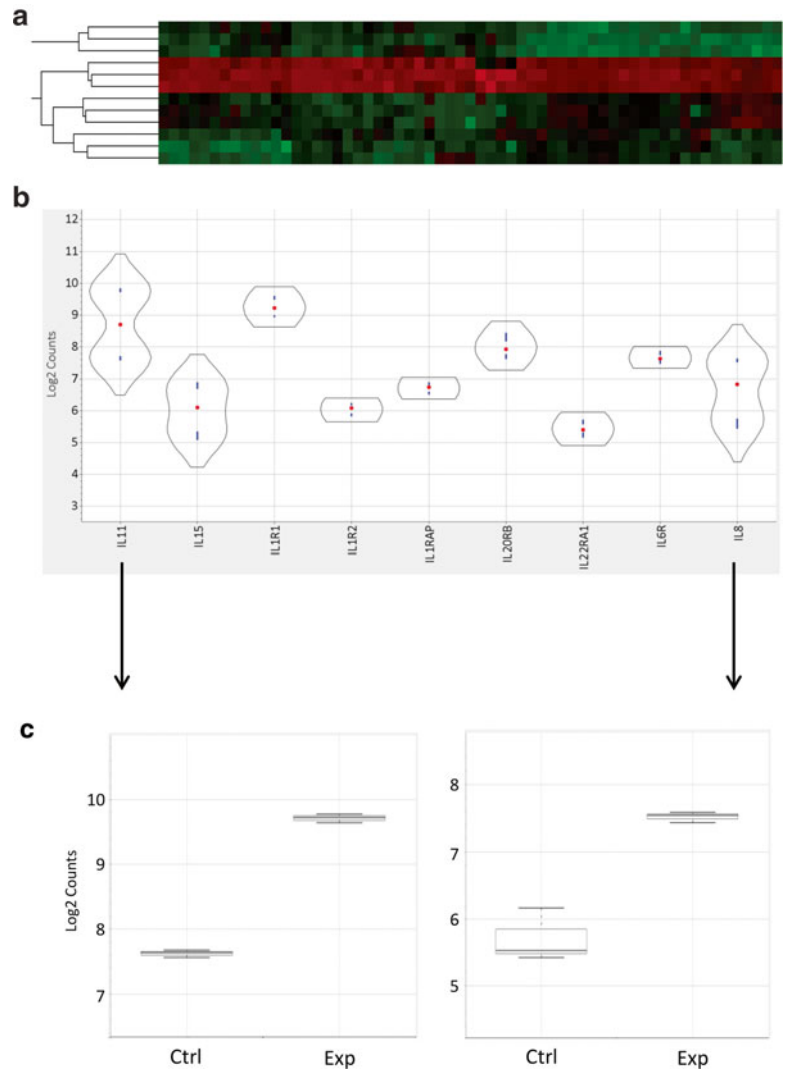

Fig. 3 Data presentation. (**a**) Gene expression data of four different biological triplicates presented as an agglomerative cluster (heat map). (**b**) Violin plot of the expression of nine genes in control and experimental samples. Each cloud per gene presents the distribution of counts in the control and experimental samples combined. A *sand clock shape* or separation of the cloud suggests that the gene is differential expressed in the two groups. (**c**) Box plots vizualizing the expression of IL11, and IL8 in the control (Ctrl) and experimental (Exp) sample are shown

3. Wipe all microtome components that can be in contact with the tissue sections and blade with RNAse-away before sectioning. Also, clean forceps with RNAse-away solution. This minimizes the risk of carryover of RNAses when the tissue in an aqueous solution.
4. All commercial RNA isolation kits yield RNA of sufficient quality and quantity for nanoString analysis.

5. For 12 samples.
6. Note the higher concentration of total RNA that is required for miRNA profiling.
7. For 12 samples.
8. Increasing the number of sections will result in a less efficient removal of paraffin. Additional xylene steps may then be necessary.
9. Collect the sample in an RNase-free tube.
10. Pipet up and down to disrupt the pellet.
11. This is the maximum volume of sample that can be added into a nanoString reaction (*see* Subheading 3.3.1, **step 8**). The variation in counts in between different tissue samples is difficult to anticipate when RNA concentration is not measured.
12. Make sure there are no bubbles.
13. A nanoString assay is performed with 12 samples. Use one vial per 12 samples.
14. Quick spin all reagents in a minicentrifuge to collect the volumes in the bottom of the tubes.
15. Program the PCR machine with a PCR volume of 30 μL and use a heated lid. The 65 °C temperature should be maintained for the whole time.
16. Minimizing the time between the addition of the Capture probe set and the placement of the reaction at 65 °C will increase the sensitivity of the assay.
17. In order to minimize the variation hybridization efficiency in between experiments, the laboratory should standardize the hybridization time, e.g., 18 h for every experiment.
18. A detailed manual can be downloaded from the nanoString website: http://www.nanoString.com/media/pdf/MAN_nCounter_Prep_Station_GEN2.pdf
19. If the cartridge and reagent plates are not at room temperature prior to processing, an increase in the assay variability may occur. The cartridge pouch should not be opened before room temperature is reached to prevent condensation of the cartridge.
20. There are two types of plates: white and green plates. One can only select high sensitivity with the green plates. The high sensitivity option increases the processing time from 2.5 to 3 h because of an increased binding time of the probes to the flow cell surface.
21. Less than 12 samples can be processed. The deck will be loaded with two Prep plates: one for lanes 1–6 and the second on for lanes 7–12. Therefore, if selecting 6 samples, choose position

1–6. If seven samples, then load the samples in position 1–7, but both Prep plates need to be loaded.

22. The 24 electrodes should insert into the 24 wells of the cartridge.
23. If the sample tubes are inverted, the sample specific information will be assigned to the incorrect data file.
24. Centrifuge the tubes briefly to collect the reagents in the bottom before opening the tubes.
25. A detailed manual can be downloaded from the nanoString website http://www.nanoString.com/media/pdf/MAN_nCounter_Digital_Analyzer_GEN2.pdf.
26. You only need to upload RLF files when you first receive a new CodeSet. Once an RLF has been uploaded, it will always be available until it is manually deleted from the digital analyzer.
27. FOV setting: low, medium, high, or max. The FOV dimension of the nCounter MAX system is 216 × 165 μm, with 25, 100, 280, and 555 FOVs for the low, medium, high, and max setting, respectively. The FOV that is required for accurate quantification depends on the RNA input and abundance of the target. It is advisable to start with High FOV and subsequently analyze the total counts and counts for the negative control (*see* Subheading 3.5 **step 8**). In case of low or high counts, recount at medium or max FOV, respectively. The absolute but not relative counts for each target will change and is especially important to discriminate changes in expression of low abundance targets from fluctuations in the noise.
28. The analyzer can analyze up to six cartridges in one run.
29. Once imaging starts, the door remains locked.
30. This will automatically download the Reporter Code Counts to the RCC folder located in the USB key.
31. PEG is very viscous. Pipet very slowly.
32. Bring Ligation Cleanup Enzyme to room temperature before adding it to the mixture.
33. Do six tubes at a time (remove caps of these 6 and when done, close caps; make six more tubes).
34. After the completion of this PCR step, the purified sample preparation reactions may be stored at −20 °C for up to 2 weeks. If no stop-step is included but when the hybridization assay will be continued, then 1 h before the end of the 2 h 15 min Purification Protocol, tubes of both the Reporter CodeSet (green cap) and Capture probe set reagent (silver cap) must be taken from the freezer (−80 °C) and thawed on ice.
35. These instructions are for 12 samples.

36. Do NOT add the Capture probe set to the master mix.
37. Leftover RNA can be stored at −80 °C.
38. Program using 30 μL volume, heated lid. Do NOT set to ramp down to 4 °C at the end of the run.
39. Minimizing the time between the addition of the Capture probe set and the placement of the reaction at 65 °C will increase the sensitivity of the assay.
40. Standardizing the hybridization time will greatly increase the inter-experiment reproducibility.
41. Free download with the purchase of an off-the-shelve of custom CodeSet.
42. RLF File is the reporter library file that contains a table that enables the conversion of the fluorescent bar code into a gene name. The RLF file can be found on the thumb drive that is delivered with the reagents.
43. The data produced by the nCounter Digital Analyzer are exported as a Reporter Code Count (RCC) file. RCC files are comma-separated text (.csv) files that contain the counts for bar code in a sample. The RCC file can be downloaded from the analyzer with a thumb drive (*see* Subheading 3.3.3, **step 11**).
44. Before the flow cell was imaged on the digital analyzer, the instrument instructed the user to upload the RLF file to the analyzer and instruct the software to link barcode counts to gene expression counts.
45. All experiments that are performed with the same CodeSet (i.e., RFL file) are collected under the same RLF name. For analysis of specific samples, individual samples can be highlighted and selected for the next steps.
46. The report file that will be created at the end contains long sample names that are not easily identified (experiment name position on flowcell.RCC). The annotation that is added here (e.g., sample name or condition) will also be shown in the report file.
47. The series of negative controls are established by the External RNA Control Consortium (ERCC). The ERCC control sequences are synthetic sequences molecules and are not homologous to any known organism, are applicable and transferable in all CodeSets, and generate consistent results in gene expression analyses.
48. Commonly mean + 3 standard deviation of the raw counts all negative controls is used to avoid any count that is a possible variation in noise. In general, the lower threshold value is between 30 and 50.

49. A nanoString experiment is performed with 12 samples simultaneously. It is not cost efficient to analyze less than 12 samples. Blank lane subtraction is not an optimal control because it does not take the complexity of the samples in which a specific binding of the negative probes can occur into account.
50. Pair wise analysis can also be performed afterwards.
51. Also note that the counts for the negative control probes are reduced to 1 and that the counts for the targets genes subtracted with the mean count of all negative values plus × times the SD, and subsequently normalized against the positive control, and the user-defined CodeSet content (e.g., reference genes or whole content).
52. The Advance analysis option allows the user to import specific analysis tools that can be downloaded from the nanoString website, e.g., PanCancer Immune Profiling Analysis Module (human and mouse) that are used in conjunction with specific CodeSets.
53. *See* also: cran.rproject.org/web/packages/NanoStringNorm/vignettes/NanoStringNorm_Introduction.pdf.
54. *See* also: http://nanostride.soe.ucsc.edu.
55. A description of the analysis pipeline is out of the scope of this chapter. For detailed information, download the white paper describing the PanCancer pathway module from the nanoString website: http://www.nanoString.com/products/pancancer_pathways/analysis_module.

Acknowledgements

The Molecular Pathology Centre at Jewish General Hospital is grateful to the Jewish General Hospital Foundation and all participants of the Enbridge Ride to Conquer Cancer® event who have enabled the purchase of the nCounter Analysis System. The images in Figs. 1 and 2 were reproduced from nanoString publications with the consent from nanoString® Technologies, Inc.

References

1. Bustin SA, Benes V, Garson J, Hellemans J, Huggett J, Kubista M et al (2013) The need for transparency and good practices in the qPCR literature. Nat Methods 10:1063–1067
2. Geiss GK, Bumgarner RE, Birditt B, Dahl T, Dowidar N, Dunaway DL et al (2008) Direct multiplexed measurement of gene expression with color-coded probe pairs. Nat Biotechnol 26:317–325
3. Reis PP, Waldron L, Goswami RS, Xu W, Xuan Y, Perez-Ordonez B et al (2011) mRNA transcript quantification in archival samples using multiplexed, color-coded probes. BMC Biotechnol 11:46

4. Koti M, Siu A, Clement I, Bidarimath M, Turashvili G, Edwards A et al (2015) A distinct pre-existing inflammatory tumour microenvironment is associated with chemotherapy resistance in high-grade serous epithelial ovarian cancer. Br J Cancer 112:1215–1222
5. Golubeva Y, Salcedo R, Mueller C, Liotta LA, Espina V (2013) Laser capture microdissection for protein and NanoString RNA analysis. In: Taatjes D, Roth J (eds) Methods in Molecular Biology 931:213–257
6. Castro NP, Fedorova-Abrams ND, Merchant AS, Rangel MC, Nagaoka T, Karasawa H et al (2015) Cripto-1 as a novel therapeutic target for triple negative breast cancer. Oncotarget 6:11910–11929
7. Waggott D, Chu K, Yin S, Wouters BG, Liu F-F, Boutros PC (2012) NanoStringNorm: an extensible R package for the pre-processing of NanoString mRNA and miRNA data. Bioinformatics 28:1546–1548
8. Brumbaugh CD, Kim HJ, Giovacchini M, Pourmand N (2011) NanoStriDE: normalization and differential expression analysis of NanoString nCounter data. BMC Bioinformatics 12:479

Chapter 22

RNA-Seq as a Tool to Study the Tumor Microenvironment

Pudchalaluck Panichnantakul, Mathieu Bourgey, Alexandre Montpetit, Guillaume Bourque, and Yasser Riazalhosseini

Abstract

The transcriptome is composed of different types of RNA molecules including mRNAs, tRNAs, rRNAs, and other noncoding RNAs that are found inside a cell at a given time. Analyzing transcriptome patterns can shed light on the functional state of the cell as well as on the dynamics of cellular behavior associated with genomic and environmental changes. Likewise, transcriptome analysis has been a major help in solving biological issues and understanding the molecular basis of many diseases including human cancers. Specifically, since targeted and whole genome sequencing studies are becoming more common in identifying the driving factors of cancer, a comprehensive and high-resolution analysis of the transcriptome, as provided by RNA-Sequencing (RNA-Seq), plays a key role in investigating the functional relevance of the identified genomic aberrations. Here, we describe experimental procedures of RNA-Seq and downstream data processing and analysis, with a focus on the identification of abnormally expressed transcripts and genes.

Key words RNA-Seq, Tumor microenvironment, Next-generation sequencing, Bioinformatics

1 Introduction

In human cancers, tumors are often heterogeneous at both the genome and phenome levels. Even in a given tumor type, these variations exist, and are referred to as *inter-tumor heterogeneity* (i.e., differences observed between tumors of individuals affected with the same tumor type) and *intra-tumor heterogeneity* (i.e., different subpopulations of malignant cells that exist within a tumor; subclones). In a tumor bulk, subclones may differ at genetic, epigenetic, and/or transcriptome levels. These heterogeneous patterns not only play a large part in the proliferative progression of the tumor as a whole, but also foster other complications such as the resistance to therapeutic drug treatments, and tumor metastasis as revealed by recent next-generation sequencing (NGS) studies (*see* examples in refs. 1, 2).

In addition to different subpopulations of malignant cells, another layer of heterogeneity occurs within a tumor bulk where

Josie Ursini-Siegel and Nicole Beauchemin (eds.), *The Tumor Microenvironment: Methods and Protocols*, Methods in Molecular Biology, vol. 1458, DOI 10.1007/978-1-4939-3801-8_22,

intrinsic tumor cells are surrounded by stroma. Interestingly, variations in the composition and abundance of stromal cells—as important constituents of tumor microenvironment—have been linked to the disease course [3, 4]. Consequently, understanding the interaction between tumor cells and their microenvironment have brought significant insight into our knowledge about molecular mechanisms involved in tumor formation and progression, that may open new therapeutic avenues. In this regard, transcriptome sequencing of RNA samples isolated from each compartment can provide valuable information. To this end, it is important to obtain pure cell subpopulations without contamination from the other cell types. Microdissection is the method of choice in many laboratories to enrich for tumor or stromal cells.

RNA-Seq is a state-of-the-art technique used to analyze the transcriptome in a global yet high-resolution manner through direct sequencing of complementary DNA (cDNA). RNA-Seq experiments begin with the production of cDNA from extracted RNA (fragmented or polyadenylated to mark coding from non-coding RNA) followed by an amplification step before the use of NGS to sequence from one end (single-end) or both ends (pair-end) of the cDNA molecules. Once sequencing is complete, the obtained sequence reads can be aligned to the reference genomes/transcripts to generate tabulated counts for the expression level of genes/transcripts. Reads obtained from RNA-Seq have to be normalized to remove inherent biases in preparation steps, particularly in the sequencing depth of a sample and the length of RNA species involved. These biases are corrected in the form of either RPKM (reads per kilobase per million reads) or FPKM (fragments per kilobase per million reads) since reads are commonly proportional to the abundance and length of transcripts [5, 6].

Popular alternatives to RNA-Seq are cDNA microarrays, in which the abundance of fluorescently tagged cDNA molecules, generated from RNA samples, is measured after hybridization to arrayed DNA probes with complementary sequences. Although microarrays are relatively inexpensive, they have several limitations. Due to the limited dynamic range of detection caused by background signals, transcripts in low or high abundance may not be accurately measured by microarrays. This is not the case with RNA-Seq where an almost unlimited dynamic range is achievable by applying appropriate depth of sequencing coverage, thereby enabling quantification of transcripts undetectable by microarrays [7, 8]. Moreover, arrays can only measure abundance of transcripts for which complementary probes can be designed, limiting their use to known transcripts [9, 10], and to species for which the genome is available, whereas RNA-Seq can provide information about new transcripts with no previous annotations [8, 11]. In addition, because RNA-Seq has a single-base resolution, information about exon connectivity can be obtained in addition to

sequence variations observed at the transcript level, thus enabling detection of splicing events as well as chromosomal rearrangements resulting in abnormal transcripts such as fusion genes. As of late, RNA-Seq advancements have allowed researchers to understand the transcriptome in greater details. For instance, the protocol for RNA-Seq can be modified to obtain information about the strand of origin (either sense or antisense) of a read; this is particularly important for the detection of alternative splicing events as well as noncoding RNAs (ncRNA) that can act as key regulators of gene expression [12]. Strand-specific RNA-Seq has significantly contributed to our knowledge about antisense transcripts (asRNAs) that are active regulators of their sense strands (usually protein coding) [13]. The identification of ncRNAs and asRNAs are proven to be important in modern molecular biology due to their function as genomic regulators and their recent association with multiple cancers [14, 15]. An emerging powerful RNA-Seq approach that can be employed to dissect intra-tumor heterogeneity is single-cell RNA-Seq, which when applied across several individual cells of a given tumor, can provide insight to the genome-wide transcriptome heterogeneity at a single-cell resolution [16, 17].

In this chapter, we describe the experimental procedures of generating sequencing libraries for stranded RNA-Seq based on the Illumina TruSeq Stranded ribosomal RNA (rRNA)-depleted protocol, and bioinformatics analysis of the corresponding sequencing data.

2 Materials

2.1 Library Generation and Quality Control

1. Filtered tips (10, 20, 100, 200, 1000 μL).
2. 1.5 and 1.7 mL boil-proof microtubes clear tubes.
3. Thermowell® GOLD 96-well PCR plates (96-well half-skirt) (e.g., Corning).
4. Full skirted 96-well plates.
5. Sealing film, AxySeal.
6. 50 mL centrifuge tubes.
7. Reservoir.
8. TruSeq® Stranded Total RNA LT (with Ribo-Zero Gold) (Illumina).
9. Agencourt RNA clean XP (Beckman Coulter).
10. Agencourt Ampure XP (Beckman Coulter).
11. Ultrapure distilled RNase-free water.
12. SuperScript II reverse transcriptase.
13. RNA adapter index tubes.
14. 100% ethanol.

15. 80% ethanol.
16. 20% ethanol.
17. 2 N NaOH.
18. Buffer EB (Qiagen).
19. Polysorbate 20 (Tween 20).
20. HT1 (Hybridization buffer), prechilled (Illumina).
21. PhiX control kit (Illumina).
22. Library Quantification kit—Illumina/Universal (Kapa).
23. 1 M Tris–HCl, pH 8.0.
24. Nuclease-free water.
25. MicroAmp clear adhesive film.
26. Powder-free gloves.
27. Mix mate with accessories.
28. LightCycler 480 (or other real-time instruments).
29. LightCycler 480 Multiwell Plate 384-well (or other 384-well plate compatible with the available real-time machine).
30. Thermocycler (with heated lid).
31. Magnetic Stand-96.
32. Mini centrifuge.
33. Plate centrifuge.
34. Vortex.

2.2 Data Processing and Analysis

1. SAMtools. Software download on SourceForge: http://sourceforge.net/projects/samtools/files/
   (a) Use version 0.1.19 or later.
2. R or other statistical software.
   (a) Command to install on Linux systems:
   sudo apt-get update.
   sudo apt-get install r-base.
   (b) Install directions available at http://cran.r-project.org/.
   (c) Use version 3.1.1 or later.
3. DESeq. In an R session use the command:
   (a) source("http://www.bioconductor.org/biocLite.R") biocLite("DESeq").
   (b) Use version 3.1.2_3.0 or later.
4. EdgeR. In an R session use the command:
   (a) Source ("http://www.bioconductor.org/biocLite.R") biocLite("edgeR").
   (b) Use version 2.2.0 or later.

5. goseq. In an R session use the command:
   (a) Source ("http://www.bioconductor.org/biocLite.R") biocLite("goseq").
   (b) Use version 1.18.0 or later.
6. STAR alignment software. Software download on GitHub: https://github.com/alexdobin/STAR/releases.
   (a) Use version 2.4.0f or later.
   (b) Installation directions available in the STAR manual: https://rna-star.googlecode.com/files/STARmanual_2.3.0.1.pdf.
7. PICARD tools. Software download on github: https://github.com/broadinstitute/picard/releases.
   (a) Use version 1.123 or later.
   (b) Requires Java installed.
8. Bwa aligner. Software download on sourceforge: http://sourceforge.net/projects/bio-bwa/files/.
   (a) Use version 0.7.10 or later.
   (b) After you acquire the source code, simply use make to compile and copy the single executable bwa to the destination you want. The only dependency required to build BWA is zlib.
9. Bvatools tools kit. Software available on Bitbucket: https://bitbucket.org/mugqic/bvatools.
   (a) Use version 1.5 or later.
   (b) Requires Java.
10. Cufflinks software. Binary version available at: http://cole-trapnell-lab.github.io/cufflinks/install/.
    (a) Use version 2.2.1 or later.
    (b) Installation directions: http://cole-trapnell-lab.github.io/cufflinks/getting_started/#installing-a-pre-compiled-binary-release.
11. Java openjdk-jdk1.7.0_60 platform available at: http://download.java.net/jdk7u60/archive/b07/binaries/jdk-7u60-ea-bin-b07-linux-x64-19_feb_2014.tar.gz.
12. Rnaseqc software available at: http://www.broadinstitute.org/cancer/cga/rnaseqc_download.
    (a) Use version 1.1.7 or later.
    (b) Requires Java.

13. Trimmomatic http://www.usadellab.org/cms/uploads/supplementary/Trimmomatic/Trimmomatic-0.33.zip.
    (a) Use version 0.33 or later.
    (b) Requires Java.
14. UCSC userApp tool kit available at: http://hgdownload.cse.ucsc.edu/admin/exe/.
    (a) Use version 305 or later.

3 Methods

3.1 RNA-Seq Library Preparation

The text below provides instructions for RNA-Seq library preparation. Here, we focus on stranded RNA-Seq using the Illumina TruSeq Stranded rRNA-depleted protocol. The protocol starts with ribosomal RNA (rRNA) depletion followed by first and second strand cDNA synthesis, purification, and ligation of adapters.

3.1.1 Ribosomal RNA (rRNA) Depletion and RNA Fragmentation

1. Remove the Ribo-Zero rRNA Removal Mix, Resuspension Buffer, Elution Buffer, the rRNA Binding Buffer and Elute, Prime, Fragment, High Mix from the −20 °C storage and let them thaw at room temperature (RT). Once thawed, put on ice. Also remove the rRNA Removal Beads from the 4 °C storage and bring them at RT.
2. On ice, in a 96-well half-skirt plate, bring 500 ng of each total RNA sample to a final volume of 10 µL with ultrapure distilled RNase-free water.
3. In a 1.5 mL boil-proof microtubes clear tube, prepare a mix with rRNA Binding Buffer and rRNA Removal Mix according to Table 1.
4. Add 10 µL of the mix prepared in the previous step to each sample. Using a multichannel, gently pipette the entire volume up and down six times to mix thoroughly.

Table 1
rRNA depletion mastermix

Reagent	For 1 reaction	For *X* reactions
rRNA binding buffer	5 µL	5 µL × *X*
rRNA removal mix	5 µL	5 µL × *X*
Total	10 µL	10 µL × *X*

5. Seal the plate with a MicroAmp™ clear adhesive film, put the sealed plate in the plate centrifuge and spin for 15 s at maximum speed.
6. In a thermal cycler, preheat the lid to 100 °C, and incubate the plate for 5 min at 68 °C. Place the sealed 96-well half-skirt plate on the thermal cycler when it reaches 68 °C. Remove the plate from the thermal cycler when it reaches 4 °C.
7. In a plate centrifuge, spin the plate for 15 s at maximum speed.
8. Incubate the 96-well half-skirt plate at RT for 1 min.
9. Vortex the rRNA Removal Beads vigorously until the beads are completely resuspended.
10. Add 35 μL of rRNA Removal Beads to each well of a new 96-well half-skirt plate.
11. Using a multichannel pipette, transfer the entire samples (20 μL) to the 96-well half-skirt plate containing the rRNA Removal Beads and pipette up and down 20 times to mix thoroughly.
12. Incubate the 96-well half-skirt plate at RT for 1 min.
13. Place the 96-well half-skirt plate on the magnetic stand at RT for 1 min.
14. Using a multichannel pipette, transfer all of the supernatant from each well (45 μL) to a new 96-well half-skirt plate.
15. Place the 96-well half-skirt plate on the magnetic stand at RT for 1 min.
16. Using a multichannel pipette, transfer all of the supernatant from each well (45 μL) to a new 96-well half-skirt plate.
17. Repeat the two previous steps until no beads remain.

3.1.2 Cleanup

1. Remove the RNA Clean XP Beads from the 4 °C storage. Let them reach RT for at least 30 min prior to use.
2. Vortex the RNA Clean XP Beads until they are completely dispersed, and pour in a reservoir.
3. Using a multichannel pipette, add 99 μL of the RNA Clean XP Beads to each sample. Gently pipette the entire volume up and down ten times to mix.
4. Incubate at RT for 15 min.
5. Place the 96-well half-skirt plate on a magnetic stand at RT for 5 min to make sure that all the beads are bound to the side of the wells.
6. Remove and discard 135 μL of the supernatant with a multichannel pipette. Do not disturb the beads. Some liquid will remain in the bottom of each well.

7. Add 200 μL of 70% ethanol to each well of the 96-well half-skirt plate while the plate is still on the magnetic stand without disturbing the beads. Pour the ethanol on the opposite side to the beads.
8. Incubate at RT for 30 s, then remove and discard all of the supernatant using a multichannel pipette.
9. Repeat the last two steps (**steps 7** and **8**).
10. Leave the 96-well half-skirt plate on the magnetic stand for 15 min to dry off all the ethanol. When the beads are dry, they will become opaque.
11. Vortex the Elution Buffer for 5 s and pour it in a new reservoir.
12. Remove the 96-well half-skirt plate from the magnetic stand and resuspend the beads completely with 11 μL of the Elution Buffer. Using a multichannel pipette, gently pipette the volume up and down ten times to mix thoroughly.
13. Incubate the 96-well half-skirt plate at RT for 2 min.
14. Place the 96-well half-skirt plate on a magnetic stand at RT for at least 5 min.
15. Using a multichannel, transfer 8.5 μL of the supernatant to a new 96-well half-skirt plate. Do not disturb the beads.
16. Using a multichannel, add 8.5 μL of Elute, Prime, Fragment High Mix to each well and gently pipette up and down ten times to mix thoroughly. Seal the plate with a MicroAmp™ clear adhesive film.
17. Put the sealed 96-well half-skirt plate in the plate centrifuge and spin for 15 s at maximum speed.
18. In a thermal cycler, preheat the lid to 100 °C, and incubate the plate for 8 min at 94 °C. Place the sealed 96-well half-skirt plate on the thermal cycler when it reaches 94 °C. Remove the plate from the thermal cycler when it reaches 4 °C.
19. Put the sealed 96-well half-skirt plate in the plate centrifuge and spin for 15 s at maximum speed, and proceed immediately to First Strand cDNA Synthesis.

3.1.3 First Strand cDNA Synthesis

1. Remove the tube of First Strand Synthesis ActD Mix from storage and thaw at RT. Once thawed vortex and centrifuge at maximum speed for 5 s and then put on ice.
2. Immediately before use, bring the SuperScript II in a CryoBox to the bench.
3. In a 1.5 mL boil-proof microtubes clear tube, prepare the First Strand Act D Master Mix at RT according to Table 2.
4. Add 8 μL of the First Strand Master mix prepared in the previous step to each sample. Using a multichannel pipette, pipette the entire volume up and down 6 times to mix thoroughly.

Table 2

First strand mastermix

Reagent	For 1 reaction	For *X* reactions
First strand synthesis act D mix	9 μL	9 μL × *X*
Super script II	1 μL	1 μL × *X*
Total	10 μL	10 μL × *X*

Table 3

Second strand mastermix

Reagent	For 1 reaction	For *X* reactions
Diluted end repair control	5 μL	5 μL × *X*
Second strand mix	20 μL	20 μL × *X*
Total	25 μL	25 μL × *X*

5. Seal the plate with a MicroAmp™ clear adhesive film. Put the sealed 96-well half-skirt plate in the plate centrifuge and spin for 15 s at maximum speed.
6. Place plate in a thermal cycler and run the following program. When the temperature reaches 25 °C, place the sealed 96-well half-skirt plate and close the lid. Remove the plate from the thermal cycler when it reaches 4 °C and place it on ice.
   (a) Choose the preheat lid option and set to 100 °C.
   (b) 25 °C for 10 min.
   (c) 42 °C for 15 min.
   (d) 70 °C for 15 min.
   (e) Hold at 4 °C.
7. Put the sealed 96-well half-skirt plate in the plate centrifuge and spin for 15 s at maximum speed, and proceed immediately to the Second Strand cDNA Synthesis.

3.1.4 Second Strand cDNA Synthesis

1. Remove the Second Strand Master Mix, End Repair Control, and Resuspension Buffer from storage and put them on ice.

2. Once thawed, vortex all the tubes and spin at maximum speed for 5 s. Put the tubes back on ice except for the Resuspension Buffer.
3. In a 1.5 mL boil-proof microtubes clear tube, prepare a 1:50 dilution of the End Repair Control.
4. In a new 1.5 mL boil-proof microtubes clear tube, prepare the Second Strand Master Mix according to Table 3.
5. Add 25 μL of the Second Strand Master Mix to each sample. Using a multichannel pipette, gently pipette the entire volume up and down six times to mix.
6. Seal the 96-well half-skirt plate with a MicroAmp™ clear adhesive film, and spin the plate for 15 sec at maximum speed in a plate centrifuge.
7. In a thermal cycler, incubate at 16 °C for 1 h. When the temperature reaches 16 °C, place the sealed 96-well half-skirt plate and let the lid open. Remove the plate from the thermal cycler when it reaches 4 °C and place it on ice.
8. Spin the plate for 15 s at maximum speed in a plate centrifuge, and proceed immediately to the Double stranded cDNA purification.

3.1.5 Purification of Double Stranded cDNA

1. Remove the Agencourt Ampure XP Beads from the 4 °C storage. Let them reach RT at least 30 min prior to use.
2. Remove the 96-well half-skirt plate from the ice and bring the samples to RT.
3. Vortex the Agencourt Ampure XP Beads until they are completely dispersed.
4. Add 90 μL of the Agencourt Ampure XP Beads to each sample. Gently pipette the entire volume up and down ten times to mix, and incubate at RT for 15 min.
5. Place the 96-well half-skirt plate on a magnetic stand at RT for 5 min to make sure that all the beads are bound to the side of the wells.
6. Remove and discard 135 μL of the supernatant. Do not disturb the beads. Some liquid may remain in the bottom of each well.
7. Add 200 μL of 80% ethanol to each well of the plate on the magnetic stand, without disturbing the beads (Pour the ethanol on the opposite side to the beads).
8. Incubate at RT for 30 s, then remove and discard all of the supernatant.
9. Repeat the last two steps (**steps 7** and **8**).
10. Leave the 96-well half-skirt plate on the magnetic stand for 15 min to dry off all the ethanol. When the beads are dry, they will become opaque.

11. Vortex the Resuspension Buffer for 5 s.
12. Remove the 96-well half-skirt plate from the magnetic stand and resuspend the beads completely with 17.5 µL of the Resuspension Buffer. Using a multichannel pipette, gently pipette the volume up and down ten times to mix thoroughly.
13. Incubate at RT for 2 min.
14. Place the 96-well half-skirt plate on a magnetic stand at RT for at least 5 min.
15. Using a multichannel, transfer 15 µL of the supernatant to a new 96-well half-skirt plate. Do not disturb the beads (*see* **Note 1**).

3.1.6 Adenylation

1. Remove the A-Tailing Mix and A-Tailing Control from storage and put them on ice.
2. Once thawed, vortex all the tubes and spin at maximum speed for 5 s. Put the tubes back on ice.
3. In a 1.5 mL boil-proof microtubes clear tube, prepare a 1:100 dilution of A-Tailing Control in Resuspension Buffer.
4. In a new 1.5 mL boil-proof microtubes clear tube, prepare the A-Tailing Master Mix according to Table 4.
5. Using a single pipette, add 15 µL of the A-tailing Master Mix to each sample and pipette up and down six times to mix thoroughly.
6. Seal the plate with a MicroAmp™ clear adhesive film, and spin the plate for 15 s at maximum speed in a plate centrifuge.
7. Place plate in a thermal cycler and run the following program. Place the sealed 96-well half-skirt plate on the thermal cycler when it reaches 37 °C. Remove the 96-well half-skirt plate from the thermal cycler when it reaches 4 °C.

Table 4

Adenylation mastermix

Reagent	For 1 reaction	For *X* reactions
Diluted A-tailing control	2.5 µL	2.5 µL × *X*
A-tailing mix	12.5 µL	12.5 µL × *X*
Total	15 µL	15 µL × *X*

(a) Choose the preheat lid option and set to 100 °C.
(b) 37 °C for 10 min.
(c) 70 °C for 5 min.
(d) Hold at 4 °C.

8. Spin the plate for 15 s at maximum speed in a plate centrifuge, and proceed immediately to the Ligation of Adapters.

3.1.7 Ligation of Adapters

1. Remove the RNA Adapter Indexes, Stop Ligation Buffer, and Ligation Control from storage and let them thaw at RT.
2. Once thawed, vortex all the tubes and spin at maximum speed for 5 s. Put the tubes back on ice.
3. Immediately before use, bring the Ligation Mix to the bench in a cryobox.
4. Vortex the Ligation Mix and spin at maximum speed for 5 s. Put the tube back in the cryobox.
5. In a 1.5 mL boil-proof microtubes clear tube, prepare a 1:100 dilution of Ligation Control in Resuspension Buffer.
6. In a new 1.5 mL boil-proof microtubes clear tube, prepare the Ligation Master Mix according to Table 5.
7. Remove the MicroAmp™ clear adhesive film from the 96-well half-skirt plate.
8. Using a single channel pipette, add 2.5 μL of the desired Adapter Index to each sample (one index per sample).
9. Using a single channel pipette, add 5 μL of the Ligation Master Mix to each sample and pipette up and down 6 times to mix thoroughly.
10. Seal the 96-well half-skirt plate with a MicroAmp™ clear adhesive film, and spin the plate for 15 s at maximum speed in a plate centrifuge.

Table 5

Ligation mastermix

Reagent	For 1 reaction	For X reactions
Diluted ligation control	2.5 μL	2.5 μL × X
Ligation mix	2.5 μL	2.5 μL × X
Total	5 μL	5 μL × X

11. In a thermal cycler, incubate at 30 °C for 10 min. When the temperature reaches 30 °C, place the sealed 96-well half-skirt plate and close the lid. Remove the plate from the thermal cycler when it reaches 4 °C.
12. Put the sealed 96-well half-skirt plate in the plate centrifuge and spin for 15 s at maximum speed.
13. Remove the seal, and add 5 μL of the Stop Ligation Buffer to each sample, and pipette up and down ten times to mix thoroughly.

3.1.8 Cleanup

1. Vortex the Agencourt Ampure XP Beads until they are completely dispersed.
2. Add 42 μL of the Agencourt Ampure XP Beads to each sample. Gently pipette the entire volume up and down 10 times to mix, then incubate at RT for 15 min.
3. Place the 96-well half-skirt plate on a magnetic stand at RT for 5 min to make sure that all the beads are bound to the side of the wells.
4. Remove and discard 79.5 μL of the supernatant with a multichannel pipette. Do not disturb the beads. Some liquid may remain in the bottom of each well.
5. Add 200 μL of 80 % ethanol to each sample in the 96-well half-skirt plate on the magnetic stand, without disturbing the beads (Pour the ethanol on the opposite side to the beads).
6. Incubate at RT for 30 s, then remove and discard all of the supernatant.
7. Repeat the last two steps (**steps 5** and **6**).
8. Leave the 96-well half-skirt plate on the magnetic stand for 15 min to dry off all the ethanol. When the beads are dry, they will become opaque.
9. Vortex the Resuspension Buffer for 5 s and pour it in a new reservoir.
10. Remove the 96-well half-skirt plate from the magnetic stand and resuspend the beads completely with 52.5 μL of the Resuspension Buffer. Using a multichannel pipette, gently pipette the volume up and down ten times to mix thoroughly, and incubate at RT for 2 min.
11. Place the 96-well half-skirt plate on a magnetic stand at RT for at least 5 min.
12. Transfer 50 μL of the supernatant to a new 96-well half-skirt plate. Do not disturb the beads.
13. Add 50 μL of the Agencourt Ampure XP Beads to each sample. Gently pipette the entire volume up and down ten times to mix, and incubate at RT for 15 min.

14. Place the 96-well half-skirt plate on a magnetic stand at RT for 5 min to make sure that all the beads are bound to the side of the wells.
15. Remove and discard 95 μL of the supernatant with a multichannel pipette. Do not disturb the beads. Some liquid may remain in the bottom of each well.
16. Remove the 96-well half-skirt plate from the magnetic stand and resuspend the beads completely with 22.5 μL of the Resuspension Buffer. Using a multichannel pipette, gently pipette the volume up and down 10 times to mix thoroughly, and incubate at RT for 2 min.
17. Place the 96-well half-skirt plate on a magnetic stand at RT for at least 5 min.
18. Using a multichannel, transfer 20 μL of the supernatant to a new 96-well half-skirt plate. Do not disturb the beads (*see* **Note 2**).

3.1.9 cDNA Fragment Enrichment by PCR

1. Remove the PCR Master Mix and PCR Primer Cocktail from storage and let them thaw at RT.
2. Once thawed, vortex all the tubes and spin at maximum speed for 5 s. Put the tubes back on ice.
3. In a new 1.5 mL boil-proof microtubes clear tube, prepare the PCR Mix according to Table 6.
4. Using a multichannel pipette, add 30 μL of the PCR Mix to each sample and pipette up and down 6 times to mix thoroughly.
5. Seal the plate with a MicroAmp™ clear adhesive film, and spin the plate for 15 s at maximum speed in a plate centrifuge.
6. Place the plate in a thermal cycler and run the following program. Place the sealed 96-well half-skirt plate on the thermal cycler when it reaches 98 °C. Remove the plate from the thermal cycler when it reaches 4 °C.

Table 6
PCR mastermix

Reagent	For 1 reaction	For *X* reactions
PCR primer cocktail	5 μL	5 μL × *X*
PCR mix	25 μL	25 μL × *X*
Total	30 μL	30 μL × *X*

(a) Choose the preheat lid option and set to 100 °C.

(b) 98 °C for 30 s.

(c) 15 cycles of:

- 98 °C for 10 s.
- 60 °C for 30 s.
- 72 °C for 30 s.

(d) 72 °C for 5 min.

(e) Hold at 4 °C.

7. Spin the plate for 15 s at maximum speed.

3.1.10 PCR Cleanup

1 Remove the MicroAmp™ clear adhesive film from the 96-well half-skirt plate.

2 Vortex the Agencourt Ampure XP Beads until they are completely dispersed and pour in a reservoir.

3 Using a multichannel pipette, add 50 μL of the Agencourt Ampure XP Beads to each sample. Gently pipette the entire volume up and down ten times to mix, and incubate at RT for 15 min.

4 Place the 96-well half-skirt plate on a magnetic stand at RT for 5 min to make sure that all the beads are bound to the side of the wells.

5 Remove and discard 95 μL of the supernatant with a multichannel pipette. Do not disturb the beads. Some liquid will remain in the bottom of each well.

6 Add 200 μL of 80 % ethanol to each sample in the 96-well half-skirt plate on the magnetic stand, without disturbing the beads (pour the ethanol on the opposite side to the beads), and incubate at RT for 30 s.

7 Using a multichannel pipette, remove and discard all of the supernatant.

8 Repeat the last two steps (**steps 6** and 7).

9 Leave the 96-well half-skirt plate on the magnetic stand for 15 min to dry off all the ethanol. When the beads are dry, they will become opaque.

10 Vortex the Resuspension Buffer for 5 s and pour it in a new reservoir.

11 Remove the 96-well half-skirt plate from the magnetic stand and resuspend the beads completely with 32.5 μL of the Resuspension Buffer. Using a multichannel pipette, gently pipette the volume up and down 10 times to mix thoroughly.

12 Incubate at RT for 2 min.

13 Place the 96-well half-skirt plate on a magnetic stand at RT for at least 5 min.

14 Using a multichannel, transfer 30 μL of the supernatant to a new Thermowell® GOLD 96-well PCR plate. Do not disturb the beads.

15 Seal the plate with a MicroAmp™ clear adhesive film, and proceed with the library quality control by quantification through qPCR.

3.2 Quantification of Libraries Using qPCR

This section addresses the quantification of the cDNA library by qPCR. It uses the KAPA SYBR® FAST Universal qPCR Kit (cat # KK4824). Quantification by qPCR provides more accurate results than fluorometric methods since it only measure molecules that have the proper adapters at each ends regardless whether they are single or double stranded. Here, we use LightCycler 480 (LC480), and present the instructions for using this system; however, the assay can be performed on other real-time instruments.

3.2.1 Preparation of the Master Mix

1. Remove the qPCR master mix tube from −20 °C and bring it to RT (minimum 30 min).
2. Once thawed, aliquot it in a 96-well Eppendorf full skirted plate. Depending on the total number of libraries to be quantified, fill each well with 29 μL starting with column 1. A total of 21 wells (A01-G03) need to be filled regardless since they will be also used for the standard curve.
3. Seal the master mix plate with an AxySeal sealing film and spin down 30 s at 1000 rpm (134 × *g*) in a plate centrifuge.
4. Identify one LightCycler 480 Multiwell Plate 384.
5. Distribute four times (4×) 6 μL from each well of the master mix plate to the four quadrants of the LC480 Multiwell Plate 384 using a multichannel or a liquid handling robot.

3.2.2 Preparation of the Dilution Plates

1. Transfer to a new full skirt 96-well plate all libraries selected for the QC (fill from column 1).
2. For quality control purpose (and if a well is empty), add 30 μL of a control library to one well.
3. Place the plate in the mix mate and mix for 5 min at 1200 rpm (195 × *g*). Spin down 1 min at 4000 rpm (2120 × *g*).
4. Place the plate on a magnet.
5. Identify four new full skirt 96-well plates to prepare samples with the appropriate dilution factor (1:7.5, 1:80, 1:800, 1:8000).
6. Using a multichannel pipette (or liquid handling robot) distribute 32.5 μL of Tris–HCl, pH 8.0 in plate 1:7.5 (only to the corresponding wells of the library plate), 145 μL of Tris–HCl,

pH 8.0 in corresponding wells of plate labeled 1:80 and 180 μL of Tris–HCl, pH 8.0 in corresponding wells of plates labeled 1:800, and 1:8000.

7. Transfer 5 μL of each library to plate 1:7.5. Mix up and down ten times.
8. Change tip. Transfer 15 μL of each diluted library from plate 1:7.5 to plate labeled 1:80. Mix up and down ten times.
9. Change tip. Transfer 20 μL of each diluted library from plate 1:80 to plate labeled 1:800. Mix up and down ten times.
10. Change tip. Transfer 20 μL of each diluted library from plate 1:800 to plate labeled 1:8000. Mix up and down ten times.

3.2.3 Loading the qPCR Plate and Performing the Assay

1. From plate 1:8000, transfer 4 μL of each well to the first three quadrants of the Lightcycler 480 Multiwell plate (384-well) that contains the master mix.
2. Transfer 4 μL of the six dilutions of the standard curve (which consist of successive tenfold dilutions from 0.0002 to 20 pM) in triplicate to the fourth quadrant of the LC480 Multiwell plate.
3. Seal the plate with a Light Cycler optimal sealing film. Do not touch the sealer face with fingers as this may interfere with the results. Use a scraper to seal the plate and remove the white sides of the seal.
4. Spin down the plate at 4000 rpm (2120 × *g*) for 1 min.
5. If the plate could not be read immediately, place it in the dark.
6. Set up the following assay parameters in a LC 480 system:

   Reaction volume: 10 μL.

   Detection Format: SYBR Green/HRM dye.

   Pre-incubation: one cycle; analysis: none; target temperature: 95 °C; acquisition mode: None; ramp rate : 4.8 °C/s.; hold: 5 min.

   Amplification: 35 cycles; analysis mode: Quantification; temperature: cycles of 95 °C for 30 s and 60 °C for 45 s.

   Melting: one cycle; analysis mode: melting curve.

   Cooling: one cycle/analysis none.
7. Load the plate in the LC480 system and Click "Start Run".
8. After the run is complete, go to the "Analysis" module and select "Abs Quant/2nd Derivative Max" in the "Create a new analysis" window.
9. Select the "High Sensitivity" option in the next window and click on "Calculate".

10. After the calculation is complete, export the data table as a text file to a USB key.

3.2.4 Analysis of qPCR Data

1. Microsoft Excel can be used for analysis. Calculate the regression parameters of the standard curve. The R^2 value should be over 0.99. If not, the qPCR experiment should be redone.
2. If the average concentration of a library falls outside the dynamic range of the DNA standards, repeat the experiment for this library using a different dilution.
3. If one of the three replicates appears to be an outlier, it may be omitted from the calculation. If more than one of the three replicates appears to be outliers, the assay should be repeated.
4. Calculate the average concentration of each library by multiplying by the factor of dilution (8000 in this example).

3.2.5 Calculating Size-Adjusted Concentration of Libraries

1. Evaluate the average size of each library using an electrophoresis-based method for example Agilent DNA Bioanalyzer, the Caliper LabChip GX, or Agilent TapeStation. The DNA BioAnalyzer can process up to 12 samples at a time while the LabChip and Tape Station can analyze 96 samples at once.
2. Calculate the size-adjusted concentration by multiplying the concentration by the ratio of 452/(average size of the library).

3.3 Sample Preparation for Clustering

This section addresses the dilution and denaturation of the cDNA libraries that must be performed immediately prior to the clustering on a cBot, a MiSeq, or a HiSeq. It is recommended to run four barcoded libraries per HiSeq lane to obtain at least 40 M reads for each sample.

3.3.1 Denature DNA Template for Libraries with a Concentration Over 2 nM

1. The HT1 tube is provided in the TruSeq PE (or SR) Cluster kit v3 cBot-HS (Box 2 of 2). Thaw the reagents according to the type of run (single-read (SR) or paired-end (PE)), at 4 °C overnight if possible. If not, it should take about 60 min using a water bath at room temperature, and then keep the reagent plate at 4 °C until used.
2. Transfer 2 μL of each library to be sequenced in separate wells of a new full skirt 96-well plate.
3. Dilute each DNA template and phiX (10 nM) using Buffer EB with Tween 20 1% to 2 nM depending on the initial concentration. For libraries with an initial concentration below 2 nM refer to Subheading 3.3.2 below.
4. Pool all samples to be sequenced on the same lane by mixing equal volume (10 μL) of each diluted library (2 nM) in a new 1.7 mL microcentrifuge tube (one for each lane).
5. Vortex briefly and pulse centrifuge.

6. Using a new 1.7 mL microcentrifuge tube, dilute the 2 N NaOH to 0.1 N as follows: 190 μL molecular biology grade water and 10 μL of 2 N NaOH.
7. Vortex to mix uniformly.
8. Combine 10 μL of each pooled DNA template and the phiX control with 10 μL of 0.1 N NaOH in independent 1.7 mL microcentrifuge tubes.
9. Vortex briefly to mix and pulse centrifuge all the tubes.
10. Incubate for 5 min at RT to denature the template into single-stranded.
11. Quickly add 980 μL of prechilled HT1 into each tube to stop the denaturation. The libraries are at 20 pM now.
12. Vortex briefly and place the denatured DNA template on ice until ready to proceed to the final dilution.
13. Dilute the 20 pM denatured DNA libraries and phiX to 9 pM using 550 μL of prechilled HT1 and 450 μL of the 20 pM denatured DNA solutions. A different concentration can be used to adjust for the number of clusters obtained on a HiSeq or MiSeq.
14. Vortex briefly to mix and pulse centrifuge the tubes.
15. Place the denatured DNA on ice until ready to use.
16. Label new 1.7 microcentrifuge tubes (one for each lane) and dispense 1.2 μL of 20 pM phiX in each of them (a typical cDNA library only requires phiX for quality control purposes. If a less complex library such as miRNA or targeted cDNA is analyzed, then higher amounts, up to 50%, of phiX can be added to increase complexity).
17. Add the 118.8 μL of each denatured template and mix by pipetting several times.
18. Set aside on ice until ready to load onto the cBot instrument.

3.3.2 Denature DNA Template for Samples Below 2 nM

1. Add 2 μL of the DNA template to a new 1.7 mL tube.
2. Calculate the amount of total volume needed to obtain a dilution of 9 pM.
3. Add 1/125 of the total volume calculated above (in **step 2**) of 0.1 N NaOH to the tube.
4. Vortex briefly to mix and pulse centrifuge all the tubes.
5. Incubate for 5 min at RT to denature the template into single strands.
6. Calculate the volume of HT1 to add by subtracting the volume of DNA and NaOH to the total volume calculated in **step 2**.

7. Quickly add the calculated volume of prechilled HT1 in each tube to stop the denaturation.
8. Vortex briefly and place the denatured DNA template on ice.
9. Place the denatured DNA on ice until ready to load.
10. In new microcentrifuge tubes add 118.8 μL of each sample and 1.2 μL of pre-denatured phiX and mix by pipetting several times.
11. If the libraries need to be sequenced, in the same lane combine the specific proportion of each denatured sample or pool (prepared with either method) to reach 120 μL in a new microcentrifuge tube.

The denatured libraries are now ready to load on a cBot for the clustering prior to sequencing on a HiSeq 2000/2500 or for clustering directly on a MiSeq or a HiSeq 2500 in rapid mode. If not used immediately, the dilutions can be kept for up to 3 days at −20 °C. We typically use 100 bp paired-end sequencing for our regular RNA-Seq experiments.

3.4 Data Analysis

This protocol provides instructions for processing of Illumina paired-end 100 bp reads for samples with a good quality reference sequence. Samples with no or low quality reference sequence should be processed differently using a de novo approach to perform a transcriptome assembly of the RNA fragments (for example using the trinity software [18]). This protocol corresponds to the methodology developed at the Canadian Centre for Computational Genomics for which an automated procedure is available at https://bitbucket.org/mugqic/mugqic_pipelines/

3.4.1 Read Trimming and Clipping of Adapters

When a sequencing centre delivers sequences (paired reads in fastq or bam format), the raw data may contain low quality bases and adapters sequences. Thus, as a first step of analysis, cleaning of the raw sequencing data is useful.

1. Illumina sequencing adapters are removed from the reads and reads are trimmed from the 3′ end to have a phred score of at least **30**. All reads with a remaining length of less than **32** bp are removed. Trimming and clipping are performed using *Trimmomatic tools* [19] with the corresponding parameters: ILLUMINACLIP:adapters.fa:2:30:15 TRAILING:30 MINLEN:32 (*see* **Note 3**).

3.4.2 Read Alignment to a Reference Genome

The filtered reads are aligned to the corresponding reference genome. Each read set is aligned using *STAR* [20] in a 2-passes approach. STAR has been shown to be one of the most efficient and fastest RNAseq aligner. Moreover, STAR is also proposed as default RNA aligner is the GATK best practice pipelines.

1. During the first pass, all samples are aligned to the generic reference using the following parameters: --runMode alignReads --runThreadN 12 --readFilesCommand zcat --outStd Log --outSAMunmapped Within --outSAMtype BAM Unsorted --limitGenomeGenerateRAM 30000000000 --limitIObufferSize 4000000000 (*see* **Note 4**).
2. All junctions, for all samples, detected in the first pass are collected, filtered using the following awk command: cat alignment_1stPass/ */SJ.out.tab | awk 'BEGIN {OFS="\t"; strChar[0]="."; strChar[1]="+"; strChar[2]="-"} {if($5>0) {print $1,$2,$3,strChar[$4]}}' | sort -k1,1 h -k2,2n > alignment_1stPass/AllSamples.SJ.out.tab.
3. Project specific junctions are used to generate a new genome index for the 2nd pass using star with the parameters: --runMode genomeGenerate --genomeDir reference.Merged --runThreadN 12 --limitGenomeGenerateRAM 30000000000 --sjdbFileChrStartEnd alignment_1stPass/AllSamples.SJ.out.tab --limitIObufferSize 4000000000 --sjdbOverhang 99 (*see* **Note 4**).
4. The second alignment pass of star for all samples is done using this new genome index as sequence reference. The following parameters are used: --genomeDir reference.Merged --runThreadN 12 --readFilesCommand zcat --outStd Log --outSAMunmapped Within --outSAMtype BAM SortedBy Coordinate --limitGenomeGenerateRAM 15000000000 --limitBAMsortRAM 15000000000 --limitIObufferSize 4000000000 --chimSegmentMin 21(*see* **Note 4**).
5. The Alignment procedure creates a sorted Binary Alignment Map files (.bam).
6. All Bam files belonging to the same individual/pool will be merge to provide a unique bam. The merging is done using the function MergeSamFiles PICARD toolkit (http://broadinstitute.github.io/picard) with the options: ASSUME_SORTED=true CREATE_INDEX=true (*see* **Note 4**).

3.4.3 Alignment Quality Control

The quality of the alignment and of the library always needs to be assessed. Different parameters can be used to assess the quality of RNAseq experiments. Among others the fraction of read aligned, the fraction of read aligned in exons, the fraction of ribosomal read and the fraction of chimeric reads allows having a rapid overview of the quality of each sample individually.

1. Compute a series of quality control metrics including the count of chimeric pairs reads, the count of transcript annotated reads and the strand specificity distribution of reads using RNA-SeqQC [21] with parameters: -n 1000 -ttype 2 (*see* **Note 5**).

2. Compute additional quality control metrics regarding the alignment of RNA reads in general and also in specific functional classes of loci in the genome (coding, intronic, UTR, intergenic, ribosomal). These metrics are collected using both CollectRnaSeqMetrics and CollectAlignmentSummaryMetrics functions from Picard with default parameters.
3. Use bwa mem to align reads on a rRNA reference fasta file and count the number of read mapped using the following parameters: -M -t 10 (*see* **Note 5**).

3.4.4 Transcripts Analysis

In RNA-Seq experiments, cDNA fragments are sequenced and mapped back to genes and ideally, individual transcripts. In paired-end RNA-Seq experiments, fragments are sequenced from both ends, providing two reads for each fragment. Properly normalized, the RNA-Seq fragment counts can be used as a measure of the relative abundance of transcripts, and Cufflinks [22] measures transcript abundances in Fragments Per Kilobase of exon per Million fragments mapped (FPKM), which is analogous to single-read "RPKM". Aligned RNA-Seq reads are assembled into transcripts and their abundance (FPKM) is estimated. These transcripts are also annotated with the known reference set of transcripts obtained from the Ensembl database.

1. Generate a hardclipped version of the bam file for the Cufflinks suite which doesn't support this official sam feature using a combination of samtools and a awk command line: awk 'BEGIN {{OFS="\t"}} {{if (substr($1,1,1)=="@") {{print;next}}; split($6,C,/[0-9]*/);split($6,L,/[SMDIN]/);if(C[2]=="S") {{$10=substr($10,L[1]+1); $11=substr($11,L[1]+1)}}; if (C[length(C)]=="S") {{L1=length($10)-L[length(L)-1]; $10=substr($10,1,L1); $11=substr($11,1,L1); }}; gsub(/[0-9]*S/,"",$6); print}}'.
2. A reference-based transcript assembly is performed using Cufflinks with the following parameters: -q --max-bundle-frags 1000000 --library-type fr-firststrand --num-threads 8.
3. Transcript assembly produces individual list of transcripts in gtf format (*see* **Note 6**).
4. Merge assemblies into a master transcriptome reference using cuffmerge in its default mode.
5. The resulting merged assembly gtf file and the hardclipped bam are used to compute expression profiles (abundances.cxb) using cuffquant with the follwing parameters: -q --max-bundle-frags 1000000 --library-type fr-firststrand --num-threads 8.
6. The differential analysis is launched for each design. Cuffdiff [23] is used to calculate differential transcript expression levels and test

them for significant differences. Cuffdiff option are: -u --max-bundle-frags 1000000 --library-type fr-firststrand --num-threads 8.

7. As Cuffdiff generates normalized data using only the sample implicated in the design comparison, we additionally apply global normalization of RNA-Seq expression levels using Cuffnorm [22] with the following options: q --max-bundle-frags 1000000 --library-type fr-firststrand --num-threads 8.

3.4.5 Gene-Level Analysis

Read counts in genes are found to be linearly related to the abundance of the target transcript [24]. If reads were independently sampled from a population with given, fixed fractions of genes, the read counts would follow a multinomial distribution, which can be approximated by the Poisson distribution. Thus, we can use statistical testing to decide whether, for a given gene, an observed difference in read counts is significant, that is, whether it is greater than what would be expected just due to natural random variation.

1. Generate temporary sam files containing only the mapped read using samtools view with the option: –F 4.
2. Launch the read counting based on a predefined set of genes (gtf format) using the htseq-count options: -m intersection-nonempty --stranded=reverse --format=sam.
3. Compile the individual gene read counts into matrix of reads counts.
4. Proceed to the differential gene expression analysis using the EdgeR [25] Bioconductor package following the instructions given in the corresponding vignette (An example of EdgeR script in R is given at the following address: https://bitbucket.org/mugqic/mugqic_tools/src/master/R-tools/edger.R).
5. Proceed to the differential gene expression analysis using the DESseq [26] Bioconductor package and following the instructions given in the corresponding vignette (An example of DESseq script in R is given at https://bitbucket.org/mugqic/mugqic_tools/src/master/R-tools/deseq.R).
6. Merge the results of these two analyses in a single csv file.

3.4.6 Additional Analyses Using FPKM Values

Additional analysis of FPKM would allow controlling the overall quality of the experiment. We regularly use correlation and saturation analyses. The correlation analysis controls the general transcripts expression consistency between samples. It can also check sample mix-up or error in name assignment. Thus, samples belonging to the same design group/condition are expected to show higher level of correlation. The saturation plots show if there is enough sequencing depth to saturate gene expression at various ranges of expression. The saturation analysis consist in resampling a series of subsets from total set of RNA reads and

then calculate the Percent Relative Error (PRE) and the median RPKM of the set of transcripts. The PRE measures how the RPKM estimated from a subset of reads deviates from real expression levels. Saturation plots are generated independently for four different sets of transcripts: high, intermediate, moderate and low expressed transcripts (corresponding to quartiles Q1 to Q4 of median RPKM).

1. Perform a pairwise sample correlation analysis (Pearson's correlation) using R (An example of script in R is given at https://bitbucket.org/mugqic/mugqic_tools/src/master/R-tools/fpkmStats.R).
2. Generate saturation plots using R (An example of script in R is given at https://bitbucket.org/mugqic/mugqic_tools/src/master/R-tools/rpkmSaturation.R).

3.4.7 Gene Ontology (GO) Analysis for the Differential Gene Expression Results

Genes are grouped into categories defined by the common biological properties (Gene Ontology or GO) and then tested to find categories that are over-represented amongst the differentially expressed genes.

1. Perform GO enrichment analysis using the *goseq* [27] R Bioconductor package following the goseq vignette instructions (An example of script in R is given at https://bitbucket.org/mugqic/mugqic_tools/src/master/R-tools/goseq.R) (*see* **Note 7**).

4 Notes

1 If you do not plan to proceed to *Adenylation* immediately, the protocol can be safely stopped here. If you are stopping, seal the plate with a MicroAmp™ clear adhesive film and store it at −15 to −25 °C for up to 7 days.

2 The samples can be stored at −20 °C overnight at this point. If you are stopping, seal the plate with a MicroAmp™ clear adhesive film and store it at −15 to −25 °C for up to 7 days.

3 The adapter.fa file should contain the sequence of the adaptors used for sequencing and the adaptor clipping parameters given here correspond to a seed Mismatches of 2, a palindrome Clip threshold of 30 and a simple clip threshold of 15. Note that parameter orders are important for trimmomatic. Be sure to place the adaptor clipping parameters before the quality read trimming parameters. Otherwise, you will trim for quality the adapter sequence in your reads. This may result in inefficient adaptor recognition and a lack of removing their non-genomic sequence.

4 During the alignment, we strongly recommend to set the correct read group for each individual alignment to be able to back track the origin of each read during the post-alignment analysis. We also recommend to keep the unmapped reads into the main bam file for more convenience and to use the –chimSegmentMin option in order to generate a separate file that displays evidences of transcript fusions. The values of the STAR options limitGenomeGenerateRAM; --limitBAMsortRAM should be adjusted based on the available RAM resources available on the host system. Note that larger genome size will require larger amount of RAM. The value of the STAR --limitIObufferSize has to be set depending on the size of the I/O blocks of the host system. Otherwise, the performance of the software will be strongly reduced.

5 During the computation of metrics, RNAseqQC uses the information of the GTF file. The "-ttype" argument allows to specify which column in GTF to use to look for rRNA transcript type. Additionally, we set the "-n" option to specify the number of transcripts to use in each category of transcripts (low, medium and highly expressed). Increasing this number will provide better estimates but we increase the time of processing. When bwa-mem is used to estimate the amount of rRNA read it is important to use the "-M" option. This option allows marking the small part of spited reads as secondary hits in order to avoid overestimating the number of rRNA reads. Additionally, the –t option can be used to indicate the number if thread to used. This option should correspond to the resource available on the host system.

6 Cufflinks uses a statistical model of paired-end sequencing experiments to derive a likelihood for the abundances of a set of transcripts given a set of fragments. Cufflinks constructs a parsimonious set of transcripts that "explains" the reads observed in an RNA-Seq experiment. The assembly algorithm explicitly handles paired-end reads by treating the alignment for a given pair as a single object in the covering relation. Cufflinks tries to find the most parsimonious set of transcripts by performing a minimum-cost maximum matching. Reference annotation based assembly seeks to build upon available information about the transcriptome of an organism to find novel genes and isoforms. When a reference GTF is provided, the reference transcripts are tiled with faux-reads that will aid in the assembly of novel isoforms. These faux-reads are combined with the sequencing reads and are input into the regular Cufflinks assembler. The assembled transfrags are then compared to the reference transcripts to determine if they are different enough to be considered novel.

7 RNA-Seq data suffer from a bias in detecting differential expression for long genes. This means that when using a standard analysis, any category containing a predominance of long genes is more likely to show up as being over-represented than a category containing genes of average lengths. Thus, we use the goseq R package, which provides methods for performing Gene Ontology analysis, taking this gene length-related bias into account.

References

1. Johnson BE, Mazor T, Hong C, Barnes M, Aihara K, McLean CY, Fouse SD, Yamamoto S, Ueda H, Tatsuno K, Asthana S, Jalbert LE, Nelson SJ, Bollen AW, Gustafson WC, Charron E, Weiss WA, Smirnov IV, Song JS, Olshen AB, Cha S, Zhao Y, Moore RA, Mungall AJ, Jones SJM, Hirst M, Marra MA, Saito N, Aburatani H, Mukasa A, Berger MS, Chang SM, Taylor BS, Costello JF (2014) Mutational analysis reveals the origin and therapy-driven evolution of recurrent glioma. Science (New York, NY) 343(6167):189–193
2. Yates LR, Gerstung M, Knappskog S, Desmedt C, Gundem G, Van Loo P, Aas T, Alexandrov LB, Larsimont D, Davies H, Li Y, Ju YS, Ramakrishna M, Haugland HK, Lilleng PK, Nik-Zainal S, McLaren S, Butler A, Martin S, Glodzik D, Menzies A, Raine K, Hinton J, Jones D, Mudie LJ, Jiang B, Vincent D, Greene-Colozzi A, Adnet P-Y, Fatima A, Maetens M, Ignatiadis M, Stratton MR, Sotiriou C, Richardson AL, Lonning PE, Wedge DC, Campbell PJ (2015) Subclonal diversification of primary breast cancer revealed by multiregion sequencing. Nat Med 21(7):751–759
3. Finak G, Bertos N, Pepin F, Sadekova S, Souleimanova M, Zhao H, Chen H, Omeroglu G, Meterissian S, Omeroglu A, Hallett M, Park M (2008) Stromal gene expression predicts clinical outcome in breast cancer. Nat Med 14(5):518–527
4. Trimboli AJ, Cantemir-Stone CZ, Li F, Wallace JA, Merchant A, Creasap N, Thompson JC, Caserta E, Wang H, Chong JL, Naidu S, Wei G, Sharma SM, Stephens JA, Fernandez SA, Gurcan MN, Weinstein MB, Barsky SH, Yee L, Rosol TJ, Stromberg PC, Robinson ML, Pepin F, Hallett M, Park M, Ostrowski MC, Leone G (2009) Pten in stromal fibroblasts suppresses mammary epithelial tumors. Nature 461(7267):1084–1091
5. Lee S, Seo CH, Lim B, Yang JO, Oh J, Kim M, Lee S, Lee B, Kang C, Lee S (2010) Accurate quantification of transcriptome from RNA-Seq data by effective length normalization. Nucleic Acids Res 39(2):e9
6. Wagner G, Kin K, Lynch V (2012) Measurement of mRNA abundance using RNA-seq data: RPKM measure is inconsistent among samples. Theory Biosci 131(4):281–285
7. Cloonan N, Forrest ARR, Kolle G, Gardiner BBA, Faulkner GJ, Brown MK, Taylor DF, Steptoe AL, Wani S, Bethel G, Robertson AJ, Perkins AC, Bruce SJ, Lee CC, Ranade SS, Peckham HE, Manning JM, McKernan KJ, Grimmond SM (2008) Stem cell transcriptome profiling via massive-scale mRNA sequencing. Nat Methods 5(7):613–619
8. Wang Z, Gerstein M, Snyder M (2009) RNA-Seq: a revolutionary tool for transcriptomics. Nat Rev Genet 10(1):57–63
9. Okoniewski MJ, Miller CJ (2006) Hybridization interactions between probesets in short oligo microarrays lead to spurious correlations. BMC Bioinformatics 7:276
10. Zhao S, Fung-Leung W-P, Bittner A, Ngo K, Liu X (2014) Comparison of RNA-seq and microarray in transcriptome profiling of activated T cells. PLoS One 9(1):e78644
11. Auer PL, Doerge RW (2010) Statistical design and analysis of RNA sequencing data. Genetics 185(2):405–416
12. Mills JD, Kawahara Y, Janitz M (2013) Strand-specific RNA-seq provides greater resolution of transcriptome profiling. Curr Genomics 14(3):173–181
13. Sigurgeirsson B, Emanuelsson O, Lundeberg J (2014) Analysis of stranded information using an automated procedure for strand specific RNA sequencing. BMC Genomics 15(1):631
14. Johnsson P, Ackley A, Vidarsdottir L, Lui W-O, Corcoran M, Grandér D, Morris KV (2013) A pseudogene long noncoding RNA network regulates PTEN transcription and translation in human cells. Nat Struct Mol Biol 20(4):440–446
15. Poliseno L, Salmena L, Zhang J, Carver B, Haveman WJ, Pandolfi PP (2010) A coding-independent function of gene and pseudogene

mRNAs regulates tumour biology. Nature 465(7301):1033–1038

16. Grun D, Lyubimova A, Kester L, Wiebrands K, Basak O, Sasaki N, Clevers H, van Oudenaarden A (2015) Single-cell messenger RNA sequencing reveals rare intestinal cell types. Nature 525(7568):251–255
17. Miyamoto DT, Zheng Y, Wittner BS, Lee RJ, Zhu H, Broderick KT, Desai R, Fox DB, Brannigan BW, Trautwein J, Arora KS, Desai N, Dahl DM, Sequist LV, Smith MR, Kapur R, Wu C-L, Shioda T, Ramaswamy S, Ting DT, Toner M, Maheswaran S, Haber DA (2015) RNA-Seq of single prostate CTCs implicates noncanonical Wnt signaling in antiandrogen resistance. Science 349(6254):1351–1356
18. Grabherr MG, Haas BJ, Yassour M, Levin JZ, Thompson DA, Amit I, Adiconis X, Fan L, Raychowdhury R, Zeng Q, Chen Z, Mauceli E, Hacohen N, Gnirke A, Rhind N, di Palma F, Birren BW, Nusbaum C, Lindblad-Toh K, Friedman N, Regev A (2011) Trinity: reconstructing a full-length transcriptome without a genome from RNA-Seq data. Nat Biotechnol 29(7):644–652
19. Bolger AM, Lohse M, Usadel B (2014) Trimmomatic: a flexible trimmer for Illumina sequence data. Bioinformatics 30(15): 2114–2120
20. Dobin A, Davis CA, Schlesinger F, Drenkow J, Zaleski C, Jha S, Batut P, Chaisson M, Gingeras TR (2013) STAR: ultrafast universal RNA-seq aligner. Bioinformatics 29(1):15–21
21. DeLuca DS, Levin JZ, Sivachenko A, Fennell T, Nazaire M-D, Williams C, Reich M, Winckler W, Getz G (2012) RNA-SeQC: RNA-seq metrics for quality control and process optimization. Bioinformatics 28(11): 1530–1532
22. Trapnell C, Roberts A, Goff L, Pertea G, Kim D, Kelley DR, Pimentel H, Salzberg SL, Rinn JL, Pachter L (2012) Differential gene and transcript expression analysis of RNA-seq experiments with TopHat and Cufflinks. Nat Protoc 7(3):562–578
23. Trapnell C, Hendrickson DG, Sauvageau M, Goff L, Rinn JL, Pachter L (2013) Differential analysis of gene regulation at transcript resolution with RNA-seq. Nat Biotechnol 31(1): 46–53
24. Mortazavi A, Williams BA, McCue K, Schaeffer L, Wold B (2008) Mapping and quantifying mammalian transcriptomes by RNA-Seq. Nat Methods 5(7):621–628
25. Robinson MD, McCarthy DJ, Smyth GK (2010) edgeR: a Bioconductor package for differential expression analysis of digital gene expression data. Bioinformatics 26(1): 139–140
26. Anders S, Huber W (2010) Differential expression analysis for sequence count data. Genome Biol 11(10):R106
27. Young MD, Wakefield MJ, Smyth GK, Oshlack A (2010) Gene ontology analysis for RNA-seq: accounting for selection bias. Genome Biol 11(2):R14

Chapter 23

Sample Preparation for Mass Spectrometry Analysis of Protein–Protein Interactions in Cancer Cell Lines and Tissues

Alice Beigbeder*, Lauriane Vélot*, D. Andrew James, and Nicolas Bisson

Abstract

A precisely controlled network of protein–protein interactions constitutes the basis for functional signaling pathways. This equilibrium is more often than not disrupted in cancer cells, by the aberrant expression or activation of oncogenic proteins. Therefore, the analysis of protein interaction networks in cancer cells has become crucial to expand our comprehension of the molecular underpinnings of tumor formation and progression. This protocol describes a sample preparation method for the analysis of signaling complexes by mass spectrometry (MS), following the affinity purification of a protein of interest from a cancer cell line or a solid tumor. In particular, we provide a spin tip-based protease digestion procedure that offers a more rapid and controlled alternative to other gel-based and gel-free methods. This sample preparation protocol represents a useful strategy to identify protein interactions and to gain insight into the molecular mechanisms that contribute to a given cancer phenotype.

Key words Protein interactions, Mass spectrometry, Sample preparation, Tryptic digestion, Spin tip

1 Introduction

Intercellular communication is a critical feature of multicellular organisms. The signaling pathways that convey messages are commonly organized via inducible protein–protein interactions. This constitutes the basis for large, complex and dynamic signaling networks whose assembly and dismantling must be highly coordinated [1]. In humans, activation of these pathways at inappropriate locations or times can have disastrous consequences such as cell transformation and cancer [2].

*Author contributed equally with all other contributors.

Josie Ursini-Siegel and Nicole Beauchemin (eds.), *The Tumor Microenvironment: Methods and Protocols*, Methods in Molecular Biology, vol. 1458, DOI 10.1007/978-1-4939-3801-8_23, © Springer Science+Business Media New York 2016

The heterogeneity of both the genomic landscape and the cancer cell phenotype, within a given tissue, highlight the complexity of the disease. It has become clear that phenotypes are not simply the result of a mutation in a single gene but rather reflect the interplay between a number of molecular interactions. In this respect, network-based approaches have become crucial for our understanding of the molecular underpinnings of tumor formation and progression [3, 4].

The analysis of protein–protein interactions within signaling networks using affinity purification followed by MS is one of the best suited methods to identify proteins that associate together directly or indirectly under physiological conditions, in normal and cancer cells [5, 6]. We provide here a sample preparation protocol for MS analysis of signaling complexes following the affinity purification of a protein of interest from a cancer cell line or solid tumor tissue.

Sample preparation is often an underestimated step in mass spectrometry analyses. Many of the current protocols can have a number of drawbacks, including: (1) being performed following gel electrophoresis, (2) extended incubation time with trypsin, and (3) requiring additional cleanup steps prior to MS analysis. This protocol provides a rapid, simple, and reproducible method for gel-free sample preparation supporting MS analysis of proteins, based on the utilization of spin tips. The digestion of protein samples directly on a chromatographic support allows for (1) gel-free digestion of a wide variety of samples with protein concentrations across a broad dynamic range, (2) a significantly shorter time of incubation with the protease, and (3) simultaneous sample purification and desalting. Moreover, the preparation of samples as described here leads to high reproducibility, as the fixed capacity of the chromatographic medium normalizes the amount of protein to be processed. This approach has been successfully applied to identify phosphorylation sites on a protein of interest [7], to characterize interaction partners following affinity purification [8, 9] and to investigate signaling network dynamics in transformed cells [10]. The method is also suitable for preparation of samples from tumor tissues for proteomic analyses.

2 Materials

In order to avoid contamination with keratins, it is recommended to handle materials with clean gloves.

2.1 Tissue Culture and Protein Extraction

1. LNCaP human prostate adenocarcinoma cells (or another cancer cell line, or tumor tissue) (*see* **Note 1**).
2. RPMI 1640 with L-glutamine culture medium supplemented with 10% fetal bovine serum (FBS).

3. Phosphate buffered saline (PBS): 137 mM NaCl, 2.7 mM KCl, 10 mM Na_2HPO_4, 1.8 mM KH_2PO_4.
4. Cell lysis buffer: 20 mM Tris–HCl, pH 7.4, 150 mM NaCl, 1 mM EDTA, 1% NP-40 (Igepal), 0.5% sodium deoxycholate, 10% glycerol. In order to prevent protein degradation, the buffer is supplemented with 1.5 μM aprotinin, 20 μM leupeptin, 15 μM pepstatin, and 1 mM phenylmethylsulfonylfluoride (PMSF) just before use. If required, phosphatase inhibitors may also be added (e.g., 10 mM β-glycerophosphate, 50 mM sodium fluoride, 10 mM sodium pyrophosphate) (*see* **Note 2**).

2.2 Affinity Purification and Sample Elution

1. Affinity resin (to be selected according to the antibody required) (*see* **Note 2**).
2. Cell lysis buffer (as in Subheading 2.1).
3. Wash buffer: 20 mM Tris–HCl, pH 7.4 (may be supplemented with protease and phosphatase inhibitors, if required).
4. Elution solution: 50 mM phosphoric acid pH 1.5–2.

2.3 Protein Digestion on Chromatography Medium in a Spin Tip

The reagents listed below should be handled with care to avoid contamination with keratins. Reagents should also be diluted in high-pressure liquid chromatography (HPLC)-grade water.

1. A 10 μL pipette tip with a 0.6 μL bed of strong cation chromatography medium (SCX) fixed at its end (e.g., Millipore ZipTip®) with adaptor.
2. Conditioned SCX resin in water: polysulfoethyl A, particle size 12 μm, pore size 300 Å (optional).
3. 10 mM potassium phosphate buffer, pH 3.0.
4. HPLC-grade water.
5. 100 mM tris (2-carboxyethyl) phosphine (TCEP) in 100 mM Tris–HCl, pH 9.0.
6. Sequencing grade-modified trypsin or other protease.
7. 100 mM iodoacetamide (light-sensitive, keep in the dark).
8. 200 mM Tris–HCl, pH 8.0.
9. 2% formic acid.

3 Methods

3.1 Tissue Culture and Protein Extraction

1. Grow LNCaP cells to 90% confluence in 10 cm petri dishes in RPMI medium with L-glutamine supplemented with 10% FBS, at 37 °C in a 5% CO_2 controlled atmosphere (*see* **Note 3**).
2. Carefully place the dishes on ice. Rinse cells once with 5 mL ice-cold PBS to remove any trace of culture medium.

3. Add 1 mL of cell lysis buffer per 10 cm dish (*see* **Note 4**). Lift cells off the plate using a scraper and harvest lysate in a 1.5 mL tube. Incubate for 20 min at 4 °C; mixing is optional (*see* **Note 5**).
4. Centrifuge at >15,000 × *g* for 20 min at 4 °C to remove insoluble material.
5. Collect supernatant in a new tube. Keep the lysate on ice for immediate use, or store at −80 °C. A small fraction of the lysate will be required to determine protein concentration (e.g., using bicinchoninic acid (BCA) assay) and for control experiments, if required (e.g., Western blotting analysis).

3.2 Affinity Purification and Sample Elution

1. Prepare the required amount of affinity resin (*see* **Note 6**) by washing with cell lysis buffer (or PBS) three times, according to the manufacturer's recommendations (*see* **Note 7**).
2. In a new tube, mix 20 mg of cell lysate to the required amount of pre-washed affinity resin (*see* **Note 8**). Rotate the tubes at 4 °C for 90 min (*see* **Note 9**).
3. Pellet beads by centrifugation at 200 × *g* for 2 min at 4 °C (*see* **Note 10**). A fraction of the post-purification lysate may be kept to confirm that this step was successful. Remove supernatant and resuspend resin in 900 µL of cell lysis buffer by gently inverting the tubes a few times. Repeat this wash step twice.
4. Pellet beads by centrifugation at 200 × *g* for 2 min at 4 °C. Remove supernatant and add 900 µL of wash buffer to resuspend the pelleted beads. Repeat once. This step is critical in removing salts and detergents, which are not compatible with later steps (*see* **Note 11**). After the last wash, aspirate as much wash buffer as possible, without disturbing the resin.
5. Add 100 µL of elution solution to the beads. Incubate at 4 °C agitation for 10 min (*see* **Note 12**).
6. Pellet beads by centrifugation at 200 × *g* for 2 min at 4 °C. Keep supernatant by transferring to a new tube. Repeat the elution twice and pool the three eluates in a single tube (*see* **Note 13**).
7. Centrifuge the pooled elutions at >15,000 × *g* for 1 min at 4 °C, then transfer the supernatant to a new 1.5 mL tube while avoiding to transfer any residual beads. This latter step is crucial. Sample can be stored at −80 °C for later use (*see* **Note 14**).

3.3 Protein Digestion on Chromatography Medium in a Spin Tip

1. Fit a 10 µL pipette tip with a 0.6 µL bed of strong cation chromatography medium (SCX) fixed at its end (e.g., Millipore ZipTip®, *see* **Note 15**) into a 1.5 mL standard collection tube, using an adaptor (*see* **Note 16**) (Fig. 1).
2. Wash column with 80 µL of potassium phosphate buffer. Centrifuge at 200 × *g* for 2 min at a time until all buffer goes through the column. Discard the flow-through. Repeat this wash step twice.

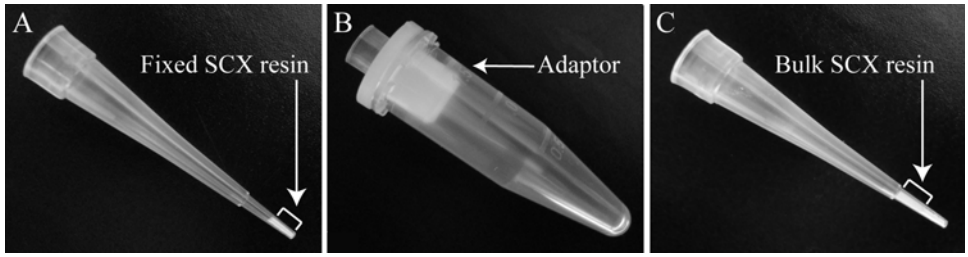

Fig. 1 Spin tip-based protein digestion setup. (**a**) A 10 μL spin tip with a 0.6 μL bed of fixed SCX resin at its end is shown. (**b**) The spin tip fits into a 1.5 mL tube with an adaptor. (**c**) Conditioned SCX resin can be added to the spin tip to increase column capacity

3. Load protein sample (eluates from Subheading 3.2) on spin tip by centrifugation at 200 × *g* for 2 min of a volume of 80 μL at a time (*see* **Note 17**). Repeat this step until the protein sample is completely loaded (*see* **Note 18**). You may keep the flow-through and analyze a fraction of it to verify that all proteins have bound the column.
4. Wash column (as in **step 2**) with 60 μL of potassium phosphate buffer.
5. Wash column with 30 μL of HPLC-grade water.
6. Transfer the column in a new 1.5 mL collection tube.
7. Incubate with 100 mM TCEP for 30 min at room temperature. To achieve this, pipette 2–3 μL of solution and centrifuge for 1–2 s, until a tiny droplet (representing less than the complete volume of solution) is seen at the bottom of the collection tube. Do not let it go through completely (*see* **Note 19**).
8. Wash column with 60 μL of HPLC-grade water.
9. Transfer spin tip into a new collection tube.
10. Resuspend MS grade tryspin in 100 mM Tris–HCl, pH 8.0, 10 mM iodoacetamide in order to get to a final concentration of 2 mg/mL (*see* **Note 20**).
11. Put trypsin solution on the resin as detailed in **step 7** above (*see* **Note 21**). Incubate with trypsin solution for 1–2 h at room temperature, in the dark (*see* **Note 22**).
12. Elute digested sample into a new collection tube by washing column with 5 μL of HPLC-grade water (*see* **Note 23**). Keep the flow-through; this is the digested sample. Repeat twice and pool eluates; total volume should be 15 μL.
13. Acidify the eluate by adding 1 μL of formic acid 2%.
14. Store at −80 °C until mass spectrometry analysis (*see* **Note 24**).

4 Notes

1. Negative controls should be planned to perform bioinformatics analysis of MS data using appropriate software (e.g., SAINT) [11].
2. The cell lysis buffer composition has to be compatible with the affinity resin that is selected.
3. The amount of cells to be grown is relative to expression levels of the protein bait (also *see* **Note 8**).
4. The volume of cell lysis buffer to be used is determined from the size of the cell pellet and the expected total protein content, which are both dependent of the cell line that is utilized. Typically, a volume of 0.3–1 mL is adequate for a 10 cm culture plate.
5. Alternatively, proteins may be extracted from tumor tissue using the same cell lysis buffer. However, the tissue will require mechanical homogenization to achieve a complete lysis.
6. The selection of the affinity resin is made following the selection of the cell line that is utilized. For example, cells stably or transiently expressing an epitope-tagged protein (e.g., GFP, Flag, HA, Myc) will require an affinity resin that recognizes the epitope. On the other hand, non-engineered (parental) cell lines will necessitate custom antibody-immobilized beads to precipitate endogenous proteins.
7. The utilization of wide-bore pipette tips will facilitate resin transfer. Bead dilutions in a larger volume (e.g., 100 µL per 10–20 µL of beads, per purification) will ensure that beads are distributed equally among all tubes, if several affinity purifications are performed simultaneously.
8. The amount of total protein to be used in each affinity purification procedure requires to be tested experimentally, as it is dependent of the bait protein expression level and the affinity of the antibody for the bait protein, among other factors. Better results are obtained when 0.5 to 1 µg of the bait protein is affinity-precipitated. In order to verify this, **step 3** of Subheading 3.2 may be followed by an extraction in Laemmli buffer to determine bait protein levels via SDS-PAGE using a BSA standard.
9. An incubation period of antibody-conjugated beads with cell lysates for 30–120 min is normally sufficient. A longer incubation period may lead to protein precipitation and to the identification of more contaminants as proteins interacting with the selected bait. Overnight incubations should be avoided. The volume in which the affinity purification is performed should not influence yields.

10. If magnetic beads are used, all centrifugation steps of the affinity purification procedure are replaced by placing the tube on the magnet for 1 min.
11. For wash steps, a prolonged incubation is not required.
12. The utilization of a temperature-controlled agitator is suggested but not required. Alternatively, tap the bottom of the tube gently a few times to resuspend beads every 2–3 min. The low pH may lead to a change of color of the beads; this will not affect subsequent steps. As elution of bait protein complexes using a peptide antigen is challenging and not compatible with gel-free tryptic digestion protocols for MS analysis, this is a significant advantage of this method.
13. This elution method was successfully performed with M2 (Flag) affinity resin, protein A Sepharose, streptavidin agarose and a variety of magnetic beads coupled to antibodies, peptides or chemicals.
14. Proteins are stable for weeks in elution solution, if stored at −80 °C. Samples may be kept to perform spin tip digestion (Subheading 3.3) simultaneously.
15. While Millipore ZipTip®-SCX are easy to use, Glygen TopTips are also suitable and available with or without chromatography media.
16. The capacity of the SCX resin is estimated to be 0.5 μg of protein per μL of resin. The amount of SCX in the spin tip may be adjusted by adding resin (Polysulfoethyl A, particle size 12 μm, pore size 300 Å) to the spin tip. This can be achieved by pipetting conditioned SCX resin resuspended in HPLC-grade water (in a 1:10 resin–water ratio), followed by centrifugation at 200 × *g* for 2 min or until the resin is packed. The equivalent of 0.5–1.5 μL of resin may be added, for a total capacity around 1 μg of protein on the spin tip (Fig. 1). This contributes to limit the amount of protein to be digested, thus increasing reproducibility of the tryptic digestion step and helping to estimate sample concentration.
17. The spin tip tryptic digestion protocol is also compatible with digestion of whole cell extracts for total proteome analysis (i.e., without the affinity purification step). The protein sample will need to be acidified prior to binding to the SCX resin. The reproducibility of the protocol described here was not specifically tested for this application.
18. A highly concentrated protein sample to be loaded on the spin tip (i.e., above 2–3 μg) or one that is contaminated with beads from the affinity purification step may block the spin tip. To overcome this problem without compromising samples, it is possible to centrifuge at a higher speed (up to 400–500 × *g*,

although this may block the column even further) or to use a closed glass capillary to stir gently the resin inside the spin tip.

19. There should also be a small volume of the TCEP solution that is visible above the SCX resin bed. If the complete volume inadvertently goes through the spin tip, this step may be repeated until successfully achieved.
20. Iodoacetamide is an alkylation agent that irreversibly transforms cysteines to prevent the reformation of disulfide bonds. It may be omitted, due to the rareness of cysteine in protein sequences. If it is used, it will increase the mass of a cysteine from 103.01 to 160.03 Da for a carboxyamidomethylcysteine. Databases should be searched accordingly.
21. It is crucial to ensure that the trypsin solution is on the column but does not go through completely. Iodoacetamide is light sensitive; therefore spin tips should be incubated in the dark (e.g., wrapping the tube rack in foil). The high concentration of trypsin that is utilized in this protocol and the small reaction volume allow an efficient digestion of proteins within 1–2 h.
22. The protocol is also compatible with proteases other than trypsin, at neutral pH.
23. Elution may also be performed in freshly prepared 200 mM ammonium bicarbonate, pH 8.0. This may be directly analyzed by mass spectrometry following acidification with formic acid to 1% final, or may require complete evaporation and resuspension in 0.1% formic acid.
24. The digested sample may be kept at –80 °C for a few weeks. It may be directly analyzed by LC/MS-MS as it is, without evaporation/resuspension or further purification.

Acknowledgements

The spin tip digestion method was initially developed in the laboratory of Dr. Tony Pawson at the Lunenfeld-Tanenbaum Research Institute, with input from Karen Colwill, Brett Larsen and Vivian Nguyen. This work was supported by grants from the Canadian Institutes for Health Research (MOP-130335) and the Canada Foundation for Innovation (32308) (to N.B.). A.B. and L.V. held Pierre J. Durand Scholarships from Université Laval Faculty of Medicine, and L.V. currently holds the Louis-Poirier Scholarship and a Université Laval Cancer Research Centre scholarship. N.B. was a scholar of the "Fonds de Recherche du Québec-Santé" in partnership with the Quebec Breast Cancer Foundation and holds a Canada Research Chair in Cancer Proteomics.

References

1. Gibson TJ (2009) Cell regulation: determined to signal discrete cooperation. Trends Biochem Sci 34:471–482
2. Pawson T (1995) Protein modules and signalling networks. Nature 373:573–580
3. Goh KI, Cusick ME, Valle D, Childs B, Vidal M, Barabasi AL (2007) The human disease network. Proc Natl Acad Sci U S A 104:8685–8690
4. Menche J, Sharma A, Kitsak M, Ghiassian SD, Vidal M, Loscalzo J, Barabasi AL (2015) Disease networks Uncovering disease-disease relationships through the incomplete interactome. Science 347:1257601
5. Lambert JP, Ivosev G, Couzens AL, Larsen B, Taipale M, Lin ZY et al (2013) Mapping differential interactomes by affinity purification coupled with data-independent mass spectrometry acquisition. Nat Methods 10:1239–1245
6. Dunham WH, Mullin M, Gingras AC (2012) Affinity-purification coupled to mass spectrometry: basic principles and strategies. Proteomics 12:1576–1590
7. Gamblin CL, Hardy EJ, Chartier FJ, Bisson N, Laprise P (2014) A bidirectional antagonism between aPKC and Yurt regulates epithelial cell polarity. J Cell Biol 204:487–495
8. Bisson N, James DA, Ivosev G, Tate SA, Bonner R, Taylor L, Pawson T (2011) Selected reaction monitoring mass spectrometry reveals the dynamics of signaling through the GRB2 adaptor. Nat Biotechnol 29:653–658
9. So J, Pasculescu A, Dai AY, Williton K, James A, Nguyen V et al (2015) Integrative analysis of kinase networks in TRAIL-induced apoptosis provides a source of potential targets for combination therapy. Sci Signal 8:rs3
10. Filteau M, Diss G, Torres-Quiroz F, Dube AK, Schraffl A, Bachmann VA et al (2015) Systematic identification of signal integration by protein kinase A. Proc Natl Acad Sci U S A 112:4501–4506
11. Choi H, Larsen B, Lin ZY, Breitkreutz A, Mellacheruvu D, Fermin D et al (2011) SAINT: probabilistic scoring of affinity purification-mass spectrometry data. Nat Methods 8:70–73

Index

Josie Ursini-Siegel and Nicole Beauchemin (eds.), *The Tumor Microenvironment: Methods and Protocols*, Methods in Molecular Biology, vol. 1458, DOI 10.1007/978-1-4939-3801-8, © Springer Science+Business Media New York 2016

C

D

E

F

G

H

I

J

K

L

M

N

O

P

Q

R

S

T

U

V

W

X

Z